Nano Chemistry: Large Molecular Capsules and Coordination Networks Based on Self-Assembly

Submitted in accordance with the requirements
for the degree of Doctor of Philosophy

By

Scott John Dalgarno, *MChem*

The candidate confirms that the work submitted is his own and that appropriate credit has been given where reference has been made to the work of others.

School of Chemistry
The University of Leeds
October 2004

The work contained in this thesis has never been submitted to any university for the award of degree. To the best of my knowledge, this thesis contains no material previously published or written by another person except where due reference is made.

Signed:.....

Acknowledgements

Firstly I would like to thank Professor Colin L. Raston and Dr. Michaele J. Hardie for their supervision and support over the last three years. I extend my gratitude to Professor Jerry L. Atwood and Professor Leonard J. Barbour for their respective supervision and help during my time in Columbia-Missouri. For help with NMR studies, I would like to thank Dr. Julie Fisher for all her efforts that extended into the late nights and weekends. I must also thank Colin Kilner for all his help with X-ray crystallography and for 'morning coffee' chats.

I have had the great fortune to work and socialise with many different characters during my time at Leeds and it would be impossible to include everybody that I have shared a drink with in one of our three seminar rooms, the Packhorse, the Eldon and the Brickies. In no particular order, I would like to thank the Kee and Kennedy groups, namely Terry, Emmanuelle (doughnut), Sylvie, Tracy, Neil, Yong, Londers, Jonathan, Mick, John and Neil. Members of the McGowan and Halcrow groups past and present; Tom, Marco, Olivia, Patrick, Stephen, Jon, Claire, Ahmed, and Osman. Finally I would like to thank all of my group for putting up with me at work and making it a pleasant environment, so thanks to Mick, Jochen, Gareth, Chris, Maria and the infidel Mark. If I have missed anybody, which I probably have, it is just another late night on the computer and I apologise.

Special thanks must go to the following people; Andy 'the bag of knowledge' Gott for quiz machine partnering, oh and darts! The French contingent, Isabelle, Jerome (jéjé), Eric, and Chokri 'use your chest' Hathroubi. I am indebted to Rox who has been a great friend to me when things were far less than great and who has listened to my rants on many an occasion. I must thank all the members of 'Real Complex' for our team efforts but unfortunately we never quite made it. Thanks to Jerome for letting me beat him at squash once (and nearly a couple of times). I must thank a very good friend and housemate, Ken, for all the drunken nights in Chapel Allerton, our drinking exploits in Aberdeen and in general just being himself.

I must of course thank all my family for being there when I needed them through this time but most of all I must thank Radia. She has shown tremendous patience with me through the past two and a half years and has nursed me from the 'lows' on many an occasion. For her many efforts, unique charm and unfaltering love, I am truly grateful.

Abstract

This thesis focuses on the characterisation of supramolecular structures containing *p*-sulfonatocalix[*n*]arenes (where *n* = 4,5,6,8) with suitable guest molecules and lanthanide metal cations. The characterisation is based primarily on X-ray diffraction but high-resolution NMR techniques have also been used to identify *p*-sulfonatocalix[4]arene/crown ether complexation in the solution phase. Notably, remarkable control can be achieved over the formation and geometries of nano-metre scale spheroids or tubules containing *p*-sulfonatocalix[4]arene *via* guest selection.

Chapter 1 gives a short overview of supramolecular chemistry, molecular recognition and the history and synthesis of calixarenes. The supramolecular chemistry of the *p*-sulfonatocalix[*n*]arenes and a selection of interesting and recently reported nano-metre scale multi-component supramolecular architectures are also reviewed.

Chapter 2 describes the pH dependent formation of a number of molecular capsule and bi-layer supramolecular architectures based on *p*-sulfonatocalix[4]arene, (di)aza-functionalised guest species and lanthanide metals.

Chapter 3 describes the formation of several bi-layer structures based on *p*-sulfonatocalix[4]arene and lanthanide metals. Incorporation of different lanthanide metal salts changed the resulting structures by either inclusion or exclusion of the anions in the supramolecular architectures formed.

Chapter 4 describes a series of Diffusion Ordered Spectroscopy experiments that were performed in collaboration with Dr. Julie Fisher at the University of Leeds. The experiments were based on calixarene/crown ether systems and the results showed 1:1 host-guest complexation in solution with a series of charged species.

Chapter 5 describes the formation of Russian doll complexes and the design and control over nano-metre scale spheroidal arrays composed of *p*-sulfonatocalix[4]arene.

Chapters 6 and 7 describe the formation of novel supramolecular complexes that are based on the *p*-sulfonatocalix[5,6,8]arenes. The resulting supramolecular architectures include unprecedented *bis*-molecular capsules, coordination polymer chains and 3-D networks.

ABBREVIATIONS

p-Sulfonatocalix[*n*]arene (where *n* = 4,5,6,8)	$SO_3[n]$
p-Alkylcalix[*n*]arenes (where *n* = 4,5,6,8)	*p*-R[*n*]
1,4-diazabicyclo[2.2.2]octane	DABCO
pyridine *N*-oxide	PyNO
4,4'-dipyridine-*N,N'*-dioxide	DiPyNO
3-pyridine sulfonic	$PySO_3$
Nuclear Magnetic Resonance	NMR
Energy Dispersive X-ray Analysis	EDX
Infra Red	IR
Strong (IR)	s
Medium (IR)	m
Weak (IR)	w
Diffusion Ordered Spectroscopy	DOSY
Pulse Field Gradient	PFG
Bi-polar Pulse Pair Stimulated Echo	BPPSTE
Dichloromethane	DCM
Toluene	Tol
Concentrated	Conc.
Hours	h
Proton (NMR)	^{1}H
Carbon (NMR)	^{13}C
Diamond square process	DS
Transition metal	TM

Table of Contents

List of Figures

List of Tables

List of Equations

Publications

1. S. J. Dalgarno, C. L. Raston, 'Capture of di-protonated [2.2.2]cryptand in the cavity of two *p*-sulfonated calixarenes as part of 2-D bi-layer lanthanide coordination polymers'. *Chem. Commun.* **2002**, 2216.
2. J. L. Atwood, L. J. Barbour, S. J. Dalgarno, C. L. Raston, H. R. Webb, 'Supramolecular assemblies of *p*-sulfonatocalix[4]arene with aquated trivalent lanthanide ions'. *J. Chem. Soc., Dalton Trans.* **2002**, 23, 4351.
3. S. J. Dalgarno, C. L. Raston, 'Rapid capture of 4,13-diaza-18-crown-6 molecules by *p*-sulfonatocalix[4]arene in the presence of trivalent lanthanide ions'. *Dalton Trans.* **2003**, 3, 287.
4. S. J. Dalgarno, M. J. Hardie, M. Makha, C. L. Raston, 'Controlling the conformation and interplay of *p*-sulfonatocalix[6]arene as lanthanide crown ether complexes', *Chem. Eur. J.*, **2003**, 9, 2834.
5. J. L. Atwood, S. J. Dalgarno, M. J. Hardie, C. L. Raston, 'Hydrogen-bonded arrays of a ytterbium(III) *p*-sulfonatocalix[6]arene complex', *New J. Chem.*, **2004**, 28. 326.
6. S. J. Dalgarno, M. J. Hardie, C. L. Raston, 'pH Dependent Formation of Molecular Capsules and Coordination Polymers', *Cryst. Growth Des.*, **2004**, 4, 227.
7. S. J. Dalgarno, M. J. Hardie, J. E. Warren, C. L. Raston, 'Lanthanide crown ether complexes of *p*-sulfonatocalix[5]arene', *Dalton Trans.*, **2004**, 16, 2413.
8. J. L. Atwood, L. J. Barbour, S. J. Dalgarno, M. J. Hardie, C. L. Raston, H. R. Webb, 'Towards mimicking viral geometry with metal organic systems', *J. Am. Chem. Soc.*, **2004**, 41, 13170.
9. S. J. Dalgarno, M. J. Hardie, J. L. Atwood, C. L. Raston, 'Bi-Layers, Corrugated Bi-Layers, and Coordination Polymers of *p*-Sulfonatocalix[6]arene', *Inorg. Chem.*, **2004**, 20, 6351.
10. S. J. Dalgarno, M. J. Hardie, C. L. Raston, 'Conformation perturbation of *p*-sulfonatocalix[5]arene *via* complexation of 1,4-diazabicyclo[2.2.2]octane', *Chem. Commun.*, **2004**, 2802.
11. J. L. Atwood, S. J. Dalgarno, M. J. Hardie, C. L. Raston, 'Confinement of amino acids: Selective single crystal *p*-Sulfonatocalix[6]arene complexation of $_{L}$ or $_{D}$-leucine'. *Chem. Commun.*, **2005**, 337.
12. S. J. Dalgarno, M. J. Hardie, J. L. Atwood, C. L. Raston, J. E. Warren, 'A 'wavy brick wall' coordination polymer linked by *p*-sulfonatocalix[8]arene', *submitted.*

Chapter one:
Literature background and introduction to the study

1.0 Introduction.

This thesis is concerned with the supramolecular chemistry of the *p*-sulfonatocalix[*n*]arenes (where *n* = 4,5,6,8), container molecules that can act as hosts when in the presence of various (in)organic guests (charged or uncharged) and lanthanide metal counterions. The work is based primarily around the formation of 'molecular capsules' comprising *p*-sulfonatocalix[4,5,6]arene and crown ethers but also extends into associated chemistry with the larger calixarenes and different guest molecules. To ensure a purposeful discussion of the work detailed within, it is first necessary to introduce the fundamentals of supramolecular chemistry and molecular recognition in addition to the history, synthesis and functionalisation of calixarenes. Latter discussion in this chapter will explore the previously reported supramolecular chemistry associated with the *p*-sulfonatocalix[*n*]arenes and solid state assemblies, highlighting some of the previously reported supramolecular architectures. A portion of the literature based around the *p*-sulfonatocalix[*n*]arenes is concerned with various aspects of behaviour in solution ranging from association with particular guests to selective catalysis. Although little of this literature will be reviewed in this chapter, it will be described in more detail in chapter four which is concerned with the study of various crown ether/*p*-sulfonatocalix[4]arene complexes in solution. The penultimate section of this chapter will describe several nano-metre scale supramolecular architectures composed of some other important supramolecular tectons (building blocks) given their relevance to both results presented within this thesis and the future direction and scope of supramolecular chemistry as a whole. Finally, this chapter will deal with a short discussion of the suitability of lanthanide ions for assembly formation with *p*-sulfonatocalix[*n*]arenes before moving on to describe the aims of the project and the guests/tectons/building blocks that will be employed in the study.

1.1 Supramolecular chemistry.

This exciting and dynamic area of chemistry was recognised over a hundred years ago by Emil Fischer but the concept lay relatively dormant until the potential of the chemistry was realised by Jean-Marie Lehn.[1] Since that time, and the subsequent publishing of his book 'Supramolecular Chemistry: Concepts and Perspectives', the field has grown enormously with entire journals such as 'Supramolecular Chemistry' or the 'Journal of Supramolecular Chemistry' being devoted to the subject alone in recent times. Lehn stated that "Just as there is a field of molecular chemistry based

on the covalent bond, there is a field of supramolecular chemistry, the chemistry of molecular assemblies and of the intermolecular bond" as shown schematically in Figure 1.1.[1]

The basic build up of a supermolecule consists of host and guest molecules that interact through intermolecular bonds. Once these supermolecules have formed and the systems understood, progression through to molecular and supramolecular devices may be possible.[1]

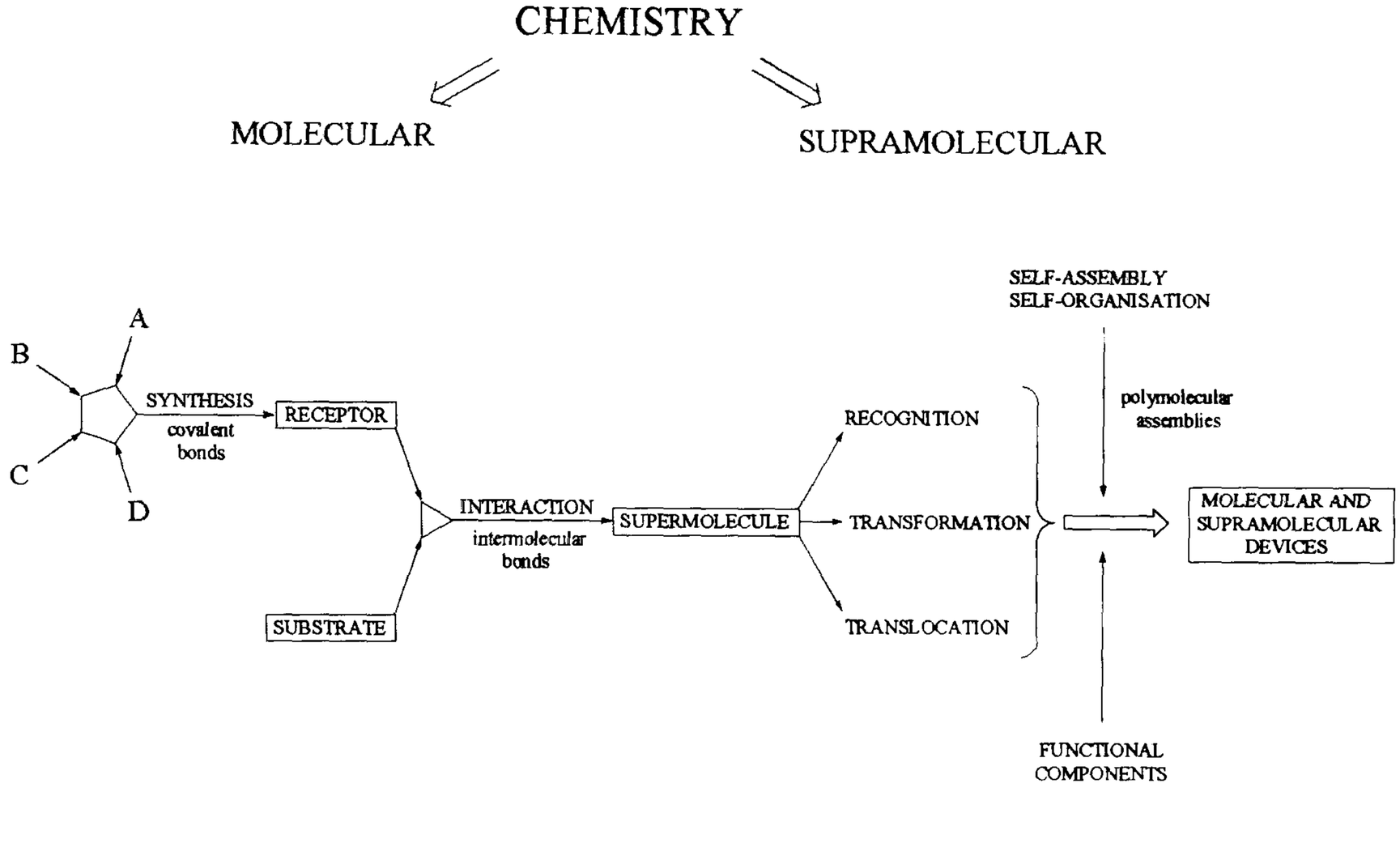

Figure 1.1 Schematic representing the shift from traditional molecular to novel supramolecular chemistry and the advance to supramolecular devices.[1]

The principles of supramolecular chemistry and/or intermolecular interactions have, and continue to be used to construct novel molecular arrangements that have application in nanotechnology. One growing research area at the forefront of supramolecular chemistry is that of molecular machines. Intermolecular forces (and covalent bonding in some cases) are used to construct molecular elevators, rotors, hydrogen-bonded shuttles and borromean rings to name but a few.[2-5] These multi-component arrangements typically build on known supramolecular motifs in order to access more complex systems or superstructures. Seeman and co-workers have used these principles to construct large DNA based molecular machines, architectures and networks.[6, 7]

Calixarenes are an incredibly useful class of host molecules that can be used to unlimited extent in supramolecular chemistry as they can (as will be shown in section 1.4) be synthesised or synthetically altered with relative ease to suit desired applications.[8, 9] This fact is reflected in the many reported articles based on the supramolecular chemistry of calixarenes, studies that often

focus on substrate binding in the cavity of the particular host.[1] Substrate binding can be selective or can, for example, allow for selective catalysis in the solution phase through intermolecular interactions.[9]

The principles of supramolecular chemistry and the theories of crystal engineering have also been used in the construction of novel and interesting solid state architectures.[4, 10] The resultant structures or networks show many interesting properties such as gas storage materials.[11-13] As highlighted by Janiak in a recent review, transition metals and pyridine or carboxylato-functionalised ligands are excellent examples of systems that form desirable rigid coordination polymers in the solid state that often display the aforementioned properties.[10]

1.2 Molecular Recognition.

For supramolecular chemistry to thrive, molecular recognition is a key pre-requisite. Molecular recognition can be described as binding with a purpose, not simply the binding of one entity to another; it is selective.[1, 14] For this to be the case, there must be molecular complimentarity between the substrate and receptor. Common terms in molecular recognition are substrate, receptor, host and guest. These terms stimulate the mind to envisage how the concept of molecular recognition in relatively small synthetic systems can be related to biological applications such as enzymatic processes. A simple but excellent example of molecular recognition is the selective binding of particular alkali metals by certain crown ether macrocycles, a phenomenon that has been known for some time and exploited by many research groups in various aspects of supramolecular chemistry (Table 1.1).[14]

Cation	Diameter (Å)	Crown Ether	Cavity Diameter (Å)
Li^+	1.36	12-crown-4	1.20 – 1.50
Na^+	1.90	15-crown-5	1.70 – 2.20
K^+	2.66	18-crown-6	2.60 – 3.20
Cs^+	3.38	21-crown-7	3.40 – 4.30

Table 1.1 The correlation of some alkali metal cation diameters with cavity diameters of particular crown ethers that lead to selective binding/molecular recognition.[14]

The complimentarity that governs the assembly of supermolecules (section 1.1) must be significant and there must be an inherently efficient recognition process that produces strong and selective binding. There are indeed many varying factors that must first be considered and then harnessed in the design of supramolecular systems in order to achieve any one particular goal. The supramolecular chemistry of this study is based primarily upon the use of *p*-sulfonatocalix[*n*]arenes and crown ethers as the host and guest respectively. The aforementioned enzymatic principles are applicable to many of the results presented within this thesis, some of which directly confirm *p*-sulfonatocalix[4]arene/crown ether pre-organisation in the solution phase (chapter four).

1.3 The History of Calixarenes.

The discovery of reactions between phenols and formaldehyde was made towards the end of the nineteenth century by Adolph von Bayer.[8] Some seventy years later, in the 1940's, Zinke discovered the formation of cyclic oligomers from reactions between *p*-alkyl phenols and formaldehyde.[8] Despite this, it was not until the 1970's that pioneering work by Gutsche *et al.* examined the chemistry further and identified the three major species found in the Zinke mixture to be cyclic tetramers, hexamers and octamers.[8, 15] Indeed it was Gutsche who eventually named these molecules 'calixarenes', a name consequent to their resembling a 'calix', Greek for cup, whilst bearing aromatic groups, hence 'arene'. This nomenclature was based on the smallest of the three macrocylces, calix[4]arene, where [4] represents the number of repeating units within the molecule. The extensive work of Gutsche *et al.* led to an explosion in the number of reported articles based on calixarenes at the turn of the century, and one which has rarely slowed due the enormous scope of chemistry related to these useful molecules.

1.4 Synthesis and Functionalisation of Calix[*n*]arenes (n = 4,5,6,...).

As stated above, there has been a dramatic increase in the number of articles reporting findings in synthetic and supramolecular calixarene chemistry. This is in part due to the term being generalised to encompass many molecules comprising a macrocyclic framework with aromatic groups connected by bridging atoms thus bearing resemblance to *p*-alkylcalix[*n*]arenes. Traditionally however, the term was used to denote two major classes of calixarene, those mentioned in section 1.3 and resorcinol based cyclo-oliogomers named resorcinarenes.[8] This thesis deals only with the supramolecular chemistry of one type of calixarene, *p*-sulfonatocalix[*n*]arenes. In the interests of brevity and given that entire books have been composed on various aspects calixarene chemistry, discussion of synthetic techniques employed will be limited. This section will however cover the

synthesis of the parent *p-tert*-butylcalix[*n*]arenes, their subsequent de-*tert*-butylation and sulfonation.[8, 16]

p-Alkylcalix[*n*]arenes (*p*-R[*n*] where R is the varying alkyl group) are formed by the base induced condensation of *p*-alkylphenols with formaldehyde. Of many such reactions reported to date, almost none are as efficient as those for the synthesis of the *p-tert*-butylcalix[*n*]arenes with respect to isolating cylo-oligomers of a chosen size in reasonable yield depending on reaction conditions.[8] Despite this, it is possible to isolate many such molecules *via* the use of continuous chromatography but this is often a lengthy, costly and time consuming exercise. Indeed it is possible to produce high purity *p*-^{t}Bu[4,5,6,8] on multi-gram scales in a matter of days in good yield although the pentamer is more synthetically challenging and is typically isolated in only a 5-15% yield.[8] In fact little progress has been made to date with respect to increasing the yield of *p*-^{t}Bu[5]. The cyclic heptamer is also isolable but is less commonly used than the more synthetically accessible calixarenes listed above. In stark contrast to the facile synthesis of *p*-R[*n*], it is not possible to synthesise calixarenes when an electron withdrawing group is present *para* to the hydroxyl group in the starting phenol.[8] Thus *p*-sulfonato, nitro, and cyano calixarenes for example must be prepared by alternative methods, one of which is shown below for the synthesis of the *p*-sulfonatocalix[*n*]arenes, Figure 1.2.

Much of the supramolecular chemistry reported to date incorporating *p*-sulfonatocalix[*n*]arene has used the calix[4]arene as a host molecule as the tetra or penta-sodium salts (Na_4SO_3[4] and Na_5SO_3[4] respectively). Tetra-sodium *p*-sulfonatocalix[4]arene is synthesised by reaction of *p*-^{t}Bu[*n*] with concentrated sulphuric acid followed by the pouring of the reaction mixture into brine to precipitate the calixarene salt.[16] The penta-sodium salt is synthesised *via* the titration of an aqueous solution containing Na_4SO_3[4] to pH~9 followed by solvent removal in *vacuo*.

Whilst route **A** reduces the number of synthetic steps in the overall sulfonation, isolation of the sulfonic acid is far more difficult *via* the use of concentrated sulphuric acid and the calixarene is typically isolated as the sodium salt (Figure 1.2).[8, 9] To circumvent this problem, *p*-^{t}Bu[4] can be de-*tert*-butylated and sulfonated *via* the use of chlorosulfonic acid, affording SO_3H[4] as a clean white hygroscopic solid (route **B**, Figure 1.2).[8, 9] Indeed as will be shown in Chapter 2 in particular, the presence of sulfonic acid groups at the *para*-position can be desirable in forming molecular capsules that are entirely pH dependent without employing alternative sources of protonation in the reaction mixture in order to achieve low pH values. The synthesis shown in Figure 1.2 highlights a simple functionalisation of the 'upper rim' of the calixarene. Given the relative ease with which sulfonation

of the calix[*n*]arenes is achieved, one can envisage the limitless possibilities of functionalisation and potential application associated with these molecules.

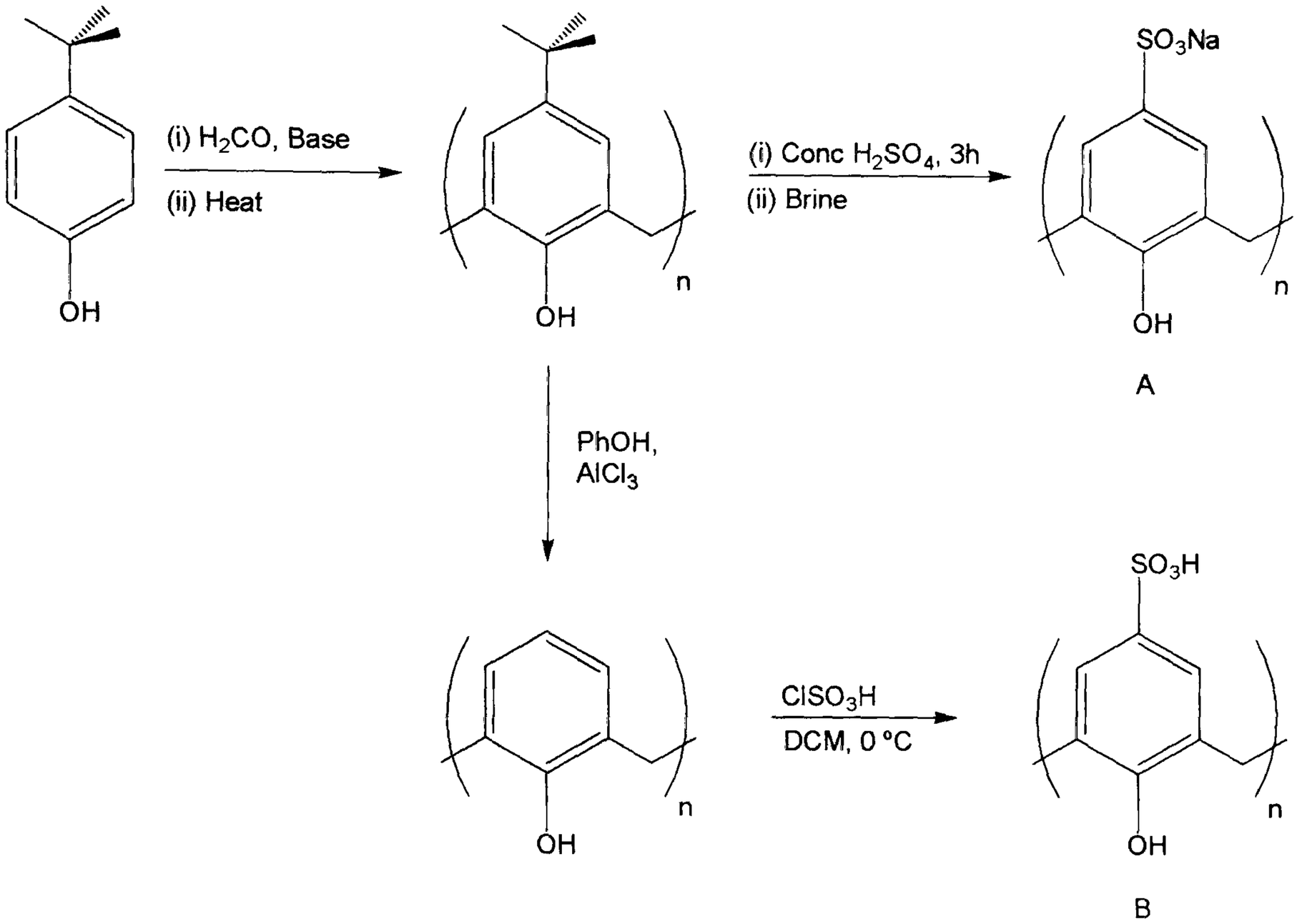

Figure 1.2 Synthetic scheme for the synthesis of the sodium salts or sulfonic acid of the *p*-sulfonatocalix[*n*]arene from *p-tert*-butylphenol starting material.[8, 9]

This is further stressed by the fact that these molecules can also be easily altered at the base or 'lower rim' thus allowing the chemist to gain access to an even greater library of container molecules.[8, 9, 15] Inherent in this library is the chemist's ability to structurally tune the calixarene framework such that the molecule possesses specific steric, electronic, or functional properties as dictated by the desired application.

1.5 Sulfonated calix[*n*]arenes

The supramolecular chemistry of the *p*-sulfonatocalix[*n*]arenes is an active area of research that is currently being pursued by several research groups worldwide. These molecules have, as will be shown in the following sections, the ability to interact in a multitude of ways in both synthetic and biological systems alike.[17-19] Much of the early work in this field was documented by Shinkai and co-workers and focused primarily on solution and catalytic properties of the *p*-sulfonatocalix[*n*]arenes.[16, 20-23] Although several other solution studies have been performed by

various research groups since this time, the literature will be reviewed in greater detail in Chapter 4 as that section deals directly with solution phase experiments with crown ether/*p*-sulfonatocalix[4]arene systems. At this point of discussion it is practical to divide this section into subsections that deal with the solid state supramolecular chemistry of each of the *p*-sulfonatocalix[*n*]arenes separately in turn (where $n = 4,5,6,8$).

1.5.1 Solid state supramolecular chemistry of *p*-sulfonatocalix[4]arene.

Toward the end of the 1980's and in the early to mid 1990's, both the Atwood and Shinkai research groups in particular began to document supramolecular architectures that were based primarily on X-ray crystallographic studies of *p*-sulfonatocalix[4]arene ($SO_3[4]$).[24-33] In all of those structures, $SO_3[4]$ is seen to adopt a truncated cone solid state conformation.[24-33] When in this conformation, the molecule typically packs in a favourable bi-layer arrangement that optimises hydrophobic-hydrophobic and hydrophilic-hydrophilic interactions (Figure 1.3). This is achieved through the formation of π-stacking or CH···π interactions between calixarene aromatic and bridging methylene groups.[34, 35] Indeed it was Atwood and co-workers that reported the structures of the alkali metal salts of *p*-sulfonatocalix[4]arene and identified them as analogues to organic clays as they exhibited bi-layers of anionic calixarenes in the solid state (Figure 1.3).[25, 26]

Of the early (and primarily 'organic only') *p*-sulfonatocalix[4]arene structural studies documented, Atwood *et al.* reported a study of the intercalation of cationic, anionic, and molecular species into the organic hosts.[24] The same group also documented the first X-ray diffraction evidence for OH···π hydrogen bonding from a cavity bound water molecule to a $SO_3[4]$ aromatic ring.[28] Shortly after, Shinkai and co-workers reported the formation of a trimethylanilinium chloride $SO_3[4]$ complex that, in the solid state, showed the aromatic ring of the guest to be directed into the hydrophobic cavity presented by the calixarene host.[27]

Indeed other interesting 'organic only' supramolecular architectures containing $SO_3[4]$ and suitable guest species were reported in the mid to late 1990's.[36] An adeninium *p*-sulfonatocalix[4]arene complex was shown to form cationic and anionic bi-layers within an extended structure that showed unusually large hydrophilic layers composed primarily of adeninium cations.[37] The development of binary metal/$SO_3[4]$ and ternary metal/ligand/$SO_3[4]$ systems was a key progression in the supramolecular chemistry of *p*-sulfonatocalix[4]arene. Shinkai *et al.* reported a molecular capsule like arrangement composed of two $SO_3[4]$ molecules that were linked *via* poly-aquo manganese ions.[38] At a similar time, Atwood and co-workers reported a series of copper or nickel pyridine

complexes that assembled with *p*-sulfonatocalix[4]arene through intermolecular interactions to generate several new supramolecular bi-layer motifs.[29-31, 39, 40]

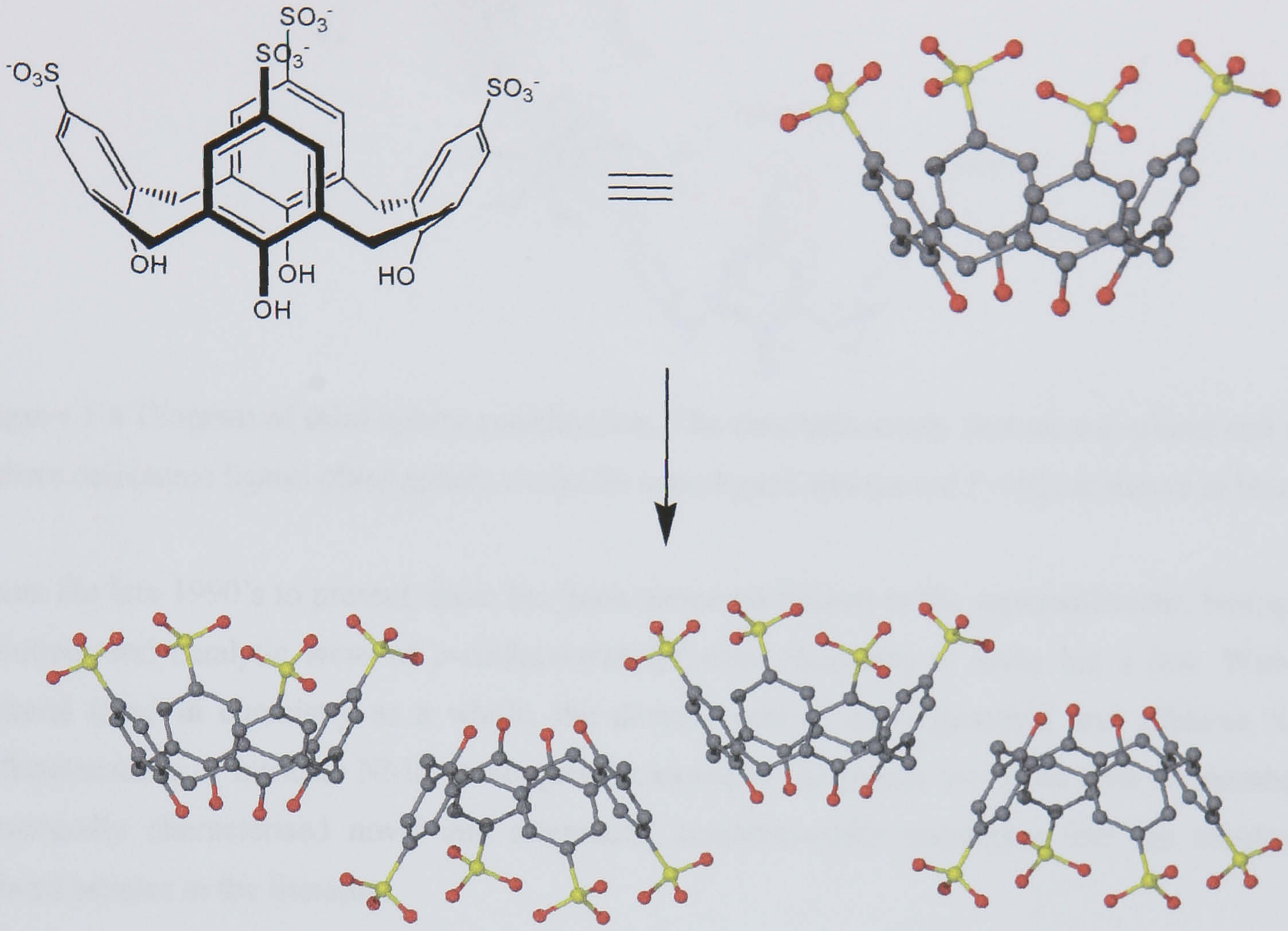

Figure 1.3 Molecular structure of a *p*-sulfonatocalix[4]arene with solid state cone representation (top). The extended solid state structure is often seen to assemble in up-down anti-parallel bi-layer motifs that mimic organic clays (bottom).[25] The bi-layer arrangement optimises both hydrophobic and hydrophilic interactions in the solid state.

Coordinated pyridine molecules were seen to intercalate into the hydrophobic layer of SO_3[4] in some of the extended structures whilst non-coordinated guest molecules occupied the cavities of *p*-sulfonatocalix[4]arene hosts.[40] Other related work by the same group adapted the above systems to suit lanthanide metals through replacement of pyridine with its *N*-oxide analogue. They reported a europium/pyridine *N*-oxide/SO_3[4] complex that showed the calixarene to simultaneously act as a first and third sphere ligand in the first structural authentication of third sphere coordination, as defined by Stoddart.[33, 41] These systems were subsequently likened them to enzyme models as they possessed metal ion binding sites in addition to hydrophobic pockets/cavities for inclusion of guest species (Figure 1.4). During this time, the potential use of *p*-sulfonatocalix[4]arene as an anti-viral or chloride channel blocking agent was realised.[19, 42, 43]

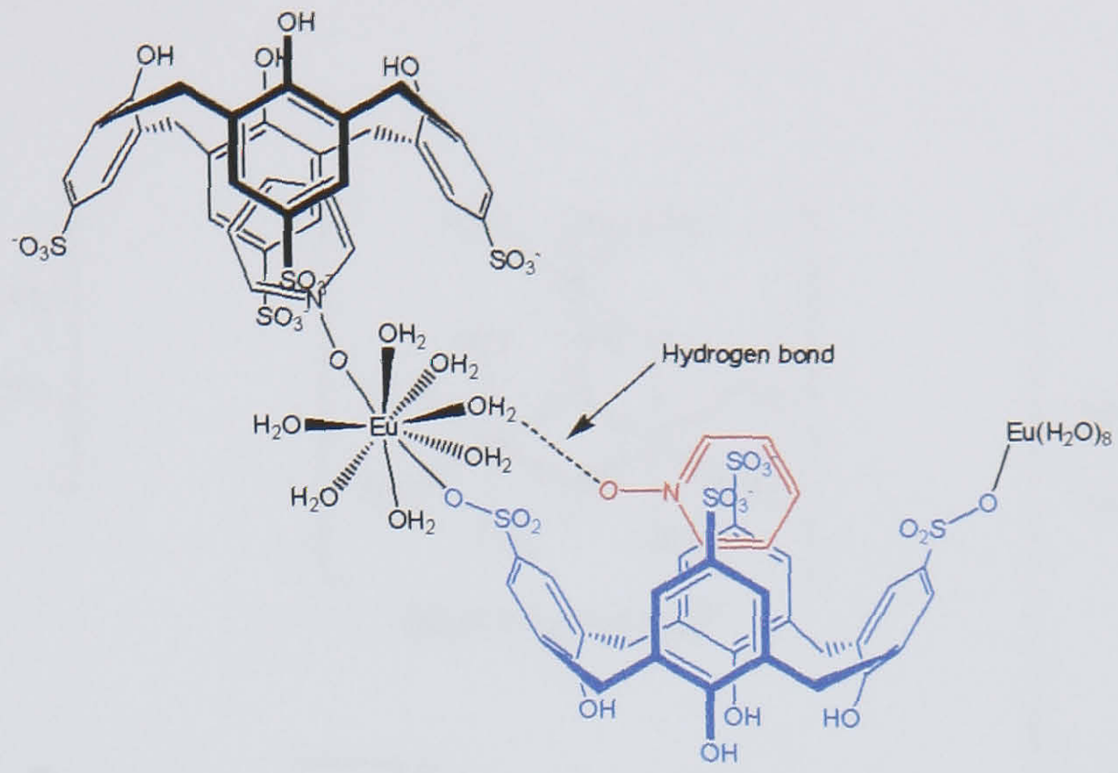

Figure 1.4 Diagram of third sphere coordination. The simultanesously first (to europium) and third sphere calixarene ligand (third sphere *via* an Eu aquo ligand and the red PyNO) is shown in blue.[41]

From the late 1990's to present, there has been increased interest in the supramolecular, biological, solution, and catalytic areas of *p*-sulfonatocalix[*n*]arene chemistry to name but a few. With the general trend in chemistry as a whole, the development of more powerful and efficient X-ray diffractometers or intricate NMR techniques for example has greatly increased both the number of structurally characterised novel and interesting supramolecular complexes and the number of related articles in the literature.

Raston and co-workers have made a significant contribution to the number of known supramolecular solid state motifs recorded in the Cambridge Crystallographic Database. Some of their studies focused on the use of 18-crown-6/SO_3[4] systems that assemble as superanions or Russian dolls (Figure 1.5).[34, 35, 44, 45] These superanions are capable of selectively crystallising a range of polynuclear hydrolytic metal super-cation complexes in bi-layer arrangements as illustrated in Figures 1.3 and 1.5.

In addition to this, the superanions can also selectively crystallise aluminium Keggin ions although there is a disturbance to the typical bi-layer packing motif of SO_3[4].[46] Alternative Russian dolls containing tetra-protonated cyclam were also capable of crystallising with dichromium(III) aquo cations, *exo*-capsule tetra-protonated cyclam, or other tetra-protonatated macrocycles in bi-layer motifs.[47, 48]

Other related studies from the Raston group used lanthanide/18-crown-6/SO_3[4] ternary systems to assemble molecular capsule or 'Ferris wheel' arrangements as shown in Figure 1.6. These studies

showed that different assemblies were formed with lanthanides of varied ionic radius and under varied pH regimes.[49, 50]

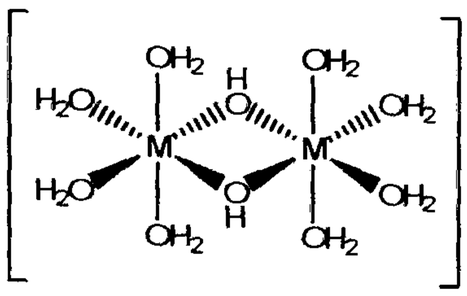

$[M_2(OH)_2(H_2O)_8]^{4+}$

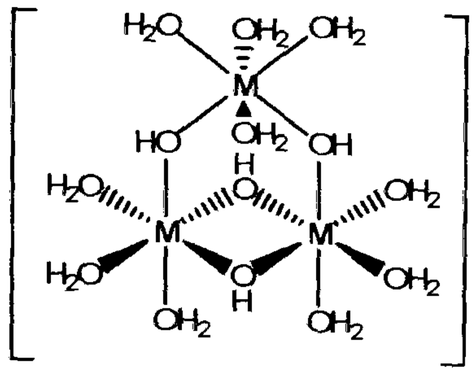

$[M_3(OH)_4(H_2O)_{10}]^{5+}$

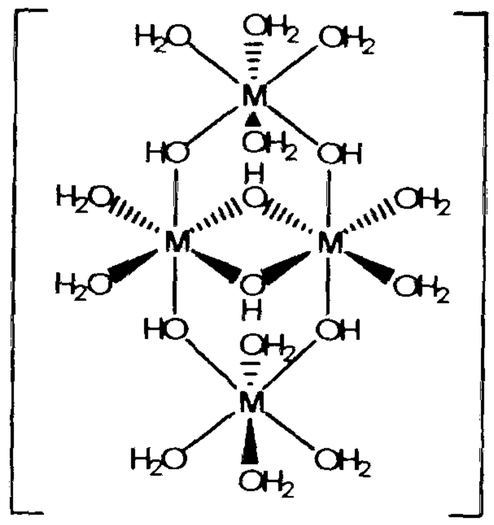

$[M_4(OH)_6(H_2O)_{12}]^{6+}$

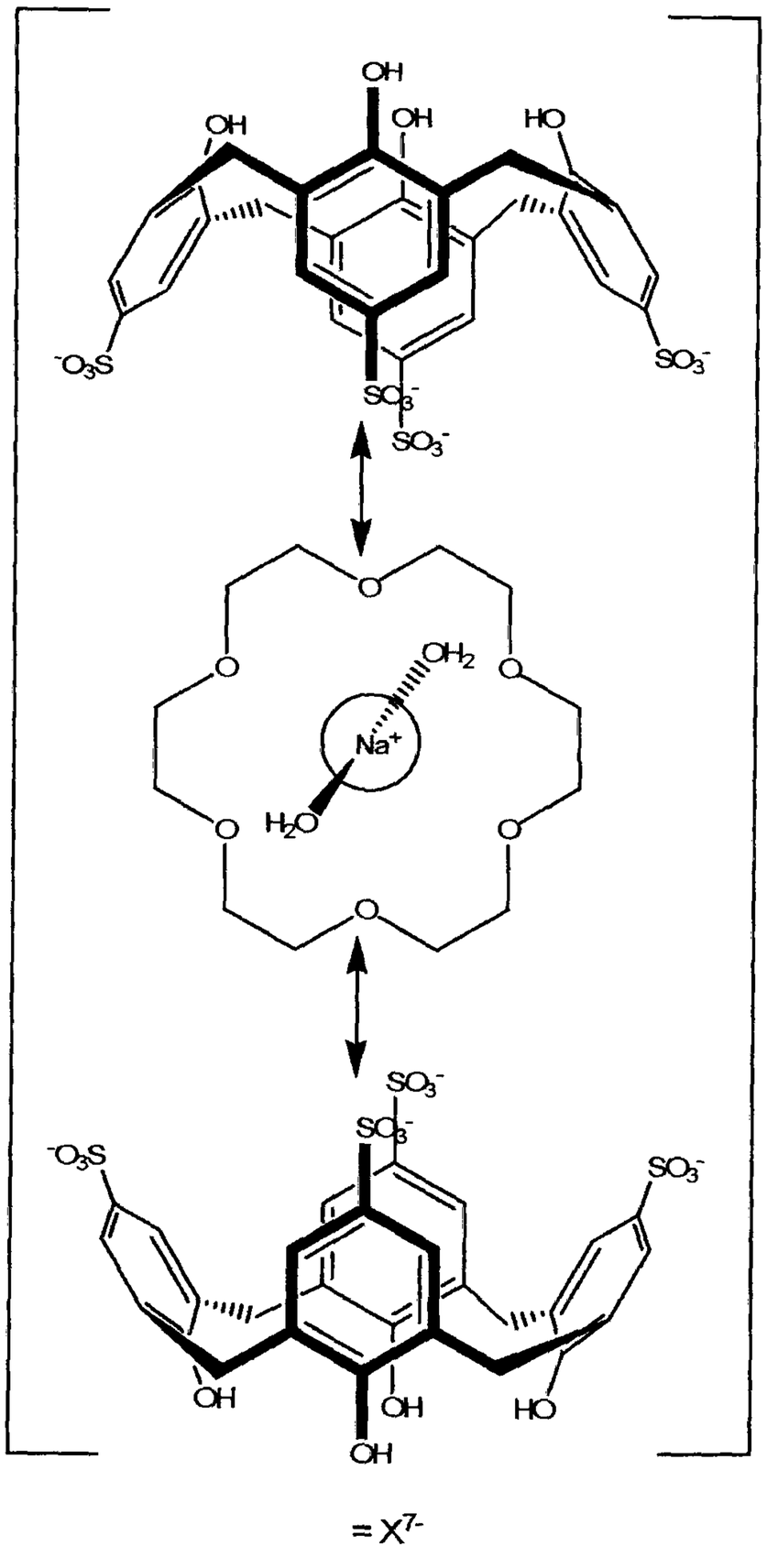

$= X^{7-}$

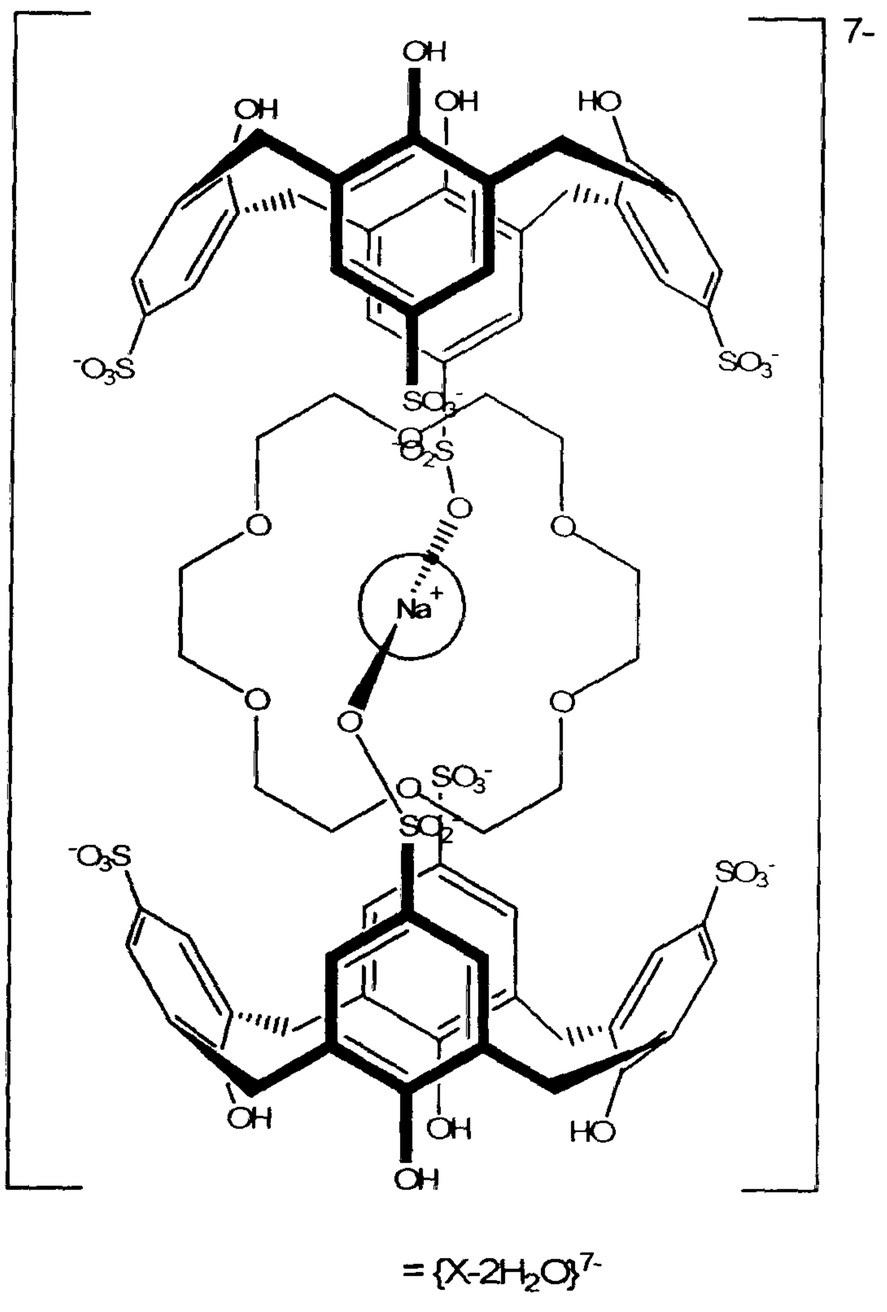

$= \{X\text{-}2H_2O\}^{7-}$

Figure 1.5 Schematic representation of the poly-nuclear hydrolytic metal super-cation complexes that are found to crystallise with the SO_3[4]/sodium 18-crown-6 Russian doll superanions in bi-layer arrangements.[35, 45, 46]

Scandium coordination polymers of SO_3[4]/18-crown-6/SO_3[4] molecular capsules were also isolated and structurally characterised.[51] Indeed pH control was used by Detellier *et al.* who reported the structure of a discrete 8:6 La(III):SO_3[4] superstructure, crystals of which grew from an acidic solution containing lanthanum(III) chloride and SO_3H[4].[52]

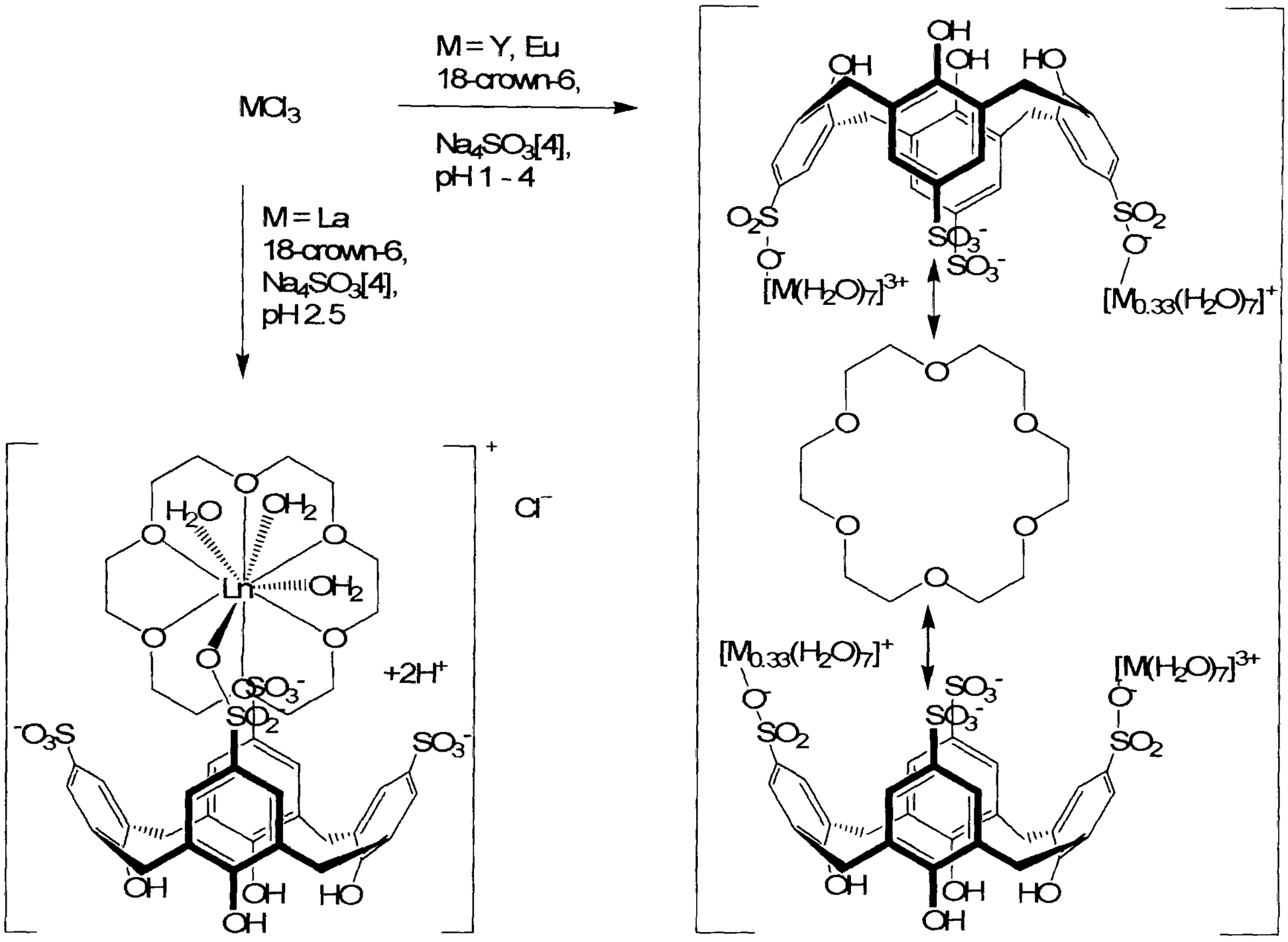

Figure 1.6 Schematic representation of the two structures formed with SO_3[4], 18-crown-6 and selected lanthanide ions, demonstrating dependence upon both ion size and pH.[35, 49, 50]

Leverd *et al.* showed that successive titration of an acidic solution of *p*-sulfonatocalix[4]arene with ehylenediamine resulted in the formation of three different structural motifs at different resulting values of pH.[53] All three had di-cationic species in the calixarene cavities and one structure assembled with the calixarenes in a head-to-head manner as for the molecular capsules described above with 18-crown-6 or related guest species (Figure 1.7).[34] More recently, Coleman *et al.* reported a comparative study of four SO_3[4]/di- and tri-ammonium cation complexes, some of which also assembled as slipped or face-to-face molecular capsules (Figure 1.7).[54]

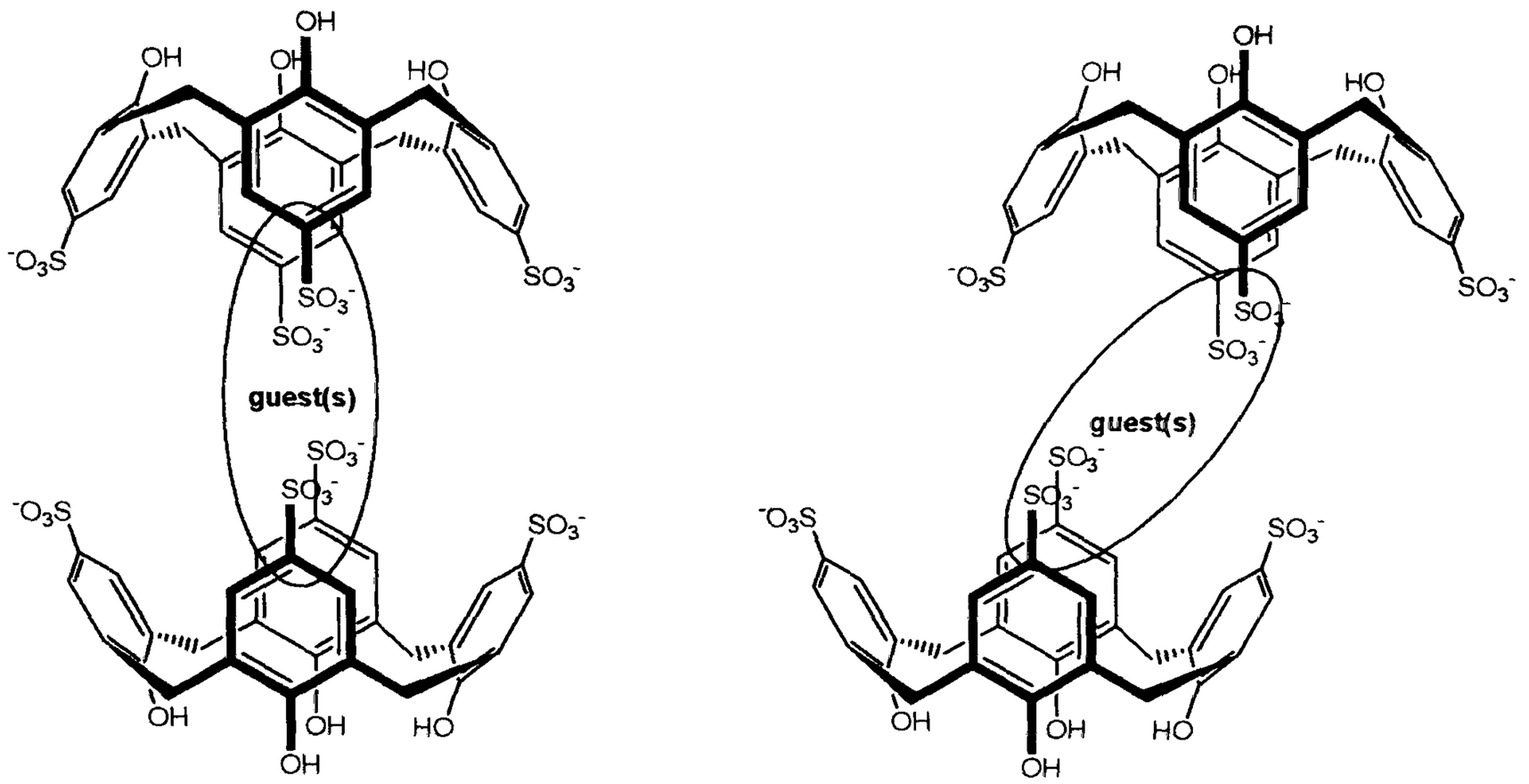

head-to-head capsule

slipped capsule

Figure 1.7 Schematic of head-to-head and slipped molecular capsules of *p*-sulfonatocalix[4]arene with guest molecules occupying the SO_3[4] cavities.

Given their biological activity, Coleman and co-workers have investigated both solution and structural aspects of SO_3[*n*]/amino acid complexes (where n = 4,6,8).[55-60] The two structural studies reported *p*-sulfonatocalix[4]arene $_L$-lysine and $_D$-arginine complexes, both of which form unusual packing arrangements. The L-lysine complex was reported as the first example of a substrate 'spanning the calix[4]arene bi-layer' in addition to being complexed directly by the calixarene.[59] Whilst this structure retained some bi-layer character, complexation of $_D$-arginine complex resulted in an entirely new packing motif for SO_3[4] that deviates from the traditional anti-parallel bi-layer (Figure 1.3). This result is one of few that *do* deviate from the bi-layer and is very interesting because, as will be shown later, 'breaking the bi-layer' can have dramatic effects on larger extended assemblies.

Joint complementary studies by the Raston/Atwood research groups investigated supramolecular assemblies with sodium *p*-sulfonatocalix[4]arene and either optically pure or racemic mixtures of several amino acids.[61, 62] Molecular capsules were found to encapsulate racemic pairs of either alanine, histidine or phenylalanine and chiral pairs of (*S*)-serine. Complexes containing (*S*)-alanine and (*S*)-histidine molecules (not as molecular capsules) were also reported.[61, 62]

More recent results by the Raston research group have exploited large globular mono- or di-cationic guests in the formation of complex supramolecular architectures.[63, 64] Co-crystallisation of SO_3[4]

with transition metal *tris*-phenanthroline di-cations resulted in the formation of a structure that showed the metal/phen complexes not only to reside partially in the calixarene cavity but also to interdigitate with the typical bi-layer motif through a large number of π-stacking interactions.[64] When different stoichiometric ratios of tetraphenylphosphonium ions are co-crystallised with SO_3[4], phenyl embraces 'break the bi-layer' and two alternative structures were characterised.[63] In one of the structures, the SO_3[4] molecules are organised into hydrophobic channels whilst in the other, the Ph_4P^+ ions isolate the *p*-sulfonatocalix[4]arenes into pairs in the solid state. Clearly the intermolecular interactions between host and potential guest species are important in determining the overall extended structure. Somewhat related studies by Atwood and Barbour showed that π-stacking and hydrogen bonding interactions dramatically altered the conformation of SO_3[4] when complexed with 4,4'-bipyridinium.[65] These results showed that the solubility of the complex was also dramatically altered with the exclusion of water from the entire structure.

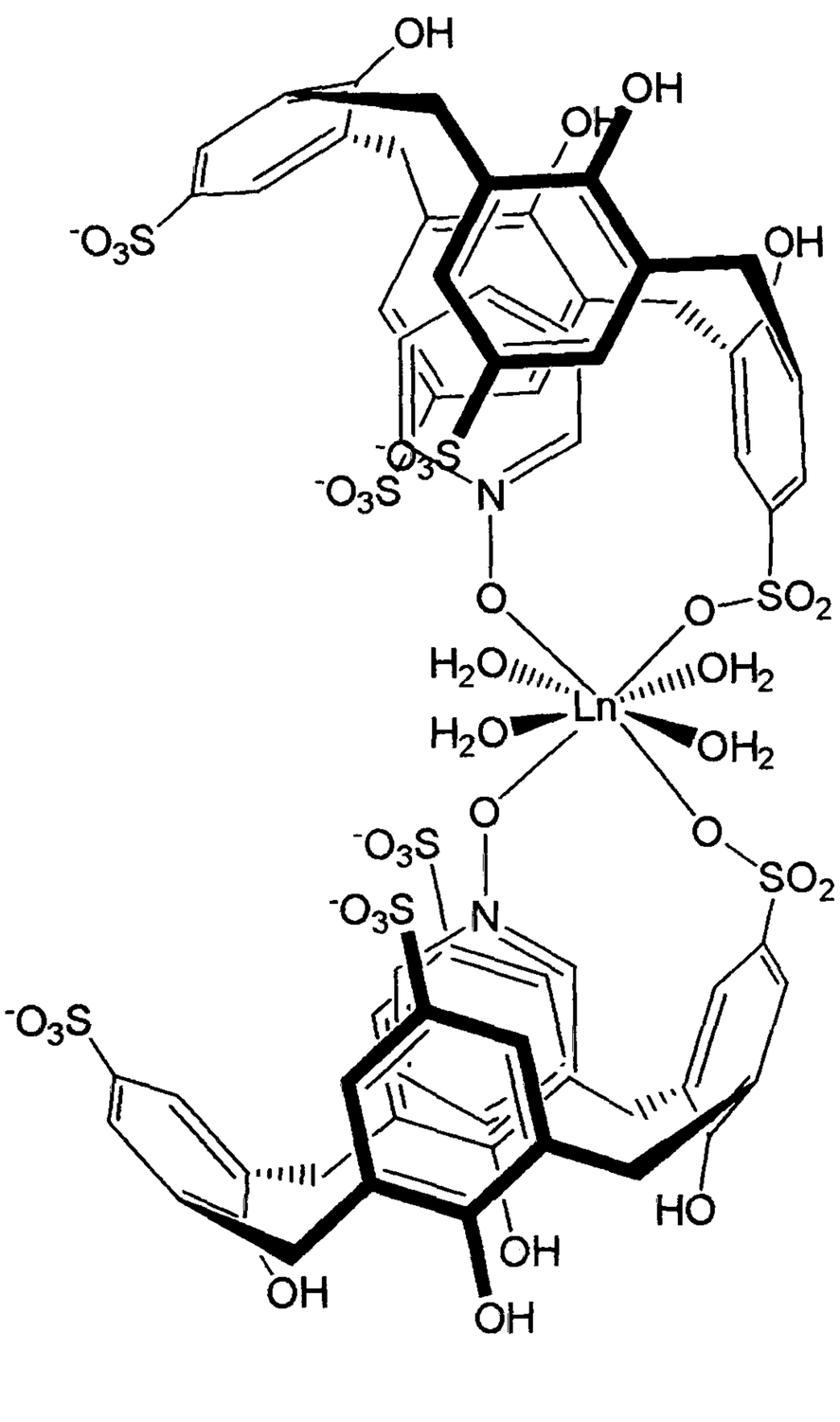

Figure 1.8 A schematic of the *C*-shaped dimer that is used to 'break the bi-layer' and to form nano-tubules or spheroids.[17]

Of the many structures described above, the majority of which are of great interest, none are as spectacular as two *p*-sulfonatocalix[4]arene based nano-structures that were reported by Atwood *et al.* and that were a result of 'breaking the bi-layer'.[17] The study reported that depending on the stoichiometries employed, the complex assembly of a ternary SO_3[4]/Ln/PyNO system could be controlled with the resultant formation of nano-scale tubules or spheres (2:1:8 and 2:1:2 molar ratios, Figures 1.9 and 1.10 respectively).[17] Remarkably, both structures formed through slight variation of a *C*-shaped dimer arrangement that consisted of two SO_3[4] molecules that are linked through a common poly-aquo lanthanide centre that has two pyridine *N*-oxide ligands (Figure 1.8). When this *C*-shaped dimer packs in the solid state, efficient packing ensures the supermolecules inherently adopt curvature in the extended structure as they pack in a parallel manner with all the calixarene base hydroxyl groups pointing to the centre of either assembly. Whilst this is true for both structures, additional PyNO molecules intercalate into the hydrophobic regions of the extended structure of the nano-tubule.

Within the nano-tubules, the SO_3[4] parallel packing is in a helical fashion, taking into account the intercalated PyNO 'spacers'.[17] The central channel of the tubule is around 15Å in diameter and is composed of hydrated lanthanum and sodium ions that participate in extensive hydrogen bonding regimes (Figure 1.9). The nano-spheroid is markedly different to the tubule and the calixarenes pack in the absence of PyNO spacers to form a tight calixarene 'shell' (Figure 1.10). Remarkably both structures have a diameter of ~28 Å. The internal volume of the spheroid was calculated to be ~1700 $Å^3$ but as will be shown in chapter five, this is an overestimation of the true internal cavity size (by a factor of ~2). The SO_3[4] molecules are arranged at the vertices of a Platonic solid, the icosahedron. The central core of the spheroid is composed of a hydrated di-nuclear sodium di-cation and a total of thirty water molecules of crystallisation, all of which partake in extensive hydrogen bonding regimes similar to those observed in the tubular structure (Figure 1.10B).

Previous work within the Raston group partially characterised another nano-spheroid that was based around SO_3[4]/18-crown-6/Ln Russian dolls that were described earlier (Figure 1.5). This structure was based around the Archimedean solid, the cuboctahedron, and has been more fully characterised through X-ray crystallographic studies during the course of this work and is presented in Chapter 5. The two nano-spheroids are very different and a detailed discussion of important structural differences between the 'cuboctahedron' and the icosahedral structure reported by Atwood *et al.* is included in Chapter 5. Latter discussion of this chapter will describe a number of large multi-component synthetic supramolecular assemblies that have been shown to assemble around Platonic or Archimedean solids as an overview of the current trends and developments in this area of supramolecular chemistry as a whole.

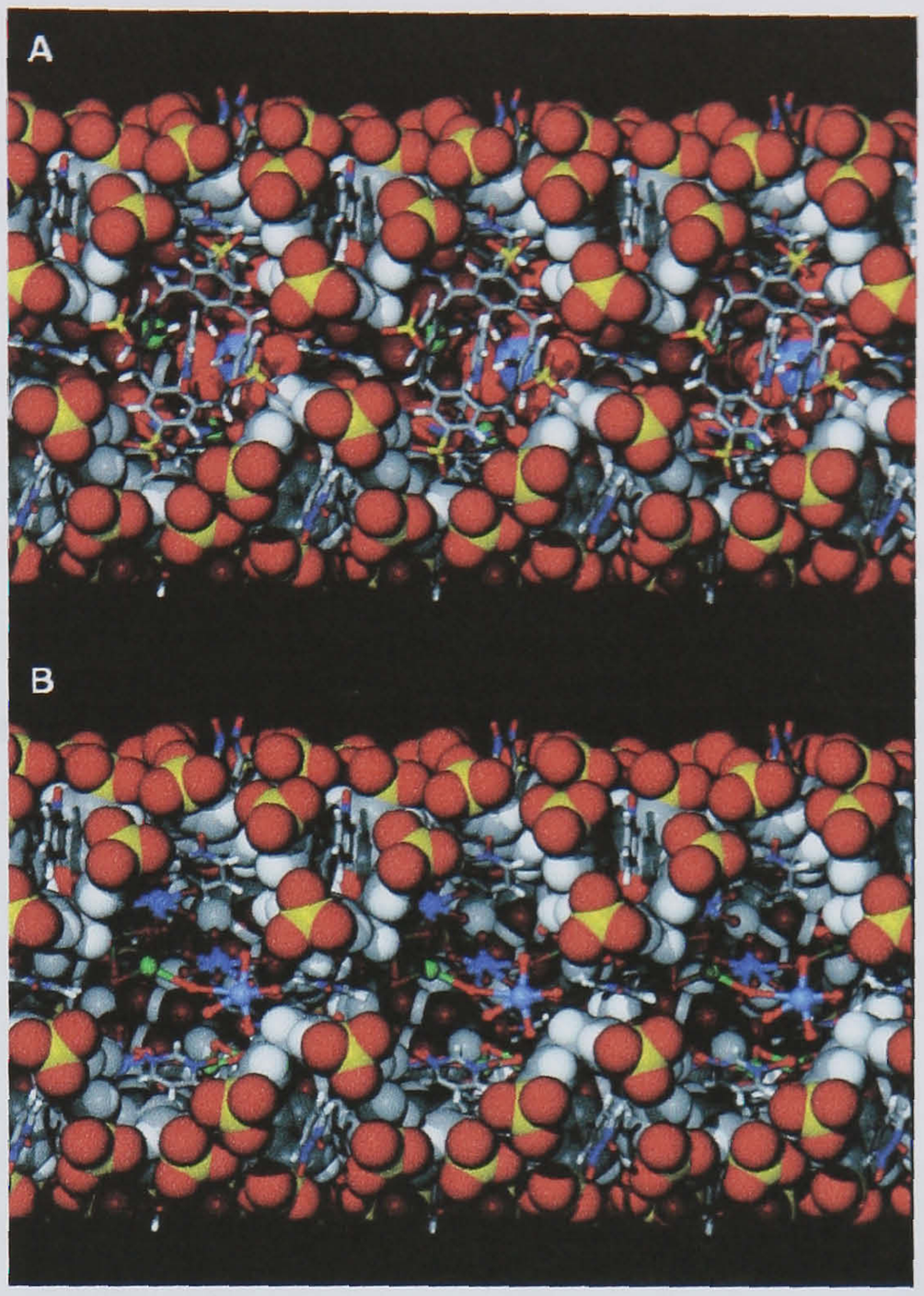

Figure 1.9 Partial space filling (A) and cutaway (B) views of the nano-scale tubules formed from a SO_3[4]/Ln/PyNO system. View (A) shows the PyNO molecules within the SO_3[4] cavities whilst (B) shows the exposed metal cations within the channel.

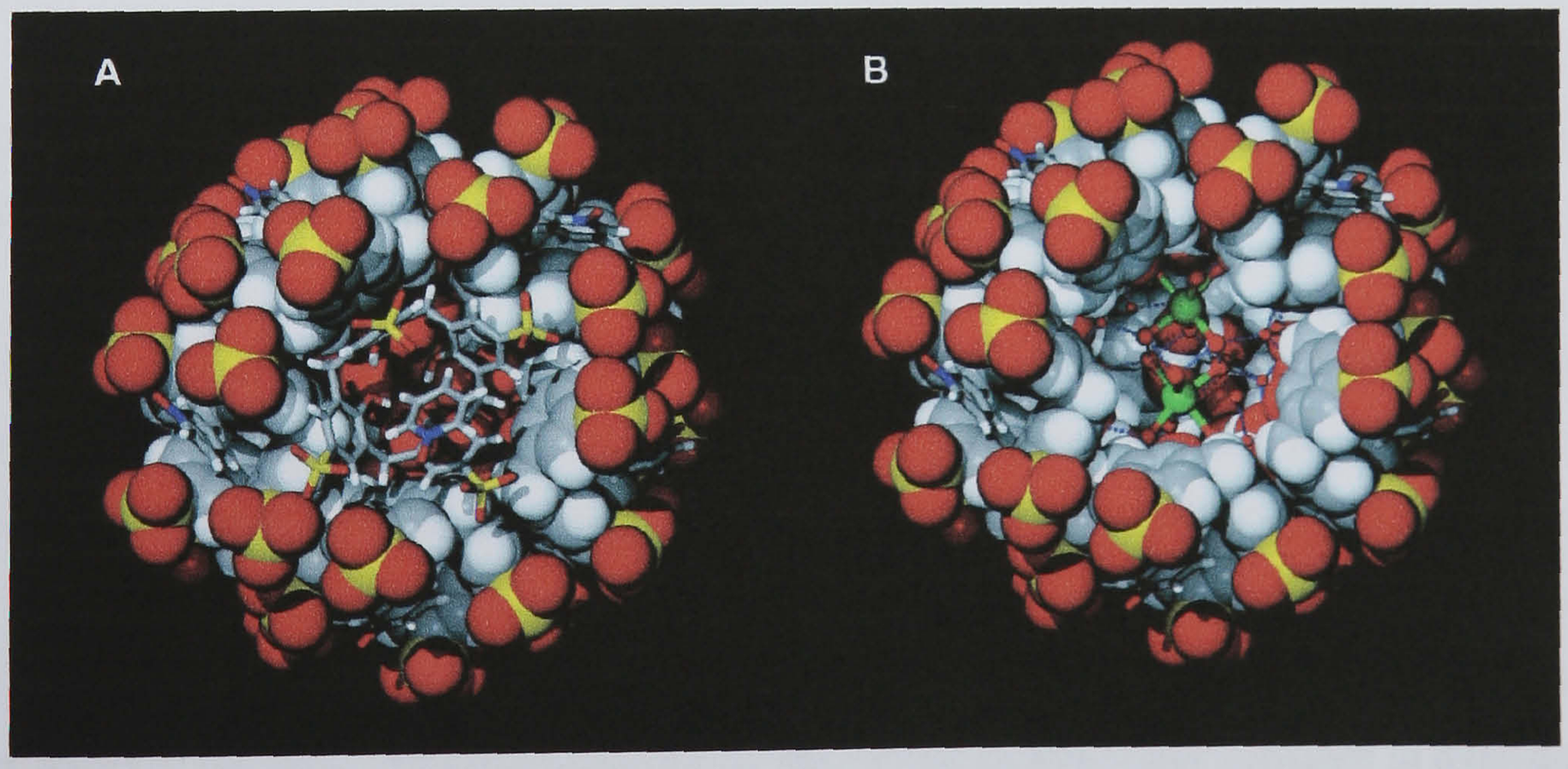

Figure 1.10 Partial space filling (A) and cutaway (B) views of the nano-scale spheres formed from a SO_3[4]/Ln/PyNO system. View (A) shows PyNO molecules within the SO_3[4] cavities whilst (B) shows the inner core metal cations of the spheroid.

1.5.2 Solid state supramolecular chemistry of *p*-sulfonatocalix[5]arene.

As described in section 1.4, the synthesis of the precursor to *p*-sulfonatocalix[5]arene, *p-tert*-butylcalix[5]arene, has been optimised to give a yield of only 5 – 15 %.[8] Given that the tetrameric, hexameric and octameric analogues are far more synthetically accessible on a much larger scale, they are, as would be expected, more widely used for research purposes. This fact is reflected by the huge difference in numbers of articles based around (un-)substituted calix[4,6,8]arenes in comparison to those of their calix[5]arene analogues. This is certainly true for the *p*-sulfonatocalix[n]arenes, and the majority of articles are primarily based on SO_3[4]. Like SO_3[4], *p*-sulfonatocalix[5]arene (SO_3[5]) adopts a cone conformation in the solid state that is capable of bearing host to suitably sized and charged guest species.[66-68] The increased calixarene size causes a concomitant splaying effect between near-opposite ring fragments within the macrocycle and it puckers to present a larger molecular cavity than that of SO_3[4] (Figure 1.11).

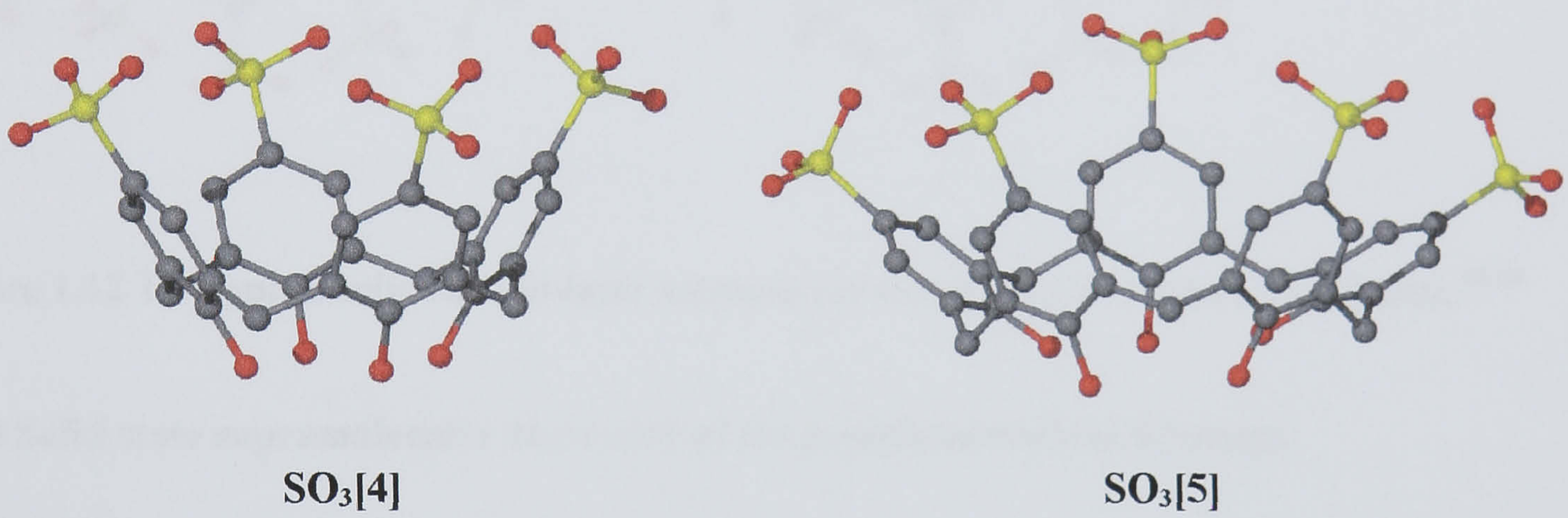

SO_3[4] **SO_3[5]**

Figure 1.11 Rough comparison between the solid state cone conformations and sizes of the *p*-sulfonatocalix[4,5]arenes (molecules not scaled accurately).

Atwood and co-workers reported the structure of the penta-sodium *p*-sulfonatocalix[5]arene and also likened them to organic clays as for SO_3[4].[25, 68] At that time, they also reported the formation of a sodium/PyNO/SO_3[5] complex and a series of sodium/lanthanide/PyNO/SO_3[5] complexes.[68] All of these complexes showed PyNO molecules (whether free or bound to a metal centre) to occupy the cavity of the calixarene in a manner similar to that of analogous SO_3[4] systems. In addition, some of the aforementioned complexes assembled as molecular capsules in a head-to-head fashion or dimers that are similar to those used to form nano-tubules or spheroids with *p*-sulfonatocalix[4]arene.[17] Atwood and co-workers then reported the structure of a cobalt *p*-sulfonatocalix[5]arene complex that also showed the calixarenes to assemble in a head-to-head, molecular capsule like manner.[67] More recently, Raston *et al.* reported the structure of a self-

assembled molecular capsule of SO_3[5] that hosted dimeric sulfuric acid in the enclosed space.[66] In all of the structures mentioned above, *p*-sulfonatocalix[5]arene is found to pack in a bi-layer arrangement and optimise hydrophobic or hydrophilic interaction in a manner similar to that found for SO_3[4].[25] Although there are few articles concerned with the structural chemistry of *p*-sulfonatocalix[5]arene, the supramolecular architectures reported thus far suggest that the molecule should be capable of forming numerous assemblies similar to those characterised for SO_3[4] such as Russian dolls, Ferris wheels, coordination polymers, or other simple host-guest assemblies.[34, 35, 40, 44, 49-53, 65]

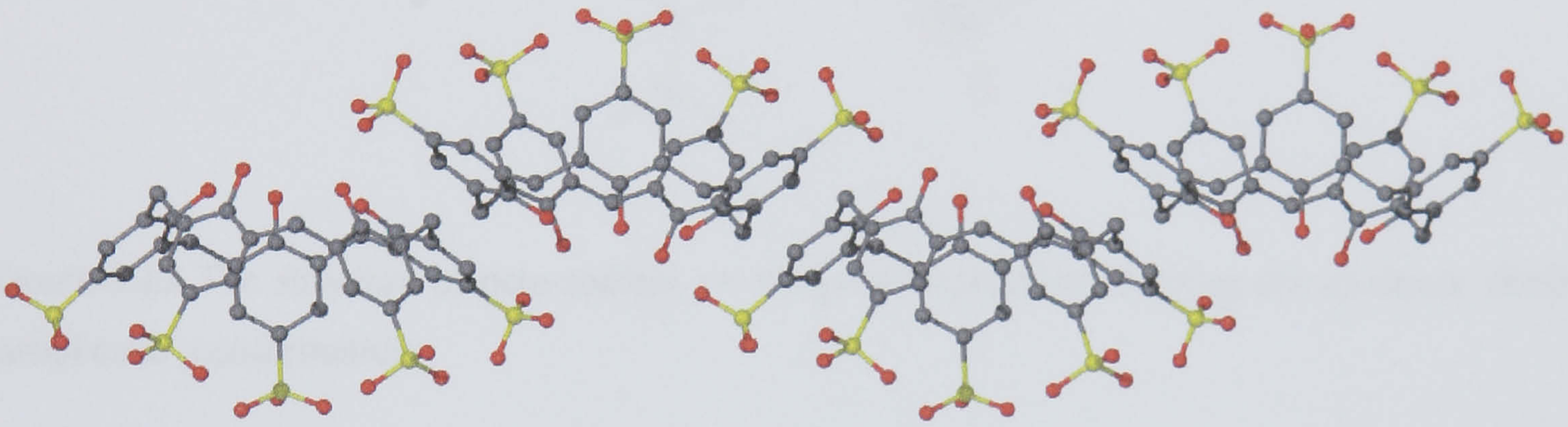

Figure 1.12 The typical solid state bi-layer arrangement found for *p*-sulfonatocalix[5]arene.[66-68]

1.5.3 Solid state supramolecular chemistry of the *p*-sulfonatocalix[6,8]arenes.

Unlike that of the *p*-sulfonatocalix[4,5]arenes, the solid state supramolecular chemistry of the SO_3[6] and SO_3[8] is limited and non-existent respectively.[69] The lack of structural authentications for both molecules may be due to the increased associated conformational freedom upon moving to these larger host molecules. Despite this increased conformational flexibility, Atwood *et al.* structurally characterised the octa-sodium salt and sulfonic acid form of *p*-sulfonatocalix[6]arene and showed the molecule to adopt an up-down 'double partial cone' conformation in the solid state (Figure 1.13).[69] In this conformation the molecule packs in a different bi-layer arrangement that once again optimises hydrophobic and hydrophilic interactions. This conformation also presents two shallow hydrophobic environments/cavities for the inclusion of guest species. In the octa-sodium salt and sulfonic acid form of calix[6]arene, these cavities are occupied by waters of crystallisation that are positioned at distances consistent with OH···π hydrogen bonding as was demonstrated for *p*-sulfonatocalix[4]arene (section 1.5.1).[28] There has to date been no characterisation of a supramolecular assembly or any other structure incorporating *p*-

sulfonatocalix[8]arene nor a structure incorporating SO_3[6] in an up-up 'double cone'/'pinched cone' conformation as has been previously observed for *p*-tert-butyl calix[6]arene.[70]

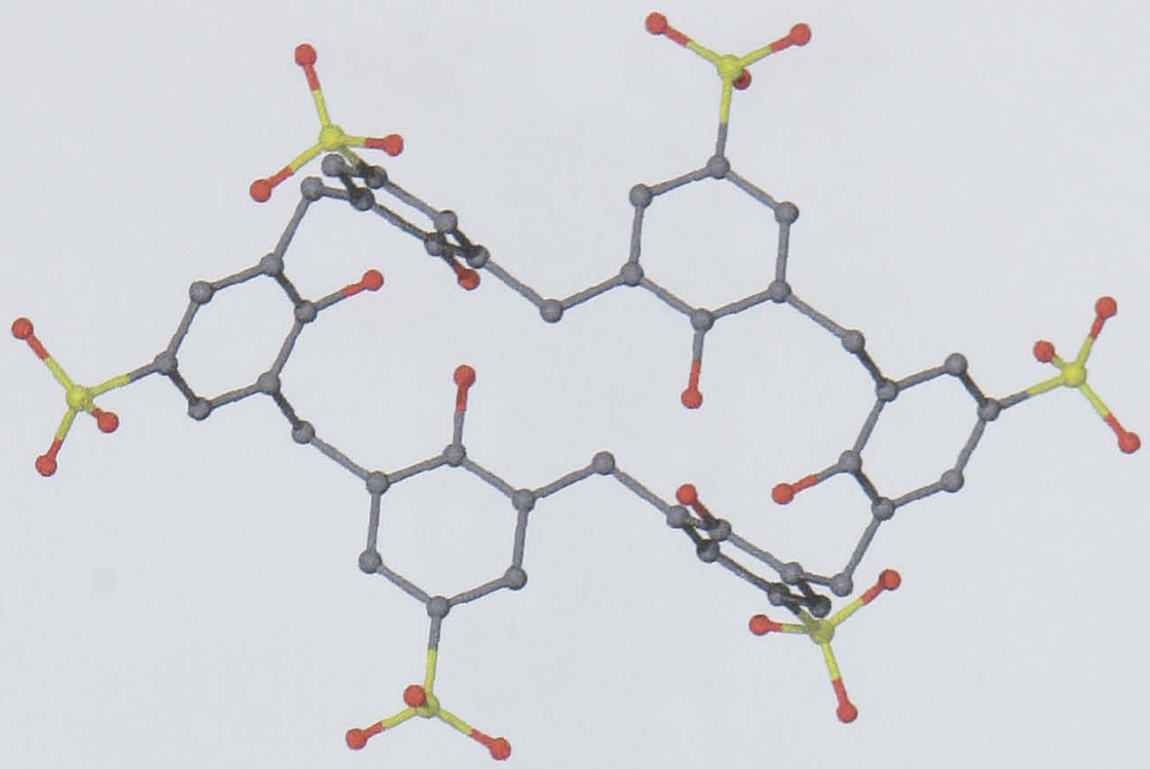

Figure 1.13 The structure of octa-sodium *p*-sulfonatocalix[6]arene showing the up-down 'double partial cone' conformation.

1.6 Related supramolecular assemblies containing other important tectons and trends in supramolecular chemistry.

The field of crystal engineering has witnessed remarkable progression in recent times.[13, 71] Rigid tectons can be used to construct metal-organic frameworks of varied size and complexity and a number of studies by Yaghi *et al.* for example have examined these structures as hydrogen storage materials.[11, 12]

Stang and co-workers have, and continue to report supramolecular assemblies that exploit coordination driven self-assembly in the formation of numerous architectures such as cages/trigonal prisms or pre-designed triangles for example.[72-74] Fujita and co-workers have also used coordination driven self assembly and have shown remarkable ability to control the assembly of several large complex nano-structures based on polypyridine containing ligands.[75, 76] They recently reported the formation of a 3.5 nm coordination nanotube that was assembled around a template, the longest tubular host documented to date (Figure 1.14).[75] Assembly could only be achieved through the use of the template but once assembled, further analysis showed that the structure remained intact even upon removal of the template. The same group also recently reported the structure if a large coordination based cuboctahedron that is composed of thirty six small components.[76] These near

spherical networks consist of twenty four equivalent ligands, twelve metal centres and the corresponding number of anions depending on the metal salt selected.

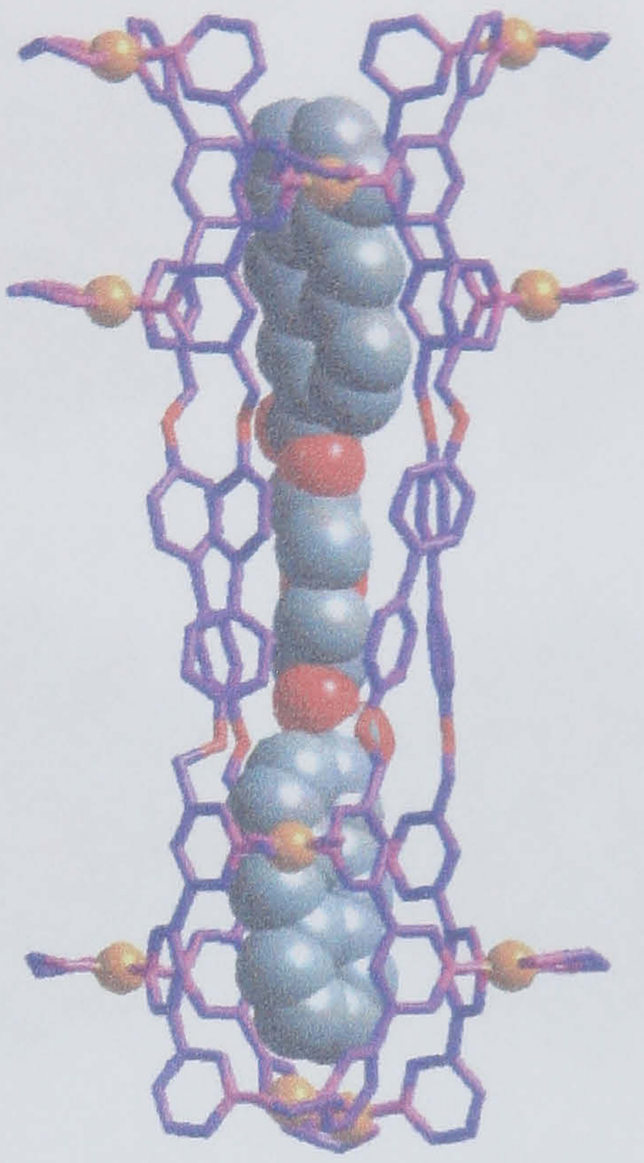

Figure 1.14 A 3.5 nm coordination tube assembled around a template as reported by Fujita *et al.*[75]

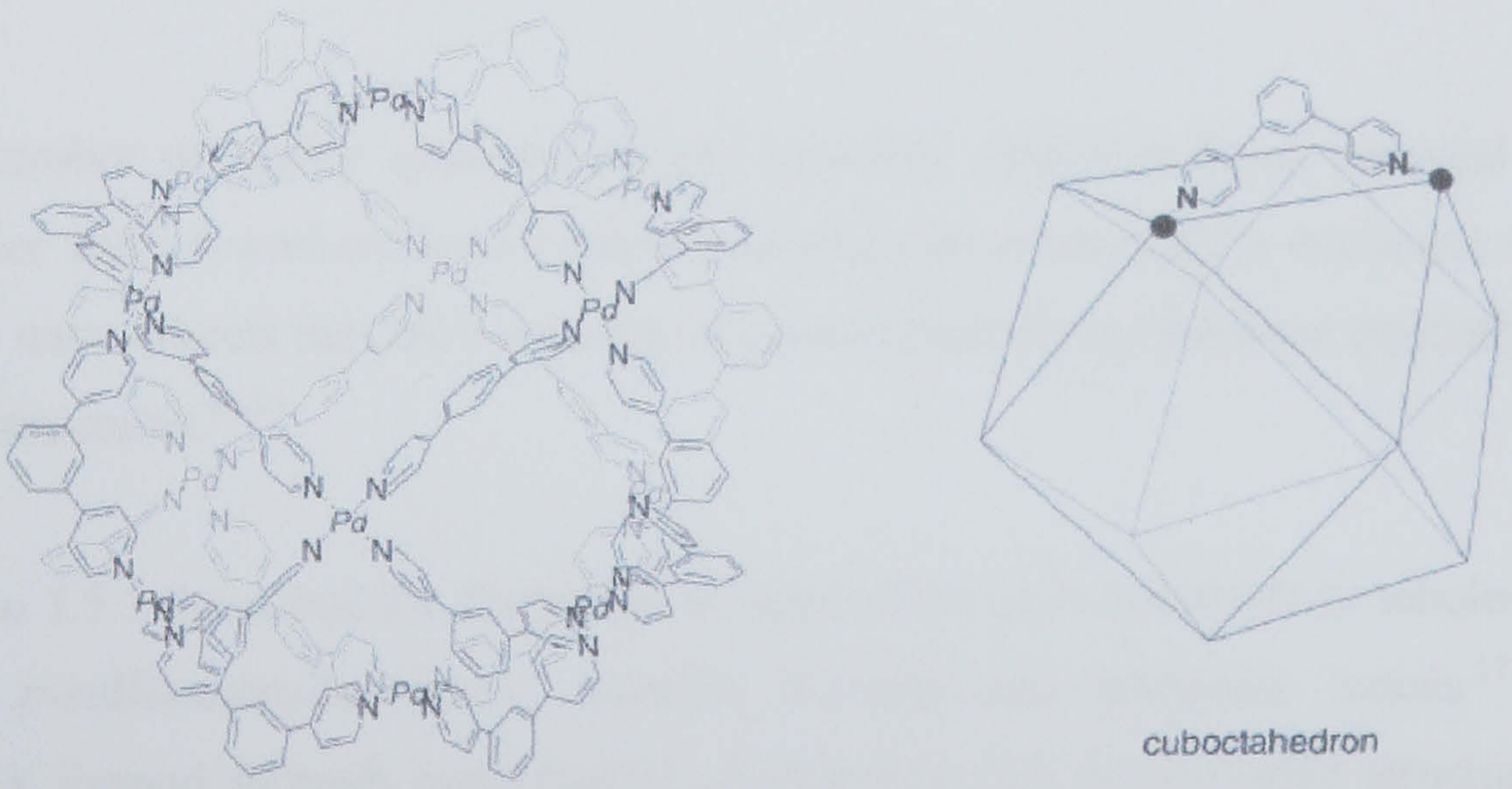

Figure 1.15 Shcmeatic of the cuboctahedral arrangements that are composed of twenty four equivalent ligands and twelve metal centres.[76]

Different but related studies by Zaworotko and co-workers have used metal-organic building blocks to assemble a series of polygons, faceted polyhedra and infinite networks.[77-80] These assemblies are

typically composed of many more components than those described above and the resultant 'nano-balls' have been shown to form as small rhombihexahedra (Figure 1.16).[77, 78]

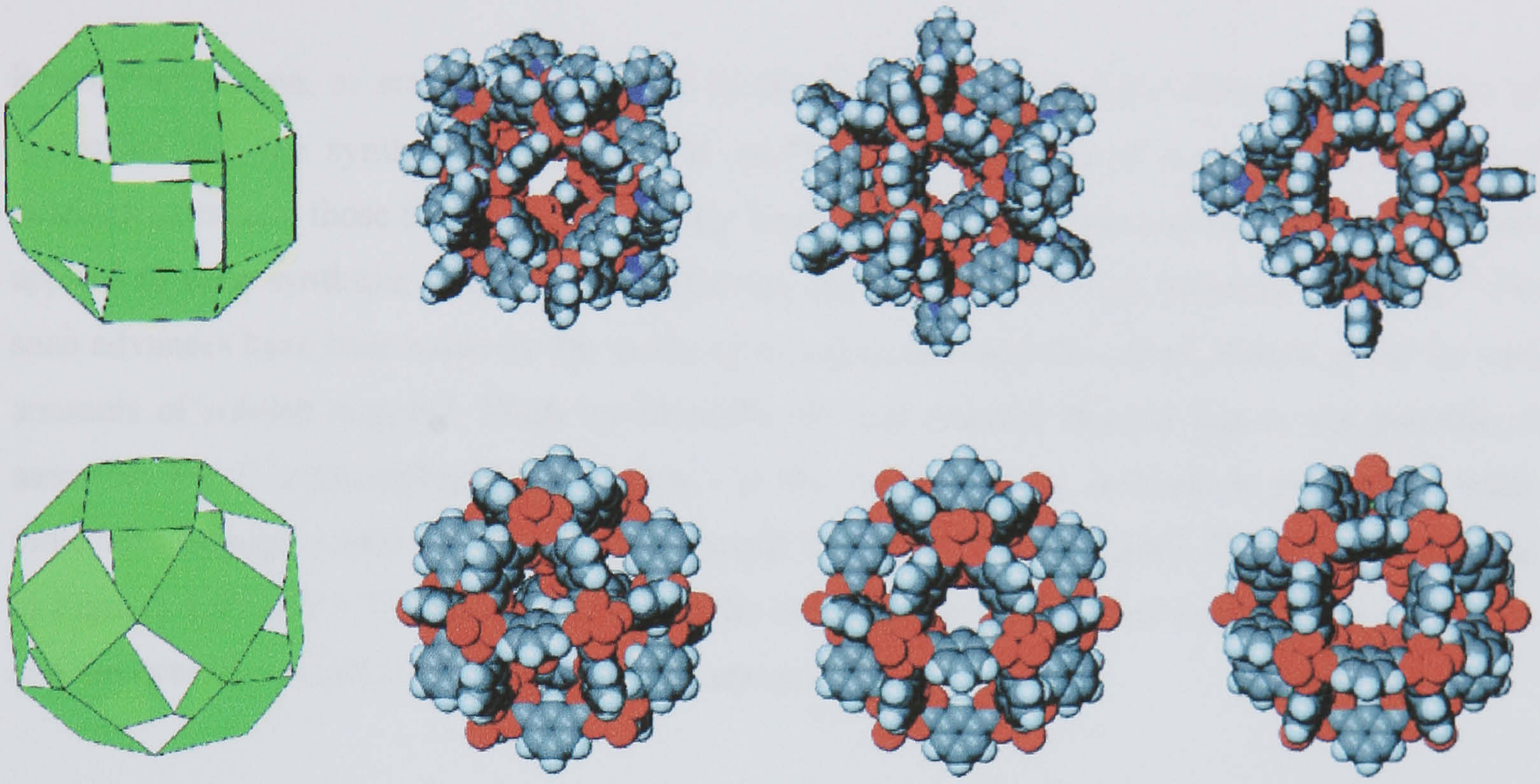

Figure 1.16 Some crystal structures of small rhombihexahedra as reported by Zarowotko and co-workers. The assemblies are comprised of many componenets and assemble through metal/ligand coordination.[77-80]

Indeed the number of highly symmetrical and complex structures being reported is increasing rapidly. Müller and co-workers have reported several poly-oxometallate structures such as nano-hedgehogs or nano-wheels that are bordering on protein periodicity and these typically adopt highly symmetrical structures.[81-84]

Part of section 1.5.1 described the formation of nano-metre scale spheroids or tubules based on the assembly of *p*-sulfonatocalix[4]arene, pyridine *N*-oxide and lanthanide metals.[17] This crucial building block formed through metal/ligand coordination but the extended structure was highly depending on π-stacking and hydrogen bonding interactions. Whilst the 'superstructures' described above are all coordination based, there are few that are as spectacular and that rely primarily upon intermolecular interactions for their formation.

One of the most famous supramolecular structures reported to date is the Rebek 'tennis ball' in which two complementary molecules wrapped around one another whilst encapsulating guest species.[85] The assembly was used to accelerate a Diels-Alder reaction by concentration

enhancement of reaction componenets within the molecular capsule arrangement. Rebek has diversified the systems to incorporate resorcinarene-based frameworks to investigate various aspects of molecular recognition with great effect.[86, 87]

Resorcinarenes are, as stated in section 1.0 of this chapter, related to the calix[4]arene family of molecules and are synthesised by the acid catalysed condensation of resorcinol with selected aldehydes (usually those that are less sterically hindered).[8, 9] Green chemistry techniques have been applied to their synthesis in recent times through the use of Ultra High Intensity Grinding.[88] No such advances have been made for the synthesis of calixarenes and this is unfortunate given the vast amounts of solvent required. Work by MacGillivray and Atwood showed that it was possible to assemble six *C*-methylcalix[4]resorcinarenes at the vertices of an octahedron with eight water molecules through a total of sixty hydrogen bonds (shown in stick and space filling representations in Figures 1.17 and 1.18 respectively).[89, 90] The hydrogen bonding regime represents a snub cube and the overall assembly is just under 2.5 nm across.[89]

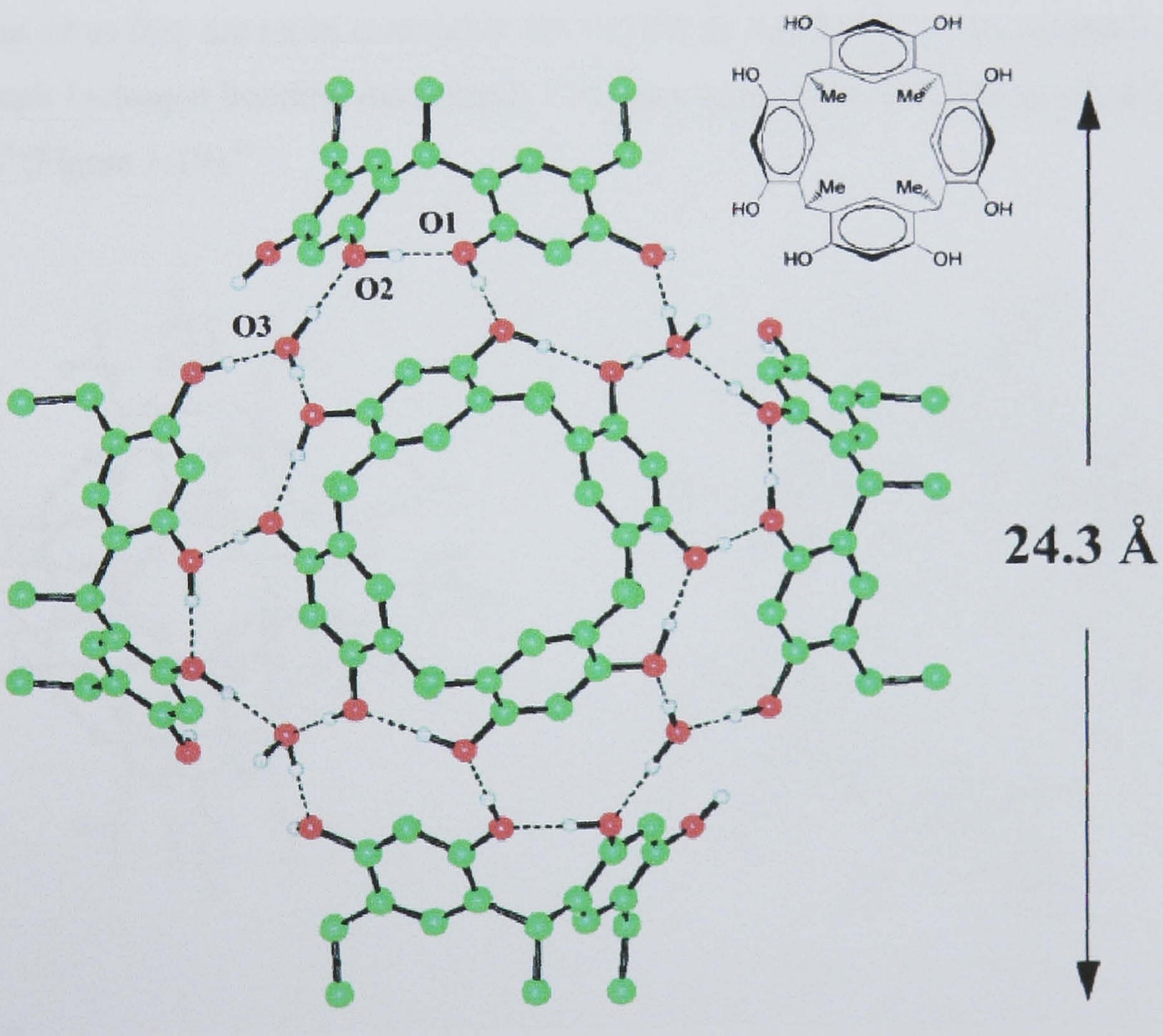

Figure 1.17 Diagram of the chiral spherical assembly formed when six *C*-methylcalix[4]resorcinarenes assemble at the vertices of an octahedron through hydrogen bonding with water molecules.[89]

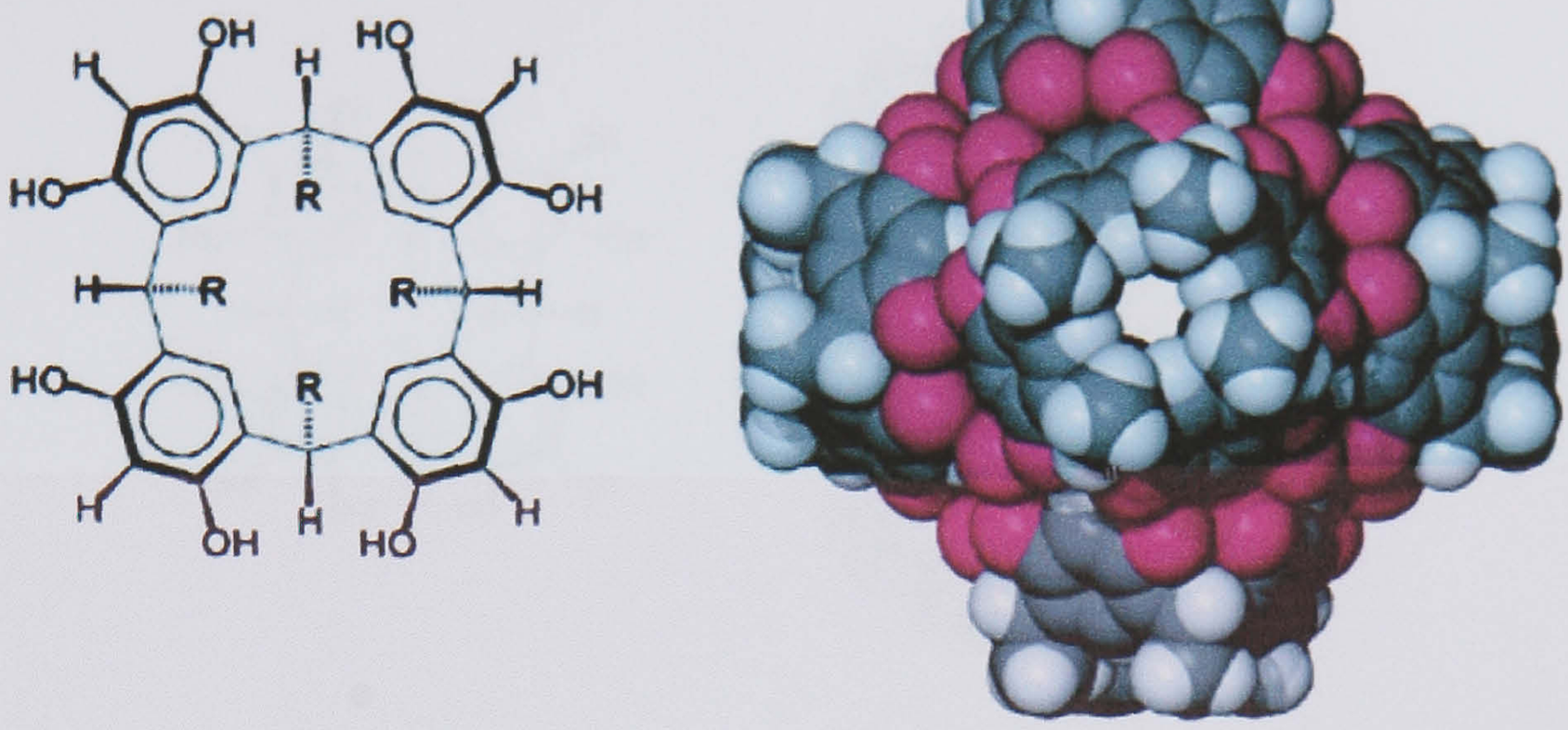

Figure 1.18 Space filling representation of the chiral spherical assembly shown in Figure 1.17, oxygen atoms are shown in purple.[89, 90]

Some time after that discovery, Mattay and co-workers showed that the related tetrahydroxy resorcinarenes or as they are more commonly known, the pyrogallol[4]arenes, assemble in a similar fashion through hydrogen bonding interactions to form a supermolecule with an internal volume of over 1500 $Å^3$ (Figure 1.19).[91]

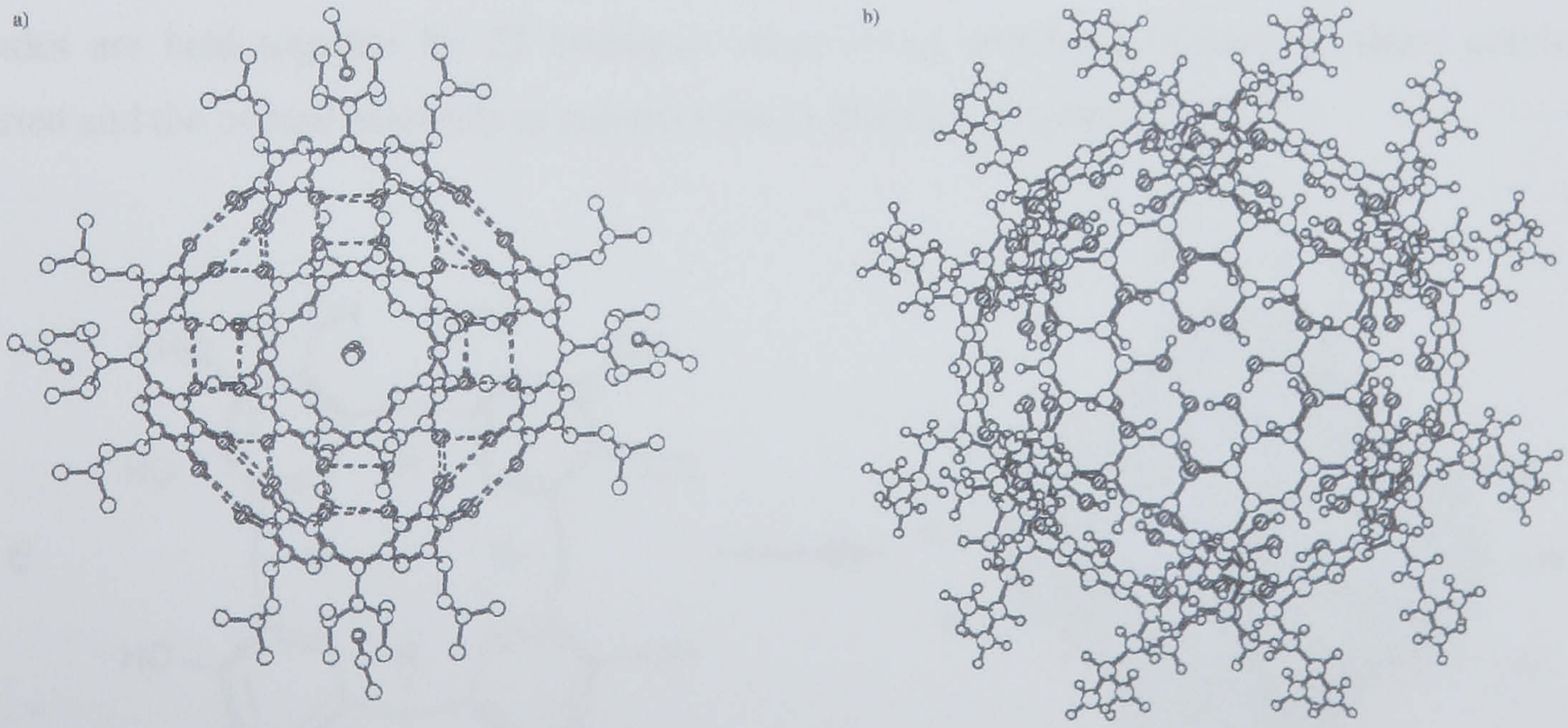

Figure 1.19 Two views of the crystal structure of the supermolecule that results from the assembly of six tetrahydroxyresorcinarenes.[91]

Complementary work by Atwood *et al.* in this area described the formation and crystal structure of a *C*-isobutylpyrogallol[4]arene hexameric capsule similar to that shown above.[90]

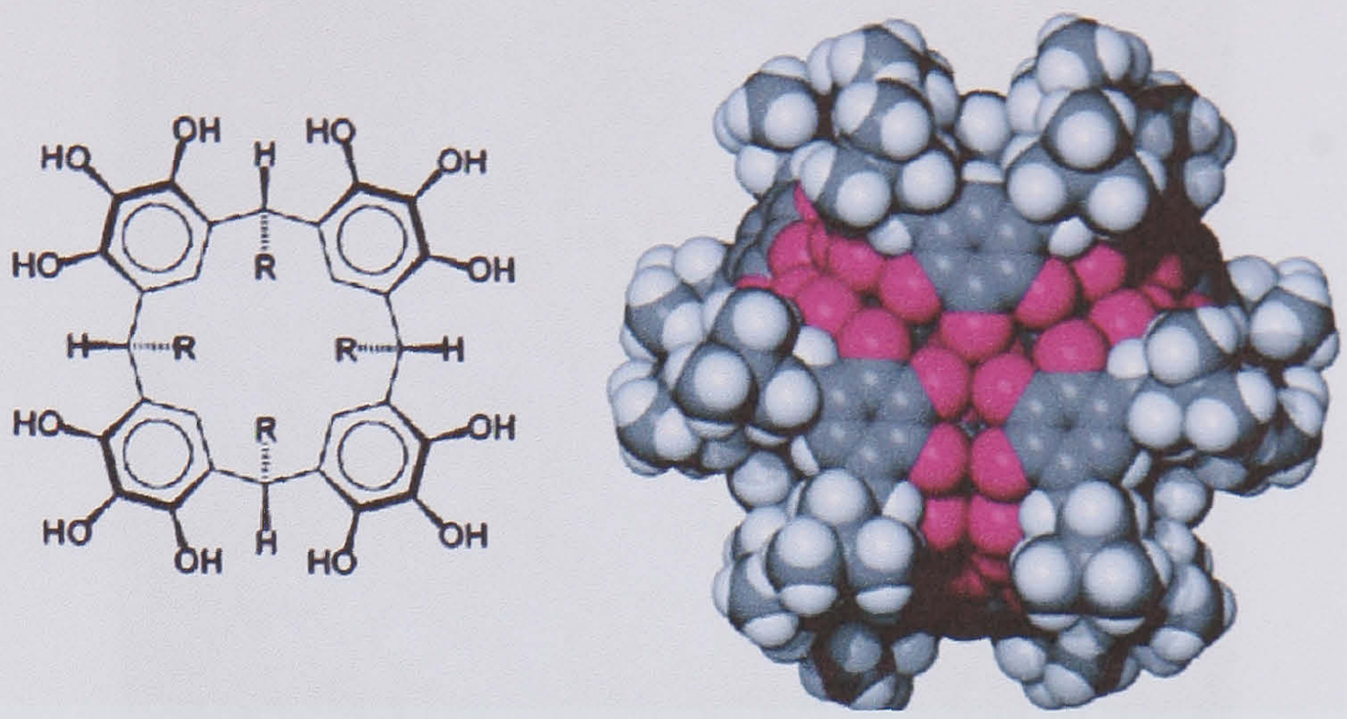

Figure 1.20 Space filling representation of the *C*-isobutylpyrogallol[4]arene hexameric capsule reported by Atwood *et al.* showing the seam of hydroxyl groups at the pyrogallol[4]arene upper rims (indicated by purple oxygen atoms).[90, 91]

More recent work by the same group described the crystal structures of three hexameric capsules based on *C*-alkylpyrogallol[4]arene precursors with ethyl acetate as guest molecules on both the interior and exterior of the capsule (Figures 1.21 and 1.22).[92] They showed that the three packing motifs between the alkyl chains on the exterior of the supermolecule affected the guest molecule orientation/interaction with the pyrogallolarene cavities on the interior of the capsule.[92] The capsules are held together by 72 hydrogen bonds in an analogous fashion to those previously reported and the overall assembly is around 4 nm in diameter (Figure 1.22).[90, 91]

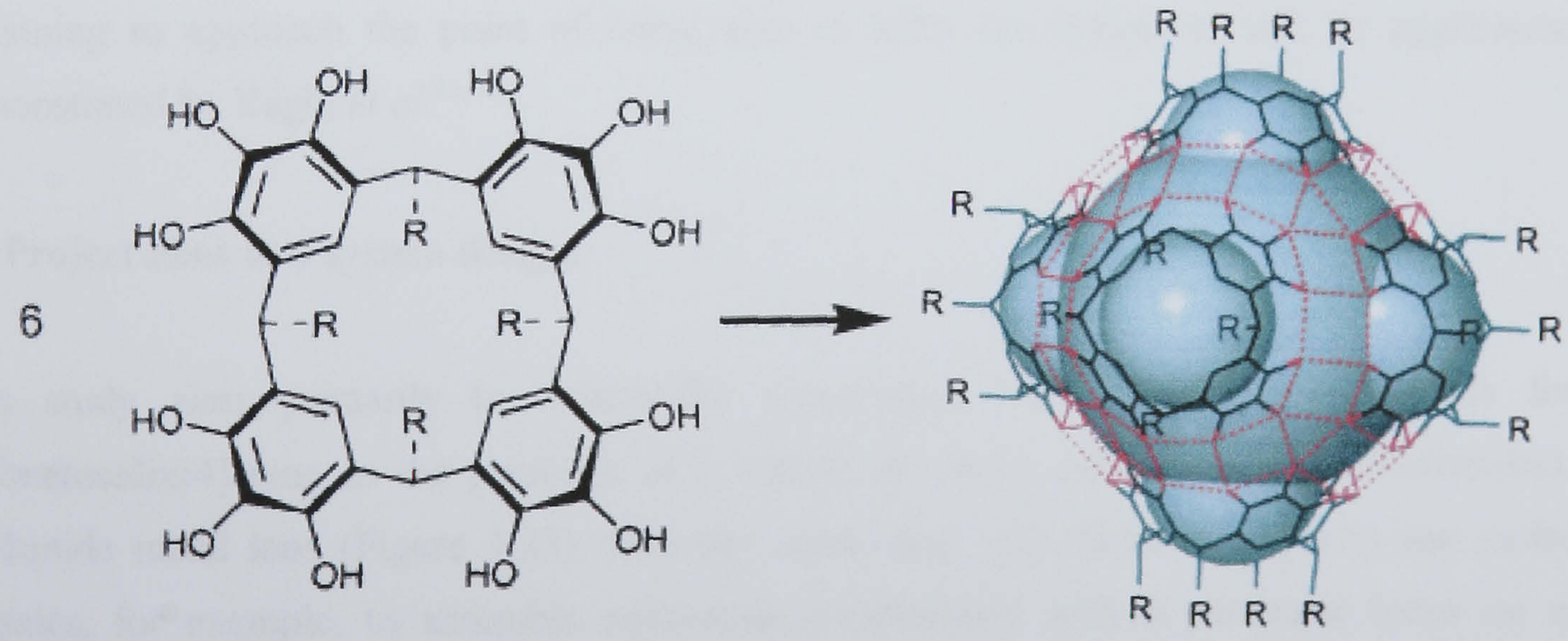

Figure 1.21 Schematic of the hexameric capsular assemblies formed with *C*-pentyl, hexyl or heptyl pyrogallol[4]arene and ethyl acetate guest molecules.[92]

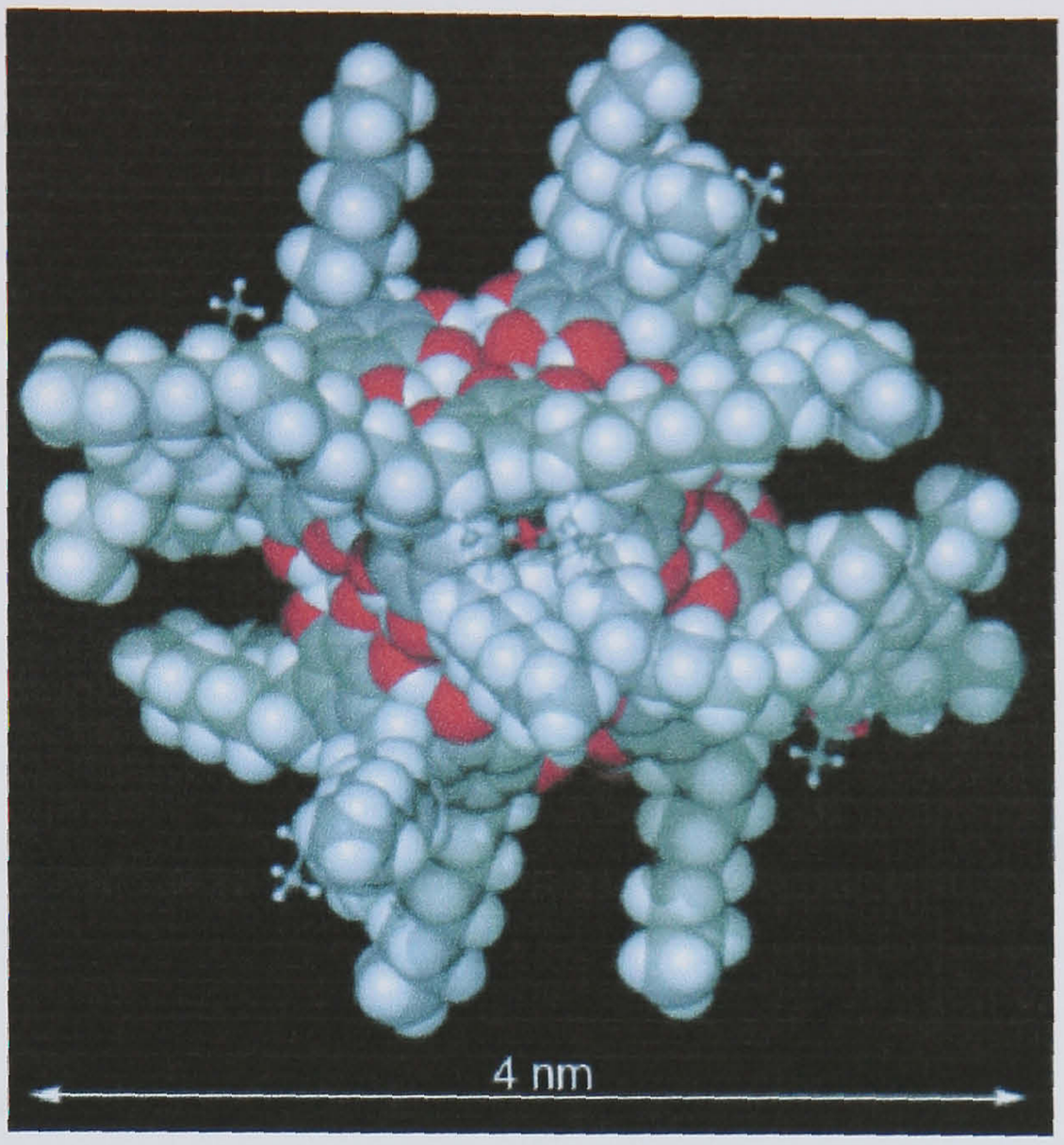

Figure 1.22 Hexameric capsule assembly formed from *C*-heptylpyrogallol[4]arene and ethyl acetate.[92]

In summary, structural characterisation of large interesting structures is becoming routine and the results are typically of great interest as they may provide a route to nano-containers, drug delivery systems etc. Several research groups are currently active in the pursuit of large coordination or hydrogen bonded superstructures for the aforementioned reasons. Given all of the above examples it is clear that the future scope of supramolecular chemistry has no bounds and the chemist is beginning to approach the point of being able to tailor the system to suit an application, as demonstrated by Yaghi *et al.*[11, 12]

1.7 Project aims and system design.

This study aims primarily to structurally characterise new supramolecular motifs for *p*-sulfonatocalix[4]arene in the presence of a variety of crown ethers (or related molecules) and lanthanide metal ions (Figure 1.23). One aim associated with these motifs is to use molecular capsules, for example, to assemble nano-scale architectures with a particular focus on nano-spheroids that can be characterised by X-ray diffraction. Additional aims are to further develop or in some cases commence the solid state supramolecular chemistry of the *p*-sulfonatocalix[5,6,8]arenes using crown ethers/pyridine *N*-oxide guests (or related molecules) and lanthanide or transition metal ions (Figure 1.23). The lanthanide ions are hard Lewis acids and have a propensity to bind

neutral or anionic species with hard donor atoms such as oxygen or nitrogen, thus making interaction with *p*-sulfonatocalix[*n*]arenes and crown ethers ideal.[93] As described in section 1.5 of this chapter, this has been used to some effect with the *p*-sulfonatocalix[4,5]arenes but not so for the *p*-sulfonatocalix[6,8]arenes.[35] For the aforementioned reason, pyridine *N*-oxide or variations thereof are also ideal ligands for lanthanide metals and bi-functional 4,4'-dipyridine-*N,N'*-dioxide has been shown to be a useful tool in the construction of lanthanide coordination networks of varied complexity (Figure 1.23).[94-96] 1,2-*bis*(4-pyridyl)ethane-*N,N'*-dioxide has also been shown to form similar types of coordination network with lanthanide ions.[97]

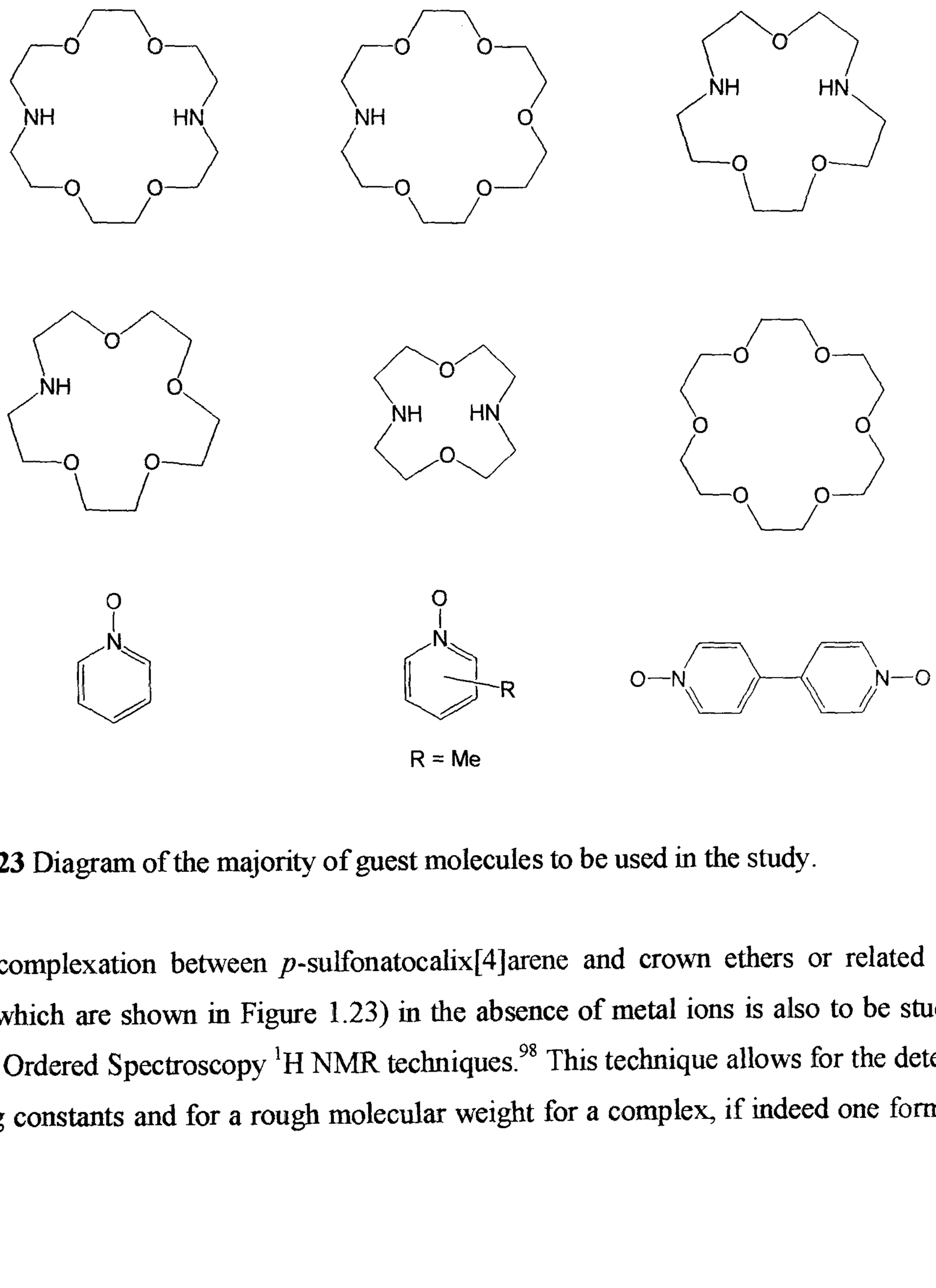

Figure 1.23 Diagram of the majority of guest molecules to be used in the study.

Solution complexation between *p*-sulfonatocalix[4]arene and crown ethers or related molecules (most of which are shown in Figure 1.23) in the absence of metal ions is also to be studied using Diffusion Ordered Spectroscopy ^{1}H NMR techniques.[98] This technique allows for the determination of binding constants and for a rough molecular weight for a complex, if indeed one forms at all in solution.

Chapter Two:

Molecular capsules and coordination polymers based on *p*-sulfonatocalix[4]arene.

2.0 Introduction.

This chapter is concerned with pH dependence in the formation of molecular capsules or coordination polymers composed of *p*-sulfonatocalix[4]arene and lanthanide metals that bear host to several (*bis*)amino-functionalised (bi)cyclic molecules in their various protonated forms. One primary goal associated with this work was to control molecular capsule formation and this has been achieved through careful control of pH and stoichiometric ratios of lanthanide metal present. Hydrogen atoms have been omitted in the majority of diagrams to aid visual clarity except where required for illustrative purposes. Water molecules of crystallisation have also been omitted for clarity, again unless included for particular purpose.

2.1 Molecular capsules and coordination polymers based on (*bis*)amino-functionalised (bi)cyclic guests.

As highlighted in Chapter 1, *p*-sulfonatocalix[4]arene (SO_3[4]) is capable of forming a range of molecular capsule motifs in the presence of 18-crown-6 and various metal counterions.[34, 35, 44-46, 50] These calixarene/crown ether assemblies adopt the role of super-anions that are capable of selectively crystallising, from solution, several polynuclear hydrolytic metal(III) cations or aluminium Keggin ions.[45, 46] Although this chemistry is well documented, the related chemistry incorporating (*bis*)amino-functionalised (bi)cyclic guests such as aza-crown ethers and cryptands is scarce or in some cases unexamined. As this was the case, we selected a range of aza-functionalised disc-shaped crown ether molecules as potential guests for inclusion within molecular capsule arrangements incorporating SO_3[4] (Figure 2.1). Exploration of this chemistry resulted in the formation and characterisation of a series of pH dependent molecular capsules or coordination polymers that display inclusion or exclusion of guest molecules depending on reaction conditions. Diaza-18-crown-6 was selected as the first guest molecule to be employed as it provided appropriate guest charge (when di-protonated) to form molecular capsules with SO_3[4]. This was based on the assumption that the calixarene would adopt a 4– charge and a molecular capsule arrangement would adopt an overall charge of 6–, ideal for crystallisation with two lanthanide metal cations. Diaza-18-crown-6 was successfully included in a molecular capsule at a pH of ≤ 3 in the presence of two nonaaquaneodymium cations as predicted. When 1-aza-18-crown-6 was employed under similar pH and reaction conditions, the crown ether was excluded from a possible molecular

capsule and an interesting bi-layer arrangement incorporating SO_3[4]/neodymium moieties formed. Crown ether exclusion was attributed to an overall capsule charge of 7– that would require either fractional lanthanide crystallisation or the sequestration of an additional 1+ charge from solution (either as a proton or a sodium ion from the glass of the crystallisation vessel). It was reasoned that significantly lowering the pH (< 0.5) would facilitate molecular capsule formation by rapid sulfonate group protonation, thus assisting molecular capsule formation with the mono-protonated guest. Crystals grew very rapidly from the reaction solution under these conditions and the structure of the molecular capsule arrangement was confirmed by X-ray crystallography. Diaza-15-crown-5 forms a molecular capsule with SO_3[4] at a pH < 3 as for diaza-18-crown-6. It was assumed that 1-aza-15-crown-5 would thus form a molecular capsule with SO_3[4] under similar conditions to 1-aza-18-crown-6 (i.e. at a pH < 0.5) but an unusual 2-D coordination polymer comprised of sealed molecular capsules was formed in the absence of the crown ether. Finally, diaza-12-crown-4 was employed as a guest and was shown to form a bi-layer arrangement with SO_3[4] but not as molecular capsules. This result was consistent with the exclusion of 1-aza-15-crown-5 from a molecular capsule on steric consideration and proves that there is a subtle balance between the importance of not only guest charge balance but the ability of any such molecule to bind more than one calixarene for molecular capsule formation. Once this series of disc-shaped guests had been examined thoroughly similar chemistry with more three-dimensional, bi-cyclic molecules was explored, notably with [2.2.2]cryptand and 1,4-diazabicyclo[2.2.2]octane. Both molecules presented the opportunity for di-protonation and consequent inclusion in molecular capsules of *p*-sulfonatocalix[4]arene.

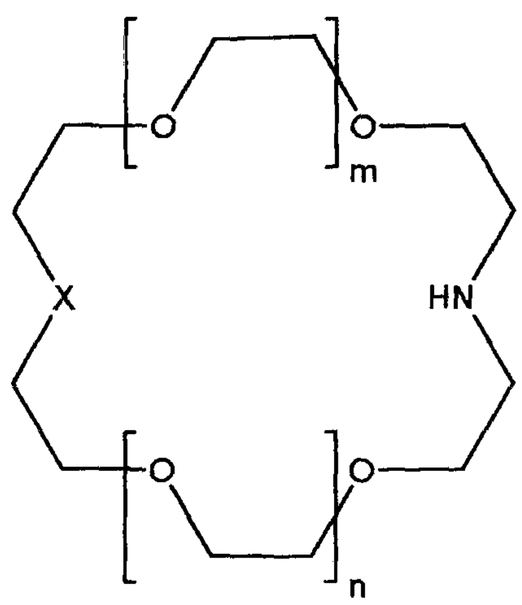

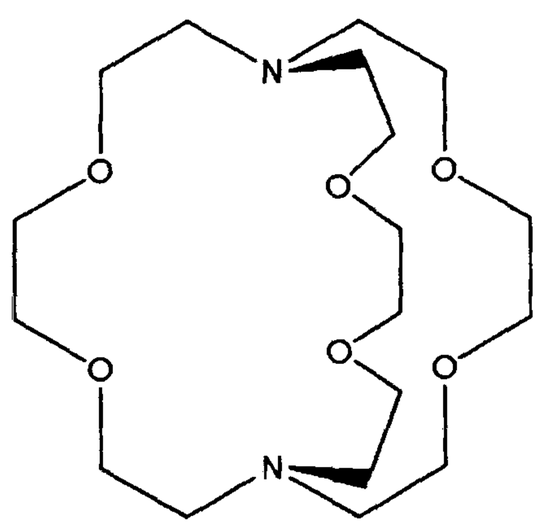

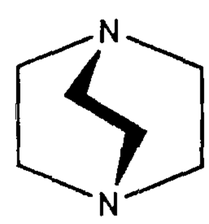

x = NH, m = 1, n = 1, diaza-18-crown-6
x = O, m = 1, n = 1, 1-aza-18-crown-6
x = NH, m = 0, n = 1, 1,7-diaza-15-crown-5
x = O, m = 0, n = 1, 1-aza-15-crown-5
x = NH, m = 0, n = 0, 1,7-diaza-12-crown-4

[2.2.2]cryptand

1,4-diazabicyclo[2.2.2]octane

Figure 2.1 Guest molecules selected for molecular capsule formation with *p*-sulfonatocalix[4]arene.

At a low pH, di-protonated cryptand was incorporated into molecular capsules of SO_3[4], as predicted, but the globular nature of the guest resulted in the calixarenes forming a 2-D coordination polymer of molecular capsules. This is in contrast to the discrete molecular capsules formed for the disc-shaped guests described above and may relate to an increase in splaying of the calixarenes and resultant proximities of sulfonate groups within hydrophobic layers. The smaller bi-cyclic 1,4-diazabicyclo[2.2.2]octane was not included within molecular capsules comprising SO_3[4] but was, in fact, incorporated (in the mono-protonated form) into a 2-D coordination polymer. The resultant structure was unexpected but the lack of molecular capsule formation is consistent with the hypothesis that DABCO molecules, like diaza-12-crown-4, are not large enough to bind two molecules of *p*-sulfonatocalix[4]arene in a capsule motif.

2.1.1 Structure of the molecular capsule [(4,13-diaza-18-crown-6 + $2H^+$)⊂[$(H_2O)_2$[$M(H_2O)_9$]$_2$[*p*-sulfonatocalix[4]arene]$_2$]]·9.5H_2O (M^{3+} = Ce, Nd, Eu, Gd), 2.1.

Crystals of the complex [(4,13-diaza-18-crown-6 + $2H^+$)⊂[$(H_2O)_2$[$Nd(H_2O)_9^{3+}$]$_2$[*p*-sulfonato-calix[4]arene]$_2$]]·9.5H_2O, **2.1**, grew rapidly (in under thirty minutes) upon addition of an excess of a lanthanide(III) chloride to a pre-prepared aqueous solution containing diaza-18-crown-6 and SO_3H[4] (Equation 2.1). The ratio of reactants in the initial solution was 10:1:2.2 of lanthanide chloride : SO_3H[4] : diaza-18-crown-6 but crystals were also grown from analogous 2:2:1 solutions. The complex was characterised by IR spectroscopy and single crystal X-ray crystallography. Complex **2.1** crystallises in a monoclinic cell and the structural solution was performed in the space group $P2_1/n$. Isostructural complexes with Ce^{3+}, Eu^{3+} or Gd^{3+} in place of Nd^{3+} were synthesised and characterised by single crystal unit cell determination, however only the Nd^{3+} complex will be discussed in any detail (unit cell parameters for isostructural complexes are listed in the experimental section for complex **2.1**). Details of data collection and structure refinement are given in Table 2.7 of this chapter. A crystallographic information file containing all bond lengths and angles for complex **2.1** can be found in appendix 2.1.1 on the attached compact disc.

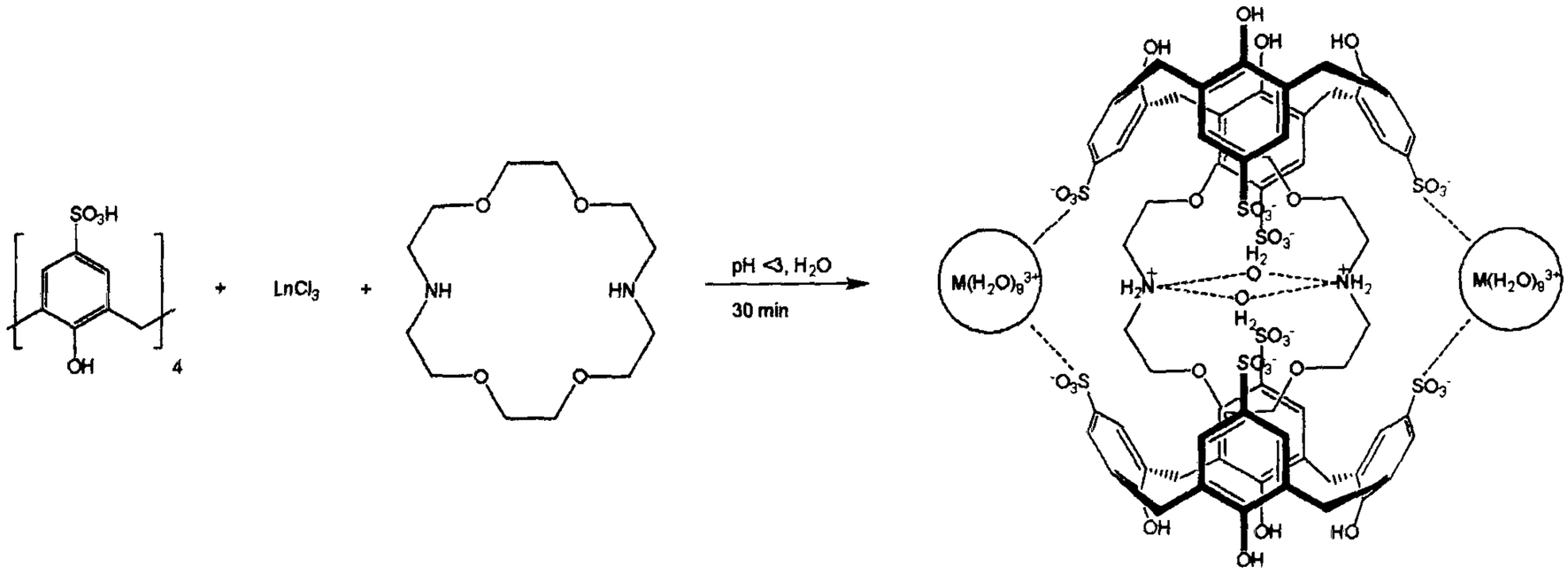

(2.1)

The asymmetric unit of **2.1** is one half of the molecular capsule comprising one calixarene, half of the di-protonated crown ether, one crown ether hydrogen bonded water molecule, one nona-aqua neodymium(III) cation and, several disordered water molecules (Figure 2.2). The crystals were, prior to data collection, anticipated to be a molecular capsule arrangement containing di-protonated diaza-18-crown-6 shrouded by two SO_3[4] anions in the presence of two neodymium(III) cations. Structural elucidation confirmed this hypothesis and the speed of crystallisation suggests pre-association of the crown ether with the calixarene prior to addition of lanthanide metal salt. Consequently, solution studies were performed on the calixarene/crown ether in solution, the results of which confirm a degree of pre-association in solution and are presented in Chapter 4.

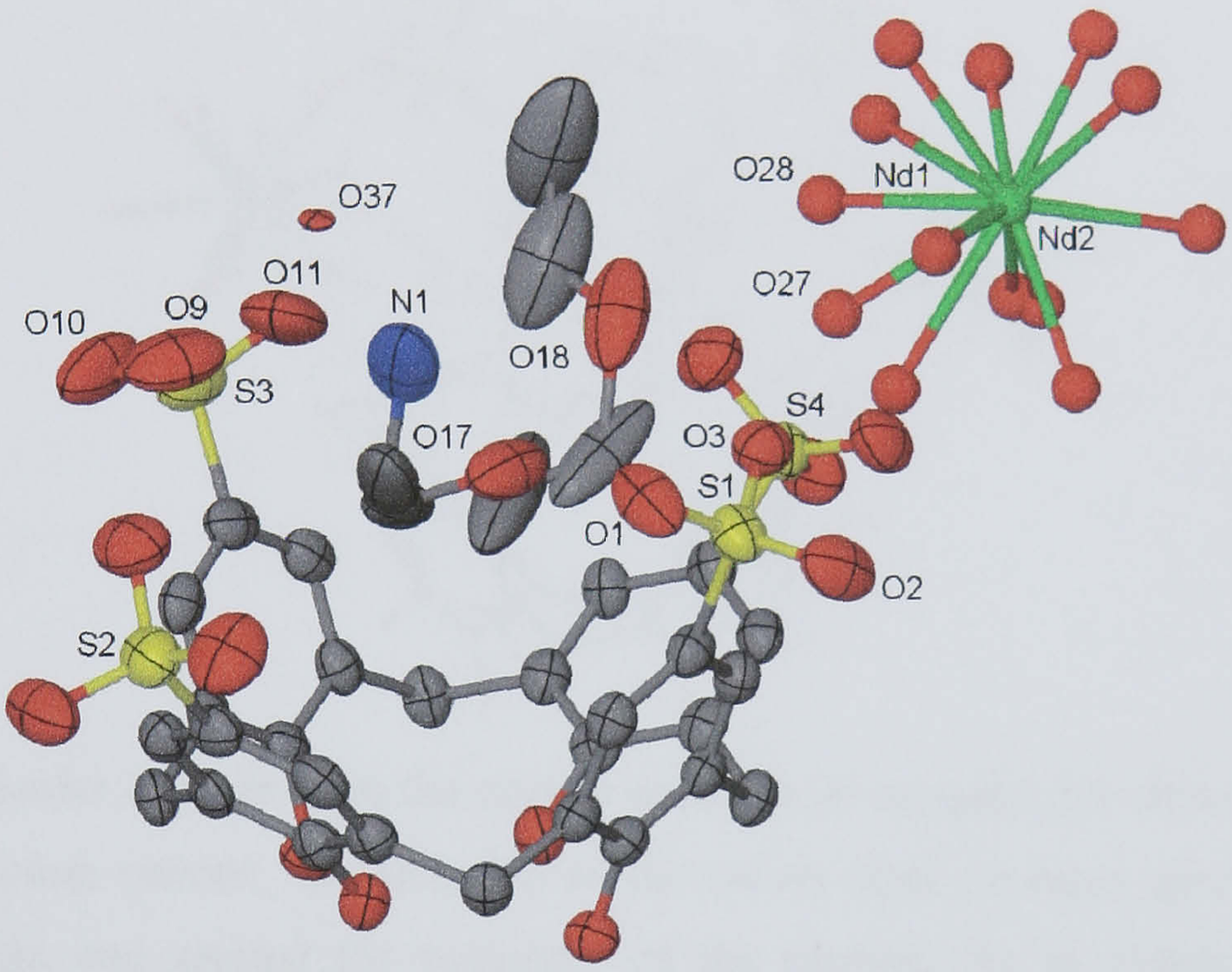

Figure 2.2 Partial asymmetric unit diagram of the crystal structure of complex **2.1**. The atoms of the calixarene, the crown ether, and the crown ether associated water molecule are shown as ellipsoids at 50% probability level. The disordered nona-aqua neodymium cation is shown in ball and stick representation. As the metal centres are located close to one another Nd1 is eclipsed by Nd2. Selected atoms have been labelled.

The molecular capsule forms with two calixarenes in a head-to-head arrangement encapsulating a di-protonated diaza-18-crown-6 guest (Figure 2.3). Within the capsular arrangement, two disordered non-coordinating nonaaquaneodymium cations reside at the sulfonate periphery of the molecular capsule. The crystallographically unique nona-aqua neodymium centre is disordered over two general positions (with partial occupancies of 0.5) and has near tri-capped trigonal prismatic geometry. Two of the disordered aquo ligands (also at partial occupancies of 0.5) hydrogen bond to an oxygen atom of the crown ether molecule with NdO(27)···O(18) and NdO(28)···O(18) distances

of 2.708 and 2.847 Å (Figures 2.2 and 2.3). There are several hydrogen bonding contacts associated with disordered aquo ligands of the metal ions and the sulfonate groups of the two calixarenes in the nearest molecular capsules (nearest NdO···OS distances consistent with hydrogen bonding ranging from 2.586 to 2.960 Å). There are additional hydrogen bonding contacts with sulfonate groups of calixarenes from neighbouring molecular capsules with similar NdO···OS distances ranging from 2.749 to 2.969 Å.

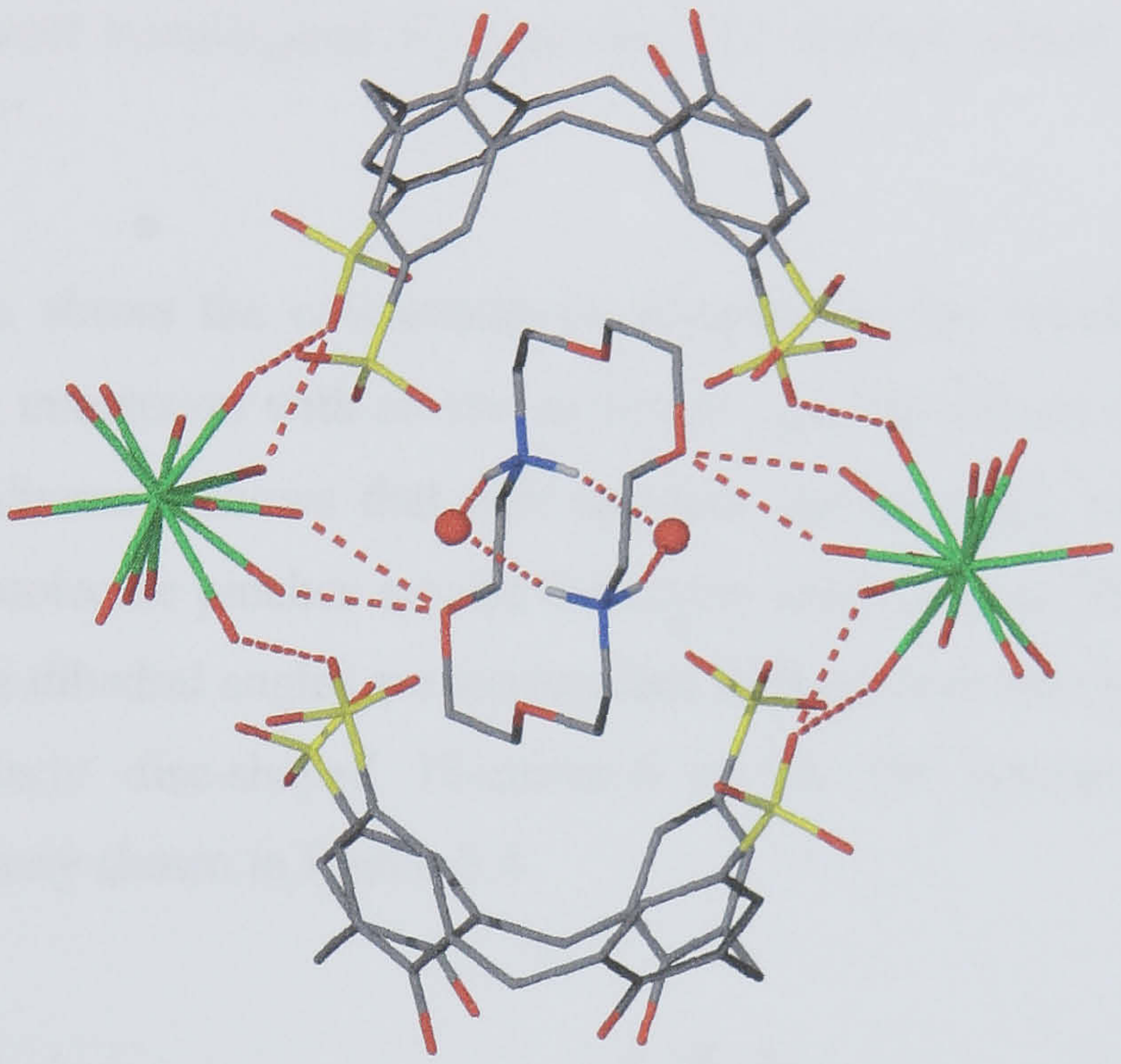

Figure 2.3 A molecular capsule from the crystal structure of complex **2.1** showing the disordered homoleptic neodymium cations, the inclusion of the crown ether *bis*-aqua species, and hydrogen bonding both within and around the periphery of the capsule. As in Figure 2.2, neodymium positions eclipse one another.

There is also a crystallographically unique water molecule that resides near the centre of the crown ether and within the molecular capsule (O(37)). The water molecule has four hydrogen bonding contacts, two to the protonated crown ether and two to the closest sulfonate groups of the calixarenes [N(1)···O(37) distances of 2.866 and 2.935 Å (corresponding NH···O distances of 2.016 and 2.072 Å respectively), and O···OS distances of 2.842 and 2.946 Å, Figures 2.3, 2.4 and 2.5]. These NH···O distances are similar to examples previously reported for di-protonated diaza-18-crown-6 and water.[99] Notably, this diaza-18-crown-6/*bis*-aqua arrangement bears both geometrical and steric resemblance to the *bis*-aqua *trans*-ligated sodium/18-crown-6 moieties that are collectively shrouded by two *p*-sulfonated calix[4]arenes in 'Russian dolls' as reported by Raston *et al.*, Figure 2.4.[34]

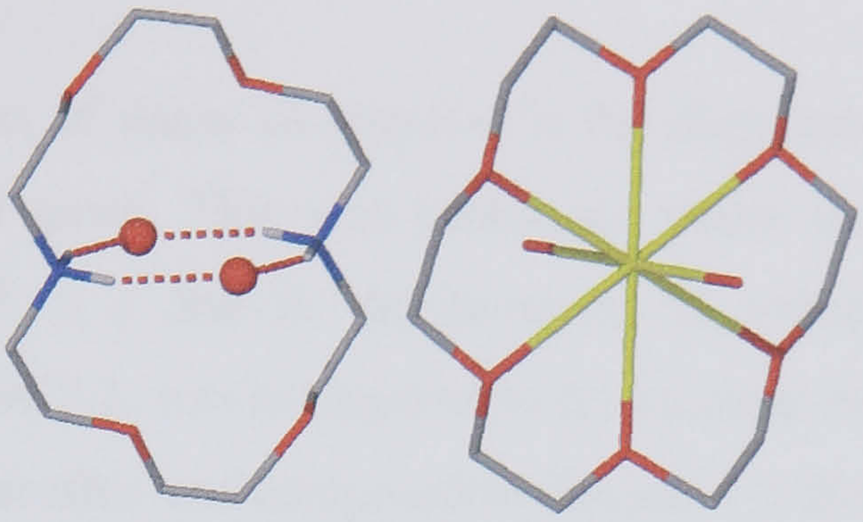

Figure 2.4 Size comparison between the di-protonated diaza-18-crown-6 *bis*-aqua guest species in complex **2.1** and a typical *trans*-ligated *bis*-aquo sodium ion held within 18-crown-6, as seen in typical 'Russian dolls'.[34]

The extended structure shows the calixarenes to assemble in the typical bi-layer arrangement through one π-stacking interaction with an aryl centroid···centroid distance of 3.774 Å, Figure 2.5. Examination of the calixarene shows that two opposite phenyl rings within the calixarene are splayed apart and the molecule pinches around the crown ether with calixarene dihedral angles of 109.0 and 129.6°. These dihedral angles are reminiscent of those seen for the calixarene when in the presence of the similarly disc-shaped 18-crown-6 or for the typical *trans*-ligated *bis*-aquo sodium/18-crown-6 moiety shown in Figure 2.4.

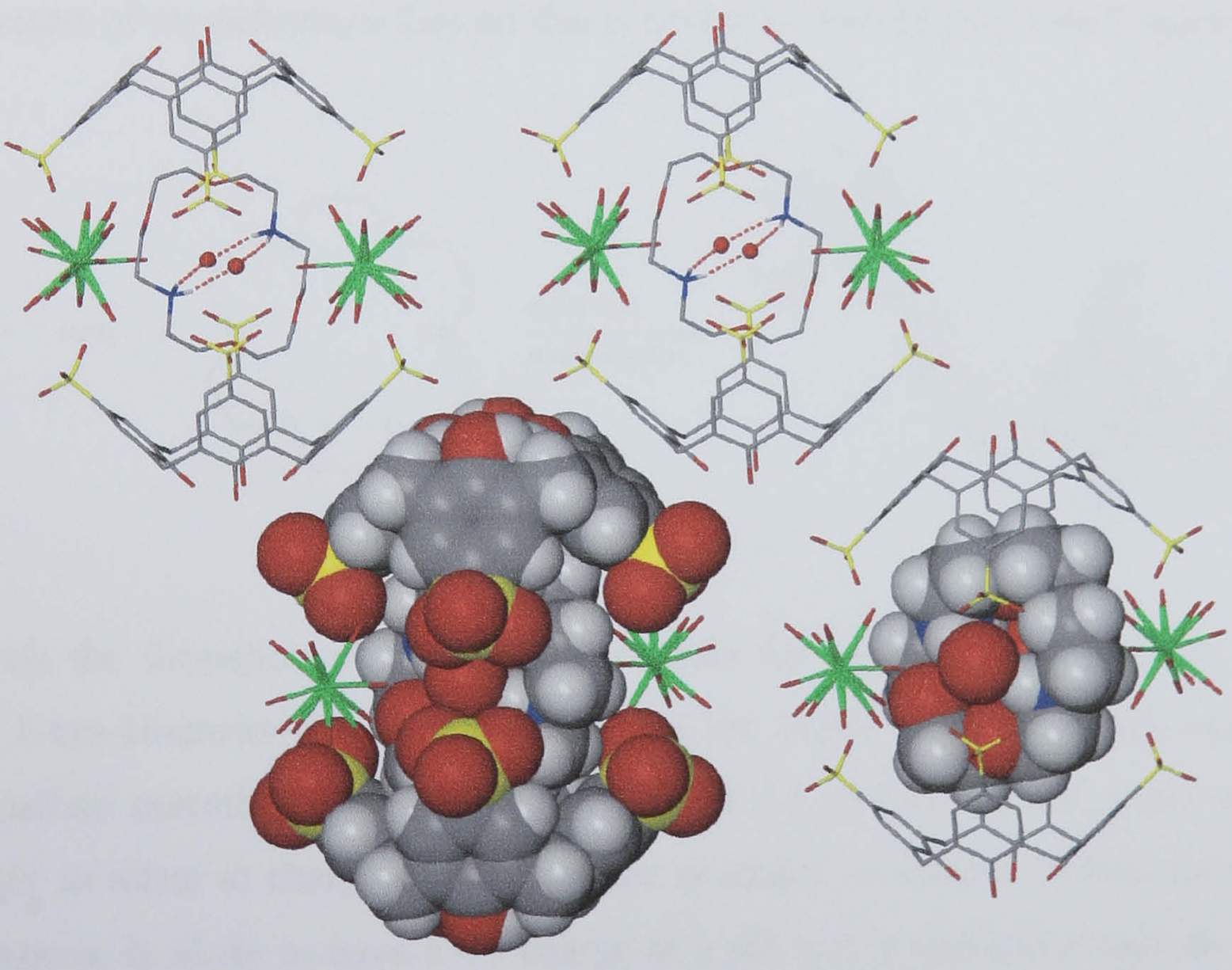

Figure 2.5 Partial space filling diagram showing the bi-layer arrangement found in the crystal structure of complex **2.1**. One molecular capsule is shown in space filling representation whilst in another, only the crown ether and associated water molecules are shown in space filling to emphasise the pinched cone conformation of the calixarene.

Given the successful inclusion of diaza-18-crown-6 in the di-protonated form, 1-aza-18-crown-6 was examined as a potential guest. This was performed under similar conditions to those for compound **2.1**, i.e. at a pH $\leq$ 3 and in the presence of excess neodymium chloride. The supramolecular structure, as for **2.1**, was anticipated to be a molecular capsule but was in fact a bi-layer structure devoid of crown ether and composed of discrete 1:1 lanthanide to SO_3[4] moieties.

2.1.2 Structure of the bi-layer arrangement $[(Nd(H_2O)_8)(p\text{-sulfonatocalix[4]arene} + H^+)]\cdot 9H_2O$, 2.2.

Crystals of the complex $[(Nd(H_2O)_8)(p\text{-sulfonatocalix[4]arene} + H^+)]\cdot 9H_2O$, **2.2**, grew slowly upon slow evaporation of a aqueous solution containing a 3:2:1 mixture of neodymium(III) chloride hydrate, 1-aza-18-crown-6, and SO_3H[4] respectively (Equation 2.2). The complex was characterised by single crystal X-ray crystallography. Complex **2.2** crystallises in a triclinic cell and the structural solution was performed in the space group $P\bar{1}$. Details of data collection and structure refinement are given in Table 2.7 of this chapter. A crystallographic information file containing all bond lengths and angles for complex **2.2** can be found in appendix 2.1.2 on the attached compact disc. The asymmetric unit consists of one octaaquaneodymium ion bound to a SO_3[4] anion and a total of nine waters of crystallisation that are disordered over thirteen positions (Figure 2.6).

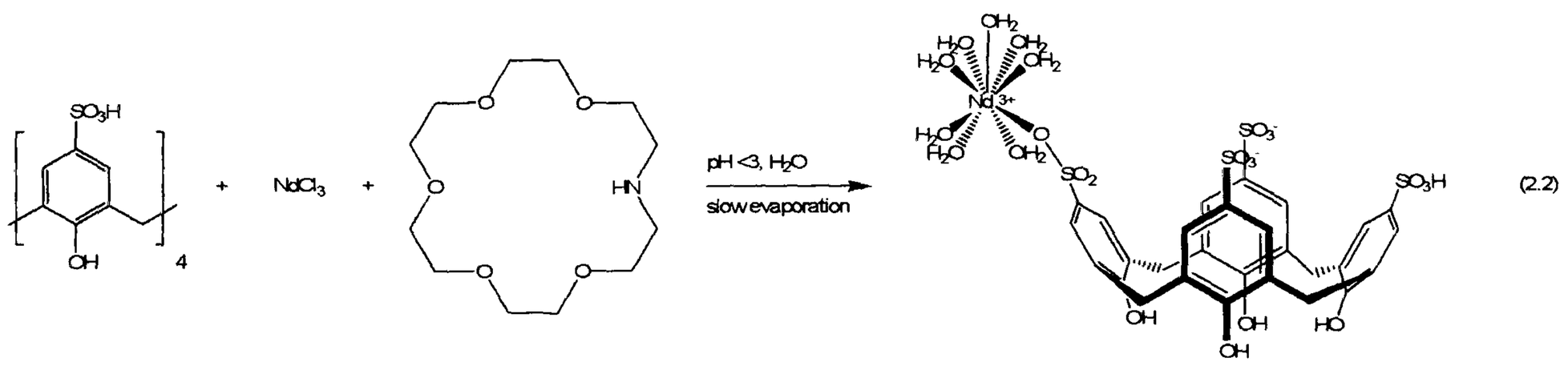

In keeping with the formation of a molecular capsule for complex **2.1**, a similar arrangement incorporating 1-aza-18-crown-6 was anticipated, but the crown ether has been wholly excluded from the crystalline assembly. As discussed in section 2.1 of this chapter, guest exclusion was initially thought to relate to charge disparity in the potential molecular capsule formation. Given that each calixarene is likely to have a 4– charge at a pH $\leq$ 3, a molecular capsule incorporating mono-protonated 1-aza-18-crown-6 would have a capsular charge of 7–. For successful capsule formation, crystallisation of a non-integral number of lanthanide cations would be required. The only other alternative route to capsule formation is the sequestration of an additional 1+ charge either as H^+ from solution or Na^+/K^+ from the crystallisation vessel, two phenomena that have been

previously observed for supramolecular systems incorporating SO_3[4].[100] Despite a relatively low solution pH (< 3), it can be assumed that exclusion of the guest and the formation of **2.2** is preferential to both proton or alkali metal ion sequestration in the potential molecular capsule formation process at this particular pH. As will be presented in section 2.1.3 in this chapter, at very low pH (< 0.5), it is indeed possible to form a molecular capsule containing mono-protonated 1-aza-18-crown-6 with crystallisation occurring in less than fifteen minutes. The present structure is, nevertheless, also interesting in that it forms a well ordered, unusually compact (or 'tight'), hydrogen-bonded bi-layer arrangement.

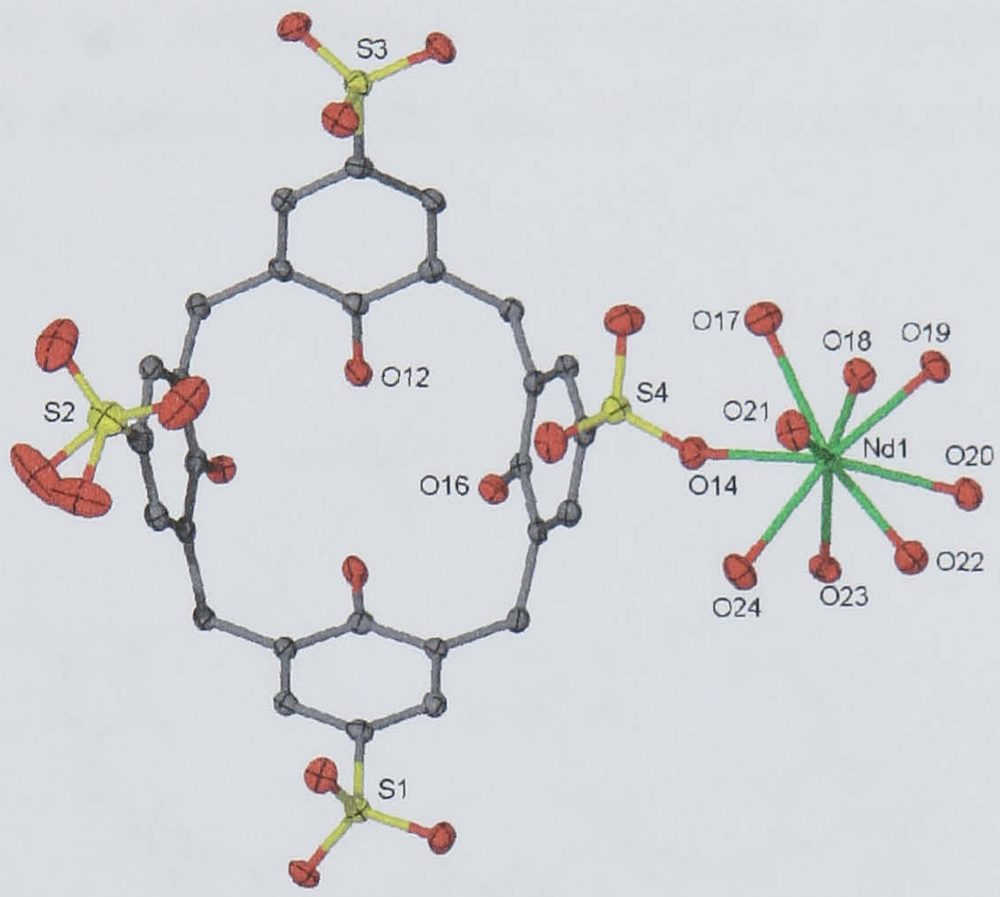

Figure 2.6 Part of the asymmetric unit from the crystal structure of complex **2.2** showing the neodymium coordination sphere, selected atom labelling, and the pinched cone conformation of the calixarene (ellipsoids shown at the 50% probability level).

Nd(1)-O(14)	2.493(3)	Nd(1)-O(17)	2.509(3)
Nd(1)-O(18)	2.486(3)	Nd(1)-O(19)	2.480(3)
Nd(1)-O(20)	2.559(3)	Nd(1)-O(21)	2.492(3)
Nd(1)-O(22)	2.508(3)	Nd(1)-O(23)	2.521(3)
Nd(1)-O(24)	2.463(3)		

Table 2.1 Interatomic distances relating to the coordination sphere of the neodymium metal centres in the crystal structure of complex **2.2** (distances given in Å with e.s.d. in parentheses).

The octa-aqua lanthanide metal centre is bound to the calixarene through the O(14) atom of the S(4) sulfonate group. The metal centre has tri-capped trigonal anti-prismatic geometry and all the metal oxygen bond distances are unexceptional to those previously reported (Table 2.1).[34, 35] The

SO_3[4]/lanthanide moieties shown in Figure 2.6 pack in the typical bi-layer fashion through a total of three crystallographically unique CH···π and π-stacking interactions (two CH···aryl centroid distances of 3.193 and 3.016 Å, and one aryl centroid···centroid distance of 3.770 Å). Each of the octa-aqua neodymium cations reside above the base of a neighbouring 'down' calixarene fragment in each layer and one of the aquo ligands hydrogen bonds to two of the hydroxyl groups at the 'base' as shown in Figures 2.7 and 2.8 (NdO(23)···O(12) and NdO(23)···O(16) distances of 2.847 and 2.925 Å respectively). The same aquo ligand also hydrogen bonds to an oxygen atom of the S3 sulfonate group of a neighbouring 'up' calixarene fragment in the bi-layer with an NdO(23)···OS distances of 2.680 Å. One other aquo ligand of the metal centre hydrogen bonds to oxygen atoms of sulfonate groups of another two neighbouring 'up' calixarene fragments (S1 and S2 sulfonate groups) with NdO(20)···OS distances of 2.721 and 2.814 Å resulting in a complicated hydrogen bonding regime, Figure 2.8.

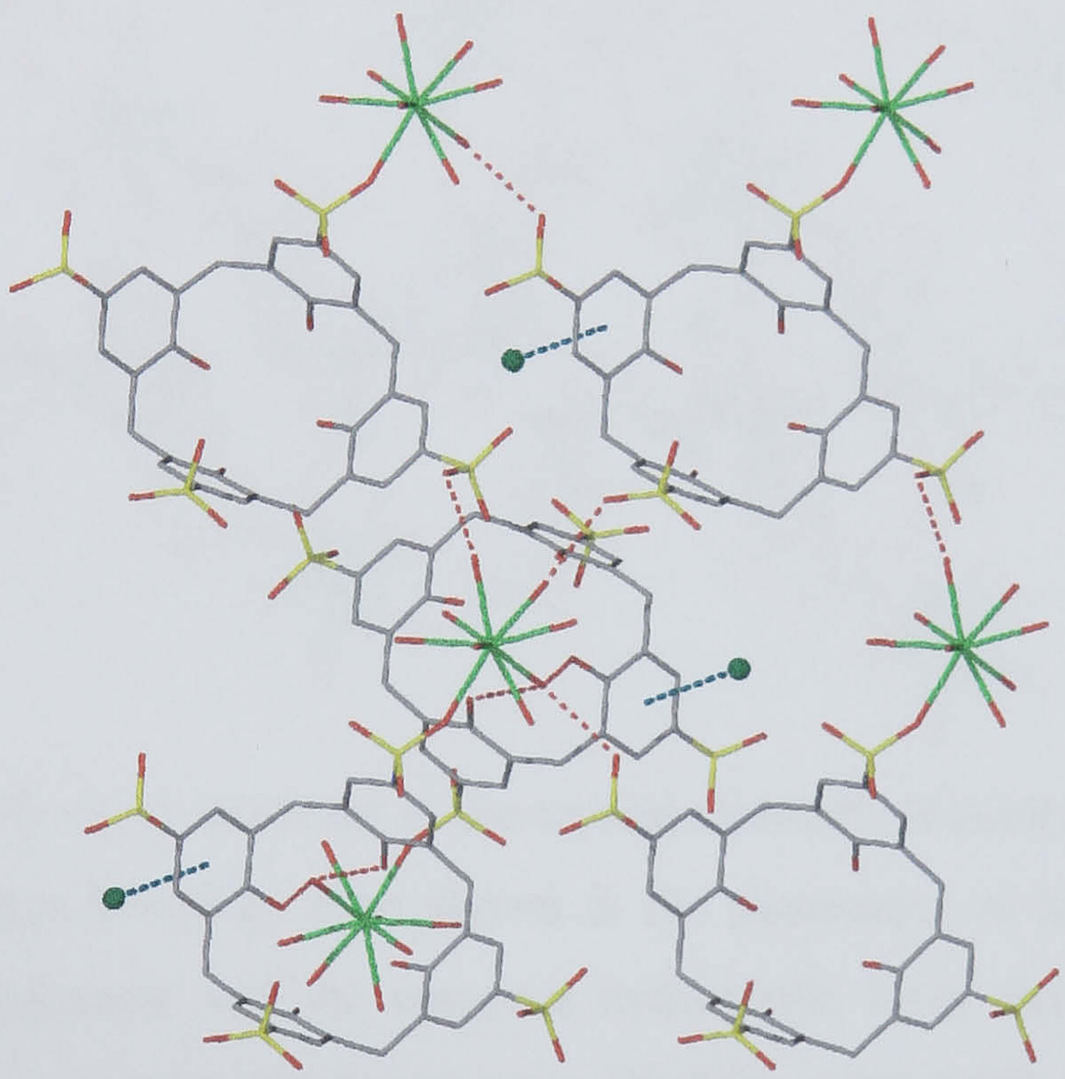

Figure 2.7 View of a hydrophobic layer in the crystal structure of complex **2.2** showing prominent hydrogen bonding contacts between aquo ligands of the metal cations to calixarene 'upper rim' sulfonate groups and 'base' hydroxyl groups. The inclusion of water molecules in the hydrophobic layer is also shown with possible OH···π interactions as dashed green lines (disordered sulfonate groups have been idealised).

In addition to intra bi-layer hydrogen bonding, there are water molecules embedded within the hydrophobic layer are in positions consistent with possible *exo*-cavity OH···π interactions to aromatic rings of the calixarenes (O···aromatic centroid distance of 3.777 Å). Unfortunately, it was

not possible to locate the hydrogen atoms in the Fourier difference map to confirm this. As mentioned in Chapter 1, the first structural evidence of this phenomenon was reported by Atwood *et al.* and showed OH···π interactions between water molecules held deep within a calixarene cavity and the aromatic rings of the macrocycle.[28] There are also water molecules (at half occupancy) held deep within the calixarene cavity in **2.2** that are also positioned so as to display three possible *endo*-cavity OH···π interactions (O···aromatic centroid distances of 3.564, 3.583, and 3.690 Å). All of these possible interactions, both *exo* and *endo* to the cavity, are of orders consistent with those documented by Atwood *et al.*[28] This is however, to our knowledge, the first structurally authenticated example of concurrent *exo* and *endo* interactions between the calixarene and water.

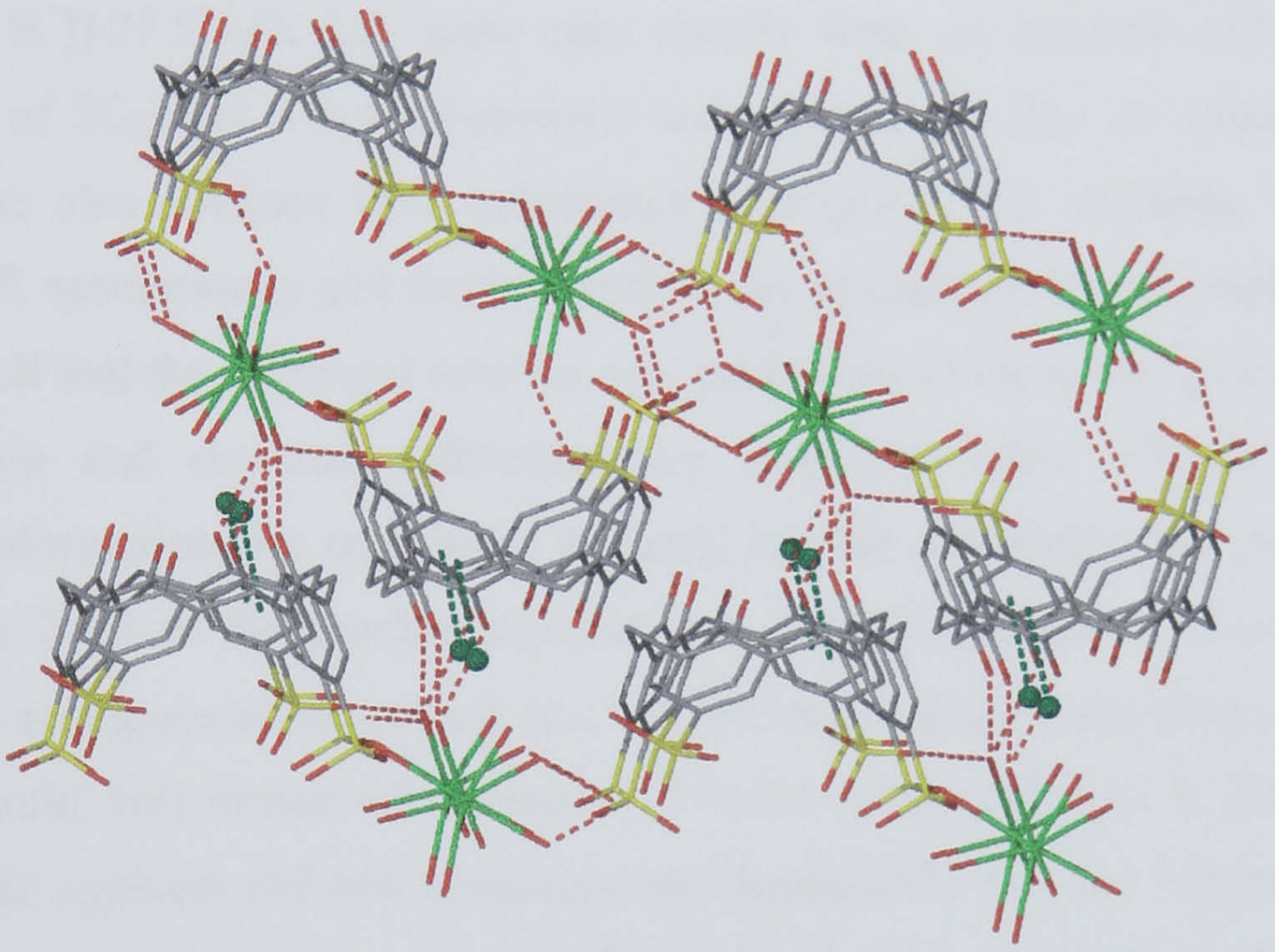

Figure 2.8 The extended bi-layer structure in the crystal structure of complex **2.2** showing the intra and inter bi-layer hydrogen bonding. Also shown is the placement of the water molecules deep within the bi-layer arrangement and the compact hydrophilic layer that results from extensive hydrogen bonding between hydrophobic layers (possible OH···π interactions shown as dashed green lines, disordered sulfonate groups have been idealised).

Within the extended bi-layer structure there are several prominent hydrogen bonding contacts between neodymium aquo ligands (that are directed into the hydrophilic layer) and sulfonate groups of the next nearest bi-layer arrangement, Figure 2.8 (relative NdO···OS distances range from 2.686 to 2.793 Å). Upon considering the disordered waters of crystallisation, an extremely extensive hydrogen bonding regime is evident within this 'tightly hydrogen-bound' supramolecular structure. It should be noted that despite exclusion of the crown ether, simple 2-D coordination polymer formation is not favoured and the calixarenes pinch in a similar fashion to those in complex **2.1**, with dihedral angles of 141.5 and 109.1°. As this is the case, it may be that at this particular pH, the

presence of the 1-aza-18-crown-6 (likely protonated but possibly neutral) influences supramolecular structure formation and prevents coordination polymer formation with neodymium. Given all of the above, it was reasoned that if very low pH was employed i.e. < 0.5, molecular capsule formation would be more likely and this was found to be the case with very rapid crystallisation of complex **2.3** occurring in under fifteen minutes.

2.1.3 Structure of the molecular capsule [(1-aza-18-crown-6 + H^+)⊂[$(H_2O)_2$[$Nd(H_2O)_9$]$_2$[(*p*-sulfonatocalix[4]arene)$_2$ + H^+]]·27.5H_2O, 2.3.

Crystals of the complex [(1-Aza-18-crown-6 + H^+)⊂[$(H_2O)_2$[$Nd(H_2O)_9^{3+}$]$_2$[(*p*-sulfonato-calix[4]arene)$_2$ + H^+]]·27.5H_2O, **2.3**, grew very rapidly from an aqueous solution containing a 1.8:1:1.3 mixture of SO_3H[4], 1-aza-18-crown-6 and neodymium chloride respectively (Equation 2.3). Crystals were also obtained from subsequent analogous 2:1:2 mixtures. The complex was characterised by IR spectroscopy and single crystal X-ray crystallography. Complex **2.3** crystallises in a monoclinic cell and the structural solution was performed in the space group $P2_1/c$. Details of the data collection and structure refinement are given in Table 2.7 of this chapter. A crystallographic information file containing all bond lengths and angles for complex **2.3** can be found in appendix 2.1.3 on the attached compact disc. The asymmetric unit consists of an entire molecular capsule arrangement comprising two SO_3[4] ions shrouding one mono-protonated 1-aza-18-crown-6 molecule, two crown ether associated water molecules (one is disordered over two positions within the capsule) and two nona-aqua neodymium(III) cations, Figures 2.9 and 2.10. In addition there are a total of twenty-seven and a half solvent water molecules in the asymmetric unit that are distributed over a total of thirty three positions.

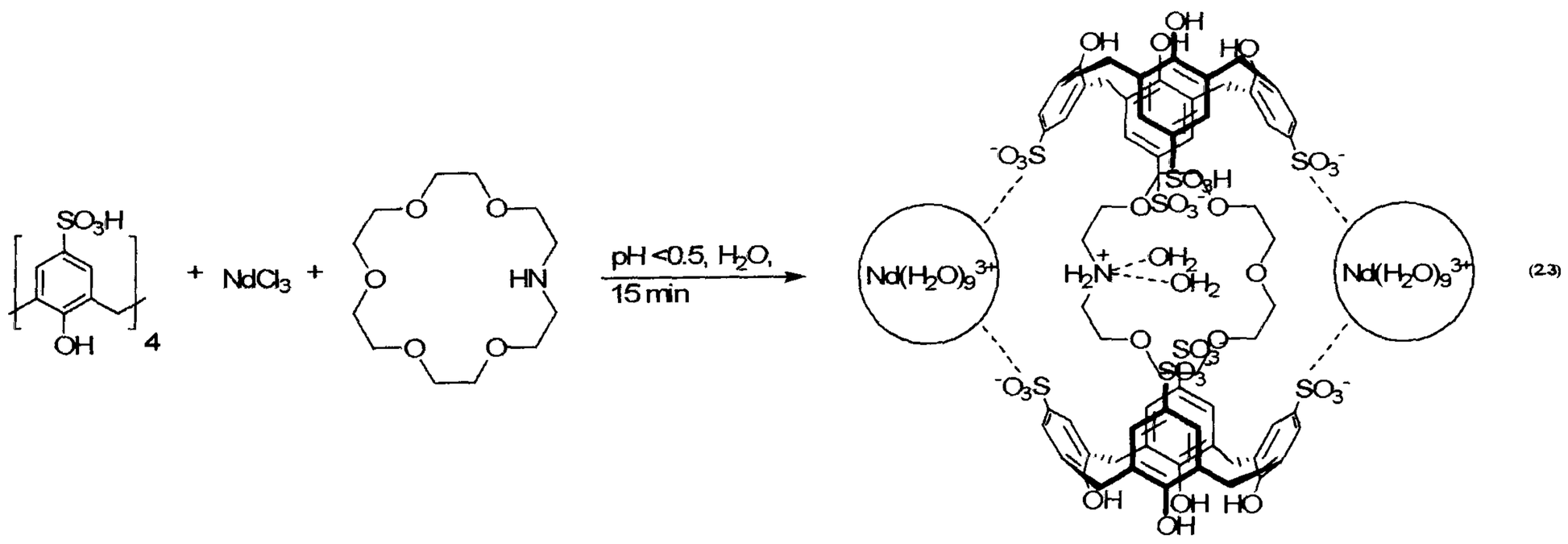

The molecular capsule is composed of two SO_3[4] molecules that shroud a mono-protonated 1-aza-18-crown-6 molecule in a head-to-head fashion with nona-aqua neodymium cations residing at the

periphery. Both nona-aqua neodymium cations have tri-capped trigonal prismatic geometry and have unexceptional Nd-O bond lengths (Table 2.2). The capsule arrangement has several interesting features, the majority of which are markedly different to those associated with the molecular capsule in compound **2.1**.

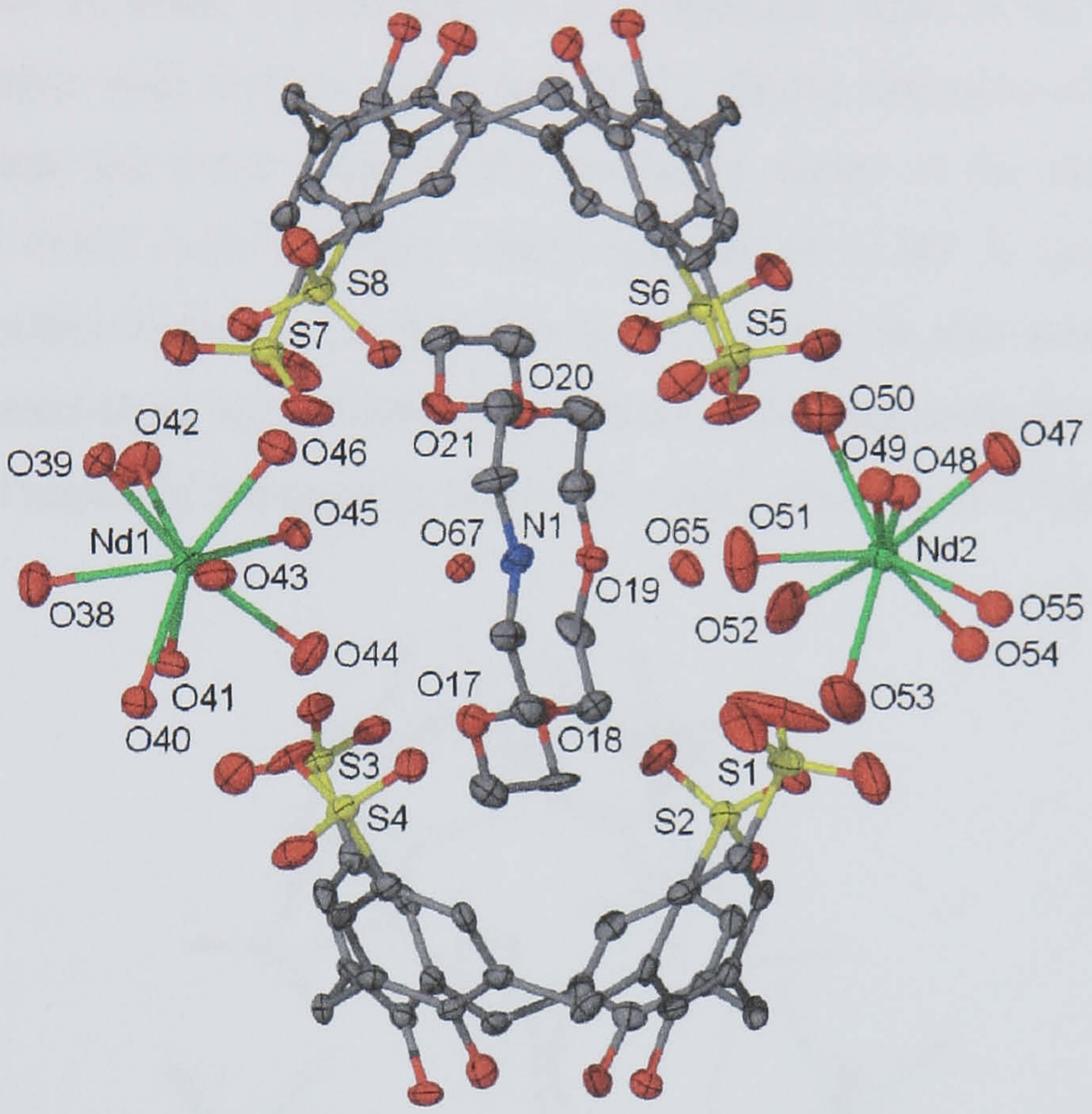

Figure 2.9 Part of the asymmetric unit from the crystal structure of complex **2.3**, ellipsoids shown at the 50% probability level. Some neodymium aquo ligands were refined isotropically and are shown in ball and stick representation and selected atoms have been labelled (one disordered water molecule within the capsule omitted for clarity).

Nd(1)-O(38)	2.498(12)	Nd(2)-O(47)	2.550(12)
Nd(1)-O(39)	2.519(12)	Nd(2)-O(48)	2.48(4)
Nd(1)-O(40)	2.617(11)	Nd(2)-O(49)	2.55(2)
Nd(1)-O(41)	2.504(12)	Nd(2)-O(50)	2.518(19)
Nd(1)-O(42)	2.481(11)	Nd(2)-O(51)	2.525(15)
Nd(1)-O(43)	2.528(13)	Nd(2)-O(52)	2.407(17)
Nd(1)-O(44)	2.486(12)	Nd(2)-O(53)	2.530(16)
Nd(1)-O(45)	2.468(10)	Nd(2)-O(54)	2.45(4)
Nd(1)-O(46)	2.477(12)	Nd(2)-O(55)	2.57(2)

Table 2.2 Interatomic distances relating to the coordination sphere of the neodymium metal centres in the crystal structure of complex **2.3** (distances given in Å with s.u.s in parentheses).

The most striking of these features is the conformational distortion of the aza-crown ether from the typically meridional conformation. This distortion is very likely attributable to the hydrogen bonding associated with O(67) that resides to the left-centre of the crown ether as shown in Figures 2.9 and 2.10. This water molecule is positioned so as to hydrogen bond to two of the oxygen donor atoms of the crown ether with O(67)···O(18) and O(67)···O(20) distances of 2.844 and 2.879 Å respectively. In addition, the protonation of the secondary amine in the crown ether results in hydrogen bonding to O(67) with an N(1)···O(67) distance of 2.798 Å (corresponding NH···O distance 1.929 Å). Another hydrogen bond to this water molecule is also associated with an aquo ligand of the closest nona-aqua neodymium cation (Nd(1)) residing at the hydrophilic rims of the calixarenes (equatorial region of the capsule, NdO(45)···O(67) distance of 2.724 Å).

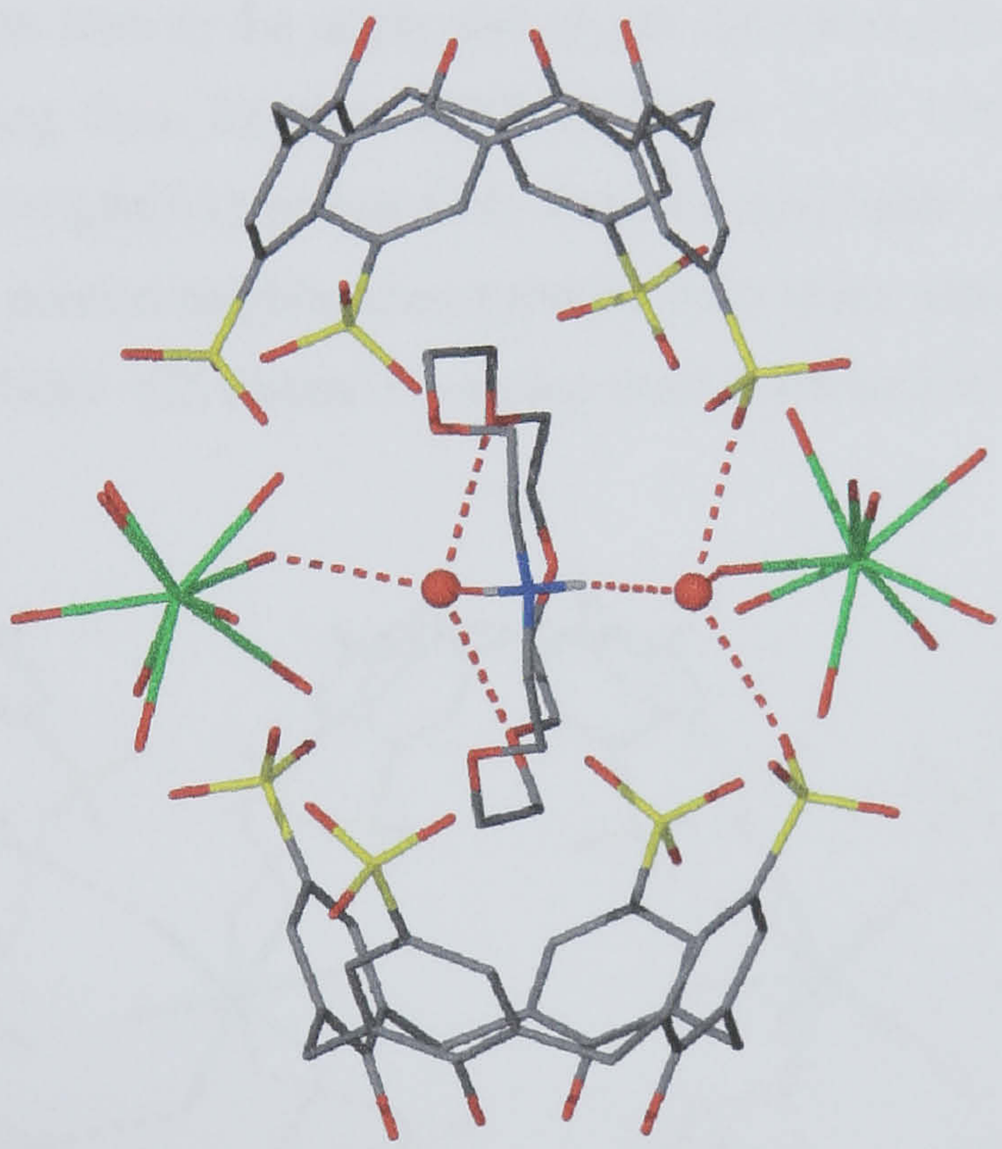

Figure 2.10 Capsular arrangement in the crystal structure of complex **2.3** showing the distortion of the mono-protonated crown ether. Also shown are the hydrogen bonding regimes associated with the included water molecules and the nona-aqua neodymium cations which reside at the periphery of the molecular capsule (one of the disordered water molecules within the capsule omitted for clarity).

The second water molecule is located to the right hand side of the crown ether in Figures 2.9 and 2.10 and is disordered over two positions. In the first position, O(65), the protonated nitrogen of the crown ether hydrogen bonds to the water molecule with an N(1)···O(65) distance of 2.909 Å (corresponding NH···O distance of 1.994 Å). There is additional hydrogen bonding to two sulfonate

groups, one from each calixarene within the capsule (O(65)···OS(7) and O(65)···OS(1) distances of 2.703 and 2.778 Å respectively). The fourth hydrogen bond associated with this water molecule is from an aquo ligand of the second nona-aqua neodymium cation (Nd(2)) with an NdO(51)···O(65) distance of 2.673 Å). In the second position, the water molecule hydrogen bonds to one sulfonate group of each of the calixarenes with O(66)···OS(7) and O(66)···OS(1) distances of 2.849 and 2.957 Å respectively. There are, however, no other hydrogen bonds from the donor atoms of the crown ether to the water molecule in this position due to the distortion of the macrocycle. The formation of the mono-protonated 1-aza-18-crown-6/*bis*-aqua arrangement here is reminiscent of both the di-protonated diaza-18-crown-6 *bis*-aqua guest species in complex **2.1** and a *trans*-ligated *bis*-aquo sodium ion/18-crown-6 fragment as seen in typical 'Russian dolls' (Figure 2.4).

Within each molecular capsule, four aquo ligands from each neodymium cation hydrogen bond to calixarene sulfonate groups (two to the upper and two to the lower calixarenes in both cases) with NdO···OS distances varying from 2.646 to 3.065 Å, Figure 2.11. There are additional hydrogen bonds from two other aquo ligands (pointing away from the molecular capsule) of each metal cation to sulfonate groups of the nearest neighbouring capsules (one to the upper calixarene and one to the lower in both cases) with NdO···OS distances varying from 2.698 to 2.969 Å.

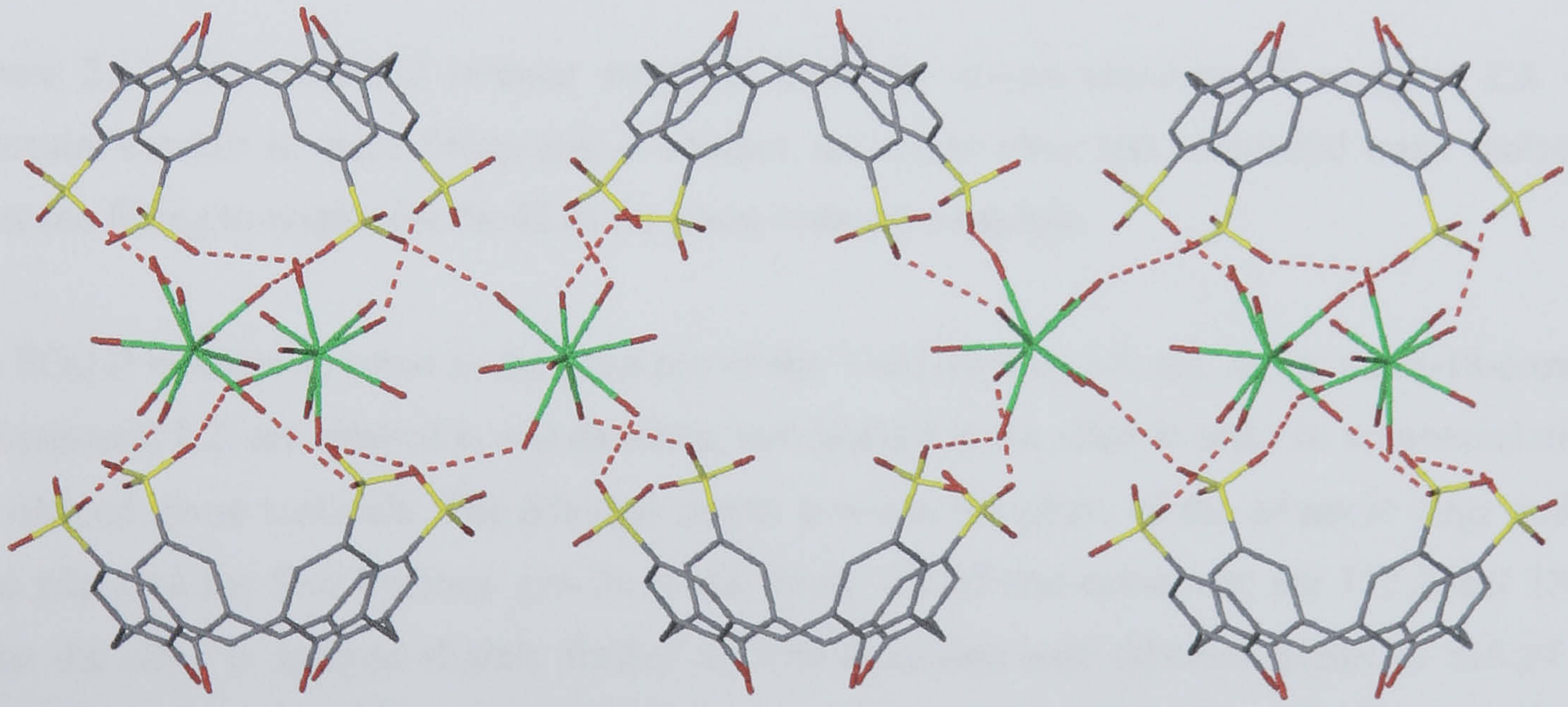

Figure 2.11 Intra and inter molecular capsule hydrogen bonding regimes in the crystal structure of complex **2.3**. The hydrogen bonds are from the neodymium aquo ligands to the sulfonate groups of the calixarenes (crown ether omitted for clarity).

The extended structure reveals the calixarenes to be arranged in the typical bi-layer arrangement with the primary hydrophobic interactions being a total of three crystallographically unique π-stacking interactions with aromatic centroid···centroid distances ranging from 3.940 to 4.109 Å

(Figure 2.11). The numerous waters of crystallisation reside in hydrophilic regions of the extended structure and have a multitude of hydrogen bonding contacts with appropriate localised functional groups.

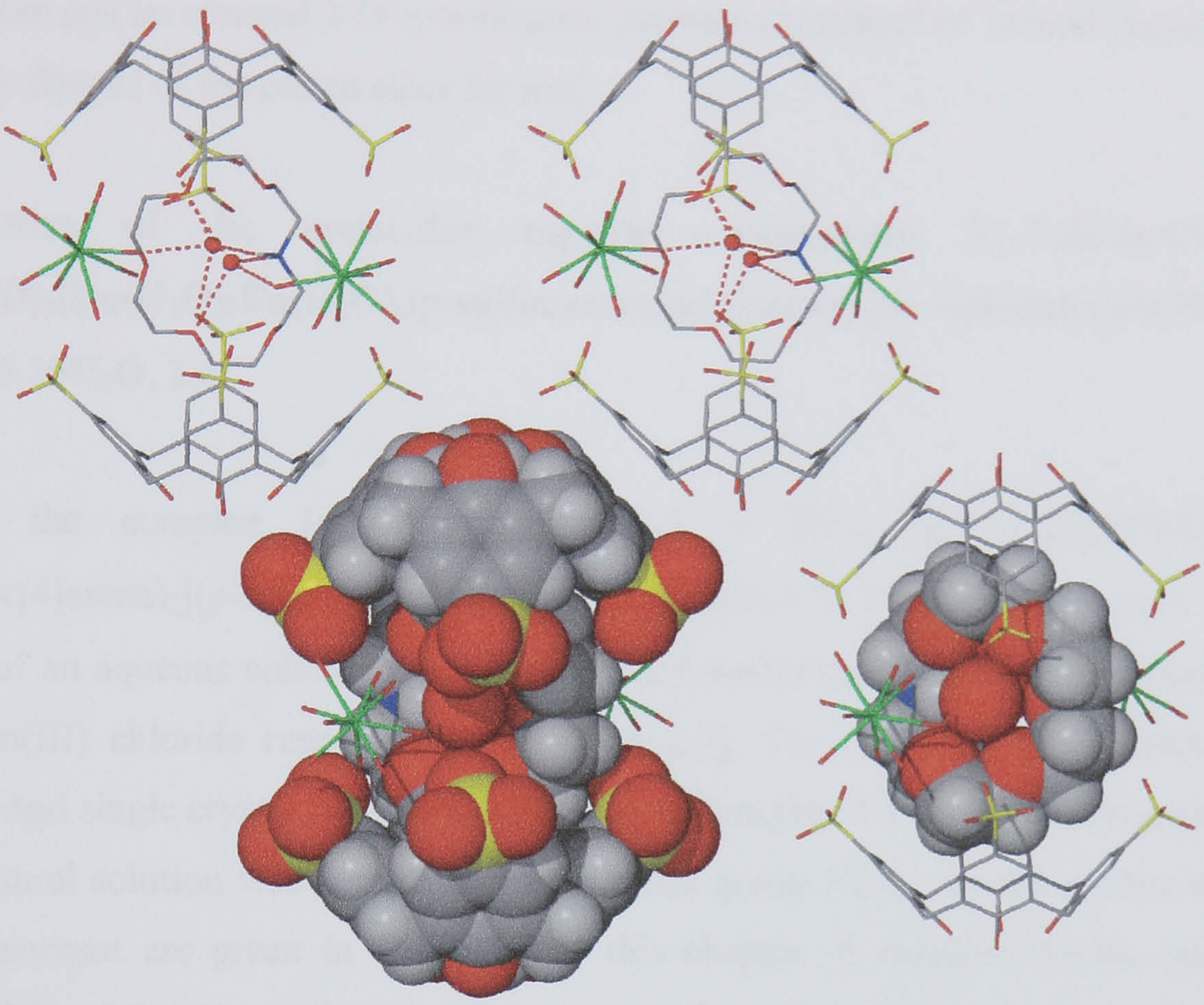

Figure 2.12 The extended bi-layer structure from the crystal structure of complex **2.3**. One molecular capsule is space filling and in another, the crown ether and associated water molecules are space filling to emphasise the fit of the guest within the capsule.

The SO_3[4] molecules, when in the presence of the 1-aza-18-crown-6 are, as for diaza-18-crown-6 in compound **2.2,** are splayed in one direction and pinched in the other in order to accommodate the disc-shaped guest molecule. The dihedral angles between the plane of the aromatic rings and the basal plane of the four hydroxy groups at the lower rim of one calixarene are 112.2 and 134.3° whilst the other is splayed slightly further in both directions with dihedral angles of 118.87 and 136.01°. These subtle differences in dihedral angles between the calixarenes in a single molecular capsule may well be attributable to both the unusual conformation of the crown ether and the crown/water/sulfonate/aquo-ligand hydrogen bonding regimes. From the successful inclusion of mono-protonated 1-aza-18-crown-6 in a molecular capsule, in conjunction with the formation of complex **2.2** at a pH $\leq$ 3, it is clear that molecular capsule formation with this guest is entirely pH dependent as sulfonate group protonation is pre-requisite. This is in stark contrast to complex **2.1** that forms at a higher (yet still acidic) pH but presents a capsule charge of 6– that is ideal for complexation with two poly-aquated trivalent lanthanide metal cations. Given the successful

inclusion of mono-protonated 1-aza-18-crown-6, the smaller analogue 1-aza-15-crown-5 was employed under similar conditions to those for complex **2.3**. The formation of a molecular capsule containing mono-protonated 1-aza-15-crown-5, similar to that of complex **2.3** was anticipated. This was not the case and an unusual 2-D coordination polymer composed of 'sealed' molecular capsules that are totally devoid of the crown ether formed.

2.1.4 Structure of the molecular capsule arrangement [(1,7-diaza-15-crown-5 + $2H^+$)$_{1.5}$⊂[$(H_2O)_3$[$Eu(H_2O)_7Eu(H_2O)_6$(*p*-sulfonatocalix[4]arene)$_2$](*p*-sulfonatocalix[4]arene)$Eu(H_2O)_8$]·$20.75H_2O$, 2.4.

Crystals of the complex [(1,7-diaza-15-crown-5 + $2H^+$)$_{1.5}$⊂[$(H_2O)_3$[$Eu(H_2O)_7Eu(H_2O)_6$(*p*-sulfonatocalix[4]arene)$_2$](*p*-sulfonatocalix[4]arene)$Eu(H_2O)_8$]·$20.75H_2O$, **2.4**, grew upon slow evaporation of an aqueous solution containing a 2:1:2 mixture of SO_3H[4], 1,7-diaza-15-crown-5, and europium(III) chloride respectively (Equation 2.5). The complex was characterised by IR spectroscopy and single crystal X-ray crystallography. Complex **2.4** crystallises in a monoclinic cell and the structural solution was performed in the space group $P2_1/c$. Details of data collection and structure refinement are given in Table 2.8 of this chapter. A crystallographic information file containing all bond lengths and angles for complex **2.4** can be found in appendix 2.1.4 on the attached compact disc.

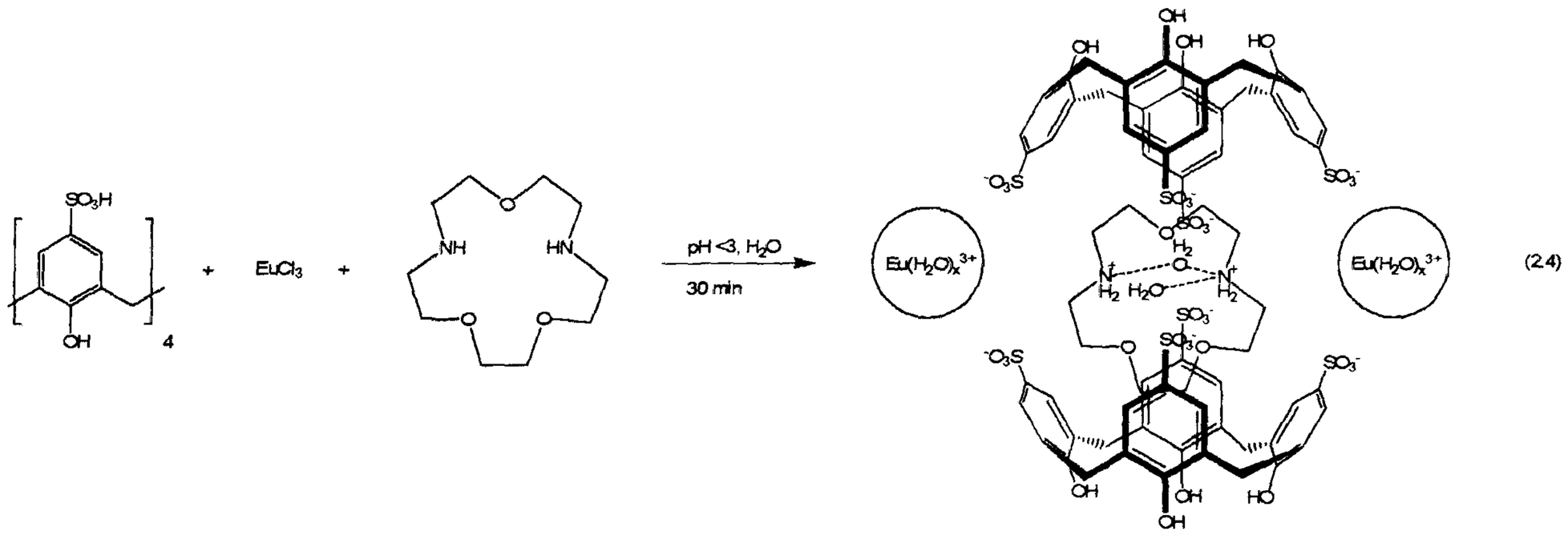

(2.4)

The asymmetric unit comprises one and a half molecular capsules that contain di-protonated diaza-15-crown-5 and two associated water molecules. In addition, there are a total of twenty and three quarter waters of crystallisation that are disordered over forty one positions. As can be seen from Figures 2.13 – 2.15, direct europium/calixarene sulfonate bonding influences the formation of the molecular capsules although homoleptic europium ions are also present. The lanthanide metal cations in molecular capsules of SO_3[4] incorporating di-protonated diaza-18-crown-6 and mono-protonated 1-aza-18-crown-6 guest species (complexes **2.1** and **2.3** respectively) have all been homoleptic. The mixture of homoleptic and coordinated europium metal centres in complex **2.4**

may be the result of the incorporation of a smaller guest. The presence of a smaller molecule in the overall capsular arrangement may cause the formation of a concomitantly narrower hydrophilic layer, thus resulting in increased head-to-head calixarene proximity and an opportunity for different lanthanide/calixarene interplay. This hypothesis would be difficult to prove as the phenomenon may also be determined by the arrangement of calixarenes within the hydrophobic layer. The bi-layer arrangement could also be dictated according to the dihedral angles of the calixarenes that may depend strongly on the steric bulk of the guest molecule(s) present.

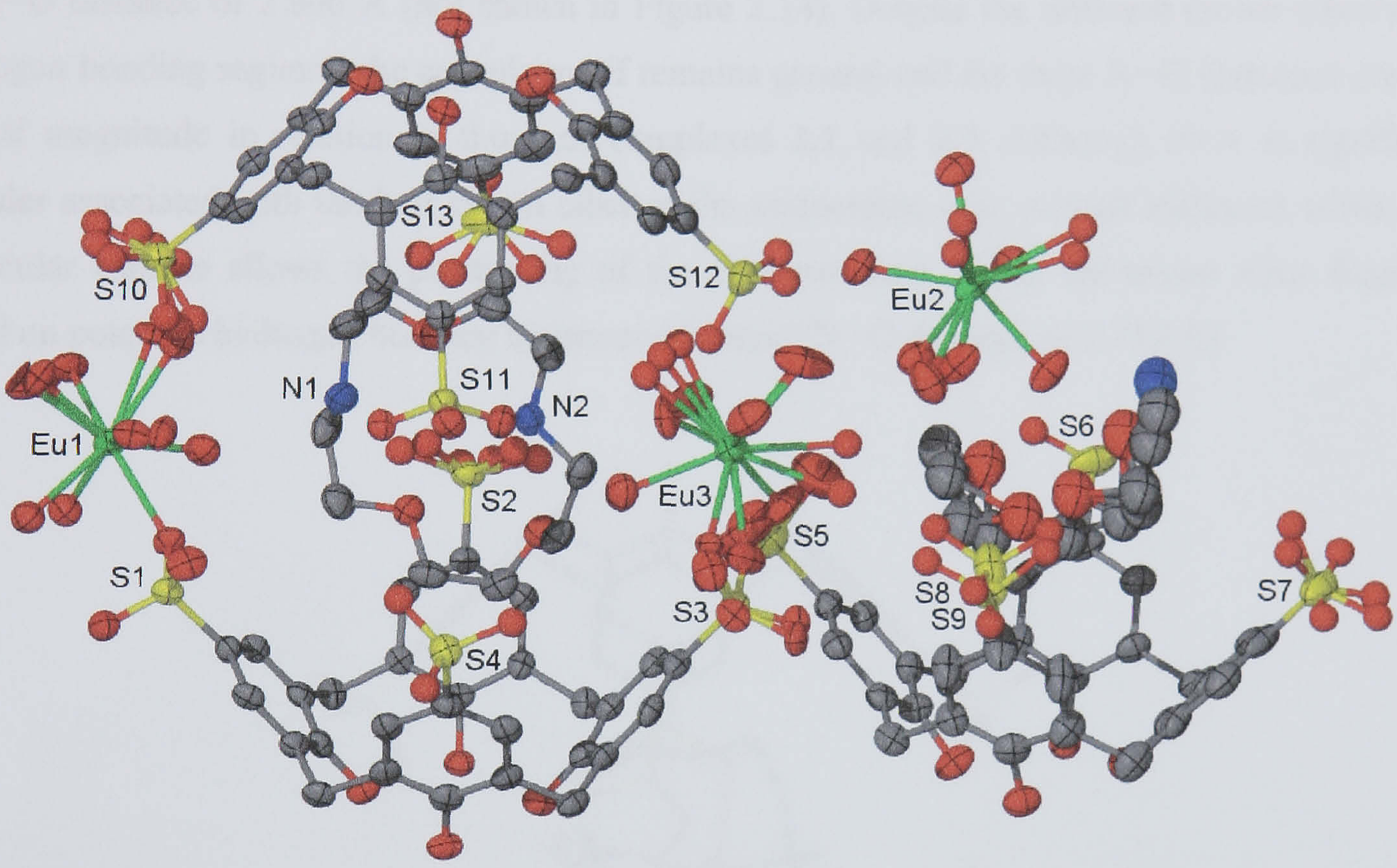

Figure 2.13 Partial asymmetric unit diagram of the crystal structure of complex **2.4**. Atoms are shown as ellipsoids at the 50% probability level except for some disordered europium aquo ligands and calixarene sulfonate groups that are in ball and stick representation. Selected atoms have been labelled.

As evident in Figure 2.13, there is significant disorder in several europium aquo ligands, several calixarene sulfonate groups and the half diaza-15-crown-5 molecule. All the europium atoms are octa-coordinate overall and have near square anti-prismatic geometry. Despite the extensive disorder in the overall structure, the contents of one molecular capsule are reasonably well resolved and allow the hydrogen bonding regime associated with the guest species to be determined (Figure 2.14). The diaza-crown ether is di-protonated and resides in the centre of the molecular capsule. A water molecule resides on each side of the di-protonated guest and there is NH···O hydrogen bonding from the protonated crown ether nitrogen atoms to the water molecules. The di-protonated

diaza-15-crown-5 is slightly distorted and the hydrogen bonding to associated water molecules is different to that in both complexes **2.1** or **2.3**. Furthermore, it no longer resembles the *trans*-ligated *bis*-aquo sodium/18-crown-6 species illustrated in Figure 2.4. The protonated N(2) atom of the crown ether is near-meridional within the capsule and hydrogen bonds to both of the associated water molecules (N···O distances of 2.839 and 2.883 Å, Figure 2.14). The protonated N(1) atom points slightly away from the centre of the capsule and hydrogen bonds to one of the crown ether associated water molecules with an N···O distance of 2.921 Å. The same protonated nitrogen also hydrogen bonds to a water molecule that is situated on the periphery of the molecular capsule with an N···O distance of 2.800 Å (not shown in Figure 2.14). Despite the different crown ether/water hydrogen bonding regimes, the capsule motif remains general and the three N···O distances are of a typical magnitude in relation to those of complexes **2.1** and **2.3**. Although there is significant disorder associated with the half crown ether in the asymmetric unit, a water molecule within this molecular capsule allows the positioning of the nitrogen atom within the crown ether fragment based on potential hydrogen bonding distances (potential N···O distance of 2.752 Å).

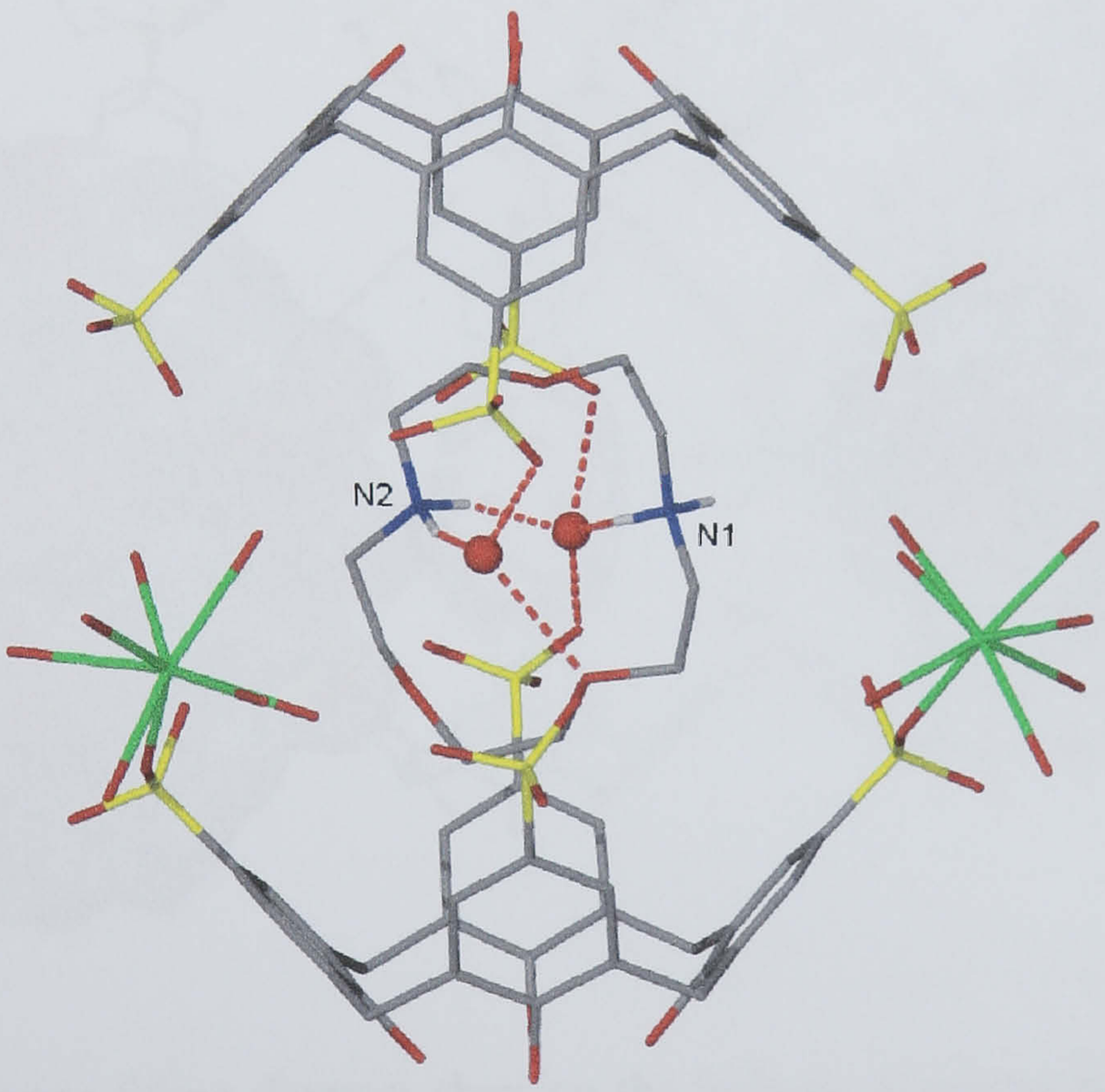

Figure 2.14 A molecular capsule from part of the crystal structure of complex **2.4** showing the inclusion of the crown ether *bis*-aqua species. For clarity some of the disordered europium aquo ligands and some of the disordered water molecules within the capsule have been omitted.

Upon symmetry expansion, the extended structure reveals the molecular capsules to pack in the expected bi-layer arrangement (Figure 2.15). There are four crystallographically unique interactions

in the bi-layer arrangement. These occur as two π-stacking interactions (aromatic centroid···centroid distances of 3.920 and 4.086 Å) and two CH···π interactions from calixarene methylene hydrogen atoms to adjacent SO_3[4] aromatic rings (CH···aromatic centroid distances of 2.757 and 3.053 Å). All the calixarenes have pinched around the crown ether guests in the C2 symmetric fashion (as described in Chapter 1). The S(10)-S(13) calixarene in the whole molecular capsule has dihedral angles of 113.0 and 134.86° (calixarene notation according to the asymmetric unit diagram, Figure 2.13). The S(1)-S(4) calixarene in the same molecular capsule has dihedral angles of 118.27 and 133.55° and the S(5)-S(9) calixarene of the crystallographically unique half molecular capsule has dihedral angles of 112.99 and 127.61°.

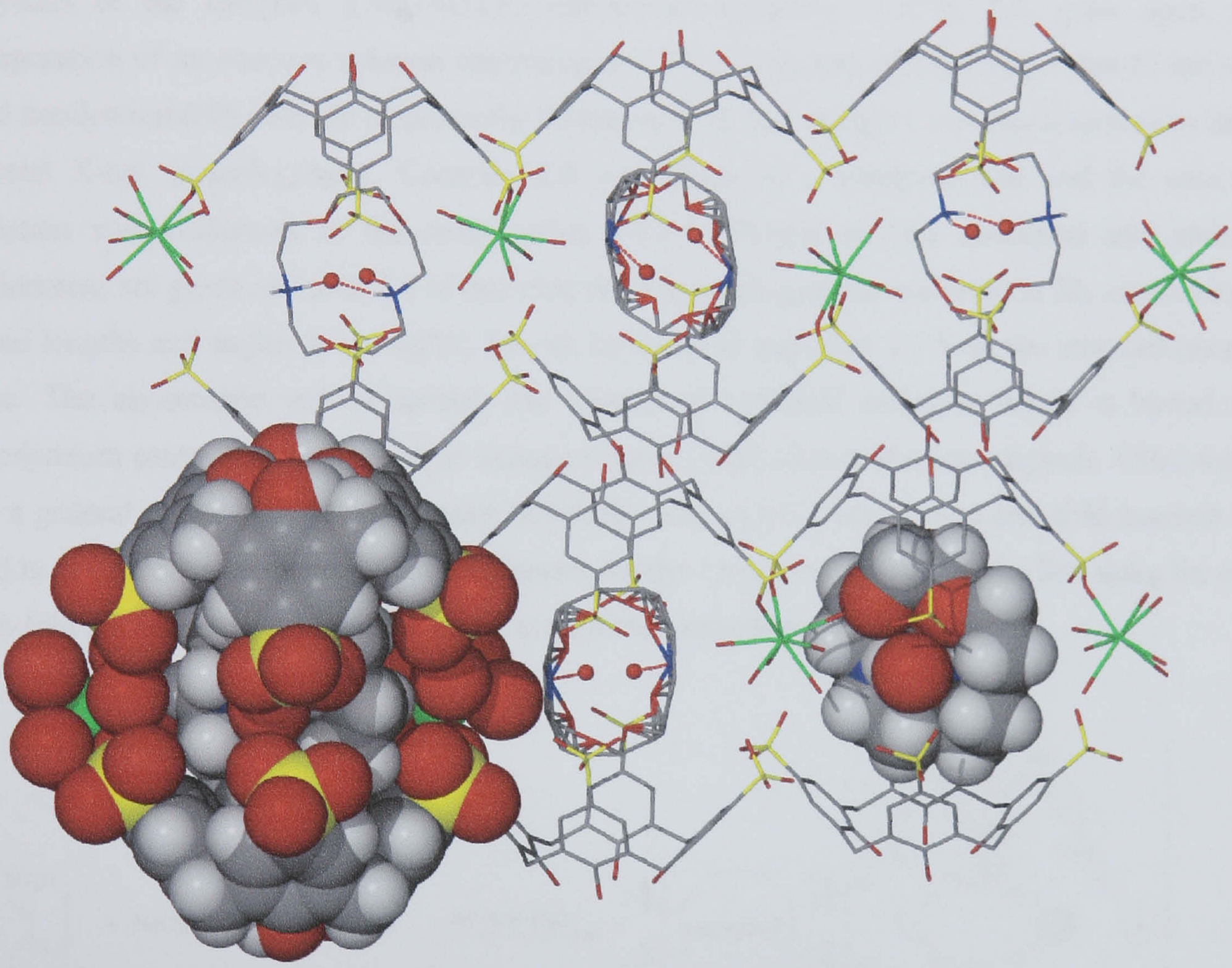

Figure 2.15 Partial space filling diagram showing the bi-layer arrangement found in the crystal structure of complex **2.4**. One molecular capsule is space filling whilst in another only the crown ether and associated water molecules are space filling to emphasise the pinched cone conformation of the calixarene. The disordered crown ether bis-aqua species are also shown but have not been rendered in space filling mode.

Given both the successful inclusion of di-protonated diaza-15-crown-5 in a molecular capsule and the ability to overcome the charge disparity in molecular capsule formation with 1-aza-18-crown-6,

it was anticipated that 1-aza-15-crown-5 would be included in a molecular capsule of SO_3[4] at a low pH (ca <1). This however was not the case and a 2-D coordination polymer completely devoid of the crown ether guest molecule resulted. The coordination polymer is an infinite array of molecular capsules sealed by neodymium sulfonate coordination around the periphery of the capsule.

2.1.5 Structure of the 2-D coordination polymer, [($Nd(H_2O)_5$)(*p*-sulfonatocalix[4]arene + H^+)], 2.5.

Crystals of the complex [($Nd(H_2O)_5$)(*p*-sulfonatocalix[4]arene + H^+)], **2.5**, grew upon slow evaporation of an aqueous solution containing a 2.3:1:1.7 mixture of SO_3H[4], 1-aza-15-crown-5, and neodymium(III) chloride respectively (Equation 2.5). The complex was characterised by single crystal X-ray crystallography. Complex **2.5** crystallises in a tetragonal cell and the structural solution was performed in the space group *P4/nnc*. Details of data collection and structure refinement are given in Table 2.8 of this chapter. A crystallographic information file containing all bond lengths and angles for complex **2.5** can be found in appendix 2.1.5 on the attached compact disc. The asymmetric unit comprises one quarter of a SO_3[4] molecule which is bound to a neodymium centre that has two aquo ligands (Figure 2.16). One of the aquo ligands, O(6), resides on a general position at full occupancy whilst the other, O(5), resides on a two-fold rotation axis and is at a quarter occupancy. The metal centre resides on a special position that lies along the same two-fold rotation axis as O(5) and is also at a quarter occupancy.

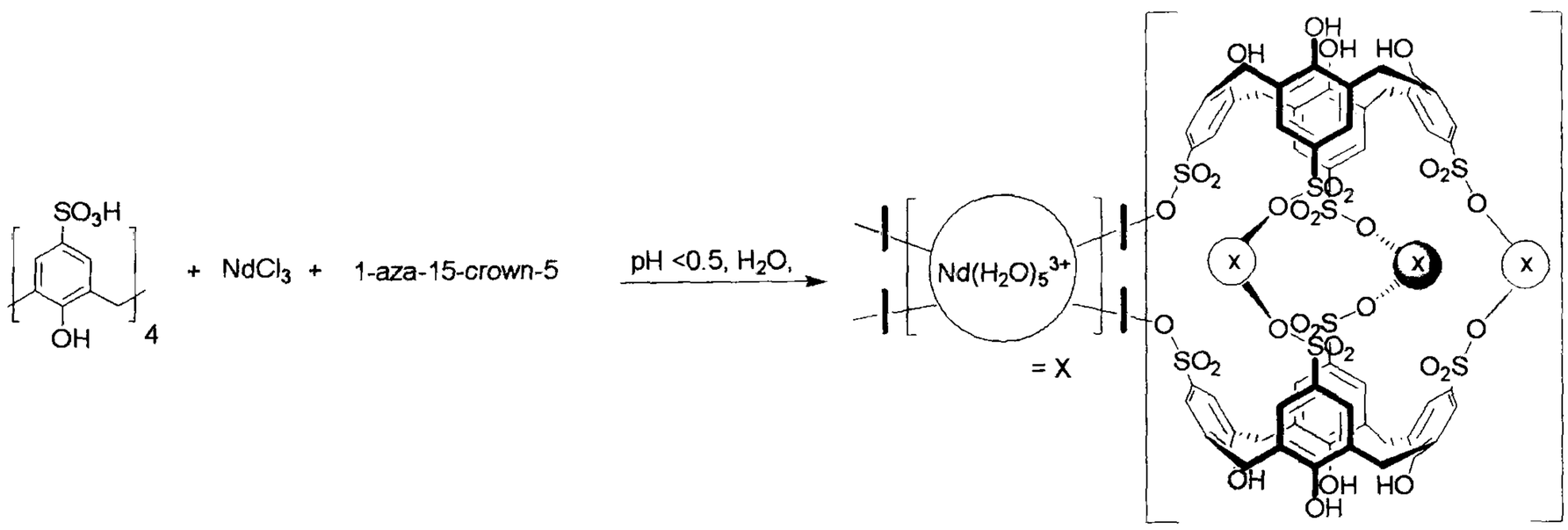

(2.5)

The overall structure is a 2-D coordination polymer built up of sealed molecular capsules based around a bi-layer arrangement of calixarenes. The most striking and prominent feature of the structure is the unprecedented sealed capsule arrangement formed by direct lanthanide sulfonate coordination through the hydrophilic layer generated by the calixarene packing (Figures 2.17 and 2.19). This type of structural motif for SO_3[4] is particularly unusual given that the hydrophobic

layers are typically separated by hydrophilic layers containing solvent water molecules. This separation is usually large enough to prevent transition or lanthanide metal ions from coordinating to sulfonate groups from adjacent layers, although a handful of examples have been reported to date.[27, 32, 39, 40, 52] None of these examples however, have been shown to form in a sealed capsular manner as is displayed in complex **2.5**.

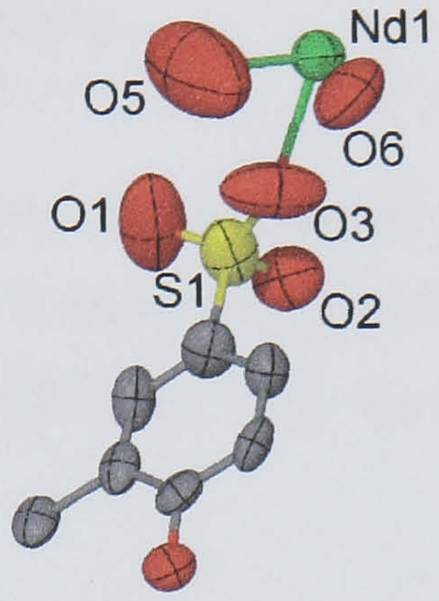

Figure 2.16 The asymmetric unit from the crystal structure of complex **2.5**, ellipsoids at the 50% probability level. Selected atoms have been labelled.

Each of the metal centres coordinates to sulfonate groups from the four nearest calixarene molecules. The penta-aqua neodymium(III) cations are disordered over two sites across a four-fold axis as show in Figure 2.19. Each metal centre, upon symmetry expansion, is of distorted tri-capped trigonal prismatic geometry. Selected bond lengths relating to the coordination sphere of the neodymium centre are listed in Table 2.3. From these bond lengths, it is immediately obvious that the neodymium aquo ligand bond distances are either slightly shorter or longer than expected. This distortion is likely due to the inherent disorder emplaced on the structure through high symmetry. Indeed, if a centroid is generated between the two disordered positions of the neodymium metal centre, the resultant centroid···oxygen bond lengths are of more typical magnitude.

Each of the centroids mentioned above coordinates to four symmetry equivalent calixarenes. Each calixarene also coordinates to four symmetry equivalent centroids to generate the 2-D coordination polymer. Both the centroids and calixarenes can be treated as 4-connecting centres within the polymer. When joined, a (4,4) grid network of vertex-sharing octahedra is generated , Figure 2.18. Within each molecular capsule, the calixarenes are in a skewed head-to-head arrangement, Figures 2.17 and 2.19. This is in contrast to molecular capsules that incorporate disc-shaped guests such as crown ethers and that have the calixarenes in a head-to-head eclipsing arrangement, as for complexes **2.1**, **2.3** and **2.4**. This skewed arrangement may perhaps be due to the unusual mode of lanthanide/calixarene coordination in this system.

Nd(1)-O(3)	2.245(9)	Nd(1)-O(6)$^{(b)}$	2.155(13)
Nd(1)-O(5)	2.25(3)	Nd(1)-O(3)$^{(c)}$	2.715(11)
Nd(1)-O(6)	2.155(13)	Nd(1)-O(6)$^{(c)}$	2.727(12)
Nd(1)-O(3)$^{(a)}$	2.715(11)	O(3)-Nd(1)$^{(a)}$	2.715(11)
Nd(1)-O(6)$^{(a)}$	2.727(12)	O(6)-Nd(1)$^{(a)}$	2.727(12)
Nd(1)-O(3)$^{(b)}$	2.245(9)		

Table 2.3 Interatomic distances relating to the coordination sphere of the neodymium metal centres in the crystal structure of complex **2.5** (distances given in Å with e.s.d. in parentheses). Key operations for symmetry related atoms: *(a)* 1/2-x, 3/2-y, +z, *(b)* 1/2-x, +y, 1/2-z, *(c)* +x, 3/2-y, 1/2-z.

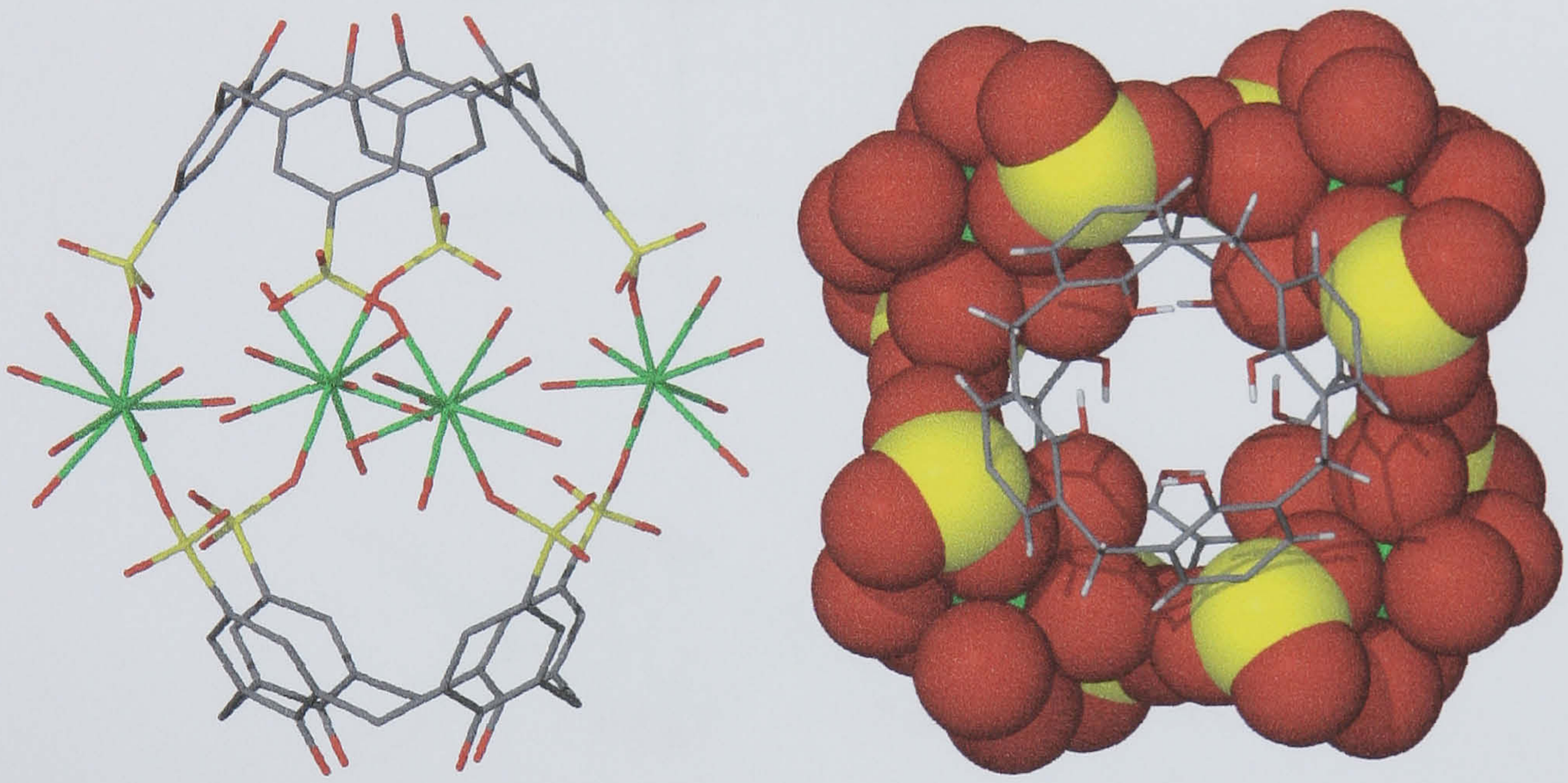

Figure 2.17 Side view and partially space filled apical view of a 'sealed' molecular capsule in the crystal structure of complex **2.5**. Both images show the neodymium metal centres in one of two disordered positions. The right hand image has been partially rendered in space filling mode so as to emphasise the reduced volume within the capsules due to the aquo ligands of the metal centres that are directed towards the centre of the capsule.

Within each skewed capsule, there is a large amount of diffuse electron density that could not be modelled effectively as either a 1-aza-15-crown-5 molecule or disordered water molecules. As some ambiguity surrounded the presence of the crown ether, several aspects of the complex were investigated. Microanalysis of the bulk sample which had been dried, ground and washed with cold water showed only traces of nitrogen which may be attributable to residual crown ether from the reaction mixture on the crystal surface. Examination of a partially space filled capsule (Figures 2.17

and 2.19) clearly shows that accommodation of 1-aza-15-crown-5 is highly unlikely since the internal cavity and equatorial region of the capsule is very sterically hindered. The NdO···ONd distance between the aquo ligands which point towards the centre of the cavity is 6.472 Å. The corresponding distance between Van der Waals radii of the aquo ligands (based on non-covalent radius of oxygen) is 5.74 Å. In addition to this, analysis of a 1-aza-15-crown-5 hydrochloride salt in the Cambridge Structural Database shows the distance between opposite carbon atoms within the macrocycle is typically to the order of at least 6 – 6.3 Å (not accounting for hydrogen atoms).[101] Given all of the above, it is likely that the diffuse electron density is disordered waters of crystallisation that are bound deep within the two calixarene cavities within the sealed capsule.

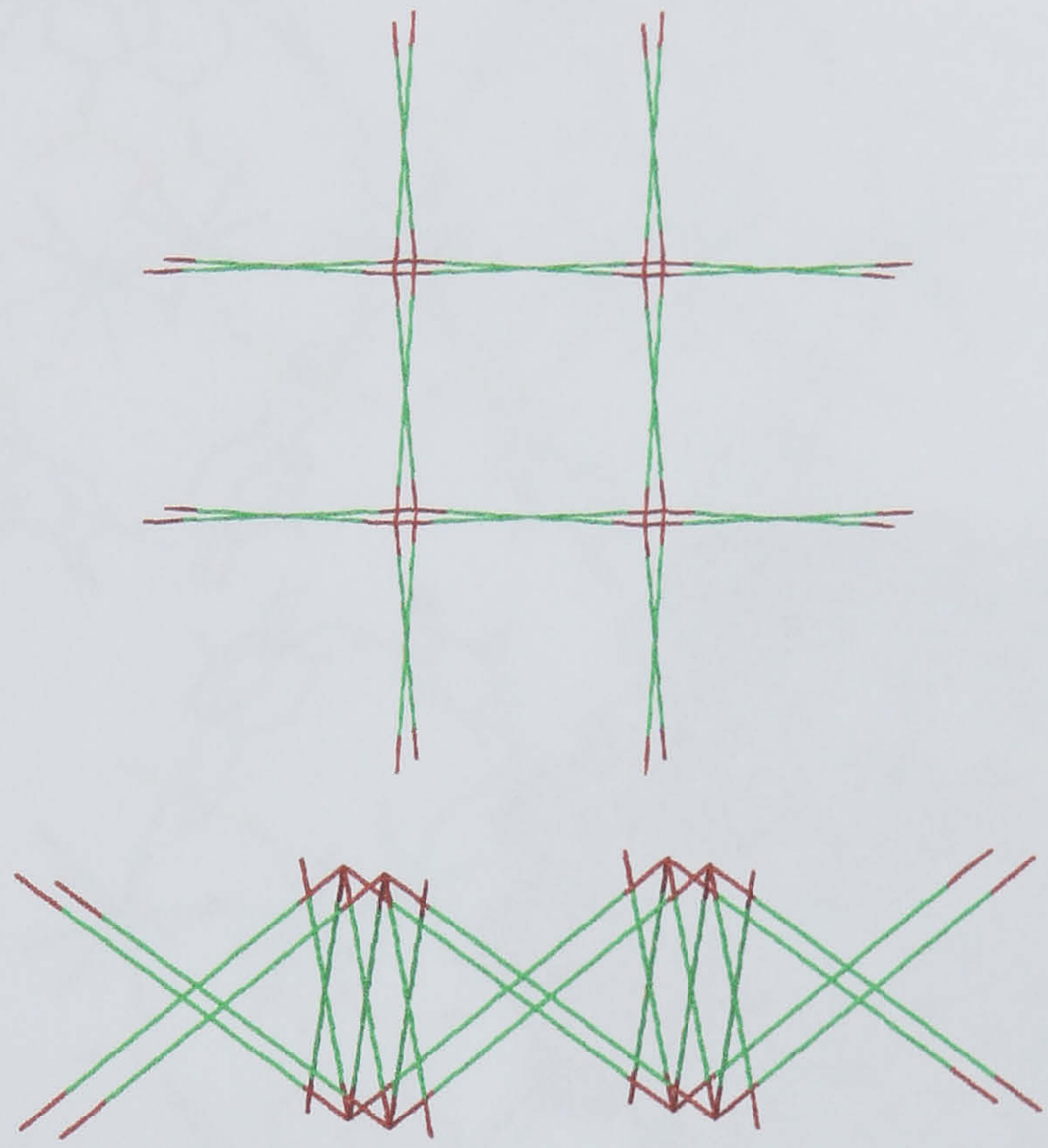

Figure 2.18 Two views of the (4,4) grid network of vertex-sharing octahedra found within the hydrophilic layers of the crystal structure of complex **2.5**. The red and green nodes represent the calixarene centroid positions and the neodymium centres respectively.

The inability to successfully model disordered solvent molecules within sealed supramolecular structures is an ongoing problem encountered in many systems displaying enclosed chemical space. Thus 1-aza-15-crown-5 is excluded as a capsule guest, and this result is consistent with any other attempts to form complexes of the crown ether with *p*-sulfonatocalix[*n*]arenes throughout the project and previous studies. Although it is likely that the crown ether has been omitted, a charge deficit of 1– prevails and at such a low pH (< 0.5) it is possible that this has been satisfied by either protonation of one sulfonate group of a calixarene or the inclusion of H_3O^+ within the capsule although there is no experimental evidence for this.

The extended bi-layer type arrangement shows the calixarenes to have splayed equally in all directions with dihedral angles of 124.6°. The primary hydrophobic interaction between calixarenes is in the form of CH···π interactions with a crystallographically unique CH···aromatic ring centroid distance of 2.90 Å. A simple 2-D coordination polymer that forms with SO_3[4] and the early lanthanide metals has been previously reported.[102] The coordination polymer differs from that in complex **2.5** as the lanthanide metals were nona-coordinate and had five aquo ligands in a coordination polymer layer.

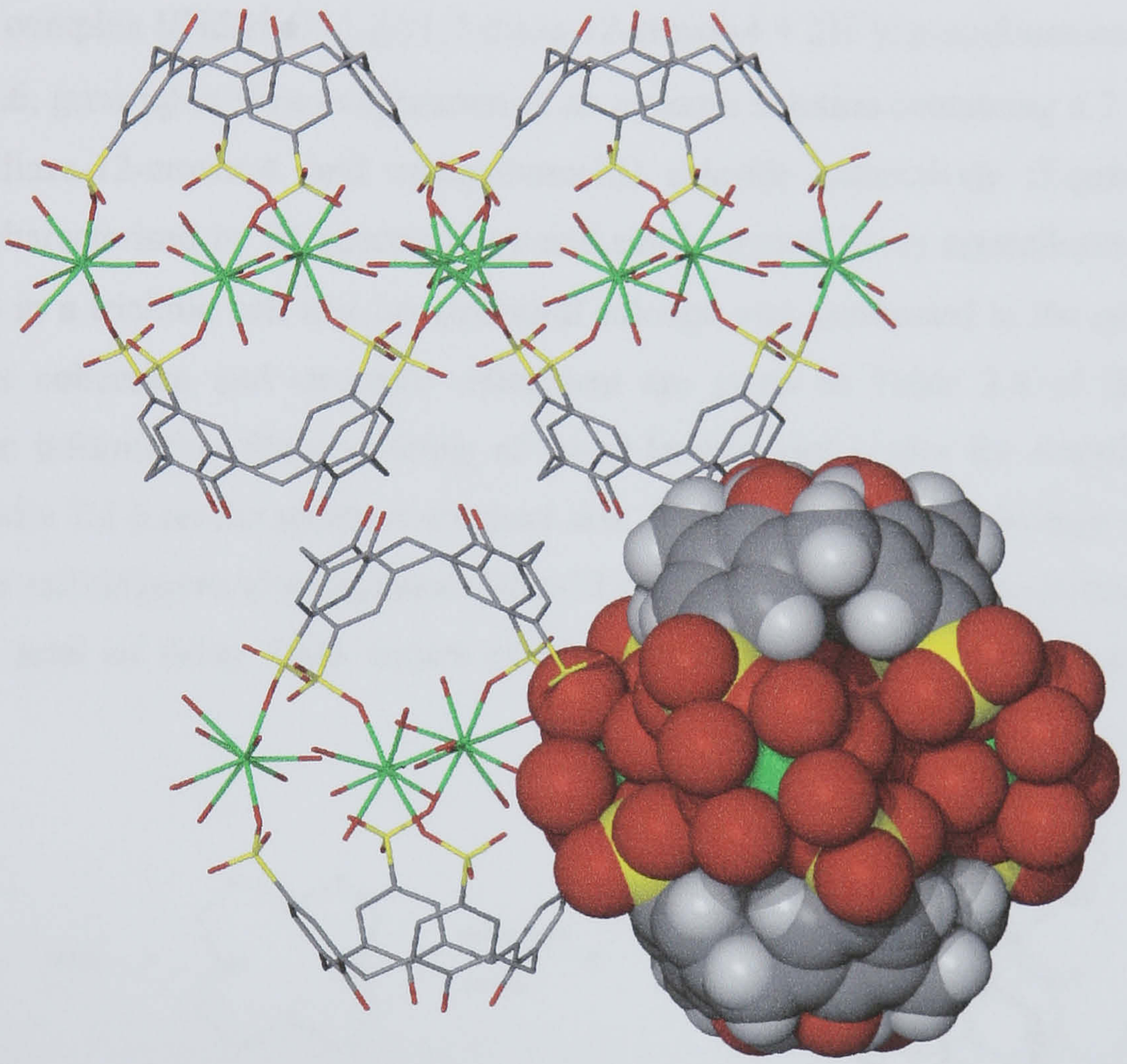

Figure 2.19 Partial space filling diagram showing the extended bi-layer arrangement from the crystal structure of complex **2.5** showing the 'sealed' molecular capsules and the skewed orientation of calixarenes within each capsule. The disordered lanthanide metals formed through symmetry constraints are also shown (top-central lanthanide position).

The metal coordination sphere was considerably different and one aquo ligand pointed into the hydrophobic layer and hydrogen-bonded to base phenolic groups of calixarenes directly beneath. Although the metal coordination sphere did not span the hydrophilic layer, the structure was of tetragonal symmetry and displayed similar topology (4,4 grid), dihedral angles (125.6°), and

hydrophobic interactions (CH···aromatic centroid distance of 2.819 Å) to those described here for complex **2.5**. A significant difference between the two structures is that the reported coordination polymer has bi-layers such that the cavities facing out of each hydrophobic layer were aligned with the bases of calixarenes in the nearest adjacent hydrophobic layer. This is in contrast to complex **2.5** where the calixarenes are aligned in a capsular fashion.

2.1.6 Structure of the bi-layer arrangement $[(Nd(H_2O)_9)_2][((1,7\text{-diaza-12-crown-4} + 2H^+)\subset p\text{-sulfonatocalix[4]arene})_4 + 2H^+]\cdot 33H_2O$, 2.6.

Crystals of the complex $[(Nd(H_2O)_9)_2][((1,7\text{-diaza-12-crown-4} + 2H^+)\subset p\text{-sulfonatocalix[4]arene})_4 + 2H^+]\cdot 33H_2O$, **2.6**, grew upon slow evaporation of an aqueous solution containing a 2:1:2 mixture of $SO_3H[4]$, 1,7-diaza-12-crown-4, and neodymium(III) chloride respectively (Equation 2.6). The complex was characterised by IR spectroscopy and single crystal X-ray crystallography. Complex **2.6** crystallises in a triclinic cell and the structural solution was performed in the space group $P\bar{1}$. Details of data collection and structure refinement are given in Table 2.8 of this chapter. A crystallographic information file containing all bond lengths and angles for complex **2.6** can be found in appendix 2.1.6 on the attached compact disc. The asymmetric unit is large and comprises four *p*-sulfonatocalix[4]arene/di-protonated diaza-12-crown-4 moieties, two nona-aqua neodymium cations, and a total of thirty three waters of crystallisation that are disordered over forty two positions.

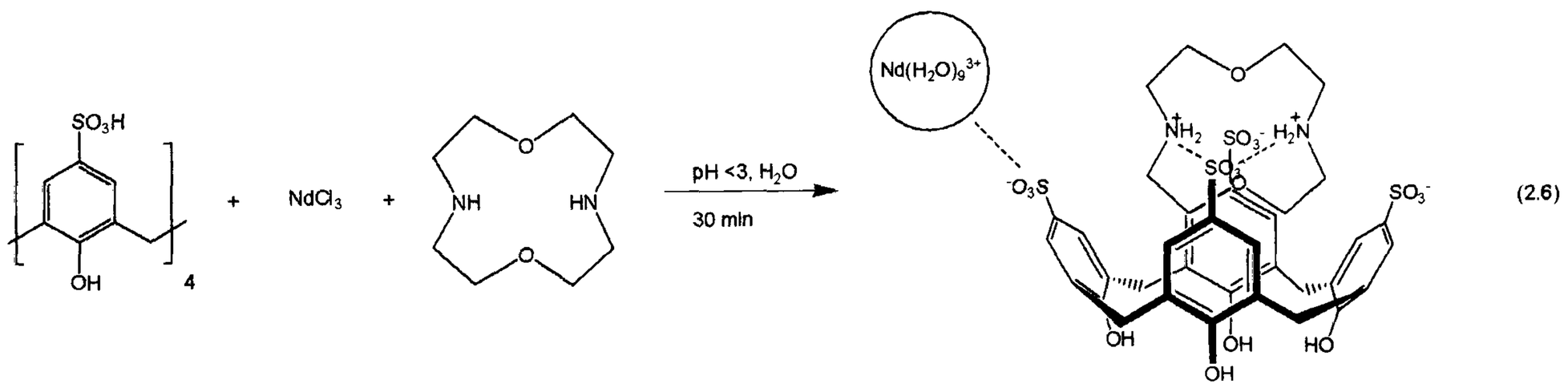

(2.6)

Complexes **2.1** – **2.4** of this chapter have shown that the formation of molecular capsules with di-protonated diaza-18-crown-6, mono-protonated 1-aza-18-crown-6, and di-protonated diaza-15-crown-5 is entirely pH dependent. Complex **2.5**, however, demonstrated that 1-aza-15-crown-5 was omitted from a molecular capsule arrangement and this may be attributable to the guest being unsuitable for the cavity of an $SO_3[4]$ molecule even when protonated and the solution is at a low pH to facilitate sulfonate group protonation. Given that a molecular capsule *was* formed with di-protonated diaza-15-crown-5 but was *not* formed with mono-protonated 1-aza-15-crown-5, it was anticipated that a molecular capsule *would* form with di-protonated diaza-12-crown-4. This

hypothesis was based on the presence of a 2+ inner capsule charge that was expected to be sufficient to overcome any possibly unfavourable steric interactions between host and guest. Unfortunately, the first and most prominent feature of complex **2.6** is that the calixarenes do not assemble as a molecular capsule but form an alternative bi-layer arrangement. The resultant structure is nevertheless interesting in that it forms an uneven bi-layer arrangement of calixarenes, a probable reason for the large number of crystallographically unique host molecules in the asymmetric unit (Figure 2.20).

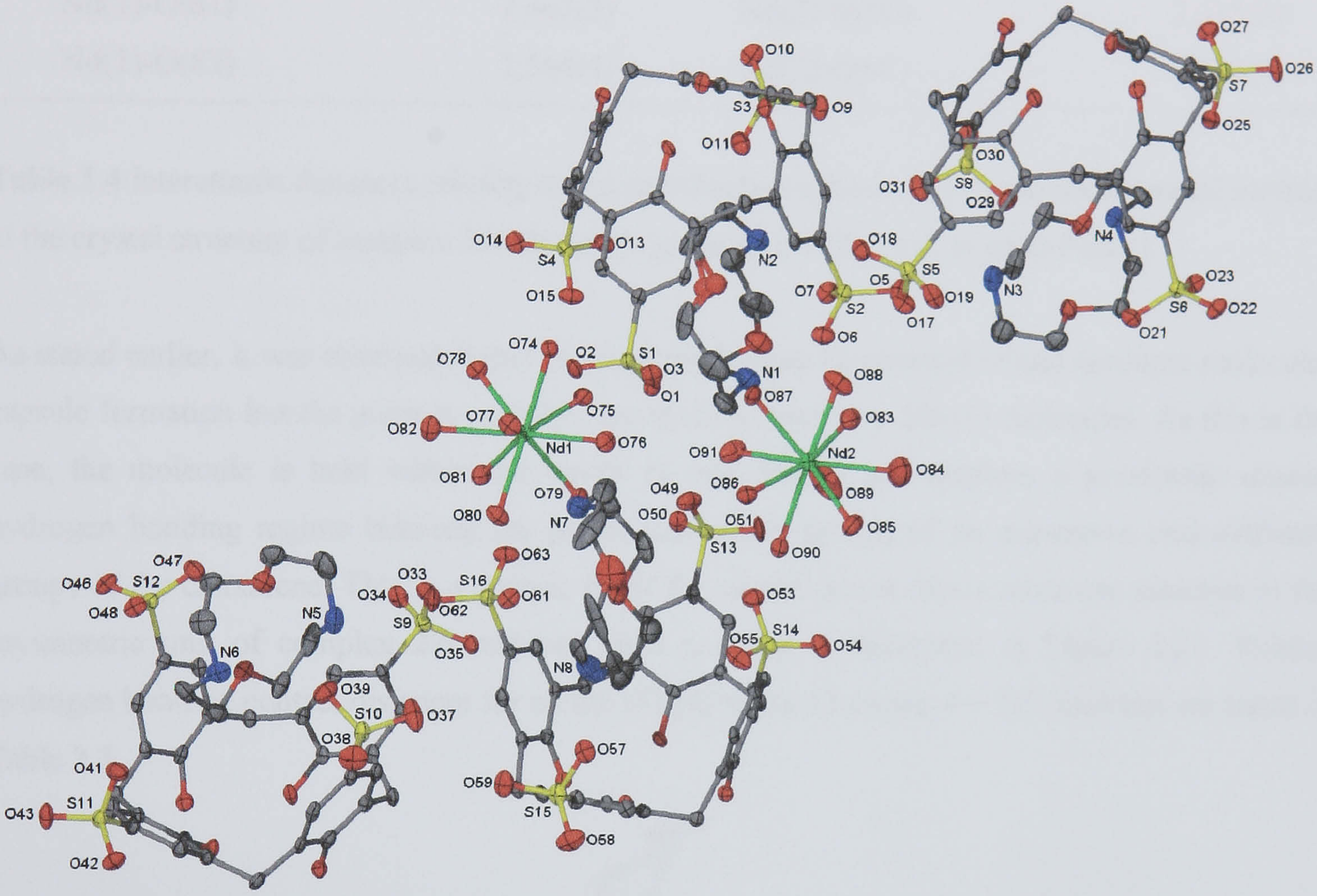

Figure 2.20 Part of the asymmetric unit from the crystal structure of complex **2.6**, ellipsoids shown at the 50% probability level. Selected atoms have been labelled. A disordered oxygen atom of the N(1) – N(2) crown ether is shown in ball and stick representation.

Both nona-aqua neodymium cations in the asymmetric unit have tri-capped trigonal prismatic geometry and have unexceptional Nd-O bond lengths (Table 2.4). There are a total of fifteen hydrogen bonding contacts between the aquo ligands of the metal cations and SO_3[4] molecules in the asymmetric unit with NdO···OS distances ranging from 2.669 to 2.953 Å. There are four other hydrogen bonding contacts between the aquo ligands of the metal cations and neighbouring SO_3[4] molecules with NdO···OS distances ranging from 2.748 to 2.961 Å.

Nd(1)-O(74)	2.504(3)	Nd(2)-O(83)	2.479(4)
Nd(1)-O(75)	2.518(3)	Nd(2)-O(84)	2.533(5)
Nd(1)-O(76)	2.499(4)	Nd(2)-O(85)	2.544(4)
Nd(1)-O(77)	2.520(4)	Nd(2)-O(86)	2.521(4)
Nd(1)-O(78)	2.529(4)	Nd(2)-O(87)	2.487(3)
Nd(1)-O(79)	2.485(3)	Nd(2)-O(88)	2.483(4)
Nd(1)-O(80)	2.506(4)	Nd(2)-O(89)	2.476(5)
Nd(1)-O(81)	2.463(3)	Nd(2)-O(90)	2.513(3)
Nd(1)-O(82)	2.564(4)	Nd(2)-O(91)	2.474(4)

Table 2.4 Interatomic distances relating to the coordination sphere of the neodymium metal centres in the crystal structure of complex **2.6** (distances given in Å with e.s.d. in parentheses).

As stated earlier, it was anticipated that di-protonated diaza-12-crown-4 would facilitate molecular capsule formation but the guest is probably too small to bind two SO_3[4] molecules. As this is the case, the molecule is held within the cavity of one SO_3[4] and displays a previously unseen hydrogen bonding regime between the protonated amine groups of an aza-crown and sulfonate groups of the calixarene. This is a generic motif for all the crown ether/calixarene moieties in the asymmetric unit of complex **2.6** and one such example is illustrated in Figure 2.21. Related hydrogen bonding contact distances for all the SO_3[4]/diaza-12-crown-4 + $2H^+$ moieties are listed in Table 2.5.

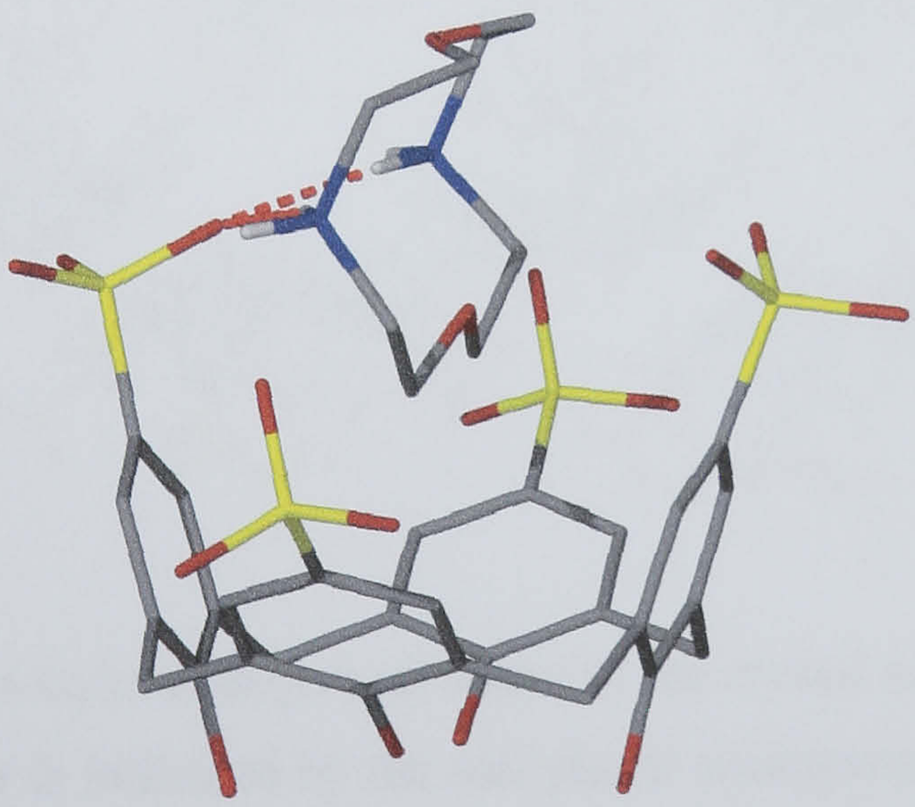

Figure 2.21 A crown ether/calixarene moiety from the crystal structure of complex **2.6**. The di-protonation of the crown ether, related sulfonate hydrogen bonding and the splaying of the calixarene are also shown.

N(1)···O(7)-S(2)	3.186	N(2)···O(7)-S(2)	2.875
N(3)···O(29)-S(8)	2.926	N(4)···O(29)-S(8)	2.965
N(5)···O(39)-S(10)	2.891	N(6)···O(39)-S(10)	2.958
N(7)···O(61)-S(16)	3.079	N(8)···O(61)-S(16)	2.964

Table 2.5 Hydrogen bonding contacts between the nitrogen atoms of the di-protonated diaza-12-crown-4 molecules and sulfonate groups of calixarenes in complex **2.6** (distances given in Å).

Although the crown ether is significantly smaller than diaza-15-crown-5 or diaza-18-crown-6, all the calixarenes in the asymmetric unit are pinched in order to accommodate the di-protonated guest. The resultant dihedral angles of the calixarenes vary between 107.31 – 108.64, and 137.91 – 149.96° for the acute and obtuse angles respectively and these values are similar to those for the inclusion of other disc shaped molecules (complexes **2.1**, **2.3** and **2.4**).[34, 35, 44-47, 50] The extended structure reveals the calixarenes are packed in a bi-layer arrangement as expected (Figure 2.22).

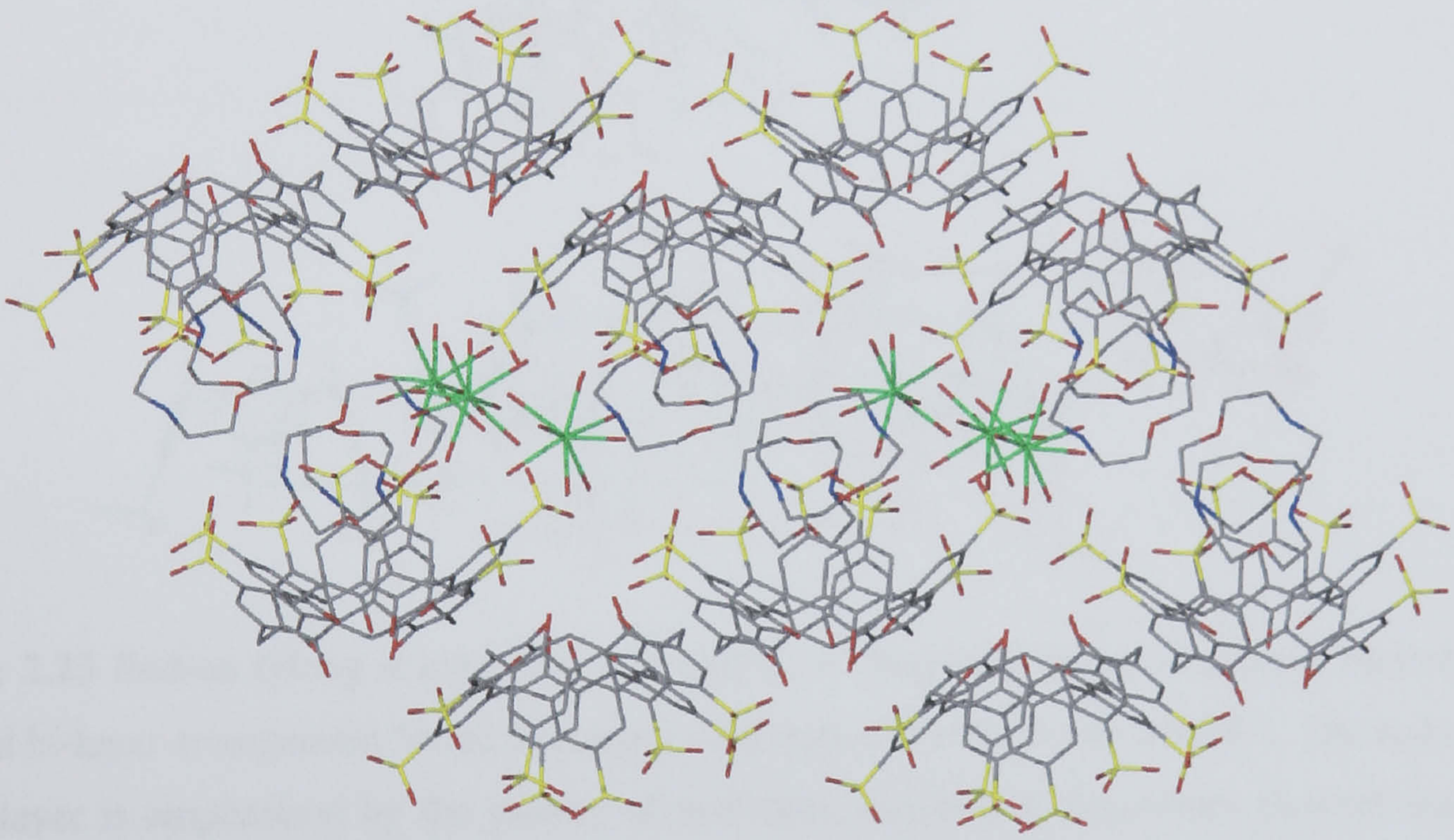

Figure 2.22 The extended bi-layer arrangement found in the crystal structure of complex **2.6**. The uneven nature of the bi-layer is indicated by the anti-planar arrangement of sulfonate groups in the hydrophilic regions of the extended structure.

There are a large number of calixarenes in the asymmetric unit involving a total of nine crystallographically unique interactions as three ArH···π, two methylene CH···π, and four π-stacking. The three ArH···π interactions have ArH···aromatic centroid distances of 2.085, 3.093 and

3.178 Å. The two methylene CH···π interactions have CH···aromatic centroid distances of 2.893 and 2.826 Å and the four π-stacking interactions have aromatic centroid···centroid distances ranging from 3.887 to 4.033 Å.

Further examination of the bi-layer arrangement reveals (as mentioned earlier) that the calixarenes pack in an uneven manner and show significant displacement from the typically observed co-planar bi-layer arrangement (Figures 2.22 and 2.23). This is particularly unusual and is likely to be a consequence of hydrogen bonding regimes associated with all or most of the hydrogen bonding components in the overall structure. Unfortunately, the quality of data prohibited determination of hydrogen positions but nevertheless the large number of molecules in the asymmetric unit also suggests that this is the case.

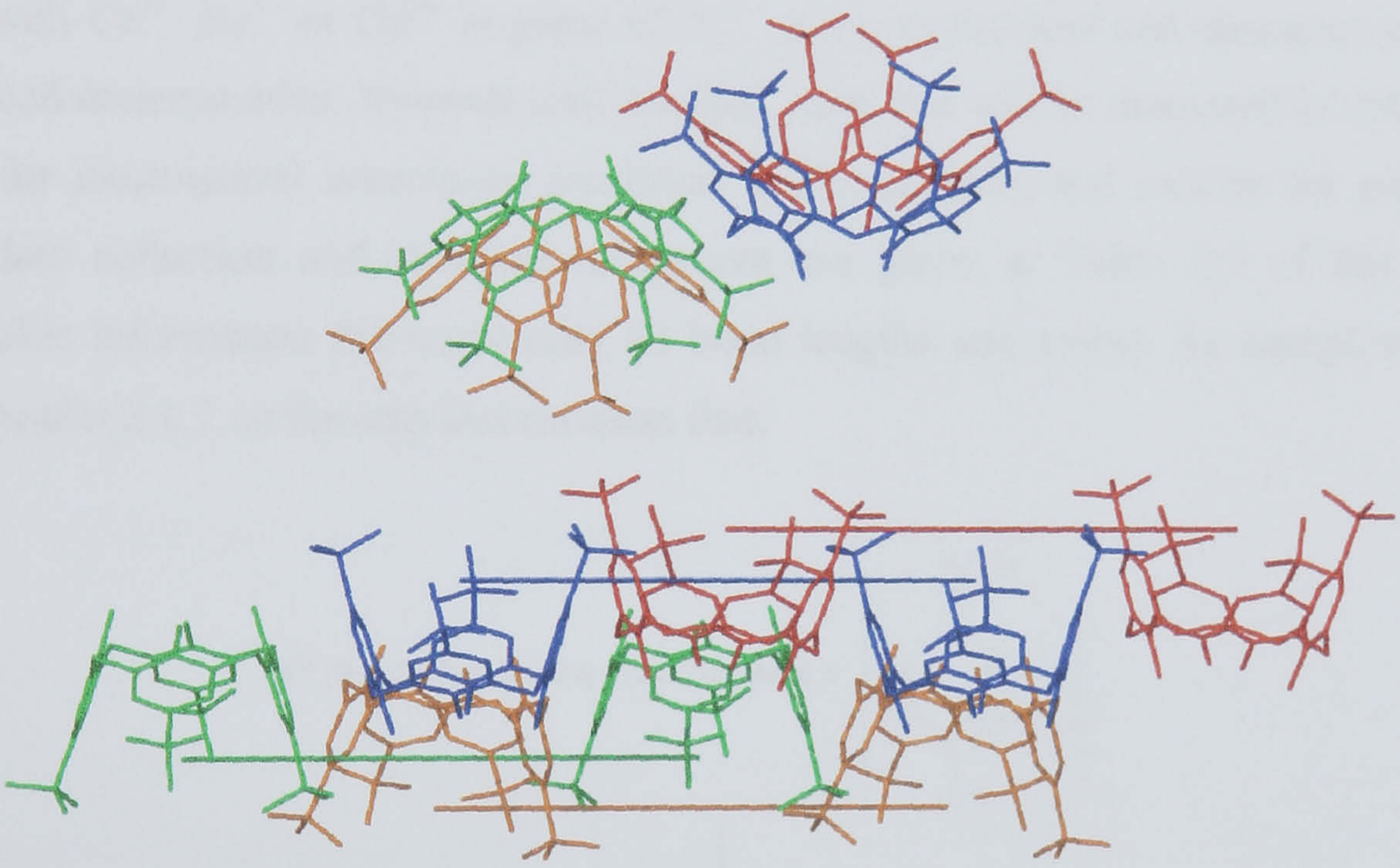

Figure 2.23 End-on (along *a* axis) and side (along *bc* diagonal) views of a cross section of the unusual bi-layer arrangement found in complex **2.6** (top and bottom respectively). The distortion of the bi-layer is emphasised by the joining of symmetry equivalent calixarenes through identically coloured lines and calixarene centroids.

Although it was anticipated that di-protonated diaza-12-crown-4 would form a molecular capsule with SO_3[4], we have defined a clear boundary at which sterics become the determining factor over electronics in the capsule formation process. As the host guest chemistry associated with lanthanide metals, SO_3[4] and disc-shaped cyclic (di)aza-functionalised guests was systematically investigated, [2.2.2]cryptand and 1,4-diazabicyclo[2.2.2]octane (DABCO) were investigated as potential guests within molecular capsules. Both molecules present the possibility of di-protonation and have more three dimensional character than the disc shaped guests employed above, and thus exploration into

this chemistry allows further investigation into guest size dependence or charge domination in molecular capsule formation.

2.1.7 Structure of the 2-D coordination polymer of molecular capsules [(2H[2.2.2]cryptand)⊂(*p*-sulfonatocalix[4]arene)$_2$(M(H$_2$O)$_4$)$_2$]·0.625H$_2$O, M = Nd, Ce, Sm, Eu, 2.7.

Crystals of the complex [(2H[2.2.2]cryptand)⊂(*p*-sulfonatocalix[4]arene)$_2$(Nd(H$_2$O)$_4$)$_2$]·0.625H$_2$O, **2.7**, grew overnight from an acidic aqueous solution containing a 5:1:3 mixture of SO$_3$H[4], [2.2.2]cryptand and neodymium(III) chloride respectively (Equation 2.7). The complex was characterised by IR spectroscopy and single crystal X-ray crystallography. Complex **2.7** crystallises in a tetragonal cell and the structure solution was performed in the space group *P*4/*nnc*. Isostructural complexes with Ce^{3+}, Eu^{3+} or Gd^{3+} in place of Nd^{3+} were synthesised and characterised by single crystal unit cell determination, however only the Nd^{3+} complex will be discussed in detail (unit cell parameters for isostructural complexes are listed in the experimental section for complex **2.7**). Details of data collection and structure refinement are given in Table 2.9 of this chapter. A crystallographic information file containing all bond lengths and angles for complex **2.7** can be found in appendix 2.1.7 on the attached compact disc.

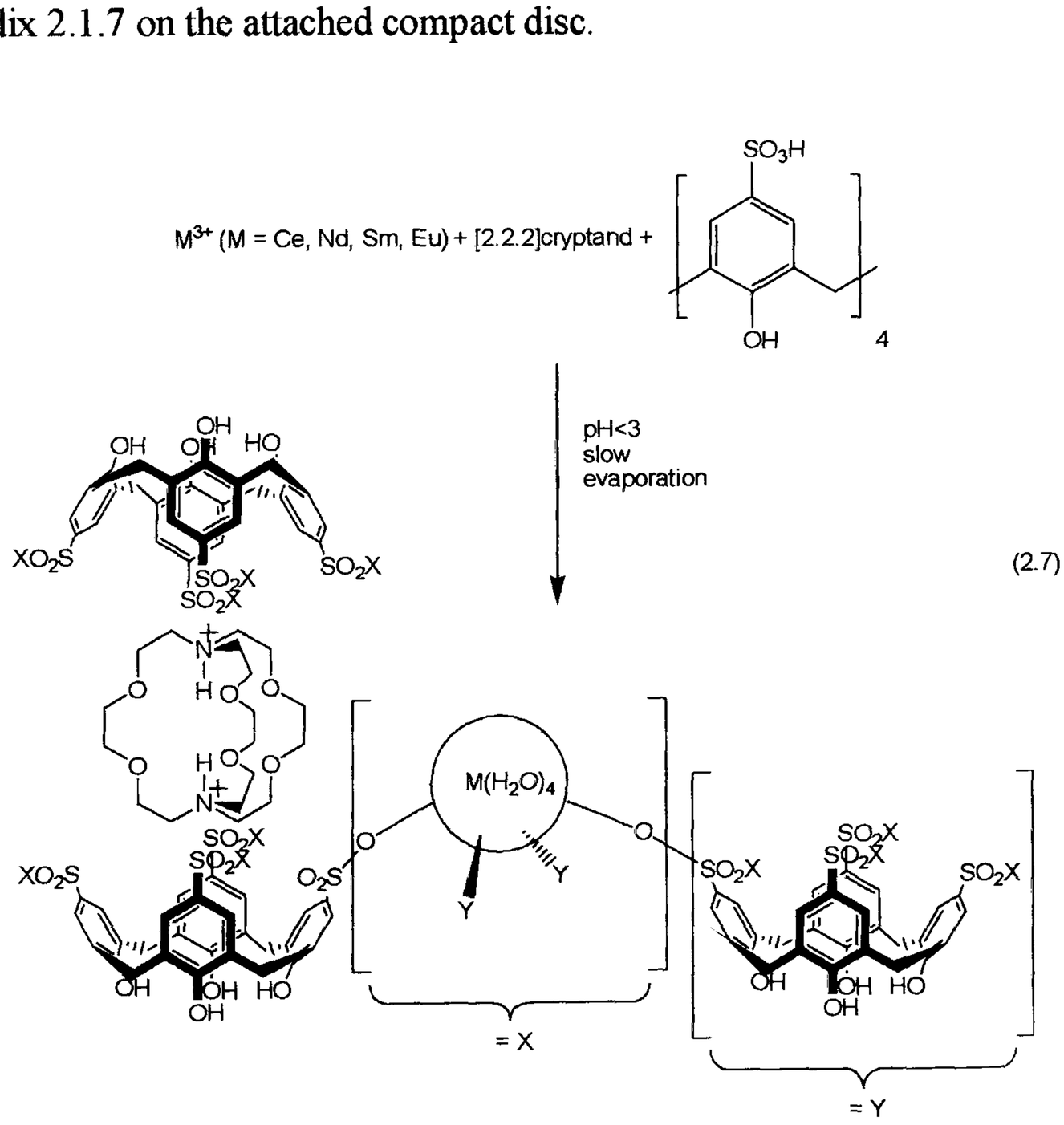

(2.7)

The asymmetric unit comprises one quarter of a SO_3[4] molecule, a section of a disordered [2.2.2]cryptand molecule (residing on a four fold rotation axis), one quarter of a neodymium atom (residing on a four fold rotation axis) with one aquo ligand, and a total of 0.625 water molecules that are distributed over two positions (Figure 2.24).

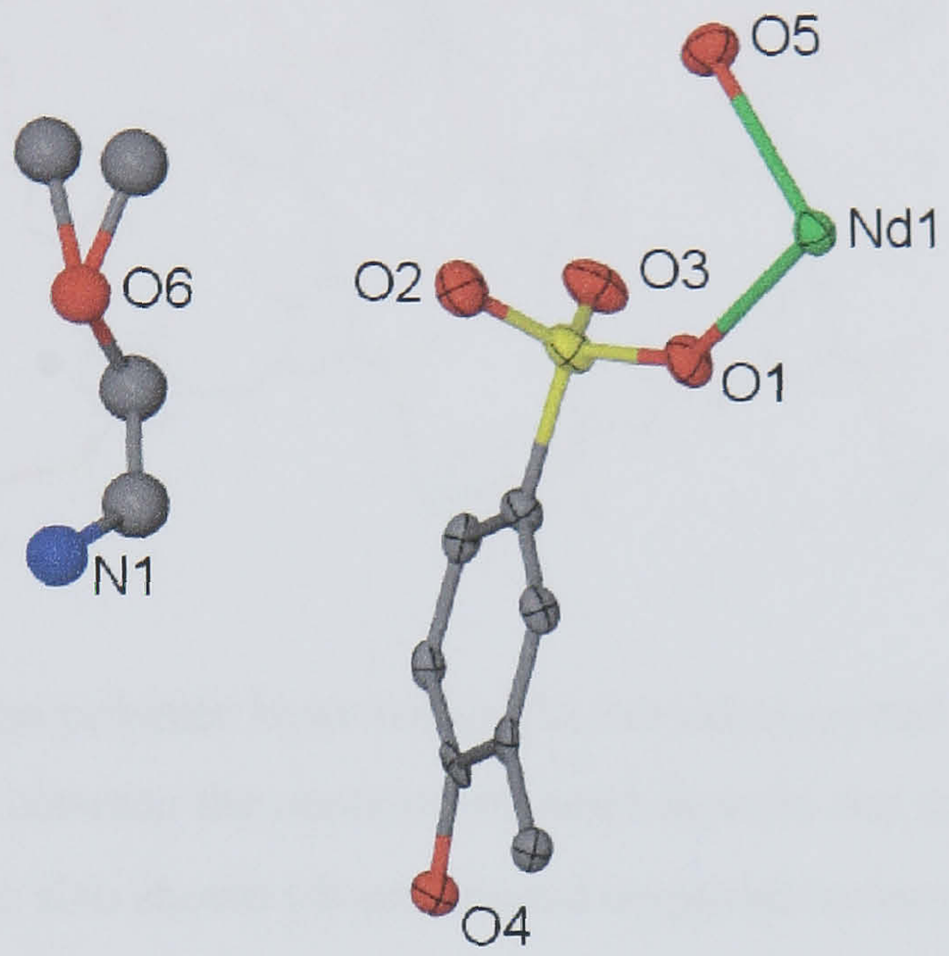

Figure 2.24 Part of the asymmetric unit in the crystal structure of complex **2.7**. The atoms are shown as ellipsoids at the 50% probability level except for the disordered cryptand atoms that are shown in ball and stick representation. Selected atoms have been labelled.

The metal centre in **2.7** resides on a four fold rotation axis and has square anti-prismatic geometry, bonding to four symmetry equivalent sulfonate oxygen atoms of four calixarene molecules, and four symmetry equivalent aquo ligands, Figures 2.25 and 2.26 (Nd(1)-O(1) and Nd(1)-O(5) bond lengths of 2.433(5) and 2.460(5) Å respectively). Upon symmetry expansion, each calixarene coordinates to four symmetry equivalent metal ions to generate a 2-D coordination polymer. Both the metal ions and calixarenes are four connecting centres within the polymer and the network topology is a (4,4) grid network of vertex sharing octahedra, similar to that shown in Figure 2.18 for complex **2.5**, despite having different lanthanide sulfonate coordination modes. All the calixarenes within the coordination polymer are arranged in a head-to-head fashion and are coplanar within each hydrophobic layer. The symmetry equivalent neodymium aquo ligands point into the hydrophilic layer but hydrogen bond to an oxygen atom (O(2)) of the nearest sulfonate groups within the coordination polymer layer (NdO(5)···O(2)S distance 2.764 Å, Figure 2.25).

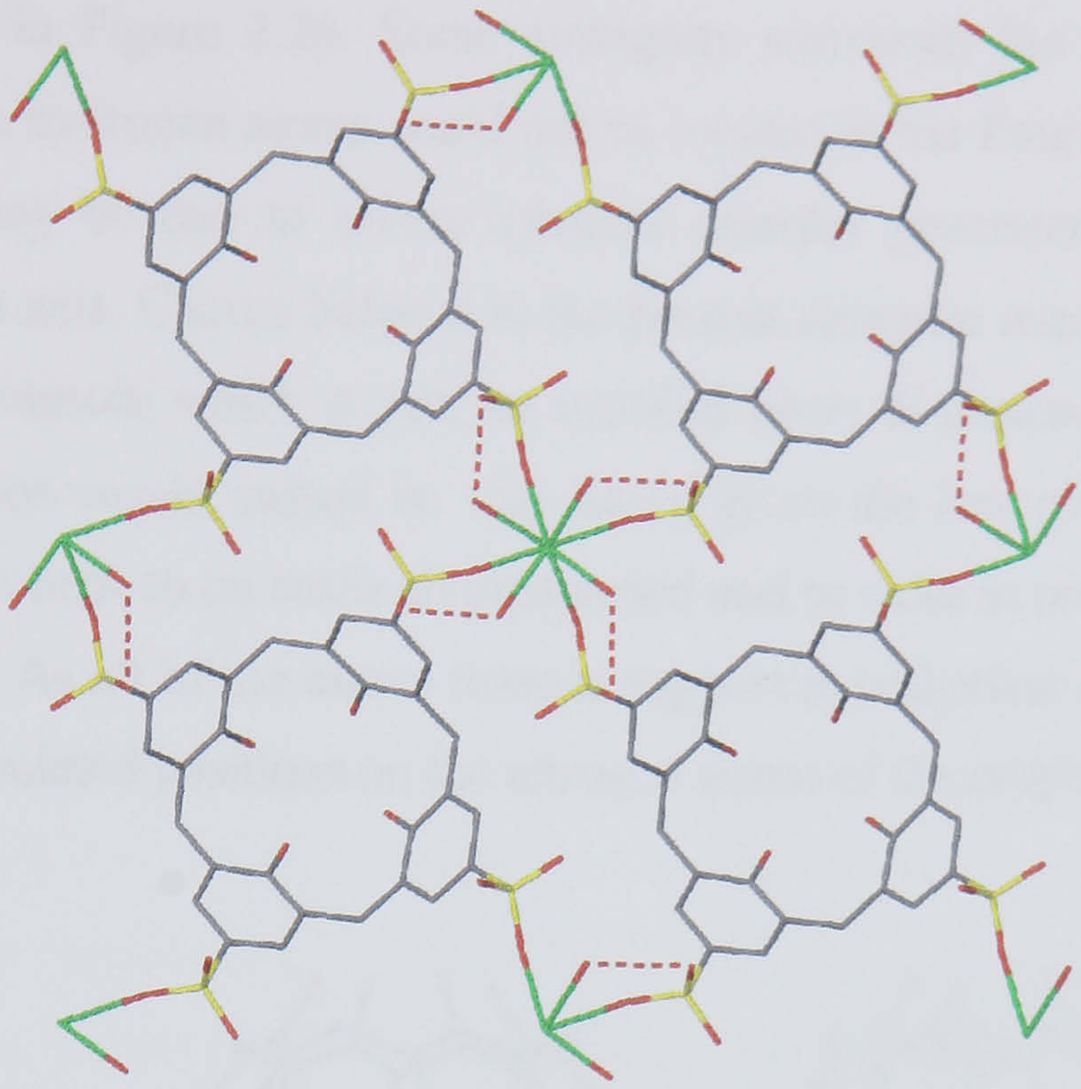

Figure 2.25 A 2-D coordination polymer layer within the extended crystal structure of complex **2.7**. Associated hydrogen bonding between the neodymium aquo ligands and nearest sulfonate groups of calixarenes within the layer are also shown (di-protonated cryptand molecules omitted for clarity).

The extended structure reveals the calixarenes to pack in the typical bi-layer arrangement as described in Chapter 1. As the structure is of high symmetry, there is only one crystallographically unique hydrophobic methylene CH···π interaction (CH···aromatic centroid distance of 2.725 Å). This is the only hydrophobic interaction within the bi-layer arrangement and this is unusual given the affinity of the calixarenes to π-stack with one another. A similar 2D coordination polymer, also of tetragonal symmetry, has been reported and involves SO_3[4] and early lanthanide metals, as described earlier in this chapter. That structure has a head-to-tail arrangement of calixarenes between hydrophobic layers, i.e. cavity facing base. The arrangement of hydrophobic layers in complex **2.7** differs in that cavities from adjacent layers face each other and, as this is the case, infinite layers of molecular capsules form with cryptand molecules residing in each capsule (Figure 2.26). It is therefore likely that the di-protonated cryptand demands this face-to-face arrangement of bi-layers, especially given the formation of the aforementioned anti-facially packed coordination polymer in the absence of the guest. The disordered water molecules in the extended structure reside in the hydrophilic regions generated by the sulfonate groups at the upper rims of the calixarenes as would be anticipated on the basis of hydrophilic interactions between them.

The nitrogen atoms of the di-protonated cryptand molecule reside on a four fold rotation axis. This is unfortunate given that cryptand is a bi-cyclic molecule and thus inherent disorder is emplaced on

the molecule as shown in Figure 2.26. Some ambiguity surrounds the protonation state of the cryptand molecule as the hydrogen atoms could not be located in the Fourier difference map of the X-ray structure. This may be due to severe inherent disorder generated by the bi-cyclic guest residing on a C_4 rotation axis. Charge balance in the present structure requires a cationic charge of 2+ for each molecular capsule which would be satisfied upon di-protonation of [2.2.2]cryptand. This degree of protonation would indeed be very likely given the low pH employed. In addition, [2.2.2]cryptand is known both to be easily di-protonated and to exist in an 'in' conformation when doubly protonated.[103, 104] As all of the above reasons support hypothetical di-protonation, hydrogen atoms were added at calculated positions on the nitrogen atoms of the cryptand.

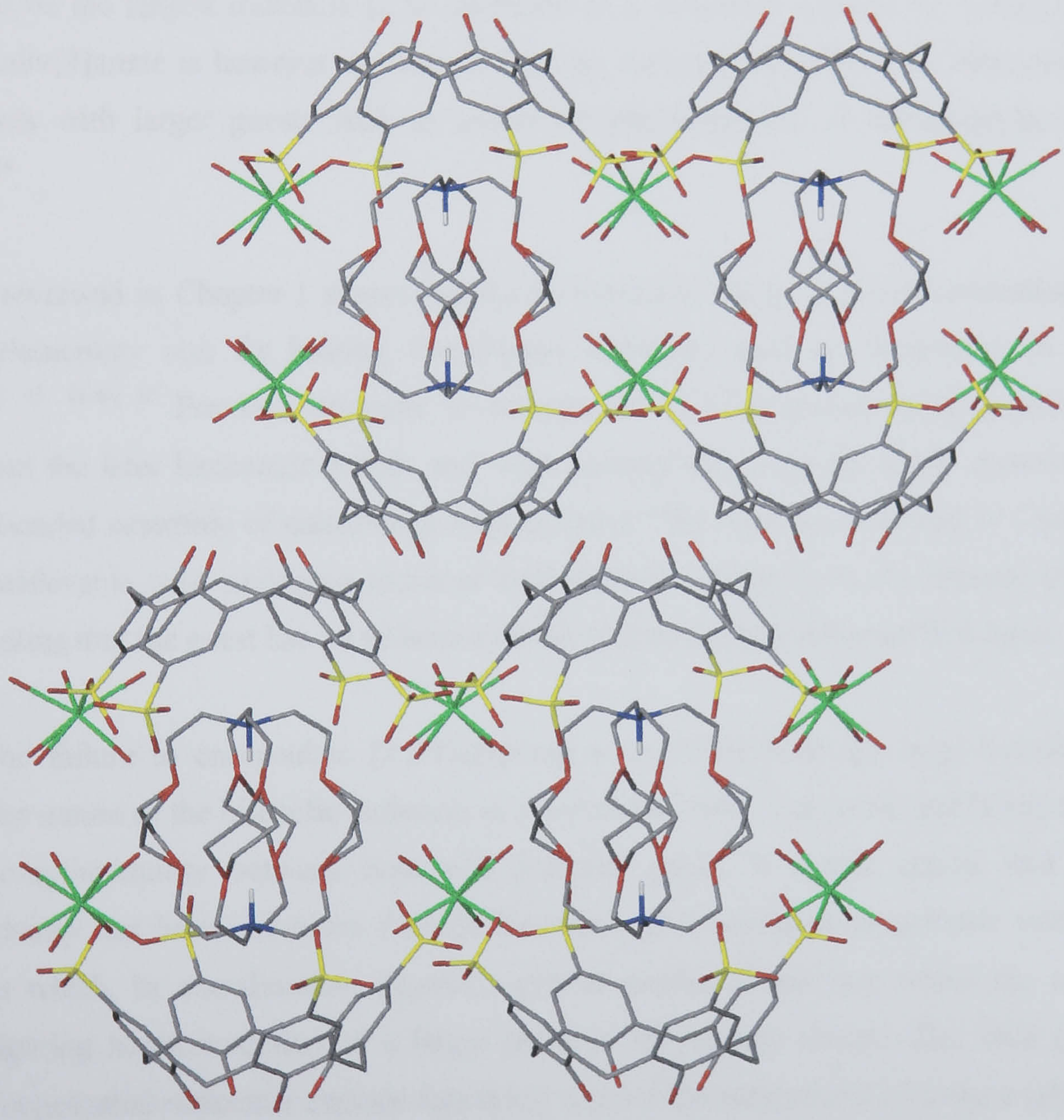

Figure 2.26 The extended bi-layer arrangement from the crystal structure of complex **2.7** showing the 2-D coordination polymers and the encapsulation of disordered di-protonated cryptand within the infinite array of molecular capsules.

One consequence of coordination polymer formation between SO_3[4] and lanthanide metals is that the calixarene splays equally in all directions, resulting in an increase in the dihedral angle between the aromatic rings and the basal plane of the four phenolic oxygens. The previously reported 2-D coordination polymer, formed in the absence of guest molecules other than water, has a dihedral angle of 125.6°. Complex **2.7** has a dihedral angle of 130.1°, one that is significantly greater than 125.6°, thus indicating the need to present a larger cavity for globular-like guest inclusion.[102] This is consistent with the accommodation of the di-protonated cryptand whilst retaining lanthanide-calixarene coordination. When disc-shaped guests such as 18-crown-6 are incorporated, pinching of the calixarene to complement the curvature of the guest molecule is prevalent with typical dihedral angles of 108.8 and 135.1°.[34] A Cambridge Structural Database search reveals di-protonated cryptand to be the largest molecule to be shrouded in a molecular capsule by SO_3[4] to date. *p*-Sulfonatocalix[4]arene is however capable of forming inclusion complexes as alternative bi-layer arrangements with larger guests such as nickel tris-phenanthroline or tetraphenylphosphonium cations.[63, 64]

Literature reviewed in Chapter 1 shows that the hydrophobic cavity of *p*-sulfonatocalix[4]arene is of a complementary size for hosting disc-shaped molecules such as 18-crown-6 in molecular capsules.[34, 35, 44-46, 50] Previous attempts to encapsulate [2.2.2]cryptand using *p*-sulfonatocalix-[4]arene and the later lanthanide metals and were unsuccessful. Instead, single crystals of a 2-D hydrogen-bonded assembly of calixarenes were isolated. This result is described in Chapter 3 and was also achievable with analogous ratios of lanthanide to calixarene in the absence of cryptand, thus suggesting that the guest has no influence on the supramolecular structure formation.

Initially, the failure to encapsulate [2.2.2]cryptand was attributed to the large overall size and globular like nature of the bi-cyclic molecule in comparison with 18-crown-6 and hence there was a lack of complimentarity between host and potential guest. It would appear that this anti-complimentarity has been overcome through formation of a coordination polymer with the early lanthanides which, by coordination, impose a greater degree of splaying within the calixarenes, thereby allowing accommodation of a larger guest of appropriate charge. The final guest to be employed in potential molecular capsule formation was 1,4-diazabicyclo[2.2.2]octane (DABCO). In relation to the series of results reported within this chapter, a molecular capsule incorporating di-protonated DABCO was anticipated. Surprisingly, a molecular capsule was not formed but an alternative, unusual, and interesting coordination polymer resulted and that shows mono-protonated DABCO to reside in the cavities of SO_3[4] molecules within hydrophobic coordination polymer layers.

2.1.8 Structure of the 2-D coordination polymer [(1,4-diazabicyclo[2.2.2]octane + H^+)⊂[(*p*-sulfonatocalix[4]arene)$^{4-}$($Nd(H_2O)_5)^{3+}$]]·$4H_2O$, 2.8.

Crystals of the complex [(1,4-diazabicyclo[2.2.2]octane + H^+)⊂[(*p*-sulfonatocalix[4]arene)$^{4-}$ ($Nd(H_2O)_5)^{3+}$]]·$4H_2O$, **2.8**, grew upon slow evaporation of an aqueous solution containing ~ a 1:1:11 mixture of SO_3H[4], DABCO and excess neodymium(III) chloride (Equation 2.8). The complex was characterised by single crystal X-ray crystallography. Complex **2.8** crystallises in a monoclinic cell and the structural solution was performed in the space group $P2_1/n$. Details of data collection and structure refinement are given in Table 2.9 in this chapter. A crystallographic information file containing all bond lengths and angles for complex **2.8** can be found in appendix 2.1.8on the attached compact disc. The asymmetric unit comprises one penta-aqua neodymium(III) cation tethered to a SO_3[4] molecule in addition to one mono-protonated DABCO and four waters of crystallisation (Figure 2.27).

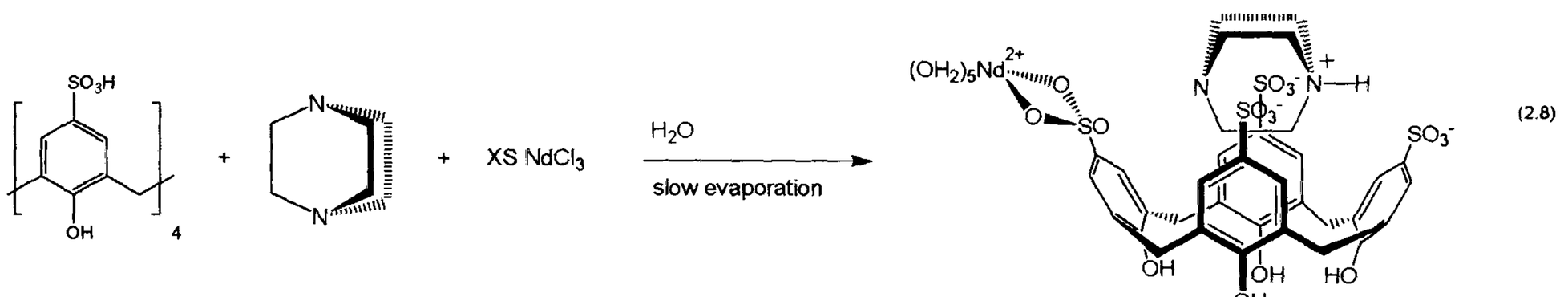

The most noticeable feature in complex **2.8** is that the compact nature of the guest molecule has markedly changed the resulting supramolecular architecture in addition to being singly, rather than doubly charged. As can be seen in Figures 2.27 – 2.30, the singly charged guest resides deep in the calixarene cavity, displays CH···π interactions with the aromatic rings of the calixarenes, and barely protrudes into the hydrophilic layer (C(33)H and C(34)H···aromatic centroid distances vary from 2.559 to 2.777Å). In addition to this, there are several interesting and unusual coordination and host-guest interactions observed in complex **2.8**.

Each neodymium centre has tri-capped trigonal prismatic geometry and possesses five aquo ligands that partake in a hydrogen bonding networks within the bi-layer assembly, Figure 2.29. Selected bond lengths relating to the coordination sphere of the neodymium centre are listed in Table 2.5. Two of the aquo ligands point down towards the base of a calixarene within the hydrophobic coordination polymer layer and the remaining three aquo ligands point upwards into the adjacent hydrophilic layer.

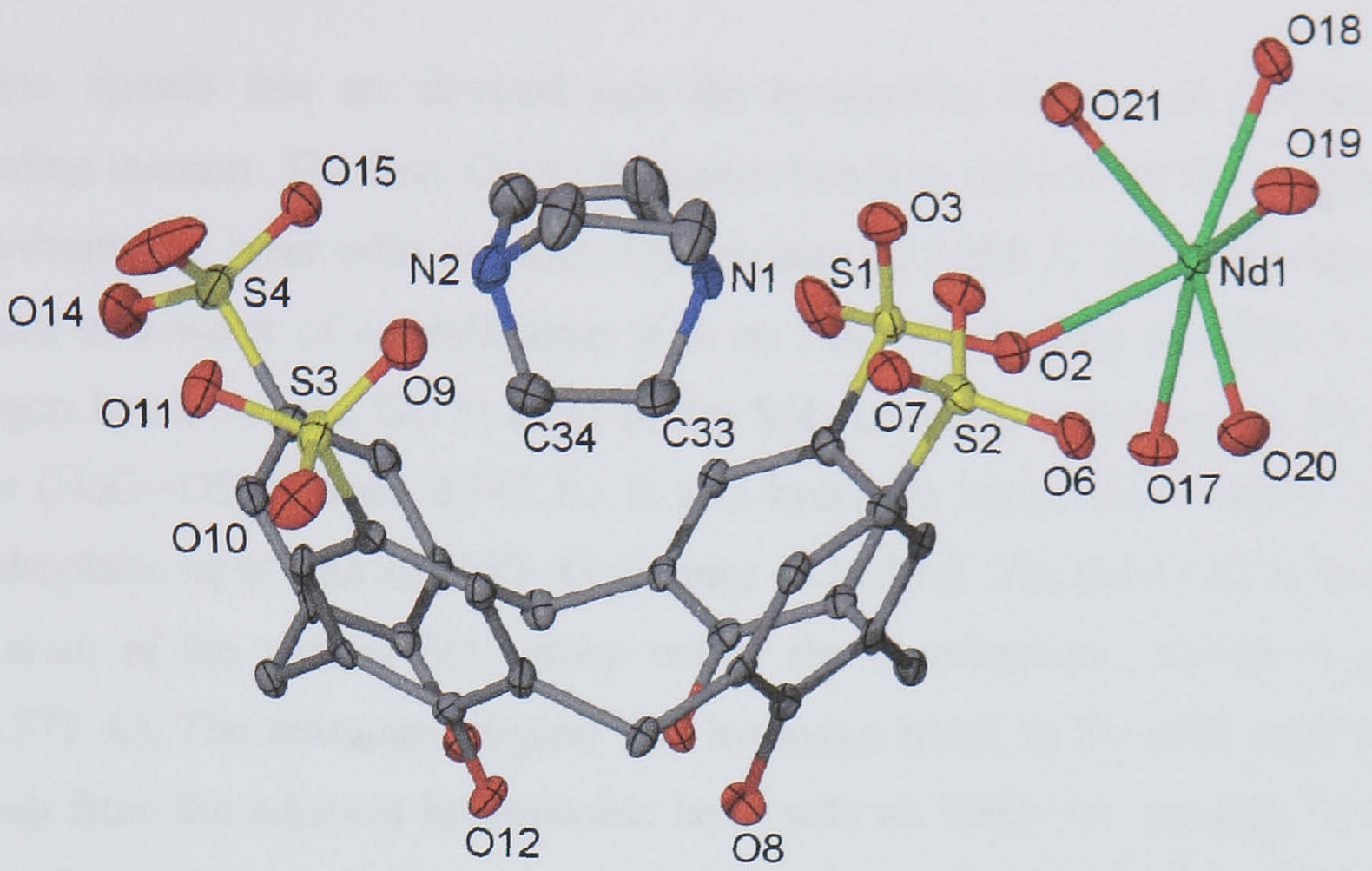

Figure 2.27 Part of the asymmetric unit from the crystal structure of complex **2.8**, ellipsoids at the 50% probability level. Selected atoms have been labelled.

Of the two aquo ligands that are directed into the hydrophobic layer, O(20) hydrogen bonds to two nearest sulfonate groups with NdO(20)···O(14)S and NdO(20)···O(10)S distances 2.797 and 2.881 Å respectively. The second aquo ligand, O(17), hydrogen bonds to two of the calixarene 'base' hydroxyl groups located directly below the neodymium centre with NdO(17)···O(12) and NdO(17)···O(8) distances of 2.707 and 2.782 Å respectively, Figure 2.30.

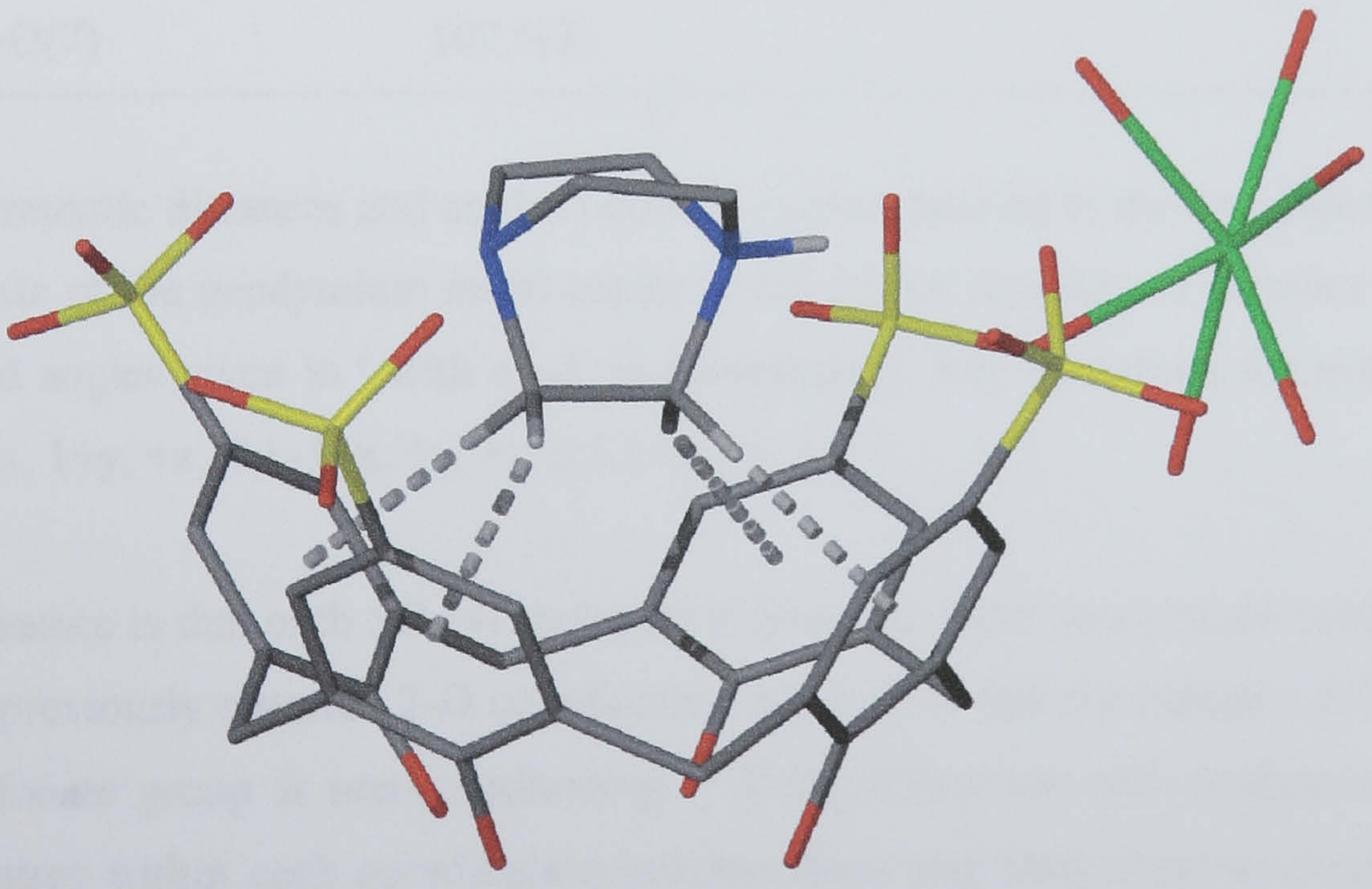

Figure 2.28 Part of the asymmetric unit in the crystal structure of complex **2.8** showing the mono-protonation of the DABCO molecule and the CH···π interactions from one DABCO ethylene 'arm' to the aromatic rings of the calixarene.

The three aquo ligands that are directed into the hydrophilic layer each partake in different hydrogen bonding regimes. The first, O(18), hydrogen bonds to O(3) of the S(1) sulfonate group in the nearest hydrophobic layer with an NdO···OS distance of 2.958 Å. The same aquo ligand also hydrogen bonds to a water of crystallisation with an NdO···O distance of 2.720 Å. The second, O(19), hydrogen bonds to the O(15) atom of the S(4) sulfonate group within the coordination polymer layer (NdO···OS distance 2.747 Å). It also hydrogen bonds to a water of crystallisation within the hydrophilic layer with an NdO···O distance of 2.636 Å. The third, O(21), hydrogen bonds to the O(3) atom of the nearest S(1) group within the coordination polymer layer (NdO···OS distance of 2.772 Å). The same aquo ligand also hydrogen bonds to the O(9) atom from the S(3) sulfonate group from the adjacent hydrophobic layer with an NdO···OS distance of 2.702 Å. The many hydrogen bonds between adjacent hydrophobic layers results in a second example of a 'tight' bi-layer arrangement similar to that for compound **2.2**. The result is a well ordered supramolecular coordination and hydrogen bonded polymer.

Nd(1)-O(2)	2.508(4)	Nd(1)-O(20)	2.503(5)
Nd(1)-O(17)	2.473(4)	Nd(1)-O(6)$^{(b)}$	2.780(5)
Nd(1)-O(18)	2.511(5)	Nd(1)-O(7)$^{(b)}$	2.496(5)
Nd(1)-O(19)	2.417(5)	Nd(1)-O(11)$^{(a)}$	2.444(4)
S(2)-O(6)-Nd(1)$^{(c)}$	94.0(2)	S(2)-O(7)-Nd(1)$^{(c)}$	105.3(2)
O(6)-S(2)-O(7)	107.5(3)		

Table 2.6 Interatomic distances and angles between vectors relating to the coordination sphere and sulfonate chelate of the neodymium metal centre in the crystal structure of complex **2.8** (distances given in Å and angles given in ° with e.s.d. in parentheses). Key operations for symmetry related atoms: *(a)* -1+x, 1+y, +z, *(b)* -1+x, +y, +z, *(c)* 1+x, +y, +z.

One unusual feature is that each SO_3[4] molecule is bound to three neodymium centres rather than four as in the previously reported 2-D coordination polymer or that for complex **2.7**, and thus one calixarene sulfonate group is non-coordinating.[102] Both calixarenes and neodymium ions are 3-connecting centres within each coordination polymer layer and these form a distorted brick-wall motif as shown in Figure 2.31. The calixarene is bound to the three neodymium centres through two mono-dentate sulfonate groups (O(2) of the S(1) sulfonate group and O(11) of the S(3) sulfonate group), and to the third sulfonate group through a four membered chelate ring system (O(6) and O(7) of the S(2) sulfonate group). Bond lengths relating to the neodymium coordination sphere and

angles relating to the neodymium sulfonate chelate ring in complex **2.8** are listed in Table 2.6. Complex **2.8**, is only the second example of lanthanide sulfonate chelation with any *p*-sulfonatocalixarene, although chelation of an aryl sulfonate to lanthanum and terbium has been reported.[102, 105, 106] The remaining non-coordinating sulfonate group participates in hydrogen bonding with a neodymium aquo ligand and two waters of crystallisation as described above. As for all the complexes described in this chapter, the extended structure reveals the calixarenes to pack in the typical bi-layer arrangement (Figure 2.30). The primary hydrophobic interactions between calixarenes in **2.8** are CH···π as described for other compounds in this chapter with CH···aromatic centroid distances varying from 2.648 to 2.921 Å.

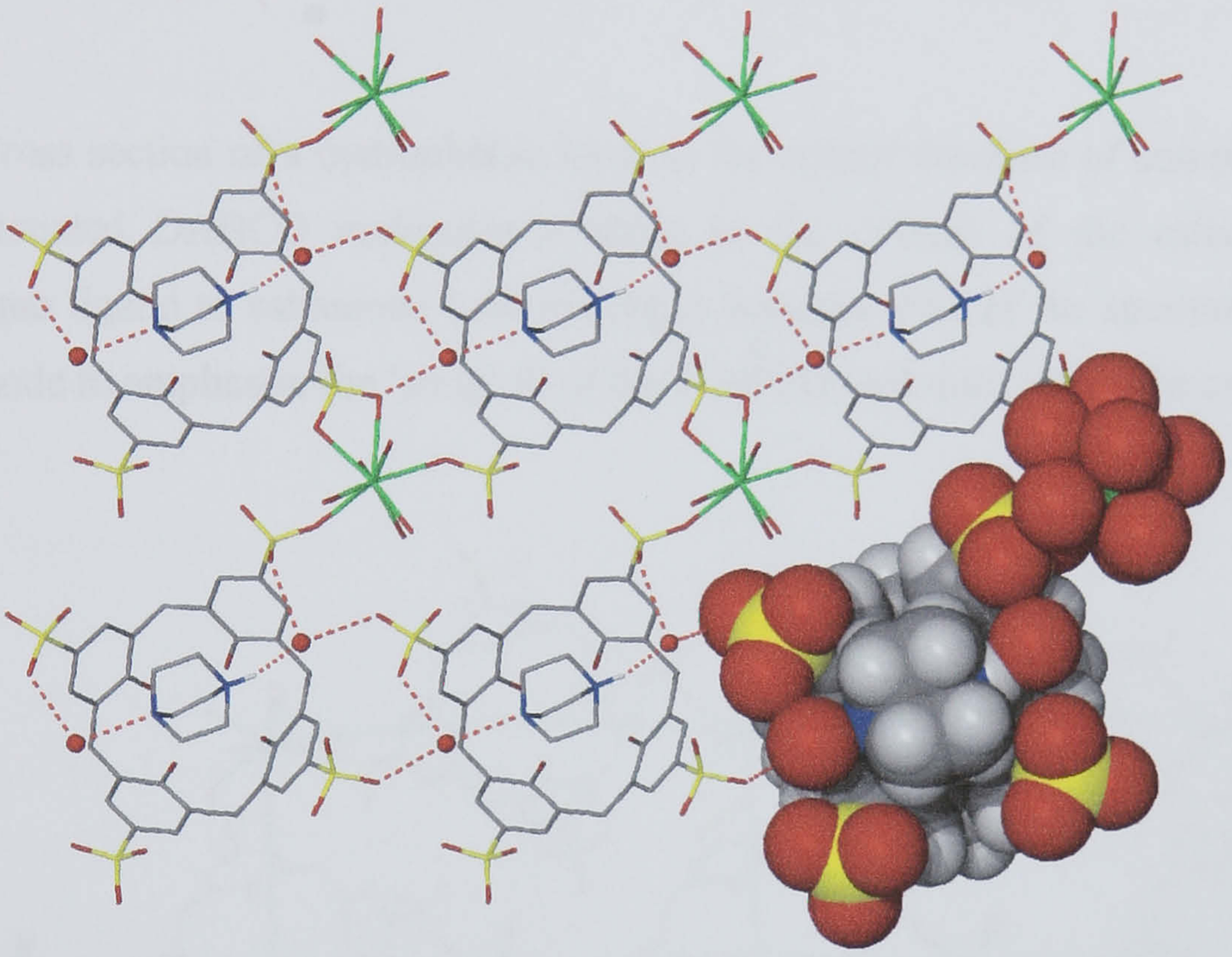

Figure 2.29 Partial space filling diagram of the 2D coordination polymer in complex **2.8**, showing the included mono-protonated DABCO and two waters of crystallisation.

Electron density located near N(1) of the DABCO molecule was assigned as hydrogen and fixed in position. This is consistent with charge balance of the complex and protonated nitrogen hydrogen bonds to the nearest water of crystallisation, N(1)···O distance of 2.717 Å, Figure 2.29 (corresponding NH···O distance of 1.825 Å). The same water molecule also hydrogen bonds to sulfonate groups from both the calixarene hosting the DABCO molecule and the nearest adjacent sulfonate group within the coordination polymer layer, O···OS distances of 2.832 and 3.087 Å, respectively. A second water of crystallisation, located around the rim of the calixarenes, hydrogen bonds to the neutral nitrogen of the DABCO with an O···N(2) distance of 2.636 Å. The water

molecule is also positioned such that it is consistent with two hydrogen bonds to two nearest neighbouring sulfonate groups, O···OS distances 2.771 and 2.773 Å (Figure 2.29).

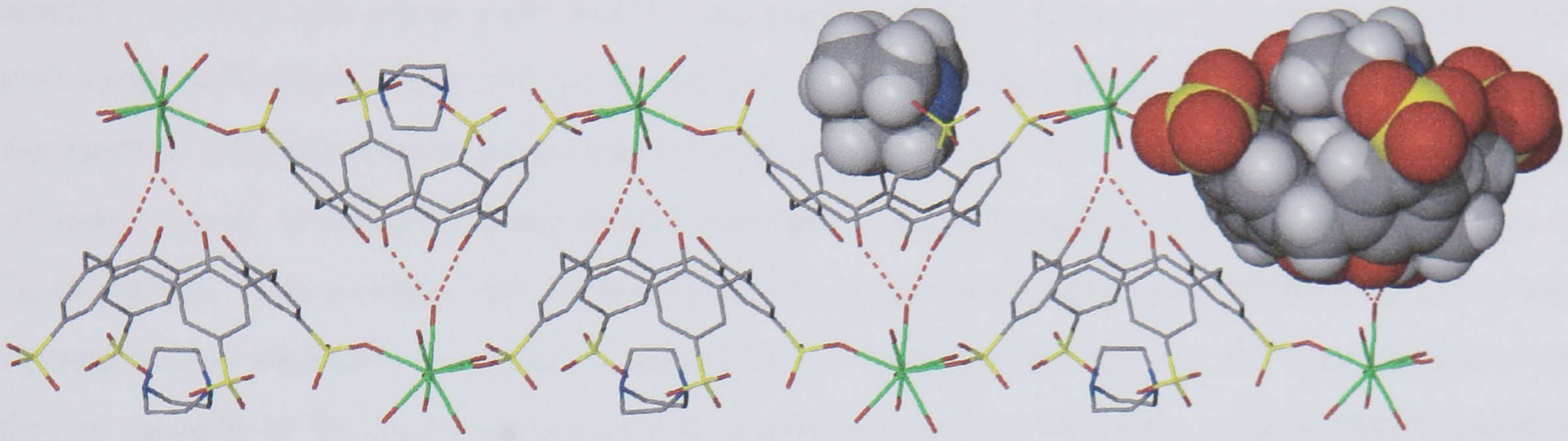

Figure 2.30 Cross section of a hydrophobic layer in the crystal structure of complex **2.8** showing the mono-protonated DABCO molecules residing in the cavities of the calixarenes and the neodymium aquo ligand to calixarene base hydrogen bonding. Part of the structure is rendered in space filling mode to emphasise the 'snug' fit of the DABCO molecule within the calixarene cavity.

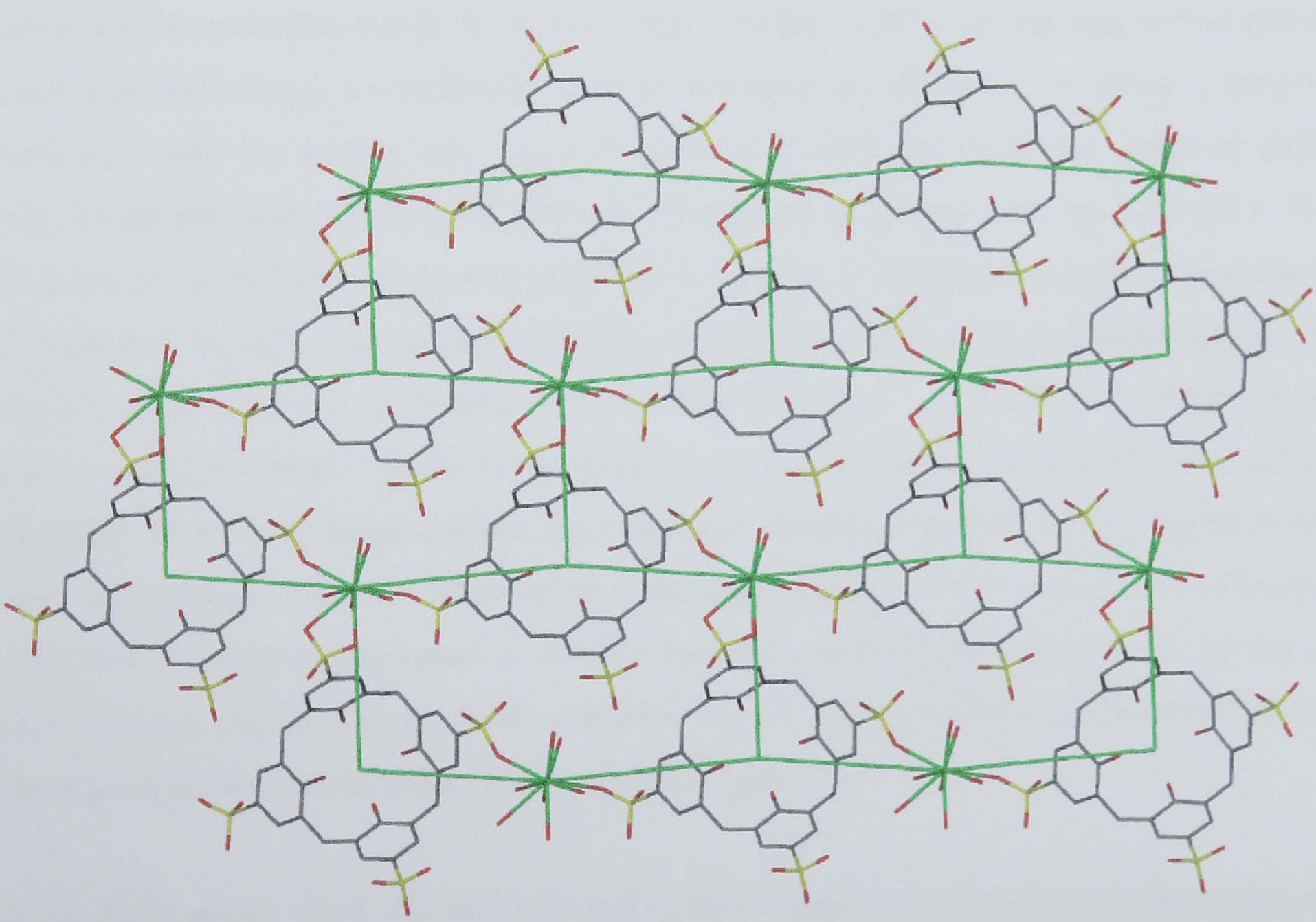

Figure 2.31 Network topology diagram from the crystal structure of complex **2.8** showing the distorted brick-wall motif formed by the 3-connecting calixarenes and neodymium ions.

As a comparison to [2.2.2]cryptand, the dihedral angles of the calixarenes in **2.8** are found to be 114.75 and 121.79°. This shows considerably less splaying relative to the inclusion of cryptand (130.1°) as would be expected given the difference in size between the two guests. As molecular capsule formation was not evident with di-protonated DABCO, it is clear that the molecule is not protruding sufficiently from the cavity to bind a second calixarene and forms an alternative coordination polymer based around mono-protonated DABCO. The guest fits 'snugly' within the calixarene cavity in a well ordered fashion through CH···π interactions with the aromatic rings of the calixarene. This structure stresses that guest size is indeed crucial in pre-determining the overall supramolecular structure. In addition, compound **2.7** demonstrates that like the host, the guest can also be versatile in the degree of protonation depending on the molar ratio of calixarene to guest in the presence of lanthanide metals.

2.2 Conclusion.

The formation of molecular capsules incorporating 18-crown-6 or sodium/18-crown-6 guests as 'Russian dolls' is well documented.[34, 35, 44-46, 50] Similar chemistry with disc-shaped aza-functionalised crown ethers has been explored here and has established that diaza-18-crown-6 is of good size and ideal charge for molecular capsule formation at a low pH (~ 3) when in the presence of lanthanide ions. At similar pH, 1-aza-18-crown-6 is excluded from the potential molecular capsule and an alternative SO_3[4]/Nd bi-layer arrangement is formed. At very low pH (~ 0.5), 1-aza-18-crown-6 is included as a mono-protonated guest in a molecular capsule, a process that is likely facilitated by sulfonate group protonation to provide overall capsule charge balance. Diaza-15-crown-5 also formed a molecular capsule with SO_3[4] at a pH of ~3 however a capsule containing 1-aza-15-crown-5 could not be isolated, even at lower pH. Despite this, the calixarenes do assemble with neodymium cations in a bi-layer coordination polymer of sealed molecular capsules, although all albeit devoid of crown ether guests. When diaza-12-crown-4 is incorporated, an alternative bi-layer arrangement is formed and this confirms that despite the presence of a potential 2+ inner capsule charge, steric considerations become dominant in the molecular capsule formation process at a certain point (summarised in Figure 2.32).

When bi-cyclic, more three dimensional and globular guests are employed, molecular capsule formation is once again dependent on guest molecule size. Cryptand, in the di-protonated form, is encapsulated by two SO_3[4] molecules as part of a 2-D coordination polymer with early lanthanide metals. The significantly smaller DABCO resides deep within the calixarene cavity and is insufficient in size to bind two SO_3[4] molecules in a molecular capsule. This results in the

formation of an unusual 2-D coordination polymer between neodymium cations and SO_3[4] molecules with mono-protonated DABCO molecules in each calixarene cavity.

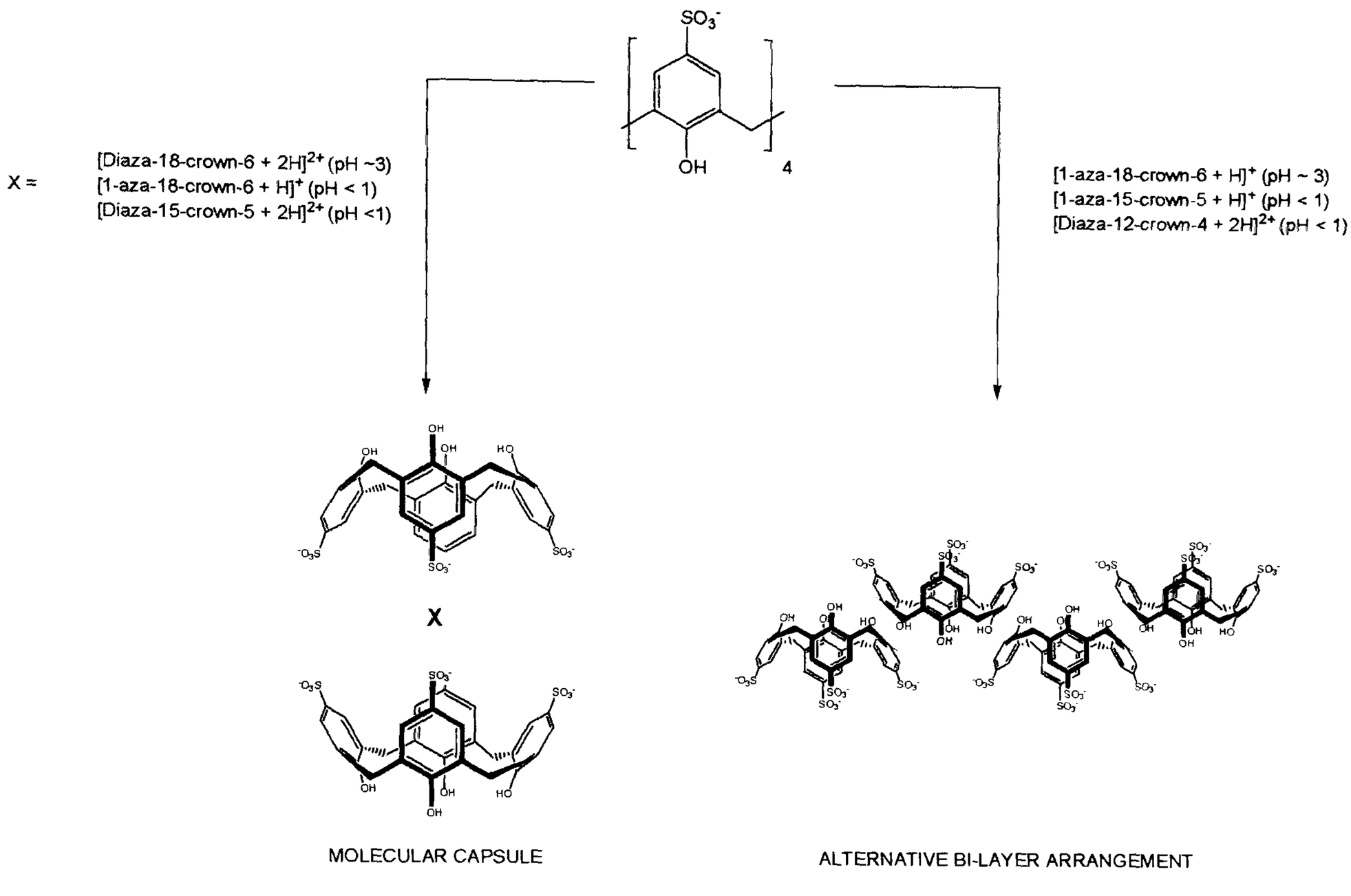

Figure 2.32 Schematic summation of the formation of molecular capsules or alternative bi-layer arrangements depending on both the aza-functionalised crown ether guest and reaction pH employed.

Clearly, *p*-sulfonatocalix[4]arene is a highly versatile material, capable of accommodating many different guest molecules in the hydrophobic cavity. When disc-shaped guest molecules of appropriate size are employed, the calixarene pinches and splays in an accommodative manner. In contrast, when more globular guests are employed, the calixarene splays equally in all directions to the required magnitude in order to accommodate the molecules.

It would appear, from the results reported in this chapter, that the formation of molecular capsules with the larger (di)aza-functionalised cyclic guests is entirely pH dependent except for 1-aza-15-crown-5. The omission of this crown ether may relate to the size of the macrocycle being unsuitable for molecular capsule or other structural formation with lanthanide metals. Indeed, this exclusion is consistent with many other attempts to form solid state complexes with various *p*-

sulfonatocalix[*n*]arenes and lanthanide metals. This hypothesis is corroborated by the formation of an alternative bi-layer arrangement with diaza-12-crown-4, neodymium cations and SO_3[4].

The results presented also suggest that molecular capsule formation with more globular guests appears to be more dependent on the size of the molecule rather than the state of protonation (pH dependence). Notably, however, both globular guests caused the calixarenes to splay in a C_4 symmetric fashion, forming supramolecular structures as 2-D coordination polymers. These results therefore suggest that increased calixarene splaying facilitates the formation of coordination polymers within bi-layers as sulfonate groups are more proximate to one another within each hydrophobic layer. When the calixarene is pinched in the C_2 symmetric manner, the sulfonate group separation is typically large enough to prevent lanthanide sulfonate bonding as part of coordination polymers. For this hypothesis to be proved, a systematic investigation of many more globular guests of various size and charge would be required. The results of that study could be compared with those relating to the calixarene in the pinched conformation to give a clearer overview and permit a more definite conclusion.

2.3 Experimental and general considerations.

p-Sulfonic acid calix[4]arene was synthesised by literature methods and purity was checked via ^{1}H NMR spectroscopy.[8] All guest molecules except 1-aza-18-crown-6 and 1-aza-15-crown-5 that were synthesised by literature methods.[107] All lanthanide metal salts were purchased from Aldrich and used as supplied without further purification. X-ray data for complexes **2.1** – **2.8** were collected at 150(2) K on an Enraf-Nonius KappaCCD diffractometer with Mo-Kα radiation. Data were corrected for Lorentz and polarisation effects and absorption corrections were applied using multi-scan techniques. The structures of complexes **2.1** – **2.8** were solved by direct methods using SHELXS-97 and refined with full-matrix least squares on F^2 using SHELXL-97. Hydrogen atoms were placed at geometrically calculated positions in all complexes. Microanalyses were not performed on crystals of complexes **2.1** – **2.8** as all showed visual degradation upon removal from the mother liquor.

Infrared spectra, where recorded throughout the thesis, were run either as a KBr disc or as a solid phase on a MIDAC FT-IR or Perkin-Elmer Spectrum One spectrometer respectively. In general, analysis of the IR spectra was performed using the typical stretching frequencies of the *p*-sulfonato-calix[4,5,6,8]arenes as an indication of complex formation (Figure 2.33).

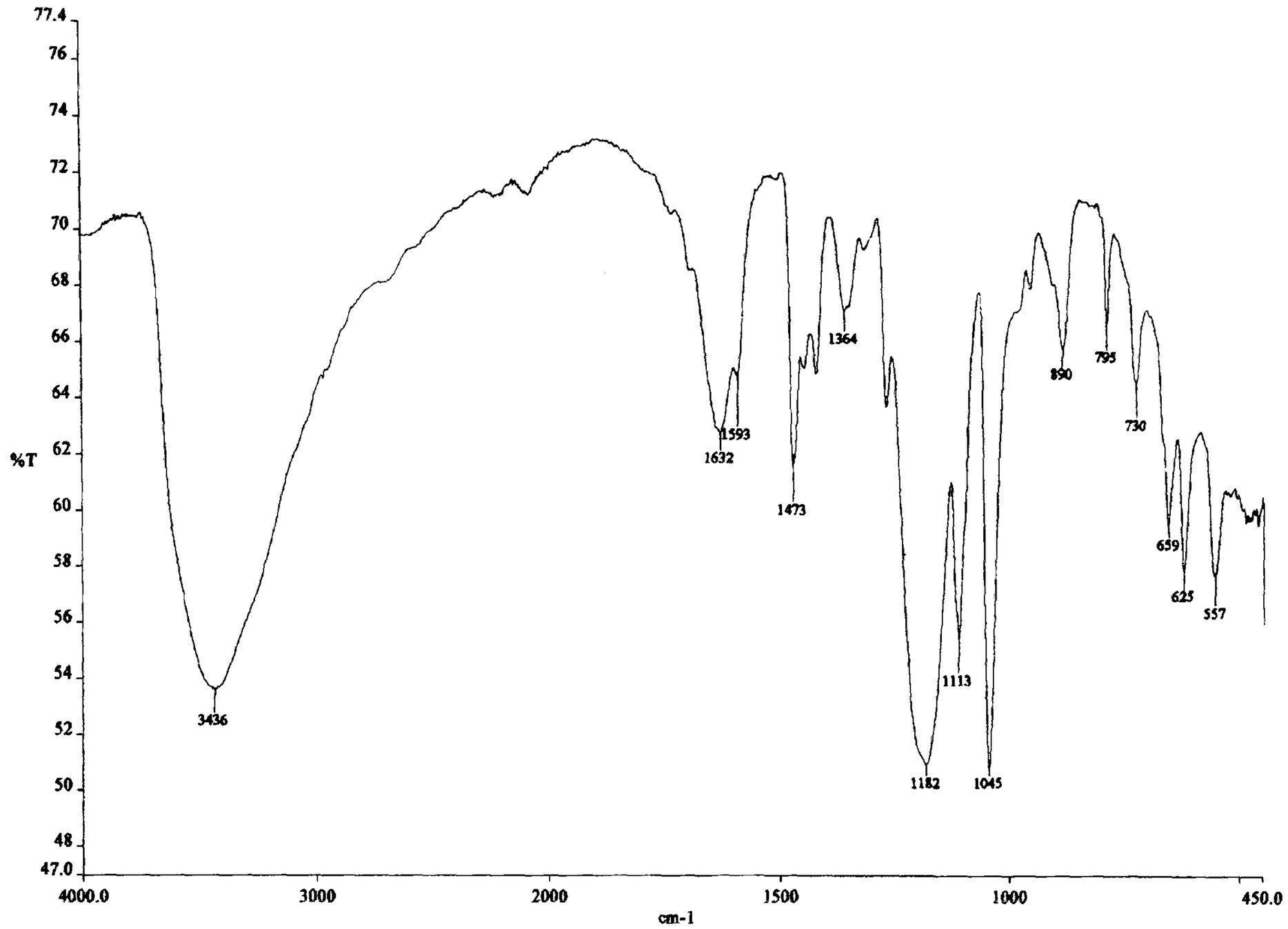

Figure 2.33 Infra-red spectrum of *p*-sulfonatocalix[4]arene showing typical stretching frequencies for sulfonate groups in the region of 1000 – 1500 $\bar{\nu}$ for comparison with calixarenes in complexes included in this thesis.

In general, reaction stoichiometries were decided through the use of combinatorial matrices within which reactant ratios were varied. The control of pH was also observed to be important in some systems and low pH was in some cases achieved *via* the use of excess of the desired calixarene sulfonic acid. In the results presented in Chapter 6, the control of pH was achieved through addition of 1M HCl as it was not possible to isolate the sulfonic acid of *p*-sulfonatocalix[5]arene in powder form for manipulation as it is an extremely hygroscopic solid. In order to establish sample homogeneity, the unit cell parameters of several crystals selected from each crystallisation batch were measured. Notably, no crystallisation batches showed obvious evidence of more than one type of crystal morphology and in all cases, unit cell measurements were indicative of those crystals for which data was collected. X-ray powder diffraction measurements were recorded for some samples but in all cases the pattern was indicative of amorphous material, likely resulting from solvent loss upon removing the crystals from the mother liquor.

2.3.1 Synthesis of the molecular capsule [(4,13-diaza-18-crown-6 + $2H^+$)⊂[$(H_2O)_2$[$M(H_2O)_9$]$_2$[*p*-sulfonatocalix[4]arene]$_2$]]·$9.5H_2O$ (M^{3+} = Ce, Nd, Eu, Gd), 2.1.

Neodymium(III) chloride (34 mg, >10 molar eq.), *p*-sulfonicacid calix[4]arene (10 mg, 13.4 μmol) and 1,4-diaza-18-crown-6 (8 mg, 30 μmol) were dissolved in distilled water (1 cm^3). On standing, large crystals of suitable quality for X-ray diffraction studies formed over 30 minutes. Yield 12 mg, 66%. IR(KBr disc, ν cm^{-1}): 3350s, 2872s, 1632m, 1595m, 1429m, 1381m, 1230s, 1157s, 1105s, 1043s. The minor change in sulfonate group stretching frequencies suggests that the calixarene is non-coordinating, as was found in the crystal structure solution. **Isostructural complexes:** For Ce^{3+}, large yellow/orange crystals formed over 30 minutes with unit cell measurements of a = 17.4035(3), b = 18.8261(2) c = 19.5930(2) Å, α = 90.0756(7), β = 67.4716(5), γ = 90.0259(13)°, T = 150(2) K.

Complex number	**2.1**	**2.2**	**2.3**
Formula	$C_{34}H_{74}NO_{37}S_4Nd_1$	$C_{28}H_{54}O_{33}S_4Nd_1$	$C_{68}H_{162}NO_{84.50}S_8Nd_2$
Mr	1348.4	1191.19	2890.95
Crystal system	Monoclinic	Triclinic	Monoclinic
Space group	$P2_1/n$	$P\bar{1}$	$P2_1/c$
T/K	150(2)	150(2)	150(2)
a /Å	17.345(4)	12.3556(3)	21.0204(2)
b /Å	18.729(4)	14.4184(3)	18.4014(2)
c /Å	19.462(4)	14.7583(3)	31.7225(4)
α /°	90	92.11(3)	90
β /°	112.31(3)	113.02(3)	98.218(1)
γ /°	90	98.35(3)	90
U Å^3	5849(2)	2381.38(9)	12144.4(2)
Z	4	2	4
F(000)	2820	1220	6004
ρ_{calc} /g cm^{-3}	1.546	1.661	1.581
μ /cm^{-1}	1.128	1.365	1.097
$\Theta_{min, max}$ /°	1.73, 25.0	2.19, 25.0	1.28, 26.0
Data collected	40525	43060	93588
Unique data	10240	8319	23822
R_{int}	0.0554	0.0841	0.1132
Obs data (I>2 $\sigma(I)$)	8081	7872	18436
Parameters	780	606	1481
Restraints	0	0	0
R_1 (observed data)	0.0951	0.0456	0.1528
ωR_2 (all data)	0.2909	0.1302	0.3504
S	1.05	1.032	1.158
Max/min residuals [e.Å^{-3}]	1.955, -2.092	2.675, -1.802	2.694, -3.093

Table 2.7 Details of data collection and structure refinement for complexes **2.1 – 2.3**.

For Eu^{3+}, preparation method was identical to that above with colourless crystals forming over 30 minutes. The unit cell measurements were a = 17.1943(3), b = 18.6962(4), c = 19.4208(5) Å, α = 90.1112(13), β = 67.7569(15), γ = 90.1442(14)°, T = 150(2) K. For Gd^{3+}, preparation method was identical to that above with colourless crystals forming over 30 minutes. The unit cell measurements were a = 17.2262(2), b = 18.7737(2), c = 19.4604(3) Å, α = 90.0184(7), β = 112.1530(17), γ = 90.0037(3)°, T = 150(2) K. On this basis, all three unit cell determinations suggest complexes isostructural to that for neodymium. **X-ray crystallography**: Residual electron density is associated with a disordered water molecule of crystallisation. Four disordered neodymium aquo ligands were disordered over two positions and refined with equal occupancies. Some waters of crystallisation were refined isotropically.

2.3.2 Synthesis of the bi-layer arrangement $[(Nd(H_2O)_8)(p\text{-sulfonatocalix[4]arene} + H^+)]\cdot 9H_2O$, 2.2.

Neodymium(III) chloride (10 mg, 40 μmol), 1-aza-18-crown-6 (10 mg, 30 μmol), and *p*-sulfonicacid calix[4]arene (10 mg, 13.4 μmol) were dissolved in distilled water (1 cm^3). Colourless crystals that were of suitable quality for X-ray diffraction studies formed upon slow evaporation. Yield 9 mg, 56%. **X-ray crystallography**: Residual electron density is associated with disordered water molecules of crystallisation that reside in the calixarene cavity. One oxygen atom of a calixarene sulfonate group was disordered over two positions, O(5A) and O(5B), with partial occupancies of 0.6 and 0.4 respectively. One water molecule of crystallisation was refined isotropically.

2.3.3 Synthesis of the molecular capsule $[(1\text{-aza-18-crown-6} + H^+)\subset[(H_2O)_2[Nd(H_2O)_9]_2[(p\text{-sulfonatocalix[4]arene})_2 + H^+]]\cdot 27.5H_2O$, 2.3.

p-Sulfonicacid calix[4]arene (40 mg, 54 μmol) and 1-aza-18-crown-6 (8 mg, 30 μmol) were dissolved in distilled water (1 cm^3) prior to addition of neodymium(III) chloride (10 mg, 40 μmol). On standing, purple crystals of suitable quality for X-ray diffraction studies formed over 15 minutes. Yield 53 mg, 61 %. IR(KBr disc, ν cm^{-1}): 3356s, 3155s, 2926m, 1642m, 1595m, 1469m, 1223s, 1159s, 1107s, 1041s. The minor changes in sulfonate group stretching frequencies suggests that the calixarene is non-coordinating, as was found in the crystal structure solution. **X-ray crystallography**: Residual electron density is located around 1 Å from the Nd(1) metal centre. Four of the Nd(2) aquo ligands (O(48), O(49), O(54) and O(55)) and some waters of crystallisation were

refined isotropically. The high R_1 (0.1528) is due to unmodelled extensive disorder associated with the large number of water molecules of crystallisation.

Complex number	**2.4**	**2.5**	**2.6**
Formula	$C_{99}H_{187.50}Eu_3N_3O_{98.25}S_{12}$	$C_7H_5Nd_{0.25}O_{5.50}S_1$	$C_{144}H_{262}N_8Nd_2O_{123}S_{16}$
Mr	3832.62	245.23	4875.06
Crystal system	Monoclinic	Tetragonal	Triclinic
Space group	$P2_1/c$	$P4/nnc$	$P\bar{1}$
T/K	150(2)	150(2)	150(2)
a /Å	30.9099(1)	12.0238(8)	19.9230(1)
b /Å	28.3481(2)	12.0238(8)	21.0935(2)
c /Å	17.4843(3)	29.3233(16)	24.7992(2)
α /°	90	90	86.4550(3)
β /°	99.36(3)	90	83.0468(3)
γ /°	90	90	80.6639(6)
U Å^3	15116.5(3)	4239.3(5)	10198.61(14)
Z	4	16	2
F(000)	7878	1464	5084
ρ_{calc} /g cm^{-3}	1.684	1.763	1.588
μ /cm^{-1}	1.511	1.124	0.782
$\Theta_{min,\ max}$ /°	2.59, 27.50	1.83, 26.42	1.89, 27.32
Data collected	156512	12635	194935
Unique data	34476	2147	45488
R_{int}	0.1523	0.0703	0.1605
Obs data (I>2 $\sigma(I)$)	23993	1394	29303
Parameters	2006	129	2677
Restraints	21	0	6
R_1 (observed data)	0.0922	0.136	0.0871
ωR_2 (all data)	0.2617	0.3658	0.2486
S	1.084	2.37	1.359
Max/min residuals [e.Å^{-3}]	1.943, -2.594	1.683, -0.819	2.982, -4.429

Table 2.8 Details of data collection and structure refinement for complexes **2.4** – **2.6**.

2.3.4 Synthesis of the molecular capsule arrangement [(1,7-diaza-15-crown-5 + $2H^+)_{1.5}\subset$[$(H_2O)_3$[$Eu(H_2O)_7Eu(H_2O)_6$(*p*-sulfonatocalix[4]arene)$_2$](*p*-sulfonatocalix[4]arene) $Eu(H_2O)_8$]·$20.75H_2O$, 2.4.

p-sulfonicacid calix[4]arene (40 mg, 54 μmol), 1,7-diaza-15-crown-5 (6 mg, 27 μmol) and europium(III) chloride (13 mg, 40 μmol) were dissolved in distilled water (2 cm^3). Upon standing, colourless crystals suitable for X-ray diffraction studies formed over 30 minutes. Yield 69 mg, 67 %. IR (solid phase, ν cm^{-1}): 3230s, 2932s, 2220m, 1818m, 1429m, 1637m, 1594m, 1467m, 1445m, 1418m, 1218m, 1141s, 1117s, 1034s. The increase in the number of sulfonate group stretching

frequencies suggests lanthanide/sulfonate coordination, as was found in the crystal structure solution. **X-ray crystallography**: Four Eu(1), two Eu(2), and three Eu(3) aquo ligands were disordered over two positions with partial occupancies of 0.7 and 0.3. One Eu(2) aquo ligand was disordered over two positions with equal occupancies. One Eu(3) aquo ligand was disordered over three positions with equal occupancies. The oxygen atoms of the S(2) sulfonate group were disordered over two positions with partial occupancies of 0.7 and 0.3. The oxygen atoms of the S(3) and S(5) sulfonate groups were disordered over two positions with partial occupancies of 0.6 and 0.4. The oxygen atoms of the S(7) sulfonate group were disordered over two positions with equal occupancies. One calixarene sulfonate group was disordered over two positions with partial occupancies of 06 and 0.4 (S(8) and S(9) respectively). Residual electron density is located around 1 Å from the Eu(2) metal centre. Several S-O bonds were restrained to maintain chemical meaning. For the disordered diaza-15-crown-5 molecules, the U_{ij} values were constrained to be the same for all atoms. Some Eu(2) and Eu(3) aquo ligands in addition to some water molecules of crystallisation were refined isotropically.

2.3.5 Synthesis of the 2-D coordination polymer, [(Nd(H$_2$O)$_5$)(*p*-sulfonatocalix[4]arene + H$^+$)], 2.5.

p-sulfonicacid calix[4]arene (40 mg, 54 μmol), 1-aza-15-crown-5 (5 mg, 23 μmol) and neodymium(III) chloride (10 mg, 40 μmol) were dissolved in distilled water (1 cm^3). Upon nearing dryness, small purple crystals which were suitable for X-ray diffraction studies grew. Yield 18 mg, 46 %. **X-ray crystallography**: The routine SQUEEZE was applied to the data for complex **2.5** due to diffuse electron density that could not be adequately modelled as disordered solvent.[108] This lowered the R_1 factor from 0.1730 to 0.1360. Residual electron density is located around 1Å from a sulfur atom. Two sulfonate group oxygen atoms were disordered over three positions, all with equal occupancies.

2.3.6 Synthesis of the bi-layer arrangement [(Nd(H$_2$O)$_9$)$_2$][((1,7-diaza-12-crown-4 + 2H$^+$)⊂*p*-sulfonatocalix[4]arene)$_4$ + 2H$^+$]·33H$_2$O, 2.6.

p-sulfonicacid calix[4]arene (40 mg, 54 μmol), 1,7-diaza-12-crown-4 (5 mg, 27 μmol) and neodymium(III) chloride (10 mg, 40 μmol) were dissolved in distilled water (2 cm^3). Upon standing, colourless crystals suitable for X-ray diffraction studies formed over 30 minutes. Yield 63 mg, 72%. IR (solid phase, ν cm^{-1}): 3472w, 2562ws, 2161wm, 1738s, 1425w, 1365m, 1217s, 1213s, 1039m. The minor change in sulfonate group stretching frequencies suggests that the calixarene is

non-coordinating, as was found in the crystal structure solution. **X-ray crystallography**: Residual electron density is located around 1 Å from the Nd(1) metal centre. Some crown ether bonds were restrained and some water molecules of crystallisation were refined isotropically.

Complex number	**2.7**	**2.8**
Formula	$C_{9.25}H_{10.50}N_{0.25}Nd_{0.25}O_{6.38}S$	$C_{34}H_{51}N_2NdO_{25}S_4$
Mr	295.3	1160.25
Crystal system	Tetragonal	Monoclinic
Space group	*P*4/*nnc*	$P2_1/n$
T/K	150(2)	150(2)
a /Å	11.9026(17)	12.4019(2)
b /Å	11.9026(17)	11.7497(1)
c /Å	32.876(7)	29.2694(5)
α /°	90	90
β /°	90	95.2780(1)
γ /°	90	90
U Å^3	4657.6(13)	4247.01(11)
Z	16	4
F(000)	2396	2372
ρ_{calc} /g cm^{-3}	1.684	1.815
μ /cm^{-1}	1.385	1.517
$\Theta_{min,\ max}$ /°	2.42, 27.52	2.39, 26.0
Data collected	17329	43281
Unique data	2701	8335
R_{int}	0.1563	0.1023
Obs data ($I>2\ \sigma(I)$)	1674	5967
Parameters	145	599
Restraints	0	1
R_1 (observed data)	0.0692	0.0566
ωR_2 (all data)	0.2015	0.1513
S	1.049	1.025
Max/min residuals [eÅ^3]	1.556, -1.436	3.384, -1.454

Table 2.9 Details of data collection and structure refinement for complexes **2.7** and **2.8**.

2.3.7 Synthesis of the 2-D coordination polymer of molecular capsules [(2H[2.2.2]cryptand)⊂(*p*-sulfonatocalix[4]arene)$_2$(M(H$_2$O)$_4$)$_2$]·0.625H$_2$O, M = Nd, Ce, Sm, Eu, 2.7.

p-sulfonicacid calix[4]arene (10 mg, 13.4 μmol), [2.2.2]cryptand (10 mg, 26.5 μmol), and neodymium(III)chloride (>10 molar eq.) were dissolved in distilled water (1cm^3). Over two days, colourless plates formed which were suitable for X-ray diffraction studies. Yield 7 mg, 44 %. IR(KBr disc, ν cm^{-1}): 3400s, 3142s, 2926m, 2735m, 2596w, 1630m, 1595m, 1469s, 1429m, 1381m, 1361m, 1224s, 1160s, 1107, 1041s. The increase in the number of sulfonate group stretching

frequencies suggests lanthanide/sulfonate coordination, as was found in the crystal structure solution. **Isostructural complexes:** For Ce^{3+}, unit cell measurements were a = 11.9527(3). b = 11.9558(6), c = 32.9301(8) Å, α = 90.004, β = 90.022, γ = 90.008°. For Sm^{3+}, unit cell measurements were a = 11.8453(2), b = 11.8625(3), c = 32.4934(9) Å, α = 90.047, β = 90.104, γ = 90.048°. For Eu^{3+}, unit cell measurements were a = 11.9291(5), b = 11.9464(3), c = 32.6602(7) Å, α = 89.961, β = 89.931, γ = 90.061°. On this basis, all three unit cell determinations suggest isostructural complexes to that for neodymium. **X-ray crystallography**: Residual electron density is associated with a disordered water molecule of crystallisation. The atoms of the disordered cryptand molecule were refined with U_{ij} values that were constrained to be the same. Disordered water molecules of crystallisation were refined isotropically. Hydrogen atoms could not be positioned on all of the carbon atoms within the cryptand due to the extensive disorder resulting from the bi-cyclic molecule residing on a four-fold rotation axis.

2.3.8 Synthesis of the 2-D coordination polymer [(1,4-diazabicyclo[2.2.2]octane + H^+)⊂[(*p*-sulfonatocalix[4]arene)$^{4-}$($Nd(H_2O)_5)^{3+}$]]·$4H_2O$, 2.8.

Slow evaporation of an aqueous solution (1 cm^3) containing *p*-sulfonic acidcalix[4]arene (35 mg, 48 μmol), 1,4-diazabicyclo[2.2.2]octane (5 mg, 45 μmol) and neodymium(III) chloride (0.125 g, 0.5 mmol) over several days afforded small purple plates which were suitable for X-ray diffraction studies. Yield 18 mg, 34 %. **X-ray crystallography**: Residual electron density is located around 1 Å from the Nd(1) metal centre. The N-H bond dista nce of the protonated DABCO molecules was restrained.

Chapter Three:

Lanthanide metal complexes of *p*-sulfonatocalix[4]arene.

3.0 Introduction.

This chapter is concerned with investigating the formation of supramolecular lanthanide/*p*-sulfonatocalix[4]arene complexes in the absence of guest molecules. The majority of complicated solid state supramolecular architectures incorporating SO_3[4], as described in Chapter 1, typically involve the calixarene bearing host to a suitably sized guest molecule, often in the form of molecular capsules, Ferris wheels, amino acid complexes or variations thereof.[34, 44-47, 50, 59-61, 109] Considering the substantial number of such supramolecular solid state complexes, relatively few metal complexes of the calixarene (other than alkali metals and some formed in the absence of guest) have been reported despite their forming interesting structural motifs in the solid state.[27, 32, 39, 110]

3.1 Transition and lanthanide metal complexes of *p*-sulfonatocalix[4]arene formed in the absence of guest molecules.

In the few 'guest absent' metal complexes reported to date, Atwood *et al.* showed that addition of copper(II) chloride to a solution of sodium *p*-sulfonatocalix[4]arene results in the formation of an interesting bi-layer motif that shows copper ions linking calixarenes in hydrophobic layers[32]. Additional copper ions span the hydrophilic layer separating adjacent hydrophobic layers, generating an unusual coordination polymer. Brechbiel and co-workers reported that addition of lead nitrate to a solution of *p*-sulfonatocalix[4]arene resulted in the formation of a complex that also showed lead ions to span the hydrophilic layer and link hydrophobic layers in a similar bi-layer motif.[110] Notably, the structure had four different lead coordination environments with varied degrees of hydration. There are a handful of solid state studies with lanthanide metals and that are more closely related to those described in this chapter. Atwood *et al.* reported the formation of a hepta-aqua yttrium/sodium/SO_3[4] complex that adopted the typical bi-layer arrangement in the extended structure.[109] The same group also reported the formation of a 3-D coordination network incorporating lanthanum nitrate, SO_3[4] and DMSO molecules.[39] That study showed there to be two different lanthanum centres participating in coordination network formation. Both of these metal centres had one coordinated nitrate anion whilst one also had a coordinated DMSO molecule that was positioned within a calixarene cavity. Detellier *et al.* reported the formation of a remarkable discrete 8:6 La(III):SO_3[4] complex from the addition of lanthanum(III) chloride to a solution of SO_3H[4].[52] They also showed that the structural formation was independent of reactant

concentration by determining the unit cell dimensions of crystals grown from several reaction mixtures. More recently, Raston *et al.* reported the formation of a simple 2-D coordination polymer *via* the addition of early lanthanide(III) trifluoromethanesulfonates to a solution containing sodium *p*-sulfonatocalix[4]arene.[102] This structure was described in Chapter 2 as it related directly to complexes **2.5**, **2,7** and **2.8** of this thesis.

The results presented within this chapter firstly describe the formation of a 2-D hydrogen-bonded network formed with the later lanthanide metal chlorides (Ln^{3+} = Gd, Tb, Tm) and $SO_3H[4]$. This result is in direct contrast to the formation of the 8:6 La(III):$SO_3[4]$ complex reported by Detellier *et al.* and that formed from a solution containing $La(III)Cl_3$ and $SO_3H[4]$.[52] The other structures described in this chapter resulted from investigating supramolecular structures resulting from a series of praseodymium salts with penta-sodium *p*-sulfonatocalix[4]arene. Of those investigated (nitrate, oxalate, perchlorate), praseodymium nitrate and perchlorate both formed complexes with $SO_3[4]$. Praseodymium nitrate formed a complicated 3-D coordination polymer that shows similarities to one reported by Atwood *et al.* that formed with $SO_3[4]$, lanthanum(III) nitrate and DMSO.[29] Praseodymium perchlorate formed a 4:3 Pr(III):$SO_3[4]$ complex that is similar in some respects to the 8:6 La(III):$SO_3[4]$ complex reported by Detellier *et al.*[52] Upon standing, and very slow evaporation, these crystals re-dissolve and re-grow in a different morphology as a praseodymium/$SO_3[4]$/sodium/perchlorate complex that is also described in this chapter. Unfortunately, single crystals did not grow from solutions containing praseodymium oxalate and $SO_3[4]$. Throughout the chapter water molecules of crystallisation have been omitted for clarity in all diagrams unless included for particular purpose.

3.1.1 Structure of the 2-D hydrogen-bonded network $[M(H_2O)_8][p\text{-sulfonatocalix[4]arene} + H^+]\cdot 4H_2O$ (M = Gd, Tb, Tm), 3.1.

Crystals of the complex $[Tb(H_2O)_8][p\text{-sulfonatocalix[4]arene} + H^+]\cdot 4H_2O$, **3.1**, grew upon slow evaporation of an aqueous solution containing a 3:1 mixture of terbium(III) chloride and $SO_3H[4]$ (Equation 3.1). The complex was characterised by IR spectroscopy and single crystal X-ray crystallography. Complex **3.1** crystallises in a tetragonal cell and the structural solution was performed in the space group *P*4/*n*. Isostructural complexes with Gd^{3+} and Tm^{3+} in place of Tb^{3+} were synthesised and characterised by single crystal unit cell determination, however only the Tb^{3+} complex will be discussed in any detail (unit cell parameters for isostructural complexes are listed in the experimental section for complex **3.1**). Details of the data collection and structure refinement are given in Table 3.5 of this chapter. A crystallographic information file containing all bond lengths and angles for complex **3.1** can be found in appendix 3.1.1 on the attached compact disc.

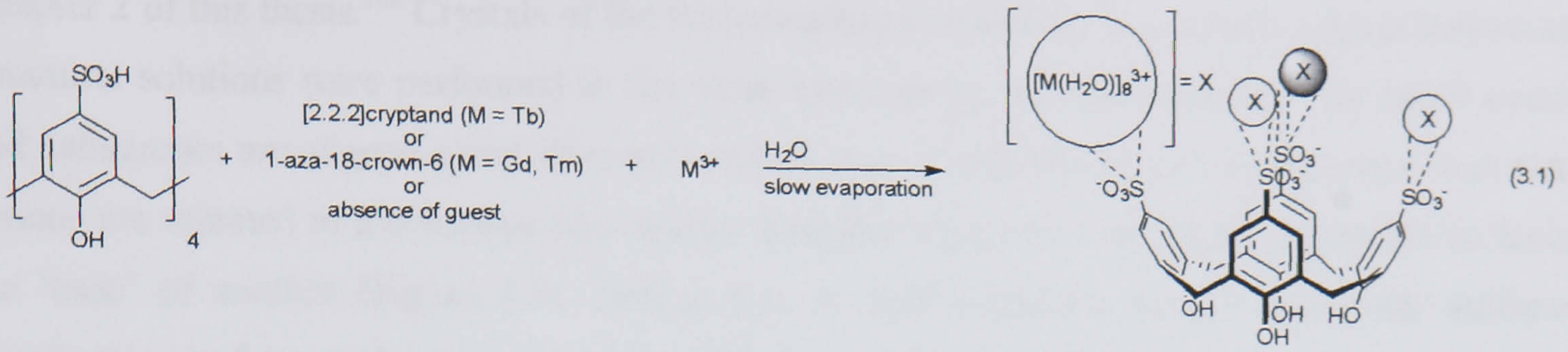

(3.1)

Notably, this structure was also obtainable when the later lanthanides were employed in attempts to form molecular capsules with [2.2.2]cryptand or 1-aza-18-crown-6 at a pH of ~3 (Equation 3.1). As was shown in Chapter 2, the use of the early lanthanide metals with the aforementioned guests at similar pH results in the formation of either an unusual neodymium/SO_3[4] bi-layer arrangement or a 2-D coordination polymer of molecular capsules shrouding di-protonated cryptand molecules (complexes **2.2** and **2.7** respectively). This phenomenon shall be discussed further below. The asymmetric unit consists of one quarter of an octa-aqua terbium cation, one quarter of an SO_3[4] molecule and a total of four water molecules disordered over nine positions (Figure 3.1).

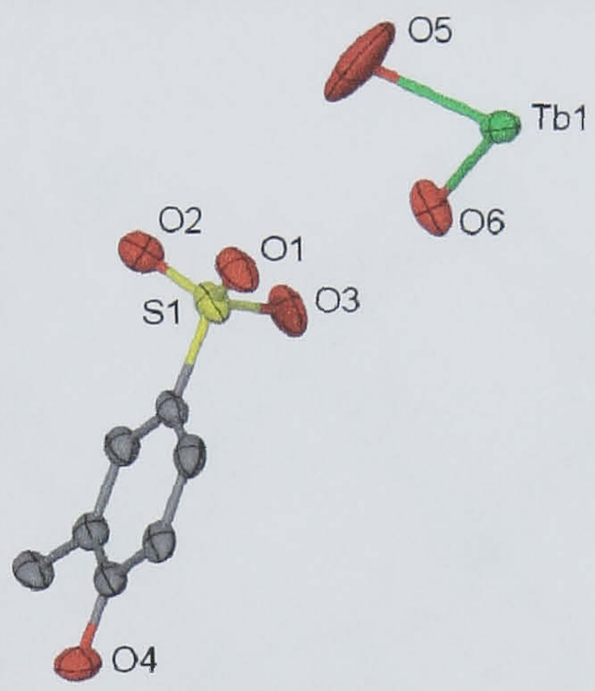

Figure 3.1 Part of the asymmetric unit from the crystal structure of complex **3.1**, anisotropic displacement ellipsoids at 50% probability. Selected atoms have been labelled.

The two major components in the crystal structure combine to form an infinite hydrogen-bonded network between $Tb(H_2O)_8^{3+}$ cations and four nearest neighbour calixarene molecules (Figures 3.2 and 3.3). This network forms by hydrogen bonding from the O(6) atom of the metal cation to both the O(3) atom of the nearest calixarene fragment and the nearest symmetry equivalent sulfonate O(1) atom (TbO(6)···O(3) and TbO(6)···O(1) distances of 2.731 and 2.751 Å respectively). The four remaining aquo ligands (O(5) and symmetry equivalents) point into the hydrophilic layer and partake in hydrogen bonding regimes with disordered waters of crystallisation. The 2-D hydrogen-bonded network, despite having non-coordinating cations, bears significant resemblance to the previously reported 2-D coordination polymer that is formed with SO_3[4] and the early lanthanide metal triflates (Ce and Pr), a structure that was highlighted for complexes **2.5**, **2.7** and **2.8** in

Chapter 2 of this thesis.[102] Crystals of the two complexes crystallise in the same crystal system and structural solutions were performed in the same space group. In both structures the metal centres and calixarenes are aligned along identical rotation axes. Given this fact, the calixarenes and metal cations are oriented in a columnar like fashion with the 'upper rim' of the SO_3[4] molecule facing the 'base' of another (Figure 3.3). This is true in both structures despite lanthanide sulfonate coordination in the coordination polymer. In fact, one of the few significant structural differences *is* the lanthanide sulfonate coordination in the 2-D coordination polymer. This lanthanide calixarene coordination is reflected in the dihedral angles of the calixarene which are 125.56° for the 2-D coordination polymer and 120.74° for complex **3.1** (dihedral angles being those between the calixarene aromatic rings and the basal plane of the calixarene phenolic oxygen atoms). This further indicates that metal sulfonate coordination dictates the degree of calixarene splaying in the overall structure. One other significant difference is the coordination sphere of the metal centres in each complex. The previously reported 2-D coordination polymer possessed nona-coordinate lanthanide metals with tri-capped trigonal prismatic geometry whereas complex **3.1** has octa-coordinate square anti-prismatic terbium cations (Tb–O(5) and Tb–O(6) bond lengths of 2.382(10) and 2.364(6) Å respectively).

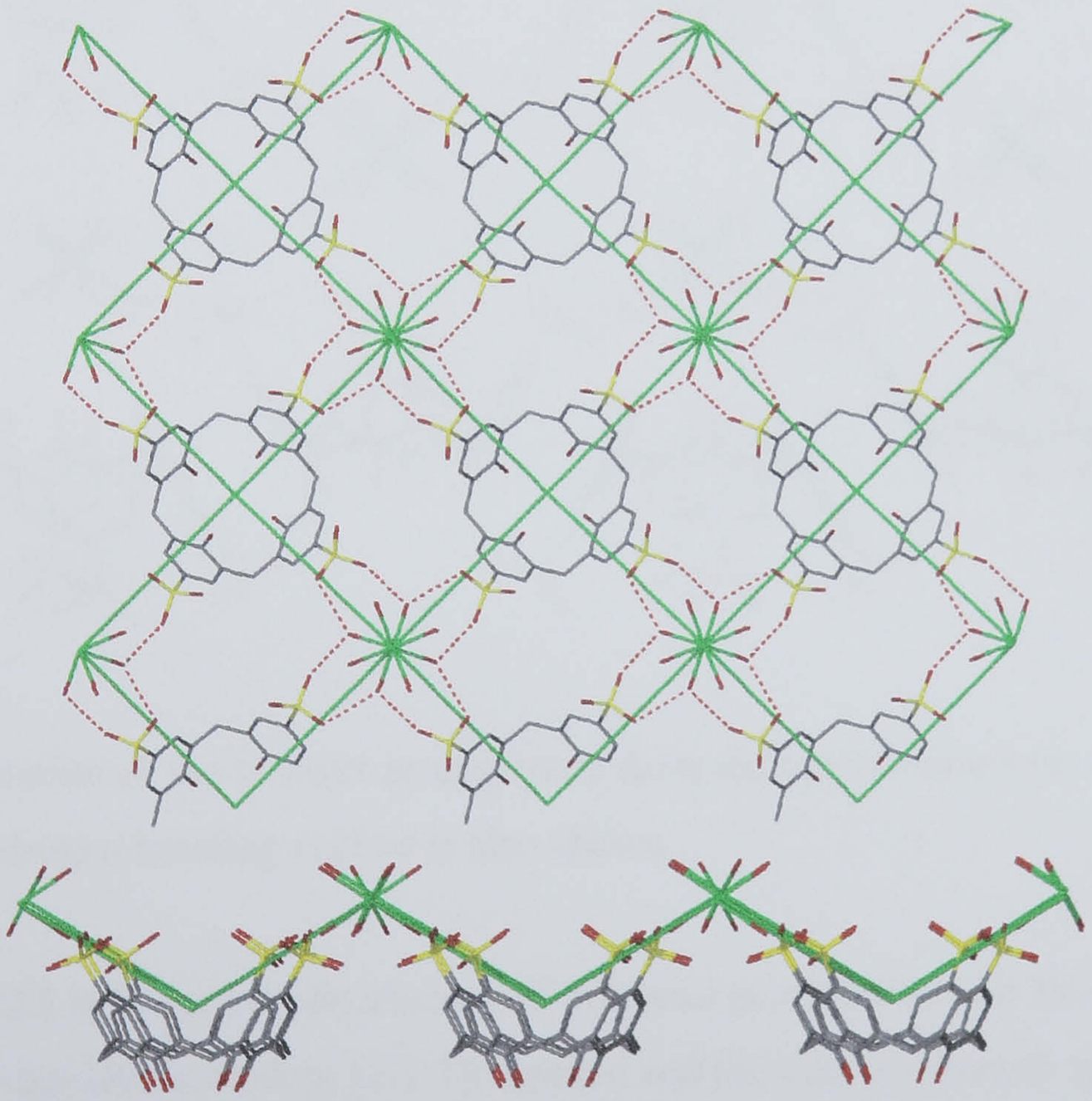

Figure 3.2 Two views of half of a hydrophobic layer from the crystal structure of complex **3.1**. The top view shows the hydrogen bonding network associated with terbium aquo ligands and sulfonate groups of the calixarenes. Both views represent the network topology associated with the complex when the calixarenes and terbium cations are treated as four connecting centres and joined by green lines.

Complex **3.1** possesses a disordered water molecule that resides in the hydrophobic cavity of the calixarene and along the same C_4 rotation axis as the SO_3[4] molecule. This water molecule is positioned 3.746 Å from the centroid of the aromatic ring of the calixarene, a distance that is consistent with previously reported examples of such OH···π interactions for this calixarene.[28] Unfortunately hydrogen atoms could not be located in the Fourier difference map to confirm this interaction.

The extended structure reveals the calixarenes to pack in the usual bi-layer arrangement as described in Chapter 1 (Figure 3.3). The 2-D hydrogen-bonded network is defined by treating both the terbium centres and calixarenes as four-connecting centres. Upon joining, these form a jagged (4,4) grid in each half of a hydrophobic layer (Figure 3.2).

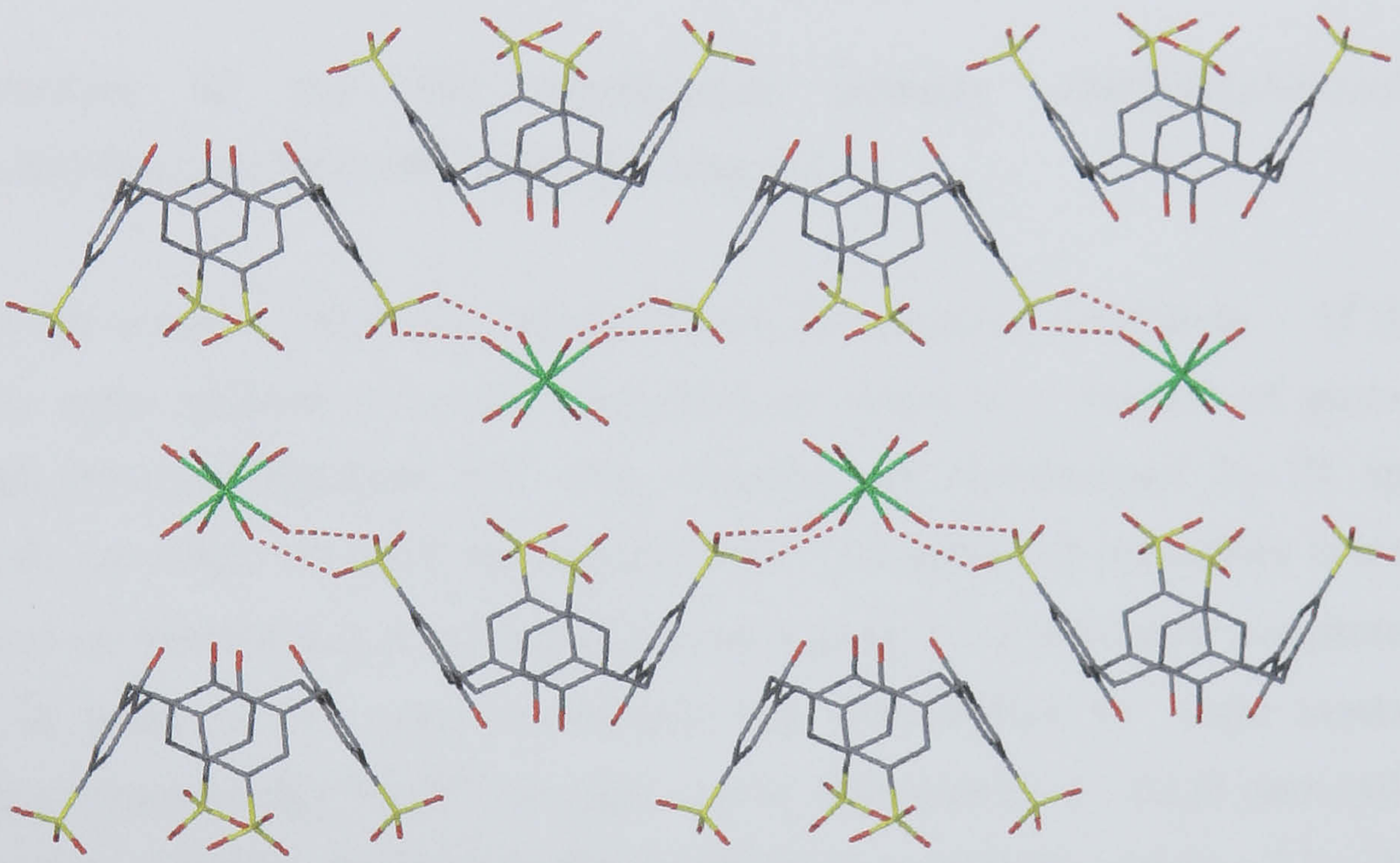

Figure 3.3 Cross section of the bi-layer arrangement from the crystal structure of complex **3.1**. Part of the TbO···OS hydrogen bonding regime is also shown.

Although complex **3.1** is formed in the absence of potential guest, it can also be isolated when in the presence of both 1-aza-18-crown-6 or [2.2.2]cryptand and the later lanthanide metals (Gd and Tm). Clearly this structural motif for SO_3[4] and the later lanthanide metals is favourable given both exclusion of these guest molecules under such conditions and that molecular capsules and alternative structures showing guest inclusion have been formed with the earlier lanthanide chlorides as described in Chapter 2. Similar behaviour is not observed with 18-crown-6 as a guest as that has been shown to form molecular capsules or Ferris wheels with SO_3[4] and several

lanthanide metals when the metal chloride salts are employed.[34, 44-46, 49, 50] The formation of complex **3.1** is markedly different to the discrete 8:6 La(III):SO_3[4] complex reported by Detellier *et al.* and which is formed when lanthanum(III) chloride is used as a reactant with SO_3H[4].[52] Notably, crystals of complex **3.1** were not formed when Tb^{3+} was substituted with Sm^{3+} or Eu^{3+} despite europium lying directly to the left of gadolinium in the lanthanide series. Thus, lanthanide metal complex formation with SO_3H[4] may be partially dependent on the position of the chosen metal chloride in the lanthanide series.

As the early lanthanides have proved useful in complex formation with SO_3[4], several praseodymium salts were examined to observe the effect of the anion on supramolecular structure formation.[17, 33, 39, 41, 52] The first of those examined was praseodymium(III) nitrate. Reaction with penta-sodium *p*-sulfonatocalix[4]arene resulted in the formation of a 3-D coordination polymer that showed the calixarenes to be joined by praseodymium atoms that have varied coordination spheres.

3.1.2 Structure of the 3-D coordination polymer $[(M(H_2O)_4(NO_3))(M(H_2O)_5)$*p*-sulfonatocalix[4]arene$]\cdot 7H_2O$ (M^{3+} = Pr, Nd, Sm), 3.2.

Crystals of the complex $[(Pr(H_2O)_4(NO_3))(Pr(H_2O)_5)$(*p*-sulfonatocalix[4]arene $- H^+$)$]\cdot 7H_2O$, **3.2**, grew slowly upon addition of excess praseodymium nitrate to a solution of penta-sodium *p*-sulfonatocalix[4]arene (Equation 3.2). The complex was characterised by IR spectroscopy, microanalysis and single crystal X-ray crystallography. Complex **3.2** crystallises in a triclinic cell and the structural solution was performed in the space group $P\bar{1}$. Isostructural complexes with Nd^{3+} and Sm^{3+} in place of Pr^{3+} were synthesised and characterised by single crystal unit cell determination, however only the Pr^{3+} complex will be discussed in any detail (unit cell parameters for isostructural complexes are listed in the experimental section for complex **3.2**). Details of the data collection and structure refinement are given in Table 3.5 of this chapter. A crystallographic information file containing all bond lengths and angles for complex **3.2** can be found in appendix 3.1.2 on the attached compact disc.

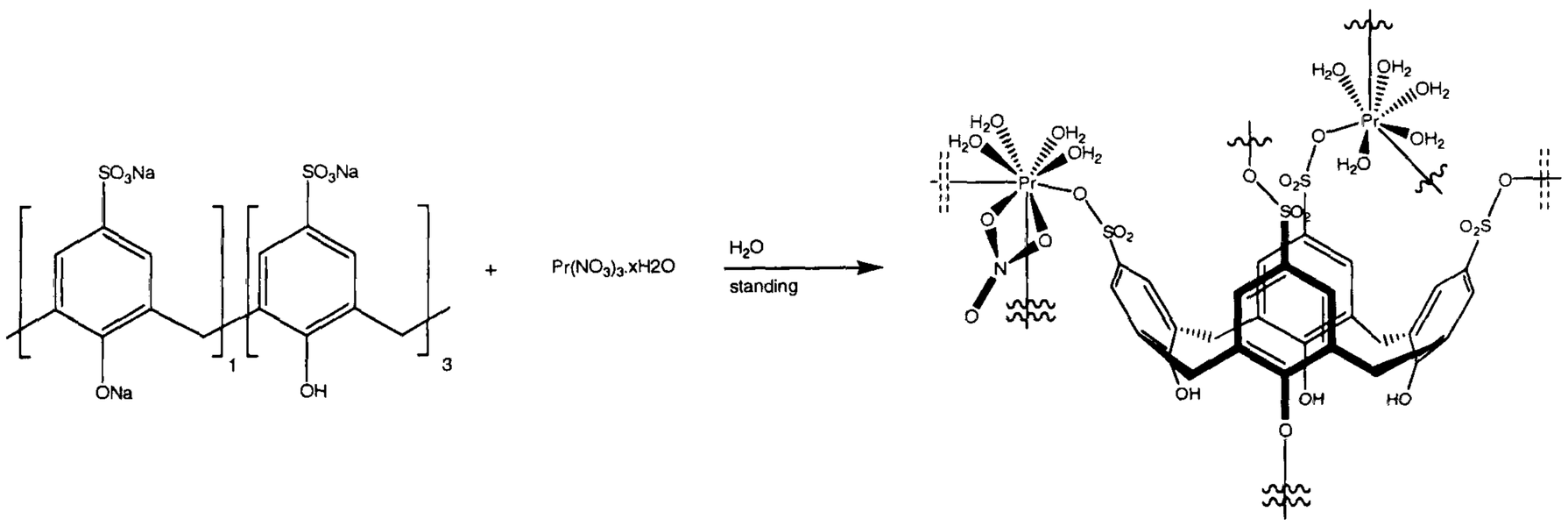

(3.2)

The asymmetric unit consists of a tetra-aquo praseodymium nitrate/SO_3[4]/penta-aquo praseodymium complex in addition to seven waters of crystallisation disordered over nine positions (Figure 3.4). There are two types of praseodymium centre in complex **3.2** and the first, Pr(1), has four aquo ligands and one coordinated nitrate anion whilst being tethered to the S(1) sulfonate group of the calixarene through the O(1) atom.

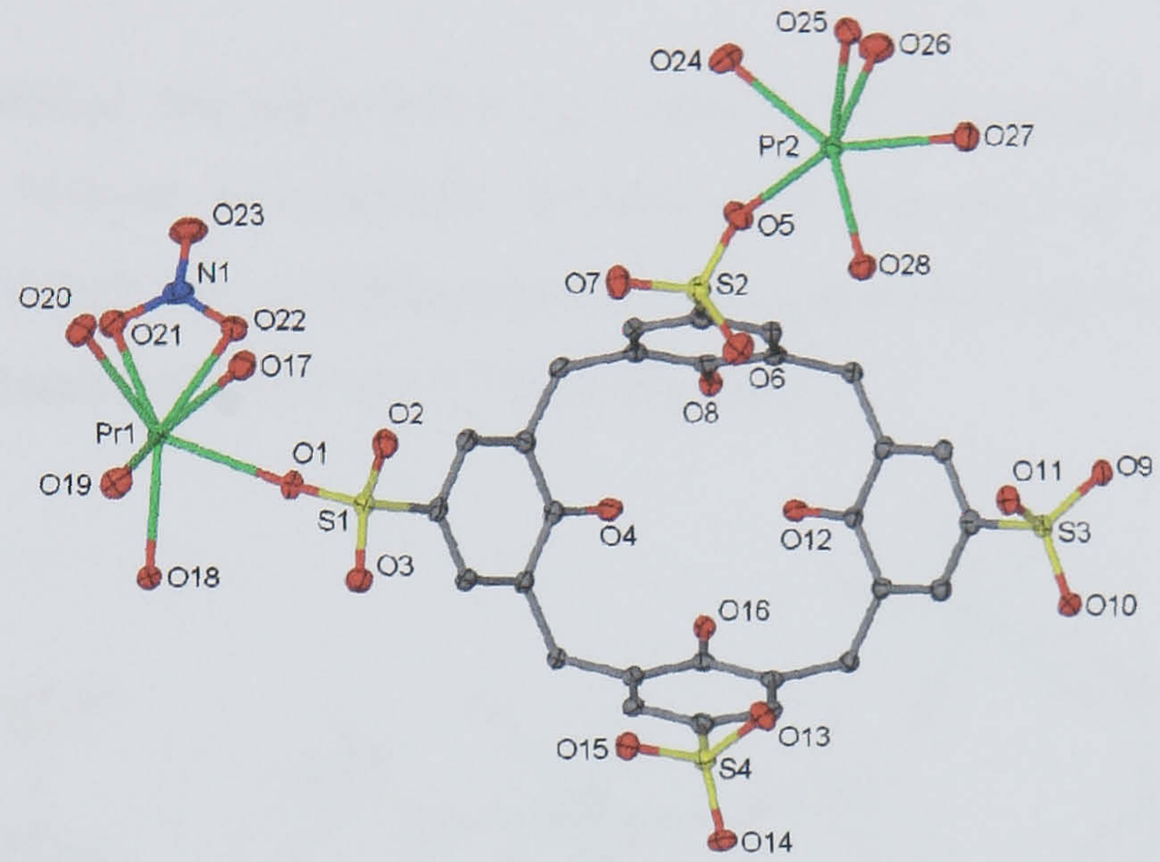

Figure 3.4 Asymmetric unit from the crystal structure of complex **3.2** (omitting uncoordinated water molecules), anisotropic displacement ellipsoids at 50% probability level. Selected atoms have been labelled.

Pr(1)-O(1)	2.4655(19)	Pr(2)-O(5)	2.445(2)
Pr(1)-O(9)[(a)]	2.4227(19)	Pr(2)-O(11)[(c)]	2.4167(19)
Pr(1)-O(16)[(b)]	2.4600(18)	Pr(2)-O(15)[(d)]	2.455(2)
Pr(1)-O(17)	2.657(2)	Pr(2)-O(24)	2.440(2)
Pr(1)-O(18)	2.486(2)	Pr(2)-O(25)	2.487(2)
Pr(1)-O(19)	2.491(2)	Pr(2)-O(26)	2.516(2)
Pr(1)-O(20)	2.540(2)	Pr(2)-O(27)	2.467(2)
Pr(1)-O(21)	2.592(2)	Pr(2)-O(28)	2.466(2)
Pr(1)-O(22)	2.499(2)		
N(1)-O(21)-Pr(1)	94.62(16)	N(1)-O(22)-Pr(1)	97.98(16)

Table 3.1 Interatomic distances between selected atoms in the crystal structure of complex **3.2** (distances given in Å with e.s.d. in parentheses). Selected angles relating to the Pr(1) coordinated nitrate anion are also listed (°). Key operations for symmetry related atoms: *(a)* 1+x, +y, -1+z, *(b)* 1-x, 2-y, -z, *(c)* -x, 1-y, 1-z, *(d)* -1+x, +y, +z.

The second, Pr(2), has five aquo ligands and is tethered to the S(2) sulfonate group of the calixarene through the O(2) atom. The two metal centres have different coordination environments. Pr(1) is nona-coordinate with tri-capped trigonal prismatic geometry (Figures 3.4 and 3.5) whereas Pr(2) is octa-coordinate and has square anti-prismatic geometry (Figures 3.4 and 3.6). The bond lengths relating to the coordination spheres of both metal centres are listed in Table 3.1.

Upon symmetry expansion, the asymmetric unit forms a 3-D coordination polymer that is based around an extended bi-layer arrangement. Inspection of this bi-layer arrangement shows the calixarenes to pack through two crystallographically unique π-stacking interactions with aromatic centroid···centroid distances of 3.616 and 3.778 Å (Figure 3.5).

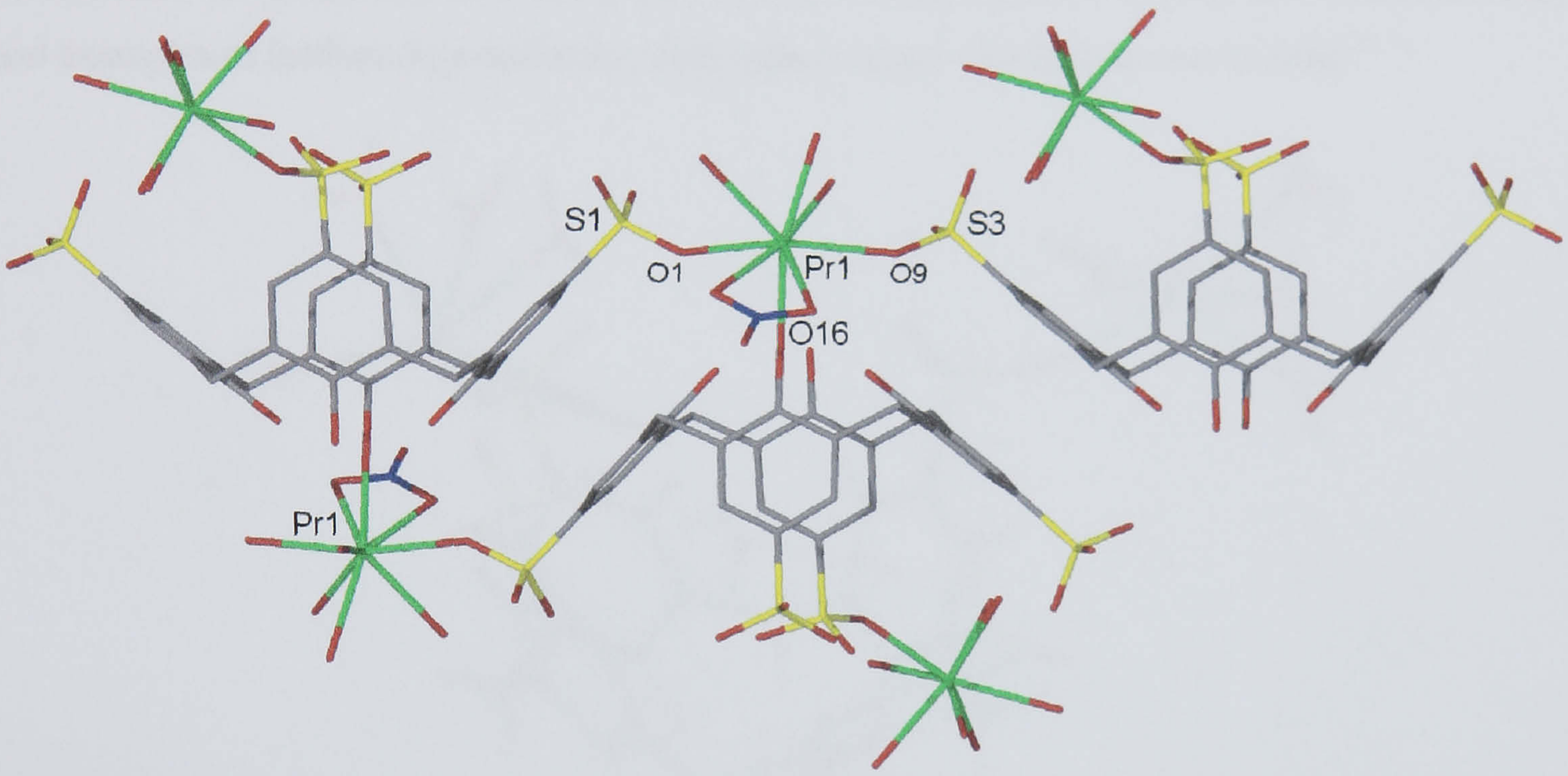

Figure 3.5 Selectively labelled section of the 3-D coordination polymer from the crystal structure of complex **3.2** emphasising the Pr(1) linkages with calixarene 'upper rim' sulfonate groups and 'base' phenoxy groups. Selected atoms have been labelled.

The calixarene is seen to pinch in the C_2 symmetric fashion and the cavity is occupied by a water molecule (SO_3[4] dihedral angles of 104.94 and 132.96°). The good quality of data allowed the refinement of the majority of hydrogen atoms on both coordinated and free water molecules. The hydrogen atoms of the water molecule (O(29)) held within the cavity were located from the Fourier difference map, assigned, refined, and show that there is an OH···π interaction to one of the calixarene aromatic rings (O(29)···aromatic centroid and OH···aromatic centroid distances of 3.623 and 2.808 Å respectively, Figure 3.6). This phenomenon, as described in chapters one and two, was first documented by Atwood *et al.* and the OH···π distance observed here is consistent with those reported.[28]

The overall 3-D coordination polymer is complex and is most easily understood in parts. Firstly, the coordination sphere of Pr(1) shows that the metal centre joins co-planar calixarenes within a hydrophobic layer of the bi-layer arrangement through coordination to the O(1) and O(9) oxygen atoms of the S(1) and S(3) sulfonate groups respectively (Figure 3.5). The metal centre also has a coordinated nitrate anion that is directed downwards into the hydrophobic layer. Indeed, a similar phenomenon is observed in the lanthanum(III) nitrate/DMSO/SO_3[4] coordination polymer reported by Atwood *et al.*[39] In addition to these features, Pr(1) also coordinates to the oxygen atom (O16) of a de-protonated base hydroxyl group of the calixarene located directly beneath the metal centre and within the same hydrophobic layer of the bi-layer arrangement. This metal/calixarene 'base' coordination is the key link in forming the 3-D coordination polymer through the hydrophobic layer and examples of lanthanide/*p*-sulfonatocalix[*n*]arene 'base' coordination are limited.[39, 41]

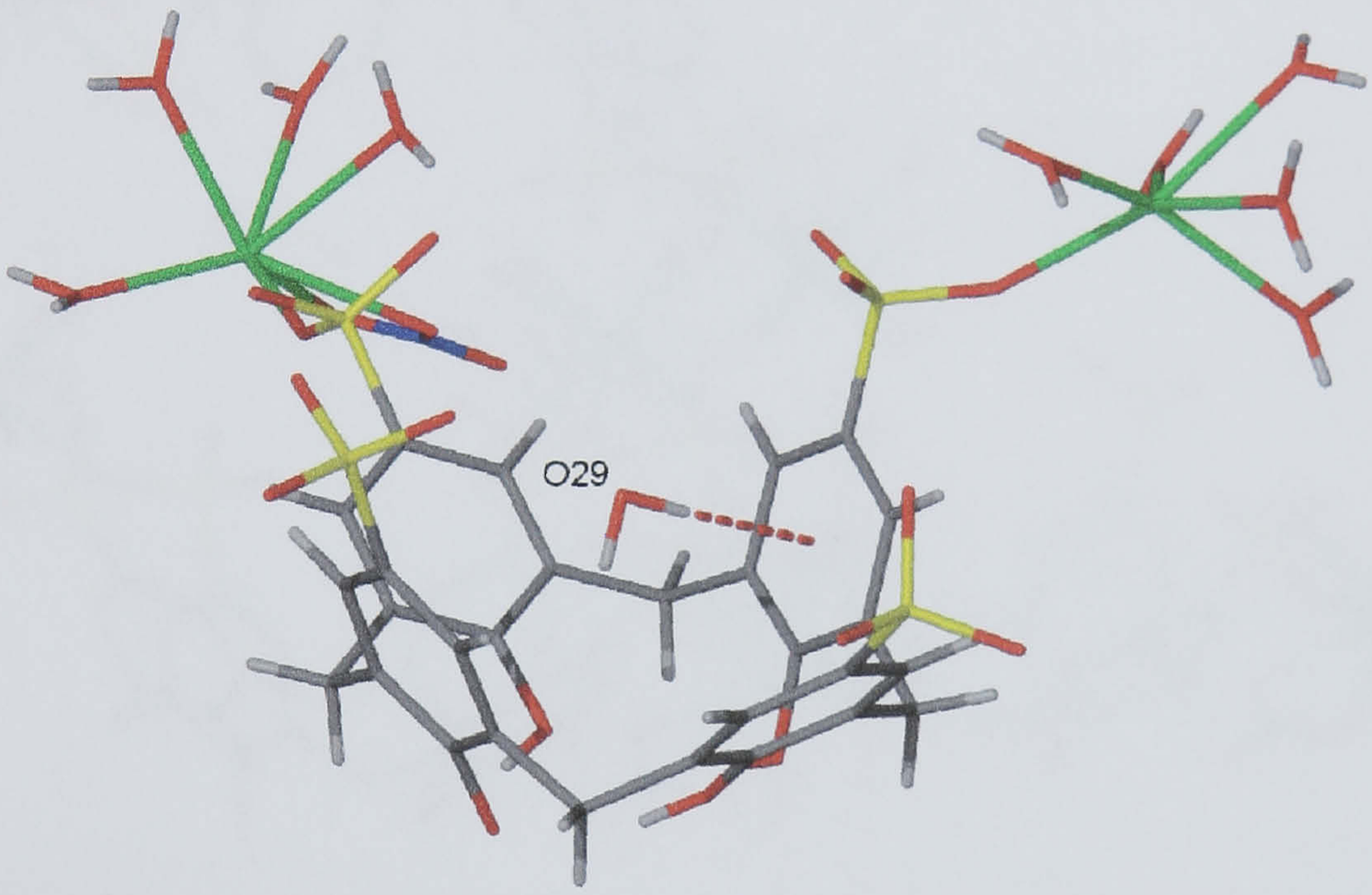

Figure 3.6 Part of the asymmetric unit from the crystal structure of complex **3.2** displaying both fixed (SO_3[4]) and located (water and praseodymium aquo ligands) hydrogen atoms. The OH···π interaction between the water molecule (O(29)) hosted in the molecular cavity and an aromatic ring of the SO_3[4] molecule is also shown (dashed red line). Selected atoms have been labelled.

Similar scrutiny of the coordination sphere of Pr(2) shows the metal centre to span the hydrophilic layer and this occurs through coordination to oxygen atoms of three different calixarene sulfonate groups (indicated by the middle Pr(2) labelled atom in Figure 3.7). The first coordination is to the O(5) atom of the S(2) calixarene sulfonate group as shown in the asymmetric unit diagram (Figure 3.4). Additionally, the metal centre coordinates to the symmetry equivalent O(11) and O(15) atoms of the S(3) and S(4) calixarene sulfonate groups respectively (Figure 3.7).

In order to understand the coordination polymer topology, each metal centre can be treated as a three-connecting centre as each connects to three symmetry equivalent calixarene molecules. Similarly, each calixarene can thus be treated as a six-connecting centre. Once connected, the Pr(1) metal centres and SO_3[4] centroids form a near linear rectangular chain (indicated as **A** in Figure 3.8). When the Pr(2) metal centres are connected to the SO_3[4] centroids, the result is the formation of a stepped ladder arrangement (indicated as **B** in Figure 3.8). As mentioned above, the SO_3[4] molecules act as six-connecting centres and the two different chains, **A** and **B**, meet at the SO_3[4]-common nodes. The overall network structure is found to be a 3-D arrangement of the chains running perpendicular to one another as illustrated in Figure 3.9 (chains **A** and **B** are represented entirely in orange and green respectively.

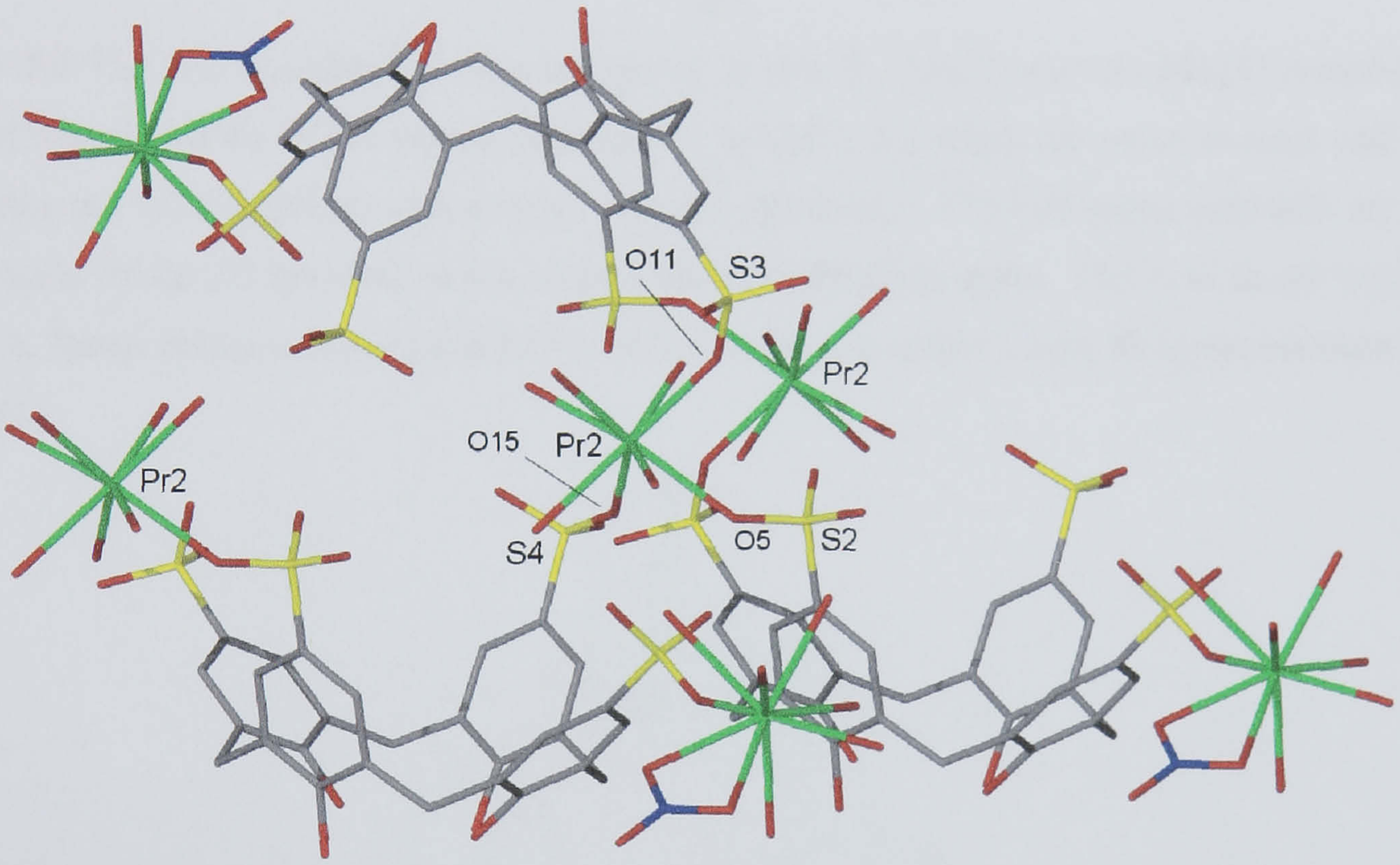

Figure 3.7 Selectively labelled section of the 3-D coordination polymer from the crystal structure of complex **3.2** emphasising the Pr(2) linkages spanning the hydrophilic layer between calixarene 'upper rim' sulfonate groups. Selected atoms have been labelled.

As different supramolecular assemblies were formed from the combination of penta-sodium p-sulfonatocalix[4]arene and praseodymium(III) triflate or nitrate salts, other anions were employed to see if further anion variation would have any effect on supramolecular structure formation. When praseodymium oxalate was employed, the reactants formed a thick oil on solution concentration and single crystals could not be obtained. Praseodymium perchlorate was then employed and excess of the metal salt was added to a solution containing Na_5SO_3[4] resulting in the formation of single crystals of a discrete 4:3 Pr(III):SO_3[4] complex.

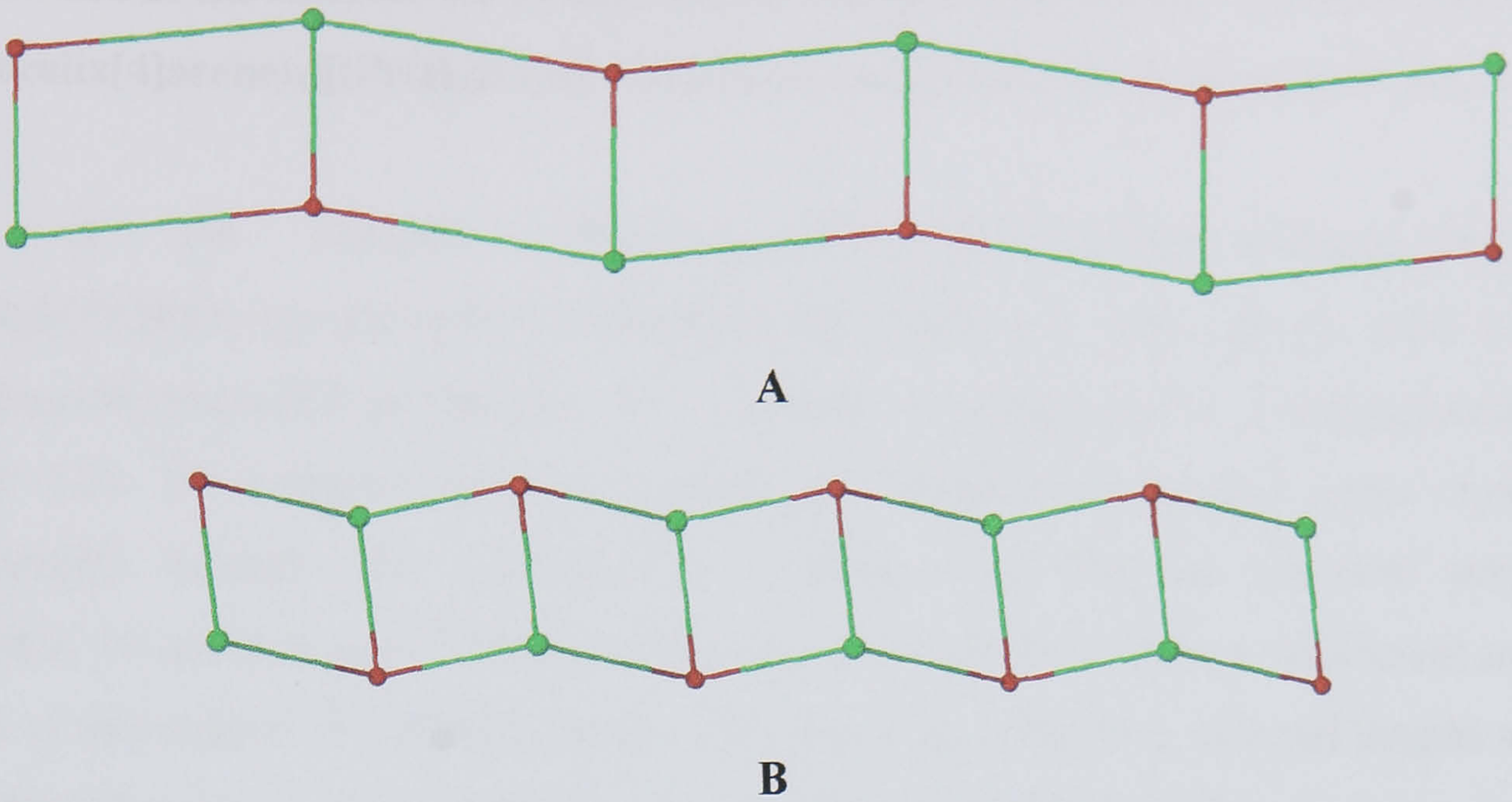

A

B

Figure 3.8 The two coordination network chains **A** and **B** formed between SO_3[4] molecules and praseodymium centres in the crystal structure of complex **3.2** when the metal centres and SO_3[4] molecules are treated and six-connecting centres respectively. The calixarene centroids are shown as red balls whilst the praseodymium centres are represented in green. The near linear rectangular chain, **A**, forms between SO_3[4] and Pr(1) whilst the stepped ladder chain, **B**, forms between SO_3[4] and Pr(2).

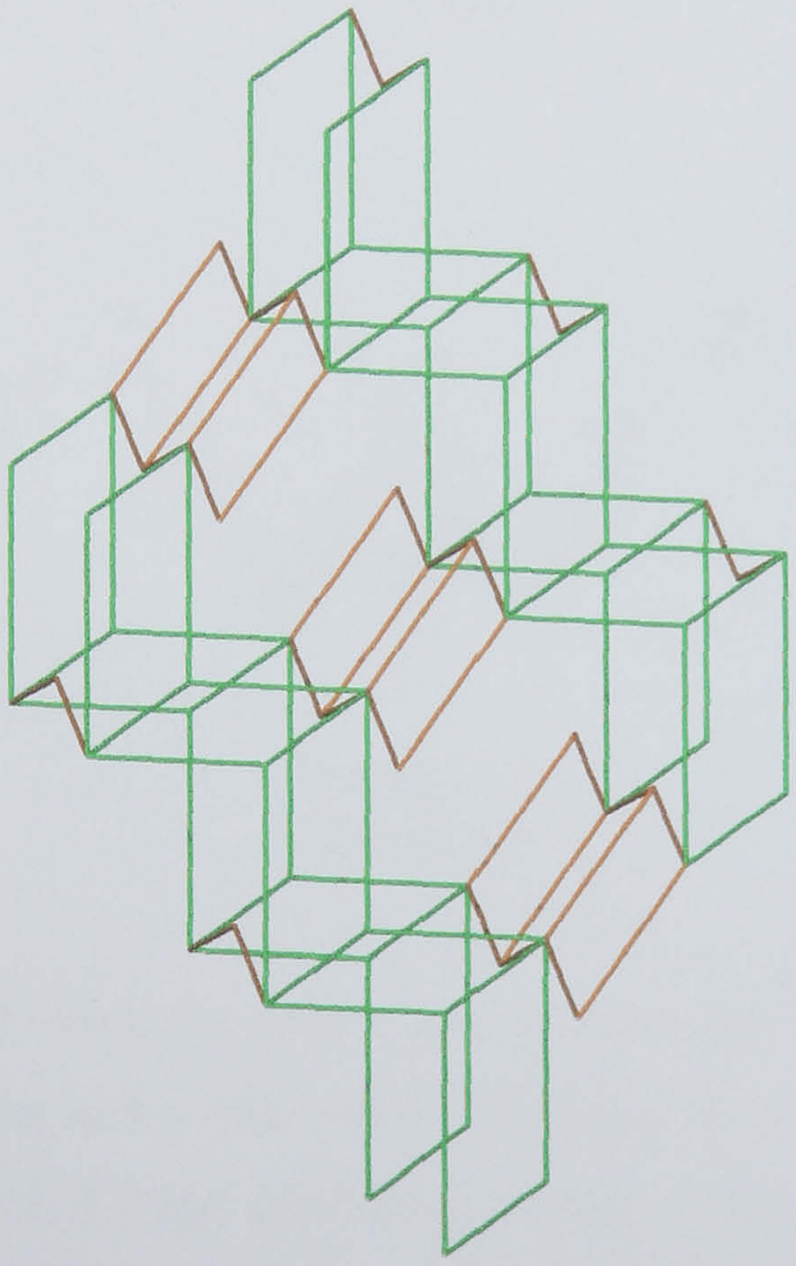

Figure 3.9 The network topology diagram from the crystal structure of complex **3.2**. The stepped ladder chains (shown as **B** in Figure 3.7) are represented entirely in green. The near linear chains (shown as **A** in Figure 3.7) are represented entirely in orange and are shown to join the stepped ladders at the six-connecting calixarene nodes.

3.1.3 Structure of the discrete 4:3 Pr(III):SO_3[4] complex $[(Pr(H_2O)_8)_2(Pr(H_2O)_6)(Pr(H_2O)_7)$(*p*-sulfonatocalix[4]arene)$_3][(Pr(H_2O)_8)_2(Pr(H_2O)_7)_2$(*p*-sulfonatocalix[4]arene)$_3]\cdot 25.5H_2O$, 3.3.

Crystals of the complex $[(Pr(H_2O)_8)_2(Pr(H_2O)_6)(Pr(H_2O)_7)$(*p*-sulfonatocalix[4]arene)$_3]$ $[(Pr(H_2O)_8)_2(Pr(H_2O)_7)_2$(*p*-sulfonatocalix[4]arene)$_3]\cdot 25.5H_2O$, **3.3**, grew slowly upon addition of excess praseodymium(III) perchlorate to a solution of penta-sodium *p*-sulfonatocalix[4]arene (Equation 3.3). The complex was characterised by IR spectroscopy and single crystal X-ray crystallography. Complex **3.3** crystallises in a triclinic cell and the structural solution was performed in the space group $P\bar{1}$. Details of the data collection and structure refinement are given in Table 3.6 of this chapter. A crystallographic information file containing all bond lengths and angles for complex **3.3** can be found in appendix 3.1.3 on the attached compact disc.

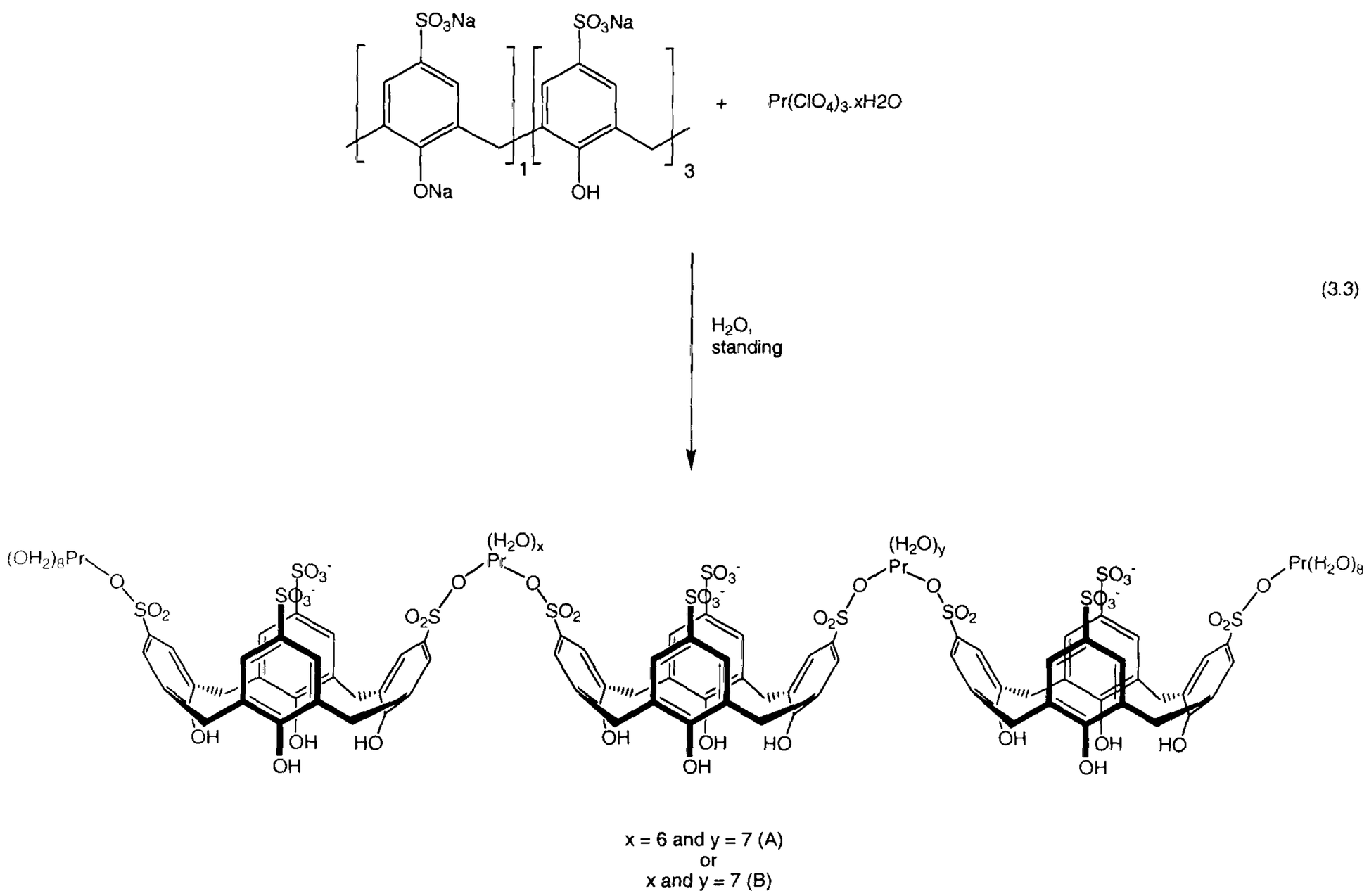

The asymmetric unit consists of two large, near-linear and discrete 4:3 Pr(III):SO_3[4] complexes, **A** and **B**, and a total of twenty five and a half water molecules of crystallisation that are disordered over forty six positions (Equation 3.2 and labelled according to Figure 3.10). All the metal centres in both complexes are nona-coordinate and the praseodymium centres that are ordered have tri-capped trigonal prismatic geometry. Despite there being significant disorder associated with some of the metal centres in addition to some of their respective aquo ligands, the praseodymium coordination spheres are of near tri-capped trigonal prismatic geometry. In addition to the disorder associated with some of the metal centres, several calixarene sulfonate groups and one SO_3[4]

molecule are also significantly disordered. Despite this extensive disorder in the overall structure, the data was modelled satisfactorily as indicated by a final value of $R_1 = 0.105$.

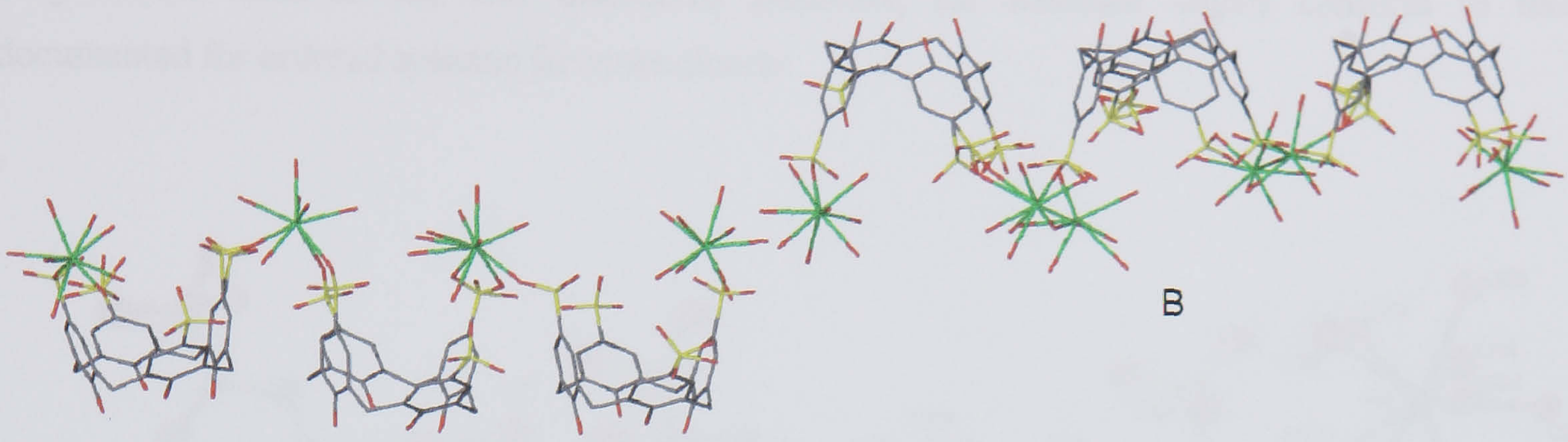

Figure 3.10 Stick representation of part of the asymmetric unit from the crystal structure of complex **3.3**. The two sections of the structure have been labelled **A** and **B** to aid discussion.

As mentioned in section 3.1 of this chapter, Detellier *et al.* reported that addition of lanthanum(III) chloride to a solution of SO_3H[4] resulted in the formation of large and discrete 8:6 La(III):SO_3[4] complexes.[52] Each of the discrete 4:3 Pr(III):SO_3[4] fragments in complex **3.3** is similar in structure to half of the superstructure reported by Detellier *et al.*[52] Although complex **3.3** formed with Na_5SO_3[4] as a starting material rather than the sulfonic acid, the presence of perchlorate anions may play a role in determining the overall supramolecular structure. This argument is strengthened by the fact that addition of praseodymium triflate to a solution containing Na_5SO_3[4] results in the formation of the 2-D coordination polymer described earlier in this chapter in relation to complex **3.2**. Given the size and varied praseodymium/sulfonate coordination associated with **A** and **B**, each will be discussed as separate entities before discussing the overall extended structure.

The two 'end' SO_3[4] molecules (S(1)-S(5) and S(10)-S(13)) in the near-linear arrangement, fragment **A**, each have a sulfonate bound octa-aqua praseodymium metal centre (Pr(1) and Pr(2), Figure 3.11). The central SO_3[4] molecule (S(6)-S(9)) is joined to the S(1)-S(5) calixarene by a hepta-aqua praseodymium metal centre (Pr(5)). The central SO_3[4] is also joined to the S(10)-S(13) calixarene by a hexa-aqua praseodymium metal centre (Pr(6)). The difference in the number of aquo ligands associated with each of the central praseodymium metal centres is due to the fact that Pr(6) forms a chelate ring with two oxygen atoms (O(34) and O(35)) of the S(7) sulfonate group of the S(6)-S(9) calixarene. There are only a few reported examples of such lanthanide chelation with *p*-sulfonatocalix[*n*]arenes although chelation of an aryl sulfonate to lanthanum has also been reported.[102, 105, 106] The bond distances and angles associated with the chelate in complex **3.3** are of a greater magnitude to the similar complexes that have been reported and to those listed for complex

2.8 in this thesis. This difference is likely to be due to the fact that the metal centre is only bound to O(34) when in one of two disordered positions (Table 3.2).[102, 105, 106] In addition to this, if a centroid is generated between the two disordered positions, the resultant angles conform to those documented for ordered systems far more closely.

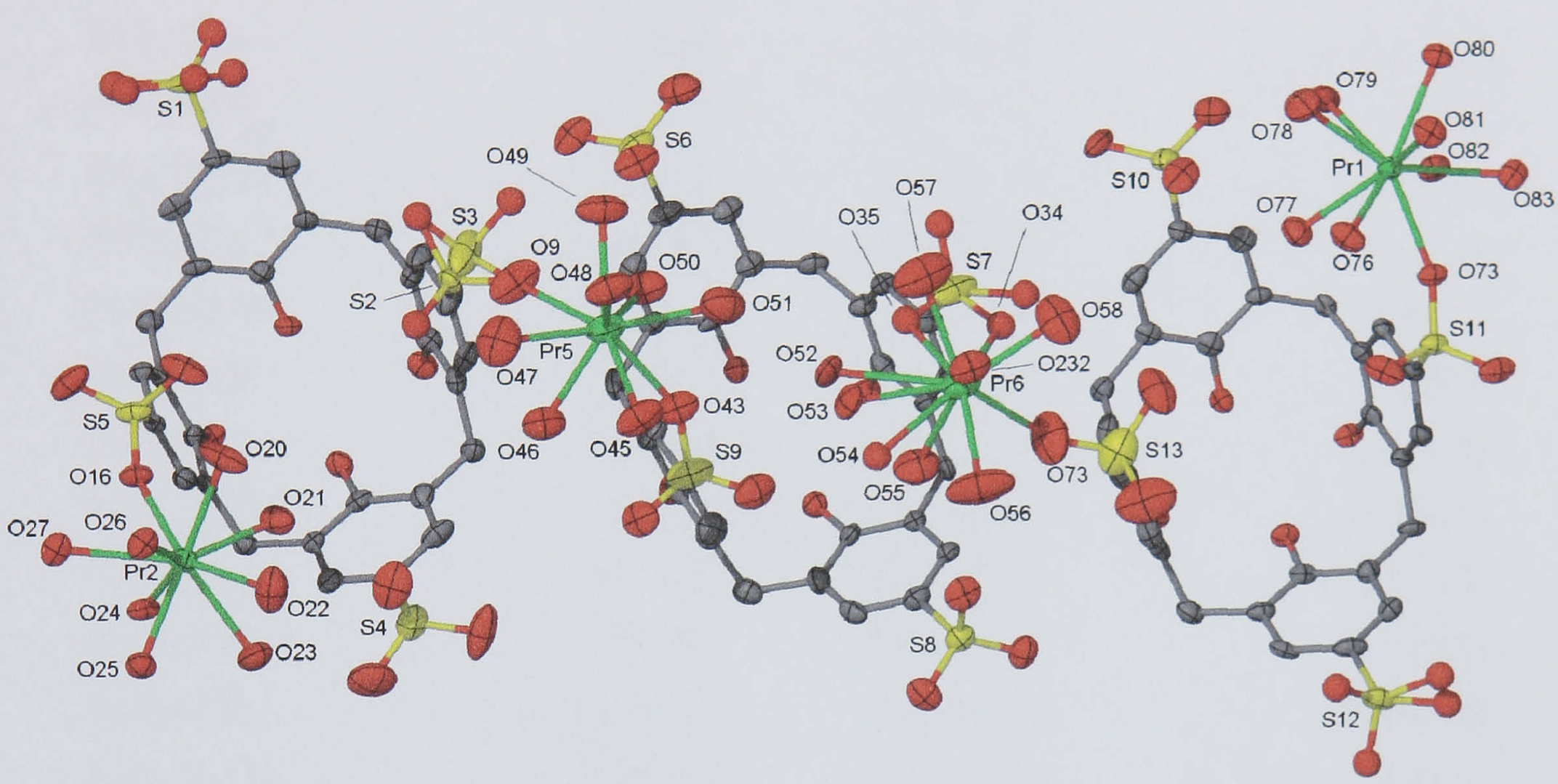

Figure 3.11 Part **A** of the asymmetric unit of the crystal structure of complex **3.3**, anisotropic displacement ellipsoids shown at the 50% probability level. Some sulfonate oxygen atoms are shown in ball and stick representation and selected atoms have been labelled.

In stark contrast to part **A,** several sulfonate groups, aquo ligands and a quarter of one SO_3[4] molecule in **B** show significant disorder (Figure 3.12). Given the disorder associated with **B**, a table of interatomic distances relating to the praseodymium coordination spheres has not been compiled. In similarity to **A**, all the praseodymium metal centres in part **B** are nona-coordinate and are of tri-capped trigonal prismatic geometry. The SO_3[4] molecules in **B** are also arranged in a similar manner to those in **A**. Essentially, the only difference between the two parts is a slight difference in the number of aquo ligands associated with the central praseodymium coordination spheres. This difference is that both of the central praseodymium atoms in **B** have seven aquo ligands whereas one central metal centre in **A** had six aquo ligands whilst the other had seven (as reflected in Equation 3.3). It should be mentioned that in order to preserve a good data to parameter ratio in the structure refinement, all of the carbon atoms in part **B** were refined isotropically. In fact similar data to parameter preservation was also required for the 8:6 discrete La(III):SO_3[4] complex reported by

Detellier *et al.*, the crystals of which presumably diffracted in a manner similar to those of complex **3.3**, that is, poorly.[52]

Pr(1)-O(63)	2.473(6)	Pr(1)-O(76)	2.540(8)
Pr(1)-O(77)	2.468(8)	Pr(1)-O(78)	2.473(8)
Pr(1)-O(79)	2.589(7)	Pr(1)-O(80)	2.508(7)
Pr(1)-O(81)	2.534(8)	Pr(1)-O(82)	2.482(8)
Pr(1)-O(83)	2.576(7)	Pr(2)-O(16)	2.495(7)
Pr(2)-O(20)	2.473(8)	Pr(2)-O(21)	2.467(8)
Pr(2)-O(22)	2.495(10)	Pr(2)-O(23)	2.595(8)
Pr(2)-O(24)	2.465(7)	Pr(2)-O(25)	2.491(7)
Pr(2)-O(26)	2.568(7)	Pr(2)-O(27)	2.628(7)
Pr(5)-O(9)	2.487(9)	Pr(5)-O(43)	2.568(8)
Pr(5)-O(45)	2.507(8)	Pr(5)-O(46)	2.538(10)
Pr(5)-O(47)	2.547(12)	Pr(5)-O(48)	2.511(9)
Pr(5)-O(49)	2.458(9)	Pr(5)-O(50)	2.540(9)
Pr(5)-O(51)	2.491(11)	Pr(6)-O(34)	2.651(16)
Pr(6)-O(35)	2.531(19)	Pr(6)-O(52)	2.81(3)
Pr(6)-O(53)	2.460(15)	Pr(6)-O(54)	2.69(3)
Pr(6)-O(55)	2.556(9)	Pr(6)-O(56)	2.473(10)
Pr(6)-O(57)	2.497(11)	Pr(6)-O(58)	2.448(12)
Pr(6)-O(73)	2.442(10)	Pr(6)-O(232)	2.532(9)
S(7)-O(34)-Pr(6)	112.3(8)	S(7)-O(35)-Pr(6)	114.4(9)
O(34)-S(7)-O(35)	87.8(10)		

Table 3.2 Interatomic distances between selected atoms in the crystal structure of complex **3.3**. Angles between vectors relating to the praseodymium/sulfonate chelate of the Pr(6) metal centre in the crystal structure of complex **3.3** are also listed (distances given in Å and angles given in ° with e.s.d. in parentheses).

One other similarity between parts **A** and **B** of complex **3.3** is that all six SO_3[4] molecules in the asymmetric unit are pinched in the C_2 symmetric fashion. This occurs with SO_3[4] dihedral angles ranging from 99.46 – 109.80° and 134.41 – 145.54° between the pinching and splaying pairs of phenyl rings respectively. There are numerous disordered water molecules residing within the molecular clefts and they are positioned within typical hydrogen-bonding distances with sulfonate

groups or praseodymium aquo ligands. Only one of these water molecules (at a partial occupancy of 0.5) is positioned with the possibility of OH···π interactions with the aromatic groups of the S(6)-S(9) SO_3[4] molecule (three possible interactions with O···aromatic centroid distances ranging from 3.154 – 3.656 Å). As is often the case, the quality of the data unfortunately did not allow location of the hydrogen atoms to confirm this phenomenon.

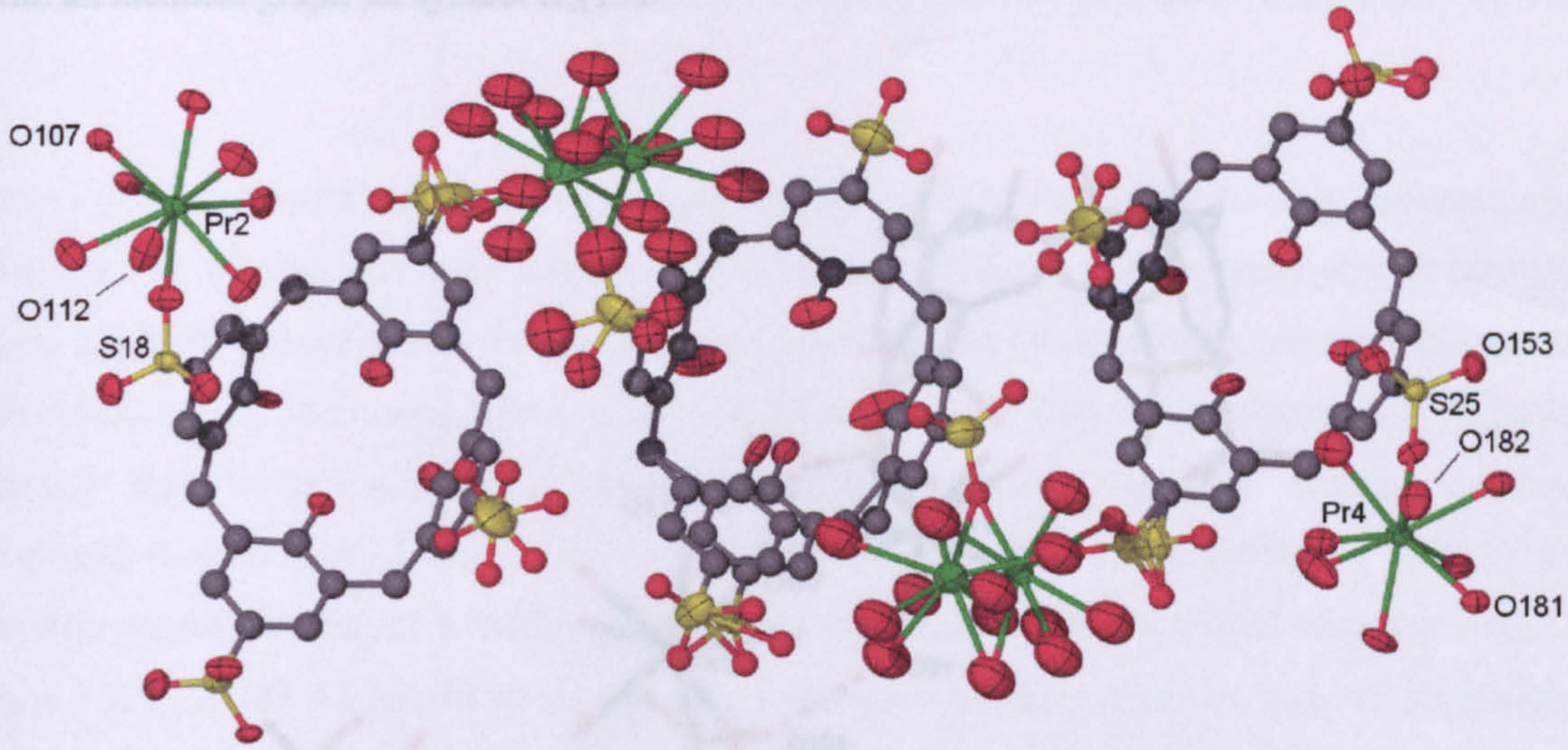

Figure 3.12 Part **B** of the asymmetric unit of the crystal structure of complex **3.3**, anisotropic displacement ellipsoids shown at the 50% probability level. All carbon and some sulfonate oxygen atoms are shown in ball and stick representation. Selected atoms have been labelled.

The extended structure of complex **3.3** shows several interesting features, the first being the hydrogen-bonding that occurs to link the 'ends' of parts A and B. This hydrogen-bonding arrangement is generic with both ends of each part and is in the form of rings between praseodymium aquo ligands and neighbouring sulfonate groups as illustrated in the Pr(1) – Pr(3) link in Figure 3.13. Praseodymium aquo ligand to SO_3[4] sulfonate hydrogen-bonding distances associated with the Pr(1) – Pr(3) and Pr(2) – Pr(4) links are listed in Table 3.3. As the importance of hydrogen bonds in determining behaviour in supramolecular chemistry became more recognised over time, a nomenclature system called Graph Set Analysis was devised by Margaret C. Etter.[14] This system was furthered by Bernstein and Davis and is used to describe any hydrogen-bonded system in terms of chains (C), rings (R), intramolecular patterns (S) or other varied finite shapes (D). Although this system could be used extensively in supramolecular systems of *p*-sulfonatocalix[n]arenes it is more useful when describing important structural features such as the hydrogen-bonding links in complex **3.3**. Each hydrogen-bonded system is assigned a descriptor that lists the type of system (C, R, S, or D), the number of donor atoms (d), the number of acceptor

atoms (a), and the total number of atoms involved in the format $C_d^a(n)$ for example. If we use the Pr(1) – Pr(3) link shown in Figure 3.13 as a working example, the hydrogen-bonding ring formed between Pr(3), O(107), O(102) and O(64) can be described by the graph set symbol $R_2^1(6)$ as there are two donor atoms, one acceptor atom and a total of four atoms in the ring. If similar treatment is applied to the two larger rings formed in the Pr(1) – Pr(3) link in Figure 3.13, we find two rings with an identical graph set symbol $R_2^2(12)$.

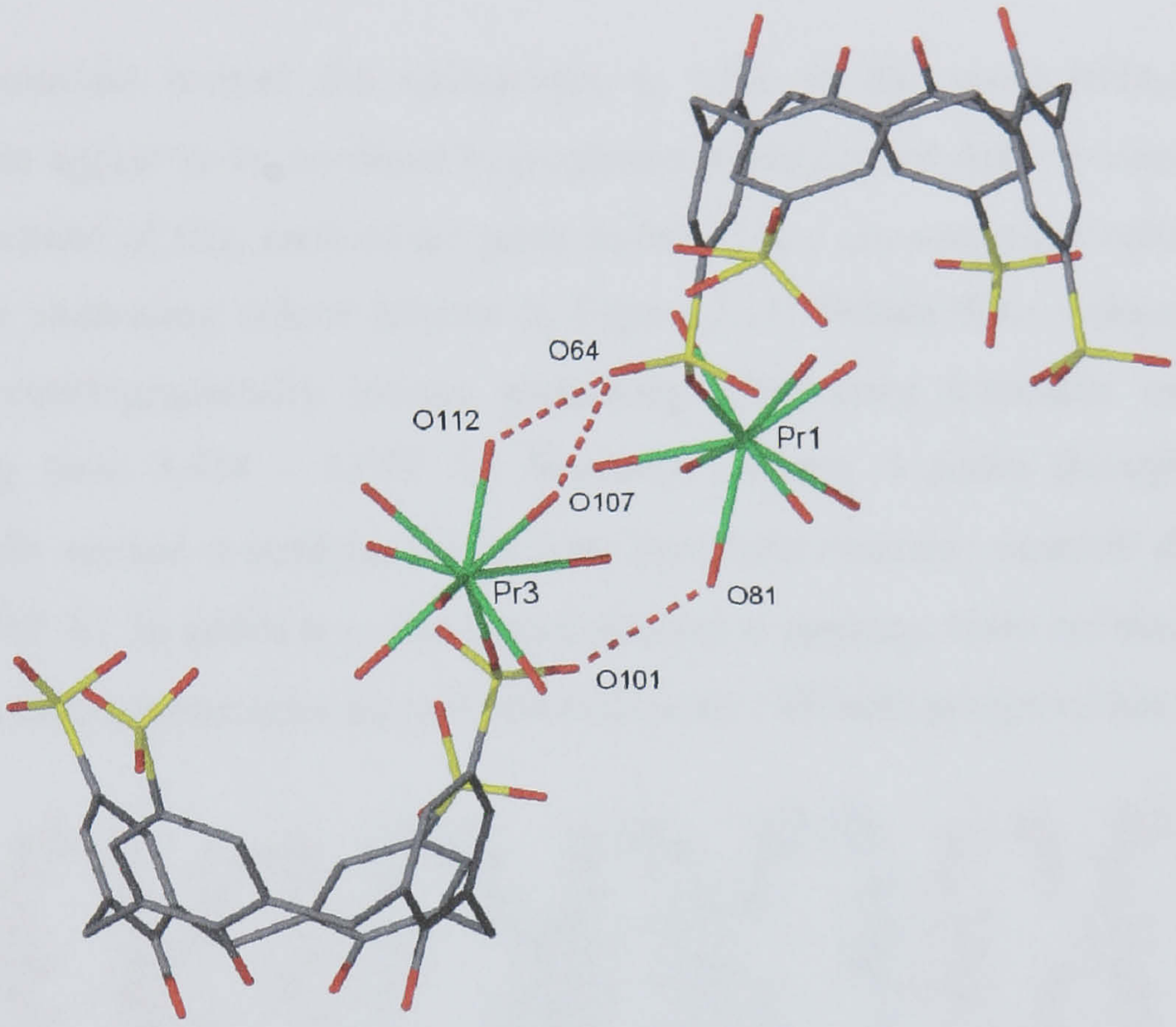

Key:

blue = donor atom
red = acceptor atom

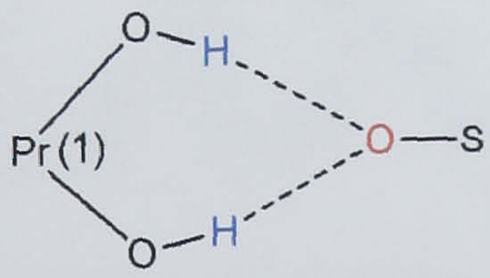

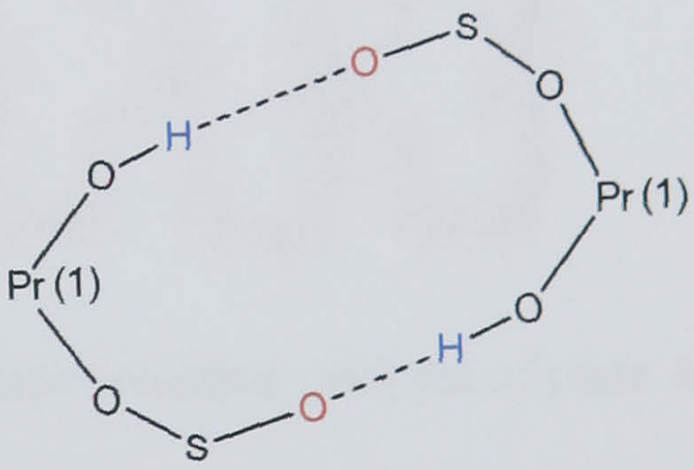

Graph Set Analysis:	$R_2^1(6)$	$R_2^2(12)$

Figure 3.13 An example of the generic hydrogen-bonding links found between the 'ends' of parts **A** and **B** in the crystal structure of complex **3.3**. A colour coded scheme for the graph set analysis associated with the hydrogen-bonding links is also shown.

O81(Pr1)···O101(S18)	2.747	O26(Pr2)···O153(S25)	2.739
O107(Pr3)···O64(S11)	2.772	O181(Pr4)···O17(S5)	2.893
O112(Pr3)···O64(S11)	2.687	O182(Pr4)···O17(S5)	2.690

Table 3.3 Praseodymium aquo ligand to SO_3[4] sulfonate hydrogen-bonding distances associated with the Pr(1) – Pr(3) and Pr(2) – Pr(4) links in the crystal structure of complex **3.3** (distances given in Å).

The extended structure reveals the calixarenes to pack in the usual bi-layer arrangement. Interestingly, there appear to be no direct hydrophobic π-stacking or ArH···π interactions between parts **A** and **B**. Instead of this, each of the parts assemble in a uni-composite columnar manner as illustrated by the alternating colour scheme in Figure 3.14. Within these columns part **A** packs through four crystallographically unique π-stacking interactions (aromatic centroid···centroid distances ranging from 3.434 – 3.679 Å). Similarly, column B packs through a total of six crystallographically unique π-stacking interactions (aromatic centroid···centroid distances ranging from 3.522 – 3.767 Å). In addition to this intra-columnar π-stacking, there are numerous hydrogen bonds between praseodymium aquo ligands and calixarene sulfonate groups within these columns.

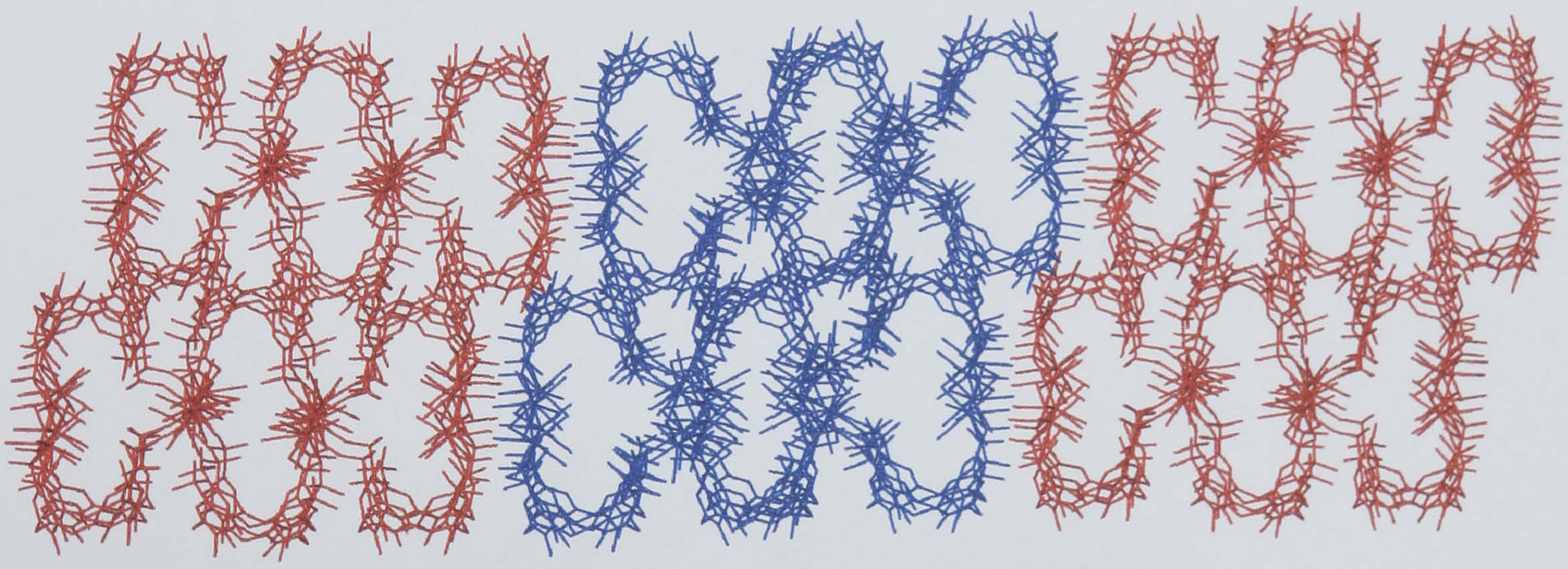

Figure 3.14 Extended structure of complex **3.3** showing the alternate columnar packing of parts **A** (red) and **B** (blue).

One of the reaction mixtures containing crystals of complex **3.3** was left to stand for some time and when undisturbed over a period of three months, very slow evaporation and reaction mixture concentration occurred. During this time the colour of the mixture darkened and upon inspection all of the crystals of complex **3.3** (colourless plates) had re-dissolved and re-grown as large green/yellow prisms. The X-ray structure revealed that the crystals were a bi-layer arrangement of an unusual praseodymium/SO_3[4]/sodium/perchlorate complex.

3.1.4 Structure of the complex $[(Pr(H_2O)_8)(p\text{-sulfonatocalix[4]arene})][(Pr(H_2O)_8)_2(Na(H_2O)_2)(ClO_4)_2(p\text{-sulfonatocalix[4]arene})]\cdot 9.5H_2O$, 3.4.

Crystals of the complex $[(Pr(H_2O)_8)(p\text{-sulfonatocalix[4]arene})][(Pr(H_2O)_8)_2(Na(H_2O)_2)(ClO_4)_2(p\text{-sulfonatocalix[4]arene})]\cdot 9.5H_2O$, **3.4**, grew over three months with very slow evaporation of a reaction mixture containing crystals of complex **3.3** (Equation 3.4). Over this period, the crystals had a new morphology and colour, re-dissolving from colourless plates to re-crystallise as large green/yellow prisms. The complex was characterised by IR spectroscopy and single crystal X-ray crystallography. Complex **3.4** crystallises in a triclinic cell and the structural solution was performed in the space group $P\bar{1}$. Details of the data collection and structure refinement are given in Table 3.6 of this chapter. A crystallographic information file containing all bond lengths and angles for complex **3.4** can be found in appendix 3.1.4 on the attached compact disc.

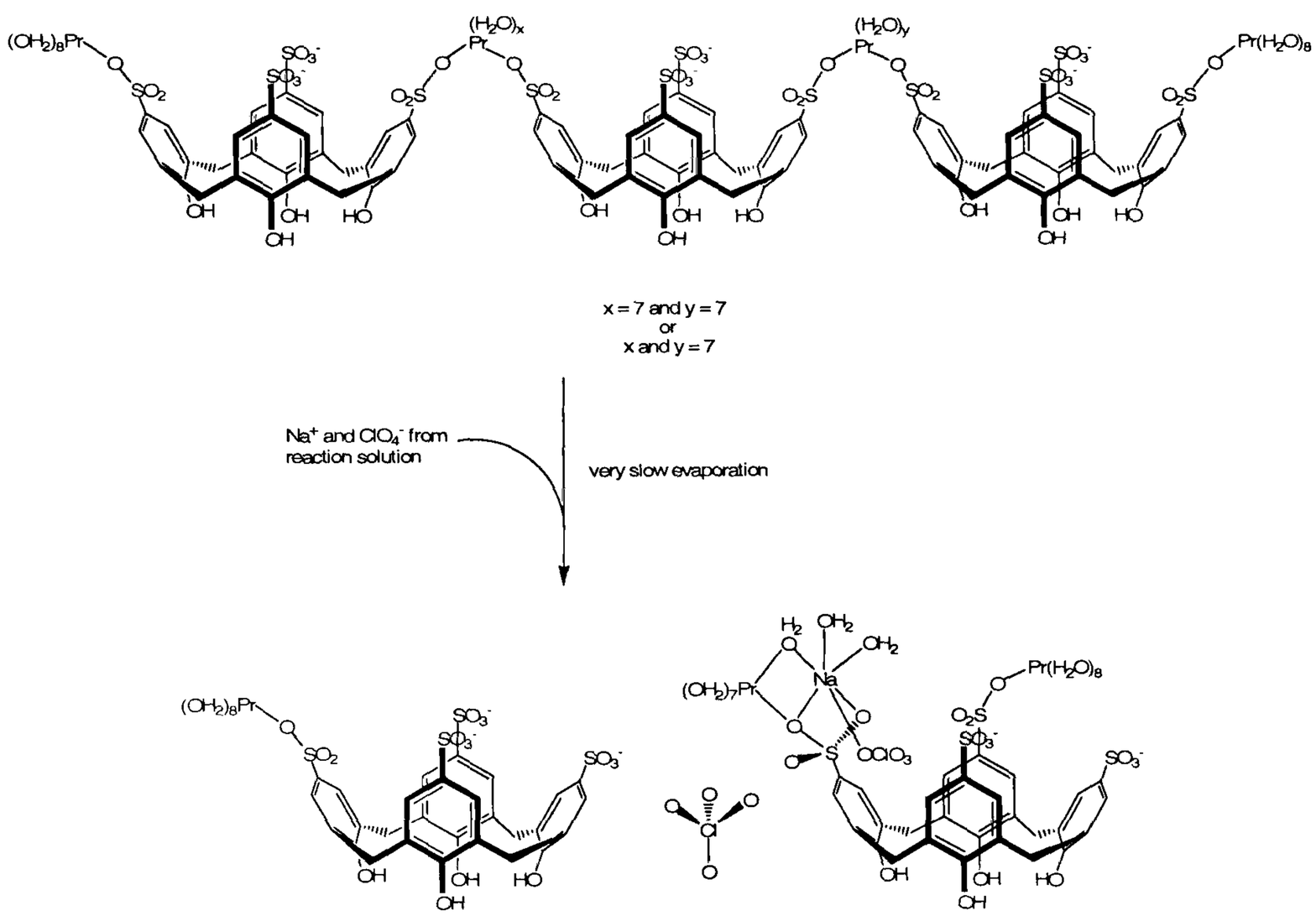

The asymmetric unit, as shown in Figure 3.15, comprises one praseodymium/SO_3[4] complex, one bi-metallic praseodymium/sodium/SO_3[4]/perchlorate complex, one free perchlorate anion and a total of nine and a half water molecules that are disordered over a total of eleven positions. To aid clarity, each of the parts **A** and **B** (as depicted by the dashed line in Figure 3.15) will be discussed separately before going on to examine the extended structure.

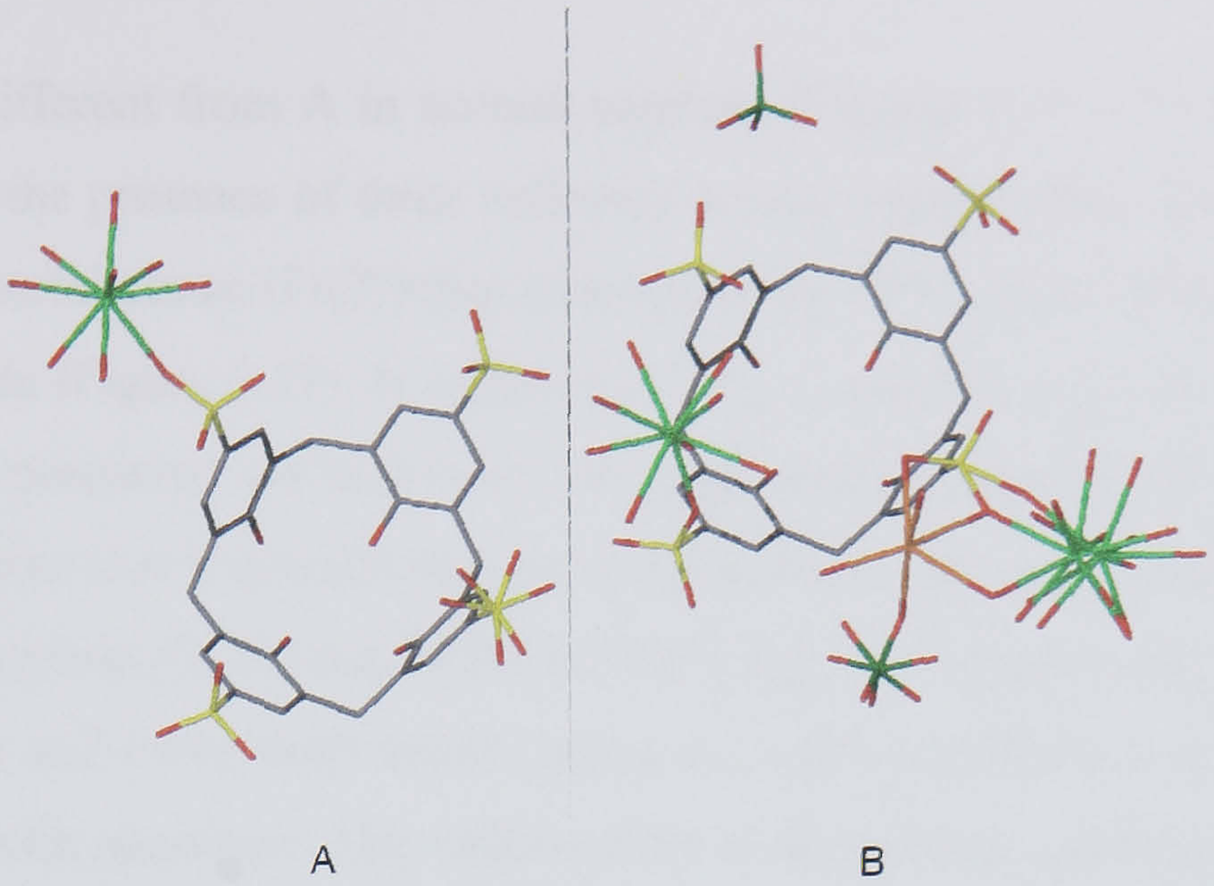

Figure 3.15 Stick representation of the asymmetric unit of the crystal structure of complex **3.4**. A dashed line has been inserted to clarify the components of the complex that are included in the discussion of parts **A** and **B**.

Part **A** is a 1:1 Pr(III):SO_3[4] moiety and Pr(1) is bound to the calixarene through the O(2) atom of the S(1) sulfonate group (Figure 3.16). In fact this structural fragment is very similar to that found in the asymmetric unit of complex **2.2** of this thesis although the dihedral angles of the calixarenes in both structures are slightly different (Figure 2.6). In complex **2.2**, the calixarene has dihedral angles of 109.1 and 141.5° whilst those of the SO_3[4] molecule in part **A** of complex **3.4** are 108.4 and 129.7°. The praseodymium metal centre Pr(1) of complex **3.4** is nona-coordinate with eight aquo ligands and has tri-capped trigonal prismatic geometry. Bond distances relating to the coordination sphere of Pr(1) are listed in Table 3.4.

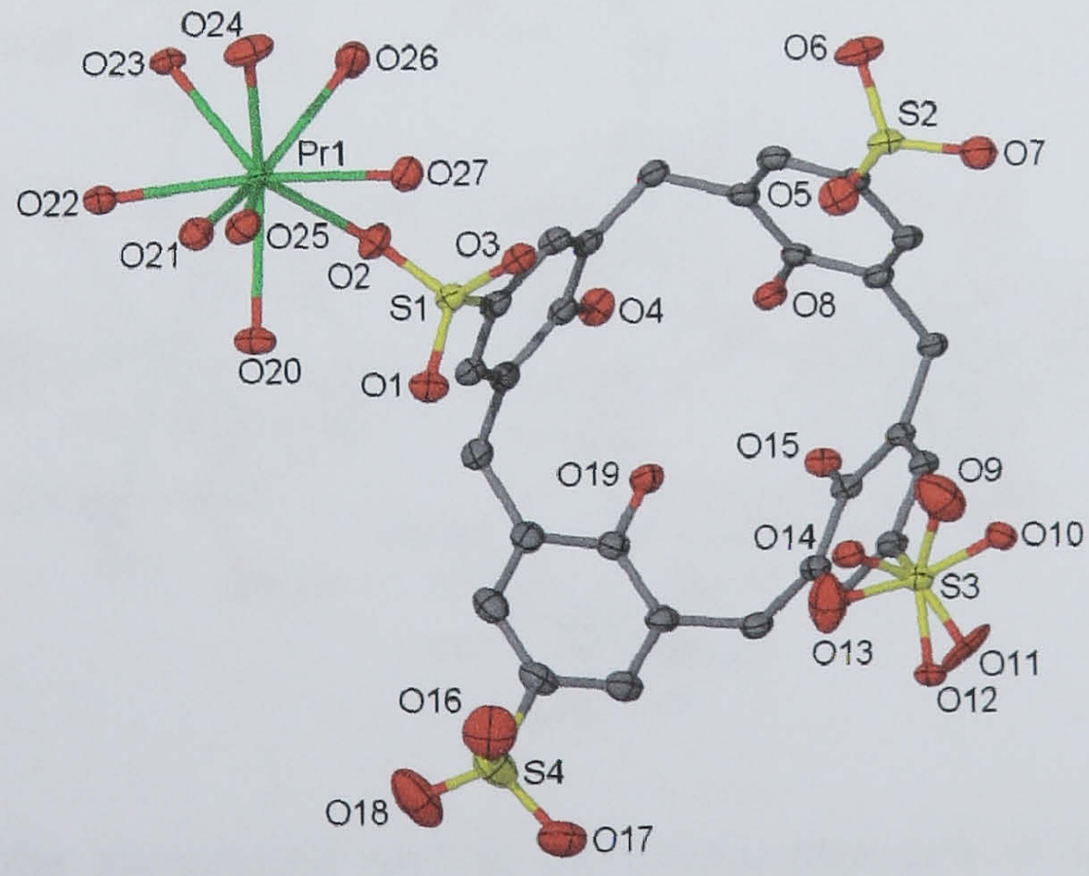

Figure 3.16 Part **A** of the asymmetric unit in the crystal structure of complex **3.4**, anisotropic displacement ellipsoids shown at the 50% probability level. Selected atoms have been labelled.

Part **B** is markedly different from **A** in several respects (Figures 3.15 – 3.17). The first and most striking difference is the presence of three sulfonate bound metal centres. One of these is an octa-aqua praseodymium metal centre (Pr(2)) that is bound to the O(33) atom of the S(6) sulfonate group of the SO_3[4] molecule (Figure 3.17). In addition to this, a sodium atom and a praseodymium atom (disordered over two positions) are both bound through oxygen atoms to the S(5) sulfonate group. The praseodymium atom that is disordered over two positions is bound through a disordered oxygen atom of the sulfonate group (O(30) and O(29) for Pr(3) and Pr(4) respectively). Despite the disorder associated with Pr(3) and Pr(4), both metal centres are nona-coordinate and have typical near tri-capped trigonal prismatic geometry. The sodium atom is of distorted octahedral geometry and forms a chelate ring with the O(30) and O(31) oxygen atoms of the SO_3[4] S(5) sulfonate group. The sodium atom has two aquo ligands, is coordinated to one of the aquo ligands of the Pr(3) metal centre (O(58)), and is also bound to a perchlorate anion through the O(63) atom (Figure 3.17). Bond distances and selected angles relating to the metal coordination spheres and the sodium/SO_3[4] sulfonate chelate ring are listed in Table 3.4. Notably, the angles relating to the sodium/sulfonate chelate ring are of comparable magnitude to those observed in the tetra-sodium salt of *p*-sulfonatocalix[4]arene reported by Atwood *et al.*[25, 26]

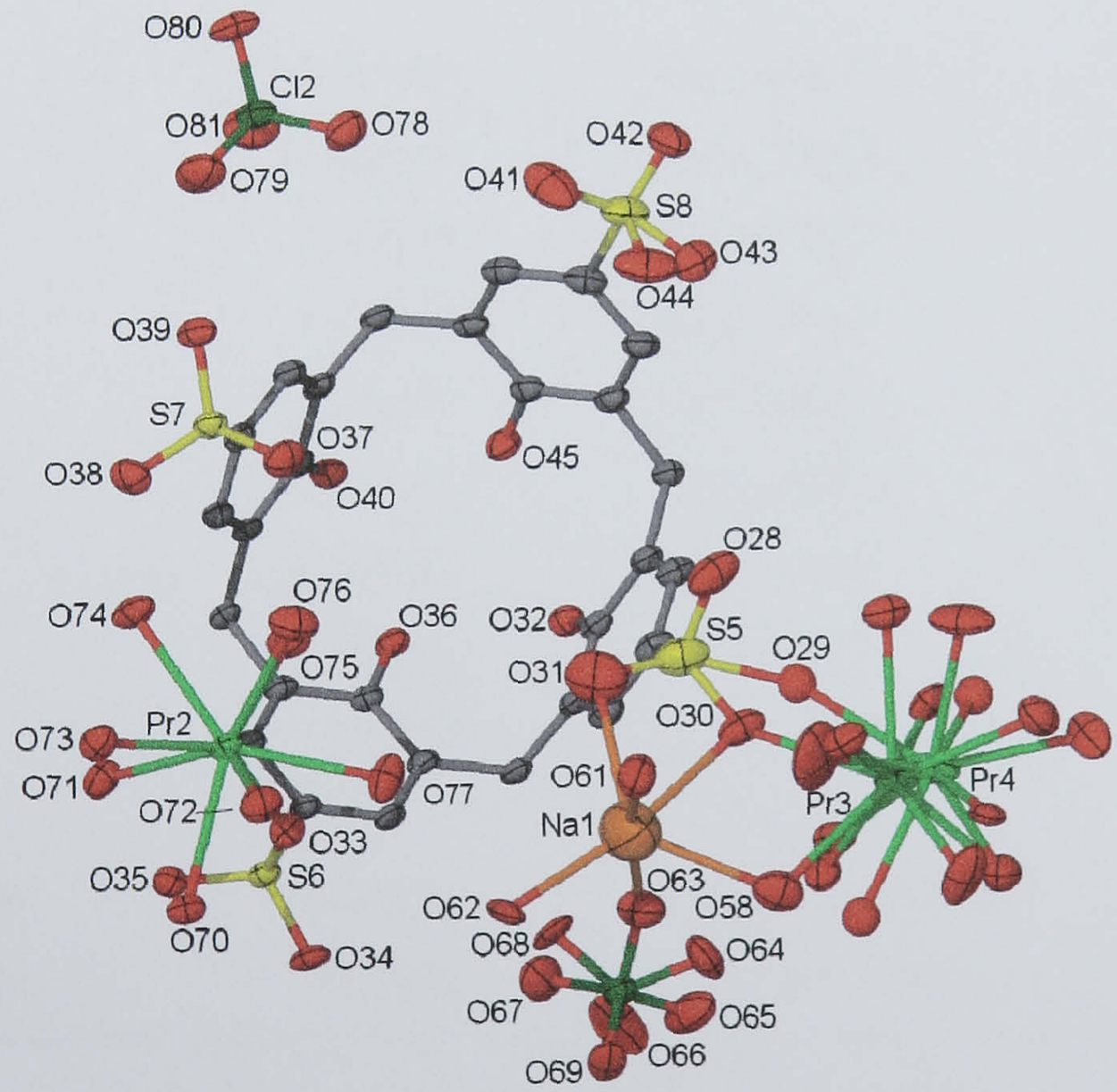

Figure 3.17 Part **B** of the asymmetric unit in the crystal structure of complex **3.4**, anisotropic displacement ellipsoids shown at the 50% probability level. Some disordered praseodymium aquo ligands and one sulfonate oxygen atom are shown in ball and stick representation. Selected atoms have been labelled.

Another unusual feature associated with complex **3.4** is that the perchlorate anions are nestled (free) or directed (bound) into voids in the hydrophobic layer (Figure 3.18). In fact a survey of all of the crystal structures containing SO_3[4] on the Cambridge Crystallographic Data Centre shows only one other structure that has an anion included in a bi-layer arrangement.[44]

Pr(1)-O(2)	2.552(3)	Pr(1)-O(20)	2.504(3)
Pr(1)-O(21)	2.487(3)	Pr(1)-O(22)	2.506(3)
Pr(1)-O(23)	2.527(3)	Pr(1)-O(24)	2.507(4)
Pr(1)-O(25)	2.490(3)	Pr(1)-O(26)	2.513(3)
Pr(1)-O(27)	2.533(3)	Pr(2)-O(33)	2.536(3)
Pr(2)-O(70)	2.561(3)	Pr(2)-O(71)	2.475(3)
Pr(2)-O(72)	2.557(3)	Pr(2)-O(73)	2.486(3)
Pr(2)-O(74)	2.520(3)	Pr(2)-O(75)	2.576(4)
Pr(2)-O(76)	2.470(3)	Pr(2)-O(77)	2.492(4)
Pr(3)-O(30)	2.550(5)	Pr(3)-O(58)	2.626(6)
Pr(4)-O(29)	2.60(2)		
Na(1)-O(31)	2.521(8)	Na(1)-O(30)	2.604(8)
Na(1)-O(61)	2.268(10)	Na(1)-O(58)	2.493(8)
Na(1)-O(63)	2.478(7)	Na(1)-O(62)	2.299(8)
Cl(1)-O(63)	1.473(5)	Cl(1)-O(64)	1.413(18)
Cl(1)-O(65)	1.396(5)	Cl(1)-O(66)	1.549(18)
Cl(1)-O(67)	1.410(5)	Cl(1)-O(68)	1.378(16)
Cl(1)-O(69)	1.445(4)	Cl(2)-O(78)	1.450(4)
Cl(2)-O(79)	1.429(4)	Cl(2)-O(80)	1.430(4)
Cl(2)-O(81)	1.428(4)		
Na(1)-O(58)-Pr(3)	107.9(2)	Pr(3)-O(30)-Na(1)	106.9(2)
S(5)-O(30)-Na(1)	95.7(3)	S(5)-O(31)-Na(1)	97.5(3)

Table 3.4 Interatomic distances between selected atoms in the crystal structure of complex **3.4**. Angles between vectors relating to the sulfonate chelate of the sodium metal centre and the metal bridging water molecules are also listed (distances given in Å and angles given in ° with e.s.d. in parentheses).

That structure, reported by Raston *et al.* showed perchlorate anions to be bound by sodium ions that also coordinated to sulfonate groups of the calixarenes. The perchlorate anions were directed into a hydrophobic layer of an extended bi-layer arrangement, a situation similar to that found in **B**. In the reported structure the calixarenes were part of 'Russian dolls' with sodium *bis*-aqua/18-crown-6 guests and poly-nuclear rhodium counterions.[44] Clearly, perchlorate anions are of a suitable size for inclusion in hydrophobic layers of SO_3[4] bi-layer arrangements and the formation of complex **3.4** has demonstrated that this can occur in the absence of metal/perchlorate coordination (Figure 3.18). In particular, the formation of complex **3.4** has demonstrated the true ability of bi-layer arrangements containing SO_3[4] to adapt to many different chemical environments whilst maintaining their common form.

The extended structure of complex **3.4** shows the calixarenes to pack in the bi-layer arrangement. This occurs through a total of four crystallographically unique π-stacking interactions with aromatic centroid···centroid distances ranging from 3.831 – 4.159 Å. There appear to be no other significant hydrophobic interactions between the SO_3[4] molecules.

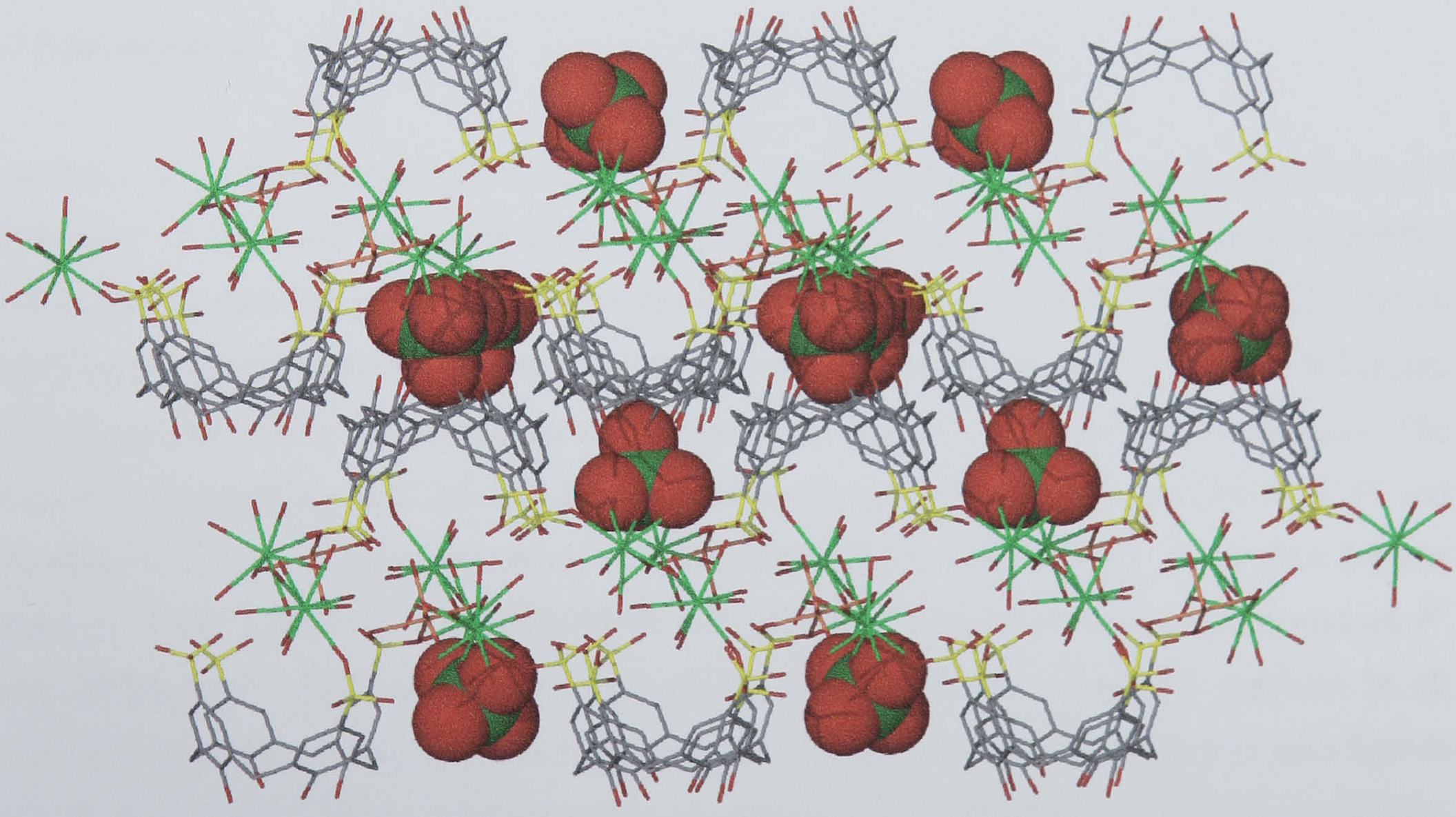

Figure 3.18 The extended bi-layer structure in the crystal structure of complex **3.4** showing the inclusion of the perchlorate anions (shown in space filling) within the hydrophobic layers.

3.2 Conclusion.

Relatively few metal complexes of *p*-sulfonatocalix[4]arene that are formed in the absence of guest molecules other than solvent molecules have been reported to date (excepting alkali metal salts). Those that have, however, have shown some interesting supramolecular structural motifs that are sometimes of surprising size and complexity. The results reported in this chapter are the result of a short study of lanthanide metals (praseodymium primarily) and anion effects in supramolecular structure formation with SO_3[4]. Yaghi *et al.* amongst others have shown that coordination polymers (amongst other materials) or 'metal organic frameworks' (MOF's) often possess desirable properties such as the ability to adsorb large quantities of various gases.[11, 12] Given the results described in this chapter, a more thorough study of an entire range of available praseodymium metal salts (as well as a range of other metal salts) would likely prove fruitful and may uncover numerous interesting and unusual supramolecular architectures. This is stressed by thte fact that in complexes **3.1 – 3.4**, incorporation of a harder anion (nitrate) dramatically alters the structure and results in the formation of a 3-D coordination polymer. The ability to control the formation of extended lanthanide/SO_3[4] complexes may prove useful in tuning these systems to suit desired applications in the future.

3.3 Experimental.

p-Sulfonic acid calix[4]arene was synthesised by literature methods and purity was checked via ^{1}H NMR spectroscopy.[8] All lanthanide metal salts were purchased from Aldrich and used as supplied without further purification. X-ray data for complexes **3.1 – 3.4** were collected at 150(2) K on an Enraf-Nonius KappaCCD diffractometer with Mo-Kα radiation. Data were corrected for Lorentz and polarisation effects and absorption corrections were applied using multi-scan techniques. The structures of complexes **3.1**, **3.2** and **3.4** were solved by direct methods using SHELXS-97 and refined with full-matrix least squares on F^2 using SHELXL-97. The structure of complex **3.3** was solved by direct methods using SHELXS-97 and refined with BLOC-matrix least squares on F^2 using SHELXL-97. Hydrogen atoms were placed at geometrically calculated positions in all complexes. Hydrogen atoms for water molecules of crystallisation and praseodymium aquo ligands were located in the Fourier difference map of complex **3.2**, assigned and refined accordingly. Infrared spectra were run as KBr discs on a MIDAC FT-IR spectrometer. Microanalyses were not performed on crystals that showed visual degradation upon removal from the mother liquor (all but complex **3.2**).

3.3.1 Synthesis of the 2-D hydrogen-bonded network $[M(H_2O)_8][p$-sulfonatocalix[4]arene + H+]$\cdot 4H_2O$ (M = Gd, Tb, Tm), 3.1.

Terbium(III) chloride (10 mg, 37.7 μmol), *p*-sulfonic acid calix[4]arene (10 mg, 13.4 μmol) and [2.2.2]cryptand (8 mg, 21.3 μmol) were dissolved in distilled water (1 cm^3). On slow evaporation over 1 week, colourless plates that were suitable for X-ray diffraction studies formed. Yield 7 mg, 42 %. IR(KBr disc, ν cm^{-1}): 3317s, 3159s, 2829m, 1634m, 1595m, 1459m, 1147s, 1117s, 1107s, 1041s. The minor changes in sulfonate group stretching frequencies suggests that the calixarene is non-coordinating, as was found in the crystal structure solution. **Isostructural complexes:** For Gd^{3+}, unit cell measurements were a = 13.4031(4), c = 15.0593(6) Å, T = 150(2) K, so it was assumed to be isostructural with the Tb^{3+} structure described earlier which was formed in the presence of [2.2.2]cryptand. Data collection and structure refinement showed the complex to be isostructural. The terbium, rather than gadolinium structure, was described in this chapter as the data of the latter was of poor quality resulting in a larger final R_1 of 0.0927. For Tm^{3+}, preparation method was identical to that of both the Tb^{3+} and Gd^{3+} analogues. The unit cell measurements were a = 13.3321(6), b = 13.3669(6), c = 14.8787(8) Å, T = 150K. The crystals were therefore assumed to be isostructural with both the Gd^{3+} and Tb^{3+} structures. Notably, crystals of the above structures could also be isolated *via* addition of the respective metal salt to a solution of SO_3H[4] in the absence of potential guest molecules, occurring with similar reaction yields. **X-ray crystallography**: Residual electron density is associated with a disordered water molecule of crystallisation.

3.3.2 Synthesis of the 3-D coordination polymer $[(M(H_2O)_4(NO_3))(M(H_2O)_5)p$-sulfonatocalix[4]arene$]\cdot 7H_2O$ (M^{3+} = Pr, Nd, Sm), 3.2.

Praseodymium(III) nitrate hexahydrate (40 mg, 90 μmol) and penta-sodium *p*-sulfonatocalix[4]arene (20 mg, 19 μmol) were dissolved in distilled water (2 cm^3). On standing over two days, large green crystals that were suitable for X-ray diffraction studies formed. Yield 22 mg, 87 %. IR (KBr disc, ν cm^{-1}): 3403s, 2937m, 1635s, 1597m, 1510s, 1475s, 1452s, 1431m, 1290s, 1269m, 1157s, 1122s, 1111s, 1045s. The increase in the number of sulfonate group stretching frequencies suggests lanthanide/sulfonate coordination, as was found in the crystal structure solution. Microanalysis calculated for $C_{28}H_{51}N_1O_{35}S_4Pr_2$: C, 24.52; H, 3.75; N, 1.02; S, 9.35. Found: C, 24.55; H, 3.65; N, 0.90; S, 9.40. **Isostructural complexes:** For Nd^{3+} the sample preparation procedure was identical except that neodymium(III) nitrate was used in place of the praseodymium analogue. The unit cell measurements were a = 10.5293(17), b = 15.1203(12), c =

16.8779(18), α = 65.9260(75), β = 84.1774(61), γ = 73.3150(80), T = 150(2) K. For Sm^{3+} the sample preparation procedure was identical except that samarium(III) nitrate was used in place of the praseodymium analogue. The unit cell measurements were a = 10.5068(15), b = 15.1559(24), c = 16.8234(21), α = 65.3561(107), β = 83.6572(84), γ = 73.0631(108), T = 150(2) K. On this basis, all three unit cell determinations suggest isostructural complexes to that for praseodymium. **X-ray crystallography**: Some bond lengths were restrained to be chemically meaningful.

Complex number	**3.1**	**3.2**
Formula	$C_{28}H_{68}O_{40}S_4Tb_1$	$C_{28}H_{51}N_1O_{35}Pr_2S_4$
*M*r	333.0	1371.76
Crystal system	Tetragonal	Triclinic
Space group	*P*4/*n*	$P\bar{1}$
T/K	150(2)	150(2)
a /Å	13.4475(4)	10.4483(1)
b /Å	13.4475(4)	15.0282(2)
c /Å	15.0257(4)	16.7750(2)
α /°	90	65.385(1)
β /°	90	83.952(1)
γ /°	90	73.595(1)
U Å^3	2717.18(14)	2296.92(5)
Z	8	2
F(000)	1370	1376
ρ_{calc} /g cm^{-3}	1.628	1.983
μ /cm^{-1}	1.56	2.389
$\Theta_{min,\ max}$ /°	3.03, 25.99	3.09, 27.5
Data collected	9583	40564
Unique data	2671	10502
R_{int}	0.0389	0.0542
Obs data (I>2 $\sigma(I)$)	2608	9778
Parameters	162	762
Restraints	0	28
R_1 (observed data)	0.0753	0.0313
ωR_2 (all data)	0.1887	0.0838
S	1.296	1.04
Max/min residuals [eÅ^3]	1.459, -0.778	1.116, -1.939

Table 3.5 Details of data collection and structure refinement for complexes **3.1** and **3.2**.

3.3.3 Synthesis of the discrete 4:3 Pr(III):SO_3[4] complex $[(Pr(H_2O)_8)_2(Pr(H_2O)_6)(Pr(H_2O)_7)$(*p*-sulfonatocalix[4]arene)$_3$][$(Pr(H_2O)_8)_2(Pr(H_2O)_7)_2$(*p*-sulfonatocalix[4]arene)$_3$]·25.5H_2O, 3.3.

Praseodymium(III) perchlorate (41 mg, 90 μmol) and penta-sodium *p*-sulfonatocalix[4]arene (20 mg, 19 μmol) were dissolved in distilled water (2 cm^3). On standing over two days, large green crystals that were suitable for X-ray diffraction studies formed. Yield 10 mg, 58 %. IR (KBr disc. ν

cm^{-1}): 3346s, 2929m, 1632m, 1470m, 1425m, 1380m, 1220s, 1157s, 1110s, 1040s. The increase in the number of sulfonate group stretching frequencies suggests lanthanide/sulfonate coordination, as was found in the crystal structure solution. **X-ray crystallography**: One Pr(6) aquo ligand was disordered over three positions with partial occupancies of 0.25, 0.5 and 0.25. A sulfonate group of the S(1) – S(5) calixarene was disordered over two positions with equal occupancies. In the third position, the atom was refined isotropically. Two oxygen atoms of the S(1) sulfonate group are disordered over two positions at equal occupancy. Two oxygen atoms of the S(12) sulfonate group are disordered over two positions at partial occupancies of 0.7 and 0.3. The oxygen atoms of the S(16) sulfonate group are disordered over two positions at equal occupancy. A sulfonate group of the S(14) – S(18) calixarene was disordered over two positions with equal occupancies.

Complex number	**3.3**	**3.4**
Formula	$C_{168}H_{299}O_{180.50}Pr_8S_{24}$	$C_{56}H_{109}Cl_2NaO_{74.50}Pr_3S_8$
*M*r	7103.79	2747.53
Crystal system	Triclinic	Triclinic
Space group	$P\bar{1}$	$P\bar{1}$
T/K	150(2)	150(2)
a /Å	15.0234(1)	17.4508(1)
b /Å	15.5928(1)	18.1033(1)
c /Å	58.5798(6)	19.1983(2)
α /°	93.8115(4)	96.5645(3)
β /°	91.1433(6)	109.229(4)
γ /°	89.9803(4)	115.5645(4)
U Å^3	13689.63(19)	4926.68(6)
Z	2	2
F(000)	7214	2782
ρ_{calc} /g cm^{-3}	1.723	1.852
μ /cm^{-1}	1.694	1.809
$\Theta_{min,\ max}$ /°	1.9, 27.5	2.86, 27.5
Data collected	187167	98651
Unique data	57777	22520
R_{int}	0.1453	0.126
Obs data (I>2 $\sigma(I)$)	30778	20038
Parameters	2841	1453
Restraints	27	0
R_1 (observed data)	0.105	0.0544
ωR_2 (all data)	0.3284	0.1595
S	1.037	1.026
Max/min residuals [eÅ^3]	4.36, -2.239	1.915, -2.14

Table 3.6 Details of data collection and structure refinement for complexes **3.3** and **3.4**.

Two praseodymium metal centres and respective aquo ligands are disordered over two positions with partial occupancies of 0.6 and 0.4. Two oxygen atoms of the S(23) sulfonate group are

disordered over two positions at equal occupancy. One quarter of the S(19) – S(23) calix[4]arene sulfonate was disordered over two positions with equal occupancies. A sulfonate group of the S(24) – S(29) calixarene was disordered over three positions with partial occupancies of 0.4, 0.2, and 0.4. The oxygen atoms of the S(29) sulfonate group are disordered over two positions at equal occupancy. One oxygen atom of the S(24) sulfonate group is disordered over two positions at equal occupancy. Some water molecules of crystallisation and several calixarene sulfonate oxygen atoms were refined isotropically.

3.3.4 Synthesis of the complex $[(Pr(H_2O)_8)(p\text{-sulfonatocalix[4]arene})][(Pr(H_2O)_8)_2(Na(H_2O)_2)(ClO_4)_2(p\text{-sulfonatocalix[4]arene})]\cdot 9.5H_2O$, 3.4 .

A sample vial containing a reaction solution and crystals of complex **3.3** was left to stand and slowly evaporate over three months. The crystals of complex 3.3 appeared to have re-dissolved and crystallised complex 3.4 as large yellow/green crystals. Yield 12 mg, 46 %. IR (KBr disc, ν cm^{-1}): 3248s, 1635m, 1601m, 1452m, 1425w, 1159s, 1120s, 1043s. The increase in the number of sulfonate group stretching frequencies suggests lanthanide/sulfonate coordination, as was found in the crystal structure solution. **X-ray crystallography**: Three oxygen atoms of the Cl(1) perchlorate anion are disordered over two positions with partial occupancies of 0.8 and 0.2. The Pr(3) and Pr(4) metal centres, in addition to related aquo ligands are disordered over two positions with partial occupancies of 0.7 and 0.3. One Pr(4) aquo ligand (O(57)) was refined isotropically. One S(5) oxygen atom is disordered over two positions (O(29) and O(30)) with partial occupancies of 0.7 and 0.3. The O(29) partial occupancy sulfonate oxygen atom was refined isotropically. The oxygen atoms of the S(3) sulfonate group are disordered over two positions at partial occupancies of 0.8 and 0.2. Residual electron density is associated with the disordered sulfonate group oxygen atoms that coordinate to the Pr(3) and Pr(4) metal centres.

Chapter four:

Diffusion Ordered spectroscopy; Determination of *p*-sulfonatocalix[4]arene/guest association in solution.

4.0 Introduction.

This chapter is concerned with determining *p*-sulfonatocalix[4]arene/guest complexation in solution *via* the use of Diffusion Ordered Spectroscopy (DOSY). This chapter will give a brief introduction to some aspects of solution phase chemistry involving *p*-sulfonatocalix[*n*]arenes (*n* = 4,5,6,8). Latter discussion focuses on pulse field gradients (PFG's) and their application in 'pulse stimulated echos' and DOSY prior to describing the experimental results in detail. Notably the experiments and data manipulation were performed in collaboration with Dr. Julie Fisher at the University of Leeds.

The supramolecular chemistry of *p*-sulfonatocalix[4]arenes has been widely studied in the solid state as described in Chapter 1. The related solution phase chemistry encompasses several areas that include selective binding of quats and acetylcholine.[111, 112] Lower rim functionalised *p*-sulfonatocalix[*n*]arenes have also been used to some extent as catalytic receptors for the hydration of 1-benzyl-1,4-dihydronicotinamide.[113]

As described in Chapter 2, rapid crystallisation of molecular capsules containing mono or di-protonated (*bis*-)amino functionalised crown ethers and *p*-sulfonatocalix[4]arene was evident upon addition of lanthanide(III) metal cations to pre-prepared reaction solutions. The speed of crystallisation suggested some pre-organisation between the host and guest prior to addition of a suitable counterion. Given this, a series of experiments were undertaken using a recently developed technique, high-resolution DOSY NMR (section 4.1). This technique allows the determination of diffusion rates of individual molecules and complexes, if, indeed, host and guest are complexed at all, in order to calculate binding constants between the two in the absence of paramagnetic lanthanide metal cations. Guest molecule selection was based primarily on the majority of the structures described in Chapter 2 but was also extended to include a comparison on the formation of SO_3[4]/18-crown-6 Russian dolls using 18-crown-6 as a guest (Figure 4.1).

The calix[4]arene sulfonic acid, **1**, was reacted with guests **3** – **8** at an acidic pH (provided by the acidic protons of the calixarene) to ensure protonation of the amine groups within the macrocycles and thus probable electrostatic interaction with the calixarene sulfonate groups in solution. Both the sulfonic acid and sodium salt of the calixarene were reacted with guest **9** to determine whether a

neutral 18-crown-6 molecule or a sodium 18-crown-6 complex would bind more strongly with SO_3[4], or if indeed at all. The reaction solutions were not buffered as any other molecular species could interact with either the calixarene and/or the crown ether and possibly affect the results of the experiments. The notation of the experiments/systems are as follows; SO_3H[4]/diaza-18-crown-6 would be represented as **1·3** (see Figure 4.1). For each system a series of host:guest ratios were examined and these were, in general, as shown in Table 4.1 (a broader range of ratios were examined for system **1·8** as the spectrum was complex).

[H]	[G]
1.0	0
1.0	0.5
1.0	1.0
1.0	2.0
0	1.0

Table 4.1 Typical host:guest stoichiometries employed in the DOSY experiments described in this chapter.

Figure 4.1 The host (**1** and **2**) and guest (**3 – 9**) molecules selected for examination with DOSY ^{1}H NMR.

The results of the experiments confirmed *p*-sulfonatocalix[4]arene/guest complexation in solution with **3** – **8** at acidic pH and binding constants were calculated for all complexes formed. The results also showed that **1** did not bind **9** as a neutral species but incorporation of sodium ions *via* the use of **2** resulted in complex formation (albeit weak to intermediate).

4.1 Introduction and background of Pulse Field Gradients (PFG's) and Diffusion Ordered Spectroscopy (DOSY).

The NMR titration is one of the most widely used methods for the investigation of intermolecular complexation processes and this technique is frequently used in the field of supramolecular chemistry. The most frequent application reported of this technique is that of K_a (association constant) determination for host-guest complexes.[98] Until relatively recently K_a would be determined by measuring the changes in proton chemical shift as the concentration of host or guest was changed. However, with the ready availability of high field spectrometers equipped with pulsed field gradients, it is becoming more common to measure diffusion coefficients as a route to K_a (section 4.1.1).[114-116]

4.1.1 Pulse field gradients and diffusion coefficients.

Pulse field gradients can be used for several purposes, one of which is the suppression of a solvent resonance and this is achieved by defocusing and selectively refocusing the desired signals in the spectrum.[117] Once shims have been optimised for a sample in a magnetic field, all of the spins are considered to be in the same magnetic environment. It is possible to apply a gradient pulse to this environment in one direction, over a finite time, the result of which is that spins in molecules at different locations over the sample volume will experience different magnetic fields. Given a random distribution, the overall magnetisation is zero as the NMR resonance has been dephased/defocused (or destroyed, Figure 4.2a).[117] Once this operation has been performed, it is indeed possible to rephase/refocus (or recover) the signal by applying an equal pulse gradient but in the opposite direction after a short time (Figure 4.2b). The result of this second operation is the production of a gradient echo/observable signal. Overall, the result of both is that now the NMR signal is encoded with a 'location'.

Diffusion coefficients directly report molecular mobility and this may be correlated with molecular weight. Moreover they may be used to probe host-guest interactions on both fast and slow NMR timescales.[118] Diffusion coefficients may be determined from T_1 measurements for example, but it

is now more usual to employ what is termed 'pulse-gradient stimulated echo' sequences (PGSE)[119] or diffusion ordered spectroscopy techniques (DOSY)[120, 121]; which is based on PGSE but results in a diffusion coefficient-chemical shift 2-D map that is particularly useful for the analysis of complex mixtures. The 'pulse-gradient stimulated echo' is a technique similar to that shown in Figure 4.2 and is based on field gradients. Once a signal is defocused, it can only be completely refocused if a particular local field around a particular spin has not changed between the two pulses of the gradient. If a molecule moves/diffuses, a different local field will apply and any signal would only be partially refocused.[117] This difference can be measured and accounted for in order to calculate how far the molecule moved from the time of the first to second pulses. Thus altering the length and strength of the pulses allows the calculation of a diffusion coefficient.

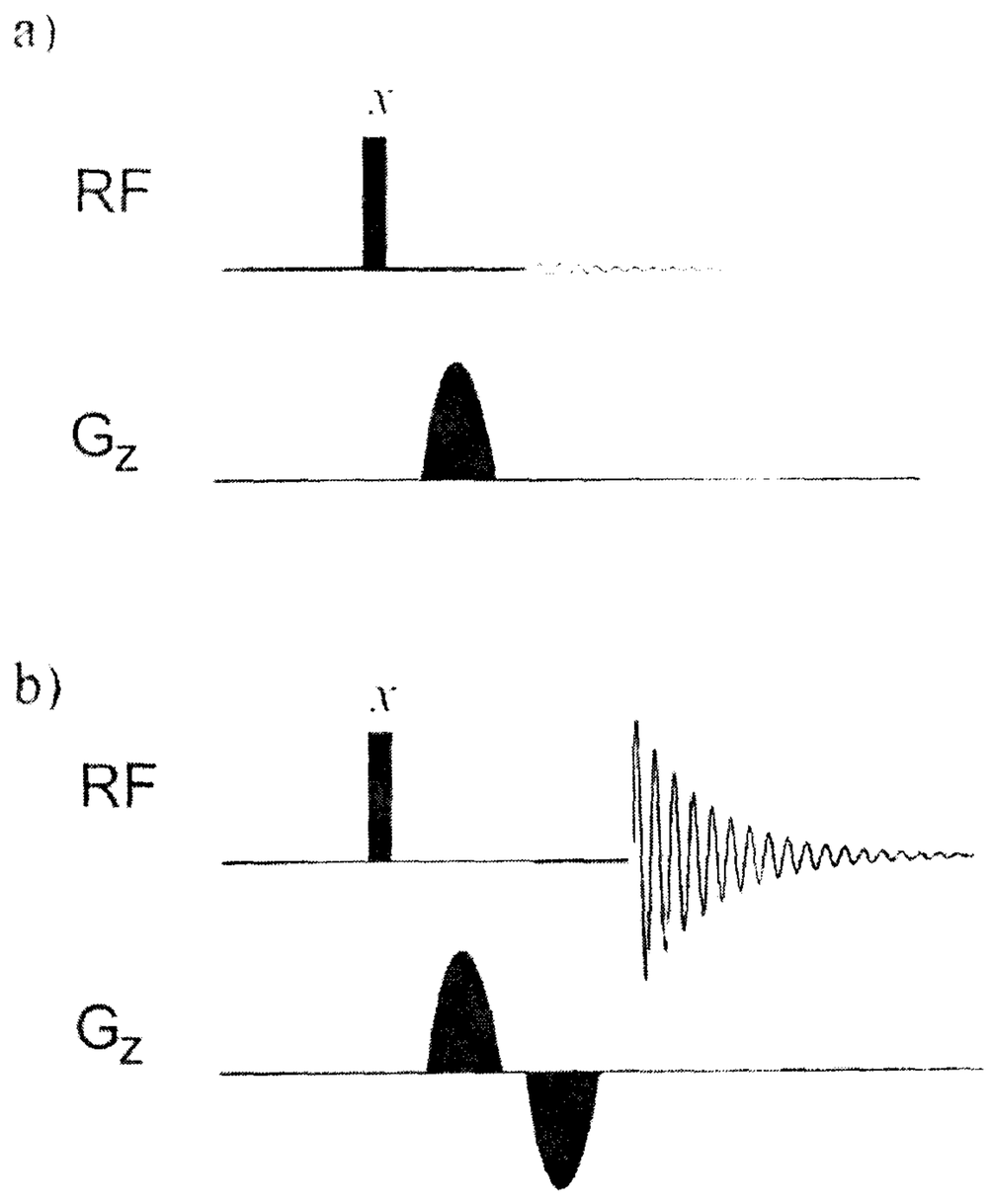

Figure 4.2 Schematic of a pulse field gradient being applied to a radiofrequency pulse channel. a) A single pulse along a z-axis for example dephases/defocuses the signal. b) Application of a second pulse in the opposite direction after a finite time recovers/refocuses the signal.[117]

Once measured, the diffusion coefficient affords the binding constant, K_a, in the following manner. If we assume a host-guest complex with 1:1 stoichiometry then K_a may be written as follows:

$$K_a = [HG]/[H][G]$$

Where [HG] is the equilibrium concentration of the host-guest complex and [H] and [G] the concentrations of the host and guest respectively.

As is true for chemical shift or T_1 measurements, the diffusion coefficient observed is a weighted average of contributions from species in exchange. Therefore the expression for the observed diffusion coefficient of a guest molecule in a solution containing a host molecule is as follows:

$$D_{obs} = X_G D_G + X_{HG} D_{HG}$$

Where D_{obs}, D_G, D_{HG} are the observed diffusion coefficient (at the guest), the diffusion coefficient of the guest on its own, and of the host-guest complex respectively. The symbols X_G and X_{HG} are the fraction of guest and host-guest complex respectively. This can be rearranged to give an expression that describes the equilibrium concentration of the complex:

$$X_{HG} = (D_G - D_{obs})/(D_G - D_{HG})$$

When the host molecule is much larger than the guest, this expression can be simplified and the diffusion coefficient for the host-guest complex (D_{HG}) can be treated as being the same as that of for the host (D_H). Thus,

$$K_a = X_{HG}/((1- X_{HG})([H]_o - X_{HG}[G]_o))$$

Where '$_o$' indicates the total concentration of host or guest.

This simplification means that from a single experiment an association constant may be determined. However this is only an approximation. For a more accurate measure of K_a or for situations when there is not a significant difference in the molecular weight of host and guest, it is probably better to measure diffusion coefficients over a range of host-guest concentration ratios.[98]

4.2 Review of solution phase chemistry associated with *p*-sulfonatocalix[4]arene.

As stated in Chapter 1, Shinkai and co-workers performed several solution phase studies.[27, 122, 123] These described the formation of aqueous $SO_3[n]$ complexes (where n = 4,6,8) with a view to the determination of association constants and template effects on the calixarene conformational freedom.[27, 122, 123] The results showed that the cavities of the *p*-sulfonatocalix[4,6,8]arenes were useful for recognition for small organic cationic species.[27, 122, 123] Since that time, Coleman and co-

workers have reported a series of successful *p*-sulfonatocalix[4,6,8]arene amino acid complexation studies.[55, 57, 58] Others have also reported on the complexation of $_{L}$-α-amino acids by SO_3[4].[124] Other literature has been concerned with the inclusion behaviour/complexation of substituted benzenes or small neutral organic molecules by SO_3[4],[125, 126] and recently Arena and co-workers have reported two studies on the recognition of aromatic ammonium cations by the *p*-sulfonatocalix[4,5]arenes.[127, 128] All of the aforementioned articles have used the NMR titration method to observe changes in chemical shift as mentioned above. Although this is clearly a useful technique for systems involving *p*-sulfonatocalix[*n*]arenes, much fewer experimental runs are required to establish changes in diffusion coefficient and thus host-guest complexation using DOSY techniques.

4.3 DOSY spectra and diffusion coefficients of systems 1·3 – 1·9 and 2·9.

In the experiments described here, the DOSY technique has been used, a technique that results in a 2-D map of the solution components (section 4.1.1). The specific pulse sequence is the bi-polar pulse pair stimulated echo (BPPSTE).[120] Spectra were recorded for 1 mM solutions of host, guest, and mixtures varying from 1:0.25 to 1:4 of host:guest in D_2O solution at 25 ^{0}C. It should be noted that while diffusion coefficients are provided for host, each of the guests, and each of the complexes, their absolute values are not reliable, but the relative values are. The actual numbers presented on their own seem unremarkable however the trend in diffusion behaviour within and across a series is informative and worthy of note. This is best appreciated by inspecting the DOSY plots, some of which have been included here. Lists of diffusion coefficients for various complexes are included in the discussion of each system. Systems **1·4** – **1·8** all use calix[4]arene tetra sulfonic acid as the host starting material to achieve a low pH in the absence of other proton sources and metal ions. Systems **1·9** and **2·9** are useful as a comparison of host starting materials and for investigation into the effect of sodium ions with 18-crown-6 as a guest molecule.

4.3.1 The SO_3H[4]/diaza-18-crown-6 system, 1·3.

As stated in section 4.0, the rapid crystal growth of a *p*-sulfonatocalix[4]arene/di-protonated diaza-18-crown-6/lanthanide capsule following addition of the metal salt prompted investigation into SO_3[4]/crown pre-organisation in solution. A series of different 1-D ^{1}H NMR spectra (not shown) were recorded and showed significant shift in the crown ether signals upon addition of SO_3[4]. Given this, the DOSY technique was considered and employed in a bid to prove the complexation and determine a binding constant. The DOSY spectra of the experimental ratios of host and guest

shown in Table 4.1 were recorded and the diffusion coefficients calculated. The spectra showed the following:

[H]:[G] 1:0

The signals for the host appear as two singlets at 7.63 and 4.08 ppm respectively (residual water referenced to 4.8 ppm, Figure 4.3 top).

[H]:[G] 0:1

The signals for the guest appear as a multiplet and triplet at around 3.7 and 2.9 ppm respectively (relative ratio 4:2, Figure 4.3 bottom).

[H]:[G] 1:0.5

The calixarene methylene signals for the calixarene host broaden and three distinct signals are seen for the guest (these lines are sharp, Figure 4.4 top).

[H]:[G] 1:1

The calixarene methylene signals have broadened to the baseline and the signals for the guest have begun to broaden (Figure 4.4 bottom).

[H]:[G] 1:2

Two doublets can be seen for the calixarene methylene protons and the guest signals are beginning to be resolved again (Figure 4.5). The presence of doublets for the calixarene methylene protons is indicative of the molecule adopting a cone conformation in solution at ambient temperature, i.e. complexed all of the time. The increased diffusion of one calixarene doublet is an experimental artefact owing to the peak lying on the shoulder of a guest signal that is at a faster diffusion rate.

The diffusion coefficients for the components in the five samples of system **1·3** are listed in Table 4.2 and show a clear reduction in the independent diffusion rates of both molecules at approximately a 1:1 [H]:[G] ratio. Indeed the data trends are typical of those previously reported for a series of 1:1 steroid:cyclodextrin complexes.[121] The presence of doublets in the 1:2 [H]:[G] spectrum indicates that the calixarene is in the cone conformation and has been restricted from the typically fluxional behaviour normally seen in the absence of guest or upon cooling to 0 °C.[123]

As a full discussion relating to the spectra of system **1·3** has been given, only tabulated data and related comments for particular spectra will be given for the remaining systems. Following this discussion, the fractions of the complexes formed and thus the binding constants will be calculated

according to the formulae shown in section 4.1.1. A short description of the Stokes-Einstein relationship will be given, and the equation used to determine 'rough' molecular weights for the complexes formed.

System 1·3

$[H]_o$ (mM)	$[G]_o$ (mM)	D_H	D_G
1.0	0	3.27 (+/- 0.01)	
1.0	0.5	3.11 (+/- 0.02)	3.08 (+/- 0.04)
1.0	1.0	3.08 (+/- 0.01)	3.32 (+/- 0.02)
1.0	2.0	2.90 (+/- 0.01)	3.67 (+/- 0.02)
0	1.0		3.85 (+/- 0.05)

Table 4.2 Diffusion rates for host and guest in system **1·3** at particular [H]:[G] ratios.

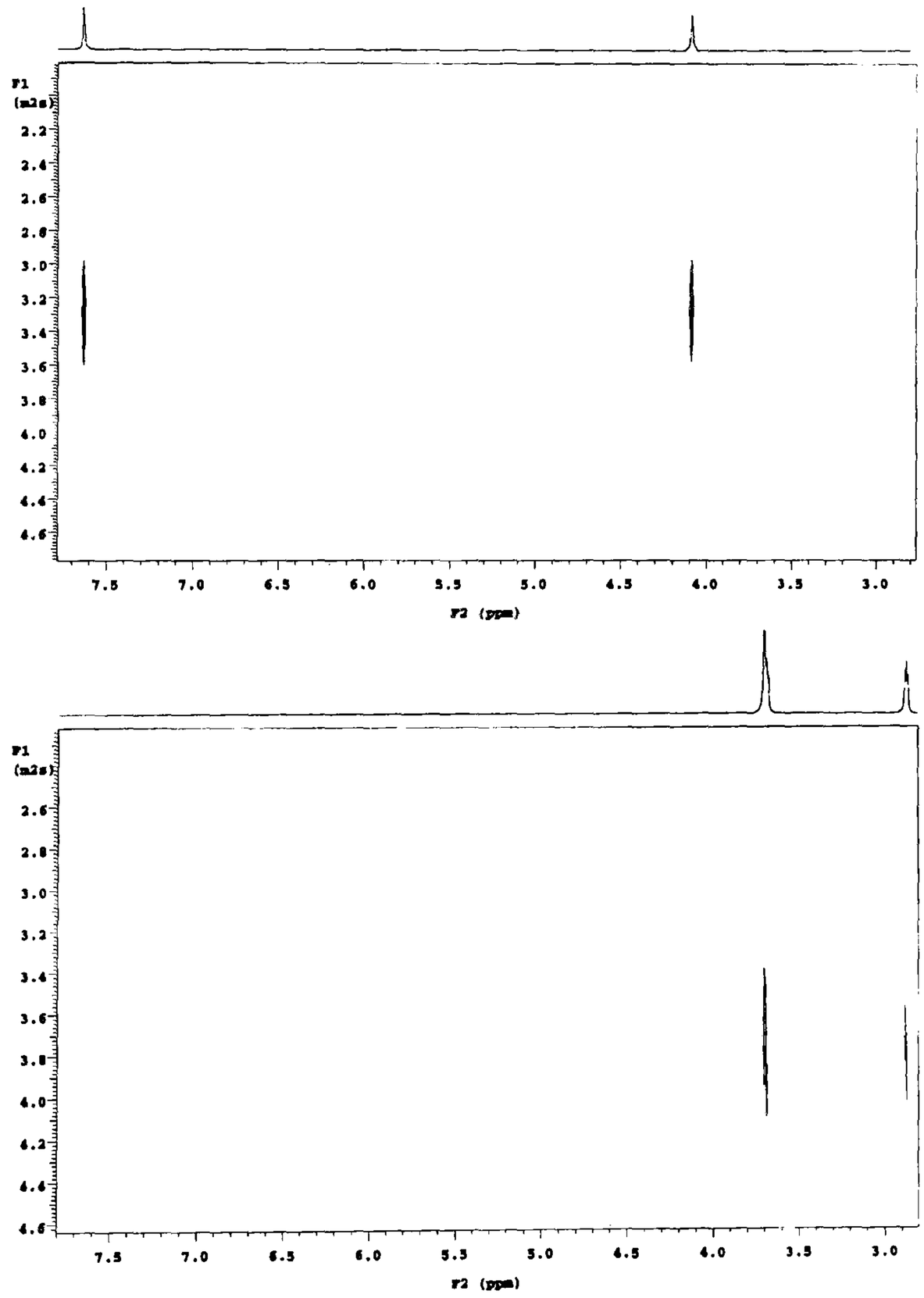

Figure 4.3 DOSY spectra of the 1:0 (top) and 0:1 (bottom) [H]:[G] samples from system **1·3** showing the peaks in the absence of either guest or host respectively.

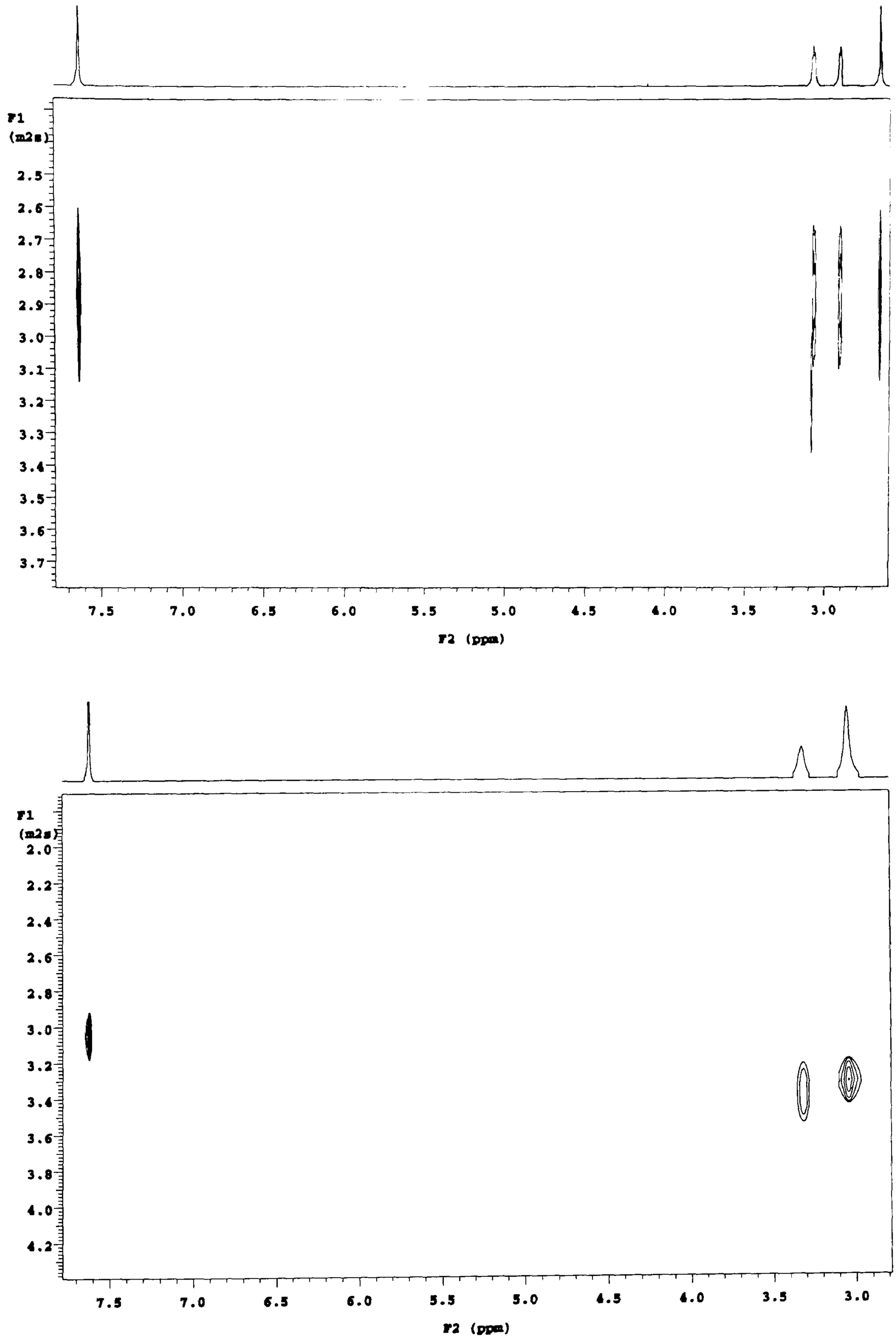

Figure 4.4 DOSY spectra of the 1:0.5 (top) and 1:1 (bottom) [H]:[G] samples of system **1**·**3**. The slower diffusion rate for all signals in the 1:0.5 spectrum indicates that all of **3** is bound by **1** (in excess).

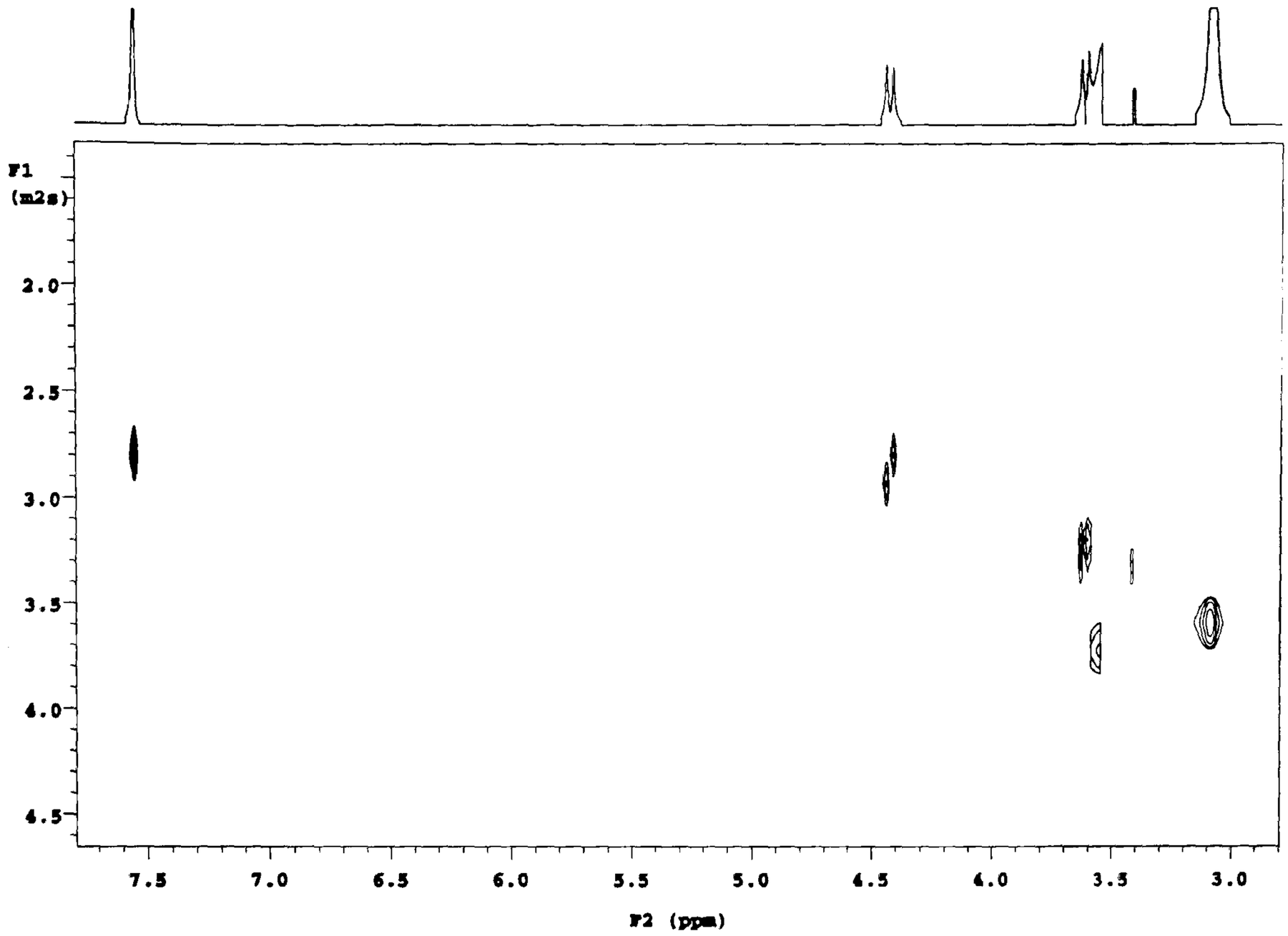

Figure 4.5 DOSY spectrum of the 1:2 [H]:[G] sample of system **1·3**. The two calixarene methylene bridge signals can be seen as two doublets, one of which has a faster diffusion rate due to a signal overlap artefact), indicating that **1** is permanently in a cone conformation, i.e. complexed. The crown ether signals are at a faster diffusion rate than those of **1,** as **3** is in excess.

4.3.2 The SO_3H[4]/1-aza-18-crown-6 system, 1·4.

[H]:[G] 1:0; As for system **1·3**.

[H]:[G] 0:1; Two signals are detected for the guest at 3.71 and 2.95 ppm.

[H]:[G] 1:0.5; The signals for the calixarene host are clearly resolved and sharp whilst six signals are resolved for the guest.

[H]:[G] 1:1; The calixarene host methylenes are slightly broadened as are the signals for the crown.

[H]:[G] 1:2; The calixarene host methylenes are broadened but clear and the guest signals have sharpened again.

System 1·4

$[H]_o$ (mM)	$[G]_o$ (mM)	D_H	D_G
1.0	0	3.27 (+/- 0.01)	
1.0	0.5	3.00 (+/- 0.04)	3.20 (+/- 0.04)
1.0	1.0	2.89 (+/- 0.08)	2.8, 3.2, 3.7*
1.0	2.0	2.93 (+/- 0.02)	3.71 (+/- 0.06)
0	1.0		3.8 (+/- 0.24)

Table 4.3 Diffusion rates for host and guest in system **1·4** at particular [H]:[G] ratios (* A complex spectrum is observed for this system consistent with slow exchange behaviour as detected in the normal spectrum).

The significant reduction in the diffusion coefficients of both host and guest suggest a strongly binding situation. The 1:1 [H]:[G] spectrum is complex and this is consistent with slow exchange that is also detected in the 1-D ^{1}H NMR spectrum.

4.3.3 The SO_3H[4]/diaza-15-crown-5 system, 1·5.

[H]:[G] 1:0; As for system **1·3**.

[H]:[G] 0:1; Two sharp signals are seen for the guest at 3.70 and 2.81 ppm.

[H]:[G] 1:0.5; The two sharp guest signals split into 5 sharp signals when the calixarene host is present, the methylene signals of which are very broad.

[H]:[G] 1:1; The calixarene host methylene signals have disappeared and the guest signals have broadened considerably.

System 1·5

$[H]_o$ (mM)	$[G]_o$ (mM)	D_H	D_G
1.0	0	3.27 (+/- 0.01)	
1.0	0.5	3.12 (+/- 0.02)	3.10 (+/- 0.04)
1.0	1.0	3.10 (+/- 0.02)	3.3 (+/- 0.1)
0	1.0		4.2 (+/- 0.1)

Table 4.4 Diffusion rates for host and guest in system **1·5** at particular [H]:[G] ratios.

Once again, the diffusion coefficients of the host are reduced, thus suggesting complexation.

4.3.4 The SO_3H[4]/1-aza-15-crown-5 system, 1·6.

[H]:[G] 1:0; As for system **1·3**.

[H]:[G] 0:1; Two sharp signals are seen for the guest at 3.70 and 2.81 ppm.

[H]:[G] 1:0.5; The calixarene host signals are sharp but the guest displays four signals with very unusual line shapes and this is presumed to be due to some 'slower' exchange phenomenon.

[H]:[G] 1:1; As for the 1:0.5 [H]:[G] sample.

System 1.6

$[H]_o$ (mM)	$[G]_o$ (mM)	D_H	D_G
1.0	0	3.27 (+/- 0.01)	
1.0	0.5	2.80 (+/- 0.02)	2.83 (+/- 0.04)
1.0	1.0	3.00 (+/- 0.01)	3.6 (+/- 0.02)
0	1.0		3.82 (+/- 0.05)

Table 4.5 Diffusion rates for host and guest in system **1·6** at particular [H]:[G] ratios.

As for the systems above, the diffusion coefficients of both host and guest are reduced upon mixing, thus indicating complexation.

4.3.5 The SO_3H[4]/diaza-12-crown-4 system, 1·7.

[H]:[G] 1:0; As for system **1·3**.

[H]:[G] 0:1; Two sharp signals are seen for the guest at 3.71 and 2.82 ppm.

[H]:[G] 1:0.5; The calixarene methylene signals are broadened whilst the guest signals remain sharp.

[H]:[G] 1:1; A huge change occurs in the spectrum and the calixarene methylene signals disappear whilst the guest signals broaden considerably.

System 1·7

$[H]_o$ (mM)	$[G]_o$ (mM)	D_H	D_G
1.0	0	3.27 (+/- 0.01)	
1.0	0.5	3.10 (+/- 0.01)	3.10 (+/- 0.01)
1.0	1.0	3.16 (+/- 0.03)	3.3 (+/- 0.3)
0	1.0		4.98 (+/- 0.01)

Table 4.6 Diffusion rates for host and guest in system **1·7** at particular [H]:[G] ratios.

The diffusion coefficients of both host and guest are reduced upon mixing, once again indicating complexation.

4.3.6 The SO_3H[4]/cyclam system, 1·8.

[H]:[G] 1:0; As for system **1·3**.

[H]:[G] 0:1; Three signals are seen for the guest at 2.96, 2.87 and 1.83 ppm.

[H]:[G] 1:0.25; The calixarene methylene signals are broad and only two signals are resolved for the guest.

[H]:[G] 1:0.5; The calixarene methylene signals are broadened whilst the guest signals remain sharp.

[H]:[G] 1:1; A dramatic change occurs and the calixarene methylene signals are resolved into two signals (still not sharp doublets). The spectrum for the guest has become hugely complex with sharp and broad components suggesting complexation in slow exchange (referred to by asterixes in Table 4.7).

[H]:[G] 1:4; Upon reaching this concentration, the calixarene methylene signals are resolved as two very sharp doublets whilst the signals of the guest are starting to collapse to a less complicated but still not resolvable form.

More stoichiometric ratios were performed for this system as the spectra were extremely complex. These results show once again that the calixarene is complexed with the guest and there are exchange effects in the spectra. This system may benefit from the use of variable concentration

studies i.e. by varying the concentration of *p*-sulfonatocalix[4]arene relative to the guest for comparison.

System 1·8

$[H]_o$ (mM)	$[G]_o$ (mM)	D_H	D_G
1.0	0	3.27 (+/- 0.01)	
1.0	0.25	3.19 (+/- 0.02)	3.36 (+/- 0.10)
1.0	0.5	3.05 (+/- 0.05)	3.07 (+/- 0.10)
1.0	1.0	3.00 (+/- 0.02)	3.04 (+/- 0.20)
1.0	2.0	2.86 (+/- 0.01)	3.3 (+/- 0.30)
1.0	3.0	2.77 (+/- 0.02)	3.8 (+/- 0.2)*
1.0	4.0	2.90 (+/- 0.01)	3.92 (+/- 0.08)*
0	1.0		4.2 (+/- 0.10)

Table 4.7 Diffusion rates for host and guest in system **1·8** at particular [H]:[G] ratios (* exchange effects apparent in spectrum).

As stated earlier, both the sulfonic acid and sodium salts of SO_3[4] were examined with 18-crown-6 as a guest molecule. This was for comparison between a neutral crown ether and a sodium 18-crown-6 complex that would likely form given the affinity of the macrocycle for sodium ions and the well documented formation of SO_3[4]/sodium 18-crown-6 based Russian dolls.[14, 34, 35, 44-46]

4.3.7 The SO_3H[4]/18-crown-6 system, 1·9.

[H]:[G] 1:0; As for system **1·3**.

[H]:[G] 0:1; One signal is seen for the guest at 3.70 ppm.

[H]:[G] 1:0.5; The calixarene host and guest signals remain sharp.

[H]:[G] 1:1; As for [H]:[G] 1:0.5 sample.

System 1·9

$[H]_o$ (mM)	$[G]_o$ (mM)	D_H	D_G
1.0	0	3.27 (+/- 0.01)	
1.0	0.5	3.19 (+/- 0.03)	4.30 (+/- 0.03)
1.0	1.0	3.11 (+/- 0.03)	4.25 (+/- 0.02)
0	1.0		3.91 (+/- 0.18)

Table 4.8 Diffusion rates for host and guest in system **1·9** at particular [H]:[G] ratios.

There diffusion coefficients of both host and guest are not reduced indicating that there is no binding.

4.3.8 The SO_3Na[4]/18-crown-6 system, 2·9.

[H]:[G] 1:0; The methylene signal of the calixarene host is broad.

[H]:[G] 0:1; As for system **1·9**.

[H]:[G] 1:0.5; The methylene signal of the calixarene host disappear as guest is introduced.

[H]:[G] 1:1; As for [H]:[G] 1:0.5 sample.

System 2·9

$[H]_o$ (mM)	$[G]_o$ (mM)	D_H	D_G
1.0	0	2.95 (+/- 0.01)	
1.0	0.5	2.72 (+/- 0.01)	4.28 (+/- 0.03)
1.0	1.0	2.85 (+/- 0.01)	3.70 (+/- 0.02)
0	1.0		3.91 (+/- 0.18)

Table 4.9 Diffusion rates for host and guest in system **2·9** at particular [H]:[G] ratios.

At a 1:1 ratio, both host and guest diffusion have been reduced and this indicates a degree of binding as for the above systems.

4.4 Determination of the fractions of complexes, resultant binding constants and 'approximate' molecular weights from systems 1·3 – 2·9.

As stated in section 4.3, fractions of complexes formed have been calculated according to the formulae given in section 4.1.1. These values are listed in Table 4.10 and have also been used to calculate the corresponding binding constants that are also listed. Literature sources suggest that strong binding can be considered as 1 x 10^5 M^{-1} and weak binding as 500 M^{-1}.[98] Thus for systems **1·3** – **1·8**, the majority of charged guests bind on an intermediate to strong scale. The protonated forms of 1-aza-15-crown-5 and diaza-12-crown-4 bind only weakly. The sulfonic acid of calix[4]arene sulfonate clearly does not bind 18-crown-6 in the cavity but introduction of sodium

ions via the use of calix[4]arene sulfonate sodium salt affects the binding, the results of which are between weak and intermediate.

System	Fraction of complex (X_{HG})	K_a (M^{-1})
1·3	0.67	$6.1(5) \times 10^3$
1·4	0.99, 0.66, 0.11	9.9×10^5 to $1.4 \times 10^{2*}$
1·5	0.73	2.5×10^4
1·6	0.27	5.1×10^2
1·7	0.92	1.4×10^5
1·8	0.97	10.8×10^5
1·9	~0	0
2·9	0.2	3.1×10^3

Table 4.10 Complex fractions and binding constants calculated for the 1:1 [H]:[G] samples from systems **1·3 – 2·9** (* System **1·4**, the fraction of the 1:0.5 [H]:[G] complex is 0.66 and K_a is 4.8×10^3 M^{-1}).

The Stokes-Einstein relationship is an equation that can be used to determine 'approximate' molecular weights of complexes in solution and is expressed as:

$$D = kT/6\pi\eta r$$

Where D is the diffusion coefficient, T the temperature, η the viscosity of the solvent and r the effective hydrodynamic radius of the molecule (r is inversely related to the cube root of the molecular mass).[121] This has been applied by Fielding et al. and used to calculate molecular weights of steroid cyclodextrin inclusion complexes (Figure 4.6).[121] This is achieved by using the expression:

$$D = 39.565(1/(\text{Molar Mass})^{1/3}) - 0.5647$$

or

$$\text{Molar Mass} = [((D + 0.5647)/39.565)^{-1}]^3$$

Calculated and averaged molecular weights for the 1:1 complexes formed in systems **1·3 – 2·9** are listed in Table 4.11. It should be noted that the resultant molecular weights for each complex are not exact but give a general trend within the results. These values help to give a clearer picture regarding the host-guest complexes formed in systems **1·3 – 1·8** and **2·9**. The value for system **1·9** is indicative of a lack of host-guest complexation. Most clearly however is the fact that the molecules, when complexed, assemble in a 1:1 stoichiometry and not as molecular capsules in solution. If this were the case, the averaged molecular weight would be much larger given that and extra calix[4]arene sulfonic acid would give an MW difference of ~ 745 $gmol^{-1}$.

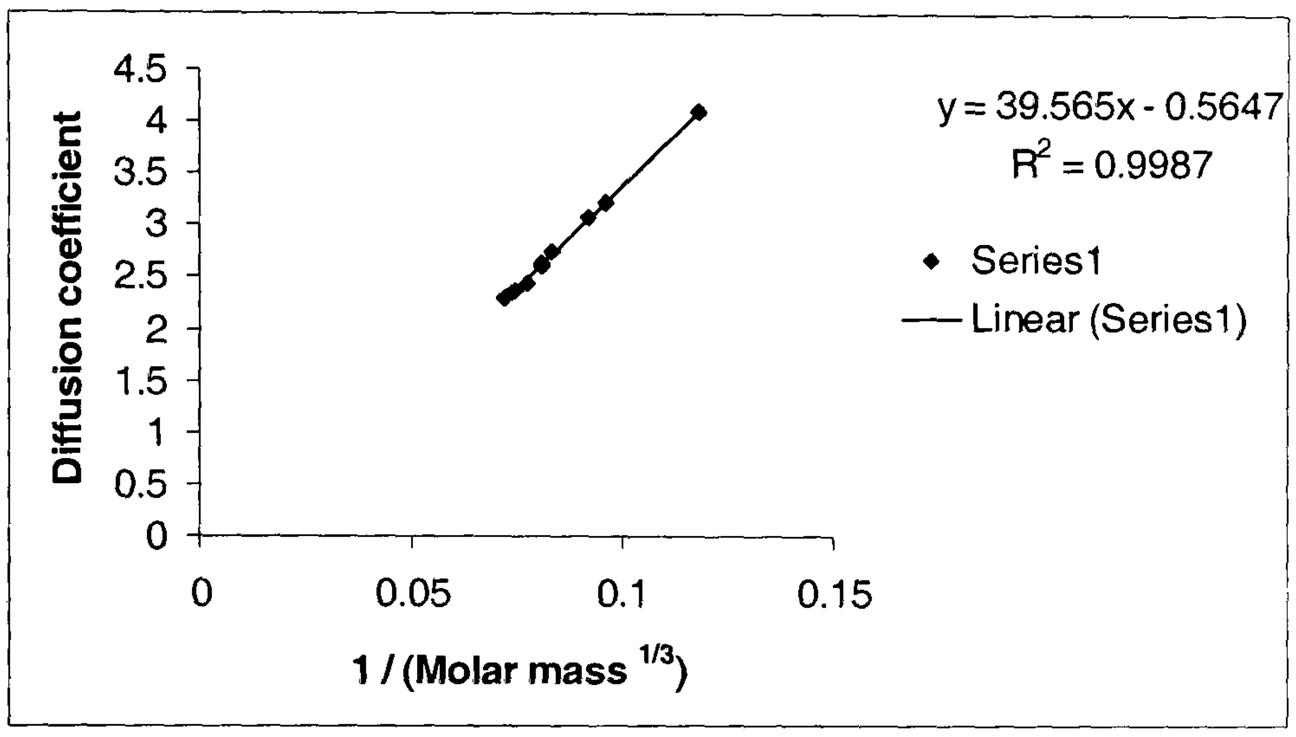

Figure 4.6 Stokes-Einstein relationship between the diffusion coefficient (D) and molecular mass (error bars not shown).[121]

System number	D_H (1:1)	MW D_H (1:1)	D_G (1:1)	MW D_G (1:1)	Average MW (1:1)	Expected MW (1:1), unsolvated
1·3	3.08	1279	3.32	1056	1167	1009.1
1·4	2.89	1502	2.8, 3.2, 3.7	1625, 1161, 799	1271	1009.1
1·5	3.10	1258	3.3	1072	1165	965.1
1.6	3.00	1367	3.6	857	1112	965.0
1·7	3.16	1198	3.3	1072	1135	921.0
1·8	3.00	1367	3.04	1322	1345	963.1
1·9	3.11	1248	4.25	555	901	1009.0
2·9	2.85	1555	3.7	799	1177	1068.1

Table 4.11 List of calculated and averaged molecular weights for the complexes in systems **1·3 – 2·9**. Three molecular weights were calculated in complex **1·4** given the complex nature of the spectrum.

4.5 Conclusion.

The results presented within this chapter have shown that SO_3[4] pre-organises with various charged crown ether (or crown ether type) molecules as host-guest complexes. The molecules, when complexed diffuse at a slower rate and the measured diffusion coefficients were used to calculate binding constants from 1:1 [H]:[G] mixtures as well as the 'approximate' molecular weight for each complex. Whilst these molecular weights do not exactly depict a 1:1 host-guest complex, they are indicative of this given that a 2:1 host-guest molecular capsule type complex would have a much larger calculated and averaged MW.

The spectra of the host-guest complex formed with cyclam (system **1·8**) were of a complex nature. Tetra-protonated cyclam has been shown to crystallise within in a molecular capsule of SO_3[4] in the presence of additional *exo*-capsule H_4 cyclam species.[47] Although this occurs in the solid state, there is no evidence of this in solution as once again the molecular weight would be far greater than that 'rough' value calculated. This very complex system could benefit from further study in order to arrive at a definitive conclusion.

The results also showed that sulfonic acid calix[4]arene does not bind 18-crown-6 as a neutral species. When the sodium salt of the calixarene is employed, binding occurs and this may be due to the formation of a sodium 18-crown-6 complex similar to those found in the solid state Russian doll superanions reported by Raston *et al.*[34, 35, 44-46]

In general, the findings of these studies help explain the phenomenon of rapid crystallisation of molecular capsules or alternative bi-layer structures that was observed with the guest molecules examined here (correlation with structures described in Chapter 2). The charged guest molecules (except 1-aza-15-crown-5) all show association with SO_3[4] in solution and this is mirrored in the speed of crystallisation of the corresponding supramolecular structures in Chapter 2. It is clear that DOSY is a valuable technique for determining binding constants, host-guest pre-organisation and for explaining such phenomena. Future studies should include a range of different charged disc shaped or globular guests that could interact with SO_3[4]. In addition, the larger *p*-sulfonatocalix[n]arenes could also be used to expand the knowledge of associated solution complexation of these useful hosts.

4.6 Experimental.

The *p*-sulfonatocalix[4]arene sulfonic acid and sodium salts were purchased from Acros and used as supplied without further purification. Similarly, all guest molecules were purchased from Aldrich and used as supplied.

All samples were prepared by a general procedure such that the concentrations were 1mM with respect to host except those which were of 0:1 [H]:[G] ratio and were made to be 1mM with respect to guest, all at a constant volume of 600 μL (D_2O). As an example, a 1:1 [H]:[G] was prepared by addition of 300 μL of a 2mM guest solution to 300 μL of a 2mM host solution.

All NMR experiments were carried out on a Varian Unity Inova 500 spectrometer equipped with a single axis field gradient unit and a 5 mm $^{1}H/^{19}F/^{13}C$ triple resonance z-gradient probe. ^{1}H NMR spectra were recorded at 25 °C and typically with 128 scans, spectral width of 4000 Hz in 8k complex points and zero filled to 32k complex points. NMR diffusion coefficients were measured from DOSY spectra using the Dbppste pulse sequence with a 50 ms delay and 1.5 ms bipolar gradient pulses. Between 10 – 15 gradient field strength increments were recorded. The spectra were deconvoluted using the 'fiddle' macro on the spectrometer prior to production of the 2-D DOSY spectrum.

Chapter Five:

Russian doll complexes and nano-metre scale spheroidal arrangements of *p*-sulfonatocalix[4]arene.

5.0 Overview.

The first section of this chapter is concerned with the formation of Russian dolls based on molecular capsules of *p*-sulfonatocalix[4]arene and metal (sodium or lanthanide)/18-crown-6 guest species. The second section of this chapter examines more closely, the formation of twelve vertex spherical assemblies of *p*-sulfonatocalix[4]arene and details how these can be controlled through the formation of Russian dolls. This control is achieved through the choice of guest molecule in molecular capsule formation with SO_3[4], a choice that has profound effects on the overall geometrical architecture of these spheroidal assemblies.

5.1 Introduction.

As a significant proportion of the literature reviewed in Chapter 1 was based on Russian dolls or molecular capsules (section 1.5.1), this topic needs little introduction. As a reminder however, Raston *et al.* documented the Russian dolls that are based on *p*-sulfonatocalix[4]arene and that are composed of superanions in the form of a di-aquo 18-crown-6 sodium complex that is shrouded by two SO_3[4] molecules (Figure 5.1).[34]

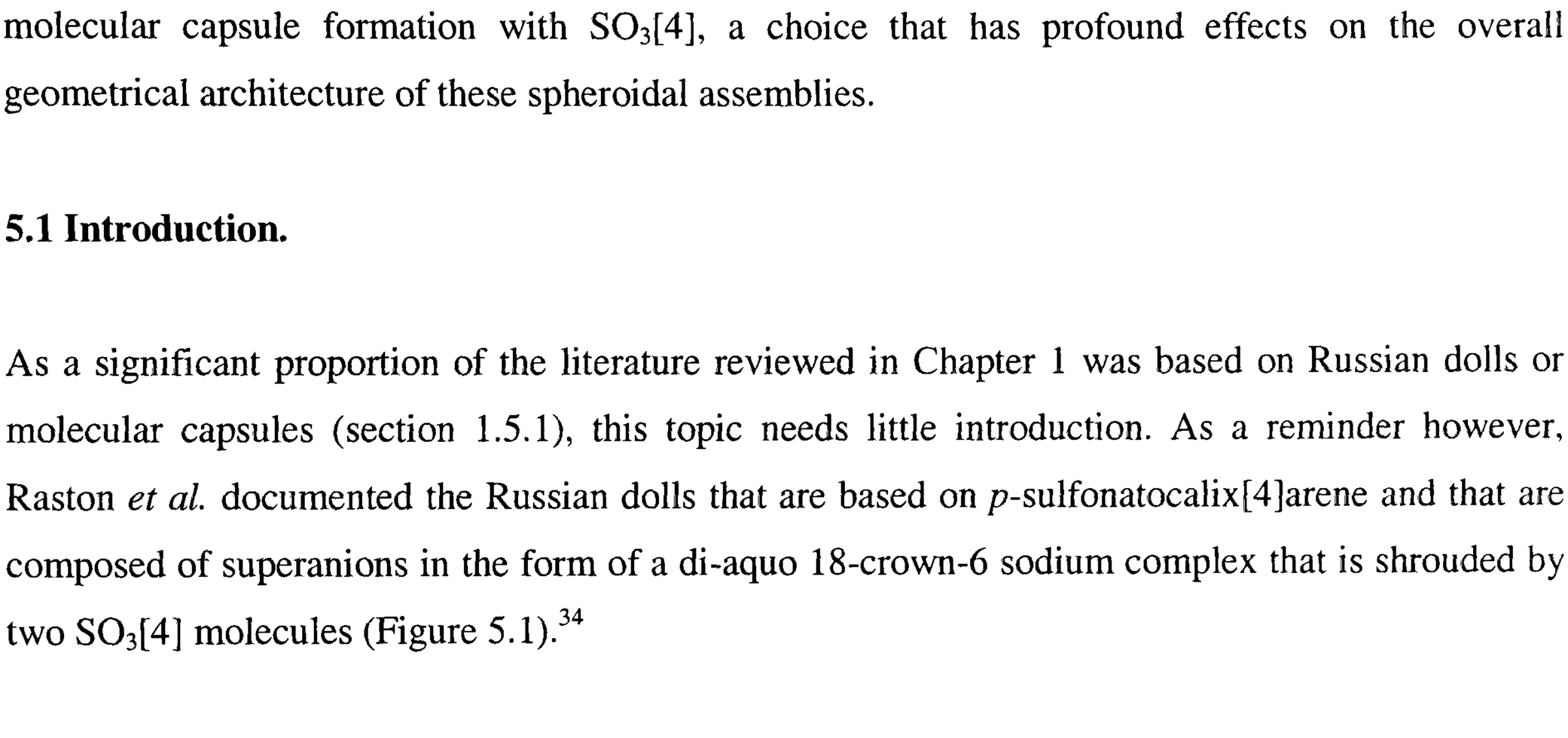

Figure 5.1 Schematic of the Russian doll superanions formed between $NaSO_3$[4] and 18-crown-6.

These superanions are capable of selectively crystallising several different poly-nuclear transition metal cations or aluminium Keggin ions from solution in bi-layer motifs.[34, 35, 44-46] The sodium centre of the *bis*-aquo 18-crown-6 complex is of bi-capped hexagonal geometry although the sodium atom is capable of losing the two *trans*-ligated water molecules and coordinating to sulfonate groups of the calixarenes (Figure 5.1). Further work by Raston and co-workers reported the formation of lanthanide based molecular capsules that had similar superanions composed of SO_3[4] and 18-crown-6 but with exclusion of sodium atoms from the crown ether macrocycle.[49, 51] These molecular capsules were formed when the corresponding metal chloride was employed as a starting material and the results showed direct lanthanide/sulfonate coordination, a structural motif not seen previously in other Russian dolls.[49, 51] Replacement of a lanthanide chloride (M^{3+} = Eu, Gd, Tb, Dy, Y, Ho, Er, Tm, Yb, Lu) with praseodymium triflate at a pH ~ 3.5 results in the formation of a new lanthanide based Russian doll. The structure has the traditional *bis*-aquo sodium 18-crown-6 guest species present rather than just a sodium-free 18-crown-6 molecule and this guest moiety is shrouded by the SO_3[4] molecules that have coordinated octa-aqua praseodymium metal centres.

5.1.1 Structure of the lanthanide based Russian doll complex $[Na(H_2O)_2\subset$18-crown-6$]\subset\{(Pr(H_2O)_9)_2$(*p*-sulfonatocalix[4]arene$)_2\}\cdot 10H_2O$, 5.1.

Crystals of the complex $[Na(H_2O)_2\subset$18-crown-6$]\subset\{(Pr(H_2O)_9)_2$(*p*-sulfonatocalix-[4]arene$)_2\}\cdot 10H_2O$, **5.1**, grew upon slow evaporation of an aqueous solution containing a 1:3:2 mixture of *p*-sulfonic acid calix[4]arene, 18-crown-6 and praseodymium triflate (pH altered to be 2.6 *via* addition of 1M NaOH, Equation 5.1). The complex was characterised by IR spectroscopy and single crystal X-ray crystallography. Complex **5.1** crystallises in a monoclinic cell and the structural solution was performed in the space group $P2_1/c$. Details of the data collection and structure refinement are given in Table 5.2 of this chapter. A crystallographic information file containing all bond lengths and angles for complex **3.1** can be found in appendix 5.1.1 on the attached compact disc.

The asymmetric unit comprises one half of a Russian doll assembly (residing around a centre of inversion) and a total of ten waters of crystallisation that are disordered over seventeen positions (Figure 5.2). The half Russian doll fragment in the asymmetric unit shows significant disorder in the praseodymium metal centres, respective aquo ligands and calixarene sulfonate groups. In addition to this, the crown ether atoms of the *trans*-ligated *bis*-aquo sodium 18-crown-6 guest are disordered over two positions. The disordered atoms of the crown ether were effectively modelled

over two positions, each position with a partial occupancy of 0.5. The same however could not be achieved for the praseodymium metal centres and hence a full table of bond lengths for the metal coordination spheres has not been compiled. Bond distances relating to the coordination sphere of the sodium atom and selected praseodymium – oxygen bond lengths have been listed in Table 5.1.

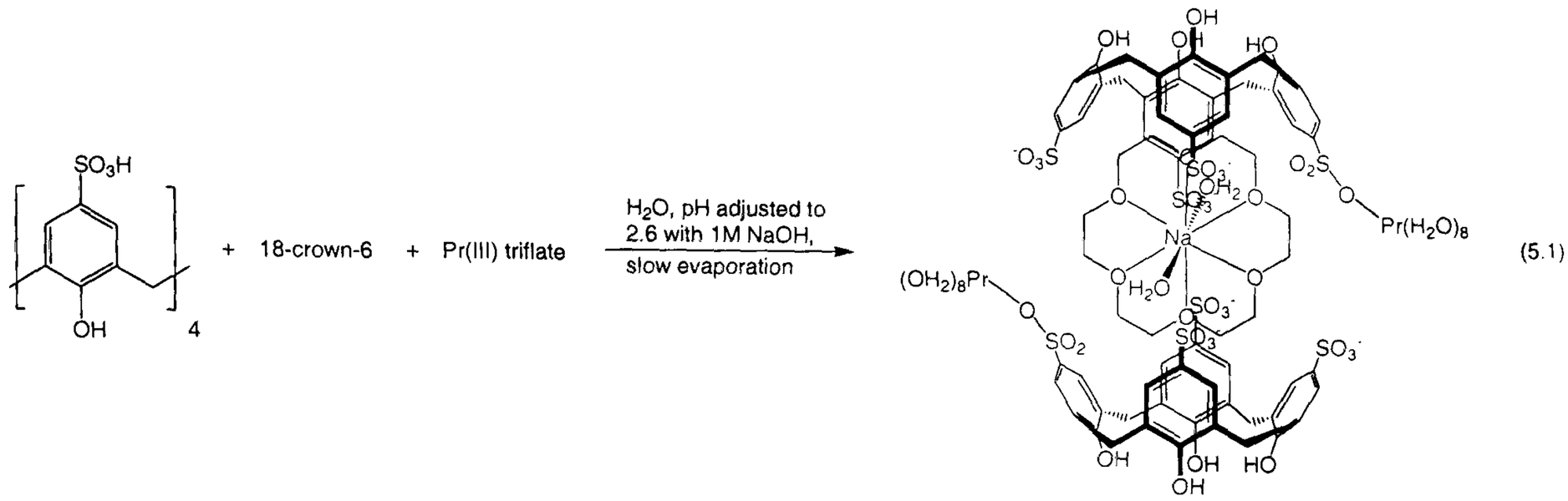

(5.1)

Within the asymmetric unit, the octa-aqua praseodymium atom is highly disordered over three positions with partial occupancies of 0.25 for Pr(1) and P(2) and 0.5 for Pr(3) (Figure 5.2). The disorder is very severe and prevents the location of the full coordination sphere for the metal centre in all three positions.

Na(1)-O(41)	2.71(2)	Na(1)-O(41)$^{(a)}$	2.71(2)
Na(1)-O(42)	2.68(2)	Na(1)-O(42)$^{(a)}$	2.68(2)
Na(1)-O(43)	2.77(2)	Na(1)-O(43)$^{(a)}$	2.77(2)
Na(1)-O(44)	2.70(3)	Na(1)-O(44)$^{(a)}$	2.70(3)
Na(1)-O(45)	2.69(3)	Na(1)-O(45)$^{(a)}$	2.69(3)
Na(1)-O(46)	2.90*	Na(1)-O(46)$^{(a)}$	2.90*
Na(1)-O(47)	2.346(8)	Na(1)-O(47)$^{(a)}$	2.346(8)
Pr(1)-O(1)	2.51(3)	Pr(2)-O(1)	2.69(3)
Pr(1)-O(2)	2.49(3)	Pr(2)-O(2)	2.74(3)

Table 5.1 Interatomic distances between atoms in the coordination sphere of the sodium atom and selected atoms from the coordination spheres of Pr(1) and Pr(2) in the crystal structure of complex **5.1** (distances given in Å with e.s.d in parentheses). Key operations for symmetry related atoms: *(a)* -x, -y, 1-z. *Long interaction between the sodium metal centre and the O(46) donor atom of the crown ether.

The metal centre, when in the Pr(1) and Pr(2) positions, is bound to a disordered oxygen atom of a calixarene sulfonate group. Bond distances relating to the praseodymium sulfonate coordination are

listed in Table 5.1. When in the third position, the metal centre is positioned such that no interaction with a sulfonate oxygen atom is possible (closest Pr – O distance of ~ 4Å). The calixarene in complex **5.1** has dihedral angles of 113.83 and 137.5° and these values are consistent for the previous inclusion of *trans*-ligated *bis*-aquo sodium 18-crown-6 guest species by SO_3[4].[34, 35, 44-46] As stated above, the asymmetric unit of complex **5.1** contains half of a *bis*-aquo sodium 18-crown-6 guest species, the sodium atom of which resides on an inversion centre. The crown ether atoms are disordered and have been modelled over two positions. The resultant sodium – oxygen bond distances are of similar magnitude to those found in previously reported *trans*-ligated *bis*-aquo sodium 18-crown-6 moieties although there is one long interaction between the sodium metal centre and the O(46) donor atom of the crown ether (bond distance of 2.90Å at a partial occupancy of 0.5).

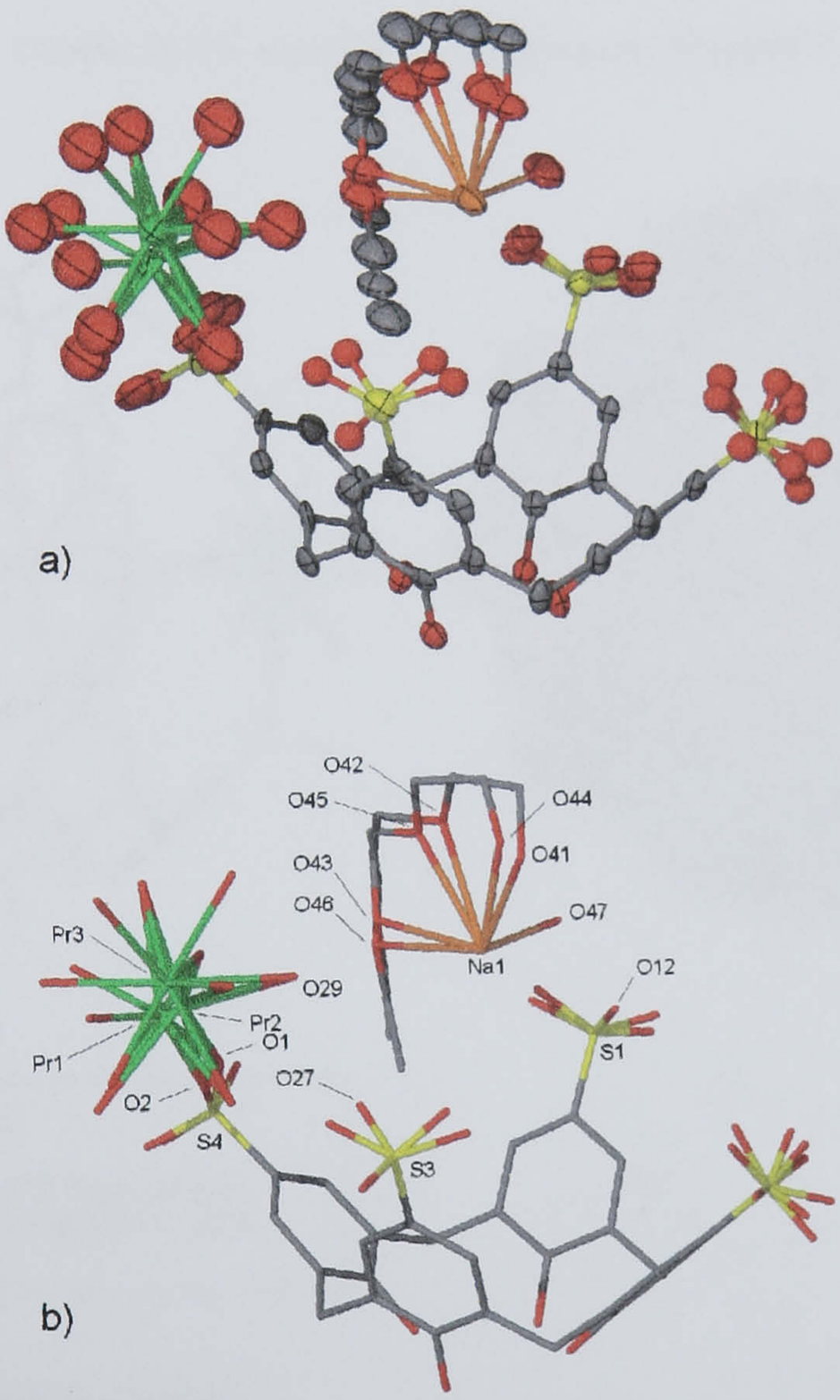

Figure 5.2 Part of the asymmetric unit from the crystal structure of complex **5.1**. a) Atoms shown as thermal ellipsoids at 50% probability (some atoms shown in ball and stick representation). b) Selected atoms have been labelled in an identical stick representation to aid visual clarity. Only half of the sodium 18-crown-6 complex is shown as the sodium centre resides on an inversion centre.

When the Russian doll assembly is examined as a whole, an intricate hydrogen-bonded network is found between the trans-ligated sodium aquo ligands, the only full occupancy praseodymium aquo ligand (O(29)) and a disordered oxygen donor atom of the crown ether macrocycle (O(43) and O(46), Figures 5.2 and 5.3). The sodium aquo ligands hydrogen bond to the two nearest sulfonate groups from the head-to-head arrangement of SO_3[4] molecules (NaO(47)···O(12)S(1) and NaO(47)···O(27)S(3) distances of 2.691 and 2.673 Å respectively, Figure 5.3a). The one full occupancy praseodymium aquo ligand (O(29)) hydrogen bonds to the sodium aquo ligand (O(47)) and a disordered crown ether oxygen donor atom (O(43) and O(46)) with PrO···ONa distances of 2.737, 2.684 and 2.732 Å respectively (Figure 5.3a). Graph set analysis (as described in Chapter 3) can be used to assign this hydrogen-bonded arrangement a descriptor $R_2^2(6)$.[14] A space filling representation of the same arrangement shows the methylene groups of the crown ether to be protruding slightly from the centre of the capsular arrangement (Figure 5.3b).

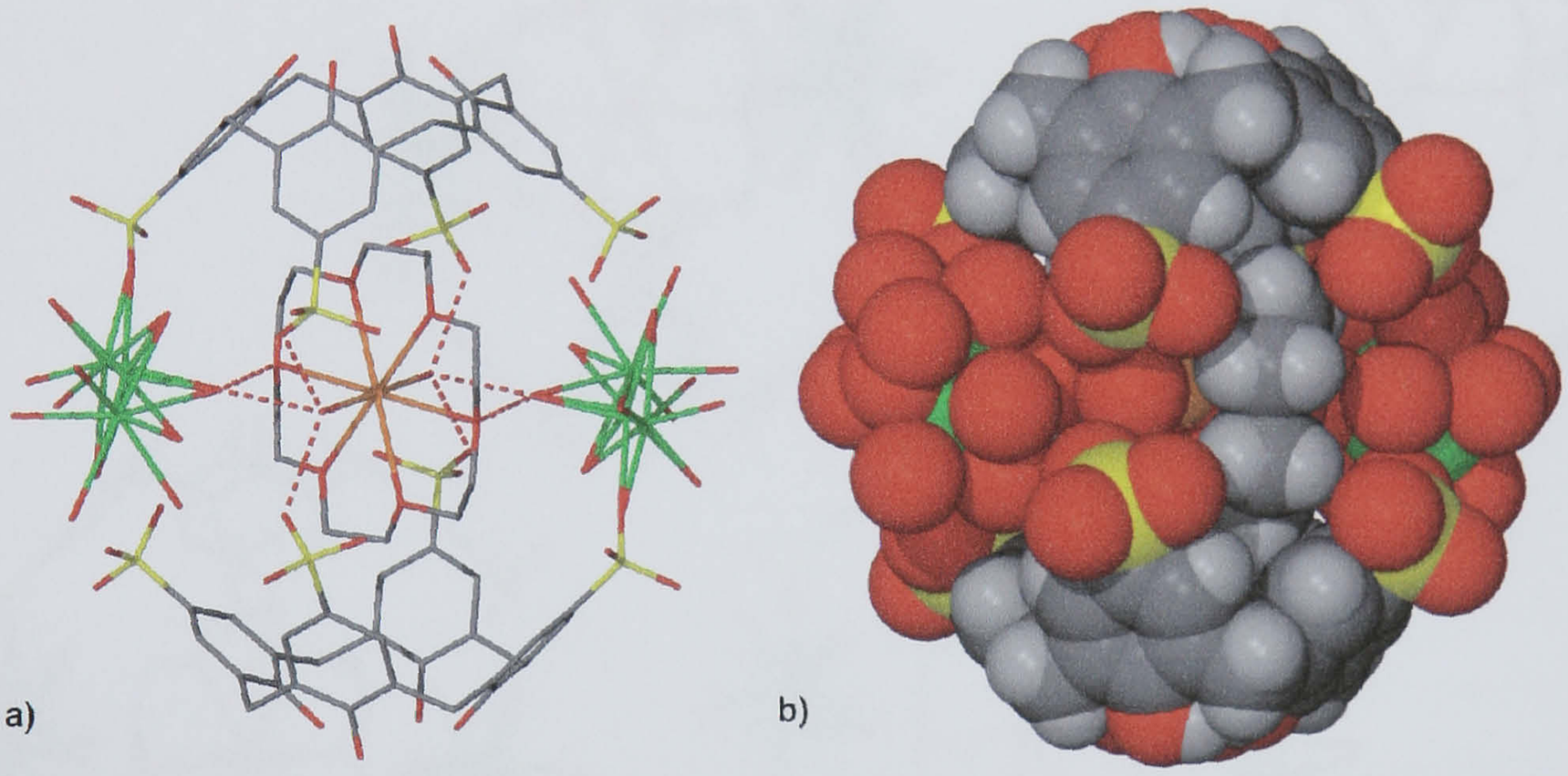

Figure 5.3 The Russian doll assembly from the crystal structure of complex **5.1**. a) The atoms are shown in stick representation and show the hydrogen bonding interactions between metal aquo ligands and calixarene sulfonate groups (disordered crown ether atoms and disordered sulfonate oxygen atoms omitted in some positions for clarity). b) The atoms are in space filling representation and show the crown ether methylene groups protruding from the centre of the cavity. c) The graph set analysis of the hydrogen bonding regime is also shown.[14]

The extended structure shows the calixarenes to pack in the usual anti-parallel bi-layer arrangement and this occurs through two crystallographically unique π-stacking interactions (aromatic centroid···centroid distances of 3.977 and 4.114 Å). These values are slightly longer than those typically observed for such interactions with SO_3[4] but are within a range of values reported in a recent survey of the Cambridge Crystallographic Data Centre.[129] A number of the disordered praseodymium aquo ligands are at distances from neighbouring calixarene sulfonate groups that are consistent with hydrogen bonding to the oxygen atoms and there are several potential contacts with PrO···OS distances ranging from 2.568 to 2.908 Å.

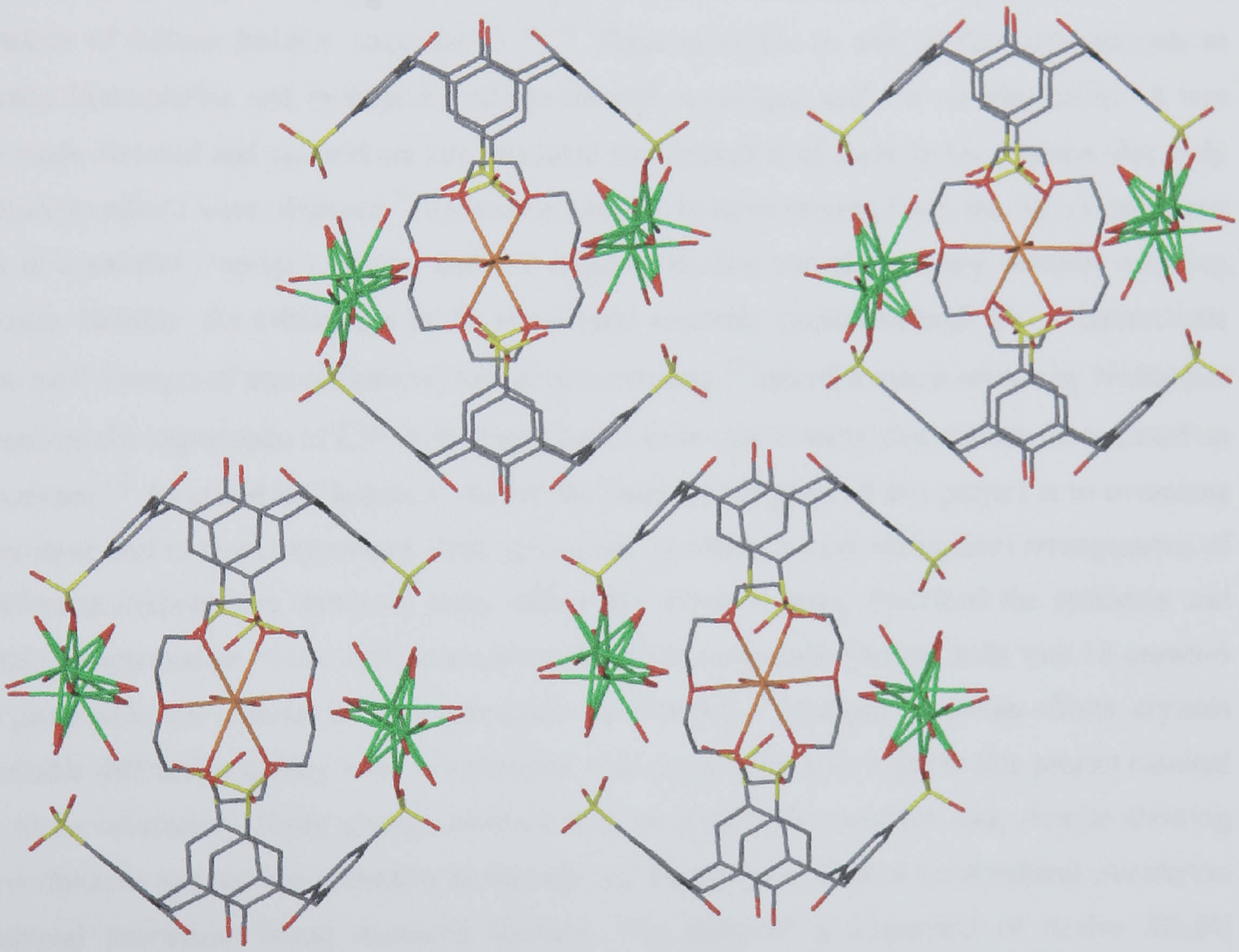

Figure 5.4 The extended bi-layer structure in the crystal structure of complex **5.1** showing the packing of the Russian dolls (some disordered sulfonate group oxygen atoms omitted for clarity).

In relation to the following section, perhaps the most important feature of complex **5.1** and other Russian dolls incorporating 18-crown-6, is that the guest molecule enforces a head-to-head arrangement of *p*-sulfonatocalix[4]arenes. Other guests that are smaller and hence less sterically demanding can form alternative *bis*-SO_3[4] arrangements such as a *C*-shaped dimer with concomitantly dramatic results in the extended structure formation.[17]

5.2 The design and control over the formation and geometry of twelve vertex spherical assemblies of *p*-sulfonatocalix[4]arene.

Atwood *et al.* reported extraordinary results that described remarkable control over the formation of nano-metre scale spheres and tubules based on *p*-sulfonatocalix[4]arene.[17] By employing different molar ratios of Na_5SO_3[4], pyridine *N*-oxide and lanthanum nitrate, the ternary system was controlled to assemble into helical tubules or twelve vertex near-spherical arrangements. As the results of Chapters 2 and 3 have shown (in addition to the numerous papers reporting structural assemblies of SO_3[4]), the truncated cone-shaped amphiphilic *p*-sulfonatocalix[4]arene favours the formation of infinite bi-layer structures.[25, 26, 38] These assemble as anti-parallel arrangements to optimise hydrophobic and hydrophilic effects through π-stacking and CH···π interactions. It was only when Atwood and co-workers circumvented the formation of these bi-layer arrays that truly spectacular effects were observed.[17] By overcoming the bi-layer driving force, the calixarenes must pack in a parallel ('up-up') fashion and this imparts inherent curvature to any possible resulting structure. Notably, the calixarenes in the icosahedral assembly packed through CH···π interactions in the total absence of any calixarene/calixarene π-stacking.[17] Indeed a recent review by Nishio has focused on the importance of CH···π hydrogen bonds in several systems that include those based on calixarenes.[130] As stated in Chapter 1, one of the fundamental goals of this project is to overcome the bi-layer and to form nano-metre scale spheroidal (or other bi-layer alternative) arrangements of *p*-sulfonatocalix[*n*]arenes. Previous work within our research group described the synthesis and partial characterisation of one such arrangement based on lanthanide Russian dolls with 18-crown-6 as a guest molecule (similar in some aspects to complex **5.1**).[100] Despite numerous efforts, crystals of suitable diffraction quality were not obtained. Continued efforts throughout this project resulted in a more satisfactory X-ray crystal structure of a praseodymium complex that, despite showing severe disorder and pseudo-symmetry in the unit cell dimensions, allowed the structural elucidation of several interesting broad structural features. The spheroid is composed of twelve SO_3[4] molecules, arranged at the vertices of a cuboctahedron and has an internal core that is occupied by six disordered poly-aquo lanthanide species. Neighbouring cuboctahedra are linked by the Russian dolls and in collaboration with the Atwood group, closer examination of the original icosahedral spheroid shows many interesting differences between the two.[17] These differences are a direct result of changing the guest species and the concomitant arrangement of SO_3[4] molecules relative to one another.

5.2.1 Structure of the cuboctahedral assembly $[Pr(H_2O)_9]_6\subset[\{((Pr\subset 18\text{-crown-6})_{0.5})\subset(p\text{-sulfonatocalix[4]arene} - H^+)\}_{12}][(Pr(H_2O)_9)_6]\cdot XH_2O$, 5.2.

Crystals of the complex **5.2**, $[Pr(H_2O)_9]_6\subset[\{((Pr\subset 18\text{-crown-6})_{0.5})\subset(p\text{-sulfonatocalix-[4]arene})\}_{12}][(Pr(H_2O)_9)_6]\cdot XH_2O$, grew within two hours from an aqueous solution containing a 1:3:1.5 mixture of $Na_5SO_3[4]$, 18-crown-6 and praseodymium triflate (Equation 5.2). The complex was previously characterised by IR spectroscopy and the structure was partially resolved through the use of single crystal X-ray crystallography although many structural features could not be determined (solution performed in the space group $P432$).[100] The quality of the data was so poor that crown ether atoms were not located and the formula $[Pr(H_2O)_9]_6\subset[(p\text{-sulfonatocalix[4]arene} - H^+)_{12}(Pr(H_2O)_9)_8]\cdot XH_2O$ was suggested.

$Na_5SO_3[4]$ + 18-crown-6 + M(III) triflate (M^{3+} = Pr, Nd, Sm)

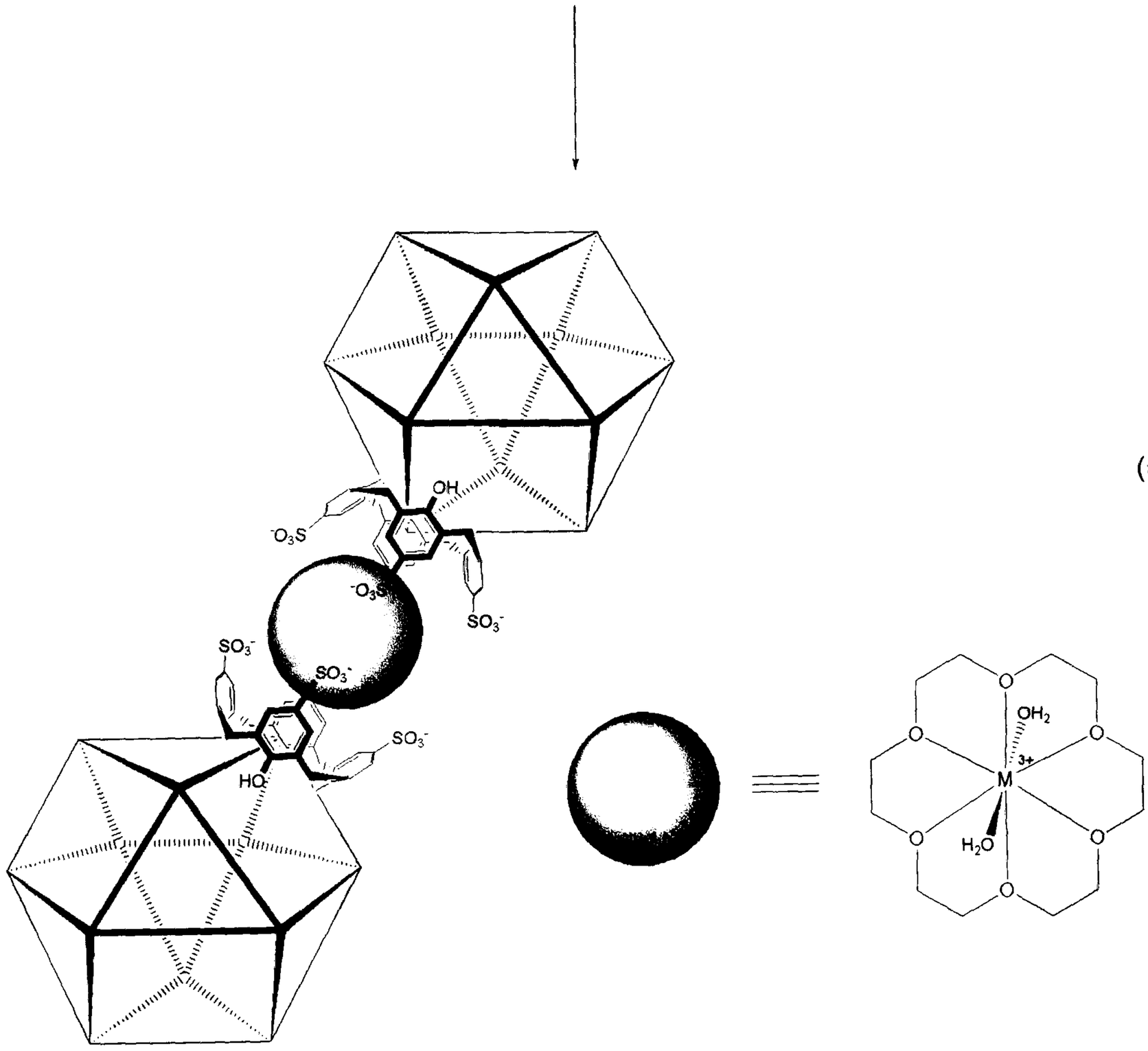

(5.2)

Complex **5.2** crystallised in a tetragonal cell and the structural solution was performed in the space group $P4/nnc$. Notably the crystals were previously found to have cubic cell dimensions and it is the

tetragonal/cubic pseudo-symmetry that is believed to be the reason for poor structural characterisation of complex **5.2** to date. Isostructural complexes with Nd^{3+} and Sm^{3-} in place of Pr^{3-} were synthesised as before and were also found to diffract poorly. X-ray diffraction data was collected but was of limited quality and gave unsatisfactory structural solutions in several space groups including *P4/nnc*. Given this, only the Pr^{3+} complex will be discussed in any detail (unit cell parameters for isostructural complexes are listed in the experimental section for complex **5.2**). Details of the data collection and structure refinement for complex **5.2** are given in Table 5.2 of this chapter. A crystallographic information file containing all bond lengths and angles for complex **5.2** can be found in appendix 5.2.1 on the attached compact disc. In a bid to further characterise complex **5.2**, transmission electron microscopy studies were performed and light scattering experiments were performed on the neodymium analogue and the results of all of these experiments will be discussed below.

As stated above, the complex is a spheroid that is composed of twelve SO_3[4] anions, arranged at the vertices of a cuboctahedron. The structure has an internal core that is occupied by six poly-aquo Pr^{3+} species (that show disorder in the aquo ligands) and neighbouring cuboctahedra are linked by Russian dolls formed with 18-crown-6/praseodymium guest species. Before complex **5.2** is discussed in detail, the original *p*-sulfonatocalix[4]arene spheroid that was reported by Atwood *et al.* will be examined more closely.[17]

That structure was elucidated and found to have twelve SO_3[4] molecules arranged at the vertices of an icosahedron.[17] The crucial building block involved in the formation of these icosahedra was a *C*-shaped dimer composed of two SO_3[4] molecules that were hinged by a tetra-aqua lanthanum metal centre. In addition to this, the lanthanum had two coordinated pyridine *N*-oxide molecules that were directed into the calixarene cavities (Figure 5.5). Once characterised, the internal volume of the cavity was estimated to be ~ 1700 $Å^3$. This was in fact an overestimation and by the use of an internal cavity volume calculation program (Cavity),[131] it was possible with the help of Professor Leonard J. Barbour to calculate the internal volume to a far greater degree of accuracy (Figure 5.6). Upon re-calculation, the true internal volume of the icosahedral arrangement was found to be 975 $Å^3$. Chapter 1 described the frequency with which large, near-spherical, multi-component supramolecular architectures, with geometries resembling the Platonic or Archimedean solids are being reported in recent times.[17, 77-80, 89, 90, 92] Pioneering work by Douglas and co-workers also showed that the virion of the cowpea chloritic mottle virus (composed of one hundred and eighty identical protein subunits) assembles into an icosahedron.[132] Under pH control, the conformation of the virion can be controlled to 'click' open, increasing the internal volume and giving rise to pores in the outer shell. These pores allow the passage of molecular material between the internal cavity

and the chemical environment. Reverse pH control can also be used to close the virion shell to trap the molecular material within.[132]

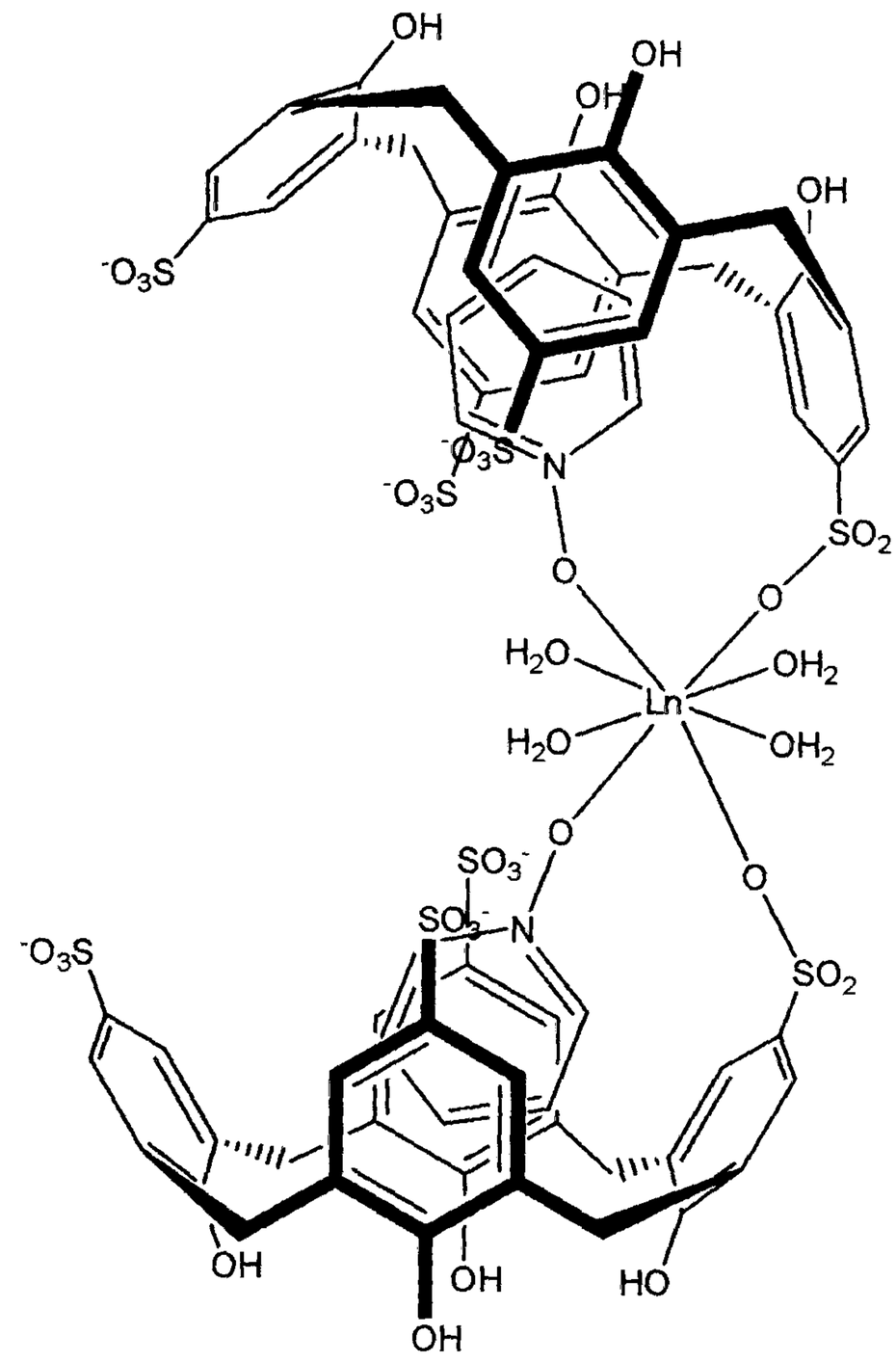

Figure 5.5 Schematic of the *C*-shaped dimer found in the icosahedral arrangement of twelve SO_3[4] molecules as reported by Atwood *et al.*[17]

In fact, the icosahedron is the most highly symmetric and most compact way to assemble twelve entities around the vertices of a twelve vertex Platonic or Archimedean solid. In the icosahedral structure reported by Atwood *et al.*, the twelve SO_3[4] molecules are seen to pack in the 'shell' of the spheroid (optimising hydrophobic and hydrophilic interactions) and are 'tightly packed' as a non-porous structure (Figure 5.7). Additionally, icosahedra can, under no circumstances, arrange in a cubic close packed manner. Each of the icosahedra are, as reported, linked *via* the *C*-shaped dimers but each icosahedron can only link to six others due to packing restrictions (Figure 5.8). The central and six nearest neighbouring icosahedra assemble in a trigonal anti-prismatic fashion (Figure 5.8 b, c). The spheroid characteristics and the packing of icosahedra are the key features that are to be used for useful comparison with complex **5.2**.

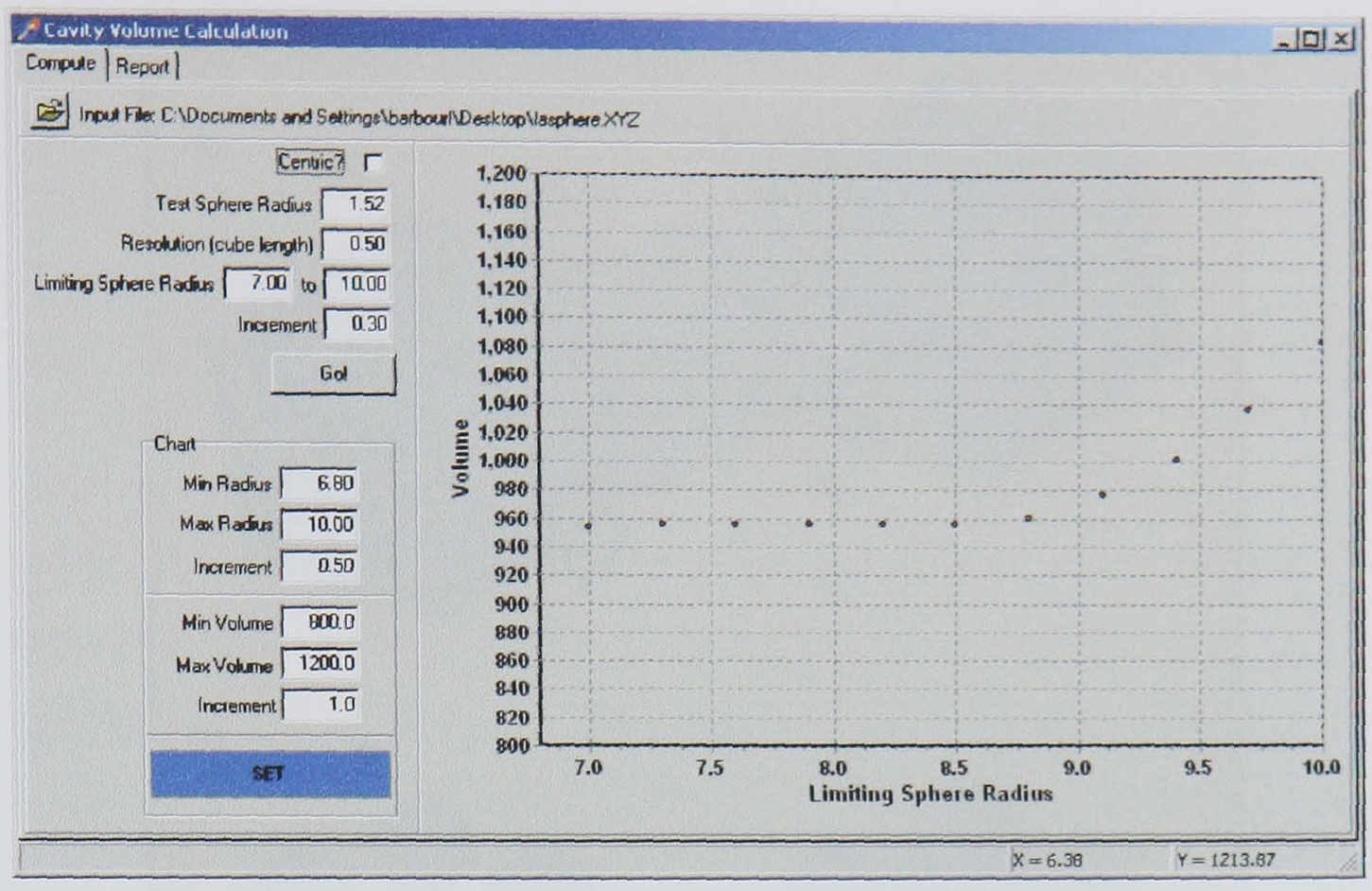

Figure 5.6 Diagram of a molecular cavity calculation performed on the icosahedral arrangement of *p*-sulfonatocalix[4]arene (reported by Atwood *et al.*) using the program Cavity.[131] Upon reaching maxiumum internal cavity volume (central plateau), a sharp increase is typically observed, indicating the calculation of exo-cavity space.

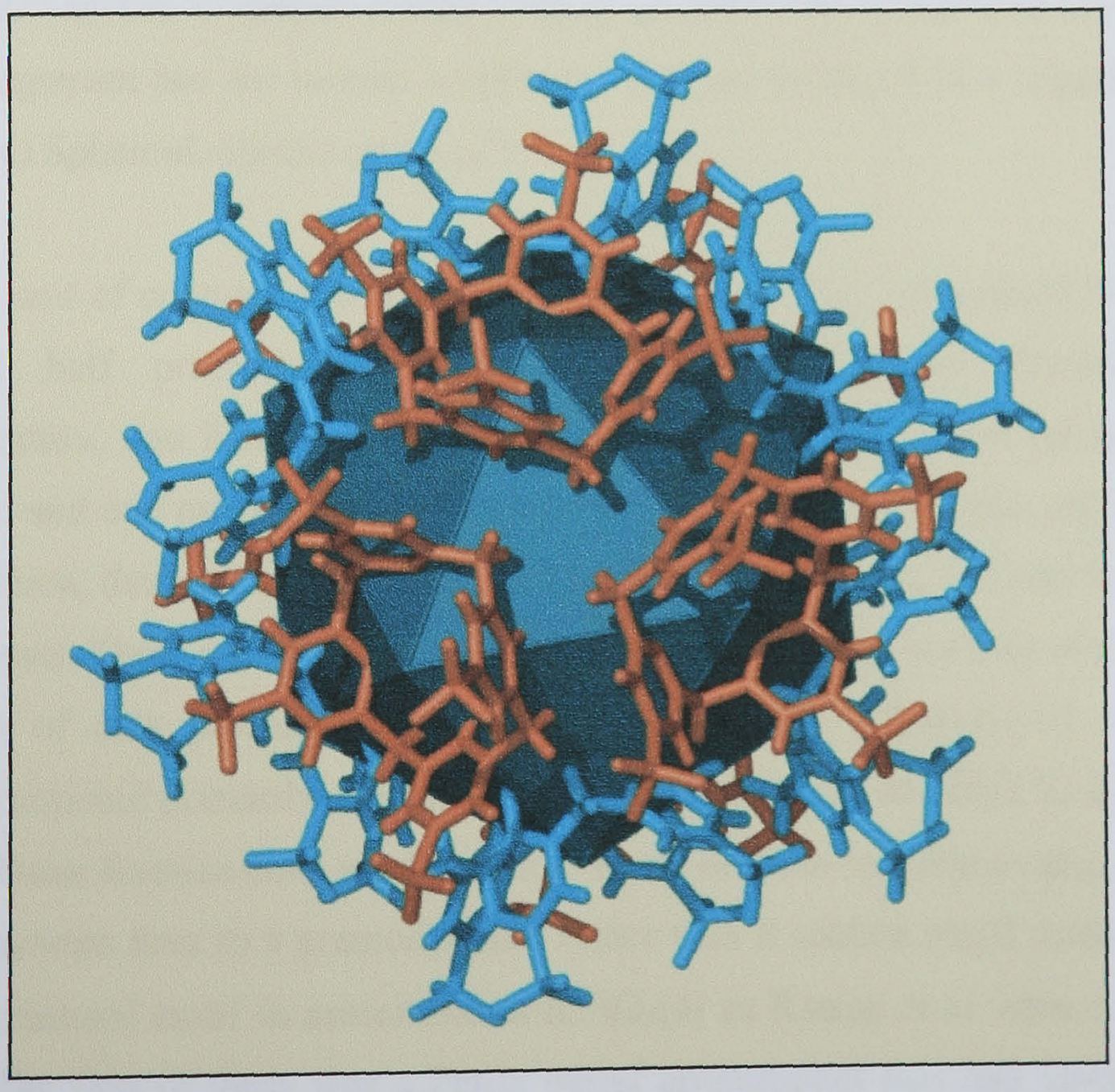

Figure 5.7 The arrangement of twelve SO_3[4] molecules at the vertices of an icosahedron showing the proximity of the calixarenes and the 'tightness' of the near-spherical array.[17]

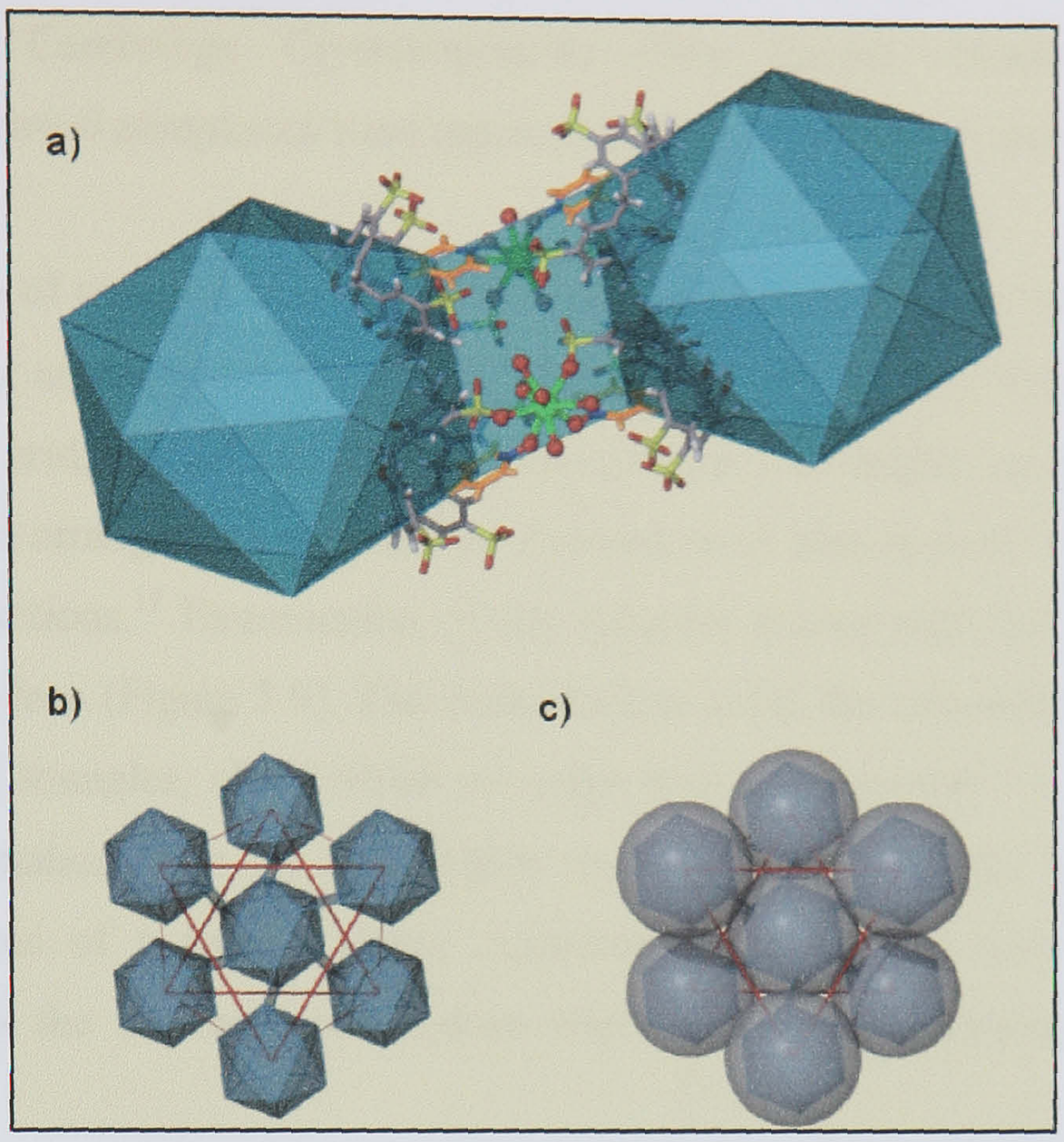

Figure 5.8 Packing diagram of the icosahedral arrangements of *p*-sulfonatocalix[4]arene reported by Atwood *et al.*[17] a) The *C*-shaped dimers joining neighbouring icosahedra are shown. b) Each icosahedral arrangement has six nearest neighbours that are arranged in a trigonal anti-prismatic formation (red). c) Spheroid representation of b).

The asymmetric unit of complex **5.2** is composed of one and a half disordered SO_3[4] molecules, two disordered half praseodymium 18-crown-6 complexes, one disordered poly-aquo praseodymium cation, one half of a disordered poly-aquo praseodymium cation (residing on a special position), and one quarter of a poly-aquo praseodymium cation (also residing on a special position). In addition, there are a total of five water molecules of crystallisation that are disordered over seven positions. There are likely many more unassigned water molecules of crystallisation but the poor quality of data precluded assignment. As illustrated schematically in Equation 5.2, complex **5.2** is composed primarily of Russian dolls, the calixarenes of which lie at the vertices of a cuboctahedron. These Russian dolls are different to many of those reported to date in that the crown ether macrocycle bears host to a praseodymium rather than a sodium metal centre. This is not an unprecedented structural motif in association with SO_3[4] as Raston *et al.* have reported two such examples.[50, 102] The first of these was a Ferris wheel arrangement that had lanthanum or cerium bound in an 18-crown-6 whilst tethered to a *p*-sulfonatocalix[4]arene.[50] The second was a Ferris wheel/Russian doll hybrid structure that also had cerium metal centres bound in 18-crown-6

molecules.[102] In addition to these results, there are many examples of lanthanide 18-crown-6 complexes on the Cambridge Crystallographic Data Centre. Noteworthy examples of praseodymium 18-crown-6 complexes were reported by Rogers and co-workers.[133, 134]

Symmetry expansion of complex **5.2** reveals the calixarenes to pack in a 'up-up' parallel manner, as for the icosahedral arrangement reported by Atwood *et al.*[17] This is achieved through CH···π interactions between bridging calixarene methylene groups and neighbouring calixarene aromatic rings. The icosahedral arrangement reported by Atwood *et al.* also showed the calixarenes to pack through CH···π interactions.[17] Examination of the spheroid shows each calixarene to reside on a vertex of a cuboctahedron (Figure 5.9). The Archimedean solid, the cuboctahedron, is composed of six squares and eight triangles, all of which are edge sharing (Equation 5.2 and Figures 5.9, 5.10 and 5.13). The cuboctahedron is the most highly symmetric and compact way to arrange twelve entities at the vertices of a twelve vertex Archimedean solid. The only other twelve vertex Archimedean solid is the truncated tetrahedron which is of lower symmetry and is of a more elliptical shape.

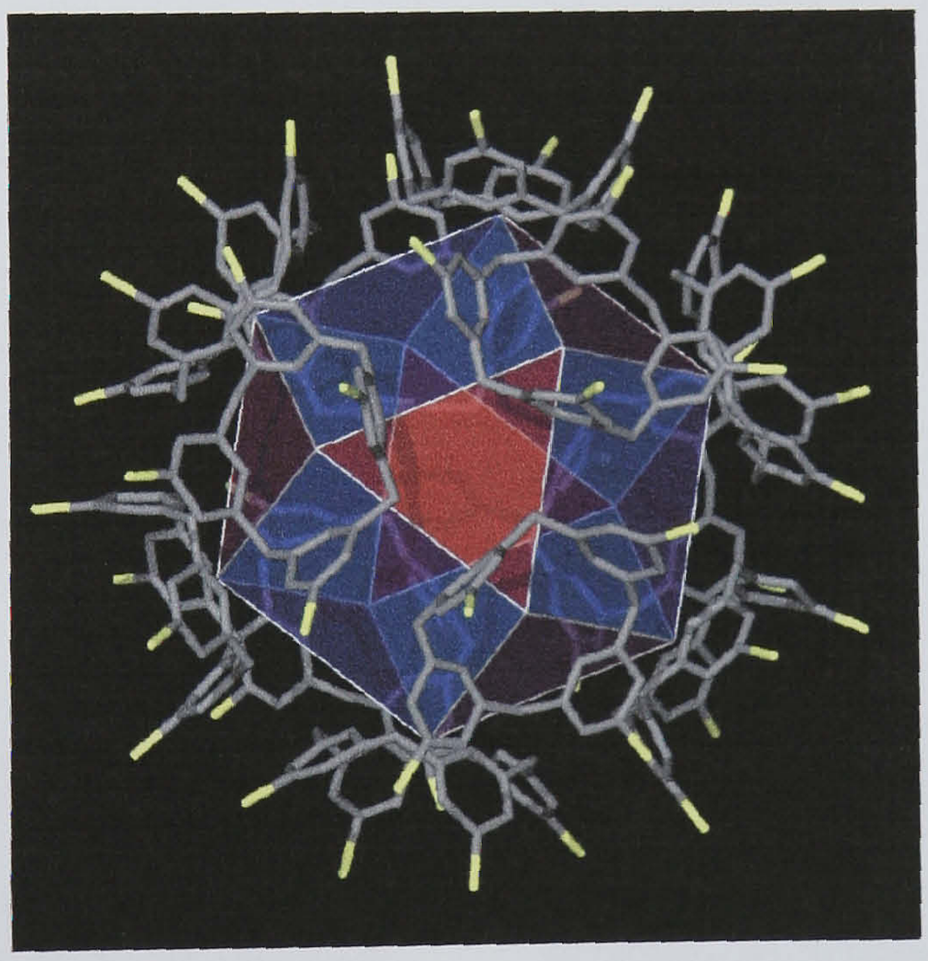

Figure 5.9 The arrangement of twelve *p*-sulfonatocalix[4]arenes around the vertices of a cuboctahedron in the crystal structure of complex **5.2**. To aid clarity, all oxygen and hydrogen atoms have been removed from the calixarenes. All other non-calixarene atoms have also been removed.

The 18-crown-6/praseodymium guest species in complex **5.2** demands the head-to-head arrangement of SO_3[4] molecules in the solid sate (as in other Russian dolls).[34, 35, 44-46] We believe that this rigid building block effect is the reason for the dramatic difference in the resulting twelve

vertex geometrical architectures as the calixarenes can only assemble in one way under such a restriction. Light scattering experiments were performed in an attempt to determine whether isolated cuboctahedra were able to form in solution prior to crystal growth or if Russian dolls were formed preferentially and then arranged into cuboctahedra upon crystallisation. Unfortunately, the rate of crystal growth is so rapid that micro-crystals grew directly after filtration of the reaction mixtures prior to the performing of the experiments, thus prohibiting useful analysis. Determination of the unit cell dimensions of the single crystals that grew from these solutions confirmed the formation of complex **5.2**. With the assumption that the building-up process *is* Russian doll to spheroid, each of the twelve SO_3[4] molecules in the spheroid shell must connect to another through the aforementioned head-to-head motif. These steric demands would inherently enforce the geometrical shape of the superstructure to be a cuboctahedron as it is the only 'regular' twelve vertex Archimedean solid capable of cubic close packing in such a way (Figure 5.10).

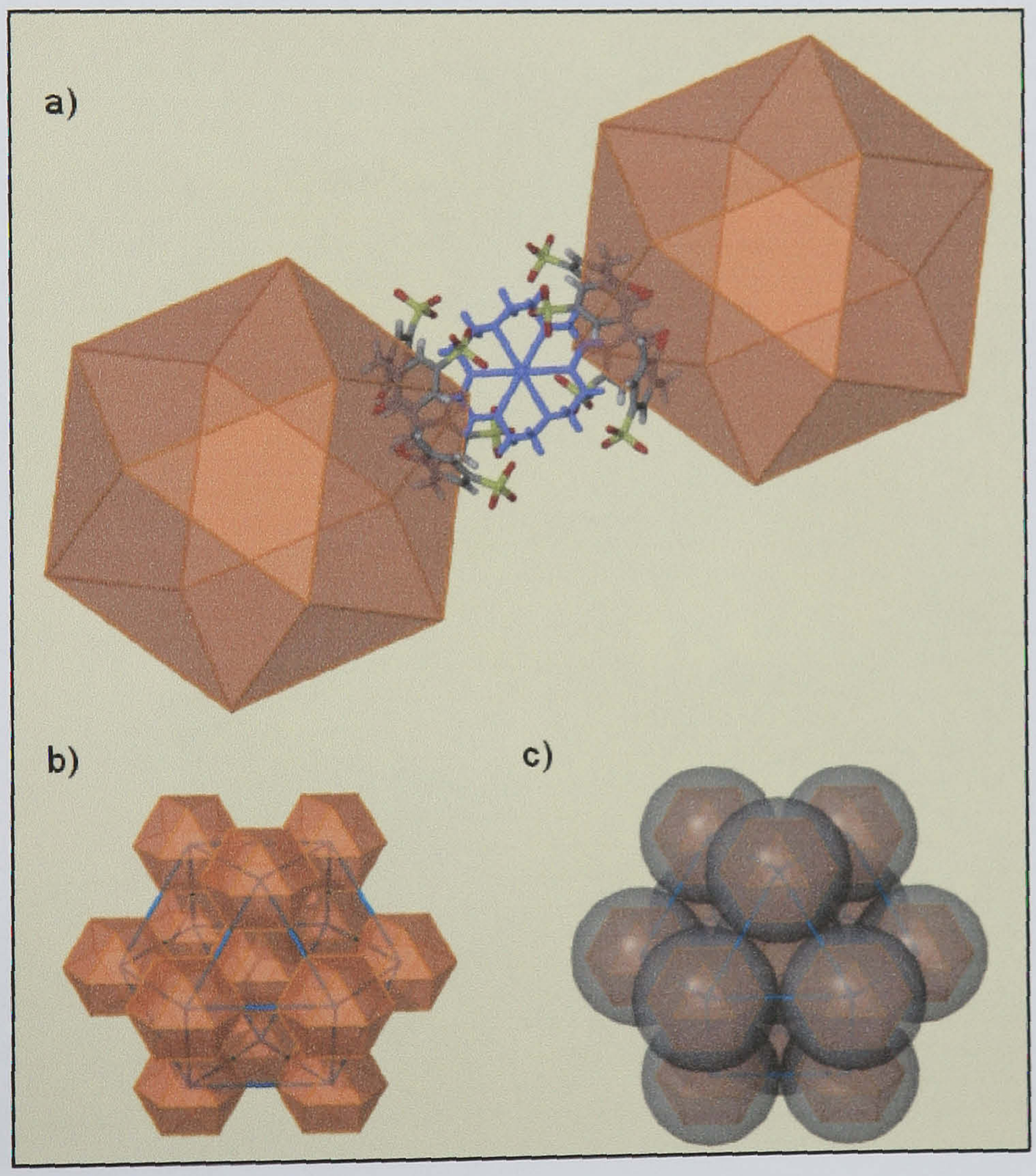

Figure 5.10 Packing diagram of the cuboctahedral arrangement found in the crystal structure of complex **5.2**. a) An idealised Russian doll linker unit is shown to join two neighbouring spheroids. b) A cubic close packed arrangement of cuboctahedra showing the ability to generate larger cuboctahedra at different nodes within the structure due to the high symmetry. c) Spheroid representation of b).

As shown above, the program Cavity can be used to accurately calculate the internal volume of spherical assemblies such as complex **5.2**.[131] Upon calculation the internal volume is found to be 1258 $Å^3$, representing an increase of ~ 30% in the internal cavity size on going from an icosahedral to cuboctahedral arrangement of twelve SO_3[4] molecules. This internal cavity is large enough to host six poly-aquo praseodymium cations and disordered waters of crystallisation (Figure 5.11) whereas the internal cavity of the icosahedral arrangement was capable of hosting thirty water molecules and two hexa-aqua sodium ions. The praseodymium cations are arranged (on special positions) at the vertices of an octahedron within the cuboctahedral arrangement of SO_3[4] (Figure 5.11). Both of the SO_3[4] arrangements are of similar diameter (~ 2.8 nm) but the icosahedron has a more elliptical shape than the cuboctahedron, thus accounting for the difference in internal volume.

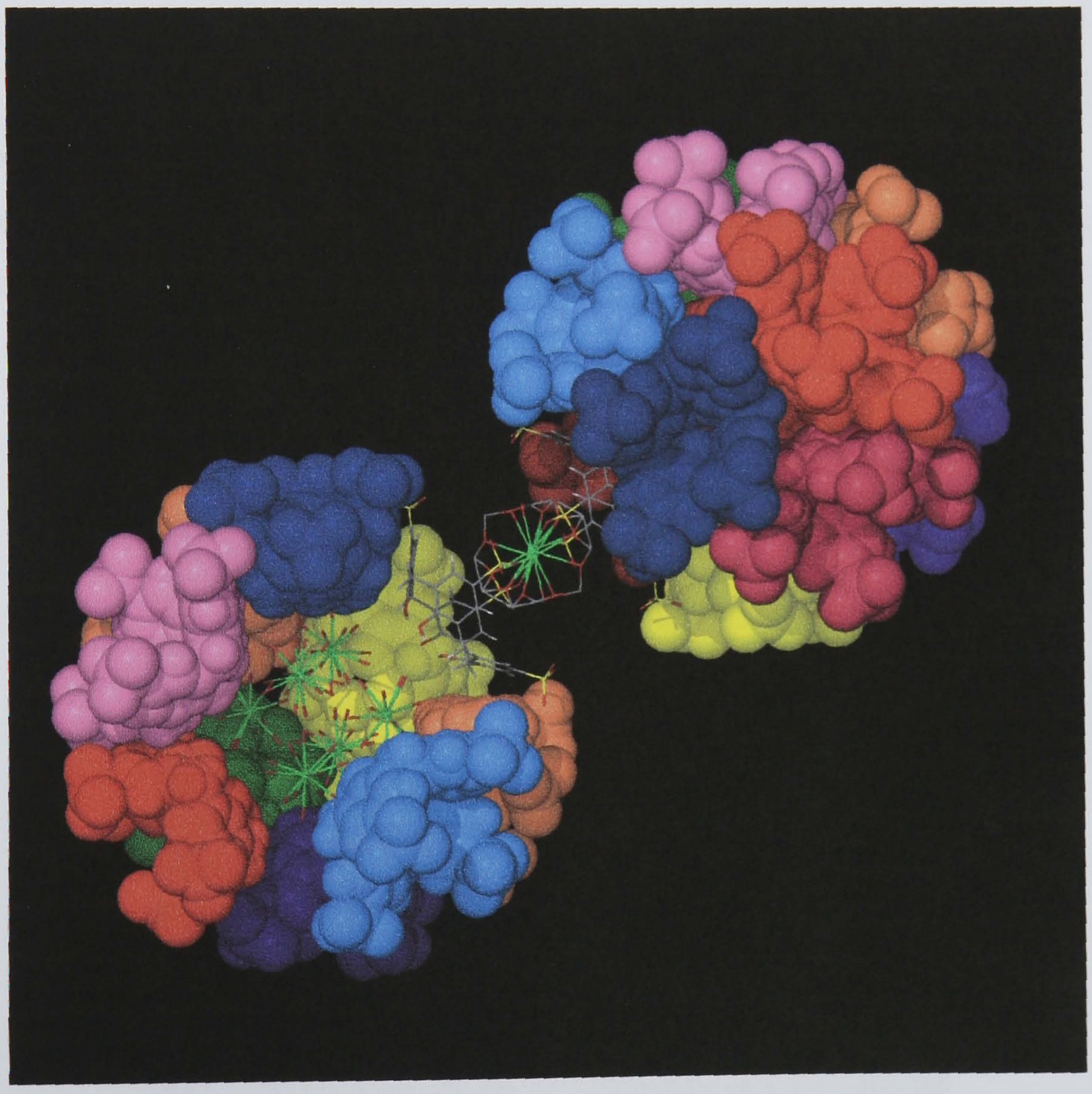

Figure 5.11 Space filling representation of two of the cuboctahedra from the crystal structure of complex **5.2**. In one cuboctahedron, one SO_3[4] molecule has been removed to show the arrangement of poly-aqua praseodymium cations in the centre of the spheroid. The Russian doll linking the two spheroids is shown in stick representation to aid visual clarity.

In fact, the icosahedron and cuboctahedron are inter-convertible *via* a sextuple diamond square (DS) process as described by Lipscomb and King.[135, 136] A DS process involves pulling the sharing vertices between two edge sharing triangles apart in order to form a square. Six of these operations transforms an icosahedron to a cuboctahedron. In addition to this, there are purportedly only two possible reasons for transforming from a icosahedral to cuboctahedral arrangement; to increase both the efficiency of packing and the volume of enclosed chemical space. [135, 136] Both of these criteria are evident upon moving from the icosahedral arrangement reported by Atwood *et al.* to the cuboctahedral arrangement in complex **5.2**.[17]

One remarkable consequence of the disparate packing described thus far is that the outer shell of the spheroid in complex **5.2** displays voids/pores (Figure 5.9 and 5.12). These pores are formed where four neighbouring calixarenes pack through one crystallographically unique CH···π interaction between the methylene hydrogen atoms and an aromatic centroid (CH···aromatic centroid distance of 2.964 Å. An example of this porosity can be seen through the blue square faces of the cuboctahedron in Figure 5.9). The pores have a Van der Waals radius of 4.18 Å and are occupied by disordered water molecules, another surprising example of a polar molecule occupying an entirely hydrophobic environment (generated by the calixarene aromatic rings surrounding the pore, Figure 5.12).

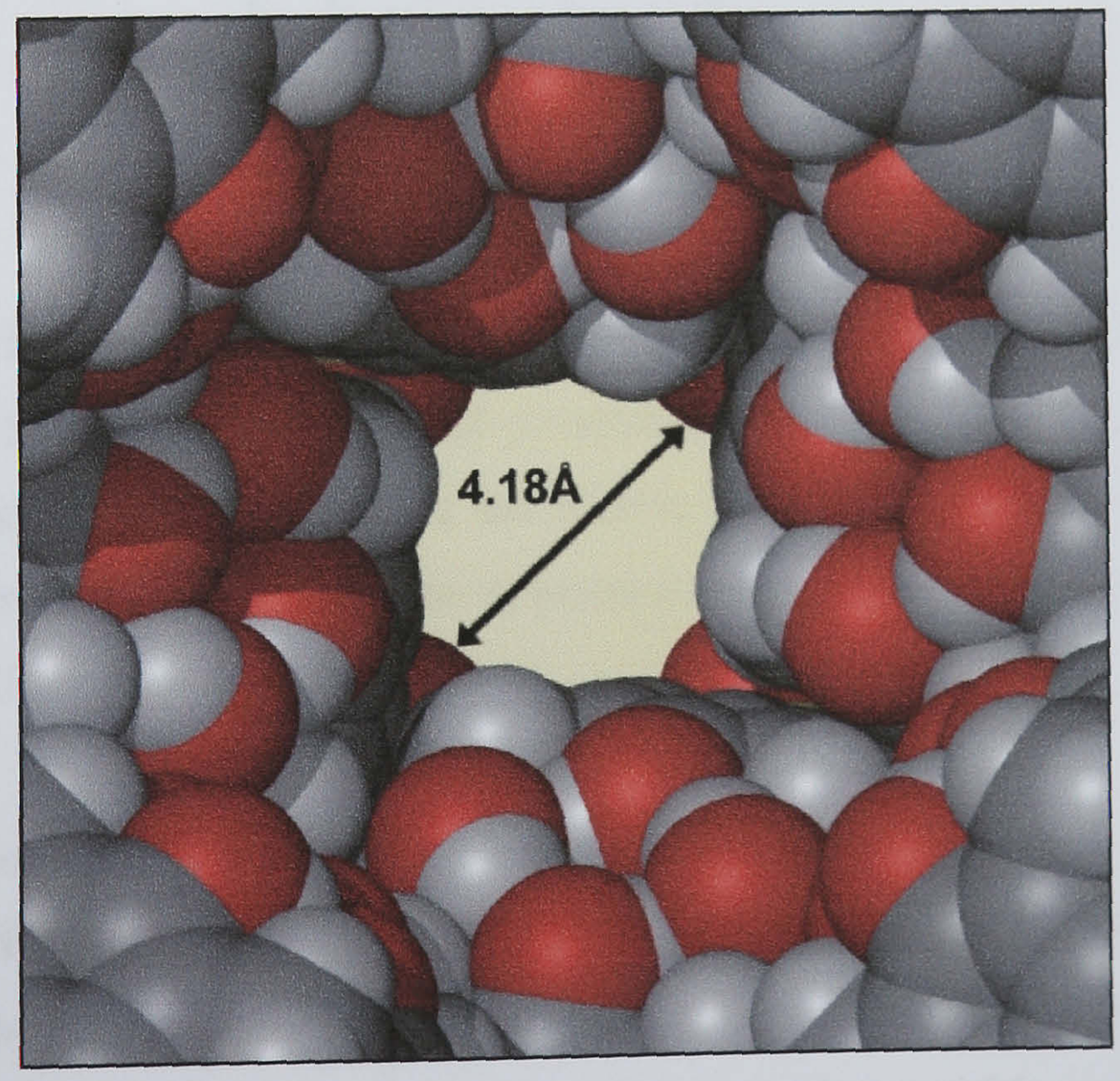

Figure 5.12 A outward view of a pore in the outer shell from the centre of the cuboctahedral arrangement of SO_3[4] molecules from the crystal structure of complex **5.2**. The van der Waals diameter is also shown.

The presence of pores in complex **5.2** is markedly different to the icosahedral structure that, as described earlier, exhibits a 'tightly packed shell' that is totally devoid of porosity. The pores in complex **5.2** are oriented along vectors radiating from the vertices of the lanthanide octahedron centred on the core of the spheroid (Figure 5.13). This arrangement can tentatively be thought of as a channel for the passage of molecular material from a hydrophilic environment, through the hydrophobic shell and into the hydrophilic interior of the spheroid and vice versa. The change of icosahedral to cuboctahedral geometry, coupled with the introduction of porosity to the calixarene 'shell' bears some resemblance to the 'clicking open' of the cowpea chloritic mottle virus virion.[122]

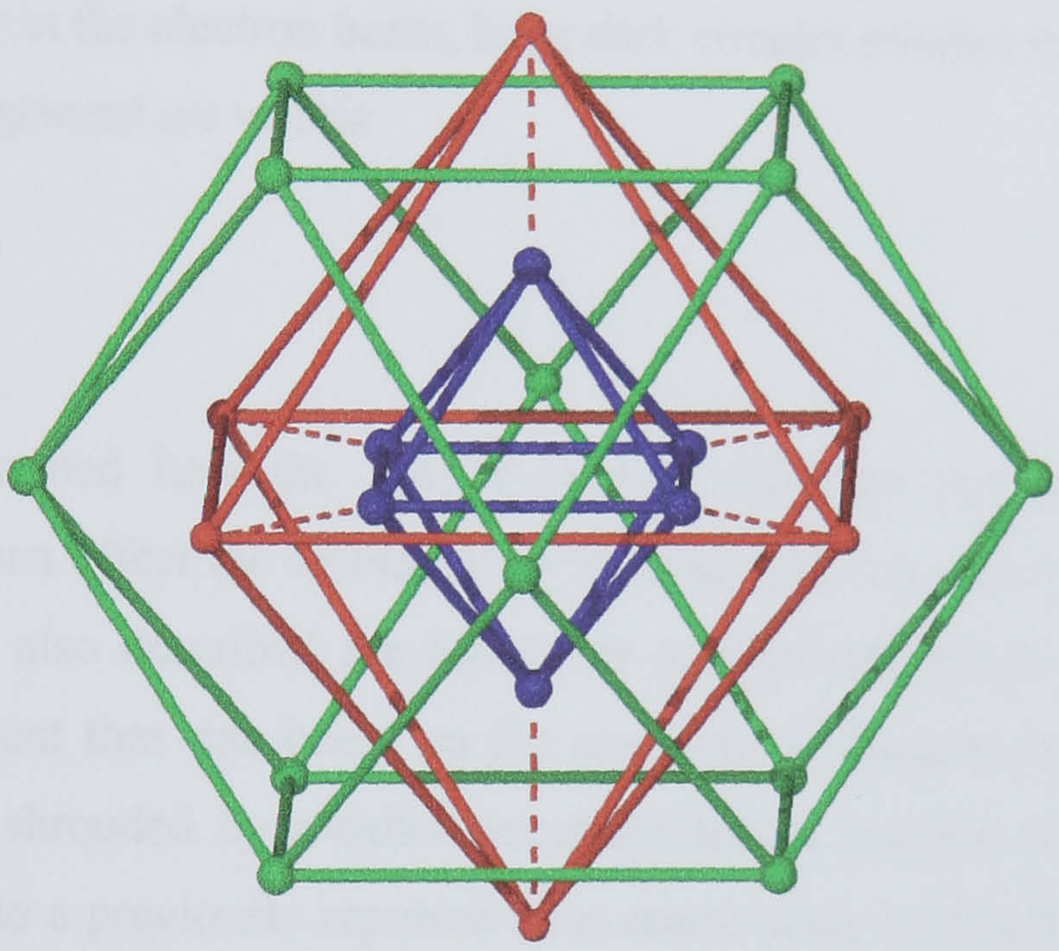

Figure 5.13 Geometrical representation of the cuboctahedral spheroid from the crystal structure of complex **5.2**. The octahedral arrangement of praseodymium metal centres in the central core are shown in purple. The calixarene centroids are shown in green to form the cuboctahedron. The porosity within the structure and the relation of pores to core praseodymium positions are shown in red balls and dashed lines.

In a further bid to characterise the spheroidal arrangements in complex **5.2**, transmission electron microscopy was performed on an analogous neodymium complex. Unfortunately, the sample degraded rapidly in the electron beam and gave less than conclusive results (Figure 5.14). Although inconclusive, some transmission electron micrographs were taken quickly and did show some large dark patches of varying size that are thought to be misaligned and degrading cuboctahedral arrangements. The dimensions of these dark patches are close to the expected values for complex **5.2** (~ 2.8 nm).

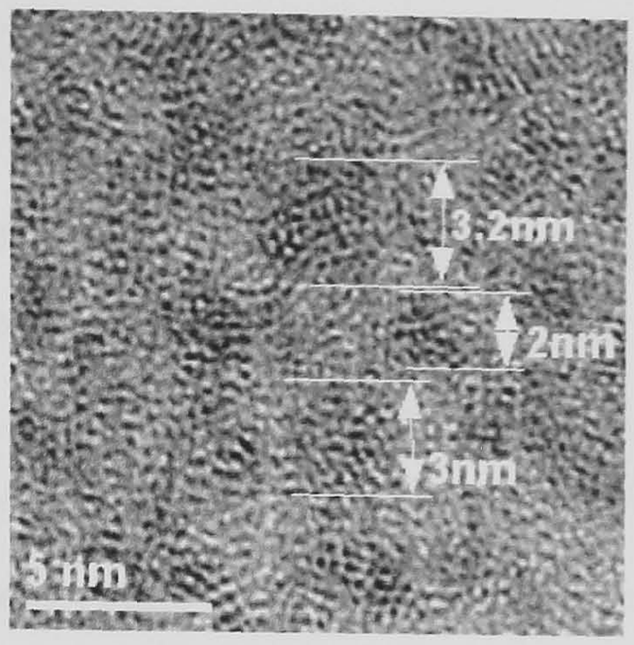

Figure 5.14 Transmission electron micrograph of complex **5.2**. Although no definite structure is observable due to decay in the electron beam, large dark circular patches that are of a size similar to the cuboctahedral arrangement are visible.

5.3 Conclusion.

This chapter first described how the use of slightly different reaction conditions (different lanthanide salt or pH) can affect the formation of Russian dolls containing 18-crown-6 as a guest molecule. This chapter also described the formation and characterisation of a nano-metre scale cuboctahedral arrangement that was based on the assembly of Russian dolls that have lanthanide 18-crown-6 complexes shrouded by *p*-sulfonatocalix[4]arenes (section 5.2). The discussion also compared complex **5.2** to a previously reported nano-metre scale icosahedral spheroid based on *p*-sulfonatocalix[4]arene and showed there to be marked differences between the two.[17] One such difference is an increase of ~ 30% in the internal spheroid volume upon moving from an icosahedral to cuboctahedral arrangement. Another result of this geometrical change is more efficient crystal packing, trigonal anti-prismatic to cubic close packed upon moving from the icosahedron to the cuboctahedron respectively.[17] Notably, both calixarene spheroid 'skins' were formed by the molecule packing through CH···π rather than π-stacking interactions that are often observed in the common 'up-down' anti-parallel solid state bi-layer motif of SO_3[4]. Clearly the presence of a calixarene head-to-head-enforcing guest species has a profound effect on the overall superstructure and future studies should include other similar species to see if similar results can be achieved.

5.4 Experimental.

p-Sulfonic acid calix[4]arene and penta-sodium *p*-sulfonatocalix[4]arene were synthesised by literature methods and purity was checked via ^{1}H NMR spectroscopy.[8] Praseodymium triflate was

purchased from Aldrich and used as supplied without further purification. X-ray data for complexes **5.1** and **5.2** were collected at 150(2) K on an Enraf-Nonius KappaCCD diffractometer with Mo-Kα radiation. Data were corrected for Lorentz and polarisation effects and absorption corrections were applied using multi-scan techniques. The structures of complexes **5.1** and **5.2** were solved by direct methods using SHELXS-97 and refined with full-matrix least squares on F^2 using SHELXL-97. Hydrogen atoms were placed at geometrically calculated positions in all complexes. Infrared spectra were run as KBr discs on a MIDAC FT-IR spectrometer. Microanalyses were not performed as crystals of both complexes showed visual degradation upon removal from the mother liquor.

5.4.1 Synthesis of the lanthanide based Russian doll $[Na(H_2O)_2\subset$18-crown-6$]\subset\{(Pr(H_2O)_9)_2$(*p*-sulfonatocalix[4]arene$)_2\}\cdot 10H_2O$, 5.1.

p-Sulfonic acid calix[4]arene (10 mg, 13.4 μmol), 18-crown-6 (11 mg, 40 μmol) and praseodymium triflate (18 mg, 27 μmol) were dissolved in distilled water (1 cm^{-3}) and the pH of the solution was altered to be 2.6 *via* addition of 1M NaOH. Slow evaporation afforded colourless crystals that were suitable for X-ray diffraction studies. Yield 10 mg, 55 %. IR(KBr disc, ν cm^{-1}): 3420s, 3200s, 1654m, 1595w, 1472m, 1422m, 1300w, 1268m, 1200s, 1165s, 1120s, 1090s, 1043s. The increase in the number of sulfonate group stretching frequencies suggests lanthanide/sulfonate coordination, as was found in the crystal structure solution. **X-ray crystallography**: Residual electron density is associated with disordered praseodymium aquo ligands. The oxygen atoms of the S(1) sulfonate group are disordered over two positions at equal occupancy. The oxygen atoms of the S(1) sulfonate group are disordered over three positions with parital occupancies of 0.2, 0.6 and 0.2. Two of the S(3) sulfonate group oxygen atoms are disordered over two positions with partial occupancies of 0.7 and 0.3. One S(3) sulfonate group oxygen atom is disordered over two positions with partial occupancies of 0.7 and 0.3 whilst another is disordered over two positions at equal occupancy. The U_{ij} values all of the crown ether atoms were constrained to be the same, as were all of the disordered praseodymium aquo ligands. Some bond lengths were restrained to be chemically meaningful.

5.4.2 Synthesis of the cuboctahedral assembly $[Pr(H_2O)_9]_6\subset[\{((Pr\subset$18-crown-6$)_{0.5})\subset$(*p*-sulfonatocalix[4]arene $- H^+)\}_{12}][(Pr(H_2O)_9)_6]\cdot XH_2O$, 5.2.

Penta-sodium *p*-sulfonatocalix[4]arene (20 mg, 19 μmol), 18-crown-6 (16 mg, 59 μmol) and praseodymium triflate (17 mg, 29 μmol) were dissolved in distilled water (2 cm^3). Upon standing over 2 – 5 hours, large green crystals that were suitable for X-ray diffraction studies formed. Yield 36 mg, no percentage given theoretical formula. **X-ray crystallography**: Residual electron density

is located around 1 Å from a praseodymium metal centre. A significant degree of disorder of the calixarene sulfonate groups as well as the water molecules of crystallization is evident. Unequivocal location of the crown ether atoms was not possible but the presence of the crown ether was inferred from circular patterns of residual electron density that comported with the overall shape of an 18-crown-6 molecule. Some crown ether atoms were assigned but not all were located. The aromatic rings of the calixarenes are distorted. The high R_1 is due to the extensive disorder problems throughout the entire structure. Notably several data sets were recorded for this complex, including one at a synchrotron source but this did not resolve the extensive disorder problem.

Complex number	**5.1**	**5.2**
Formula	$C_{34}H_{70.50}Na_{0.50}O_{37.25}PrS_4$	$C_{66}H_{100}O_{40}Pr_{3.75}S_6$
*M*r	1356.05	2254.23
Crystal system	Monoclinic	Tetragonal
Space group	$P2_1/c$	$P4/nnc$
T/K	150(2)	150(2)
a /Å	17.319(3)	30.052(4)
b /Å	18.702(4)	30.052(4)
c /Å	20.782(9)	42.551(9)
α /°	90	90
β /°	118.18(2)	90
γ /°	90	90
U Å^3	5933(3)	38428(11)
Z	4	18
F(000)	2804	20399
ρ_{calc} /g cm^{-3}	1.518	1.753
μ /cm^{-1}	1.061	2.339
$\Theta_{min,\ max}$ /°	1.33, 25.0	1.35, 18.18
Data collected	70997	121530
Unique data	10440	6728
R_{int}	0.1425	0.1718
Obs data ($I>2\ \sigma(I)$)	6608	5015
Parameters	646	526
Restraints	10	0
R_1 (observed data)	0.137	0.291
ωR_2 (all data)	0.3488	0.6174
S	2.063	4.674
Max/min residuals [eÅ^3]	2.052, -1.881	5.699, -2.516

Table 5.2 Details of data collection and structure refinement for complexes **5.1** and **5.2**.

Chapter six:

Host-guest, coordination polymer, Ferris wheel and (bis)molecular capsule arrangements incorporating *p*-sulfonatocalix[5]arene.

6.0 Introduction.

This chapter is composed of three sections and is focussed on developing the solid state supramolecular chemistry of *p*-sulfonatocalix[5]arene (SO_3[5]) *via* the use of appropriate guest molecules in the presence or absence of lanthanide or sodium metal cations (Figure 6.1). The majority of reported structural chemistry incorporating SO_3[5] has focused on lanthanide (Ln) or transition metal (TM) pyridine *N*-oxide complexes.[67, 68] The relative lack of progress in this area of supramolecular chemistry is likely owing to the fact that preparation of SO_3[5] is more synthetically challenging in comparison to the *p*-sulfonatocalix[4,6,8]arenes that can be readily synthesised on a multi-gram scale.[8]

The first section of this chapter is describes the formation of host-guest europium/SO_3[5]/4-picoline *N*-oxide (4-PicNO) or 4,4'-dipyridine-*N,N'*-dioxide (DiPyNO) complexes, the results of which are effectively an extension to the Ln/SO_3[5]/PyNO or transition metal/SO_3[5]/pyridine complexes reported by Atwood *et al.*[67, 68] The second section of this chapter describes the formation of two lanthanide/crown ether/SO_3[5] host-guest complexes that incorporate diaza-18-crown-6 or diaza-15-crown-5, both in their di-protonated forms.

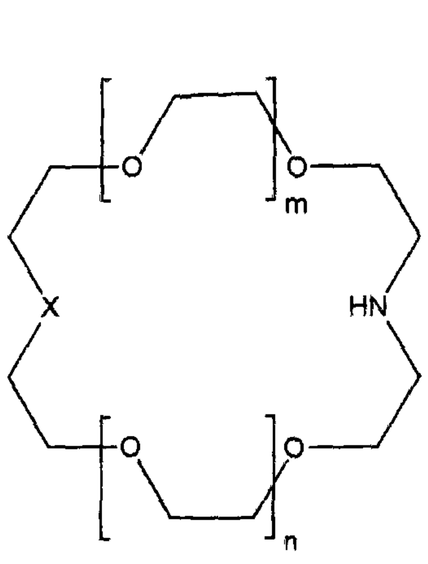

x = NH, m = 1, n = 1, diaza-18-crown-6
x = O, m = 1, n = 1, 1-aza-18-crown-6
x = NH, m = 0, n = 1, 1,7-diaza-15-crown-5
x = O, m = 0, n = 1, 1-aza-15-crown-5
x = NH, m = 0, n = 0, 1,7-diaza-12-crown-4

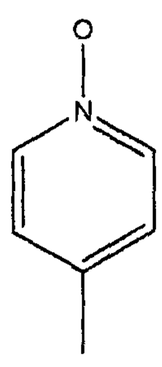

pyridine *N*-oxide

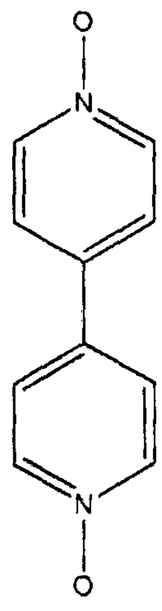

4,4'-dipyridine-*N,N'*-dioxide

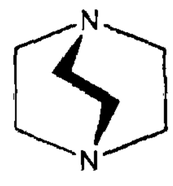

1,4-diazabicyclo[2.2.2]octane

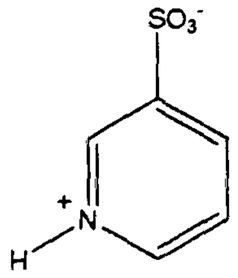

3-pyridine sulfonic acid

Figure 6.1 Guest molecules selected for supramolecular assembly formation with *p*-sulfonatocalix[5]arene.

The second section also describes the formation of a lanthanide/1-aza-18-crown-6/Na/SO_3[5] coordination polymer that has extended Ferris wheels similar to those reported by Raston *et al.* for *p*-sulfonatocalix[4]arene.[35, 50] The third section describes two alternative supramolecular structures that form when Na_5SO_3[5] is reacted with either 1,4-diazabicyclo[2.2.2]octane (DABCO) or 3-pyridine sulfonic acid ($PySO_3$) at a pH of <1. The former of the two, when di-protonated, causes a solid state conformational distortion of SO_3[5], the result of which is the formation of a *bis*-molecular capsule arrangement. When 3-pyridine sulfonic acid is reacted with Na_5SO_3[5]. a coordination polymer of molecular capsules containing two $PySO_3$ molecules results.

p-Sulfonatocalix[5]arene, in the solid state, typically adopts a truncated cone shape similar to that observed for the tetrameric analogue.[25, 26, 68] The cone of *p*-sulfonatocalix[5]arene is splayed to a greater extent due to the increased number of aromatic rings in the macrocycle and all the structural examples of SO_3[5] reported to date show the host to assemble in a bi-layer arrangement that is similar to that found for *p*-sulfonatocalix[4]arene.[35, 66-68] All but one of the structures described in this chapter adopt a similar arrangement but this shall be discussed further below. Hydrogen atoms have been omitted in the majority of diagrams to aid visual clarity except where required for illustrative purposes. Water molecules of crystallisation have also been omitted for clarity, again unless included for particular purpose.

6.1 Lanthanide 4-picoline-*N*-oxide or 4,4'-dipyridine-*N,N'*-dioxide complexes of *p*-sulfonatocalix[5]arene.

As described in the introduction to this chapter, much of the structural chemistry relating to *p*-sulfonatocalix[5]arene has been reported by Atwood *et al.*[35, 67, 68] This work focused primarily on the formation of lanthanide pyridine *N*-oxide complexes of SO_3[5] and showed the molecule capable of assembling in molecular capsules or other capsular resembling assemblies.[67, 68] Chapter five described the formation of a nano-metre scale spheroid that incorporated PyNO as guest molecule in the cavity of *p*-sulfonatocalix[4]arene. Given that this particular guest had been examined extensively with the *p*-sulfonatocalix[4,5]arenes, the 2, 3 and 4-picoline *N*-oxides were employed as guest molecules in lanthanide/SO_3[4,5,6] systems. Unfortunately from all guest and calixarene combinations examined, success was only achieved in the formation of a 4-PicNO/SO_3[5]/europium complex. When 4,4'-dipyridine-*N,N'*-dioxide (DiPyNO) is employed as a potential guest in a europium/SO_3[5] system, an interesting host-guest complex results.

6.1.1 Structure of the complex [((4-picoline *N*-oxide)⊂(*p*-sulfonatocalix[5]arene))$_2$ + 3H$^+$)(Na(H$_2$O)$_3$)][Eu(H$_2$O)$_9$]·9.75H$_2$O, 6.1.

Crystals of the complex [(4-picoline *N*-oxide)$_2$⊂[(*p*-sulfonatocalix[5]arene + H$^+$)(Na(H$_2$O)$_2$)][(Eu(H$_2$O)$_9$)$_2$]·9.75H$_2$O, **6.1**, grew upon slow evaporation of an acidic aqueous solution containing a 1:3:1 mixture of Na$_5$SO$_3$[5], 4-picoline *N*-oxide and europium(III) nitrate (pH adjusted to be <1 with 1M HCl, Equation 6.1). The complex was characterised by IR spectroscopy and single crystal X-ray crystallography. Complex **6.1** crystallises in an orthorhombic cell and the structural solution was performed in the space group *Pbcn*. Details of data collection and structure refinement are given in Table 6.9 of this chapter. A crystallographic information file containing all bond lengths and angles for complex **6.1** can be found in appendix 6.1.1 on the attached compact disc.

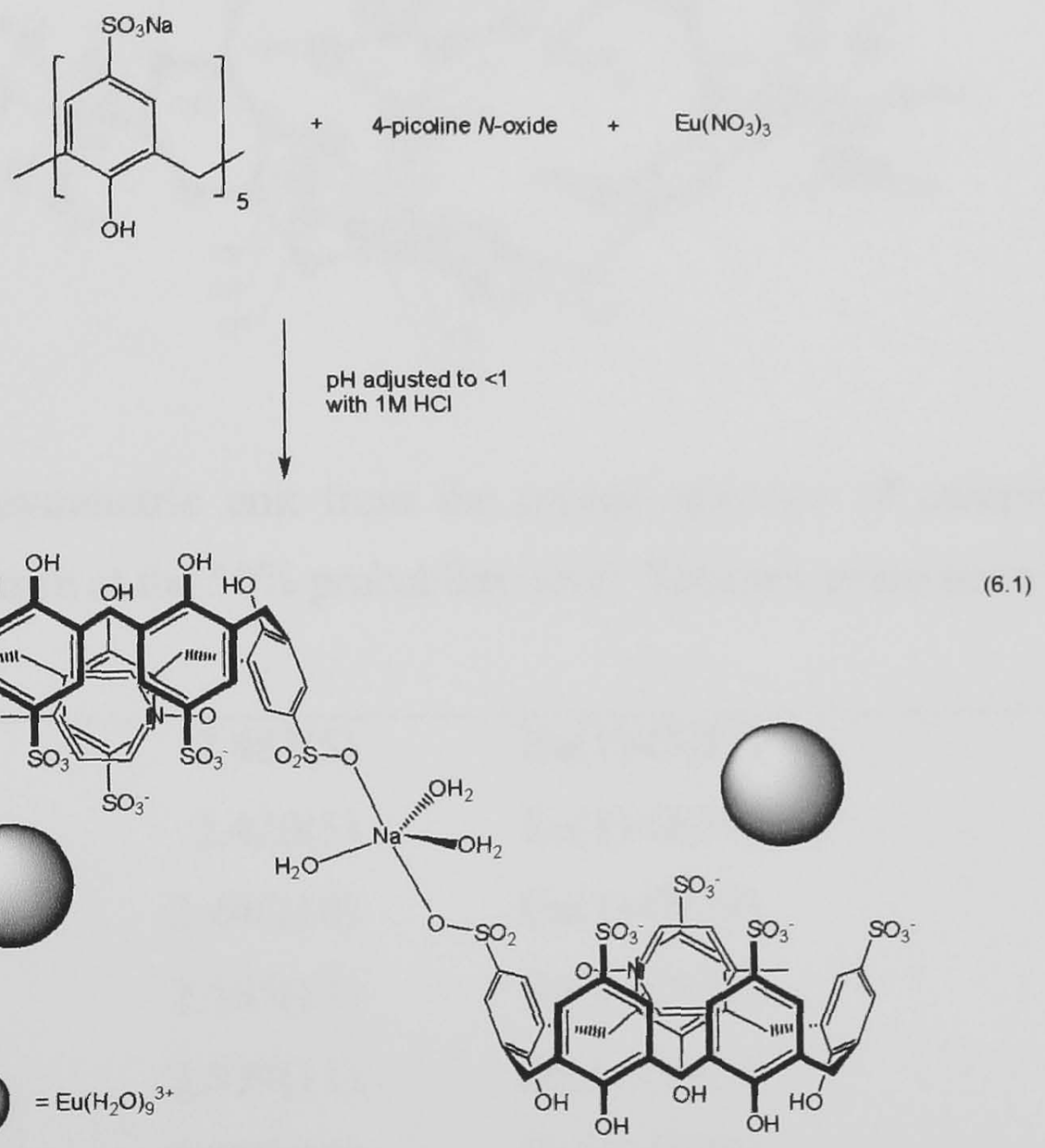

The asymmetric unit consists of one *p*-sulfonatocalix[5]arene, one 4-picoline *N*-oxide, one disordered nona-aqua europium cation, one half of a sulfonate bound tris-aquo sodium centre (residing on a special position) and a total of nine and three quarter water molecules that are disordered over fifteen positions (Figure 6.2). The SO$_3$[5] is seen to adopt a cone conformation and the cavity hosts the 4-PicNO molecule (Figures 6.2 and 6.3). Although the nona-aqua europium cation is disordered, the species is of near tri-capped trigonal prismatic geometry. Symmetry expansion of the coordination sphere of the sodium atom in complex **6.1** shows the metal to be five

coordinate and of trigonal bi-pyramidal geometry. Within the asymmetric unit, O(47) and Na(1) lie along a two fold rotation axis whilst O(46) is on a general position (Figures 6.2 and 6.3). Bond lengths relating to the coordination spheres of both the europium and sodium metal centres are listed in Table 6.1.

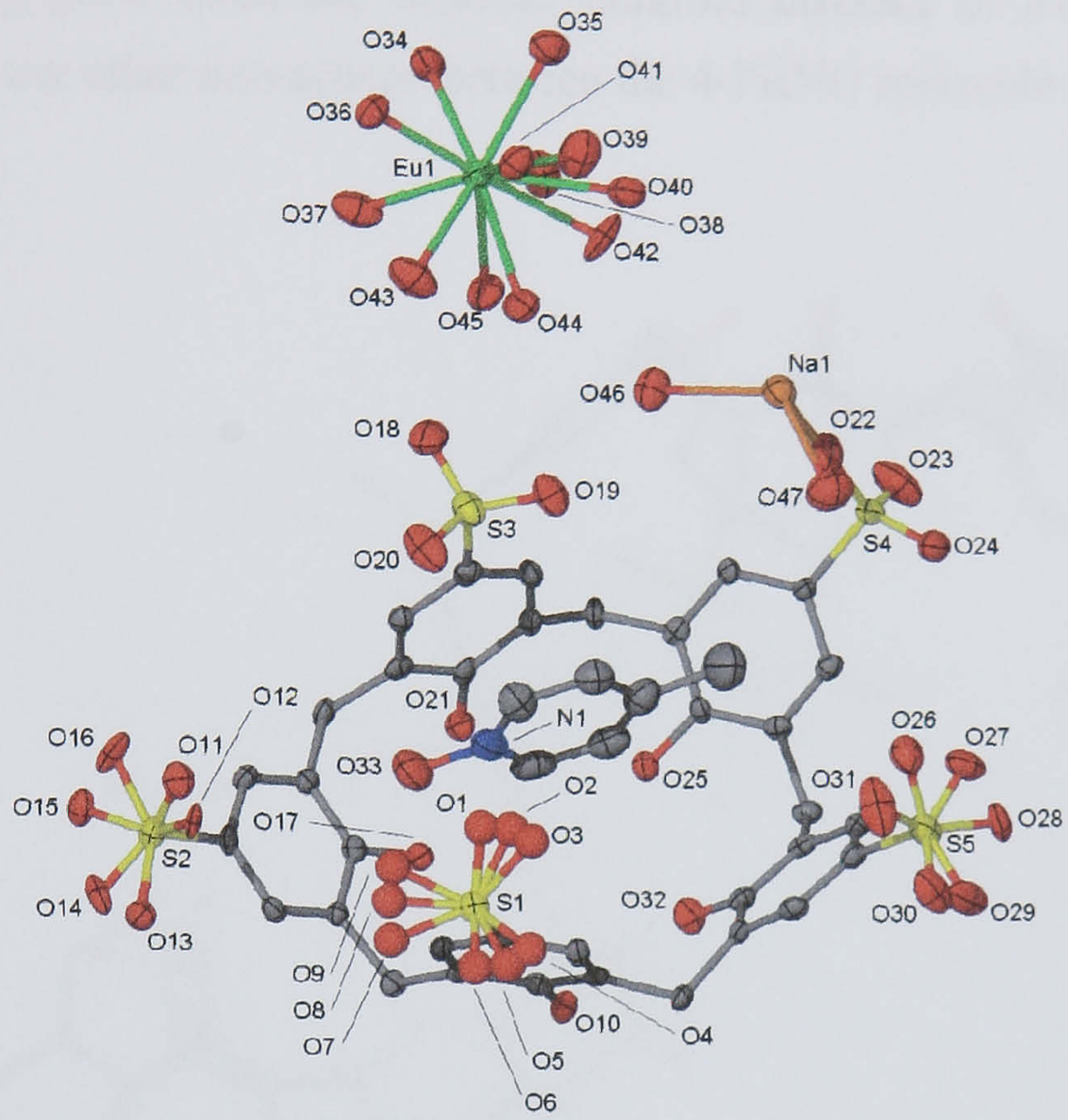

Figure 6.2 Part of the asymmetric unit from the crystal structure of complex **6.1**, anisotropic displacement ellipsoids shown at the 50% probability level. Selected atoms have been labelled.

Eu(1)-O(34)	2.487(5)	Eu(1)-O(35)	2.487(5)
Eu(1)-O(36)	2.420(5)	Eu(1)-O(37)	2.462(6)
Eu(1)-O(38)	2.446(10)	Eu(1)-O(39)	2.525(16)
Eu(1)-O(40)	2.565(12)	Eu(1)-O(41)	2.586(5)
Eu(1)-O(42)	2.379(11)	Eu(1)-O(43)	2.459(5)
Eu(1)-O(44)	2.367(10)	Eu(1)-O(45)	2.506(9)
Na(1)-O(46)	2.357(6)	Na(1)-O(47)	2.319(9)
Na(1)-O(46)$^{(a)}$	2.357(6)	Na(1)-O(22)$^{(b)}$	2.409(6)
Na(1)-O(22)$^{(c)}$	2.409(6)		

Table 6.1 Interatomic distances relating to the coordination spheres of the europium and sodium metal centres in the crystal structure of complex **6.1** (distances given in Å with e.s.d. in parentheses). Key operations for symmetry related atoms: *(a)* -x, +y, 1/2-z, *(b)* 1/2-x, 1/2-y, 1/2+z, *(c)* -1/2+x, 1/2-y, -z.

Further symmetry expansion around the sodium coordination sphere reveals an up-down *bis*-SO_3[5] arrangement that is linked *via* calixarene sulfonate groups through the penta-coordinate sodium centre (Figure 6.3). As described earlier, the cavity of the *p*-sulfonatocalix[5]arene is occupied by a 4-PicNO molecule and there is a π-stacking interaction between the aromatic ring of the calixarene S(3) fragment and the guest (aromatic centroid···centroid distance of 3.885 Å). There do not however appear to be any other interactions between the 4-PicNO molecule and any other aromatic rings of the calixarene.

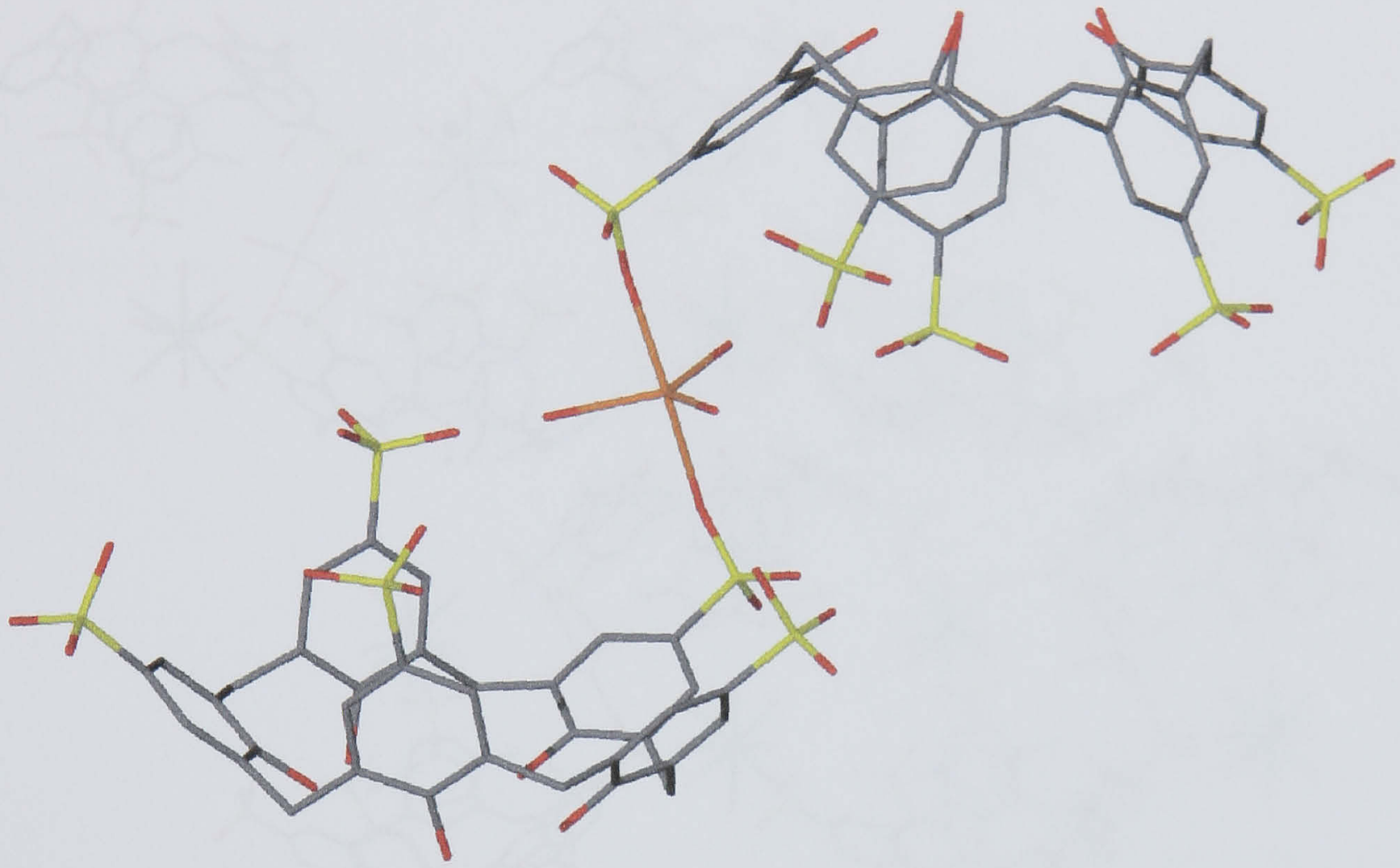

Figure 6.3 The SO_3[5] – Na – SO_3[5] link found in the crystal structure of complex **6.1** showing the full coordination sphere of the sodium centre and the up-down *bis*-SO_3[5] arrangement. 4-Picoline *N*-oxide molecules, homoleptic europium cations and some disordered calixarene sulfonate oxygen atoms have been omitted for clarity.

Examination of the extended structure reveals the calixarenes to pack in a bi-layer arrangement similar to those described by Atwood *et al.* for the Ln/PyNO/SO_3[5] complexes described above (Figure 6.4). The SO_3[5] molecules in the bi-layer arrangement pack through two crystallographically unique interactions. There is one π-stacking interaction between aromatic groups of neighbouring calixarenes with an aromatic centroid···centroid distance of 3.803 Å. There is also one CH···π interaction from a methylene bridging group to an aromatic ring of a neighbouring calixarene with a CH···aromatic centroid distance of 2.774 Å. Given the extent of the disorder associated with the homoleptic europium cation and calixarene sulfonate groups, coupled with the locally disordered water molecules, numerous possible EuO···OS or EuO···O hydrogen bonding interactions are evident. Some ambiguity arises when the overall charge of the arrangement

is considered. In one *bis*-asymmetric unit arrangement, there are two SO_3[5] molecules presenting a probable 10– charge. This charge is partially counterbalanced by the presence of two nona-aqua europium cations and a tris-aqua sodium metal centre, all of which have a cumulative charge of 7+. Hence there is an overall charge deficit of 3–. This deficit may be balanced by sulfonate group protonation given that the pH adjusted solution (pH <1) undergoes slow evaporation to achieve crystal growth.

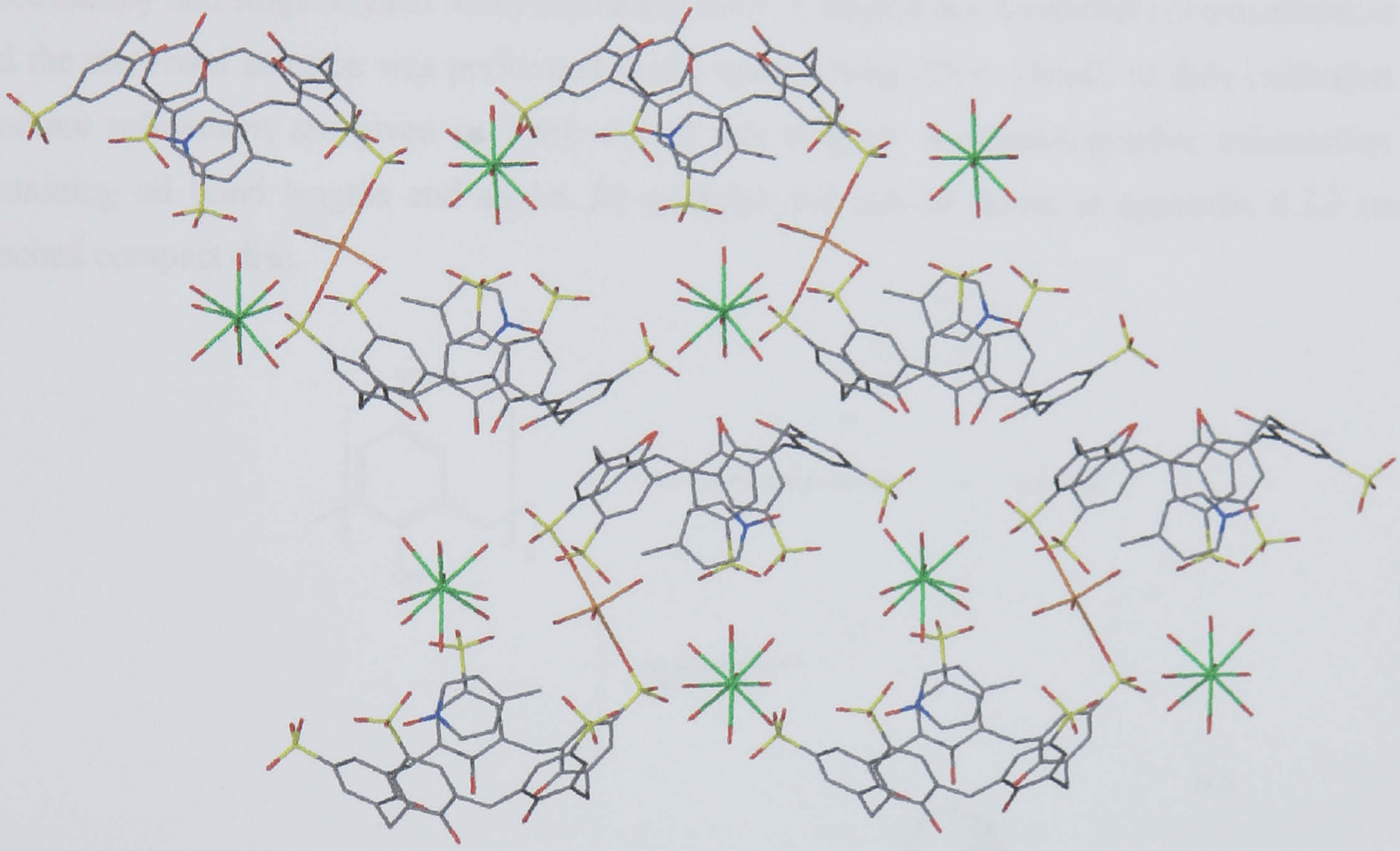

Figure 6.4 Extended symmetry expansion of the crystal structure of complex **6.1** showing the bi-layer arrangement of *p*-sulfonatocalix[5]arenes, the up-down SO_3[5] dimers and the positioning of the nona-aqua europium cations within the extended structure. Some disordered calixarene sulfonate oxygen atoms and europium aquo ligands have been omitted for clarity.

The non-coordinated 4-PicNO in complex 6.1 partially resembles a PyNO/La/Na/SO_3[5] complex that was reported by Atwood et al. in which PyNO was included in the molecular cavity but was also non-coordinating. When 4-PicNO in the above ternary system is replaced with 4,4'-dipyridine-*N,N'*-dioxide, a Eu/SO_3[5]/DiPyNO host-guest complex forms. The complex shows partial inclusion of the guest within the cavity of SO_3[5] and the host-guest assemblies dimerise through intermolecular π-stacking interactions and hydrogen bonding.

6.1.2 Structure of the complex [((4,4'-dipyridine-*N,N'*-dioxide)⊂(*p*-sulfonatocalix[5]-arene))$_2$ + $4H^+$][$(Eu(H_2O)_9)_2$]·$17H_2O$, 6.2.

Crystals of the complex [((4,4'-dipyridine-*N,N'*-dioxide)⊂(*p*-sulfonatocalix[5]-arene))$_2$ + $4H^+$][$(Eu(H_2O)_9)_2$]·$17H_2O$, **6.2**, grew upon slow evaporation of an acidic aqueous solution containing a 1:3:1 mixture of Na_5SO_3[5], 4,4'-dipyridine-*N,N'*-dioxide and europium(III) nitrate (pH adjusted to be <1 with 1M HCl, Equation 6.2). The complex was characterised by IR spectroscopy and single crystal X-ray crystallography. Complex **6.2** crystallises in a monoclinic cell and the structural solution was performed in the space group $P2_1/c$. Details of data collection and structure refinement are given in Table 6.9 of this chapter. A crystallographic information file containing all bond lengths and angles for complex **6.2** can be found in appendix 6.1.2 on the attached compact disc.

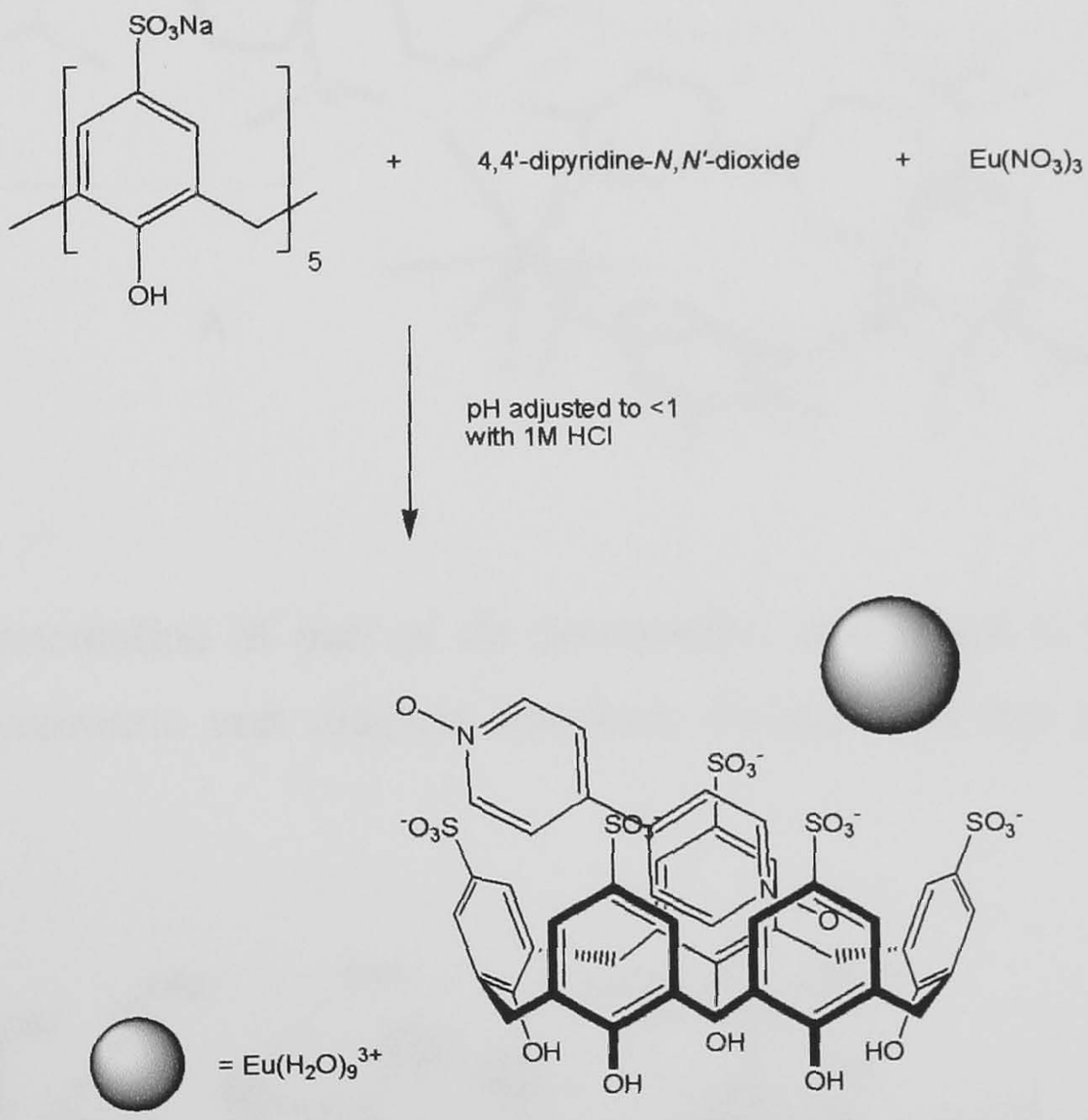

(6.2)

The asymmetric unit consists of two *p*-sulfonatocalix[5]arenes, two 4,4'-dipyridine-*N,N'*-dioxides, two nona-aqua europium cations (one of which is disordered) and a total of seventeen water molecules that are disordered over twenty four positions (Figure 6.5). The most noticeable feature of complex **6.2** is that the DiPyNO molecules in the asymmetric unit are non-coordinating and form a dimer like arrangement. As the asymmetric unit is large, it has been divided into two parts, **A** and **B,** to aid clarity and early discussion (indicated by the dashed grey line in Figure 6.5). Latter discussion relating to complex **6.2** will focus on the extended structure and encompasses both **A** and

B. Prior to discussion, it should be noted that the extended structure reveals the *p*-sulfonatocalix[5]arenes to pack in the previously seen bi-layer arrangement.[66-68]

In part **A**, the DiPyNO molecule is clearly too large for the cavity of SO_3[5] and the N(2)/O(42) group of the N(1)/N(2) DiPyNO molecule is directed into the cavity of the SO_3[5] whilst the N(1)/O(41) group is directed into the hydrophilic layer generated by the sulfonate groups of the calixarenes (Figure 6.6). The nona-aqua Eu(1) cation is of tri-capped trigonal prismatic geometry and bond lengths relating to the europium coordination sphere are listed in Table 6.2.

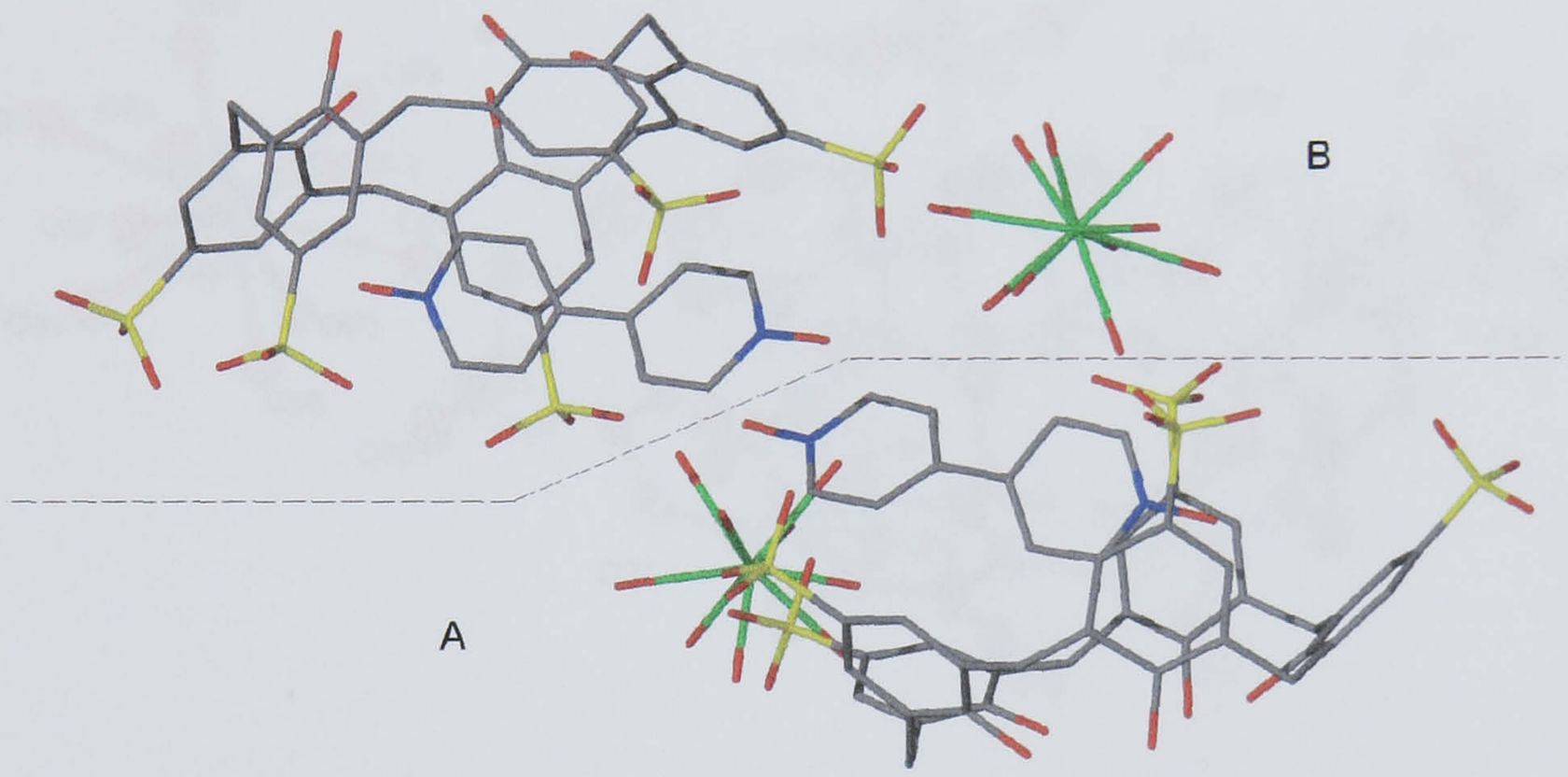

Figure 6.5 Stick representation of part of the asymmetric unit found in the crystal structure of complex **6.2**. The asymmetric unit diagram has been divided into two parts (**A** and **B**) to aid discussion.

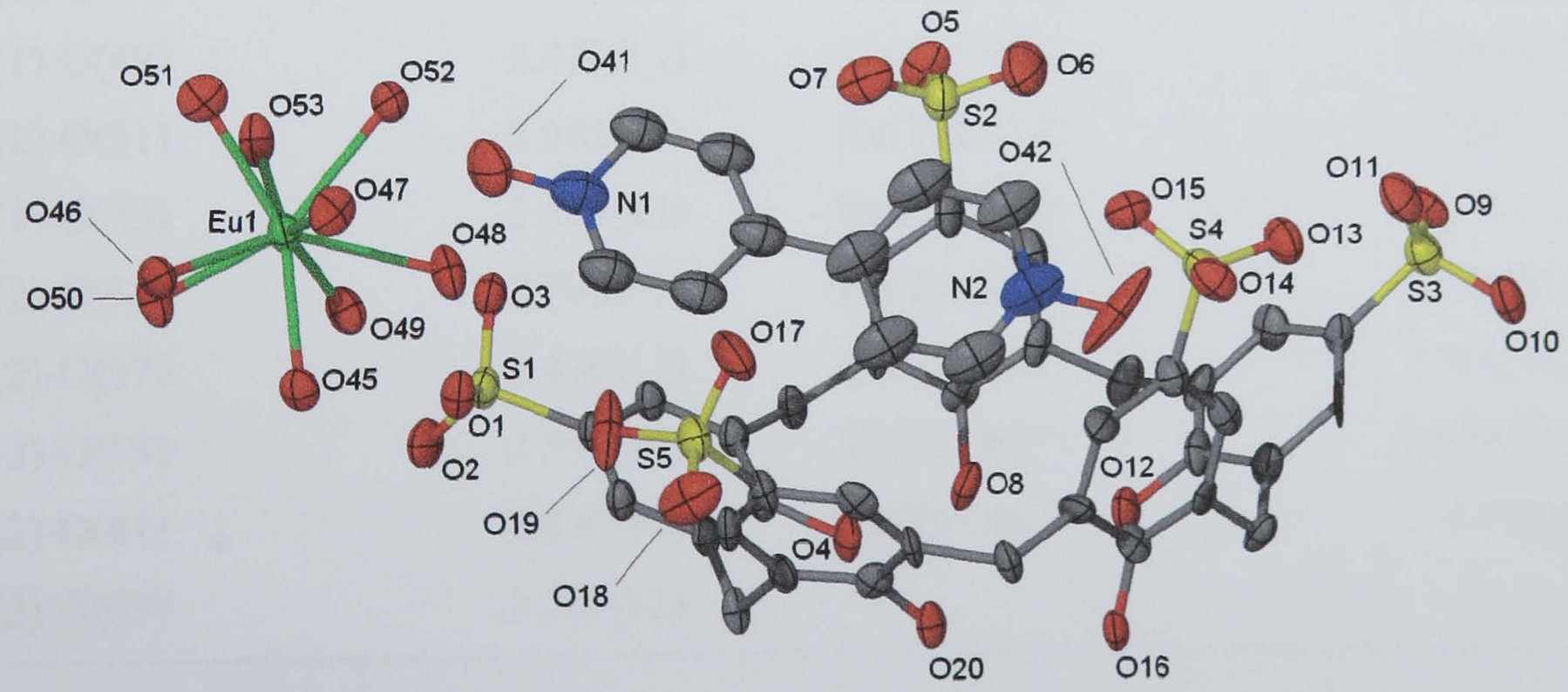

Figure 6.6 Part **A** of the asymmetric unit from the crystal structure of complex **6.2**, anisotropic displacement ellipsoids shown at the 50% probability level. Selected atoms have been labelled.

The arrangement in part **B** is similar to that of **A** and the N(3)/O(43) group of the N(3)/N(4) DiPyNO molecule is directed into the cavity of the SO_3[5] whilst the N(4)/O(44) group is directed into the hydrophilic layer generated by the sulfonate groups of the calixarenes (Figure 6.7). One of the aquo ligands of the nona-aqua Eu(2) cation is disordered equally over two positions (O(55) and O(62)) and the cation is of distorted tri-capped trigonal prismatic geometry. The aquo ligands of Eu(2) were refined isotropically and the bond lengths relating to the europium coordination sphere are listed in Table 6.2.

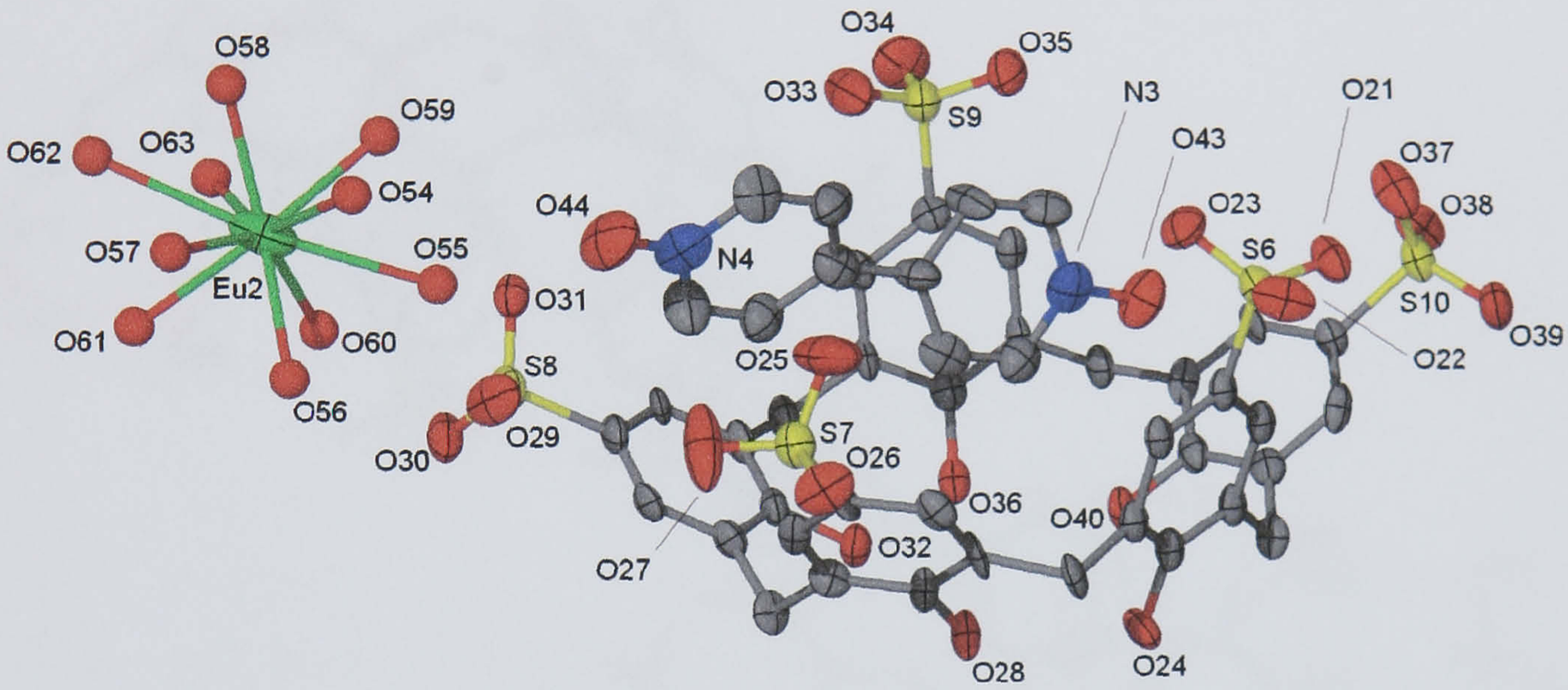

Figure 6.7 Part **B** of the asymmetric unit from the crystal structure of complex **6.2**, anisotropic displacement ellipsoids shown at the 50% probability level. Selected atoms have been labelled.

Eu(1)-O(45)	2.424(11)	Eu(1)-O(46)	2.519(10)
Eu(1)-O(47)	2.482(11)	Eu(1)-O(48)	2.512(12)
Eu(1)-O(49)	2.470(11)	Eu(1)-O(50)	2.446(11)
Eu(1)-O(51)	2.502(12)	Eu(1)-O(52)	2.494(11)
Eu(1)-O(53)	2.455(13)	Eu(2)-O(54)	2.490(17)
Eu(2)-O(55)	2.706(19)	Eu(2)-O(56)	2.420(12)
Eu(2)-O(57)	2.426(17)	Eu(2)-O(58)	2.385(17)
Eu(2)-O(59)	2.530(15)	Eu(2)-O(60)	2.424(13)
Eu(2)-O(61)	2.436(14)	Eu(2)-O(62)	2.79(4)
Eu(2)-O(63)	2.368(12)		

Table 6.2 Interatomic distances relating to the europium coordination spheres in the crystal structure of complex **6.2** (distances given in Å with e.s.d. in parentheses).

There are several intermolecular interactions between the SO_3[5], DiPyNO and selected water molecules that link parts **A** and **B** (Figure 6.8). In part **A** there is a π-stacking interaction between the N(2) pyridine ring of the N(1)/N(2) DiPyNO molecule and the aromatic ring of the calixarene S(2) fragment (aromatic centroid···centroid distance of 3.687 Å, Figure 6.8). There is a hydrogen bond from the O(83) water molecule of crystallisation and the O(42) atom of the N(1)/N(2) DiPyNO (O···O distance of 2.486 Å). The same water molecule also hydrogen bonds to the O(11) oxygen atom of the calixarene S(3) sulfonate group with an O···OS distance of 2.886 Å.

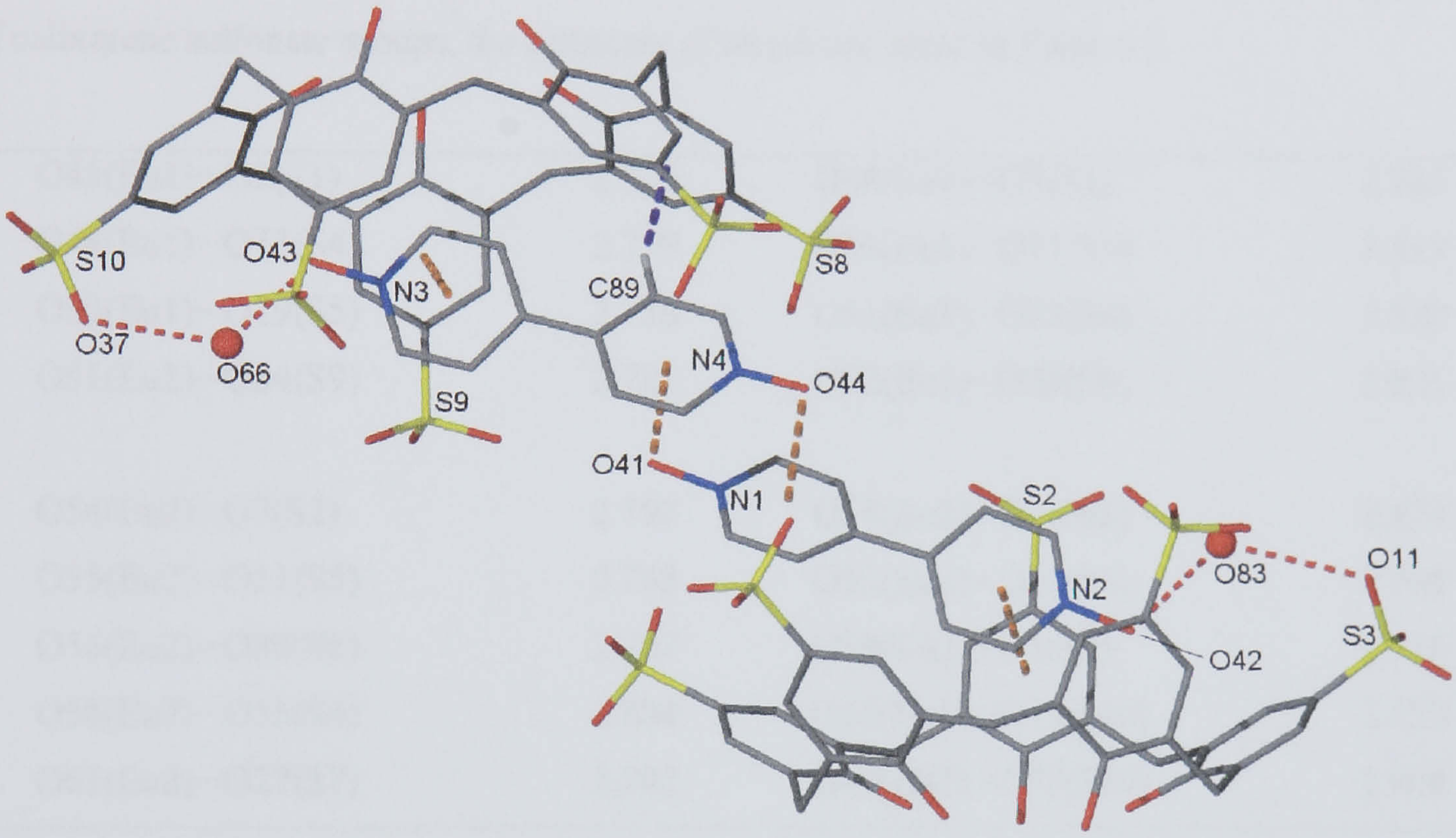

Figure 6.8 Intermolecular interactions found between DiPyNO, SO_3[5] and selected waters of crystallisation in the crystal structure of complex **6.2**. Selected atoms have been labelled.

In part **B** there is a π-stacking interaction between the N(3) pyridine ring of the N(3)/N(4) DiPyNO molecule and the aromatic ring of the S(9) part of the calixarene (aromatic centroid···centroid distance of 3.843 Å, Figure 6.8). There is a CH···π interaction from the C(89) carbon atom of the N(3)/N(4) DiPyNO molecule to the aromatic ring of the S(8) part of the calixarene (CH···aromatic centroid distance of 2.763 Å). There is a hydrogen bonding from a disordered water molecule of crystallisation (O(66) and O(67), occupancies of 0.3 and 0.7 respectively) to the O(43) atom of the N(3)/N(4) DiPyNO (O···O distances of 2.336 and 2.516 Å for O(66) and O(67) respectively). The same disordered water molecule also hydrogen bonds to the O(37) oxygen atom of the calixarene S(10) sulfonate group (O···OS distances of 2.740 and 2.773 Å for O(66) and O(67) respectively).

One of the links between parts **A** and **B** is the central dimerisation through the *N*-oxide groups of the DiPyNO molecules (Figure 6.8). In complex **6.2** they are arranged such that the oxygen atoms of the *N*-oxide groups are positioned above the pyridine ring of the neighbouring DiPyNO molecule. The O(41) atom of the N(1)/N(2) DiPyNO molecule is above the N(4) pyridine ring of the N(3)/N(4) DiPyNO molecule (N(1)O(41)···aromatic centroid distance of 3.226 Å). Similarly, the O(44) atom of the N(3)/N(4) DiPyNO molecule is above the N(1) pyridine ring of the N(1)/N(2) DiPyNO molecule (N(4)O(44) ···aromatic centroid distance of 3.284 Å). In addition to all of the above, there are several hydrogen bonds between the europium aquo ligands and the oxygen atoms of calixarene sulfonate groups, the distances of which are listed in Table 6.3.

O45(Eu1)···O2(S1)	2.810	O48(Eu1)···O3(S1)	2.785
O48(Eu1)···O13(S4)	2.759	O49(Eu1)···O11(S3)	2.819
O50(Eu1)···O19(S5)	2.756	O51(Eu1)···O23(S6)	2.820
O51(Eu1)···O34(S9)	2.781	O52(Eu1)···O23(S6)	2.821
O54(Eu2)···O7(S2)	2.792	O54(Eu2)···O31(S8)	2.874
O55(Eu2)···O21(S5)	2.765	O55(Eu2)···O31(S8)	2.708
O56(Eu2)···O30(S8)	2.757	O58(Eu2)···O5(S2)	2.715
O58(Eu2)···O15(S4)	2.804	O60(Eu2)···O39(S10)	2.850
O61(Eu2)···O27(S7)	2.782	O63(Eu2)···O37(S10)	2.904

Table 6.3 Hydrogen bonding contacts between europium aquo ligands and SO_3[5] sulfonate groups from the crystal structure of complex **6.2** (distances given in Å).

As stated above, the *p*-sulfonatocalix[5]arenes assemble in a bi-layer arrangement in the extended structure (Figure 6.9). Each hydrophobic layer is composed of calixarenes from either part **A** or **B**. The calixarene packing within each uni-composite layer is similar and both are formed through two CH···π and one π-stacking interaction. For the SO_3[5] in **A,** the two CH···aromatic centroid and aromatic centroid···centroid distances are 2.651, 2.774 and 3.691 Å respectively. For the SO_3[5] in **B,** the two CH···aromatic centroid and aromatic centroid···centroid distances are 2.988, 2.870 and 3.598 Å respectively. In addition to all of the aforementioned interactions, the numerous disordered waters of crystallisation reside in the hydrophilic layer and are in positions consistent with hydrogen bonding with appropriate functional groups as expected.

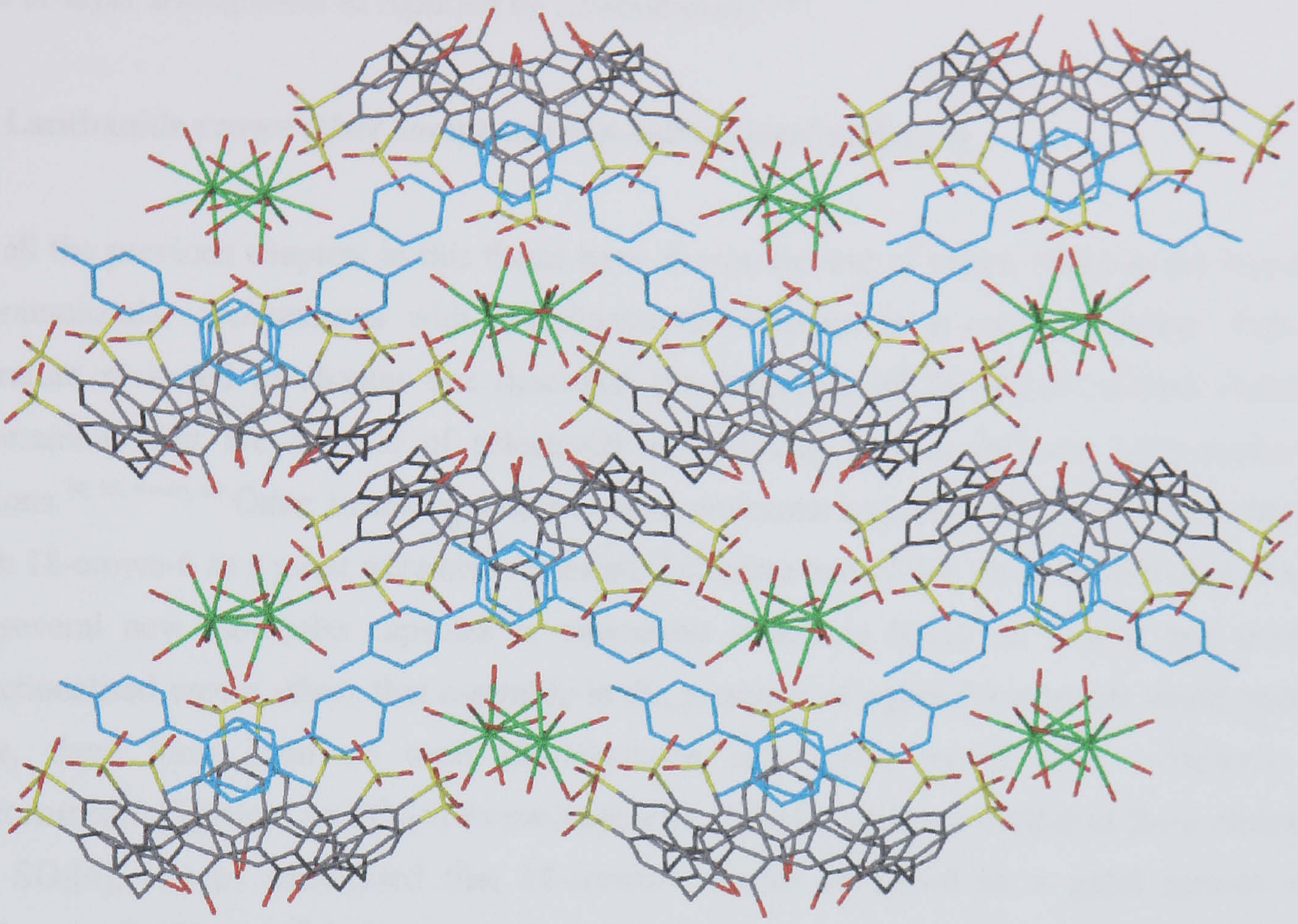

Figure 6.9 Crystal structure of complex **6.2** showing the bi-layer arrangement of *p*-sulfonatocalix[5]arene. The DiPyNO molecules are shown in blue to emphasise the traversing of the hydrophilic layer.

6.1.3 Summary of lanthanide 4-picoline-*N*-oxide or 4,4'-dipyridine-*N,N'*-dioxide complexes of *p*-sulfonatocalix[5]arene.

When the 2,3,4-picoline *N*-oxides were employed as potential guest molecules in several ternary lanthanide *p*-sulfonatocalix[4,5,6]arene systems, single crystals formed only for a SO_3[5]/4-PicNO/Eu complex. Pyridine *N*-oxide has previously been shown to be an excellent guest in various lanthanide *p*-sulfonatocalix[4,5]arene complexes. Clearly the presence of an additional methyl group upon moving to the picoline *N*-oxides has a generally negative effect in solid state complex formation with the *p*-sulfonatocalix[4,6]arenes. Depending on the position of the methyl group however, complex formation is possible with SO_3[5] as shown in complex **6.1** but the guest is not coordinated to the lanthanide metal centre as expected. When 4,4'-dipyridine-*N,N'*-dioxide is employed as a guest in a ternary lanthanide *p*-sulfonatocalix[5]arene system, a complex forms that shows the guest to be too large for inclusion within the cavity of SO_3[5]. Once again the guest is not coordinated to the europium metal centre and the SO_3[5]/DiPyNO/Eu complexes dimerise through a

series of intermolecular interactions. In both complexes, the calixarene assembles in the previously seen bi-layer arrangement as reported by Atwood *et al.*[67, 68]

6.2 Lanthanide crown ether complexes of *p*-sulfonatocalix[5]arene.

As all the previous chapters in this thesis have shown, the use of crown ethers in the formation of supramolecular architectures with *p*-sulfonatocalix[*n*]arenes is a common theme. Part of the literature reviewed in chapter one described the formation of SO_3[4]/18-crown-6 Russian doll superanions that are capable of selectively crystallising various different (polynuclear-)metal cations.[34, 35, 44-46, 49] Other structural motifs such as molecular capsules and Ferris wheels that formed with 18-crown-6 as a guest were also reviewed.[50] Chapter two of this thesis described the formation of several new molecular capsules or alternative structures based on SO_3[4] and (*bis*)amino-functionalised crown ethers that assemble in the presence of aquated lanthanide metal cations. To date, there have been no such investigations into metal crown ether complexes of *p*-sulfonatocalix[5]arene. As SO_3[5] forms lanthanide PyNO complexes similar to those characterised for SO_3[4], it was anticipated that 18-crown-6 would be useful as a guest species with *p*-sulfonatocalix[5]arene.[68] In fact several metal cations were examined for complex formation with SO_3[5] and 18-crown-6 but single crystals could not be obtained. When 18-crown-6 is replaced with several (*bis*)amino-functionalised crown ethers (Figure 6.1) at a low pH, single crystals of four complexes grew rapidly. Di-protonated diaza-18-crown-6 forms a host-guest complex with SO_3[5] and europium counterions. When 1-aza-18-crown-6 is employed, a extended Ferris wheel type coordination polymer forms with sodium ions in the centre of the crown ether molecules. Di-protonated diaza-15-crown-5 forms a host-guest complex similar to that found for diaza-18-crown-6. Di-protonated diaza-12-crown-4 also forms a similar complex although the crystals are twinned (structure not included).

6.2.1 Structure of the complex [[({4,13-diaza-18-crown-6 + 2H}.H_2O)⊂*p*-sulfonatocalix[5]-arene][$Eu(H_2O)_9$]]$_2$.24H_2O, 6.3.

Crystals of the complex [[({4,13-diaza-18-crown-6 + 2H}.H_2O)⊂*p*-sulfonatocalix[5]arene][$Eu(H_2O)_9$]]$_2$.24H_2O, **6.3**, grew upon standing over two hours from an acidic aqueous solution containing a 1:2:2 mixture of Na_5SO_3[5], diaza-18-crown-6 and europium(III) nitrate hexahydrate (pH adjusted to be <1 with 1M HCl, Equation 6.3). The complex was characterised by IR spectroscopy and single crystal X-ray crystallography. Complex **6.3** crystallises in an monoclinic cell and the structural solution was performed in the space group $P2_1/c$. Details of

data collection and structure refinement are given in Table 6.10 of this chapter. A crystallographic information file containing all bond lengths and angles for complex **6.3** can be found in appendix 6.2.1 on the attached compact disc.

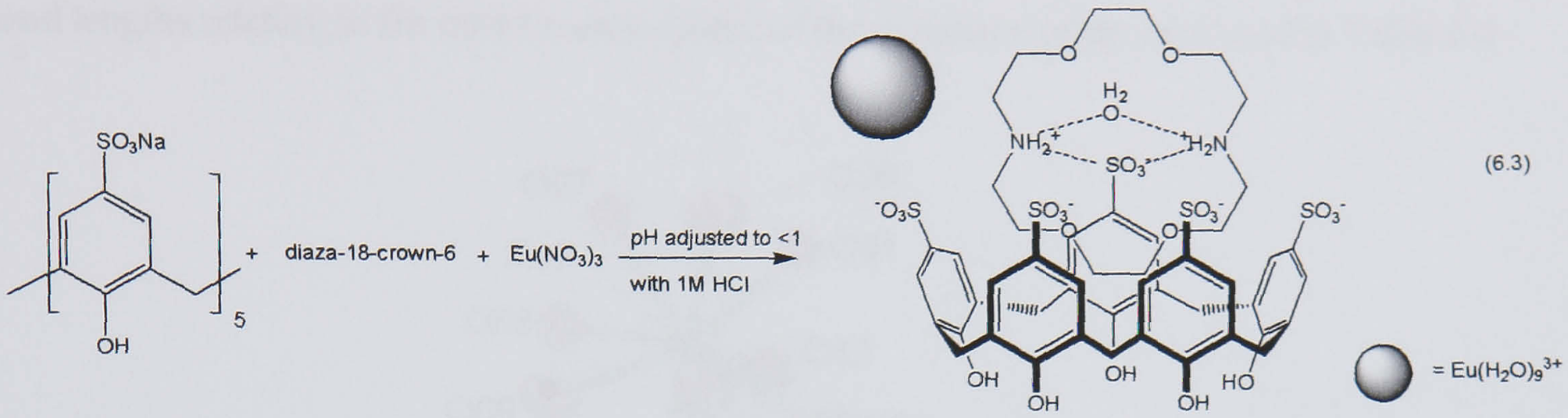

(6.3)

The asymmetric unit consists of two *p*-sulfonatocalix[5]arenes, two di-protonated diaza-18-crown-6 molecules, two nona-aqua europium cations and a total of twenty four water molecules that are disordered over thirty four positions (Figure 6.10). As the asymmetric unit is large, it has been divided into two parts, **A** and **B,** to aid clarity and early discussion (indicated by the dashed grey line in Figure 6.10). Latter discussion relating to complex **6.3** will focus on the extended structure and hydrogen bonding links found between **A** and **B**.

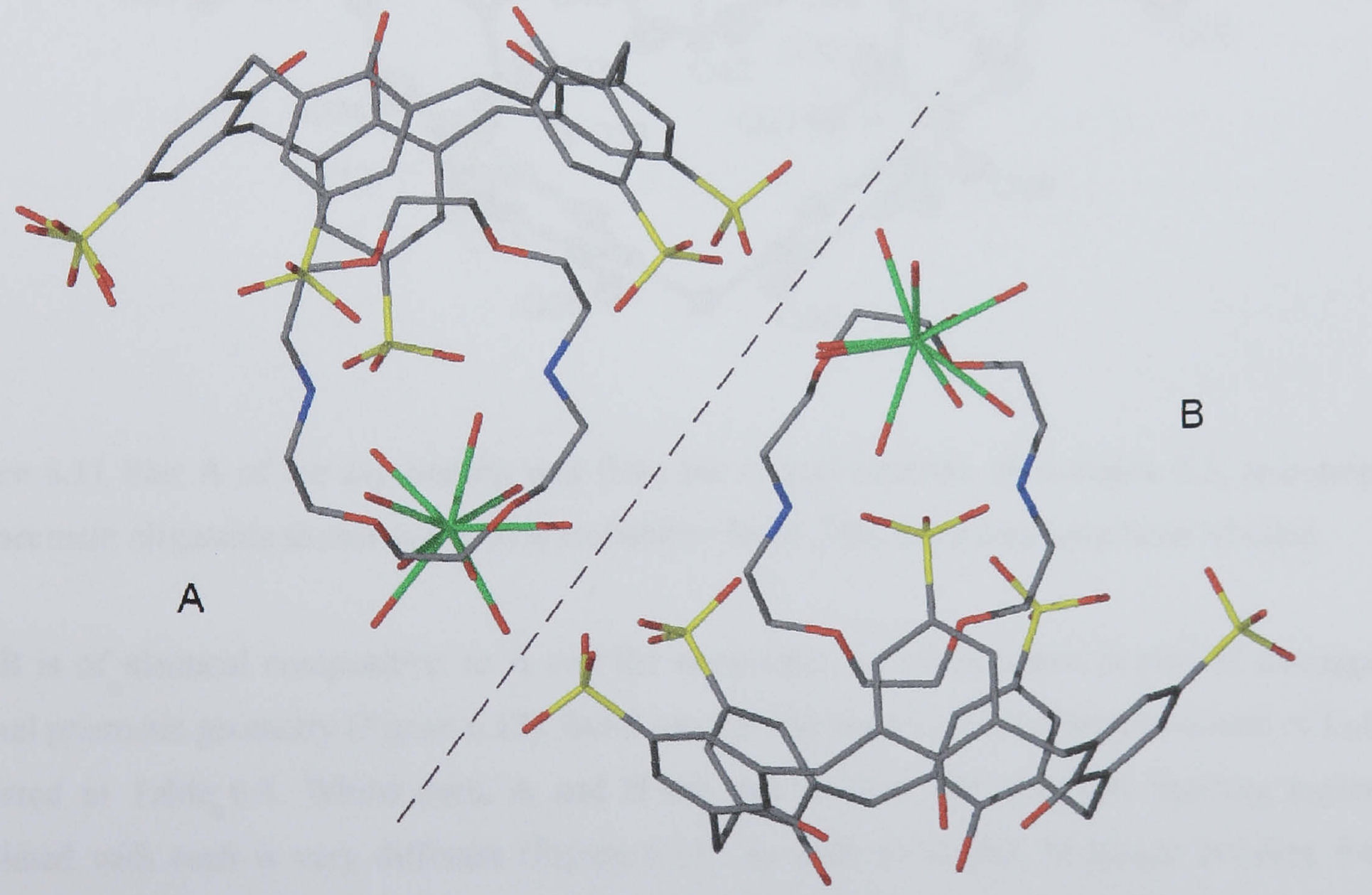

Figure 6.10 Stick representation of part of the asymmetric unit found in the crystal structure of complex **6.3**. The asymmetric unit diagram has been divided into two parts (**A** and **B**) to aid discussion.

Part **A** comprises one SO_3[5], one di-protonated diaza-18-crown-6 and one nona-aqua europium metal centre. The oxygen atoms of the S(8) sulfonate group are disordered over two positions with partial occupancies of 0.8 and 0.2. The Eu(2) cation is of tri-capped trigonal prismatic geometry and bond lengths relating to the coordination sphere of the europium centre are listed in Table 6.4

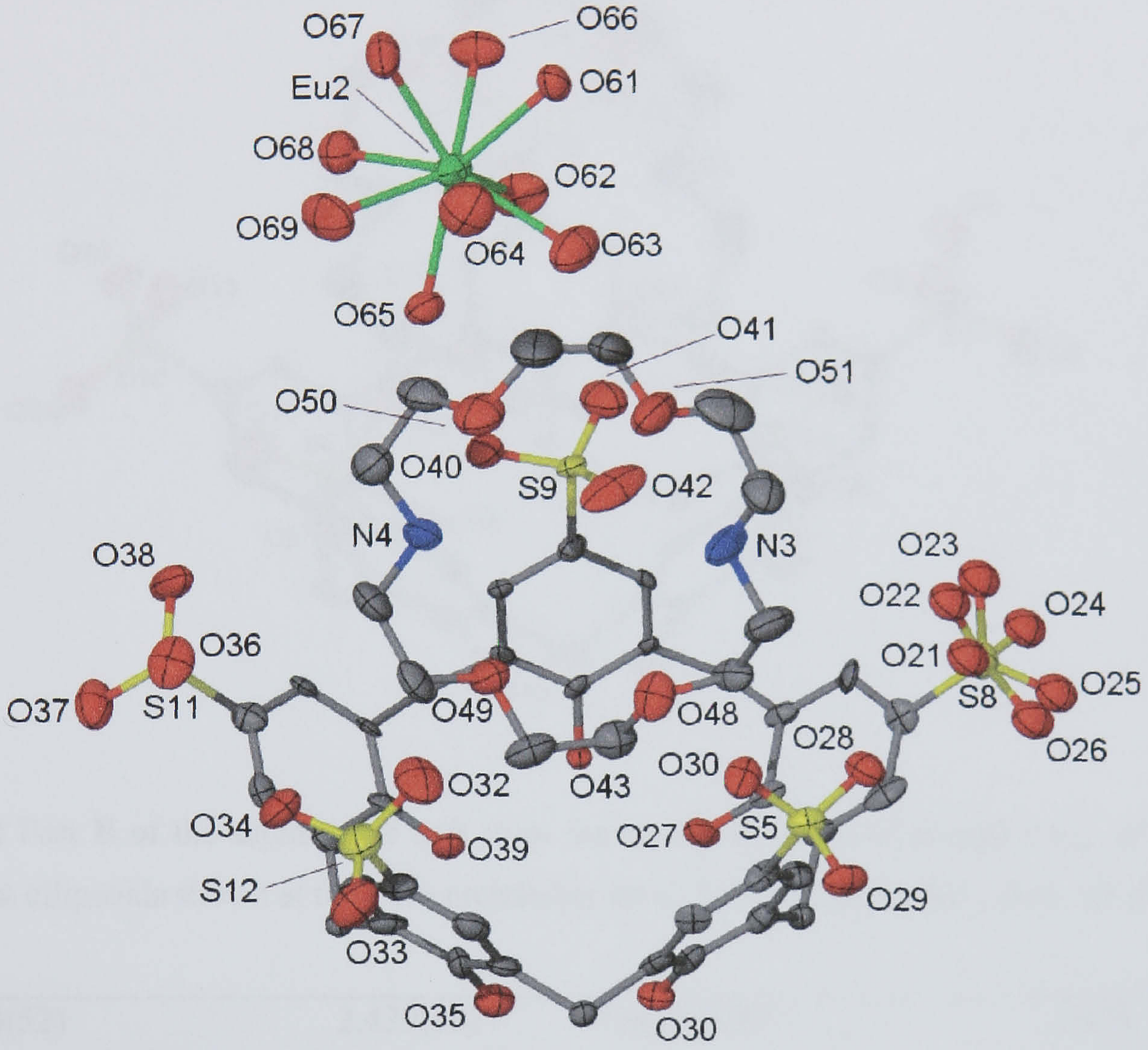

Figure 6.11 Part **A** of the asymmetric unit from the crystal structure of complex **6.3**, anisotropic displacement ellipsoids shown at the 50% probability level. Selected atoms have been labelled.

Part **B** is of identical composition to **A** and the nona-aqua europium centre is also of tri-capped trigonal prismatic geometry (Figure 6.12). Bond lengths relating to the coordination sphere of Eu(1) are listed in Table 6.4. Whilst parts **A** and **B** are very similar, the hydrogen bonding regimes associated with each is very different (Figure 6.13). In addition to this, hydrogen bonding from europium aquo ligands to neighbouring calixarene sulfonate oxygen atoms links parts **A** and **B** (Figure 6.13).

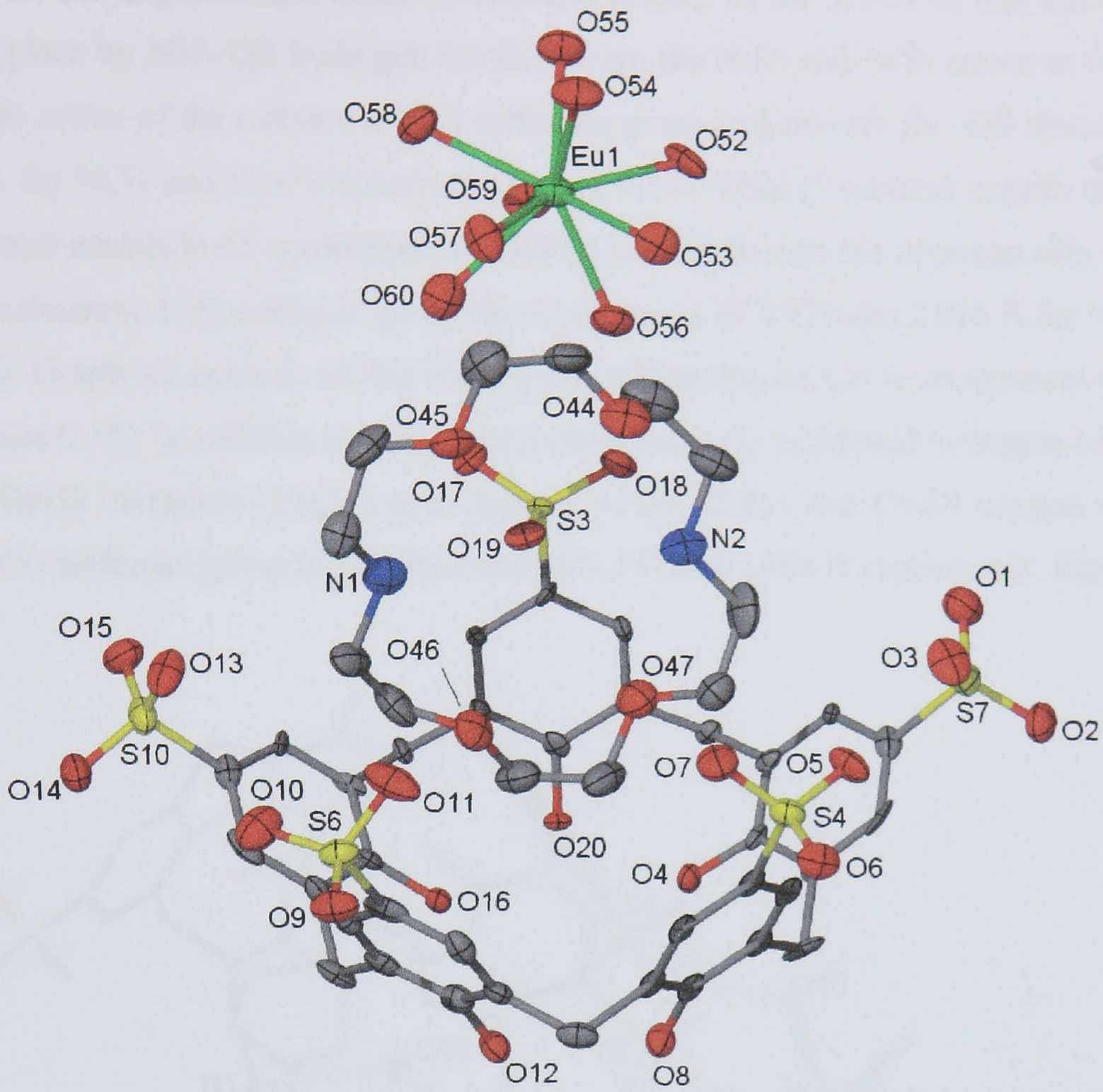

Figure 6.12 Part **B** of the asymmetric unit from the crystal structure of complex **6.2**, anisotropic displacement ellipsoids shown at the 50% probability level. Selected atoms have been labelled.

Eu(1)-O(52)	2.439(10)	Eu(1)-O(53)	2.490(10)
Eu(1)-O(54)	2.421(10)	Eu(1)-O(55)	2.496(9)
Eu(1)-O(56)	2.419(10)	Eu(1)-O(57)	2.431(10)
Eu(1)-O(58)	2.468(10)	Eu(1)-O(59)	2.427(10)
Eu(1)-O(60)	2.554(12)	Eu(2)-O(61)	2.481(10)
Eu(2)-O(62)	2.421(11)	Eu(2)-O(63)	2.429(12)
Eu(2)-O(64)	2.496(15)	Eu(2)-O(65)	2.452(9)
Eu(2)-O(66)	2.448(11)	Eu(2)-O(67)	2.460(11)
Eu(2)-O(68)	2.436(11)	Eu(2)-O(69)	2.494(13)

Table 6.4 Interatomic distances relating to the europium coordination spheres in the crystal structure of complex **6.3** (distances given in Å with e.s.d. in parentheses).

Within part **A**, the di-protonated diaza-18-crown-6 resides in the cavity of the calixarene and is anchored in place by NH···OS hydrogen bonding from the N(3) and N(4) atoms to the O(42) and O(40) oxygen atoms of the calixarene S(9) sulfonate group respectively (N···OS distances of 2.728 and 2.879 Å for N(3) and N(4) respectively, Figure 6.13). Both protonated amines also hydrogen bond to a water molecule of crystallisation (O(86)) that resides on the opposite side of the crown ether to the calixarene S(9) sulfonate group (N···O distances of 2.929 and 2.816 Å for N(3) and N(4) respectively). Graph set analysis of this hydrogen bonding ring results in assignment of the $R_4^3(10)$ symbol (Figure 6.14). In addition to these interactions, there are additional hydrogen bonds from the O(63) and O(65) europium (Eu(2)) aquo ligands to the O(41) and O(40) oxygen atoms of the calixarene S(9) sulfonate group (O···O distances of 2.797 and 2.804 Å respectively, Figure 6.13).

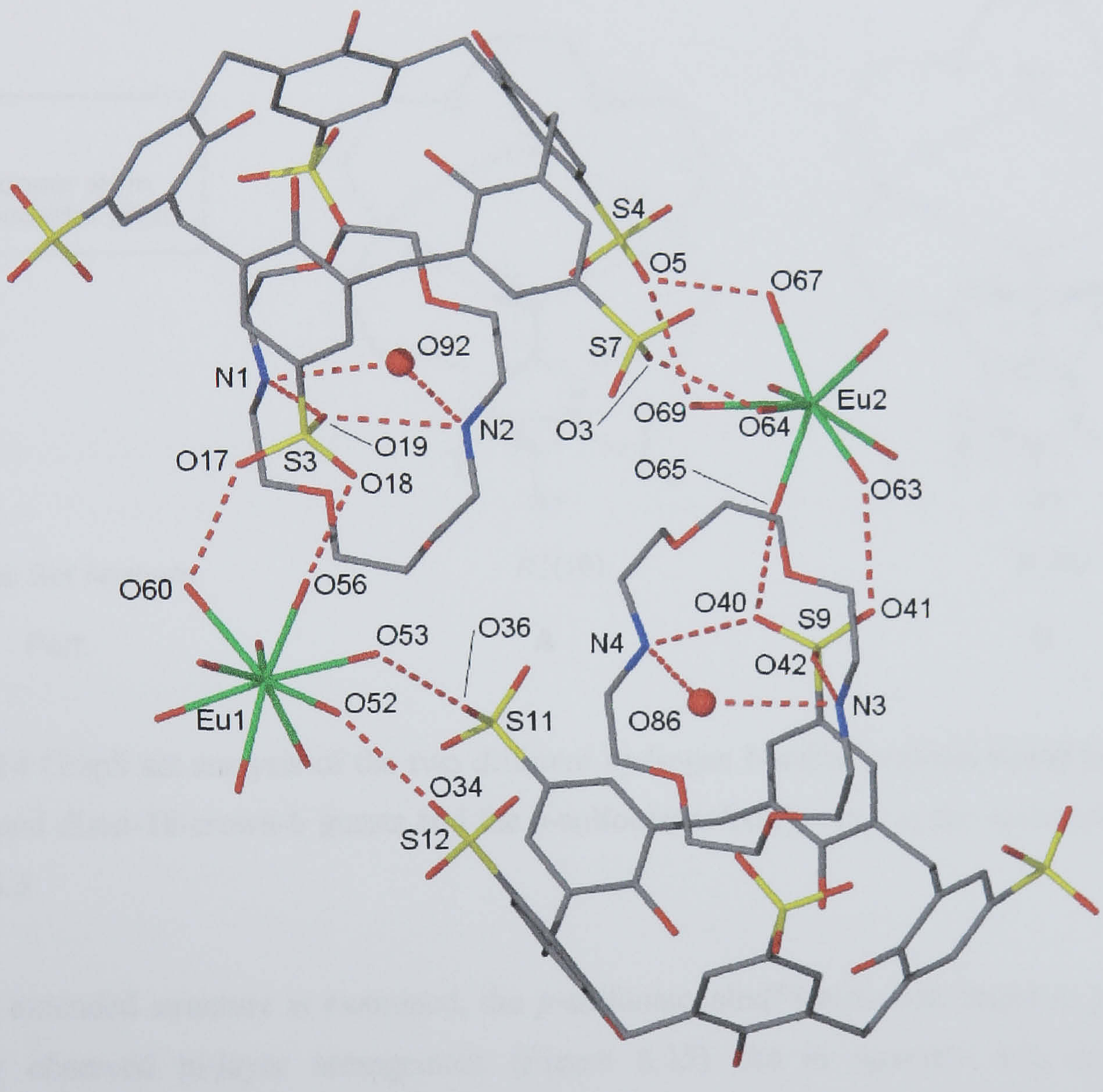

Figure 6.13 Some hydrogen bonding interactions found between the molecular components in the asymmetric unit of the crystal structure of complex **6.3**. The different crown ether associated hydrogen bonding regimes are shown in addition to the hydrogen bonding links between the components of **A** and **B**. Selected atoms have been labelled and disordered S(8) sulfonate oxygen atoms have been shown in only one position for clarity.

Within part **B**, the di-protonated diaza-18-crown-6 also resides in the cavity of the calixarene but is anchored in place by a different NH···OS hydrogen bonding regime to that observed for **A**. The protonated amines both hydrogen bond to the O(19) oxygen atom of the calixarene S(3) sulfonate group with N···O distances of 3.073 and 2.962 Å for N(1) and N(2) respectively. Both protonated amines also hydrogen bond to a crown ether associated water of crystallisation (O(92)) in a similar fashion to that observed for **A** (N···O distances of 2.838 and 2.881 Å for N(1) and N(2) respectively). Graph set analysis of this hydrogen bonding ring results in assignment of the $R_4^2(8)$ symbol (Figure 6.14). Parts **A** and **B** are partially linked through five crystallographically unique EuO···OS hydrogen bonds (EuO···OS distances ranging from 2.649 to 2.906 Å, Figure 6.13).

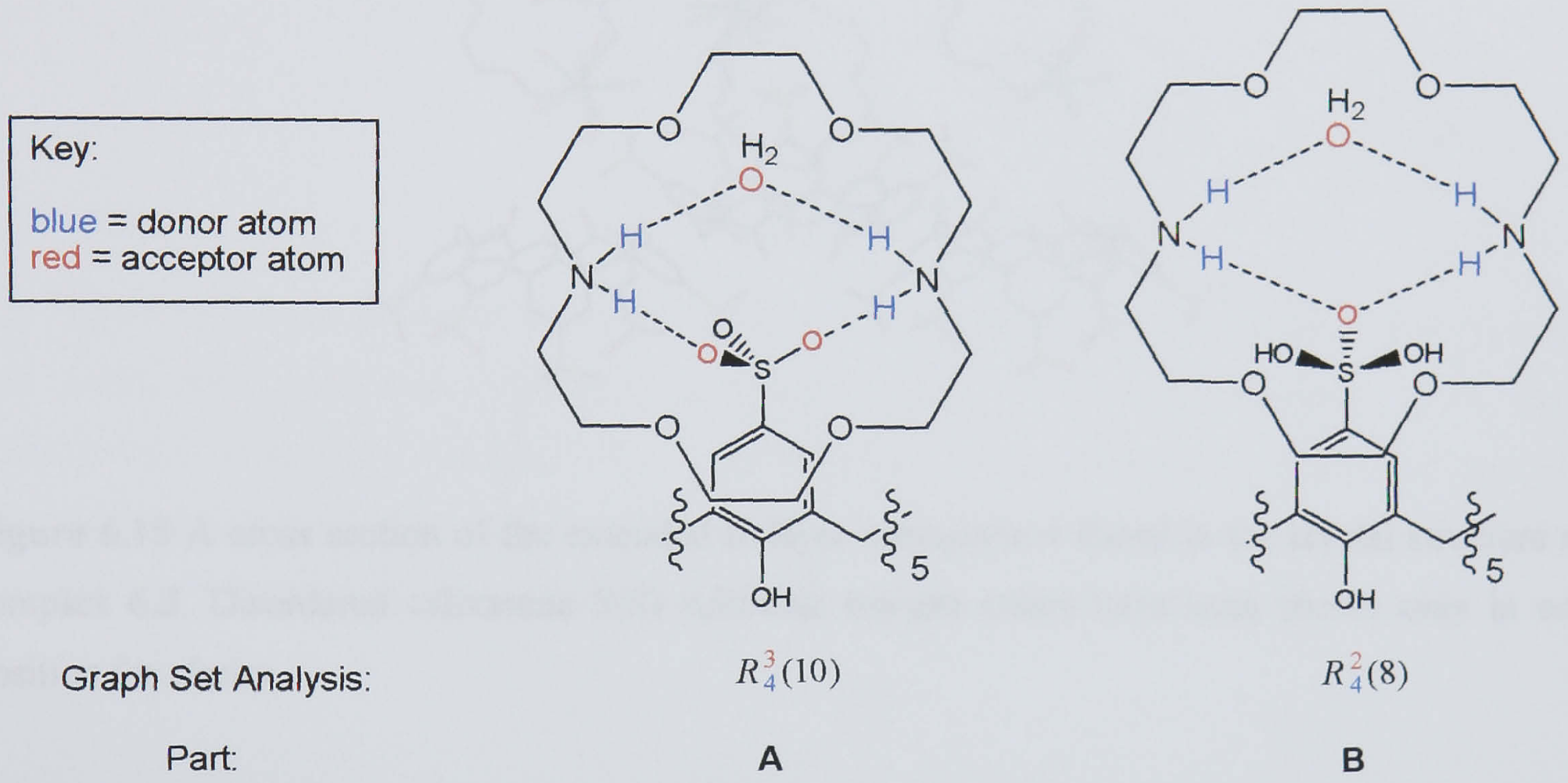

Figure 6.14 Graph set analysis of the two different hydrogen bonding regimes found between the di-protonated diaza-18-crown-6 guests and the *p*-sulfonatocalix[5]arenes in the asymmetric unit of complex **6.3**.

When the extended structure is examined, the *p*-sulfonatocalix[5]arenes are found to pack in the previously observed bi-layer arrangement (Figure 6.15). As in complex **6.2**, each of the hydrophobic layers is composed of calixarenes from either part **A** or **B**. The uni-composite layers in complex form through two crystallographically unique π-stacking interactions for each calixarene. The SO_3[5] from part **A** assembles with aromatic centroid···centroid distances of 3.596 and 3.994 Å. The SO_3[5] from part **B** assembles with aromatic centroid···centroid distances of 3.481 and 3.708 Å. Also evident in the extended structure are numerous additional EuO···OS hydrogen bonds from nona-aqua europium cations to symmetry equivalent calixarene sulfonate groups.

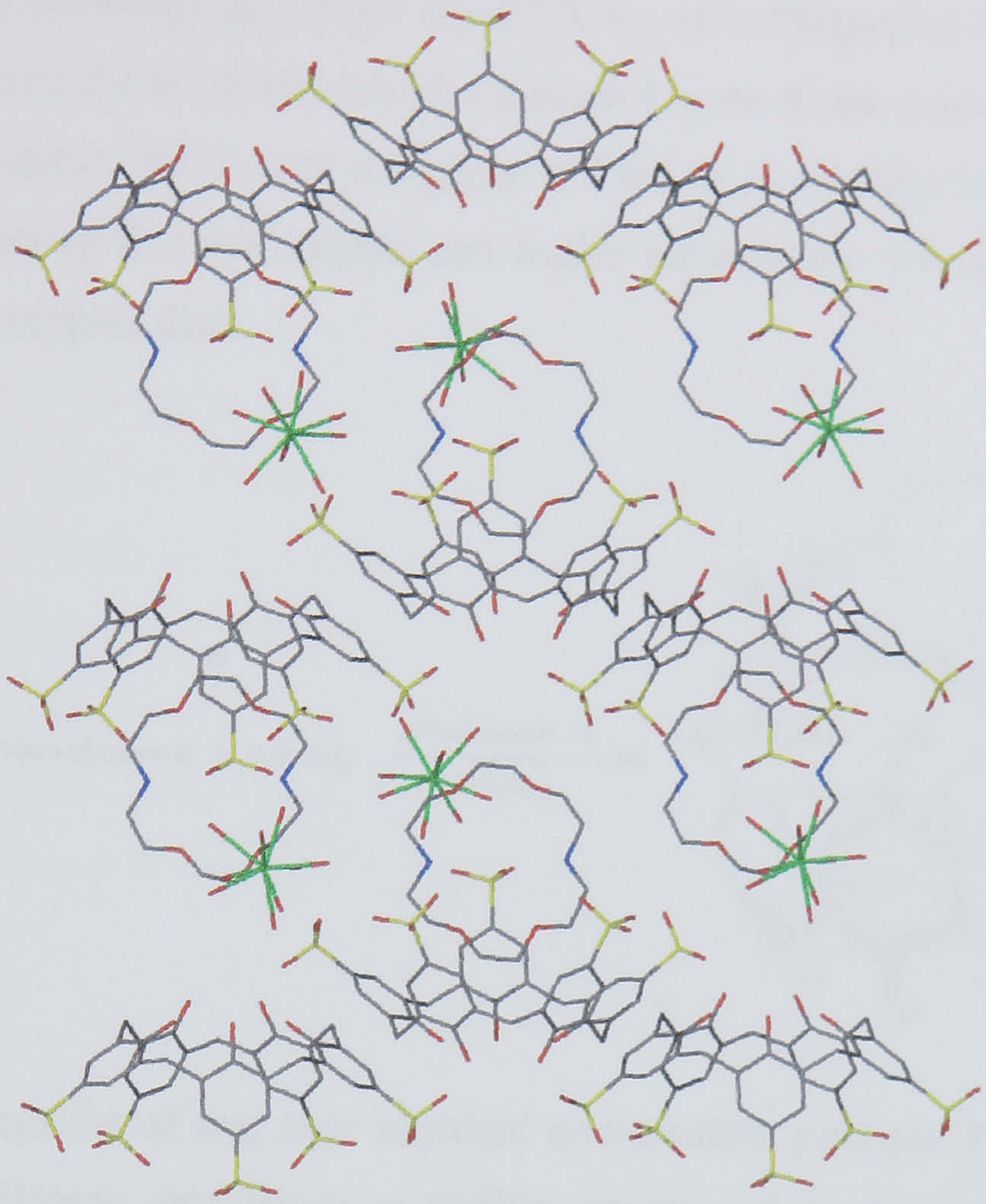

Figure 6.15 A cross section of the extended bi-layer arrangement found in the crystal structure of complex **6.3**. Disordered calixarene S(8) sulfonate oxygen atoms have been shown only in one position for clarity.

When diaza-18-crown-6 is replaced by 1-aza-18-crown-6 in the above ternary system, an interesting coordination polymer forms between SO_3[5] and europium or sodium metal centres. In addition to this, each SO_3[5] cavity is occupied by a sodium bound 1-aza-18-crown-6 that is anchored to a europium aquo ligand and can be considered an extended Ferris wheel. This arrangement bears some resemblance to a previously reported Ferris wheel that incorporates Na_4SO_3[4], 18-crown-6 and lanthanum.[50]

6.2.2 Structure of the coordination polymer [(Na⊂1-aza-18-crown-6)][(Eu(H$_2$O)$_6$)(Na(H$_2$O)$_3$)(*p*-sulfonatocalix[5]arene)].10.5H$_2$O, 6.4.

Crystals of the complex [(Na⊂1-aza-18-crown-6)][(Eu(H$_2$O)$_6$)(Na(H$_2$O)$_3$)(*p*-sulfonatocalix[5]arene)].10.5H$_2$O, **6.4**, grew upon standing over several days from an acidic aqueous solution containing a 1:2:2 mixture of Na_5SO_3[5], 1-aza-18-crown-6 and europium(III)

nitrate hexahydrate (pH adjusted to be <1 with 1M HCl, Equation 6.4). The complex was characterised by IR spectroscopy and single crystal X-ray crystallography. Complex **6.4** crystallises in an monoclinic cell and the structural solution was performed in the space group $P2_1/c$. Details of data collection and structure refinement are given in Table 6.10 of this chapter. A crystallographic information file containing all bond lengths and angles for complex **6.4** can be found in appendix 6.2.2 on the attached compact disc.

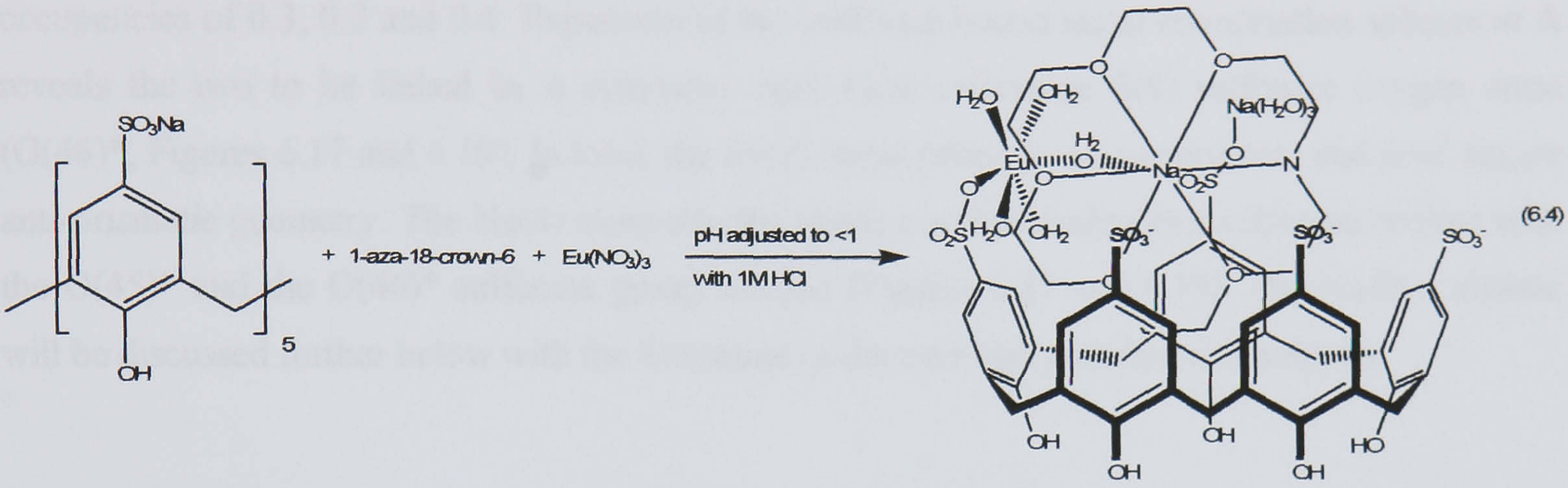

(6.4)

The asymmetric unit consist of two near identical coordination polymer fragments that comprise one *p*-sulfonatocalix[5]arene, one tris-aqua sodium centre, a hexa-aqua europium centre and a sodium/1-aza-18-crown-6 complex that is anchored to the primary coordination polymer structure through sodium coordination to a europium aquo ligand (Figure 6.16). To aid discussion, the two coordination polymer fragments have been labelled **A** and **B**.

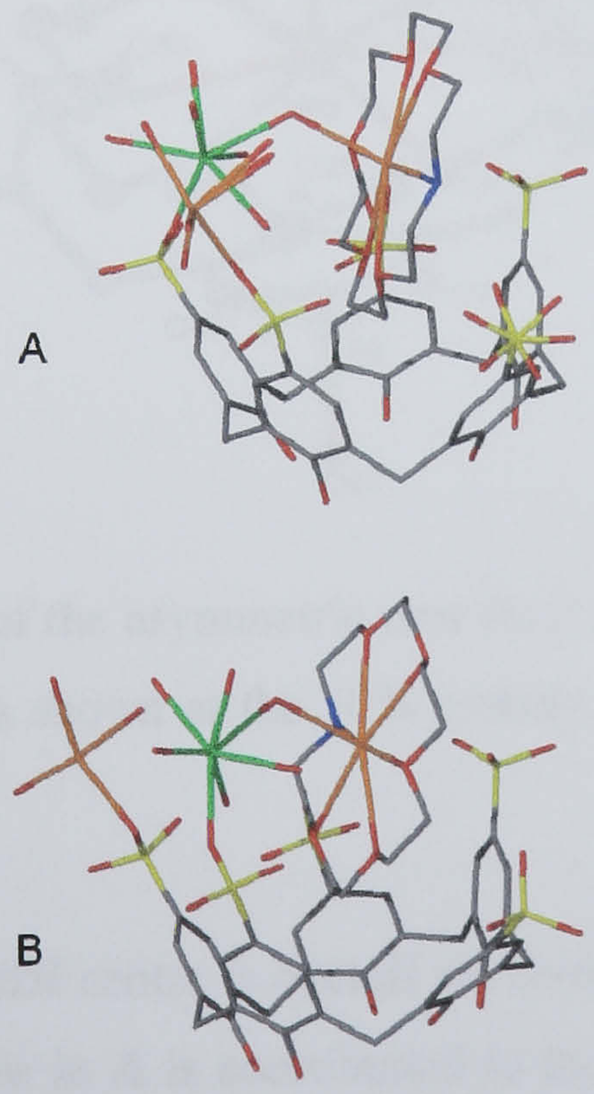

Figure 6.16 Stick representation of the two coordination polymer fragments found in the crystal structure of complex **6.4**. Each fragment has been labelled **A** and **B** to aid discussion.

There is some disorder associated with two SO_3[5] sulfonate groups and two sodium aquo ligands within fragment **A** (Figure 6.17). The oxygen atoms of the calixarene S(9) sulfonate group are disordered over two positions with partial occupancies of 0.55 and 0.45. Two oxygen atoms of the calixarene S(7) sulfonate group are disordered over two positions with partial occupancies of 0.7 and 0.3. Finally one of the sodium aquo ligands is disordered over two positions with partial occupancies of 0.8 and 0.2 whilst another aquo ligand is disordered over three positions with occupancies of 0.3, 0.3 and 0.4. Expansion of the sulfonate bound metal coordination spheres in **A** reveals the two to be linked by a symmetry equivalent calixarene S(8) sulfonate oxygen atom (O(46)*, Figures 6.17 and 6.19). In total, the Eu(2) metal centre is octa-coordinate and is of square anti-prismatic geometry. The Na(4) atom also the forms a sodium/calixarene sulfonate chelate with the O(45)* and the O(46)* sulfonate group oxygen (Figures 6.17 and 6.19). The Na/SO_3 chelate will be discussed further below with the formation of the extended coordination polymer.

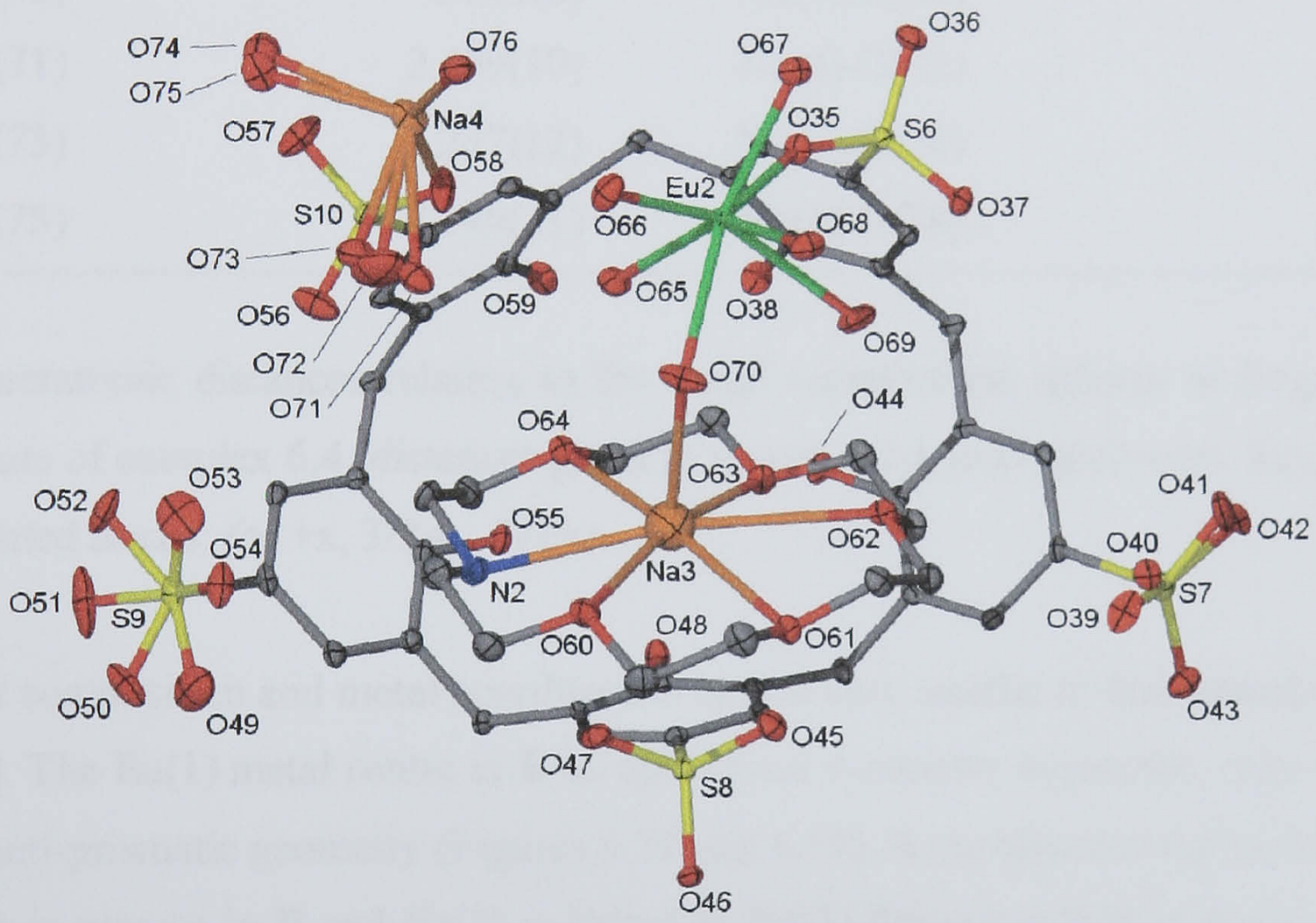

Figure 6.17 View of fragment **A** of the asymmetric unit from the crystal structure of complex **6.4**, anisotropic displacement ellipsoids shown at the 50% probability level. Selected atoms have been labelled.

Although disordered, the Na(4) metal centre is overall six coordinate and is of distorted octahedral geometry. The Na(3) sodium centre in **A** is coordinated to the donor atoms of the N(2) 1-aza-18-crown-6 guest, is also coordinated to the O(70) europium aquo ligand, is hepta-coordinate and is of distorted capped hexagonal geometry (Figure 6.17). The sodium/water/europium bonding is

particularly unusual and a search of the Cambridge Crystallographic Data Centre reveals that for these metals at least, there are no structural examples of this phenomenon. A similar type of bridging has been achieved however with oxygen atoms of an asymmetric macrocyclic compartmental Schiff base. Bond lengths relating to the coordination spheres of the metal centres in **A** are listed in Table 6.5.

Eu(2)-O(35)	2.3859(19)	Eu(2)-O(46)$^{(a)}$	2.4415(19)
Eu(2)-O(65)	2.449(2)	Eu(2)-O(66)	2.386(2)
Eu(2)-O(67)	2.4247(19)	Eu(2)-O(68)	2.4406(19)
Eu(2)-O(69)	2.428(2)	Eu(2)-O(70)	2.386(2)
Na(3)-O(60)	2.874(2)	Na(3)-O(61)	2.937(2)
Na(3)-O(62)	2.957(2)	Na(3)-O(63)	2.795(2)
Na(3)-O(64)	2.935(2)	Na(3)-O(70)	2.697(2)
N(2)-Na(3)	2.773(3)	Na(4)-O(45)$^{(a)}$	2.438(2)
Na(4)-O(46)$^{(a)}$	2.841(2)	Na(4)-O(58)	2.382(2)
Na(4)-O(71)	2.499(10)	Na(4)-O(72)	2.37(3)
Na(4)-O(73)	2.237(12)	Na(4)-O(74)	2.380(3)
Na(4)-O(75)	2.149(11)	Na(4)-O(76)	2.402(2)

Table 6.5 Interatomic distances relating to the metal coordination spheres in fragment **A** of the crystal structure of complex **6.4** (distances given in Å with e.s.d. in parentheses). Key operations for symmetry related atoms: *(a)* +x, 3/2-y, -1/2+z.

The fragment composition and metal coordination in **B** is very similar to that described above for **A** (Figure 6.18). The Eu(1) metal centre in **B** is, upon local symmetry expansion, octa-coordinate and is of square anti-prismatic geometry (Figures 6.18 and 6.19). A europium/water/sodium link similar to found in **A** is present in **B** and Eu(1) is linked to Na(2) through a S(4) sulfonate group oxygen atom (O(14)*, Figure 6.18). There is also a sodium/calixarene sulfonate chelate similar to that found in **A** and this will also be described further below with the formation of the extended coordination polymer. The Na(1) sodium centre is coordinated to all of the donor atoms of the N(1) 1-aza-18-crown-6 guest, is coordinated to the O(30) europium aquo ligand, is hepta-coordinate and is of distorted capped hexagonal geometry. Bond lengths relating to the coordination spheres of the metal centres in **B** are listed in Table 6.6.

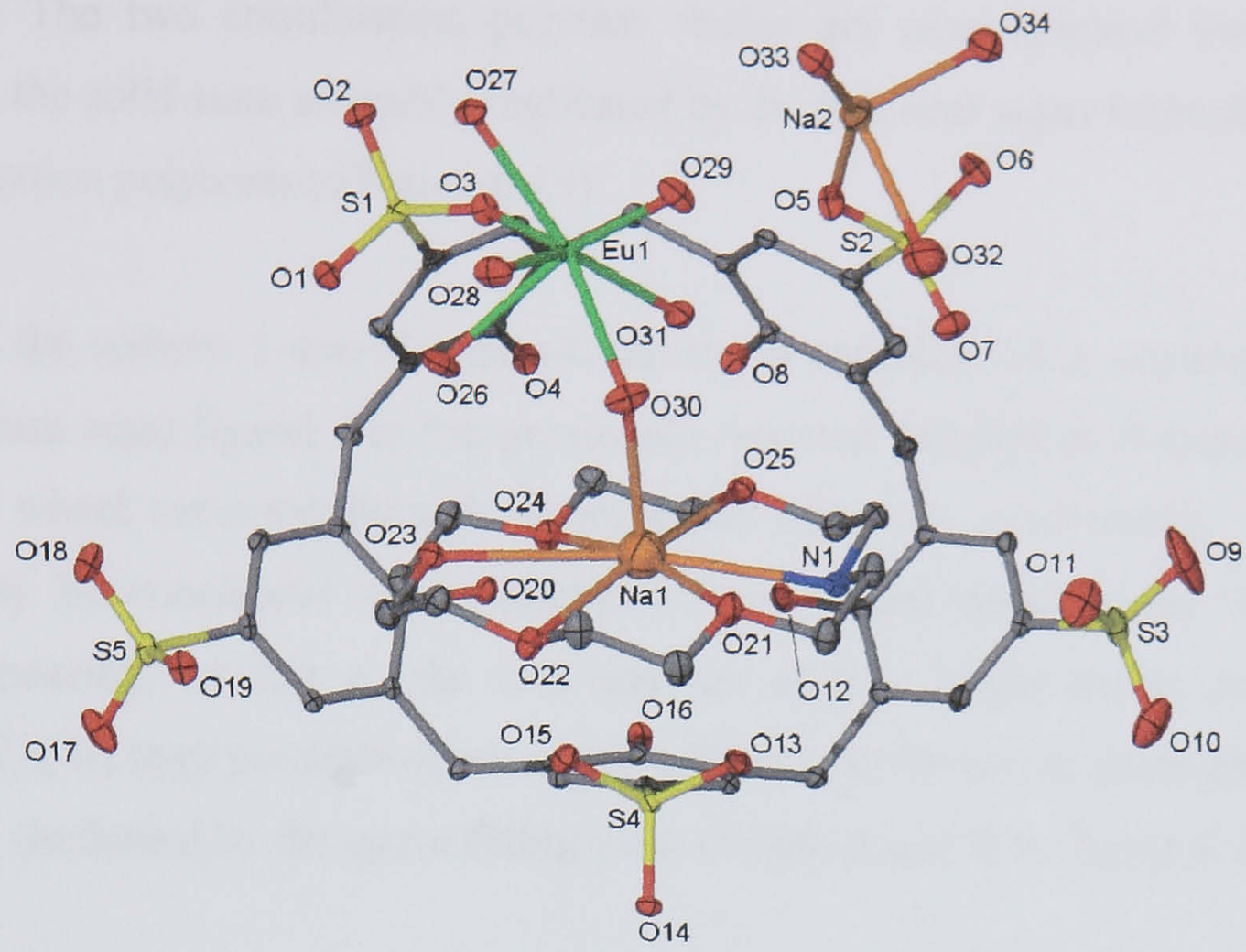

Figure 6.18 Fragment **B** of the asymmetric unit from the crystal structure of complex **6.4**, anisotropic displacement ellipsoids shown at the 50% probability level. Selected atoms have been labelled.

Eu(1)-O(3)	2.4165(19)	Eu(1)-O(14)$^{(a)}$	2.4318(18)
Eu(1)-O(26)	2.426(2)	Eu(1)-O(27)	2.4108(19)
Eu(1)-O(28)	2.413(2)	Eu(1)-O(29)	2.387(2)
Eu(1)-O(30)	2.403(2)	Eu(1)-O(31)	2.457(2)
Na(1)-O(21)	2.836(3)	Na(1)-O(22)	3.005(3)
Na(1)-O(23)	2.950(3)	Na(1)-O(24)	2.782(3)
Na(1)-O(25)	2.923(3)	Na(1)-O(30)	2.676(3)
Na(1)-N(1)	2.777(3)	Na(2)-O(5)	2.376(2)
Na(2)-O(14)$^{(a)}$	2.822(2)	Na(2)-O(15)$^{(a)}$	2.465(2)
Na(2)-O(32)	2.356(3)	Na(2)-O(33)	2.315(3)
Na(2)-O(34)	2.318(3)		

Table 6.6 Interatomic distances relating to the metal coordination spheres in fragment **B** of the crystal structure of complex **6.4** (distances given in Å with e.s.d. in parentheses). Key operations for symmetry related atoms: *(a)* +x, 3/2-y, -1/2+z.

When the extended structure is examined, sodium centres from both fragments (as stated above) form chelate rings with symmetry equivalent calixarene sulfonate groups (Figure 6.19). The angles associated with the sodium/calixarene sulfonate chelates are of typical magnitude and are listed in

Table 6.7.[105, 106] The two coordination polymer chains are near identical but run in opposite directions within the solid state assembly (indicated by the two near super imposable images for the extended coordination polymers in Figure 6.19).

The tethering of the sodium 1-aza-18-crown-6 moiety in complex **6.4** is unusual in that it occurs through a europium aquo ligand. For the previously reported SO_3[4]/La/18-crown-6 Ferris wheel, tethering of the wheel occurred through direct metal sulfonate coordination. The formation of complex **6.4** may be considered as an extended Ferris wheel arrangement. The need for this extension may possibly be due to the fact that the slightly larger cavity size of SO_3[5] (in comparison to SO_3[4]) may preclude direct metal sulfonate as the crown ether guest resides deeper within the cavity (indicated by the space filling view of both **A** and **B** in Figure 6.20).

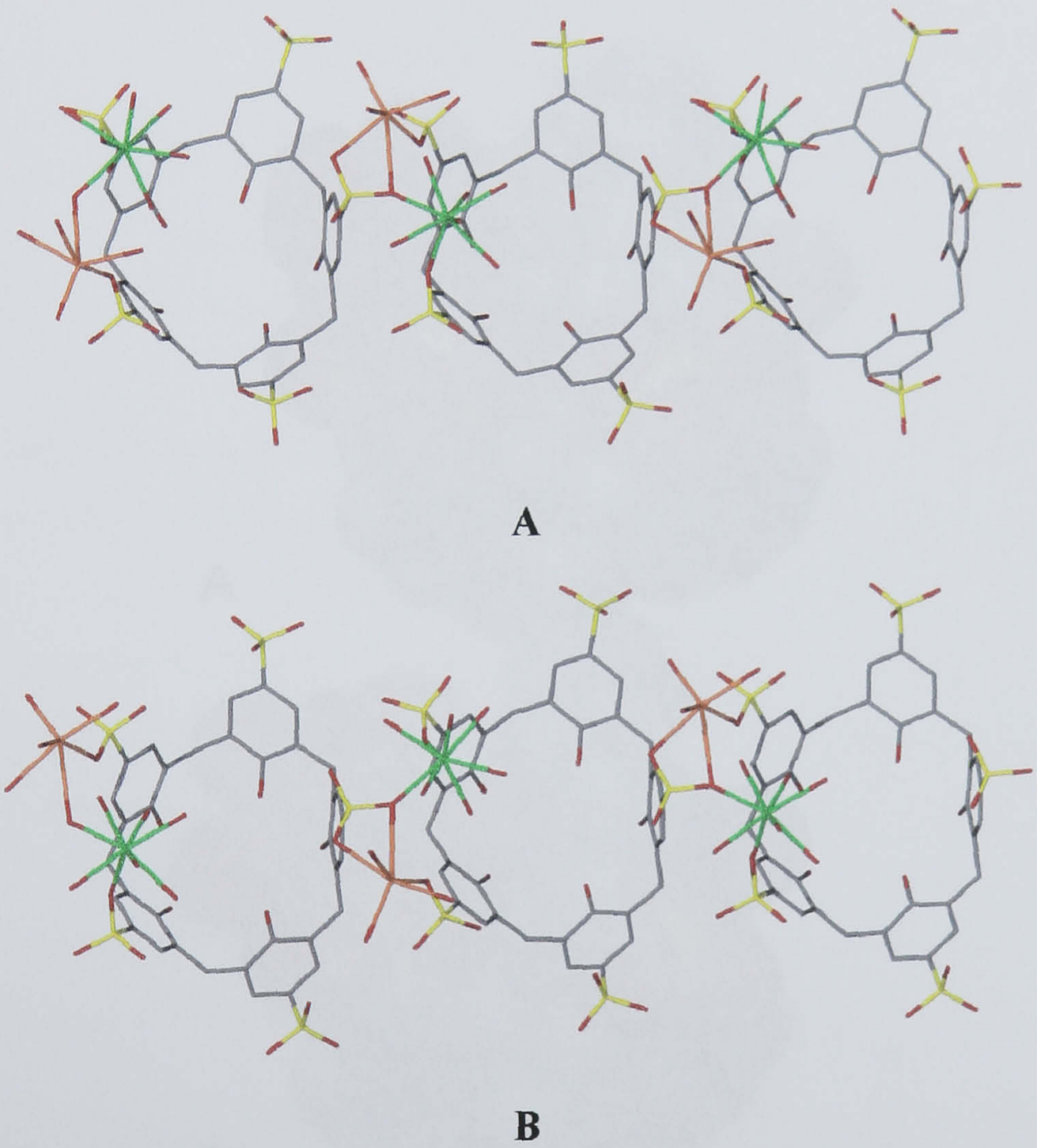

A

B

Figure 6.19 Individual views of the coordination polymer chains formed by the symmetry expansion of fragments **A** an **B** in the crystal structure of complex **6.4** showing the europium sulfonate bonding and sodium sulfonate chelate rings. Some oxygen atoms of disordered sulfonate groups or sodium aquo ligands have been omitted for clarity as have the sodium/aza-crown ether moieties.

S(4)-O(14)-Na(2)$^{(b)}$	88.39(9)	S(8)-O(45)-Na(4)$^{(b)}$	105.80(12)
S(4)-O(15)-Na(2)$^{(b)}$	104.17(11)	S(8)-O(46)-Na(4)$^{(b)}$	87.93(9)

Table 6.7 Angles between vectors relating to the sulfonate chelate of the sodium metal centres in the crystal structure of complex **6.4** (angles given in ° with e.s.d. in parentheses). Key operations for symmetry related atoms: *(b)* +x, 3/2-y, 1/2+z.

Further examination of the extended structure reveals that as for complexes **6.1 – 6.3** of this chapter, the *p*-sulfonatocalix[5]arenes pack into a bi-layer arrangement. Unlike complexes **6.2** and **6.3** however, the two SO_3[5] molecules from the asymmetric unit combine within the same hydrophobic layer and pack through a total of two crystallographically unique π-stacking interactions with aromatic centroid···centroid distances of 3.576 and 3.653 Å.

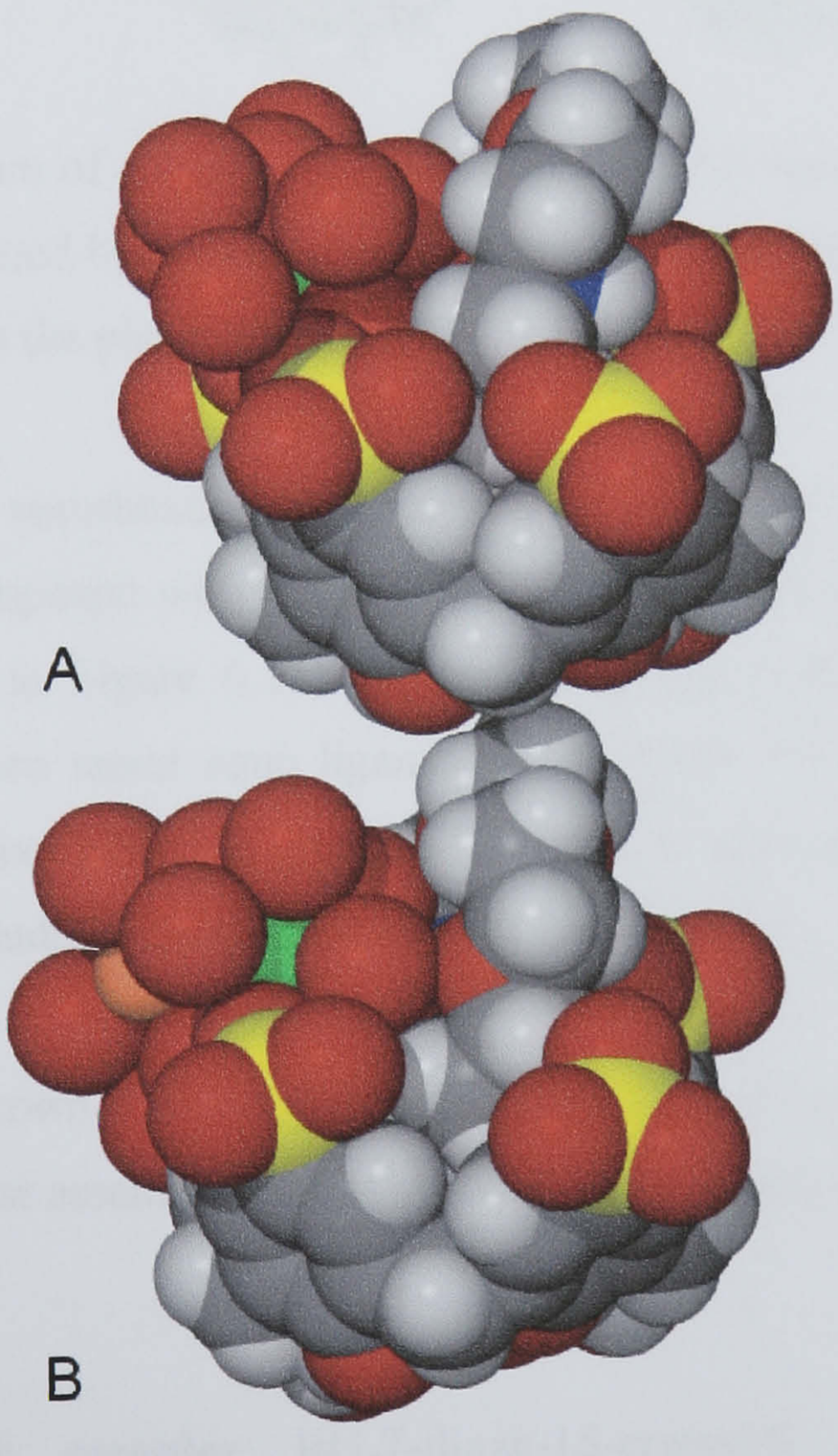

Figure 6.20 Space filling representation of parts **A** and **B** from the asymmetric unit from the crystal structure of complex **6.4** showing the 'snug fit' of the sodium bound 1-aza-18-crown-6 molecules within the cavities of the *p*-sulfonatocalix[5]arenes.

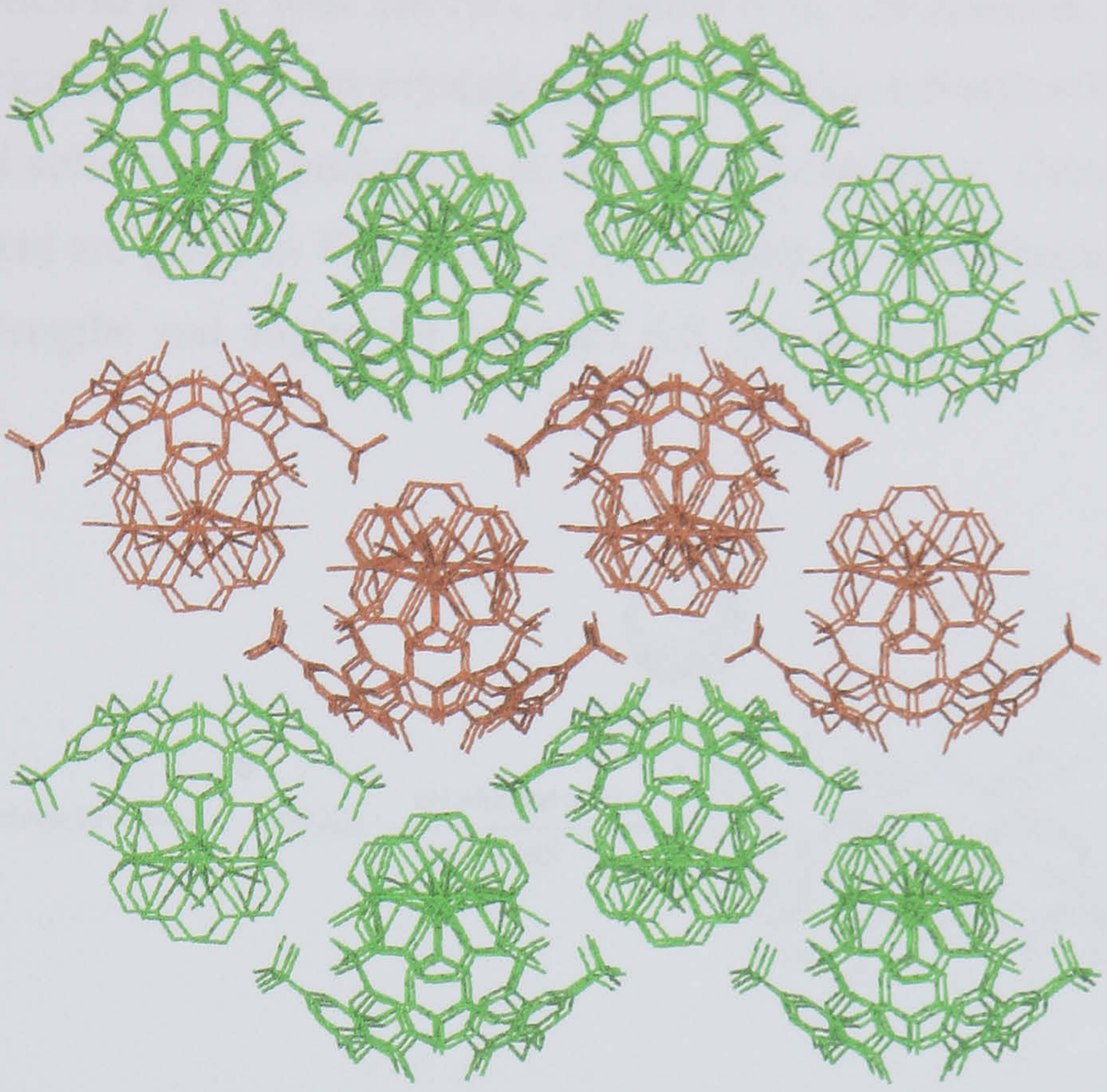

Figure 6.21 Packing diagram of complex **6.4** showing the uni-composite layers within the overall bi-layer arrangement (indicated by the alternating colour scheme). The coordination polymer chains are running perpendicular to the plane of the page.

In contrast, however, the coordination polymer chains of **A** and **B** assemble such that each hydrophilic layer is uni-composite with regard to crown ethers and metal centres (indicated by the alternating colour scheme in Figure 6.21). There are numerous intra and inter-chain hydrogen bonding interactions between metal aquo ligands, crown ether donor atoms, water molecules of crystallisation and calixarene sulfonate groups. These many interactions link chains of identical composition within the extended structure but will not be described.

Replacement of 1-aza-18-crown-6 with 1,7-diaza-15-crown-5 in the above ternary system results in the formation of a host-guest assembly that bears some resemblance to the SO_3[5]/diaza-18-crown-6/Eu complex, **6.3**.

6.2.3 Structure of the complex [[(1,7-diaza-15-crown-5 + 2H)⊂*p*-sulfonatocalix[5]-arene][$Eu(H_2O)_9$]]$_2$.11.75H_2O, 6.5.

Crystals of the complex [[(1,7-diaza-15-crown-5 + 2H)⊂*p*-sulfonatocalix[5]-arene][$Eu(H_2O)_9$]]$_2$.11.75H_2O, **6.5**, grew upon standing over thirty minutes from an acidic aqueous solution containing a 1:2:2 mixture of Na_5SO_3[5], 1,7-diaza-15-crown-5 and europium(III) nitrate

hexahydrate (pH adjusted to be <1 with 1M HCl, Equation 6.5). The complex was characterised by IR spectroscopy and single crystal X-ray crystallography. Complex **6.5** crystallises in an monoclinic cell and the structural solution was performed in the space group $P2_1/c$. Details of data collection and structure refinement are given in Table 6.11 of this chapter. A crystallographic information file containing all bond lengths and angles for complex **6.5** can be found in appendix 6.2.3 on the attached compact disc.

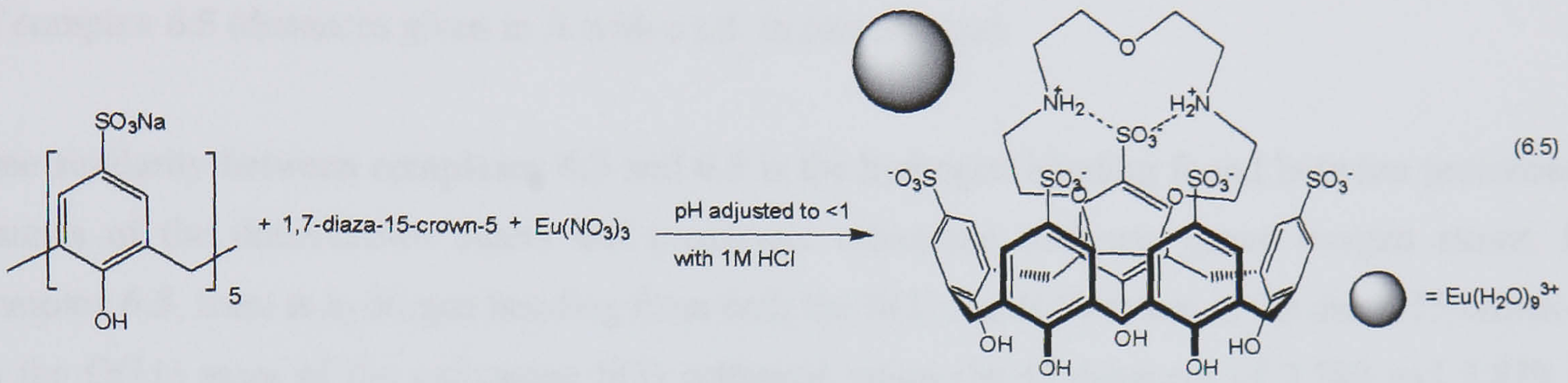

(6.5)

The asymmetric unit consists of one *p*-sulfonatocalix[5]arene, one di-protonated diaza-15-crown-5 molecule, one nona-aqua europium cation and a total of eleven and three quarter water molecules of crystallisation that are disordered over thirteen positions (Figure 6.22). The europium centre is nona-coordinate and is of tri-capped trigonal prismatic geometry. Bond lengths relating to the coordination sphere of Eu(1) are listed in Table 6.8. As stated above, the present structure bears some resemblance to complex **6.3** in that the crown ether is non-coordinating and is located within the cavity of the SO_3[5].

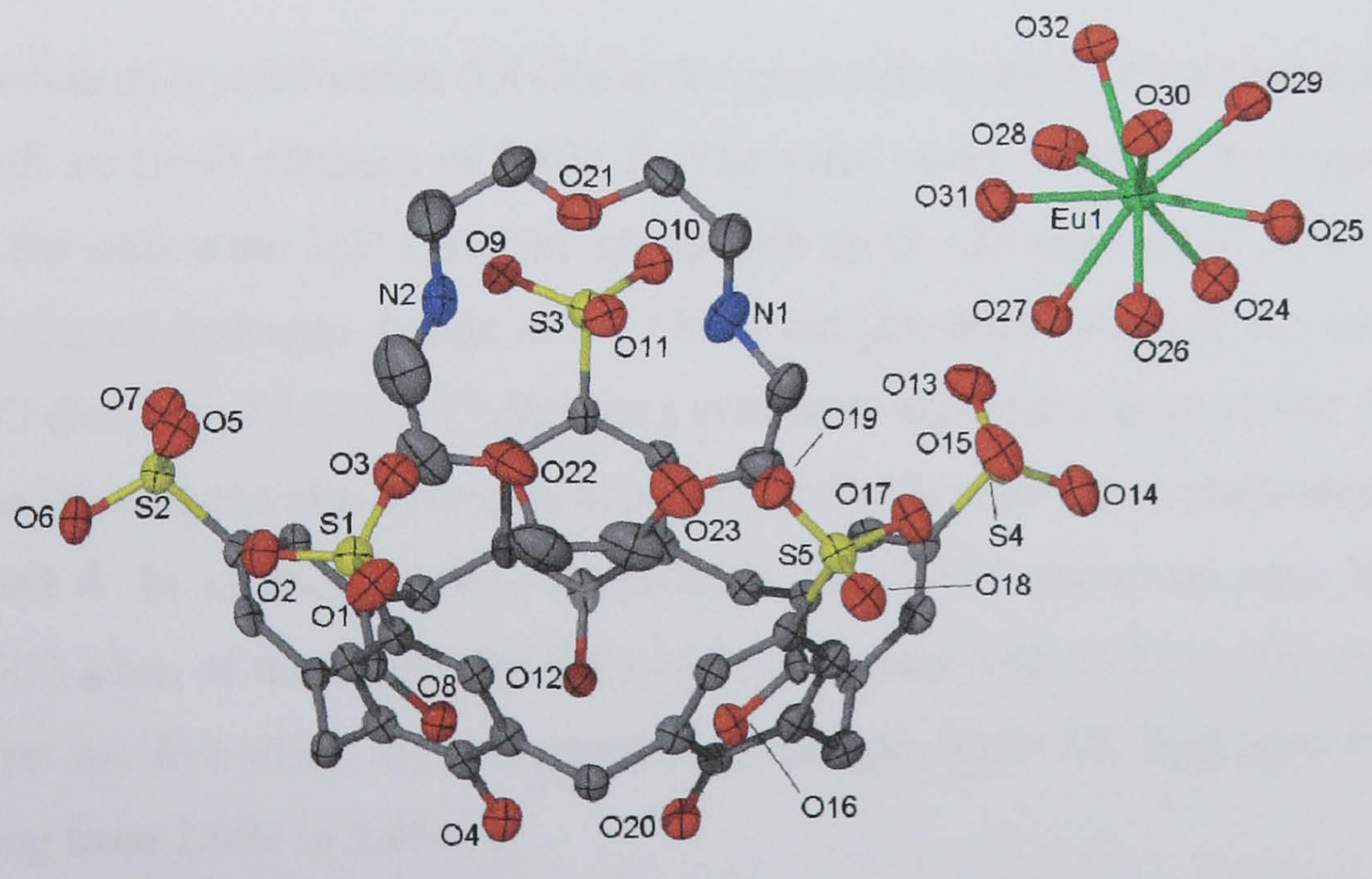

Figure 6.22 Part of the asymmetric unit from the crystal structure of complex **6.5**, anisotropic displacement ellipsoids shown at the 50% probability level. Selected atoms have been labelled.

Eu(1)-O(24)	2.411(9)	Eu(1)-O(25)	2.520(8)
Eu(1)-O(26)	2.406(8)	Eu(1)-O(27)	2.582(8)
Eu(1)-O(28)	2.463(8)	Eu(1)-O(29)	2.485(8)
Eu(1)-O(30)	2.471(9)	Eu(1)-O(31)	2.432(8)
Eu(1)-O(32)	2.467(8)		

Table 6.8 Interatomic distances relating to the europium coordination sphere in the crystal structure of complex **6.5** (distances given in Å with e.s.d. in parentheses).

One similarity between complexes **6.3** and **6.5** is the hydrogen bonding found between protonated amines of the diaza-crown ethers and proximate calixarene sulfonate group oxygen atoms. In complex **6.5**, there is hydrogen bonding from both the N(1) and N(2) atoms of the diaza-15-crown-5 to the O(11) atom of the calixarene S(3) sulfonate group (N···O distances of 2.780 and 2.879 Å respectively, Figure 6.23). In complex **6.3**, the di-protonated diaza-18-crown-6 guest adopts near meridional geometry and there is hydrogen bonding to a calixarene sulfonate group and a crown ether associated water molecule of crystallisation (Figure 6.13). The di-protonated diaza-15-crown-5 in complex **6.5** has a distorted geometry and the two protonated amines are directed towards the calixarene S(3) sulfonate group. As this is the case, hydrogen bonding to a water molecule of crystallisation on the opposite side of the crown ether from the from the calixarene S(3) sulfonate group is not possible. Despite this, alternative hydrogen bonding regimes involving two crown ether oxygen donor atoms, one water of crystallisation and a europium aquo ligand are evident (Figure 6.23).

The water molecule of crystallisation (O(43)) hydrogen bonds to the O(23) donor atom of the diaza-15-crown-5 with an O···O distance of 2.803 Å. The same water molecule hydrogen bonds to the O(19) atom of the calixarene S(5) sulfonate group with an O···OS distance of 2.835 Å. The O(30)* europium aquo ligand hydrogen bonds to the O(21) oxygen donor atom of the diaza-15-crown-5 with an EuO···O distance of 2.921 Å (* denotes a symmetry equivalent atom to that shown in Figure 6.22). The same aquo ligand also hydrogen bonds to the O(43) water of crystallisation with an O···O distance of 2.693 Å. In addition to these interactions, the O(32)* europium aquo ligand hydrogen bonds to the O(3) atom of the calixarene S(1) sulfonate group with an EuO···OS distance of 2.855 Å. In total there are five other crystallographically unique EuO···OS hydrogen bonds that have distances ranging from 2.692 to 2.844 Å.

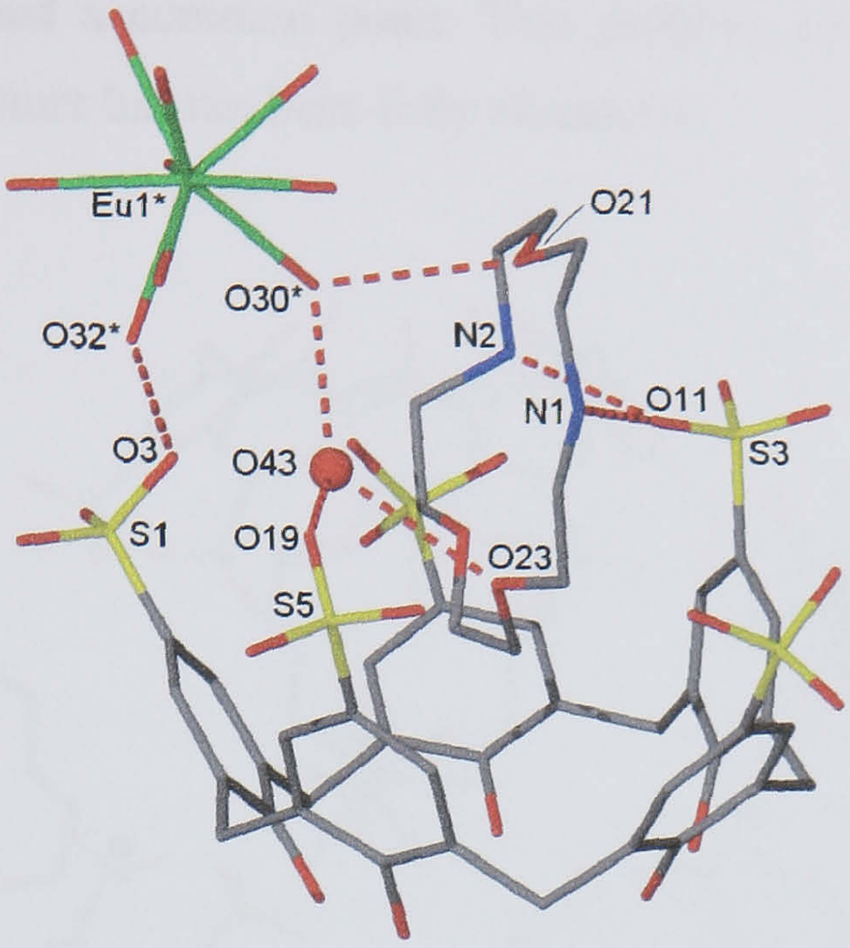

Figure 6.23 Some of the hydrogen bonding interactions found between the molecular components in the crystal structure of complex **6.5**. Selected atoms have been labelled and a * denotes a symmetry equivalent atom.

When the extended structure is examined, the calixarenes are seen to pack in a bi-layer arrangement similar to those described both above and in the literature.[66-68] This packing occurs through one CH···π and two π-stacking interactions (crystallographically unique). The CH···π interaction is from a calixarene methylene bridge and an aromatic ring of a neighbouring SO_3[5] molecule (CH···aromatic centroid distance of 2.933 Å). The two π-stacking interactions occur with aromatic centroid···centroid distances of 3.575 and 3.767 Å. When the numerous other waters of crystallisation are taken into account, complicated hydrogen bonding regimes are evident within the extended structure.

Replacement of diaza-15-crown-5 with 1-aza-15-crown-5 in the above ternary system did not result in single crystal formation despite several attempts. Incorporation of a 1+ charged guest in the cavity of SO_3[5] would require crystallisation of a non-integer number of lanthanide metal cations or sequestration of additional sodium ions or protons from solution to achieve charge balance, and clearly this is unfavourable in the present system. This fact, coupled with the continual exclusion of 1-aza-15-crown-5 from supramolecular architectures with *p*-sulfonatocalix[4]arene, as described in chapter two, further suggests that the molecule is unsuitable for solid state complex formation with the smaller *p*-sulfonatocalix[*n*]arenes (where $n = 4$ or 5). When diaza-12-crown-4 is used as a guest in a ternary system analogous to those described above, crystals of a europium complex similar to **6.3** and **6.5** grow rapidly (in under thirty minutes). Unfortunately the crystals appeared to be twinned and the structural solution was of poor quality and suggested superimposition of two *p*-

sulfonatocalix[5]arenes around a common point. This problem could not be overcome through recrystallisation and the structure has not been fully elucidated.

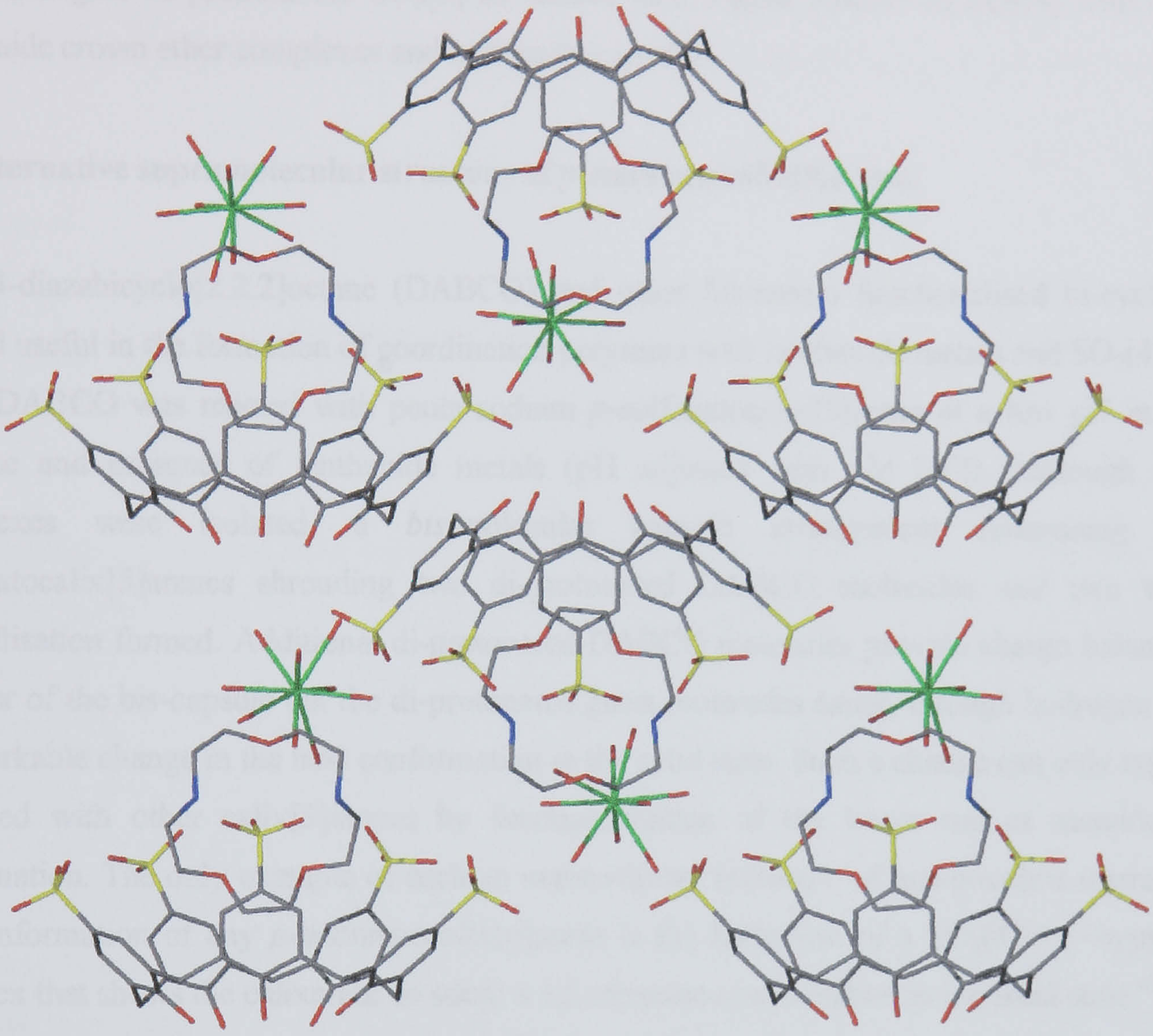

Figure 6.24 A cross section of the extended bi-layer arrangement found in the crystal structure of complex **6.5**.

6.2.4 Summary of lanthanide crown ether complexes of *p*-sulfonatocalix[5]arene.

This section described the formation of three host-guest complexes (one of which could not be fully resolved) and the formation of an extended Ferris wheel structure, all of which formed with (*bis*)amino functionalised crown ether guests of varied size. Unfortunately, none of the above complexes assembled as molecular capsules as was predicted. In hindsight this would be unlikely given that a SO_3[5] with a charge of 5– will of course crystallise as a 1:1 host guest complex with a 2+ guest and a 3+ counterion. Additional attempts to incorporate a variety of 2+ transition metal cations were unsuccessful but this should be examined further. Unfortunately finding a route to molecular capsule formation with SO_3[5] may involve the use of a large amount of the calixarene in a combinatorial approach and isolation of the required amount of starting material would be costly

with respect to time. If molecular capsules composed of SO_3[5] were to be accessed, they may prove useful in nano-spheroid formation (chapter five) and should be investigated further with other (bi)cyclic guest molecules. Given that an extended Ferris wheel arrangement was characterised, this shows a degree of promise for SO_3[5] to behave in a similar manner to SO_3[4] with respect to lanthanide crown ether complexes and molecular capsules.

6.3 Alternative supramolecular structure of *p*-sulfonatocalix[5]arene.

As 1,4-diazabicyclo[2.2.2]octane (DABCO) and other *bis*-amino functionalised bi-cyclic guests proved useful in the formation of coordination polymers with lanthanide metals and SO_3[4] (chapter two), DABCO was reacted with penta-sodium *p*-sulfonatocalix[5]arene at a low pH in both the absence and presence of lanthanide metals (pH adjusted with 1M HCl). Although no metal complexes were isolated, a *bis*-molecular capsule arrangement comprising two *p*-sulfonatocalix[5]arenes shrouding two di-protonated DABCO molecules and two waters of crystallisation formed. Additional di-protonated DABCO molecules provide charge balance on the exterior of the bis-capsule but the di-protonated guest molecules cause, through hydrogen bonding, a remarkable change in the host conformation in the solid state. Such a change can only typically be achieved with other calix[5]arenes by functionalisation of the lower rim or metal/lower rim coordination. The only example of such an extraordinary influence of non-covalent interactions on the conformation of any *p*-sulfonatocalix[*n*]arene is the formation of a SO_3[4]/4,4`-bypyridinium complex that shows the calixarene to adopt a 1,3-alternate conformation in the solid state.[65] Another molecule examined as a potential guest for the cavity of SO_3[5] was 3-pyridine sulfonic acid ($PySO_3$). A recent review showed $PySO_3$ to be flexible in its ability to form coordination networks that used both the pyridine and sulfonate functionalities as connection points.[137] Given this, $PySO_3$ was reacted with Na_5SO_3[5] at a low pH (altered by addition of 1M HCl) afforded a molecular capsule arrangement comprising two *p*-sulfonatocalix[5]arenes shrouding two $PySO_3$ molecules as part of a sodium/SO_3[5] coordination polymer.

6.3.1 Structure of the complex *bis*-molecular capsule [{(DABCO + 2 H^+)(H_2O)}⊂(*p*-sulfonatocalix[5]arene + H^+)][(DABCO + 2 H^+)$_{1.5}$]·9.25H_2O, 6.6.

Crystals of the complex [{(DABCO + 2 H^+)(H_2O)}⊂(*p*-sulfonatocalix[5]arene + H^+)][(DABCO + 2 H^+)$_{1.5}$]·9.25H_2O, **6.6**, grew upon standing over two days from an acidic aqueous solution containing a ~1:5 mixture of Na_5SO_3[5] and 1,4-diazabicyclo[2.2.2]octane (pH adjusted to be <1 with 1M HCl, Equation 6.6). The complex was characterised by IR and NMR spectroscopy and single crystal X-

ray crystallography. ^{1}H NMR spectroscopy of re-dissolved crystals of complex **6.6** confirmed the SO_3[5]:DABCO stoichiometry to be 1:2.5. Complex **6.6** crystallises in a triclinic cell and the structural solution was performed in the space group $P\bar{1}$. Details of data collection and structure refinement are given in Table 6.11 of this chapter. A crystallographic information file containing all bond lengths and angles for complex **6.6** can be found in appendix 6.3.1 on the attached compact disc.

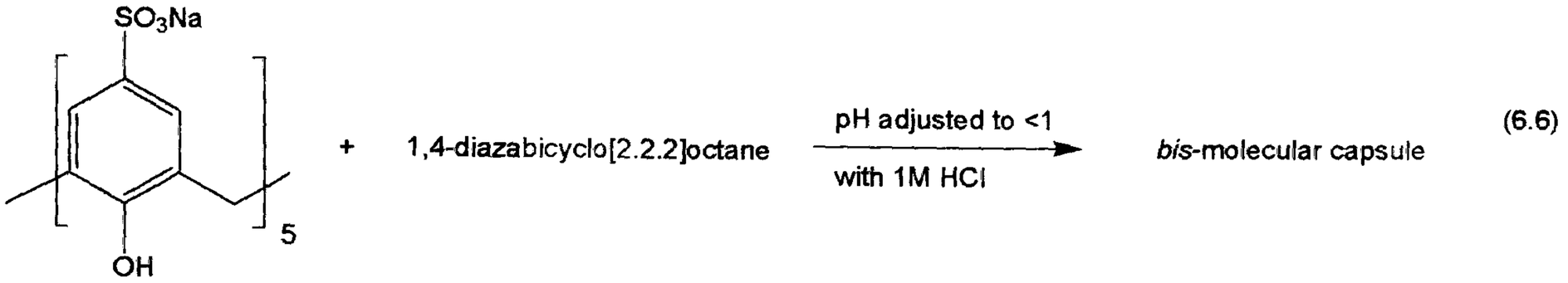

The asymmetric unit consists of one *p*-sulfonatocalix[5]arene, two and a half di-protonated DABCO molecules (some of which are disordered) and a total of nine and a quarter molecules that are disordered over twenty four positions (Figure 6.25). One di-protonated DABCO molecule is disordered over two positions (N(1)/N(2) and N(7)/N(9) with partial occupancies of 0.75 and 0.25 respectively. One half di-protonated DABCO molecule is also disordered over two positions (N(3) and N(4), both with partial occupancies of 0.5). In addition, one ethyl arm of the N(5)/N(6) di-protonated DABO molecule is disordered over two positions each with a partial occupancy of 0.5. The most notable feature of the asymmetric unit is the surprising distortion of the typically truncated cone shape of *p*-sulfonatocalix[5]arene (Figure 6.22 and 6.23). In this conformation the molecule presents two partial cavities that are occupied by the N(5)/N(6) di-protonated DABCO molecule and a water of crystallisation (O(28), Figure 6.22).

As cited in section 6.3, there is only one reported example in which non-covalent interactions dramatically influence the conformation of any *p*-sulfonatocalix[*n*]arene. That example showed that complexation of SO_3[4] with 4,4'-bipyridinium results in the calixarene adopting a 1,3-alternate conformation in the solid state.

Indeed there are no such examples for *p*-sulfonatocalix[5]arene and a survey of all the calix[5]arene structures on the Cambridge Crystallographic Data Centre reveals that a dramatic conformational perturbation such as that shown in Figure 6.23 can only normally be achieved by either calixarene lower rim functionalisation or lower rim/metal coordination. The conformational distortion results in the formation of two partial cavities that, as stated above are occupied by the N(5)/N(6) di-protonated DABCO molecule and a water of crystallisation (O(28), Figures 6.22 and 6.24).

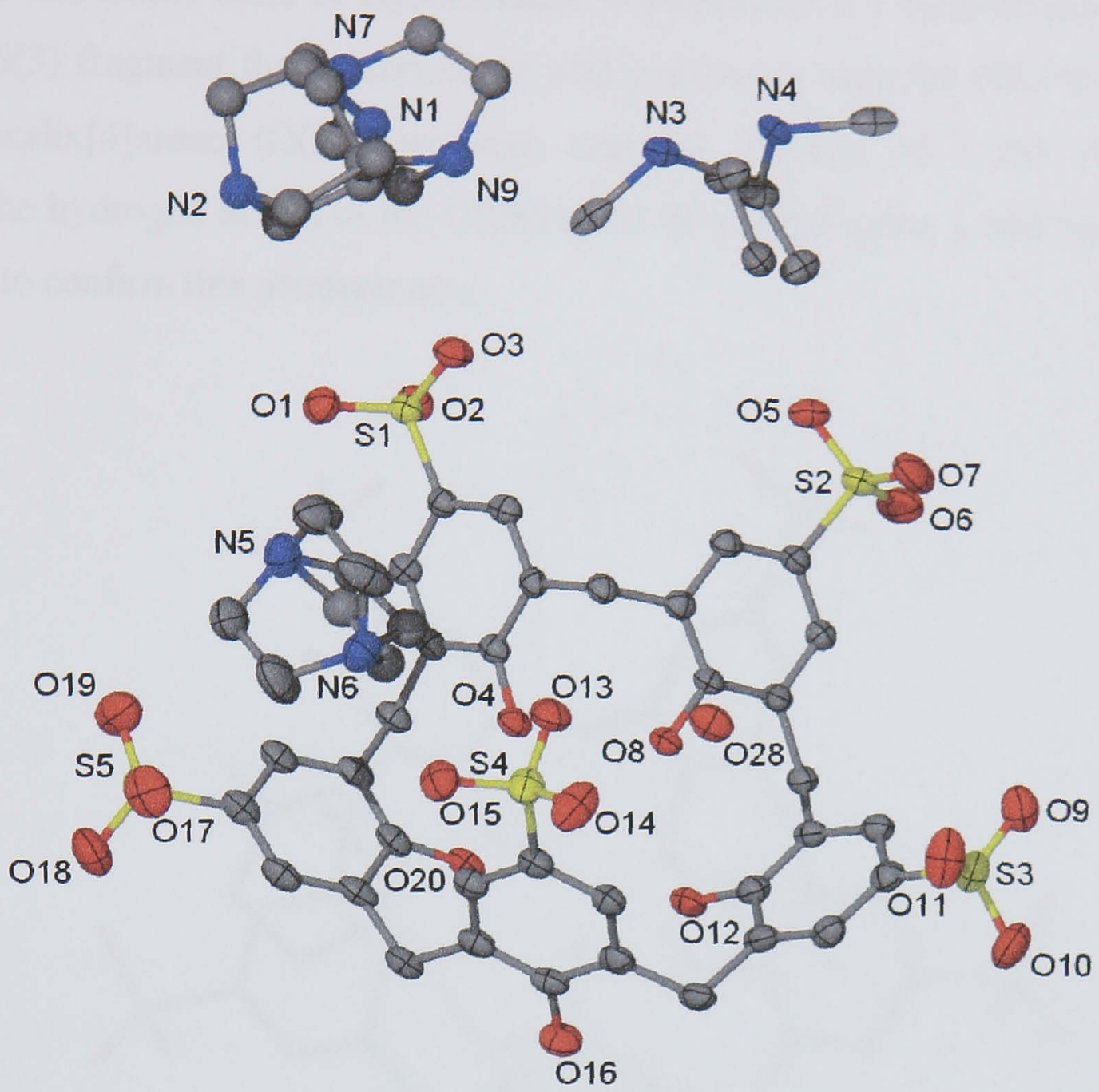

Figure 6.22 Part of the asymmetric unit from the crystal structure of complex **6.6**, anisotropic displacement ellipsoids shown at the 50% probability level. Isotropically refined atoms are shown in ball and stick representation. Selected atoms have been labelled.

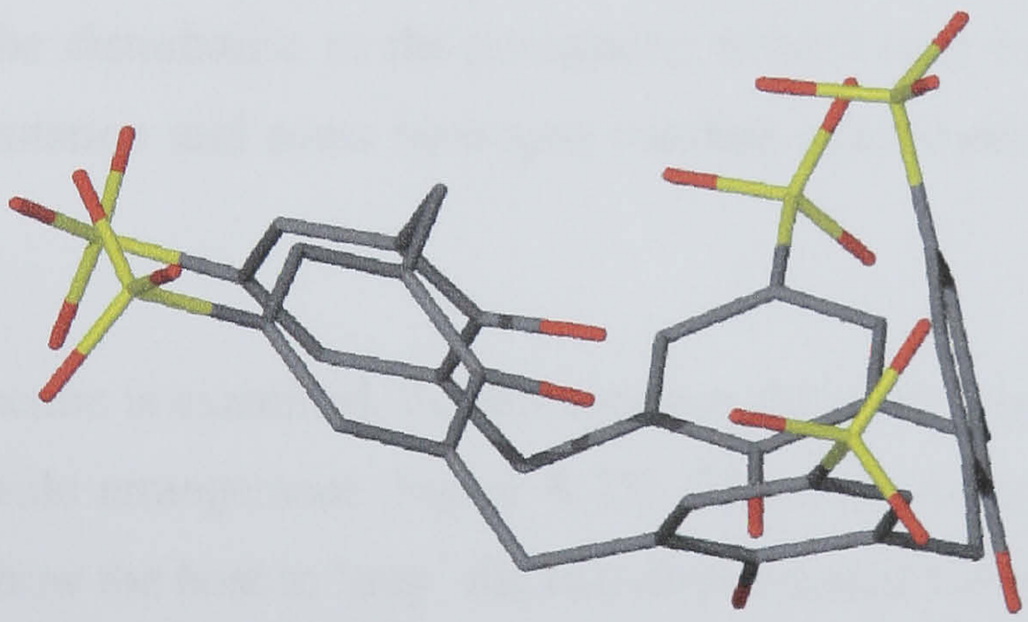

Figure 6.23 Side view of the conformational distortion of the *p*-sulfonatocalix[5]arene from the crystal structure of complex **6.6**.

The protonated N(6) atom of the DABCO hydrogen bonds to the O(15) atom of the calixarene S(4) sulfonate group with a N···OS distance of 2.750 Å (corresponding NH···OS distance of 1.853 Å, Figure 6.24). There is a hydrogen bond from the O(8) calixarene base hydroxy group to the O(28) water of crystallisation with an O···O distance of 2.681 Å (corresponding OH···O distance of 1.912

Å, Figure 6.24). The O(28) water of crystallisation is positioned at a distance from aromatic ring of the calixarene S(3) fragment that is consistent with previously reported OH···π interactions found for *p*-sulfonatocalix[4]arene (O(28)···aromatic centroid distance of 3.785 Å, Figure 6.24).[28] Unfortunately the hydrogen atoms of the O(28) water of crystallisation could not be located in the difference map to confirm this phenomenon.

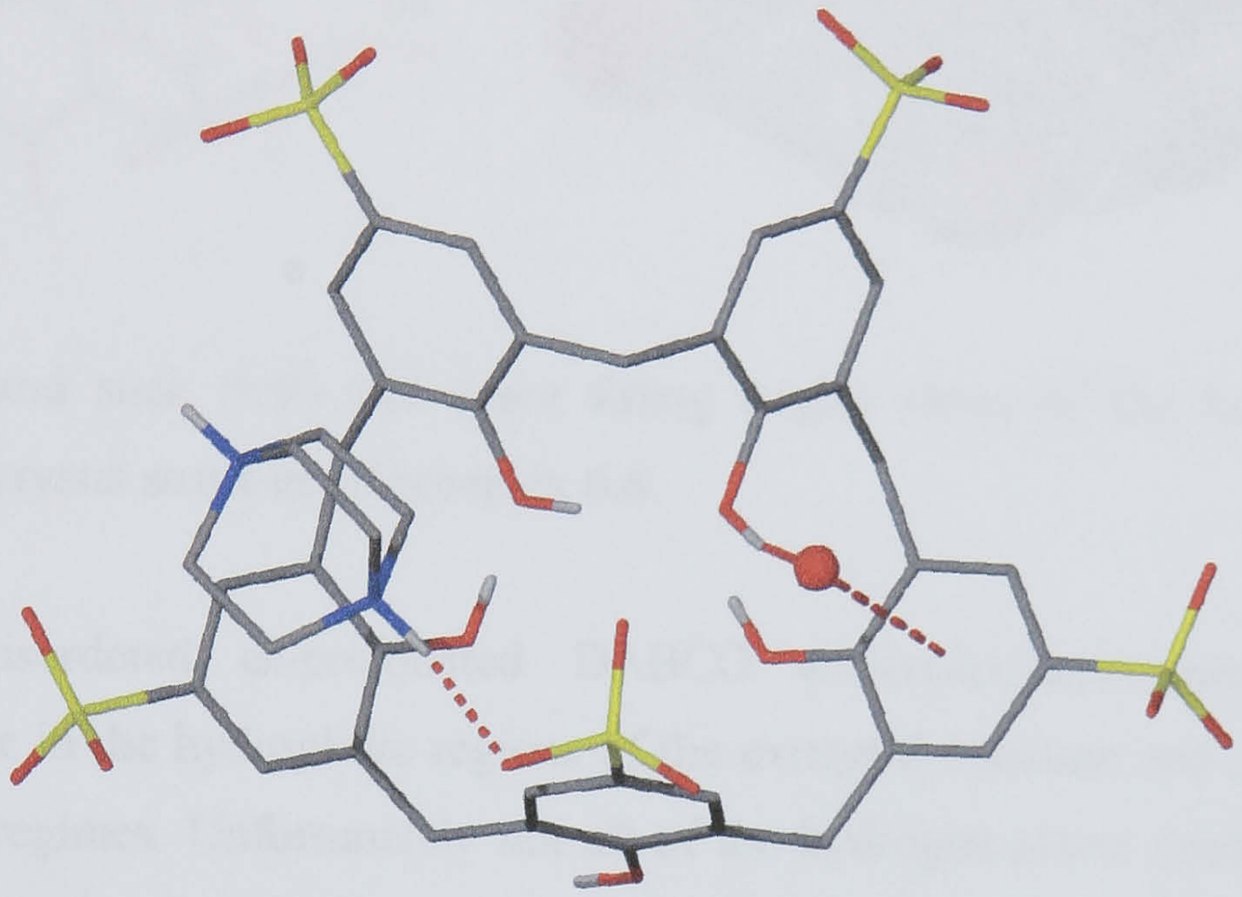

Figure 6.24 View of the *p*-sulfonatocalix[5]arene cavity and the two included guest species in the crystal structure of complex **6.6**. All atoms except the guest water of crystallisation are shown in stick representation. The disturbance to the pentameric SO_3[5] base hydrogen bonding regime is clear from this representation and some hydrogen bonding interactions are shown as dashed red lines.

When the extended structure is examined, the arrangement shown in Figure 6.24 is seen to assemble in a *bis*-molecular capsule arrangement (Figure 6.25). The stick and space filling representations shown in Figure 6.25 show the host to 'trap' the two di-protonated DABCO molecules and the two waters of crystallisation through the series of hydrogen bonds described above. The extended structure also reveals that the calixarenes do not pack in the typical bi-layer arrangement but in hydrophobic chains (Figure 6.26). This occurs through two CH···π and one π-stacking interaction (crystallographically unique). The two CH···π interactions are from aromatic ring hydrogen atoms to adjacent calixarene aromatic rings and have CH···aromatic centroid distances of 2.934 and 3.001 Å. The crystallographically unique π-stacking interaction occurs with an aromatic centroid···centroid distance of 4.004 Å.

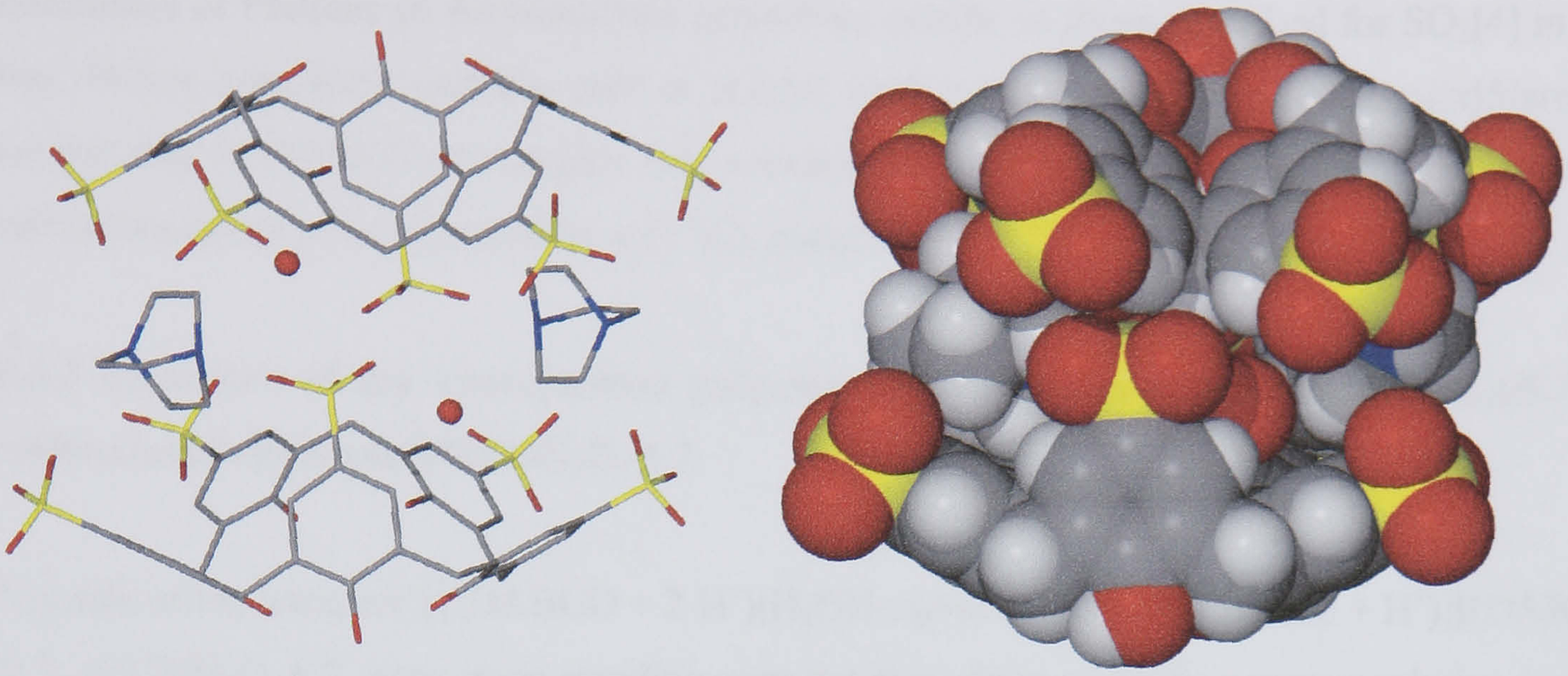

Figure 6.25 Ball and stick (left) and space filling (right) views of the *bis*-molecular capsule arrangement in the crystal structure of complex **6.6**.

The additional disordered di-protonated DABCO molecules/counterions and waters of crystallisation reside in the hydrophilic regions of the extended structure and partake in numerous hydrogen bonding regimes. Unfortunately not all of the hydrogen atoms could be located on the disordered DABCO molecules therefore precise hydrogen bonding regimes cannot be determined.

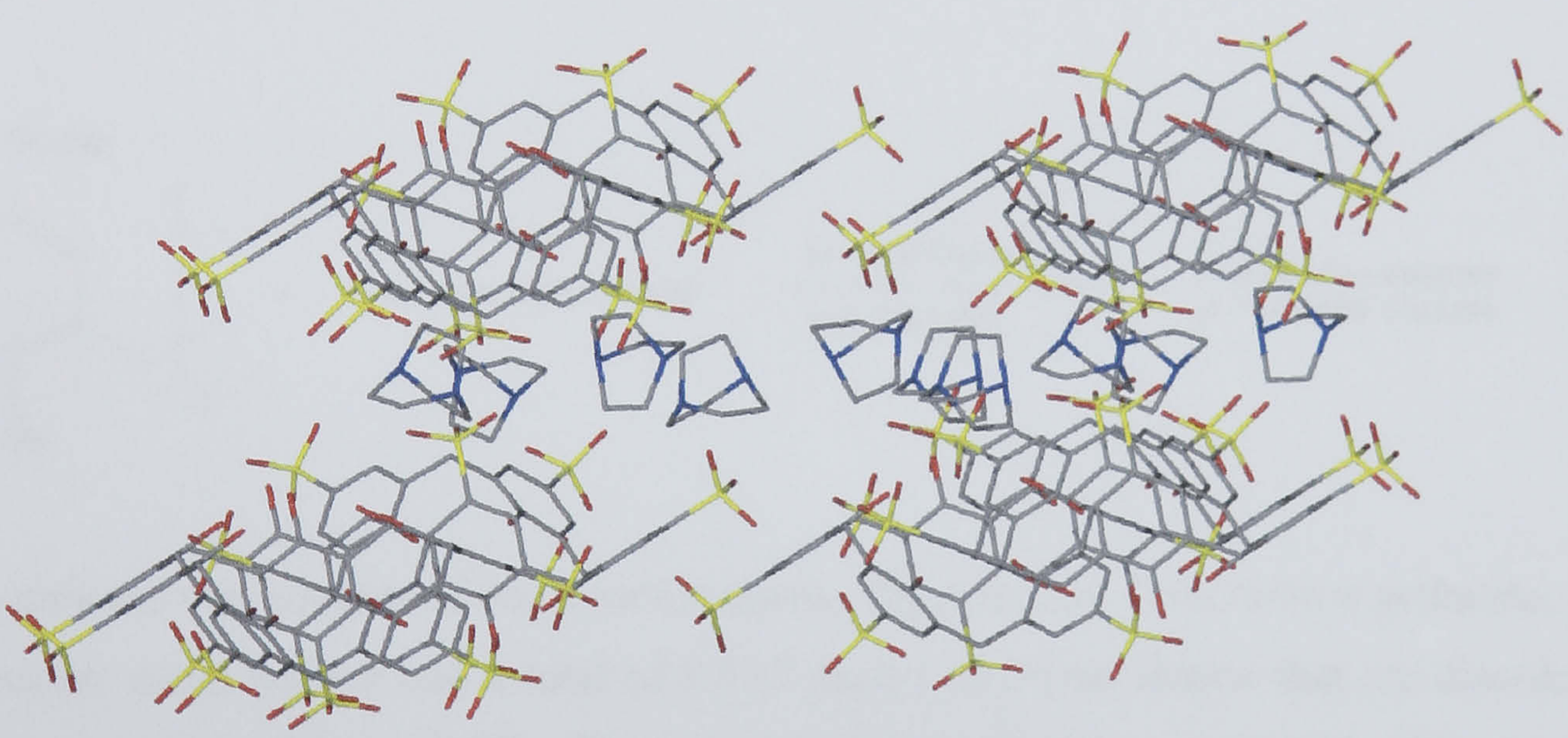

Figure 6.26 Packing diagram of the hydrophobic chains found in the crystal structure of complex **6.6**. The chains run perpendicular to the plane of the page. The additional di-protonated DABCO molecules that reside in hydrophilic environments are also shown.

Complex **6.6** shows that non-covalent interactions can have a profound effect on the conformation of *p*-sulfonatocalix[5]arene in the absence of metal counterions. The complex also shows that the molecule could perhaps act as a two-vertex species were it to be incorporated into nano-spheroid

assemblies of Platonic or Archimedean geometries similar to those described for SO_3[4] in chapter five. When 3-pyridine sulfonic acid is reacted with penta-sodium *p*-sulfonatocalix[5]arene in a similar way to DABCO in complex **6.6**, a molecular capsule arrangement forms that shows each calixarene cavity to be occupied by a $PySO_3$ molecule.

6.3.2 Structure of the coordination polymer [(3-pyridinium sulfonate·H_2O)($Na_2(H_2O)_{2.5}$)(*p*-sulfonatocalix[5]arene)]·9.833H_2O, 6.7.

Crystals of the complex [{(DABCO + 2 H^+)(H_2O)}⊂(*p*-sulfonatocalix[5]arene + H^+)][(DABCO + 2 H^+)$_{1.5}$]·9.25H_2O, **6.7**, grew upon standing over two days from an acidic aqueous solution containing a ~1:5 mixture of Na_5SO_3[5] and 3-pyridine sulfonic acid (pH adjusted to be <1 with 1M HCl, Equation 6.7). The complex was characterised by NMR spectroscopy and single crystal X-ray crystallography. ^{1}H NMR spectroscopy of re-dissolved crystals of complex **6.7** confirmed the SO_3[5]:$PySO_3$ stoichiometry to be 1:1. Complex **6.7** crystallises in a monoclinic cell and the structural solution was performed in the space group *C*2/*c*. Details of data collection and structure refinement are given in Table 6.12 of this chapter. A crystallographic information file containing all bond lengths and angles for complex **6.7** can be found in appendix 6.3.2 on the attached compact disc.

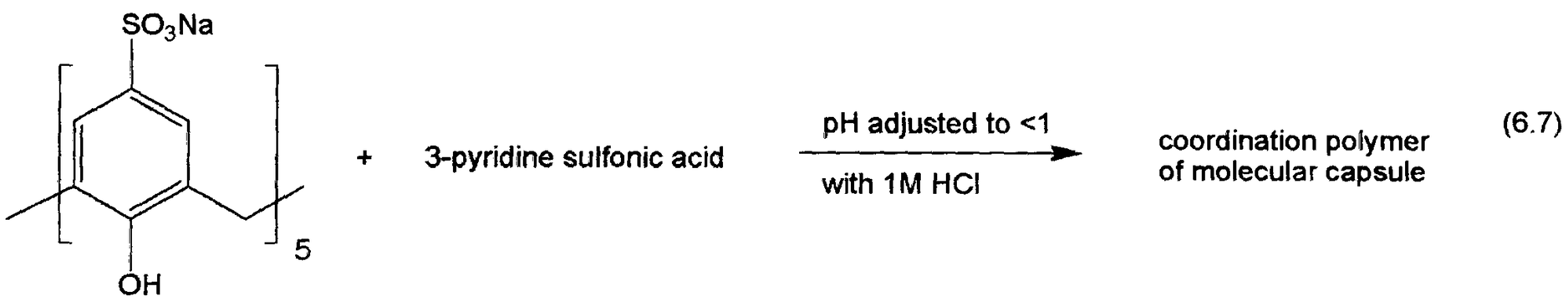

The asymmetric unit consists of one *p*-sulfonatocalix[5]arene, one 3-pyridinium sulfonate, two poly aquo sodium metal centres and a total of 9.833 waters of crystallisation that are disordered over thirty six positions (Figure 6.27). There is significant disorder associated with three of the calixarene sulfonate groups, the $PySO_3$ molecule (parts of which are disordered over either two or three positions) and some of the sodium aquo ligands in the asymmetric unit (Figure 6.27). The oxygen atoms of the calixarene S(1) sulfonate group are disordered over two positions with partial occupancies of 0.8 and 0.2 (Figure 6.27). The oxygen atoms of the calixarene sulfonate group S(3) are disordered over three positions with partial occupancies of 0.6, 0.2 and 0.2 (Figure 6.27). Two of the oxygen atoms of the calixarene S(5) sulfonate group are disordered over two positions with partial occupancies of 0.8 and 0.2 (Figure 6.27). The $PySO_3$ molecule is badly disordered and given the extensive disorder associated with the sodium terminal or bridging aquo ligands and particular

calixarene sulfonate groups, a table of interatomic distances for the sodium coordination spheres has not been constructed. Upon local symmetry expansion, the sodium centres in the asymmetric unit retain some vestige of octahedral geometry (albeit distorted) as shown in Figure 6.28.

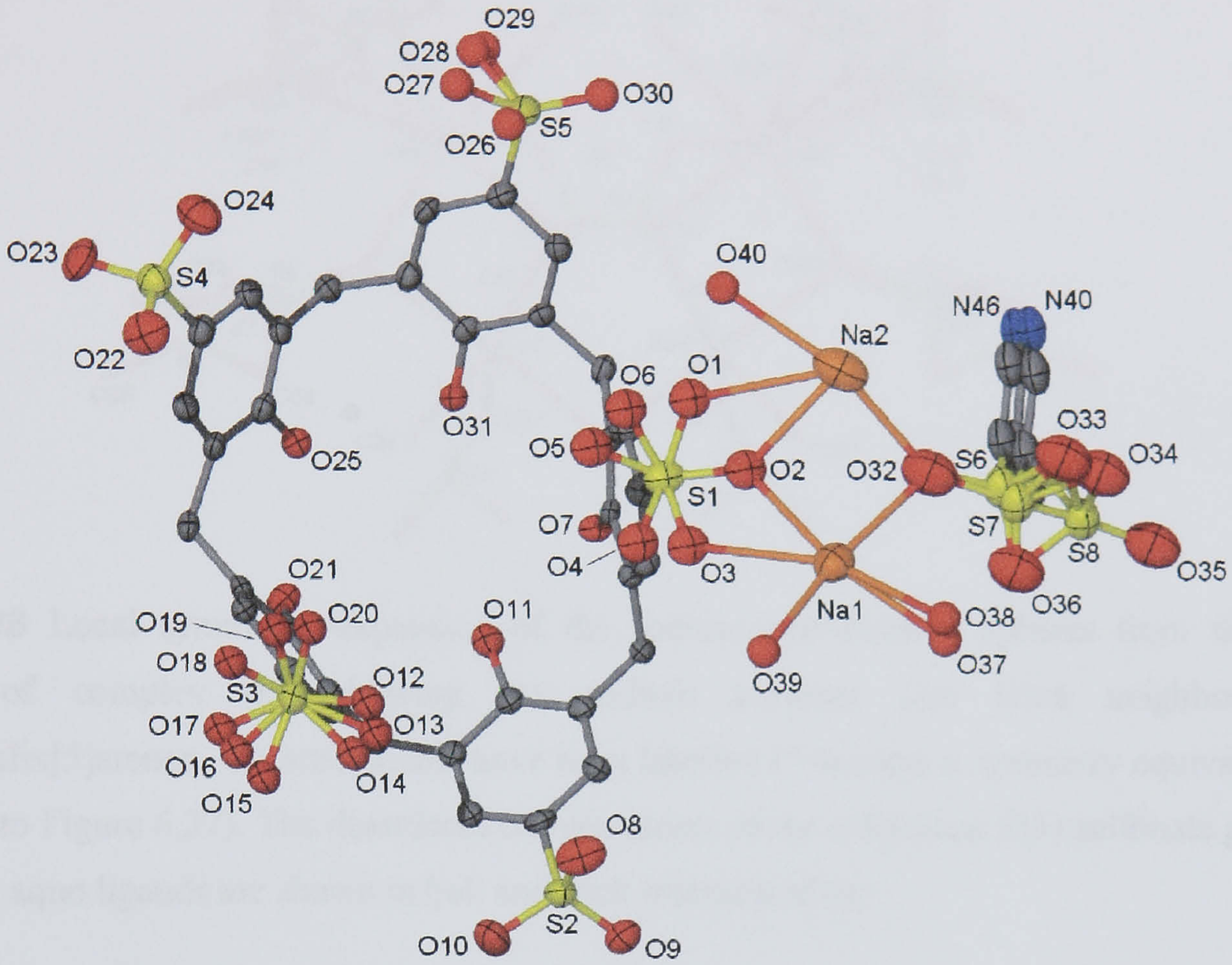

Figure 6.27 Part of the asymmetric unit from the crystal structure of complex **6.7**, anisotropic displacement ellipsoids shown at the 50% probability level. Selected atoms have been labelled. The disordered oxygen atoms of the calixarene S(5) sulfonate group and the sodium aquo ligands are shown in ball and stick representation.

Expansion from the asymmetric unit reveals a sodium tetramer that links four neighbouring *p*-sulfonatocalix[5]arenes in two adjacent molecular capsule arrangements (Figures 6.28 and 6.29). These molecular capsules assemble with $PySO_3$ molecules occupying part of the calixarene cavities (Figure 6.29). In addition to this, a water of crystallisation that is disordered over three positions occupies part of the SO_3[5] cavity and is in a position consistent with hydrogen bonding from the protonated nitrogen atom (that is disordered over two positions) of the $PySO_3$ guest (six N···O distances ranging from2.575 to 3.015 Å. Several groups have reported solid state structures of poly-aquo poly-nuclear sodium clusters but we believe that this is the first to adopt a trapezoidal 'horseshoe' shape as is shown in Figure 6.28.[138-143] Unfortunately the quality of data did not permit the location or refinement of the $PySO_3$ hydrogen atoms and there is some ambiguity surrounding the protonation state of the overall complex. Assuming the calixarene adopts a 5– charge, the presence of two sodium centres and a zwitterionic $PySO_3$ molecule leaves a charge deficit of 3–. As

the crystals grew from very acidic aqueous media, it is possible that charge balance may be provided through protonation of the sulfonate groups of both the calixarene and $PySO_3$ molecules.

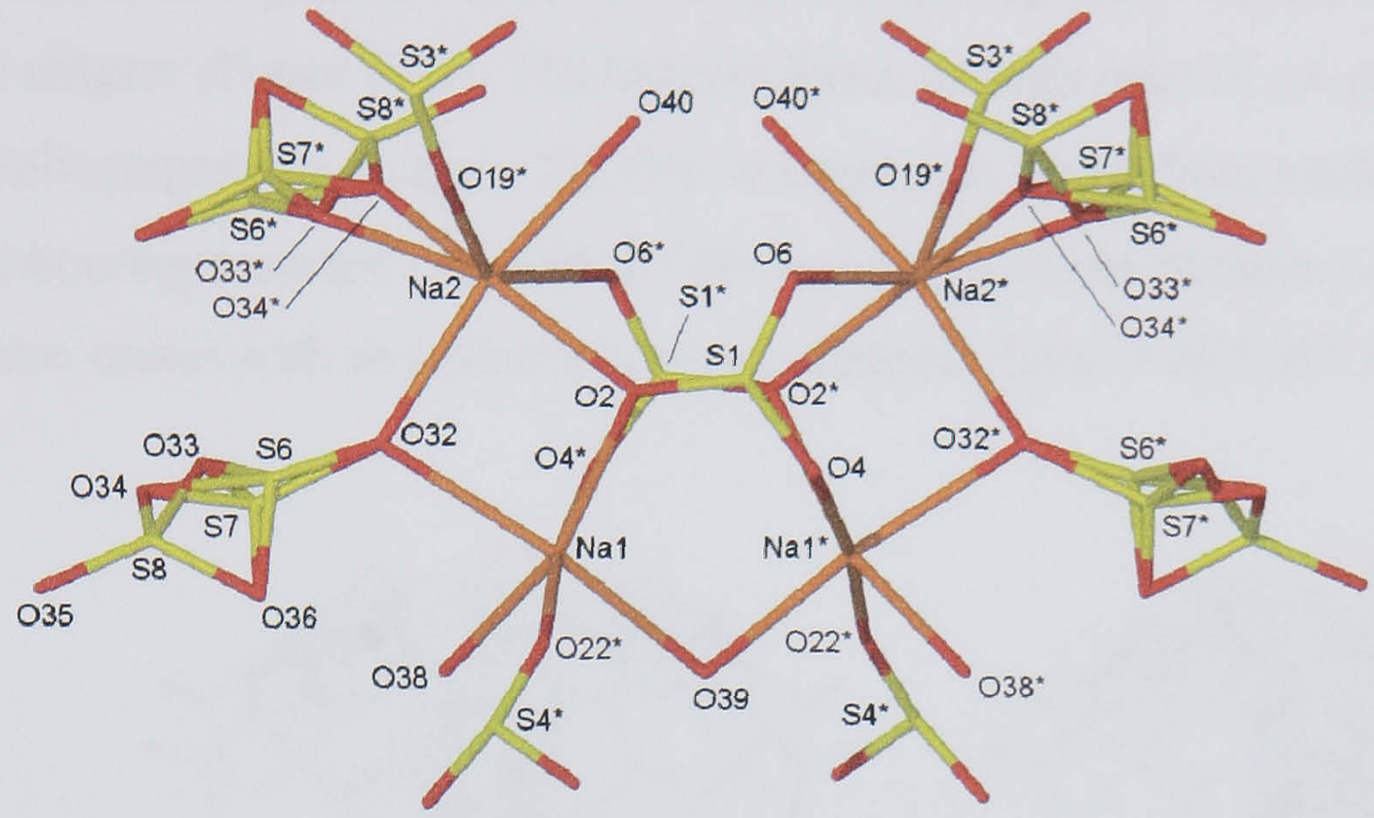

Figure 6.28 Local symmetry expansion of the sodium coordination spheres from the crystal structure of complex **6.7** showing the sodium tetramer that links neighbouring *p*-sulfonatocalix[5]arenes. Selected atoms have been labelled (* denotes a symmetry equivalent atom in relation to Figure 6.27). The disordered oxygen atoms of the calixarene S(5) sulfonate group and the sodium aquo ligands are shown in ball and stick representation.

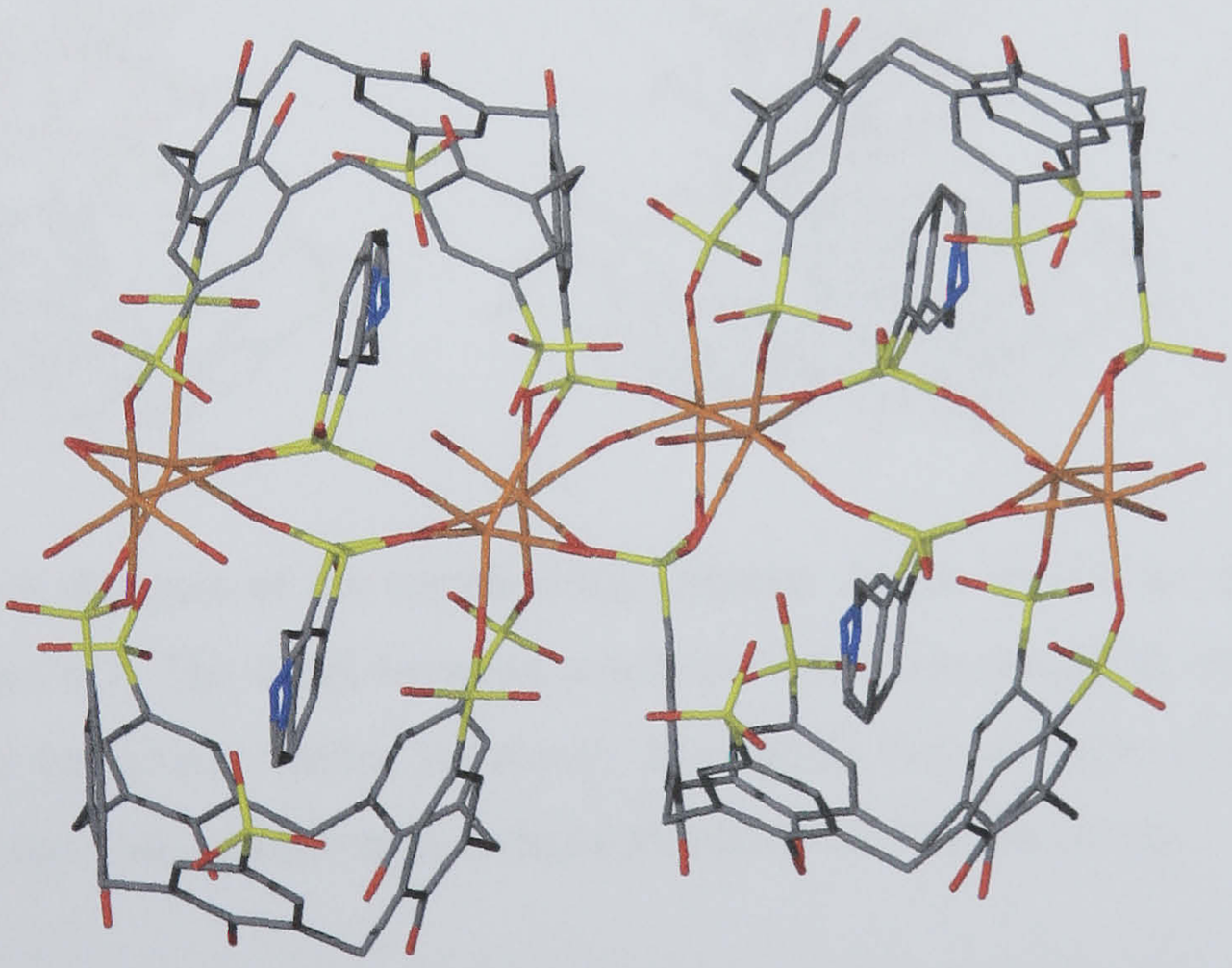

Figure 6.29 Stick representation of two adjacent molecular capsules from the extended crystal structure of complex **6.7**. The molecular capsules are linked by the central sodium tetramers shown in Figure 6.28. Disordered oxygen atoms of calixarene sulfonate groups, the $PySO_3$ and sodium aquo ligands have been omitted for clarity.

The extended structure also shows the calixarenes to assemble in coordination polymer chains that are based on a bi-layer arrangement similar to both previously reported examples and to complexes **6.1 – 6.5** of this chapter (Figure 6.29). The bi-layer forms through one CH···π and one π-stacking interaction (crystallographically unique). The CH···π interaction occurs from a calixarene methylene bridge to a neighbouring aromatic ring with a CH···aromatic centroid distance of 2.737 Å. The π-stacking interaction occurs with an aromatic centroid···centroid distance of 3.737 Å.

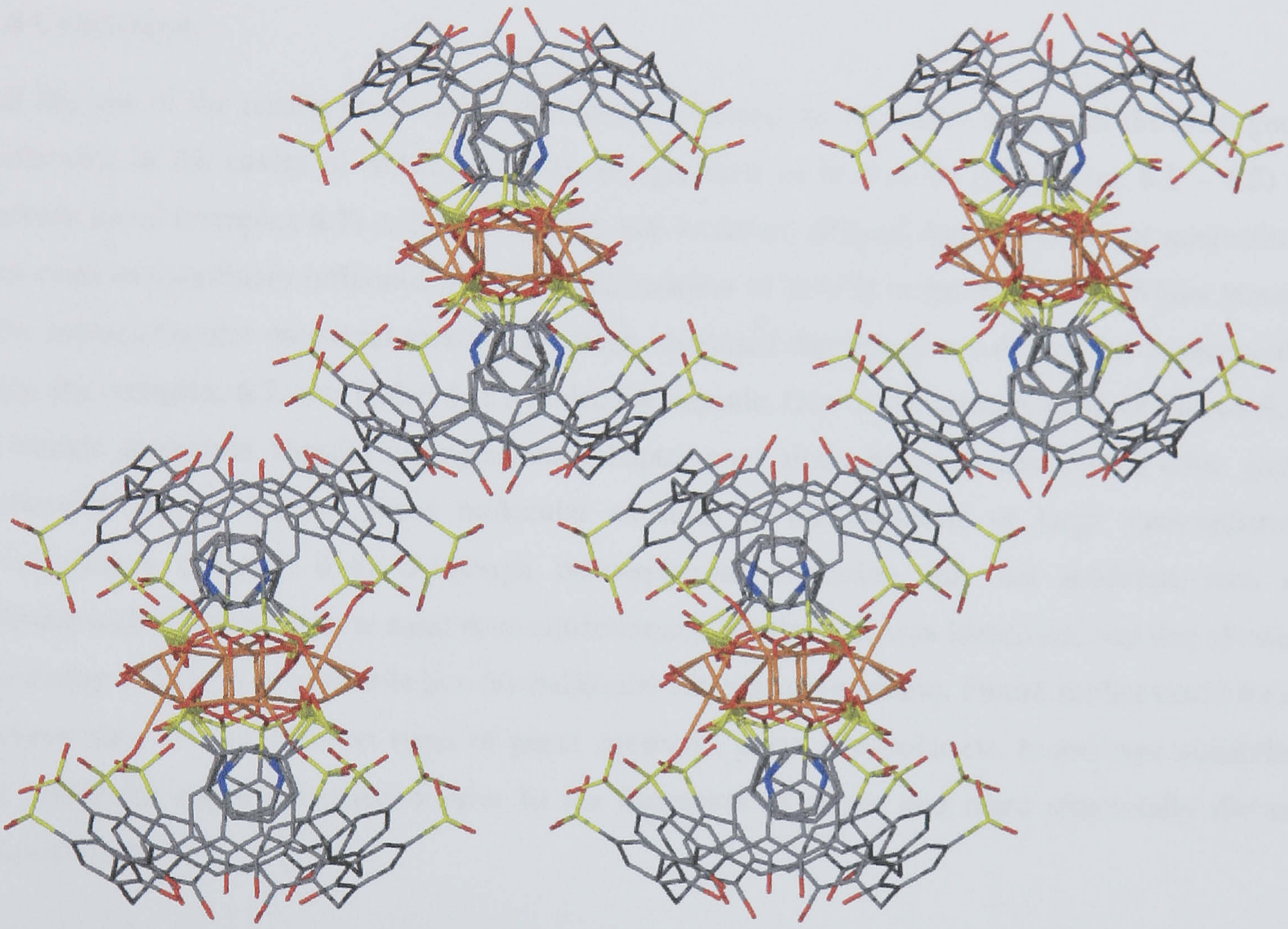

Figure 6.29 Packing diagram of the coordination polymer chains formed in the extended crystal structure of complex **6.7**. The voids between neighbouring chains are filled with disordered water molecules but these have been omitted for clarity. Disordered oxygen atoms of calixarene sulfonate groups, the $PySO_3$ and sodium aquo ligands have also been omitted for clarity.

6.3.2 Summary of alternative supramolecular structures incorporating *p*-sulfonatocalix-[5]arene.

Complex **6.6** shows that non-covalent interactions can exert extraordinary influence over the conformational properties of *p*-sulfonatocalix[5]arene in the solid state. Di-protonated DABCO molecules are clearly of perfect fit to the resultant partial cones that are generated by the

conformational distortion to the SO_3[5] host. The result of this is the formation of an unprecedented *bis*-molecular capsule arrangement in which two *p*-sulfonatocalix[5]arenes shroud two di-protonated DABCO molecules and two waters of crystallisation. Although double inclusion of small molecular species in a molecular capsule of SO_3[5] has been previously reported, perturbation of the solid state conformation through the formation of such influential non-covalent interactions is a new phenomenon. Indeed complex **6.7** is a typical example of multi-guest inclusion within a molecular capsule of SO_3[5] but there is no deviation from the typical solid state cone conformation for *p*-sulfonatocalix[5]arene. .

6.4 Conclusion.

All but one of the results presented in this chapter showed the inclusion of several different guest molecules in the cavity of SO_3[5] when in the presence of lanthanide (complexes **6.1** – **6.5**) or sodium metal (complex **6.7**) cations. Complex **6.6**, however, showed that non-covalent interactions can exert extraordinary influence over the conformation of SO_3[5] in the solid state. Whilst several new supramolecular structural motifs have been identified through X-ray diffraction experiments, only one complex, **6.7**, was isolated as a molecular capsule. One of the primary goals of this work is to isolate molecular capsule arrangements (chapter one: aims) based around crown ether guest molecules and to employ these molecular capsules in the synthesis of large nano-spheroid arrangements (chapter five). Although nano-spheroid formation was not achieved with *p*-sulfonatocalix[5]arene, a new solid state conformation for the host was identified, one that showed the ability of SO_3[5] to assemble in a *bis*-molecular capsule arrangement. Future studies could focus on screening several different types of guest, aromatic, polar, non-polar etc. to estimate suitability for molecular capsule formation prior to the formation of larger and more structurally diverse arrangements.

6.5 Experimental.

Penta-sodium *p*-sulfonatocalix[5]arene was synthesised by literature methods and purity was checked via ^{1}H NMR spectroscopy.[8] All guest molecules except 1-aza-18-crown-6 were synthesised by literature methods.[107] All other guest molecules and all lanthanide metal salts were purchased from Aldrich and used as supplied without further purification. X-ray data for complexes **6.1** – **6.3** and **6.5** – **6.8** were collected at 150(2) K on an Enraf-Nonius KappaCCD diffractometer with Mo-Kα radiation. X-ray data for complex **6.4** was collected using synchotron radiation at wavelength of 0.6894 Å. Data were corrected for Lorentz and polarisation effects and absorption corrections were applied using multi-scan techniques. The structures of complexes **6.1** and **6.4** – **6.8** were solved by direct methods using SHELXS-97 and refined with full-matrix least squares on F^2 using SHELXL-

97. The structures of complexes **6.2** and **6.3** were solved by direct methods using SHELXS-97 and refined with BLOC-matrix least squares on F^2 using SHELXL-97. Hydrogen atoms were placed at geometrically calculated positions in all complexes. Infrared spectra were run either as a KBr disc or as a solid phase on a MIDAC FT-IR or Perkin-Elmer Spectrum One spectrometer respectively. Microanalyses were not performed on crystals of complexes **6.1** – **6.7** as all showed visual degradation upon removal from the mother liquor.

Complex number	**6.1**	**6.2**
Formula	$C_{41}H_{79.50}EuNNaO_{41.25}S_5$	$C_{90}H_{120}Eu_2N_2NaO_{80}S_{10}$
Mr	1581.81	3157.39
Crystal system	Orthorhombic	Monoclinic
Space group	*Pbcn*	$P2_1/c$
T/K	150(2)	150(2)
a /Å	19.1391(3)	30.0333(4)
b /Å	21.8802(3)	19.4301(3)
c /Å	29.5140(5)	21.3461(7)
α /°	90	90
β /°	90	92.940(1)
γ /°	90	90
U Å^3	12359.5(3)	12440.1(5)
Z	8	4
F(000)	6532	6444
ρ_{calc} /g cm^{-3}	1.7	1.686
μ /cm^{-1}	1.298	1.286
$\Theta_{min,\ max}$ /°	2.42, 27.44	1.25, 22.22
Data collected	47652	77243
Unique data	13417	15039
R_{int}	0.0978	0.0998
Obs data ($I>2\ \sigma(I)$)	9296	11904
Parameters	924	1448
Restraints	0	0
R_1 (observed data)	0.068	0.1115
ωR_2 (all data)	0.2102	0.2792
S	1.032	1.168
Max/min residuals [eÅ^3]	1.876, -2.124	1.838, -2.644

Table 6.9 Details of data collection and structure refinement for complexes **6.1** and **6.2**.

6.5.1 Synthesis of the complex [((4-picoline *N*-oxide)⊂(*p*-sulfonatocalix[5]arene))$_2$ + 3H$^+$)(Na(H$_2$O)$_3$)][Eu(H$_2$O)$_9$]·9.75H$_2$O, 6.1.

Penta-sodium *p*-sulfonatocalix[5]arene (10 mg, 10 μmol), 4-picoline *N*-oxide (3 mg, 30 μmol) and europium(III) nitrate hexahydrate (5 mg, 10 μmol) were dissolved in distilled water (2 cm^3). Upon

slow evaporation, crystals that were suitable for X-ray diffraction studies formed. Yield 8 mg, 51 %. IR(solid phase, ν cm^{-1}): 3365s, 2926s, 1608m, 1583m, 1519m, 1472m, 1336s, 1160s, 1107s, 1043s. The minor changes in sulfonate group stretching frequencies suggests that the calixarene is non-coordinating, as was found in the crystal structure solution. **X-ray crystallography**: The oxygen atoms of the S(5) sulfonate group are disordered over two positions at equal occupancy. The oxygen atoms of the S(1) sulfonate group are disordered over three positions and are at partial occupancies of 0.2, 0.6 and 0.2. The oxygen atoms of the S(2) sulfonate group are disordered over two positions and are at partial occupancies of 0.7 and 0.3. Two europium aquo ligands were disordered over two positions at equal occupancy. Another europium aquo ligand is disordered over two positions with partial occupancies of 0.6 and 0.4. Residual electron density is located ~ 1 Å from the europium metal centre. Some water molecules of crystallisation were refined isotropically.

Complex number	**6.3**	**6.4**
Formula	$C_{94}H_{176}Eu_2N_4O_{93}S_{10}$	$C_{94}H_{157}Eu_2N_2Na_4O_{78.50}S_{10}$
*M*r	3474.91	3287.7
Crystal system	Monoclinic	Monoclinic
Space group	$P2_1/c$	$P2_1/c$
T/K	150(2)	115(2)
a /Å	31.7846(2)	28.6783(11)
b /Å	20.1234(2)	20.5174(9)
c /Å	22.5742(4)	22.1845(11)
α /°	90	90
β /°	96.6820(10)	95.954(1)
γ /°	90	90
U Å^3	14340.7(3)	12983.0(10)
Z	4	4
F(000)	7192	6772
ρ_{calc} /g cm^{-3}	1.609	1.682
μ /cm^{-1}	1.127	1.243
$\Theta_{min,\ max}$ /°	1.2, 22.71	1.53, 27.5
Data collected	109813	86872
Unique data	19182	32453
R_{int}	0.0901	0.0457
Obs data (I>2 $\sigma(I)$)	16379	26635
Parameters	1664	1792
Restraints	6	0
R_1 (observed data)	0.1407	0.0414
ωR_2 (all data)	0.3852	0.1217
S	3.02	1.016
Max/min residuals [eÅ^3]	10.404, -3.374	1.205, -1.396

Table 6.10 Details of data collection and structure refinement for complexes **6.3** and **6.4.**

6.5.2 Synthesis of the complex [((4,4'-dipyridine-*N,N'*-dioxide)⊂(*p*-sulfonatocalix[5]-arene))$_2$ + $4H^+$][$(Eu(H_2O)_9)_2$]·$17H_2O$, 6.2.

Penta-sodium *p*-sulfonatocalix[5]arene (10 mg, 10 μmol), 4,4'-dipyridine-*N,N'*-dioxide (6 mg, 30 μmol) and europium(III) nitrate hexahydrate (5 mg, 10 μmol) were dissolved in distilled water (2 cm^3). Upon slow evaporation, crystals that were suitable for X-ray diffraction studies formed. Yield 7 mg, 43 %. IR(solid phase disc, ν cm^{-1}): 3373s, 2879s, 1698m, 1610m, 1588m, 1514m, 1470m, 1338s, 1273m, 1162s, 1102s, 1042s, 1034s. The minor changes in sulfonate group stretching frequencies suggests that the calixarene is non-coordinating, as was found in the crystal structure solution. **X-ray crystallography**: One Eu(2) aquo ligand is disordered over two positions at equal occupancy. Residual electron density is located ~ 1 Å from the Eu(2) metal centre. For the 4,4'-dipyridine-*N,N'*-dioxide molecules, the U_{ij} values of three of the aromatic rings were constrained to be the same within each ring. The Eu(2) aquo ligands and some water molecules of crystallisation were refined isotropically.

6.5.3 Synthesis of the complex [[({4,13-diaza-18-crown-6 + 2H}.H_2O)⊂*p*-sulfonatocalix[5]-arene][$Eu(H_2O)_9$]]$_2$.$24H_2O$, 6.3.

Europium(III) nitrate hexahydrate (10 mg, 20 μmol) was added to an aqueous solution (1.5 cm^3) containing penta-sodium *p*-sulfonatocalix[5]arene (10 mg, 10 μmol) and diaza-18-crown-6 (5 mg, 20 μmol). 1M HCl was added drop-wise until the solution pH was < 1. Large colourless crystals grew upon standing over a period of ~ 2 hours. 18 mg, 51 %. IR (KBr disc, ν cm^{-1}); 3358s, 3100s, 2891s, 1650m, 1595m, 1450m, 1174s, 1122s, 1043s. The minor changes in sulfonate group stretching frequencies suggests that the calixarene is non-coordinating, as was found in the crystal structure solution. **X-ray crystallography**: Residual electron density is located ~ 1 Å from the Eu(1) metal centre and given the size of the maximum residual peak (10.404 e$Å^3$), energy dispersive X-ray analysis (EDX) was used to confirm the Eu:S ratio to be ~ 1:5 as expected. The oxygen atoms of the S(8) sulfonate group are disordered over two positions at partial occupancies of 0.8 and 0.2. The U_{ij} values of the oxygen atoms of the S(8) sulfonate group, the methylene bridging carbon atoms of the C(36)-C(70) SO_3[5] molecule, and the C(8)-C(13) aromatic ring of the C(1)-C(35) SO_3[5] molecule were all constrained to be the same within each particular group. Some disordered water molecules of crystallisation were refined isotropically. Some bond lengths were restrained to be chemically meaningful.

Complex number	**6.5**	**6.6**
Formula	$C_{45}H_{90.50}EuN_2O_{43.75}S_5$	$C_{50}H_{74.50}N_5O_{29.25}S_5$
Mr	1671.95	1373.95
Crystal system	Monoclinic	Triclinic
Space group	$P2_1/c$	$P\bar{1}$
T/K	150(2)	150(2)
a /Å	11.3620(4)	12.7511(2)
b /Å	19.9020(6)	15.9188(3)
c /Å	30.3716(12)	16.7800(4)
α /°	90	85.795(1)
β /°	96.627(2)	79.554(1)
γ /°	90	74.439(1)
U Å^3	6821.9(4)	3225.72(11)
Z	4	2
F(000)	3470	1447
ρ_{calc} /g cm^{-3}	1.628	1.415
μ /cm^{-1}	1.178	0.268
$\Theta_{min,\ max}$ /°	2.7, 23.59	2.66, 27.34
Data collected	12949	68394
Unique data	7561	14404
R_{int}	0.0689	0.0941
Obs data ($I>2\ \sigma(I)$)	5829	9211
Parameters	818	913
Restraints	0	14
R_1 (observed data)	0.0728	0.0977
ωR_2 (all data)	0.2162	0.2862
S	1.046	1.751
Max/min residuals [eÅ^3]	1.25, -0.973	1.955, -0.632

Table 6.11 Details of data collection and structure refinement for complexes **6.5** and **6.6**.

6.5.4 Synthesis of the coordination polymer [(Na⊂1-aza-18-crown-6)] [(Eu(H$_2$O)$_6$)(Na(H$_2$O)$_3$)(*p*-sulfonatocalix[5]arene)].10.5H$_2$O, 6.4.

Europium nitrate hexahydrate (10 mg, 20 μmol) was added to an aqueous solution (1.5 cm^3) containing penta-sodium *p*-sulfonatocalix[5]arene (10 mg, 10 μmol) and 1-aza-18-crown-6 (5 mg, 20 μmol). 1M HCl was added drop-wise until the solution pH was < 1. On standing over several days, small colourless crystals suitable for X-ray diffraction studies formed, 14 mg, 42 %. IR (KBr disc, υ cm-1); 3410s, 3132s, 2924s, 1647m, 1595m, 1473m, 1454m, 1161s, 1113s, 1097s, 1080s, 1047s. The increase in the number of sulfonate group stretching frequencies suggests metal/sulfonate coordination, as was found in the crystal structure solution. **X-ray crystallography**: Residual electron density is located ~ 1 Å from the Eu(1) metal centre. The oxygen atoms of the S(9) sulfonate group are disordered over two positions with partial occupancies of 0.45 and 0.55.

One Na(4) aquo ligand is disordered over two positions with partial occupancies of 0.8 and 0.2. Another Na(4) aquo ligand is disordered over three positions with partial occupancies of 0.3, 0.3 and 0.4. Two oxygen atoms of the S(7) sulfonate group are disordered over two positions with partial occupancies of 0.7 and 0.3.

Complex number	**6.7**
Formula	$C_{40}H_{55.67}N_1Na_2O_{35.83}S_6$
*M*r	1362.19
Crystal system	Monoclinic
Space group	*C*2/*c*
T/K	150(2)
a /Å	30.8338(7)
b /Å	19.2303(6)
c /Å	21.7518(6)
α /°	90
β /°	101.206(2)
γ /°	90
U Å^3	12651.7(6)
Z	8
F(000)	5659
ρ_{calc} /g cm^{-3}	1.43
μ /cm^{-1}	0.323
$\Theta_{min,\ max}$ /°	2.51, 27.49
Data collected	41122
Unique data	13768
R_{int}	0.1655
Obs data (I>2 $\sigma(I)$)	8159
Parameters	828
Restraints	5
R_1 (observed data)	0.1277
ωR_2 (all data)	0.3583
S	1.871
Max/min residuals [eÅ^3]	1.111, -0.892

Table 6.12 Details of data collection and structure refinement for complex **6.7**.

6.5.5 Synthesis of the complex [[(1,7-diaza-15-crown-5 + 2H)⊂*p*-sulfonatocalix[5]-arene][Eu(H$_2$O)$_9$]]$_2$.11.75H$_2$O, 6.5.

Europium nitrate hexahydrate (10 mg, 20 μmol) was added to an aqueous solution (1.5 cm^3) containing penta-sodium *p*-sulfonatocalix[5]arene (10 mg, 10 μmol) and 1,7-diaza-15-crown-8 (5 mg, 20 μmol). 1M HCl was added drop-wise until the solution pH was < 1. On standing over thirty minutes colourless crystals suitable for X-ray diffraction studies formed, 14 mg, 42 %. IR (KBr disc, υ cm-1); 326s, 2879s, 2368m, 1653m, 1591m, 1467m, 1448m, 1421m, 1209s, 1114s, 1041s.

The minor changes in sulfonate group stretching frequencies suggests that the calixarene is non-coordinating, as was found in the crystal structure solution. **X-ray crystallography**: Residual electron density is associated with disordered water molecules of crystallisation. Some water molecules of crystallisation were refined isotropically.

6.5.6 Synthesis of the complex *bis*-molecular capsule [{(DABCO + 2 H^+)(H_2O)}⊂(*p*-sulfonatocalix[5]arene + H^+)][(DABCO + 2 H^+)$_{1.5}$]·9.25H_2O, 6.6.

A solution containing penta-sodium *p*-sulfonatocalix[5]arene (10 mg, 9.6 μmol) and DABCO (5 mg, 45 μmol) was acidified using 1M hydrochloric acid until the pH < 1. Over two days large prismatic colourless crystals that were suitable for X-ray diffraction studies formed. Yield 8 mg, 66%. ^{1}H NMR (D_2O) δ = 7.58 (s, 10H, Ar**H**), 3.93 (s, 10H, ArC**H**$_2$), 3.48 (s, 30H, NC**H**$_2$). IR(KBr disc, ν cm^{-1}): 3402s, 2930s, 2594s, 2336m, 1635m, 1589m, 1469s, 1421s, 1387s, 1178s, 1107s, 1043s. The minor changes in sulfonate group stretching frequencies suggests that the calixarene is non-coordinating, as was found in the crystal structure solution. **X-ray crystallography**: Residual electron density is associated with an ethyl arm of the disordered N(1)/N(2) DABCO molecule. One ethyl arm of the N(5)/N(6) DABCO molecule is disordered over two positions at equal occupancy and the disordered atoms were refined isotropically. One DABCO molecule is disordered over two positions (N(1)/N(2) and N(7)/N(9)) with partial occupancies of 0.75 and 0.25 (respectively). One half DABCO molecule (N(3)/N(4)) is disordered over two positions at equal occupancy and the U_{ij} values of the carbon atoms were constrained to be the same. The N(1)/N(2) and N(7)/N(9) DABCO molecules and some water molecules of crystallisation were refined isotropically. Some bond lengths were restrained to be chemically meaningful.

6.5.7 Synthesis of the coordination polymer [(3-pyridinium sulfonate·H_2O)(Na_2(H_2O)$_{2.5}$)(*p*-sulfonatocalix[5]arene)]·9.833H_2O, 6.7.

Penta-sodium *p*-sulfonatocalix[5]arene (10 mg, 9.6 μmol) and 3-pyridine sulfonic acid (7 mg, 45 μmol) was acidified using 1M hydrochloric acid until the pH < 1. Upon slow evaporation over several days, large colourless crystals that were suitable for X-ray diffraction studies formed. Yield 7 mg, 54 %. **X-ray crystallography**: Residual electron density is associated with disordered water molecules of crystallisation. The oxygen atoms of the S(3) sulfonate group are disordered over three positions with partial occupancies of 0.6, 0.2 and 0.2. Two oxygen atoms of the S(5) sulfonate group are disordered over two positions with partial occupancies of 0.8 and 0.2 as are all of the oxygen atoms of the S(1) sulfonate group. The aromatic ring of the $PySO_3$ molecule is d isordered

over two positions with partial occupancies of 0.6 and 0.4 whilst the sulfonate group of the $PySO_3$ is disordered over three positions with partial occupancies of 0.6, 0.2 and 0.2. Sodium aquo ligands and some water molecules of crystallisation were refined isotropically. Some bond lengths were restrained to be chemically meaningful.

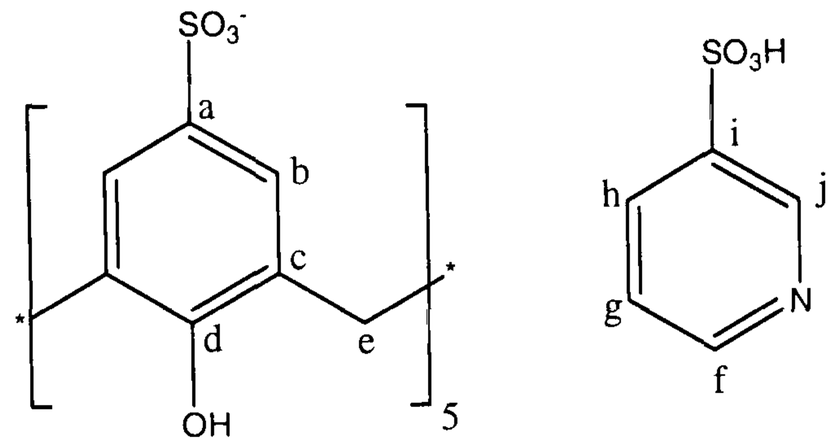

^{1}H NMR (250 MHz, D_2O) δ = 9.21 (s, 1H, C_jH), 8.21 (d, 1H, C_hH or C_fH), 8.20 (d, 1H, C_hH or C_fH), 8.03 (dd, 1H, C_gH), 7.35, (s, 10H, C_bH), 3.62 (s, 10H, C_eH). ^{13}C NMR (D_2O) δ = 153.3, 144.0, 143.8, 143.4, 139.7, 135.8, 128.3, 126.8, 31.1.

Chapter Seven:

Supramolecular assemblies of the *p*-sulfonatocalix[6,8]arenes.

7.0 Introduction.

This chapter is composed of five sections and is focussed on developing the solid state supramolecular chemistry of the *p*-sulfonatocalix[6,8]arenes via the use of suitable guest molecules (Figure 7.1) and various metal counterions. The first four sections are focussed on *p*-sulfonatocalix[6]arene whilst the last section describes some related supramolecular chemistry with SO_3[8]. Very little progress has been made in the solid state supramolecular chemistry of *p*-sulfonatocalix[6]arene for over a decade and at that time Atwood *et al.* reported the structures of both the octa-sodium salt and sulfonic acid of SO_3[6].[69] These structures showed the calixarene to adopt 'double partial cone' conformation with three sulfonate groups pointing up and three down. More recent work by Asfari *et al.* reported the structures of alkali metal salts of SO_3[6] and showed the calixarene to act as a poly-hapto aromatic ligand for rubidium and caesium metal centres.[144] One other related structure was published by Castro et al. and reported the formation of a cobalt sepulchrate complex with *O*-methylated SO_3[6]. In that structure the calixarene adopted 'near-double cone' conformation ('double cone' has all sulfonate groups pointing upwards) although one aromatic sulfonate fragment was inverted.[145] These structures show that SO_3[6] is inherently flexible and conformational control may be difficult. Notably there have been no structures reported to date that have incorporated *p*-sulfonatocalix[8]arene as a supramolecular building block.

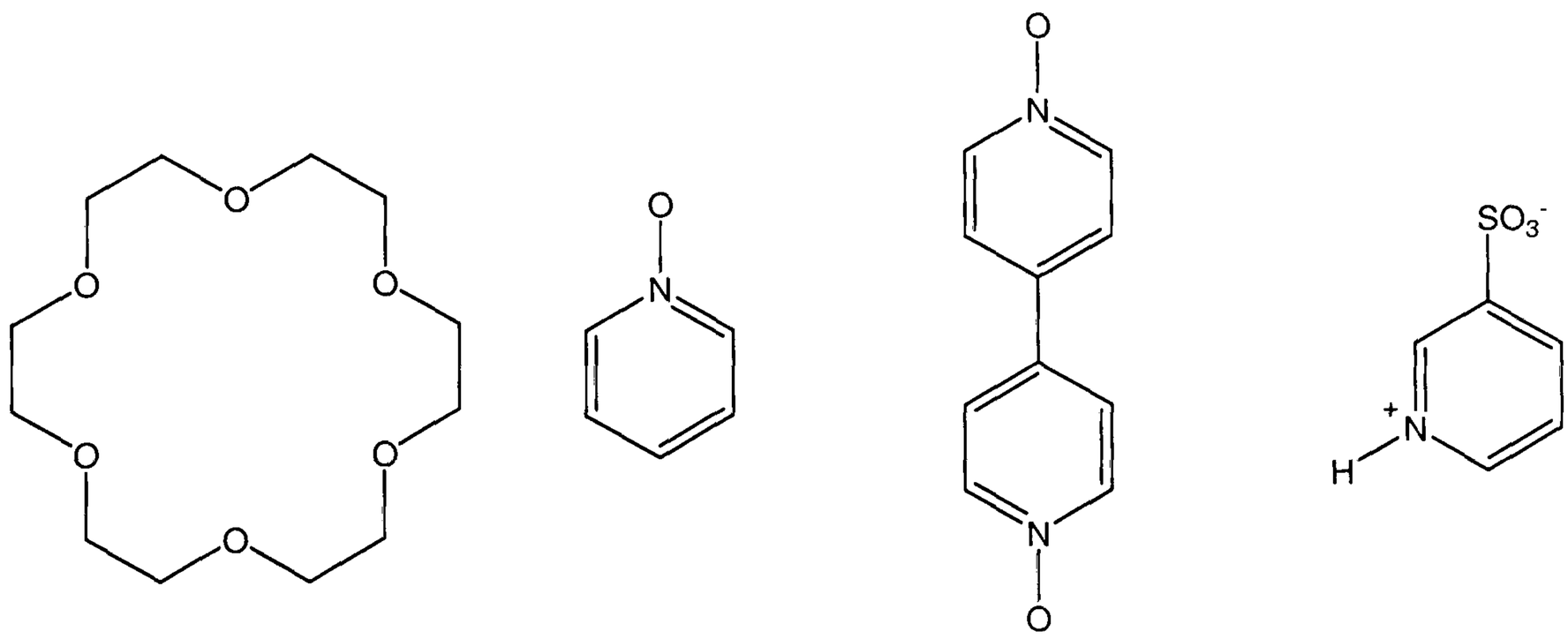

18-crown-6 pyridine *N*-oxide 4,4'-dipyridine-*N,N'*-dioxide 3-pyridine sulfonic acid

Figure 7.1 Guest molecules selected for lanthanide complex formation with *p*-sulfonatocalix[6]arene.

The first section of this chapter shows that the formation of lanthanide crown ether complexes can be used to control the conformation of SO_3[6] in the solid state. These structures all employ 18-crown-6 as a guest molecule with different lanthanide metal cations and the calixarene is found to adopt the previously unseen 'double cone' conformation under certain conditions. The second section of this chapter focuses on solid state formation of amino acid complexes of SO_3[6]. Although solution studies have been reported by others on such systems, the first SO_3[6]/amino acid complex is described ($_L$-leucine).[55, 56, 58] The complex shows not only amino acid complexation but also that the calixarene is also capable of selectively crystallising the $_L$- or $_D$-isomers from a racemic mixture. The third section focuses primarily on lanthanide and pyridine *N*-oxide (or 4,4'-dipyridine-*N,N'*-dioxide) complexes of *p*-sulfonatocalix[6]arene that were investigated and resulted in the discovery of some interesting new supramolecular architectures either as host-guest complexes or coordination polymers. A nickel/PyNO/SO_3[6] bi-layer complex that resulted from investigation into related transition metal chemistry is also described. The fourth section shows an alternative, multifaceted and interesting structure formed with 3-pyridine sulfonic acid ($PySO_3$) and Na_8SO_3[6] in which poly-aquo sodium hexamers assemble in hexagonally packed sheets. Finally, this chapter describes the formation of a complex 3-D coordination polymer incorporating *p*-sulfonatocalix[8]arene, 4,4'-dipyridine-*N,N'*-dioxide and lanthanide metals as the first structural authentication of SO_3[8].

As shown in both previous chapters of this thesis and much of the literature relating to the structural chemistry of *p*-sulfonatocalix[4]arene, the molecule adopts a truncated cone shape in the solid state and typically packs in bi-layer arrangements. Under certain circumstances, this bi-layer formation with SO_3[4] can be circumvented and spheroidal or tubular arrangements are formed instead (chapter five). The structures described in this chapter show that SO_3[6] is capable of packing in at least four different ways, either as bi-layers, helical chains, end-to-end chains or corrugated bi-layers and that SO_3[8] packs in a pleated loop conformation. Once the supramolecular coordination and host-guest chemistry is better understood, it may be possible not only to control the conformation of the *p*-sulfonatocalix[6,8]arenes with many different guest molecules (as is possible for SO_3[4]), but also to assemble the hosts in spheroidal Platonic or Archimedean arrangements or variations thereof when the calixarenes can act as a two (or more – SO_3[8]) vertex species. For clarity, waters of crystallisation have been omitted from the majority of diagrams unless included for particular purpose.

7.1 Controlling the conformation and interplay of *p*-sulfonatocalix[6]arene as lanthanide crown ether complexes.

When varied stoichiometric ratios of SO_3[6]/18-crown-6/Ln(III)Cl_3 are employed, a level of conformational control over *p*-sulfonatocalix[6]arene is achievable. A 1:4:5.5 mixture of the reactants (where Ln^{3+} = Tb, Tm) results in the formation of an unprecedented *bis*-molecular capsule that shows the calixarene to adopt the unseen 'double cone' conformation. The capsule contains two 18-crown-6 molecules and each calixarene has one hepta-aqua metal centre bound through a sulfonate group. There are two additional homoleptic octa-aqua metal cations that reside at the periphery of the capsule providing overall charge balance. When a 1:3:4.5 mixture of reactants (where Ln^{3+} = Nd, Eu) is employed, a new Ferris wheel arrangement is formed also with the calixarene in the 'double cone' conformation. One *bis*-aqua metal centre is bound within an 18-crown-6 macrocyle and is coordinated to the calixarene through a sulfonate group. Another hepta-aqua metal centre is coordinated to another sulfonate group of the calixarene to provide the overall charge balance. Finally, when a 1:8:3.5 mixture of reactants (where Ln^{3+} = Eu, Tb) is employed, the calixarene adopts the 'double partial cone' conformation and an 18-crown-6 molecule resides in each partial cone. Nona-aqua metal cations hydrogen bond to oxygen donor atoms of the crown ether macrocycles (amongst others) whilst also providing overall charge balance.

7.1.1 Structure of the *bis*-molecular capsule [{(H_2O⊂18-crown-6)·2H_2O}$_2$⊂[{(Tb(H_2O)$_8$(*p*-sulfonatocalix[6]arene)}$_2$][Tb(H_2O)$_8$]$_2$]·23.5H_2O, 7.1.

Crystals of the complex [{(H_2O⊂18-crown-6)·2H_2O}$_2$⊂[{(Tb(H_2O)$_7$(*p*-sulfonatocalix[6]arene)}$_2$][Tb(H_2O)$_8$]$_2$]·23.5H_2O, **7.1**, grew upon standing over three days from an aqueous solution containing a 1:4:5.5 mixture of SO_3H[6], 18-crown-6 and anhydrous terbium(III) chloride (Equation 7.1). The complex was characterised by IR spectroscopy and single crystal X-ray crystallography. Complex **7.1** crystallises in a monoclinic cell and the structural solution was performed in the space group $P2_1/n$.

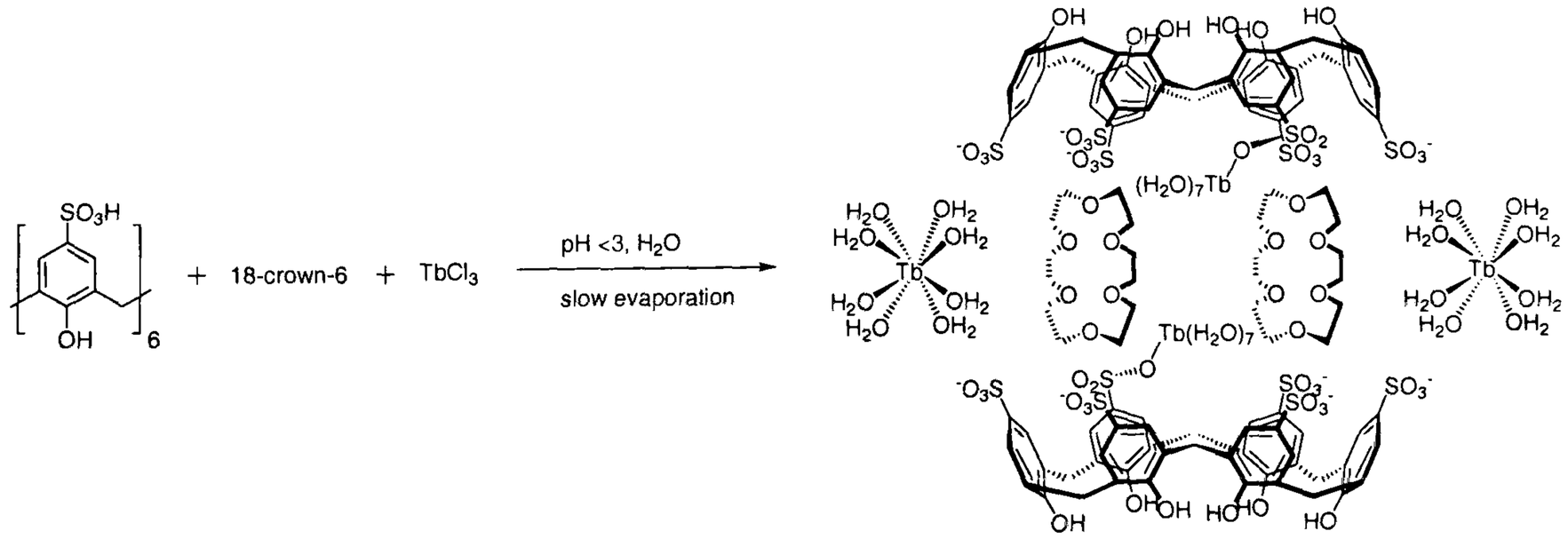

(7.1)

The isostructural complex with Tm^{3+} in place of Tb^{3+} was synthesised and characterised by single crystal unit cell determination, however only the Tb^{3+} complex will be discussed in any detail (unit cell parameters for isostructural complex are listed in the experimental section for complex **7.1**). Details of data collection and structure refinement are given in Table 7.16 of this chapter. A crystallographic information file containing all bond lengths and angles for complex **7.1** can be found in appendix 7.1.1 on the attached compact disc.

The asymmetric unit consists of one half of the *bis*-molecular capsule arrangement and this includes a hepta-aqua terbium/*p*-sulfonatocalix[6]arene moiety, an 18-crown-6 molecule and an octa-aqua terbium cation (Figure 7.2). In addition to this, there are a total of three crystallographically unique waters of crystallisation within the semi-capsular arrangement that are disordered over a total of seven positions. There are also twenty three and a half waters of crystallisation on the exterior of the capsule that are disordered over a total of thirty five positions. The most striking feature of the structure is that the SO_3[6] molecule of the asymmetric unit is in the previously unseen 'double cone' conformation (Figure 7.3).

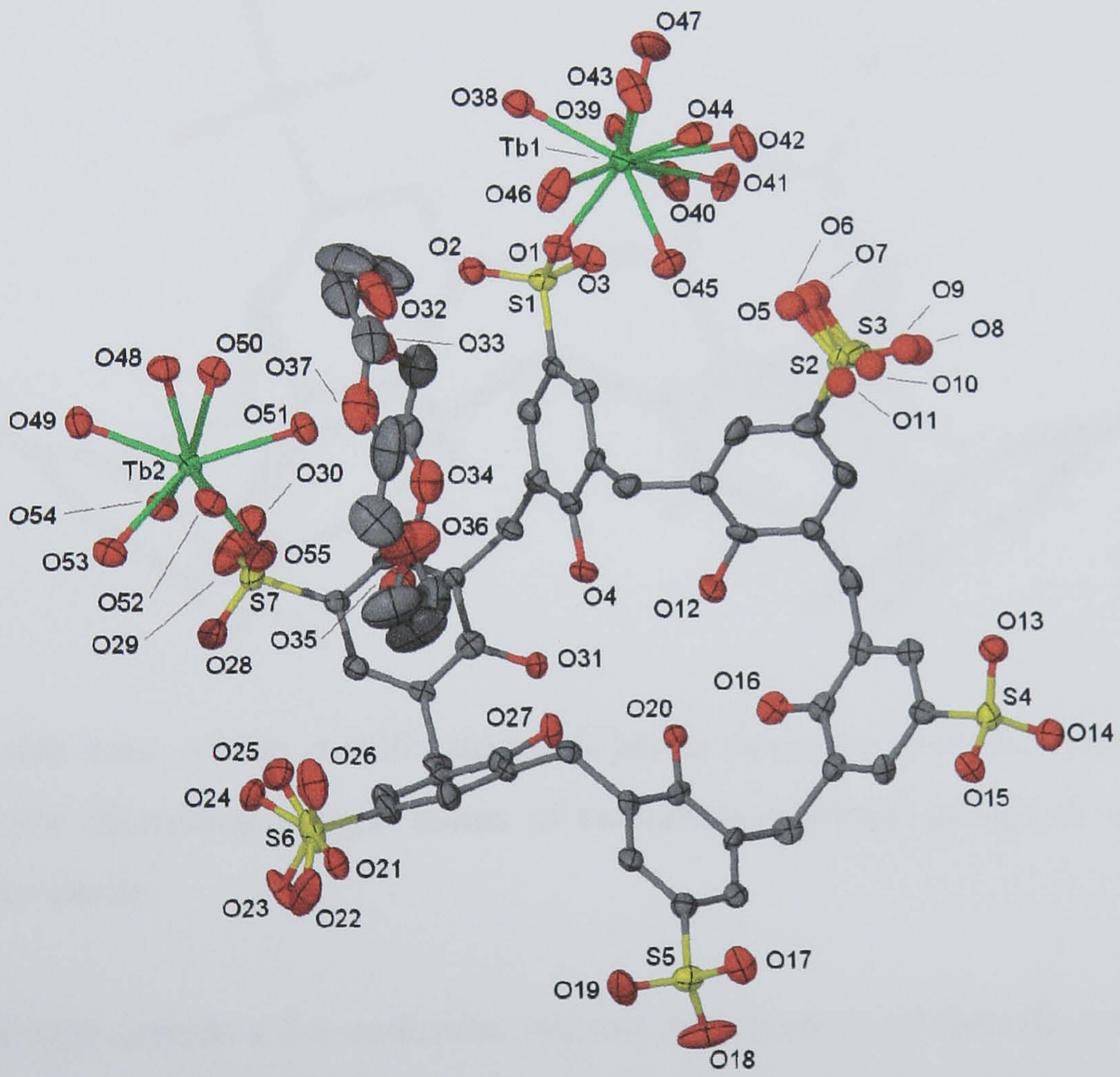

Figure 7.2 Part of the asymmetric unit from the crystal structure of complex **7.1**, anisotropic displacement ellipsoids shown at the 50% probability level. Some sulfonate oxygen atoms were refined isotropically and are shown in ball and stick representation. Selected atoms have been labelled (disordered water molecules within the capsule omitted for clarity).

Although this conformation has been documented for *p*-tert-butyl calix[6]arene, *p*-sulfonatocalix[6]arene has never been structurally characterised in this conformation to date.[9] The SO_3[6] is seen to pinch in a near C_2-symmetric fashion and a hydrogen bonding regime is evident between the six calixarene base hydroxyl groups (O(4), O(12), O(16), O(20), O(27) and O(31), six O···O distances ranging from 2.638 – 2.795 Å) (Figure 7.2). This hydrogen bonding likely stabilises the double cone conformation and is similar to that found in many structures of SO_3[4] when in the cone or pinched cone conformations.[34, 35] The terbium metal centre that is bound to the calixarene has eight aquo ligands, three of which are disordered over two positions each (Figure 7.2). Although the Tb – O bond lengths are of a typical magnitude, disorder makes it difficult to observe tri-capped trigonal prismatic geometry for the metal centre as would be expected for a nine-coordinate lanthanide species (Table 7.1).[105] The second terbium cation has eight aquo ligands, is not coordinated to the calixarene and has square anti-prismatic geometry. Bond distances relating to the coordination spheres of both terbium metal centres are listed in Table 7.1.

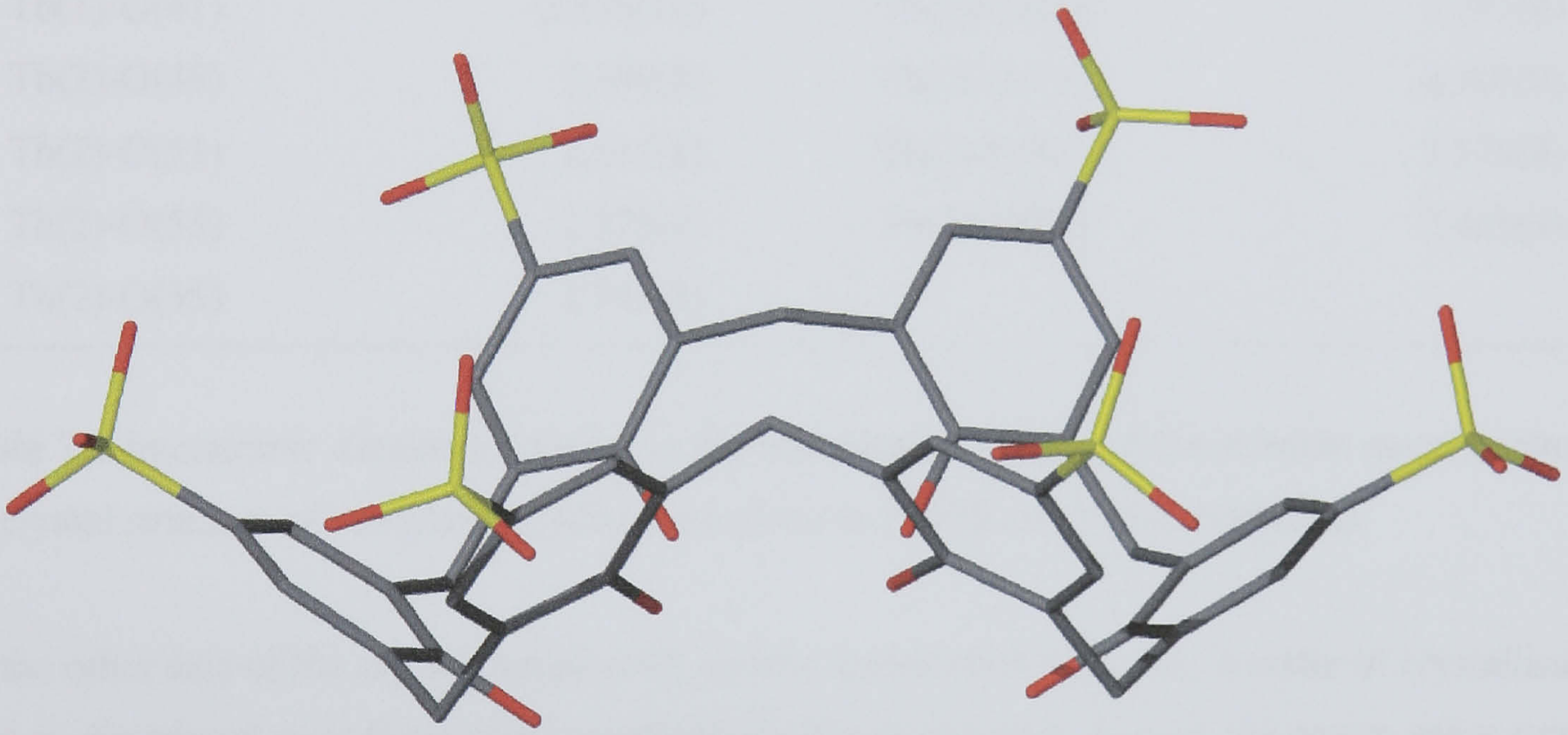

Figure 7.3 A side view of the *p*-sulfonatocalix[6]arene molecule from the crystal structure of complex **7.1**, some disordered oxygen atoms of calixarene sulfonate groups as well as all other atoms omitted for clarity.

Symmetry expansion reveals a *bis*-molecular capsule arrangement of two 18-crown-6 molecules shrouded by two Tb/*p*-sulfonatocalix[6]arene moieties and two homoleptic terbium cations. Examination of the *bis*-molecular capsule as a whole reveals several intricate hydrogen bonding systems inside and around the periphery of the arrangement (Figure 7.4a). One of the aquo ligands of the Tb(1) cation hydrogen bonds to an oxygen atom of the closest sulfonate group of the same SO_3[6] molecule (Tb(1)-O(45)···O(7)-S(3) distance of 2.962 Å, not shown in Figure 7.4a). Three

aquo ligands of the homoleptic terbium cation (Tb(2)) hydrogen bond to oxygen atoms of sulfonate groups (Tb(2)-O(48)···O(15)-S(4), Tb(2)-O(52)···O(13)-S(4), and Tb(2)-O(54)···O(30)-S(7) distances of 2.782, 2.704 and 2.790 Å respectively, Figure 7.4a). Two aquo ligands of the same metal centre also hydrogen bond to the donor atoms of the crown ether macrocycle. One aquo ligand, O(51), hydrogen bonds to two donor atoms with Tb(2)-O(51)···O(33) and Tb(2)-O(51)···O(37) distances of 2.818 and 2.873 Å respectively (Figure 7.4a). The other aquo ligand, O(51), hydrogen bonds to one of the crown ether donor atoms with a Tb(2)-O(55)···O(35) distance of 2.758 Å.

Tb(1)-O(1)	2.384(8)	Tb(1)-O(38)	2.371(9)
Tb(1)-O(39)	2.495(16)	Tb(1)-O(40)	2.333(19)
Tb(1)-O(41)	2.373(16)	Tb(1)-O(42)	2.436(18)
Tb(1)-O(43)	2.457(18)	Tb(1)-O(44)	2.350(17)
Tb(1)-O(45)	2.436(9)	Tb(1)-O(46)	2.382(9)
Tb(1)-O(47)	2.376(10)	Tb(2)-O(48)	2.395(8)
Tb(2)-O(49)	2.380(8)	Tb(2)-O(50)	2.399(8)
Tb(2)-O(51)	2.417(8)	Tb(2)-O(52)	2.370(8)
Tb(2)-O(53)	2.370(9)	Tb(2)-O(54)	2.409(8)
Tb(2)-O(55)	2.343(8)		

Table 7.1 Interatomic distances relating to the coordination sphere of the terbium metal centres in the crystal structure of complex **7.1** (distances given in Å with e.s.d. in parentheses).

On the other side of the crystallographically unique crown ether molecule, a water of crystallisation (that is disordered over three close positions) hydrogen bonds to two of the crown ether oxygen donor atoms. A centroid generated between the three oxygen positions results in O(centroid)···O(34) and O(centroid)···O(36) distances of 2.887 and 2.881 Å respectively (Figure 7.4a). Other disordered waters of crystallisation within the capsule are within hydrogen bonding distances of these molecules and a possible hydrogen bonded link between crown ether molecules can be constructed (a total of three O(centroid)···O and O···O distances ranging from 2.694 to 3.074 Å, Figure 7.4a). The pinching of the SO_3[6] mentioned earlier results in the 'double cone' conformation with two effective pseudo-calix[3]arenes. The crown ethers fit snugly within these resultant cavities as shown in Figure 7.4b. Given that the calixarene has been shown to adopt a new conformation, the packing is as expected very different to that found for the octa-sodium salt of SO_3[6].[69]

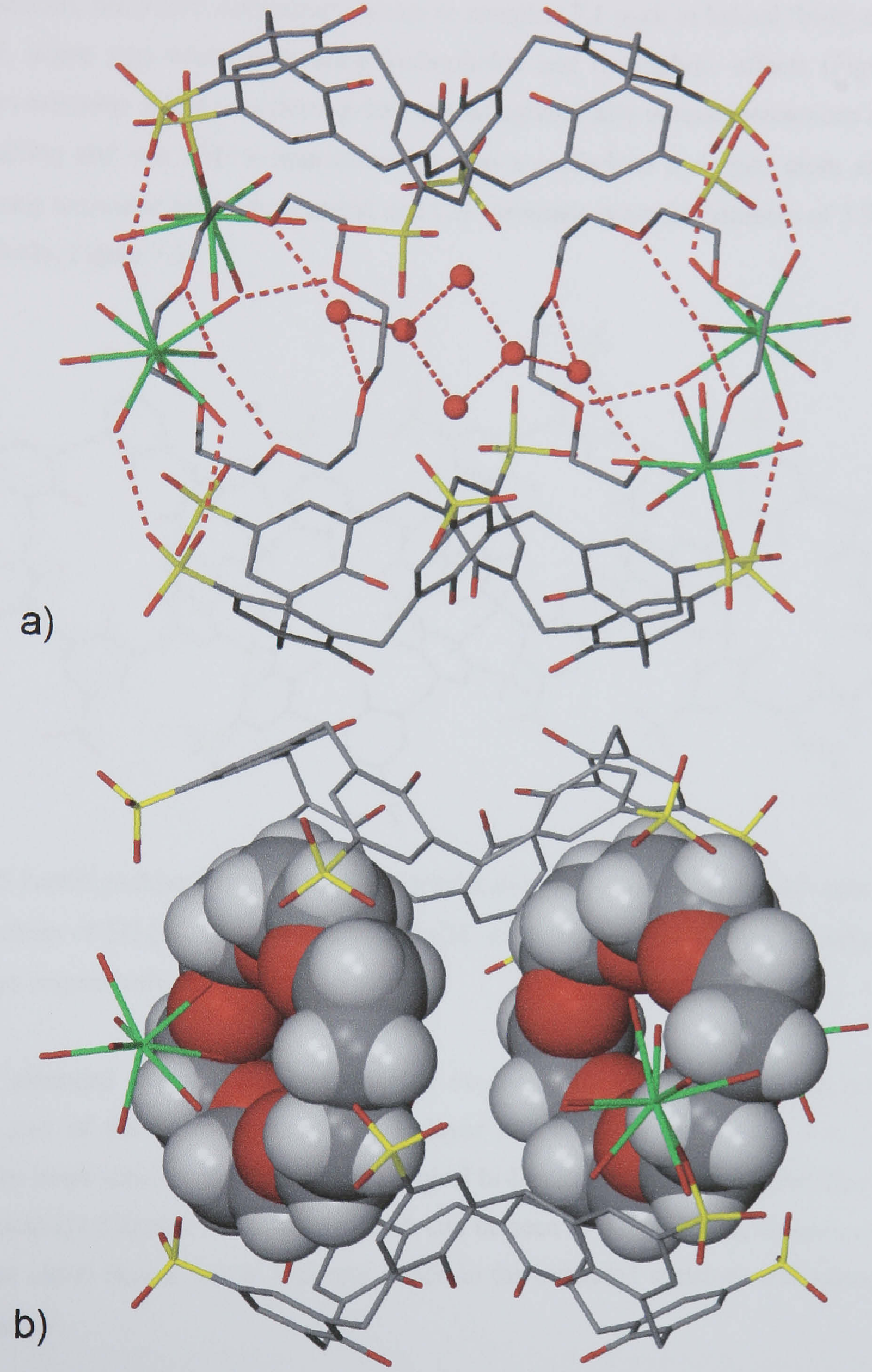

Figure 7.4 The *bis*-molecular capsule arrangement from the crystal structure of complex **7.1**. a) The capsule is skewed slightly to show the hydrogen bonding regimes within and around the periphery of the capsule (inner capsule water molecules shown in ball representation). b) A space filling representation to the arrangement showing the 'snug fit' of the pseudo-calix[3]arene cavities to the 18-crown-6 molecules.

When examined, the *p*-sulfonatocalix[6]arenes in complex **7.1** pack in helical 'bi-layer like' chains along a 2_1 screw axis whilst optimising hydrophobic and hydrophilic effects (Figure 7.5). The calixarenes assemble in this way through two crystallographically unique interactions in the form of one π-stacking and one CH···π interaction between a methylene hydrogen atom and an SO_3[6] aromatic ring (aromatic centroid···centroid and CH···aromatic centroid distances of 3.952 and 2.641 Å respectively, Figure 7.5).

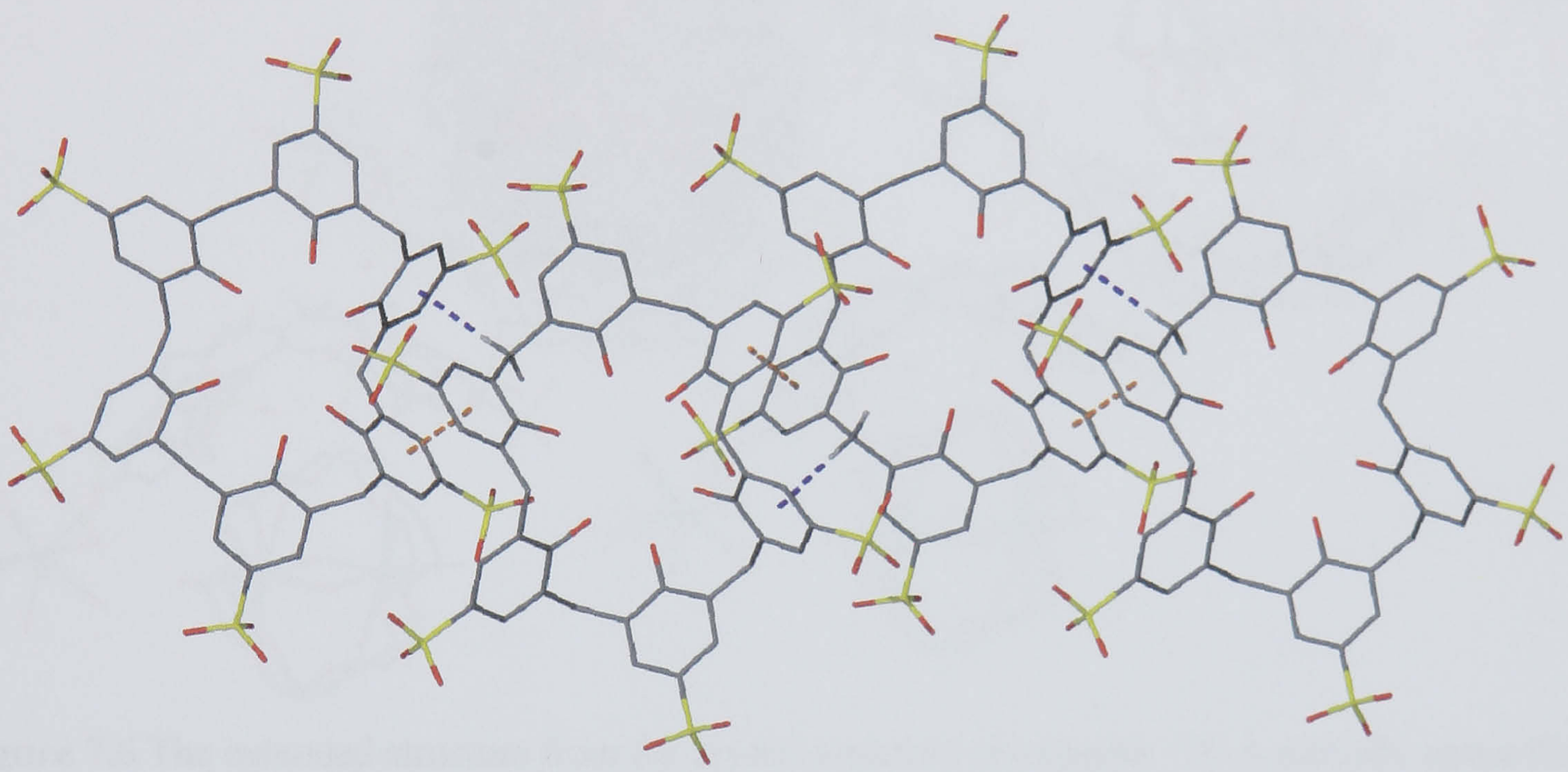

Figure 7.5 Partial packing diagram from the crystal structure of complex **7.1** showing a helical bi-layer like chain of SO_3[6]. The π-stacking and CH···π interactions are shown as orange and purple dashed lines respectively.

When the extended structure is examined, the *bis*-molecular capsules are found to pack as an integrated part of the helical chains, in a bi-layer like arrangement (Figure 7.6). This type of arrangement bears some resemblance to the typical bi-layer motifs found in solid state structure of *p*-sulfonatocalix[4,5]arenes examples of which can be seen in the preceding chapters of this thesis. Notably the chiral chains run in different hands in the extended structure and hence there is no overall chirality.

Complex 7.1 resulted from a 1:4:5.5 mixture of SO_3H[6], 18-crown-6 and anhydrous lanthanide(III) chloride (where Ln^{3+} = Tb, Tm). When a 1:3:4.5 mixture of the same reactants (except Ln^{3+} = Nd, Eu) is employed, a new complex results that shows the calixarene to adopt the cone conformation, and to bear host to a Ferris wheel type arrangement with a lanthanide cation and the 18-crown-6.

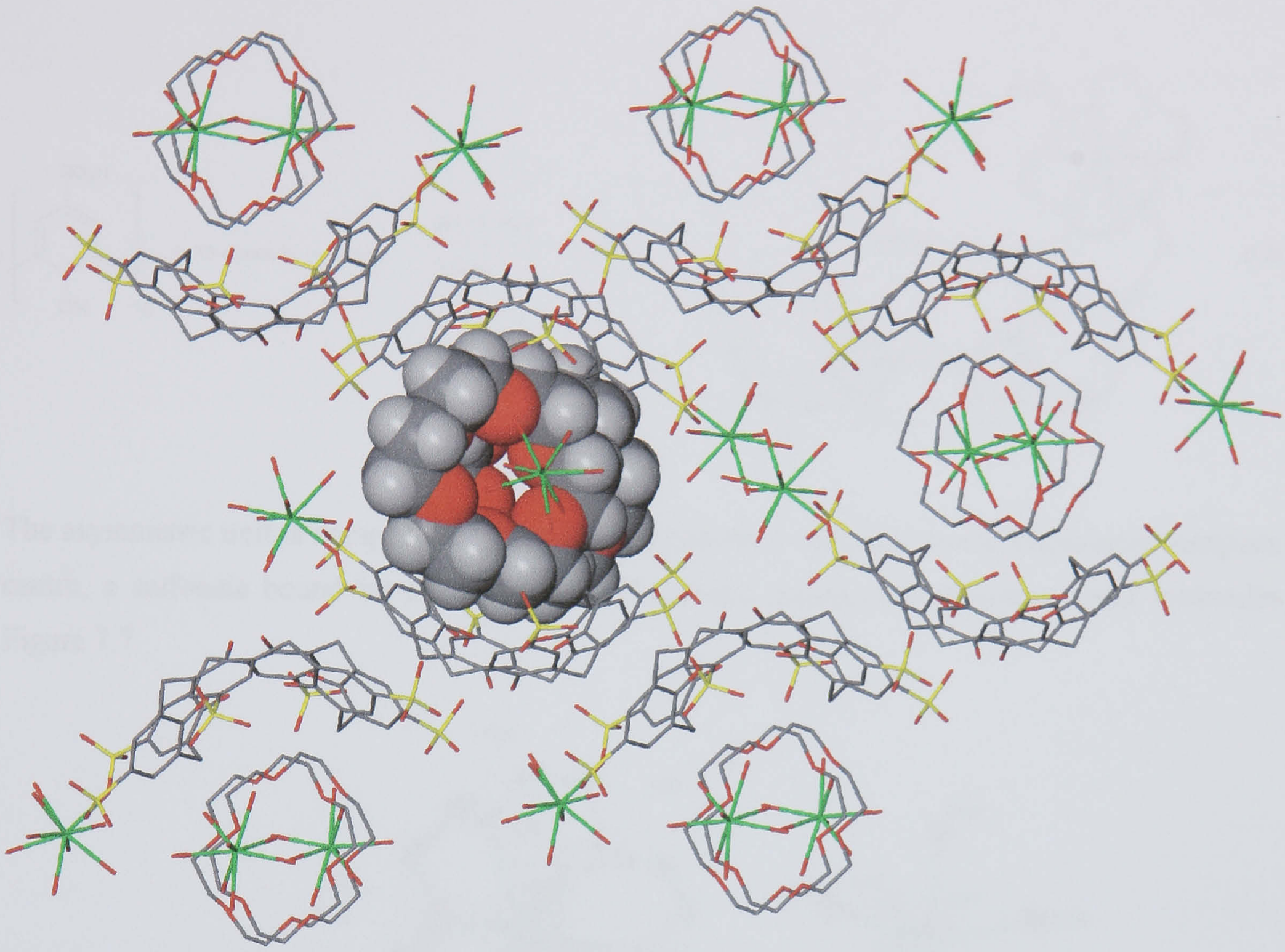

Figure 7.6 The extended structure from the crystal structure of complex **7.1**. A partially space filled *bis*-molecular capsule is shown whilst others are shown in stick representation. The helical bi-layer like chains (shown in Figure 7.3) run across the plane of the page.

7.1.2 Structure of the Ferris wheel arrangement [(Eu(H$_2$O)$_2$⊂18-crown-6)∩(*p*-sulfonatocalix[6]arene)(Eu(H$_2$O)$_7$]·17H$_2$O, 7.2.

Crystals of the complex [(Eu(H$_2$O)$_2$⊂18-crown-6)∩(*p*-sulfonatocalix[6]arene)(Tb(H$_2$O)$_7$]·17H$_2$O, **7.2**, grew upon standing over three days from an aqueous solution containing a 1:3:4.5 mixture of SO$_3$H[6], 18-crown-6 and anhydrous europium(III) chloride (Equation 7.2). The complex was characterised by IR spectroscopy and single crystal X-ray crystallography. Complex **7.2** crystallises in an orthorhombic cell and the structural solution was performed in the space group $P2_12_12_1$. The isostructural complex with Nd^{3+} in place of Eu^{3+} was synthesised and characterised by single crystal unit cell determination, however only the Eu^{3+} complex will be discussed in any detail (unit cell parameters for isostructural complex are listed in the experimental section for complex **7.2**). Details of data collection and structure refinement are given in Table 7.16 of this chapter. A crystallographic information file containing all bond lengths and angles for complex **7.2** can be found in appendix 7.1.2 on the attached compact disc.

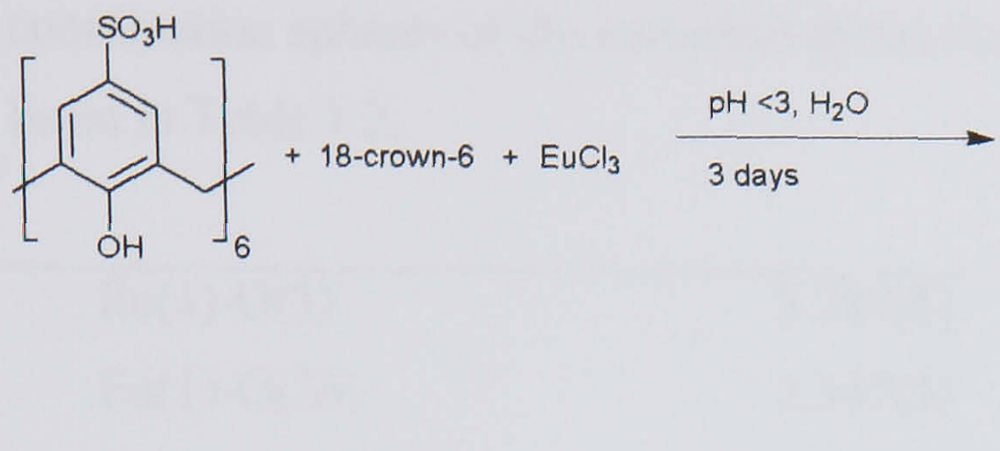

(7.2)

The asymmetric unit is composed of one SO_3[6] molecule, a sulfonate bound hepta-aqua europium centre, a sulfonate bound bis-aqua europium/18-crown-6 moiety and seventeen water molecules Figure 7.7.

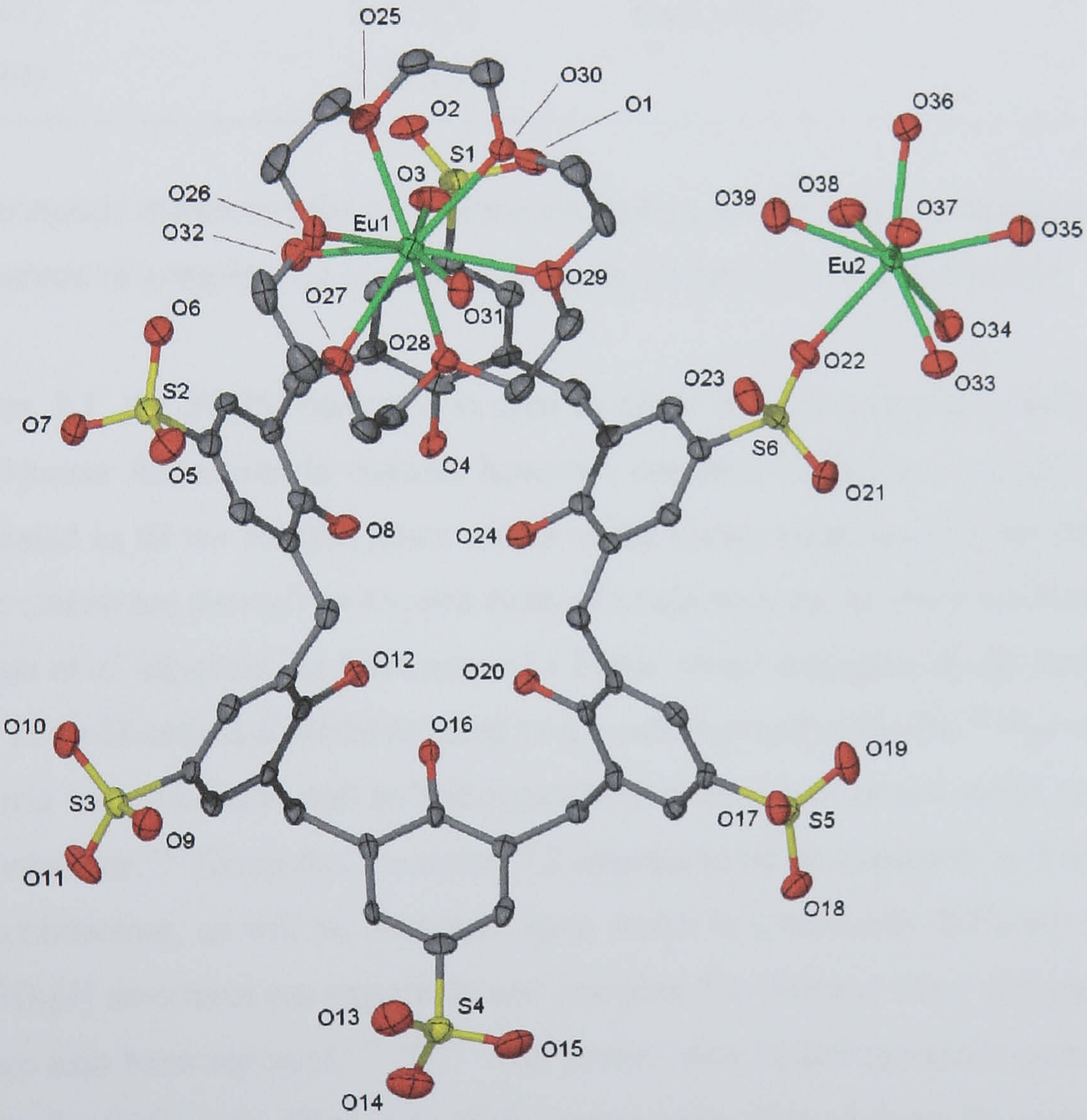

Figure 7.7 Part of the asymmetric unit from the crystal structure of complex **7.2**, anisotropic displacement ellipsoids shown at the 50% probability level. Selected atoms have been labelled.

The europium metal centre Eu(1) is nona-coordinate and has tri-capped trigonal prismatic geometry whilst Eu(2) is octa-coordinate and of square anti-prismatic geometry. Bond lengths relating to the coordination spheres of the europium metal centres in complex **7.2** are of typical magnitude and are listed in Table 7.2.

Eu(1)-O(3)	2.284(5)	Eu(1)-O(25)	2.534(5)
Eu(1)-O(26)	2.547(5)	Eu(1)-O(27)	2.525(5)
Eu(1)-O(28)	2.501(5)	Eu(1)-O(29)	2.579(5)
Eu(1)-O(30)	2.527(5)	Eu(1)-O(31)	2.360(5)
Eu(1)-O(32)	2.396(5)	Eu(2)-O(22)	2.417(5)
Eu(2)-O(33)	2.406(5)	Eu(2)-O(34)	2.415(5)
Eu(2)-O(35)	2.427(5)	Eu(2)-O(36)	2.442(5)
Eu(2)-O(37)	2.425(5)	Eu(2)-O(38)	2.351(6)
Eu(2)-O(39)	2.381(6)		

Table 7.2 Interatomic distances relating to the coordination sphere of the europium metal centres in the crystal structure of complex **7.2** (distances given in Å with e.s.d. in parentheses).

As for complex **7.1**, the SO_3[6] molecule is seen to pinch in a C_2-symmetric fashion to give two pseudo-calix[3]arene fragments. In contrast however, complex **7.2** has one europium metal centre that is coordinated to all the oxygen donor atoms of the crown ether macrocycle whilst also being tethered to the calixarene through an oxygen atom of a sulfonate group. As described in Chapters 1, 2 and 5, Raston *et al.* reported the formation of a Ferris wheel arrangement that had lanthanum or cerium bound in an 18-crown-6 whilst tethered to a *p*-sulfonatocalix[4]arene.[50] The same group also reported a Ferris wheel/Russian doll hybrid structure that also had cerium metal centres bound in 18-crown-6 molecules.[102] Given this, complex **7.2** appears to be an extension to this chemistry and the resultant architecture, as will be described later, packs in a markedly different manner to both the reported SO_3[4] structures (as expected) and complex **7.1**. Several other europium/18-crown-6 complexes have also been reported.[134, 146-149] The crown ether bound europium centre also has two aquo ligands each residing on either side of the macrocycle. One of these aquo ligands hydrogen bonds to an oxygen atom of a sulfonate group with an Eu(1)-O(32)···O(1)-S(1) distance of 2.854 Å, as illustrated on the underside of the crown ether in Figure 7.8. The second europium centre has seven aquo ligands, all of which are too distant to hydrogen bond to any sulfonate group of the SO_3[6] molecule it is bound to. It does however have four aquo ligands that are positioned so as to

form nine hydrogen bonds to oxygen atoms of four sulfonate groups from four symmetry equivalent neighbouring calixarenes.

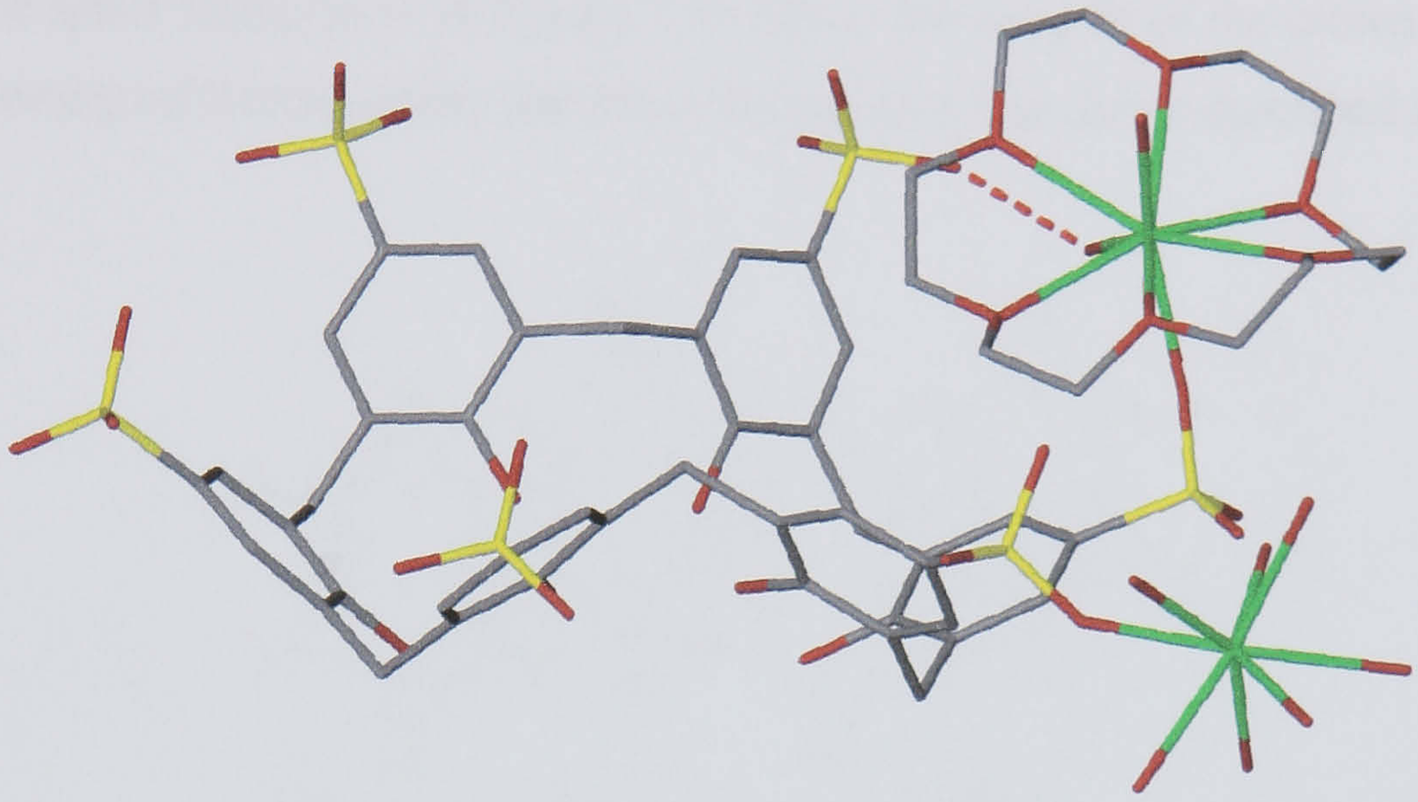

Figure 7.8 A stick representation of part of the asymmetric unit from the crystal structure of complex **7.2**. The C_2-symmetric nature of the calixarene is shown in addition to the europium crown ether coordination. Hydrogen bonding from a europium aquo ligand to a calixarene sulfonate group is also shown.

Tb(2)-(O34)···O(7)-S(2)	2.760	Tb(2)-(O34)···O(14)-S(4)	2.823
Tb(2)-(O35)···O(6)-S(2)	2.796	Tb(2)-(O35)···O(17)-S(5)	2.653
Tb(2)-(O36)···O(10)-S(3)	2.774	Tb(2)-(O36)···O(19)-S(5)	2.707
Tb(2)-(O39)···O(9)-S(3)	2.691		

Table 7.3 Hydrogen bonding contacts between the europium aquo ligands and sulfonate groups of calixarenes in complex **7.2** (distances given in Å).

The SO_3[6] molecules in complex **7.2** pack in a manner different to that in complex **7.1** but in a chiral manner. The calixarenes pack through one π-stacking and two CH···π interactions in hydrophobic helical bi-layer like chains (aromatic centroid···centroid and CH···aromatic centroid distances of 3.870, 2.841 and 2.806 Å respectively, Figure 7.9). The chains are similar (differing in the number of intermolecular interactions) as those described for complex **7.1** but the chains in complex **7.2** pack in an entirely different way. This difference in packing may well be dictated by the fact that the part of the crown ether that protrudes from a pseudo-calix[3]arene cavity of one SO_3[6] is hosted by the empty pseudo-calix[3]arene cavity of the neighbouring complex (Figure 7.10). In fact the chains of complexes pack in a herringbone like arrangement through this intermolecular hosting phenomenon. In addition to this interaction, each complex is linked to

another through a hydrogen bonding chain formed that starts at the Eu(1) aquo ligand (O(31)) that points upwards from the crown ether macrocycle (as in Figure 7.8), connects through three waters of crystallisation and finishes by hydrogen bonding to the Eu(1) aquo ligand on the underside of the crown ether. The space filling view in Figure 7.10 shows the snug fit of the crown ether molecules into the neighbouring calixarene cavity and the hydrogen bonding chains described above.

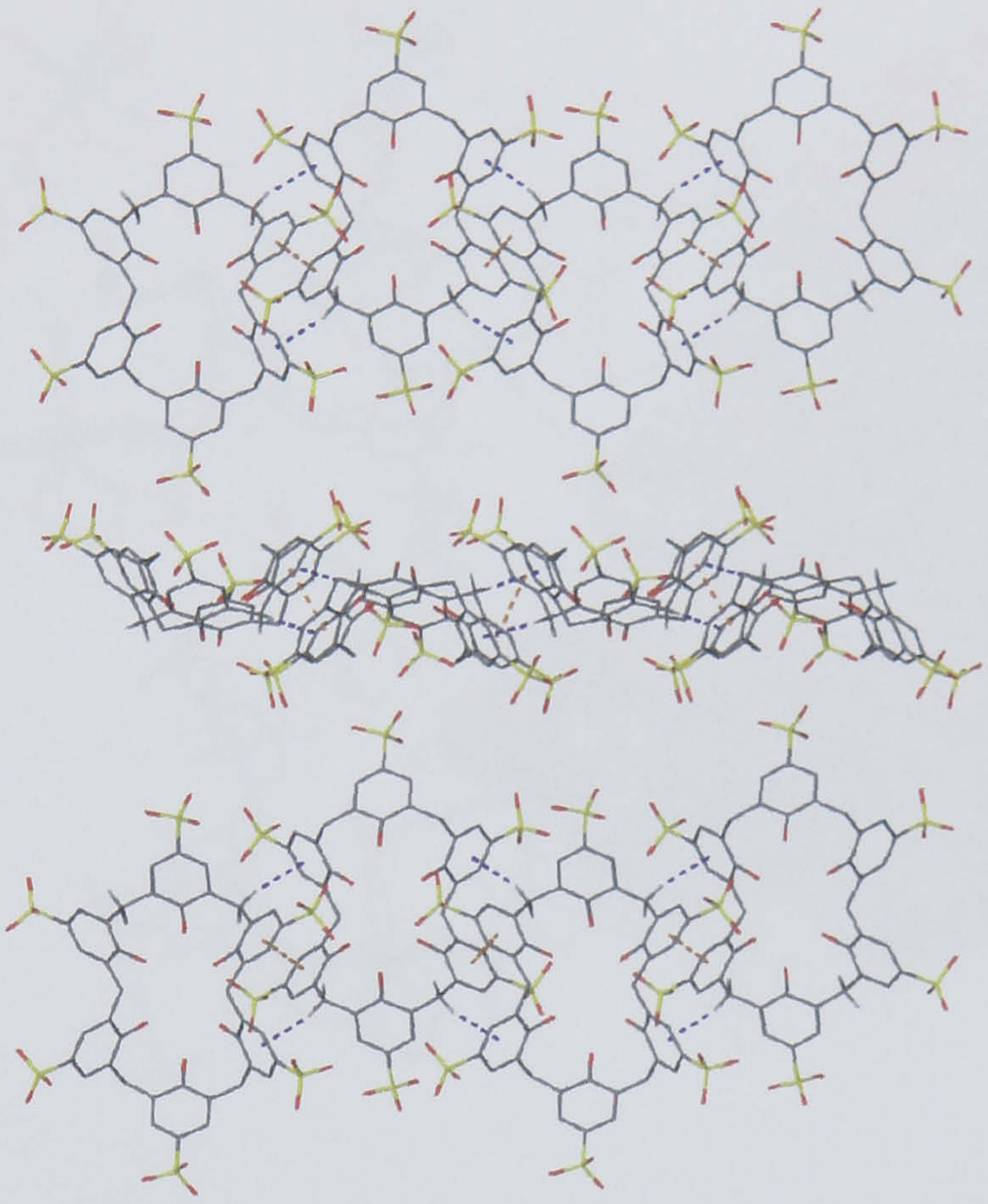

Figure 7.9 *p*-Sulfonatocalix[6]arene packing diagram from the crystal structure of complex **7.2**. The π-stacking and CH···π interactions within the helical chains are shown as dashed orange and purple lines respectively. The alternating chain packing motif is also shown. The crown ether/europium moieties and other coordinated europium cations have been omitted for clarity.

As a 1:4:5.5 ratio of *p*-sulfonatocalix[6]arene, 18-crown-6 and lanthanide(III) chloride gave rise to a *bis*-molecular capsule and a 1:3:4.5 ratio (albeit with different lanthanide metals) resulted in the formation of a new Ferris wheel type arrangement, a larger ratio of 18-crown-6 was employed with a smaller ratio of lanthanide(III) metal chloride and a constant SO_3[6] concentration. When a 1:8:3.5 ratio is present (where Ln^{3+} = Eu, Tb), an interesting and multifaceted complex is formed with the calixarene in the up-down 'double partial cone' conformation. The increased 18-crown-6 concentration disrupts the hydrogen bonding regime at the base of the calixarene, the result of which is deviation from the expected SO_3[6] conformation. Nona-aqua metal cations participate in an extended hydrogen bonding regime with the calixarenes assembling in a new end-to-end chain-like fashion.

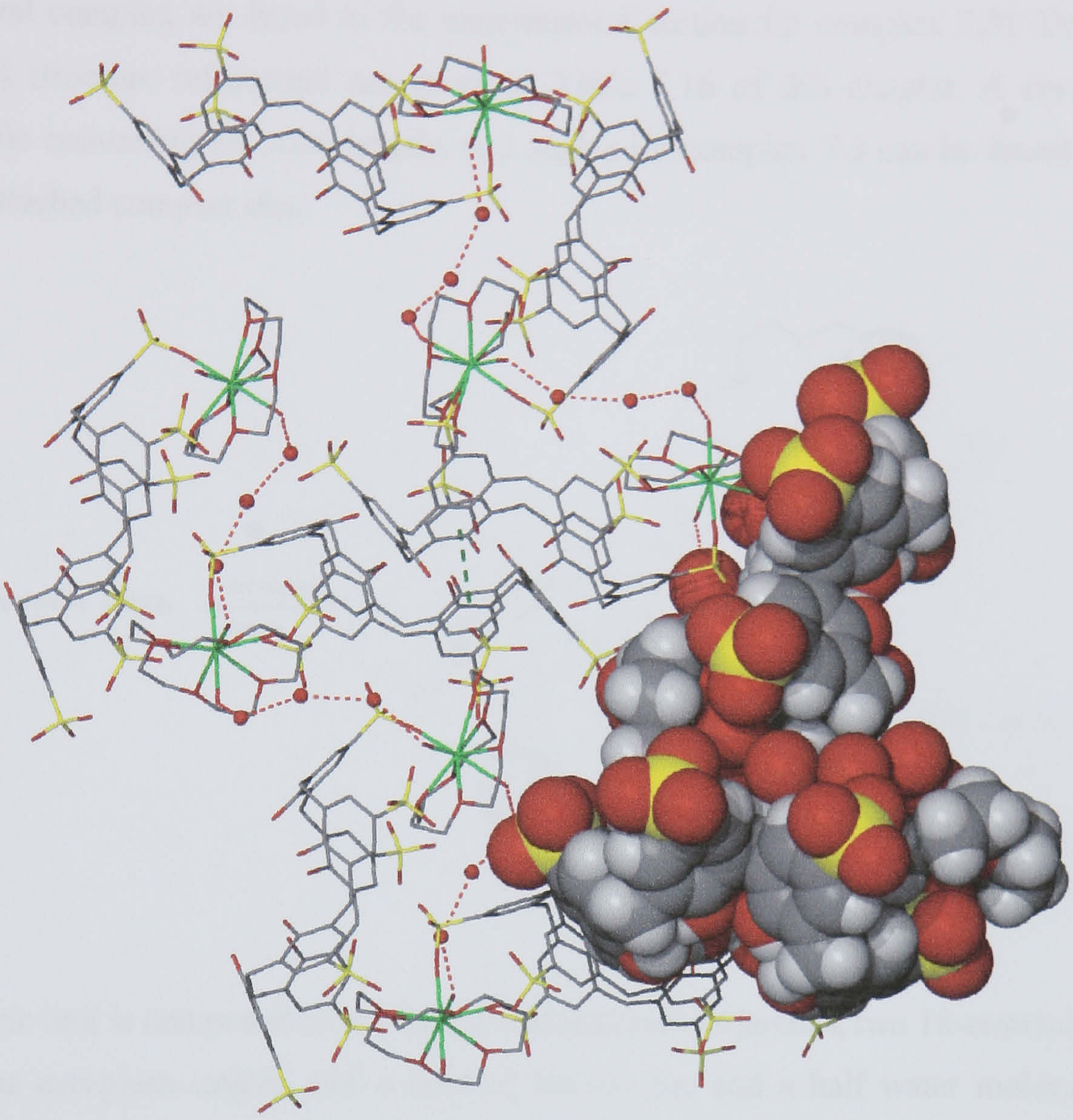

Figure 7.10 Cross section of a partial space filling diagram from the crystal structure of complex **7.2**. The packing of the Ferris wheel moieties within one another and the hydrogen bonding interactions between europium aquo ligands and waters of crystallisation is shown (coordinated europium hepta-aqua cations and other waters of crystallisation omitted for clarity). A π-stacking interaction between the central calixarenes is also shown as a dashed green line.

7.1.3 Structure of the complex $[Eu(H_2O)_9][\{18\text{-crown-6} \cap (p\text{-sulfonatocalix-[6]arene})_{0.5}\}_2]\cdot 21.5H_2O$, 7.3.

Crystals of the complex $[Eu(H_2O)_9][\{18\text{-crown-6} \cap (p\text{-sulfonatocalix-[6]arene})_{0.5}\}_2]\cdot 21.5H_2O$, **7.3**, grew upon standing over three days from an aqueous solution containing a 1:8:3.5 mixture of SO_3H[6], 18-crown-6 and anhydrous europium(III) chloride (Equation 7.3). The complex was characterised by IR spectroscopy and single crystal X-ray crystallography. Complex **7.3** crystallises in a triclinic cell and the structural solution was performed in the space group $P\bar{1}$. The isostructural complex with Tb^{3+} in place of Eu^{3+} was synthesised and characterised by single crystal unit cell

determination, however only the Eu^{3+} complex will be discussed in any detail (unit cell parameters for isostructural complex are listed in the experimental section for complex **7.3**). Details of data collection and structure refinement are given in Table 7.16 of this chapter. A crystallographic information file containing all bond lengths and angles for complex **7.3** can be found in appendix 7.1.3 on the attached compact disc.

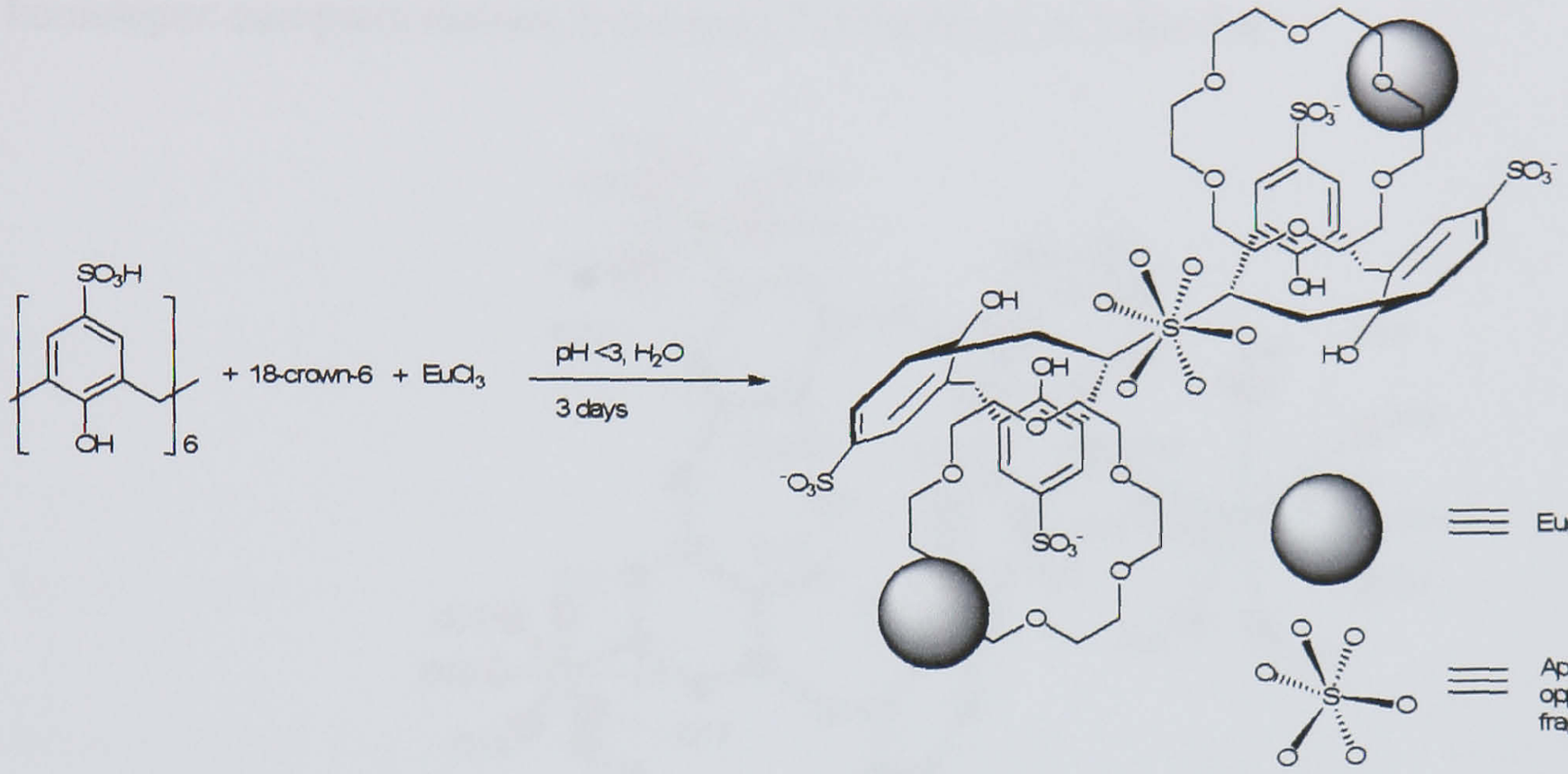

(7.3)

The asymmetric unit is composed of two half *p*-sulfonatocalix[6]arenes, two 18-crown-6 molecules, two nona-aqua europium cations and a total of twenty one and a half water molecules that are disordered over twenty four positions (Figure 7.11). Each of the half calixarenes in the asymmetric unit is positioned around a centre of inversion so each fragment shall be discussed separately.

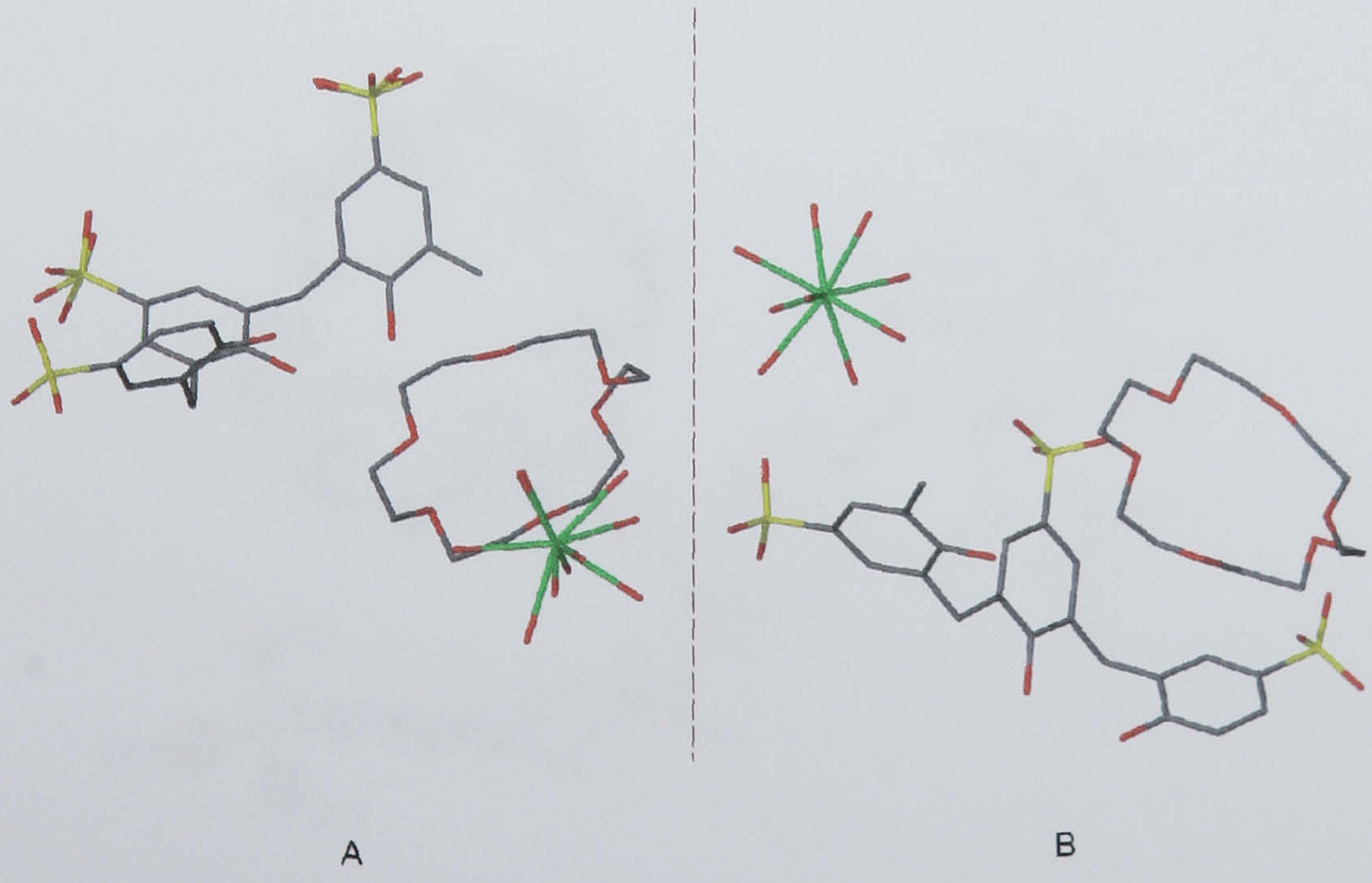

Figure 7.11 Stick representation of part of the asymmetric unit from the crystal structure of complex **7.3**. The two sections have been labelled **A** and **B** to aid discussion.

Two of the sulfonate groups of the half calixarene in part **A** show disorder. In addition to this, one of the europium aquo ligands is also disordered over two positions (O(54) and O(55), Figure 7.12). Despite this disorder, the europium cation is of near tri-capped trigonal prismatic geometry. The atoms of part **B** show no disorder and the nona-aqua europium metal centre is of tri-capped trigonal prismatic geometry (Figure 7.13). Bond distances relating to the coordination spheres of the homoleptic europium cations in complex **7.3** are listed in Table 7.4.

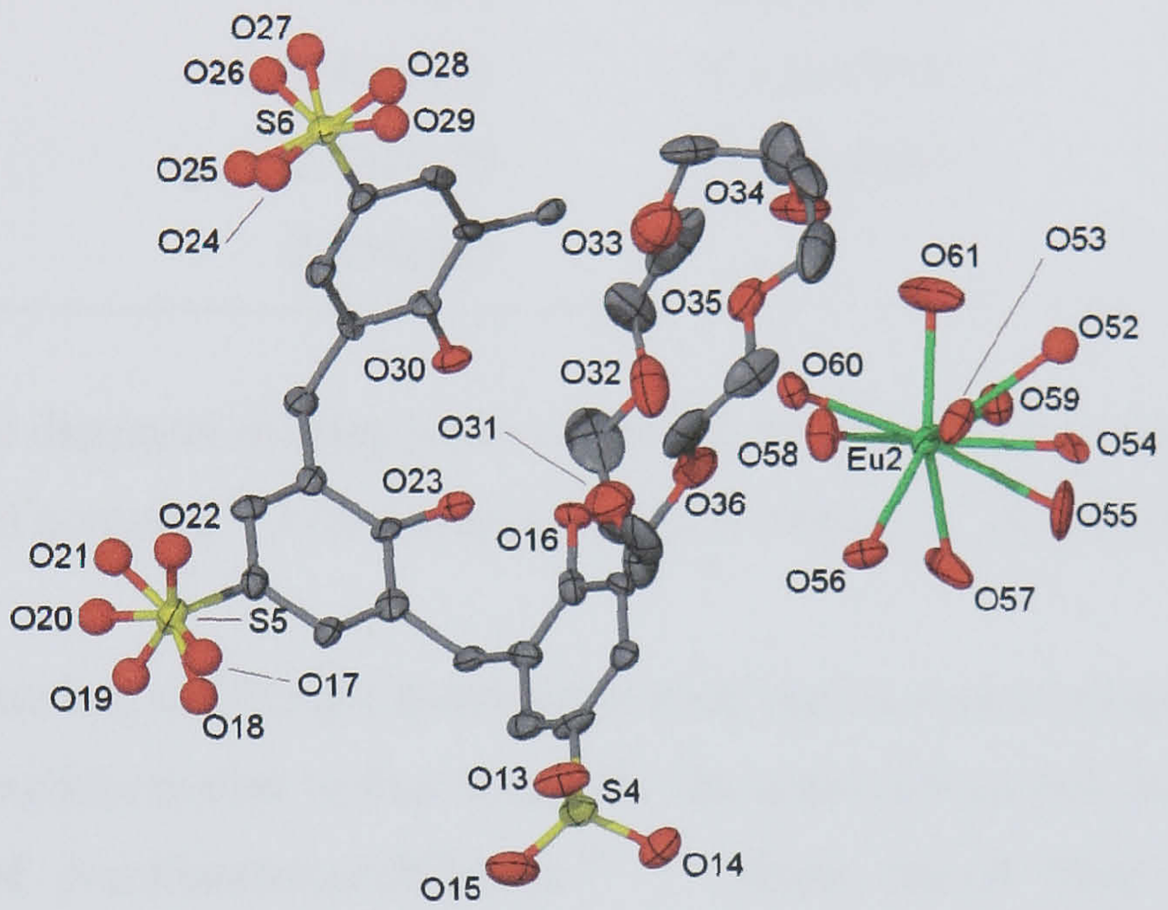

Figure 7.12 Part **A** of the asymmetric unit from the crystal structure of complex **7.3**, anisotropic displacement ellipsoids shown at the 50% probability level. Some sulfonate oxygen atoms were refined isotropically and are shown in ball and stick representation. Selected atoms have been labelled.

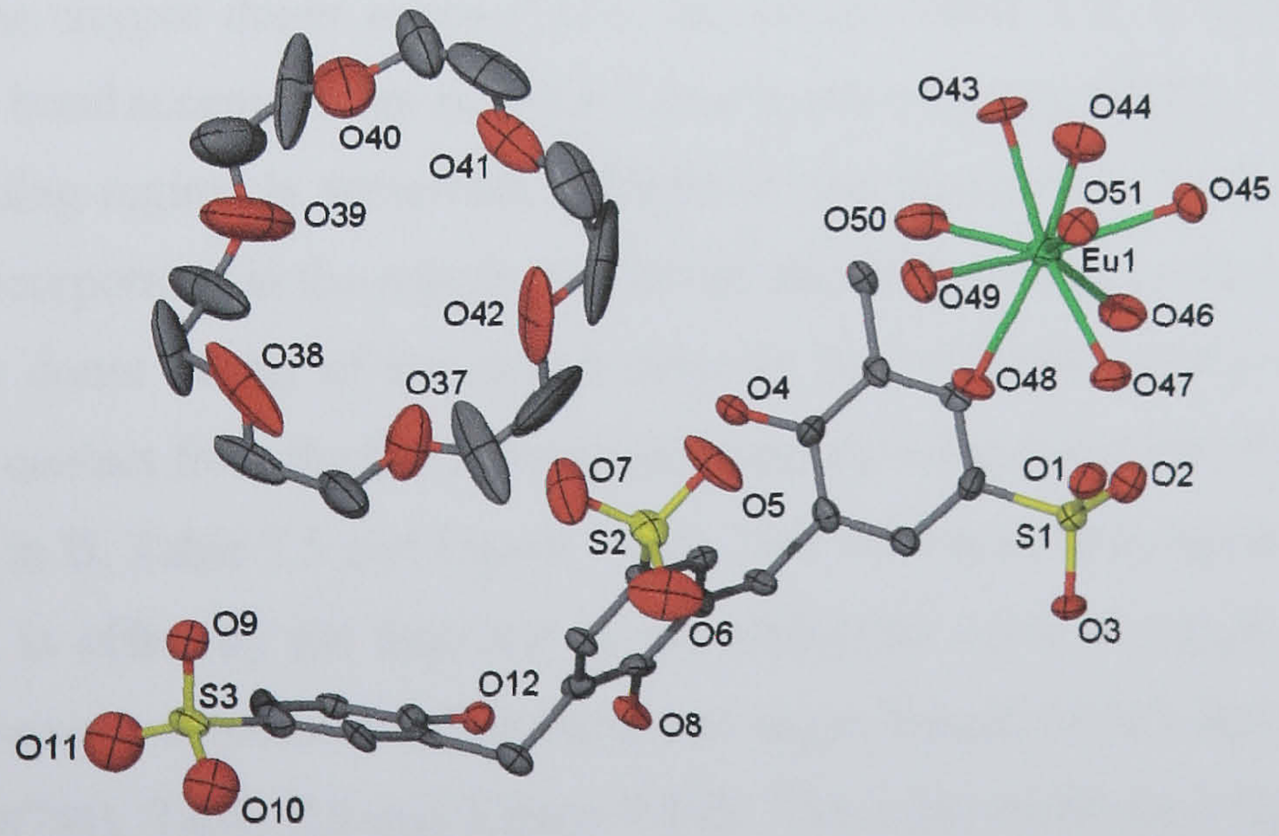

Figure 7.13 Part **B** of the asymmetric unit from the crystal structure of complex **7.3**, anisotropic displacement ellipsoids shown at the 50% probability level. Selected atoms have been labelled.

Eu(1)-O(43)	2.499(13)	Eu(1)-O(44)	2.515(15)
Eu(1)-O(45)	2.456(13)	Eu(1)-O(46)	2.472(14)
Eu(1)-O(47)	2.443(14)	Eu(1)-O(48)	2.497(12)
Eu(1)-O(49)	2.475(14)	Eu(1)-O(50)	2.463(16)
Eu(1)-O(51)	2.516(13)	Eu(2)-O(52)	2.62(6)
Eu(2)-O(53)	2.436(14)	Eu(2)-O(54)	2.38(3)
Eu(2)-O(55)	2.45(3)	Eu(2)-O(56)	2.422(14)
Eu(2)-O(57)	2.426(15)	Eu(2)-O(58)	2.440(14)
Eu(2)-O(59)	2.437(17)	Eu(2)-O(60)	2.455(13)
Eu(2)-O(61)	2.358(18)		

Table 7.4 Interatomic distances relating to the coordination sphere of the europium metal centres in the crystal structure of complex **7.3** (distances given in Å with e.s.d. in parentheses).

Upon symmetry expansion, the SO_3[6] molecule in each part is seen to adopt the up-down 'double partial cone' conformation similar to that found for the octa-sodium salt, sulfonic acid, and other alkali metal salts of *p*-sulfonatocalix[6]arene.[69, 144] When crown ether proximate waters of crystallisation are taken into account, hydrogen bonding regimes link the metal cations, 18-crown-6, selected water, and *p*-sulfonatocalix[6]arene molecules in both fragments (Figure 7.14). In part **A**, there are a total of four hydrogen bonds from three of the europium aquo ligands to three oxygen donor atoms of the 18-crown-6 molecule (Table 7.5 and Figure 7.14a, one hydrogen bond omitted for visual clarity). On the other side of the 18-crown-6, a water of crystallisation (O(67)) hydrogen bonds to two of the oxygen donor atoms (O(31) and O(33), Table 7.5). In addition to this, O(67) acts as a hydrogen bond acceptor from an SO_3[6] base hydroxyl group (O(30), Table 7.5). In part **B**, the hydrogen bonding regime is somewhat different to that found in **A**. In **B**, one more water of crystallisation is incorporated in the regime and the number of hydrogen bonds from europium aquo ligands to oxygen donor atoms of the crown ether is also different. There is in fact only one hydrogen bonding contact from the O(51) europium aquo ligand to the O(38) donor atom of the 18-crown-6 molecule in **B**, Table 7.5 and Figure 7.14b. This difference in europium aquo/crown ether hydrogen bonding is offset by the insertion of the additional water molecule between the metal cation and the 18-crown-6 molecule. One europium aquo ligand, O(49), hydrogen bonds to the water molecule (O(79)), Table 7.5 and Figure 7.14b. The same water molecule (O(79) hydrogen bonds to two of the oxygen donor atoms of the crown ether to the O(38) donor atom of the 18-crown-6 molecule, Table 7.5 and Figure 7.14b. On the other side of the crown ether, the europium/18-crown-6 moeity is linked to the calixarene through a hydrogen bonding regime similar

to that found in **A**. A water of crystallisation, O(71), hydrogen bonds to two of the donor atoms of the crown ether and acts as a hydrogen bond acceptor from an SO_3[6] base hydroxyl group (O(8), Table 7.5, Figure 7.14b).

Eu(2)-(O58)···O(32)	2.901	Eu(2)-(O60)···O(34)	2.964
Eu(2)-(O60)···O(36)	2.716	Eu(2)-(O61)···O(34)	2.709
(O67)···O(31)	2.758	(O67)···O(33)	2.903
(O30)···O(67)	2.645		
Eu(1)-(O51)···O(38)	2.887	Eu(1)-(O49)···O(79)	2.693
(O79)···O(38)	2.924	(O79)···O(42)	2.823
(O71)···O(39)	3.071	(O71)···O(41)	2.746
(O8)···O(71)	2.575		

Table 7.5 Hydrogen bonding contacts between europium aquo ligands, water molecules, crown ether oxygen atoms and SO_3[6] base hydroxyl groups in parts **A** and **B** from the crystal structure of complex **7.3** (distances given in Å).

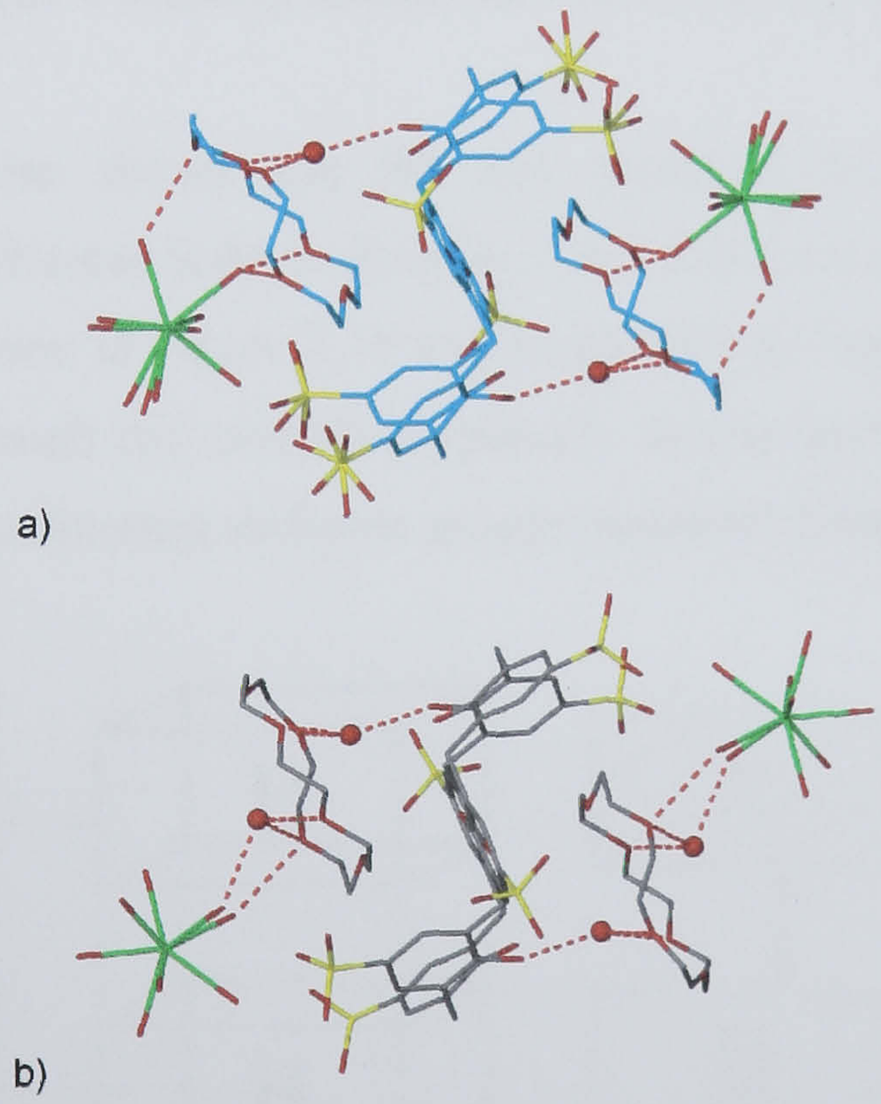

Figure 7.14 Symmetry expansion of parts **A** and **B** of the asymmetric unit from the crystal structure of complex **7.3**. The atoms are shown in stick representation except for the waters of crystallisation that are shown as balls. a) The carbon atoms of part **A** are shown in blue (to aid further discussion) and the hydrogen bonding regime is shown as dashed red lines. b) The carbon atoms of part **B** are shown in grey and the different hydrogen bonding regime is also shown.

The extended structure is very complex and is best examined in parts. The SO_3[6] molecules pack through one crystallographically unique π-stacking interaction along the diagonal of the unit cell to form end-to-end chains with an aryl centroid···centroid separation of 3.613 Å, Figure 7.15. The end-to-end chains are composed of alternating calixarenes (from **A** and **B**) as indicated by the colour scheme in Figure 7.15.

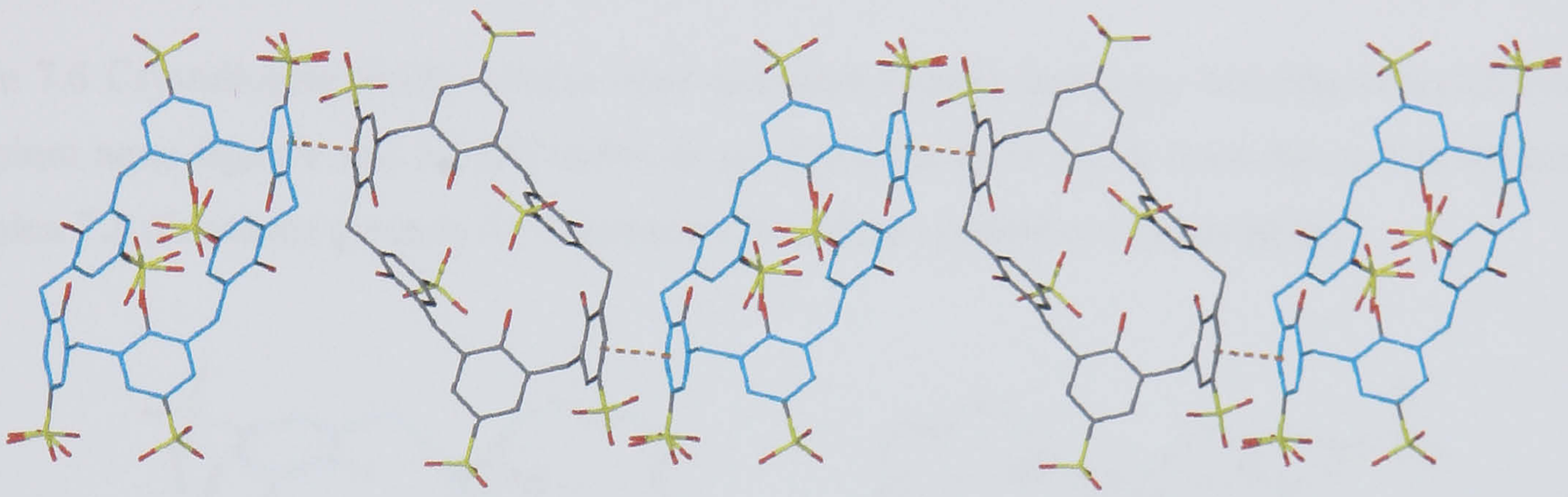

Figure 7.15 Partial packing diagram from the crystal structure of complex **7.3**. An end-to-end chain of alternating *p*-sulfonatocalix[6]arenes (from parts **A** {blue} and **B** {grey}) is shown in addition to the crystallographically unique π-stacking interaction (dashed orange line).

The extended structure also shows that the two expanded fragments **A** and **B** alternate independently in an intra-columnar fashion along the *a* axis and these columns are assembled in a 2-D grid (shown in cartoon form in Figure 7.16 and graphically in Figure 7.17). The uni-composite columns both assemble through two crystallographically unique hydrogen bonds formed between europium aquo ligands and calixarene sulfonate groups (distances listed in Table 7.6).

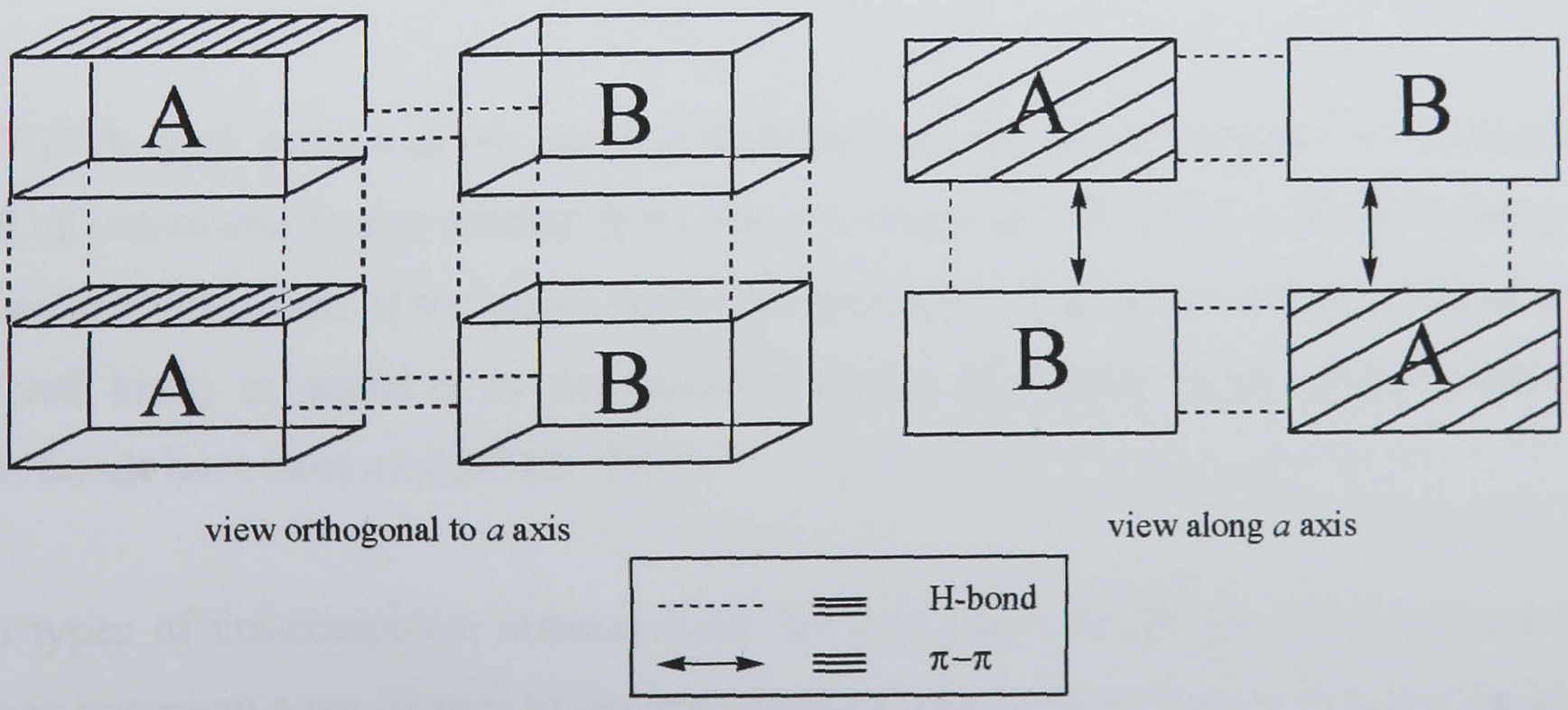

Figure 7.16 Schematic of the intra and inter-column hydrogen bonding found in the crystal structure of complex **7.3**.

INTRA-COLUMN		INTER-COLUMN	
Eu(1)-(O46)···O(1)-S(1)	2.758	Eu(1)-(O47)···O(13)-S(4)	2.838
Eu(1)-(O48)···O(1)-S(1)	2.875	Eu(1)-(O51)···O(15)-S(4)	2.802
Eu(2)-(O56)···O(27*)-S(6)	2.724	Eu(1)-(O45)···O(18*)-S(5)	2.917
Eu(2)-(O59)···O(14)-S(4)	2.744	Eu(2)-(O59)···O(2)-S(1)	2.758
		Eu(2)-(O61)···O(2)-S(1)	2.940

Table 7.6 Crystallographically unique intra and inter-column hydrogen bonding contacts between europium aquo ligands and SO_3[6] sulfonate groups of parts **A** and **B** from the crystal structure of complex **7.3** (distances given in Å, * denotes a disordered sulfonate oxygen atom).

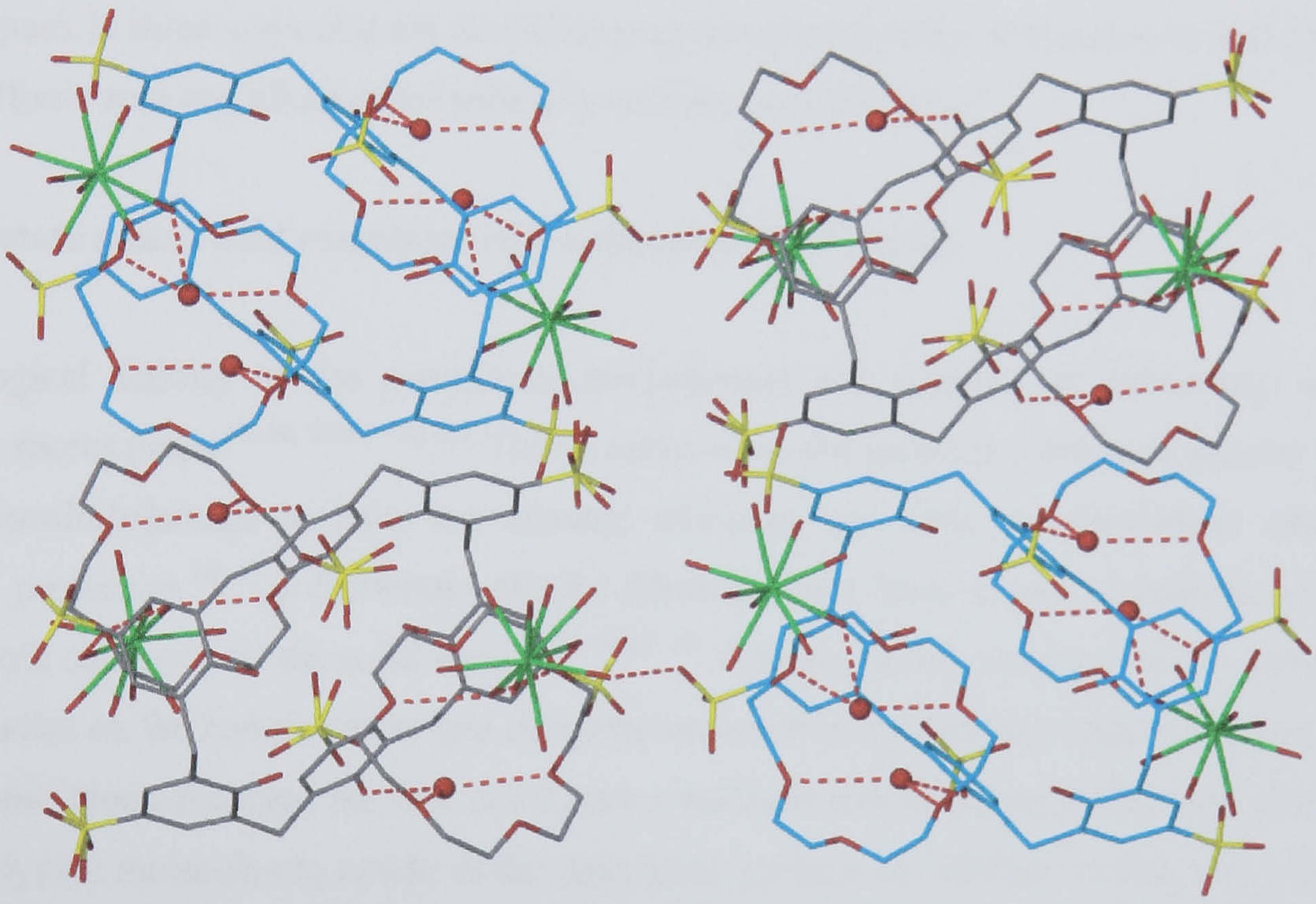

Figure 7.17 A cross section of the packing diagram from the crystal structure of complex **7.3**.The 2-D grid of end-to-end chains formed from parts **A** (blue) and **B** (grey) is shown (chains running perpendicular to the plane of the page). Intra and inter-chain hydrogen bonding contacts are shown (dashed red lines) in addition to the selected waters of crystallisation. Some inter-columnar hydrogen bonds have been omitted for clarity.

The two types of uni-composite column form the 2-D grid through five inter-column hydrogen bonds from europium aquo ligands to oxygen atoms of calixarene sulfonate groups (partially shown in Figure 7.17). The numerous remaining waters of crystallisation are in positions consistent with

very extensive hydrogen bonding regimes with europium aquo ligands and calixarene sulfonate groups.

7.1.4 Summary of lanthanide crown ether complexes of *p*-sulfonatocalix[6]arene.

This section has shown three structures that are obtainable through the use of different stoichiometries of 18-crown-6 and lanthanide metal chloride with respect to *p*-sulfonatocalix[6]arene. A new solid state conformation for SO_3[6] was isolated, characterised and shows the host molecule to be suited to multi-guest inclusion and multi-faceted complex formation. Notably, complexes **7.1** and **7.2** show a type of extension to work reported by Raston *et al.* that has shown *p*-sulfonatocalix[4]arene capable of forming molecular capsules and Ferris wheel arrangements with lanthanide metals and 18-crown-6.[50, 102] In addition to this, SO_3[6] has been shown to pack in three ways that are all different to those reported by Atwood *et al.* and Asfari *et al.* for the sulfonic acid and alkali metal salts of *p*-sulfonatocalix[6]arene.[69, 144]

7.2 Solid state amino acid complexes of *p*-sulfonatocalix[6]arene.

The biological activity of the *p*-sulfonatocalix[*n*]arenes has received an increasing amount of interest in recent times.[55, 56, 58-60, 150, 151] This is reflected in the growing number of patents that show *p*-sulfonatocalix[*n*]arenes to have ion channel blocking, anti-viral, antithrombotic and enzyme inhibition properties.[18, 19] *p*-Sulfonatocalix[4,6,8]arenes have been shown to interact with amino acids in both solution and the solid state.[55, 56, 58-62, 151] Coleman *et al.*, amongst others, have reported several studies on the complexation and characterisation of several amino acids in solution.[55, 56, 58-60, 151] The same group reported the first solid state *p*-sulfonatocalix[4]arene/amino acid complex that showed L-lysine molecules to reside in the calixarene cavities. In addition to this, one L-lysine was shown to traverse the bi-layer arrangement, a particularly unique phenomenon.[59] Raston *et al.* reported the solid state structures of several other *p*-sulfonatocalix[4]arene/amino acid complexes.[61, 62] They showed that racemic pairs of alanine, histidine, and phenylalanine were shrouded by two SO_3[4] molecules in molecular capsule arrangements with additional poly-aquo sodium cations in the structures. They also reported in the same article that chiral amino acids ((*S*)-alanine, (*S*)-histidine, and (*S*)-tyrosine) formed 1:1 complexes with *p*-sulfonatocalix[4]arene with additional poly-aquo sodium cations in the resultant structures. More recent work by Raston *et al.* has shown the formation of di-sodium, penta-sodium, and di-caesium/di-sodium complexes of *p*-sulfonatocalix[4]arene and (*S*)-serine.[62] Whilst all of the structures described above show SO_3[4] to adopt the typical bi-layer arrangement, recent work by Coleman *et al.* has reported the formation of a new packing motif for *p*-sulfonatocalix[4]arene as part of a D-arginine complex.[60] The typical bi-

layer arrangement of SO_3[4] has been disturbed, the result being concomitant formation of water channels within the extended structure. Although several amino acid complexes of *p*-sulfonatocalix[6]arene have been reported to date (or with *O*-substituted variations of SO_3[6]), there are no solid state examples of such complexation.[55, 56, 58, 150] Given this, a series of amino acids (racemic and chiral) were investigated as potential guest molecules for complexation of *p*-sulfonatocalix[6]arene as a potential extension to the analogous structural SO_3[4] chemistry described above. Of those examined (arginine, histidine, phenylalanine, serine, leucine, tyrosine, and proline, Figure 7.18), leucine was the only amino acid to form single crystals with *p*-sulfonatocalix[6]arene that were suitable for X-ray diffraction studies.

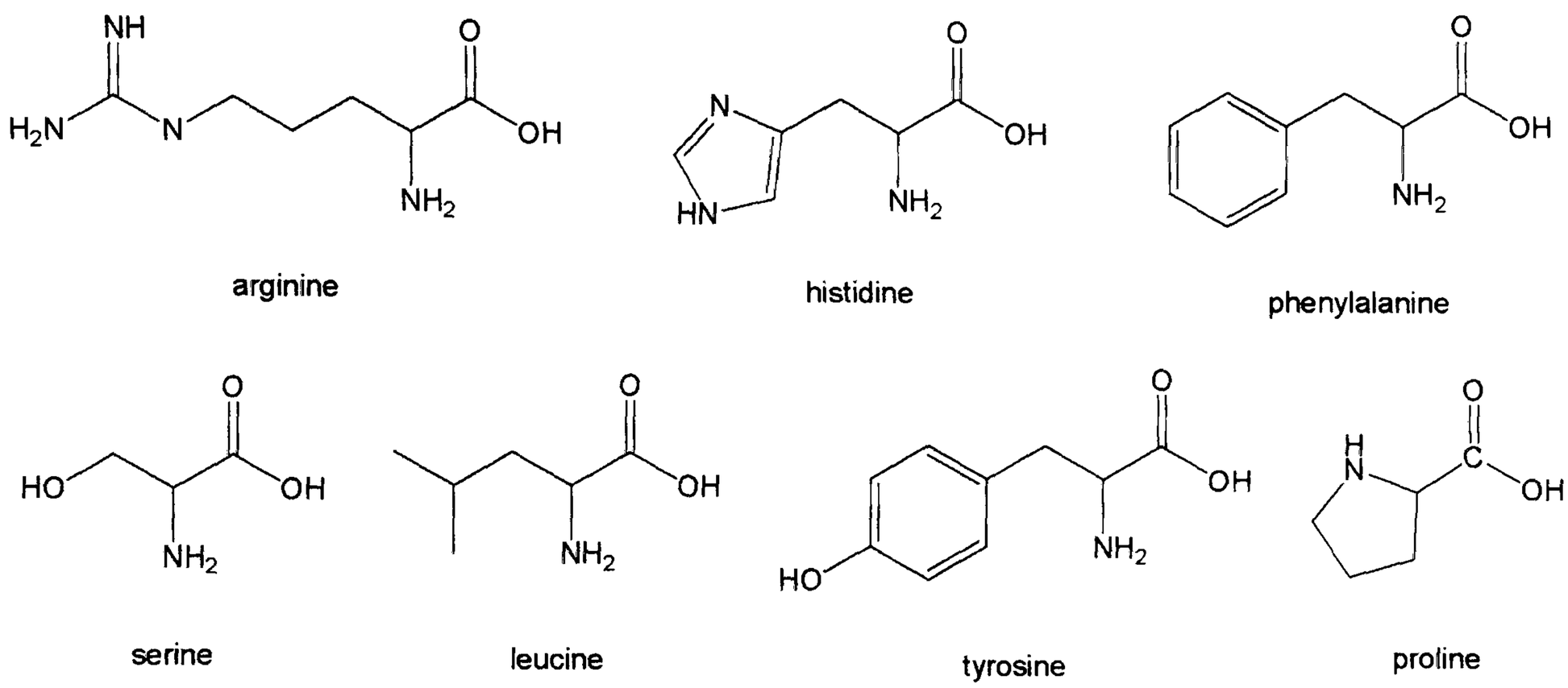

Figure 7.18 The amino acids used in attempted solid state complex formation with *p*-sulfonato-calix[6]arene.

7.2.1 Structure of the amino acid complex [($_L$-leucine + H^+)$_2$⊂*p*-sulfonatocalix[6]arene][$_L$-leucine + H^+)$_4$].3.25H_2O, 7.4.

Crystals of the complex [($_L$-leucine + H^+)$_2$⊂*p*-sulfonatocalix[6]arene][$_L$-leucine + H^+)$_4$].3.25H_2O, **7.4**, grew upon slow evaporation of a pH adjusted aqueous solution containing a 1:6 mixture of Na_8SO_3[6] and either racemic or optically pure $_L$-leucine (pH adjusted to be <1 using 1M HCl, Equation 7.4). The complex was characterised by IR, NMR spectroscopy and single crystal X-ray crystallography. Complex **7.4** crystallises in an orthorhombic cell and the structural solution was performed in the space group $P2_12_12_1$. Details of data collection and structure refinement are given in Table 7.17 of this chapter. A crystallographic information file containing all bond lengths and angles for complex **7.4** can be found in appendix 7.2.1 on the attached compact disc.

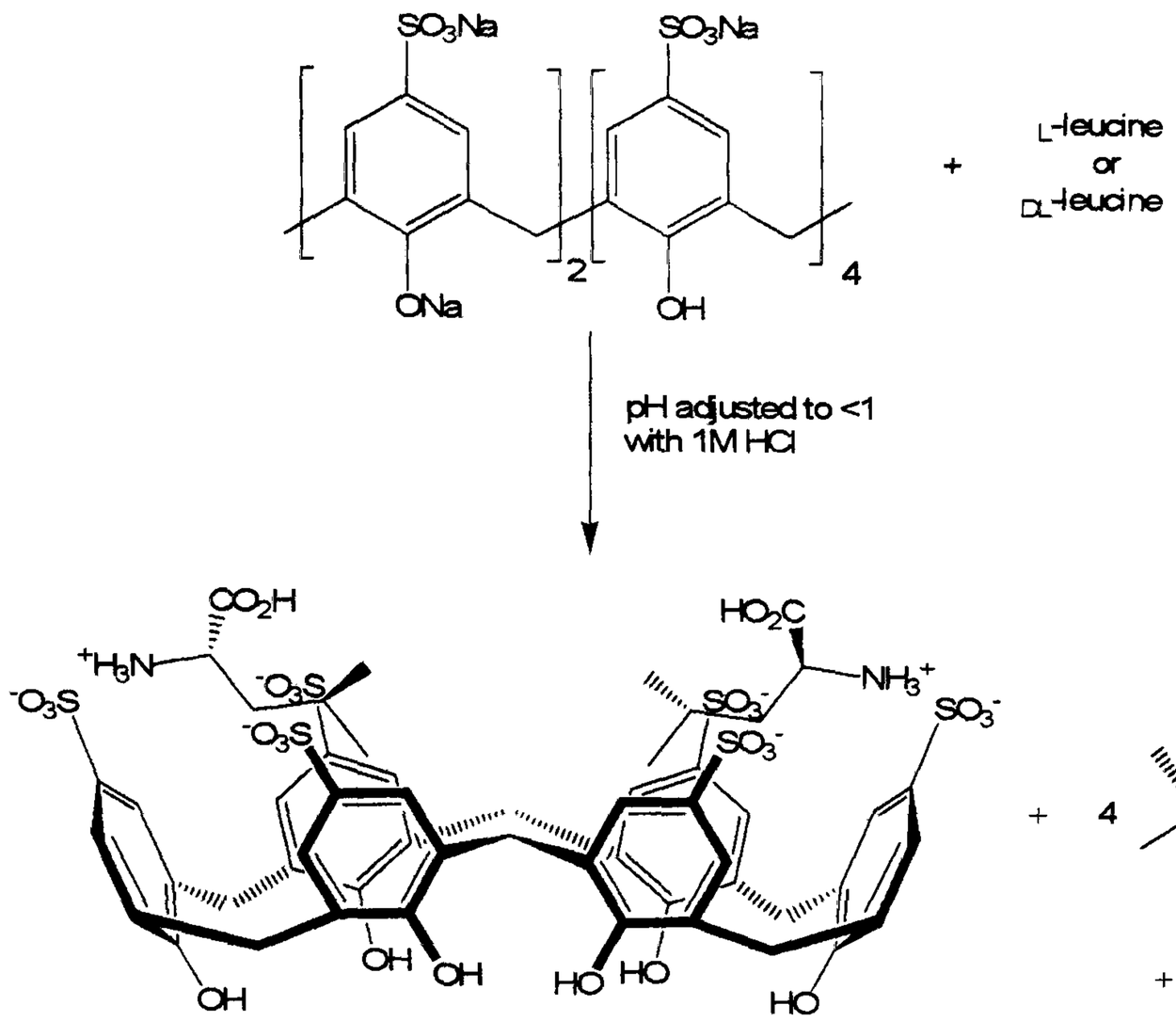

(7.4)

The asymmetric unit consists of one *p*-sulfonatocalix[6]arene, a total of six $_{L}$-leucine molecules, and a total of three and a quarter water molecules that are disordered over eight positions (Figure 7.19). Two of the $_{L}$-leucine molecules are at a partial occupancy of 0.5, and in one position the molecule is poorly resolved. As some ambiguity surrounded the 1:6 SO_3[6]:$_{L}$-leucine stoichiometry from the crystal structure, the ratio was confirmed by NMR spectroscopy. A notable feature of complex **7.4** is that the calixarene has adopted the 'double cone' conformation. When in this conformation, the SO_3[6] has a molecule of $_{L}$-leucine residing in each of the pseudo-calix[3]arene cavities that result from the pinching effect between two opposite methylene bridging groups within the calixarene (Figures 7.19 and 7.20). This conformation is similar to that observed for *p*-sulfonatocalix[6]arene in complexes **7.1** and **7.2** (Figures 7.3 and 7.8 respectively). The amino acid molecules in complex **7.4** are anchored in place through the formation of NH···OS and C-OH···OS hydrogen bonds from the hydrophilic $_{L}$-leucine functional groups to the calixarene sulfonate groups. The protonated amine groups of the N(1) and N(2) $_{L}$-leucine molecules have N···OS hydrogen bonding distances of 2.887 and 2.878 Å respectively, Figure 7.20 (corresponding NH···O distances of 2.008 and 2.083 Å). The carboxylic acid groups of the N(1) and N(2) $_{L}$-leucine molecules also hydrogen bond to sulfonate group oxygen atoms with CO···OS distances of 2.603 and 2.649 Å respectively (Figure 7.20). Although the hydrogen atoms were not located for these interactions, the distances are consistent with an identified $_{L}$-leucine C-OH···OS interaction found within the crystal structure (N(3) L-leucine to the S(5) calixarene sulfonate group). That interaction was identified by residual electron density that suggested hydrogen atom positioning with a C(55)O(36)···O(24)S(5) distance of 2.638 Å (corresponding C-OH···OS distance of 1.799 Å).

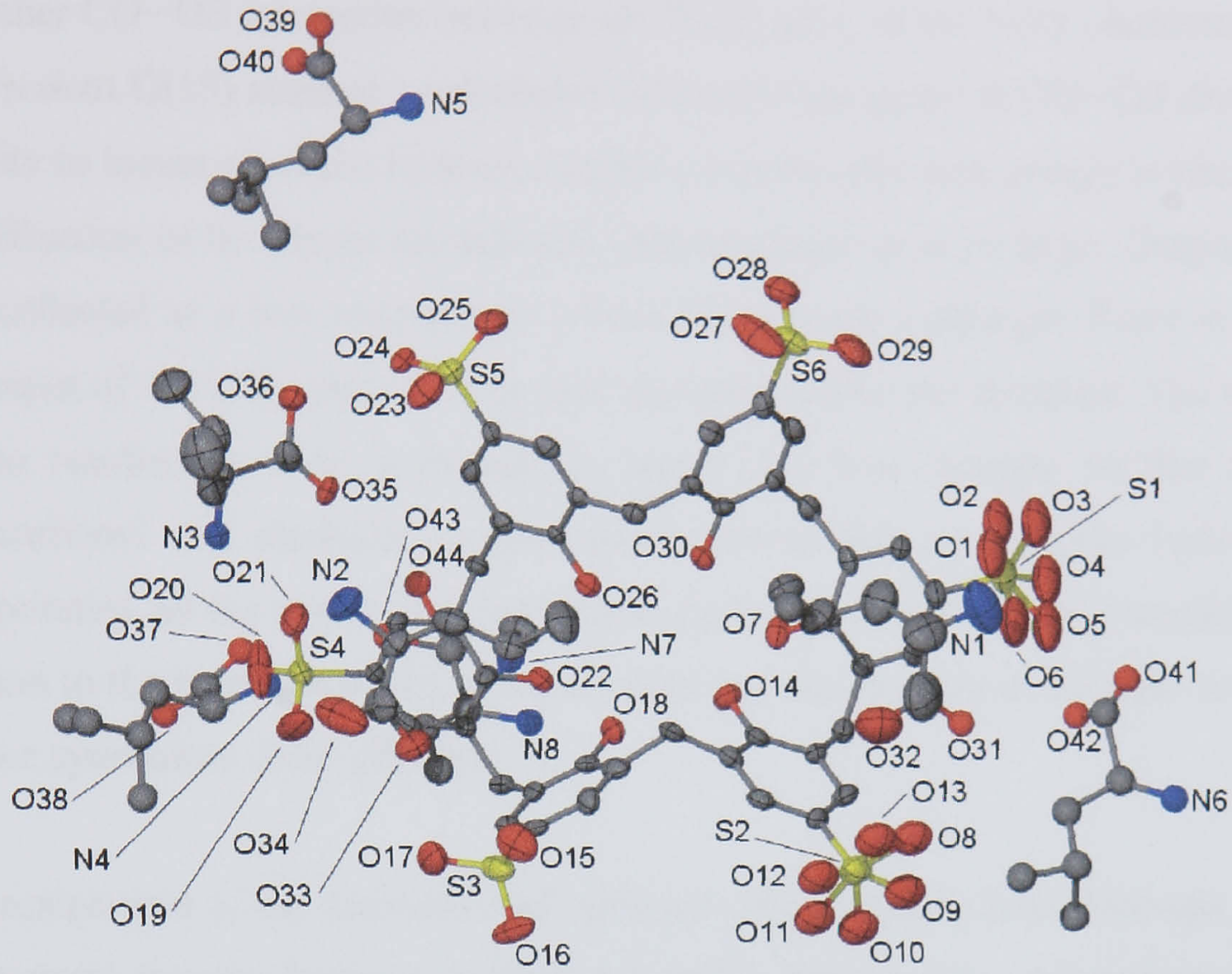

Figure 7.19 Part of the asymmetric unit from the crystal structure of complex **7.4**, anisotropic displacement ellipsoids shown at the 50% probability level. Some of the L-leucine molecules and some atoms from other L-leucine molecules are shown in ball and stick representation. The badly disordered and poorly resolved L-leucine molecule is obscured by the L-leucine⊂SO_3[6] arrangement. Selected atoms have been labelled.

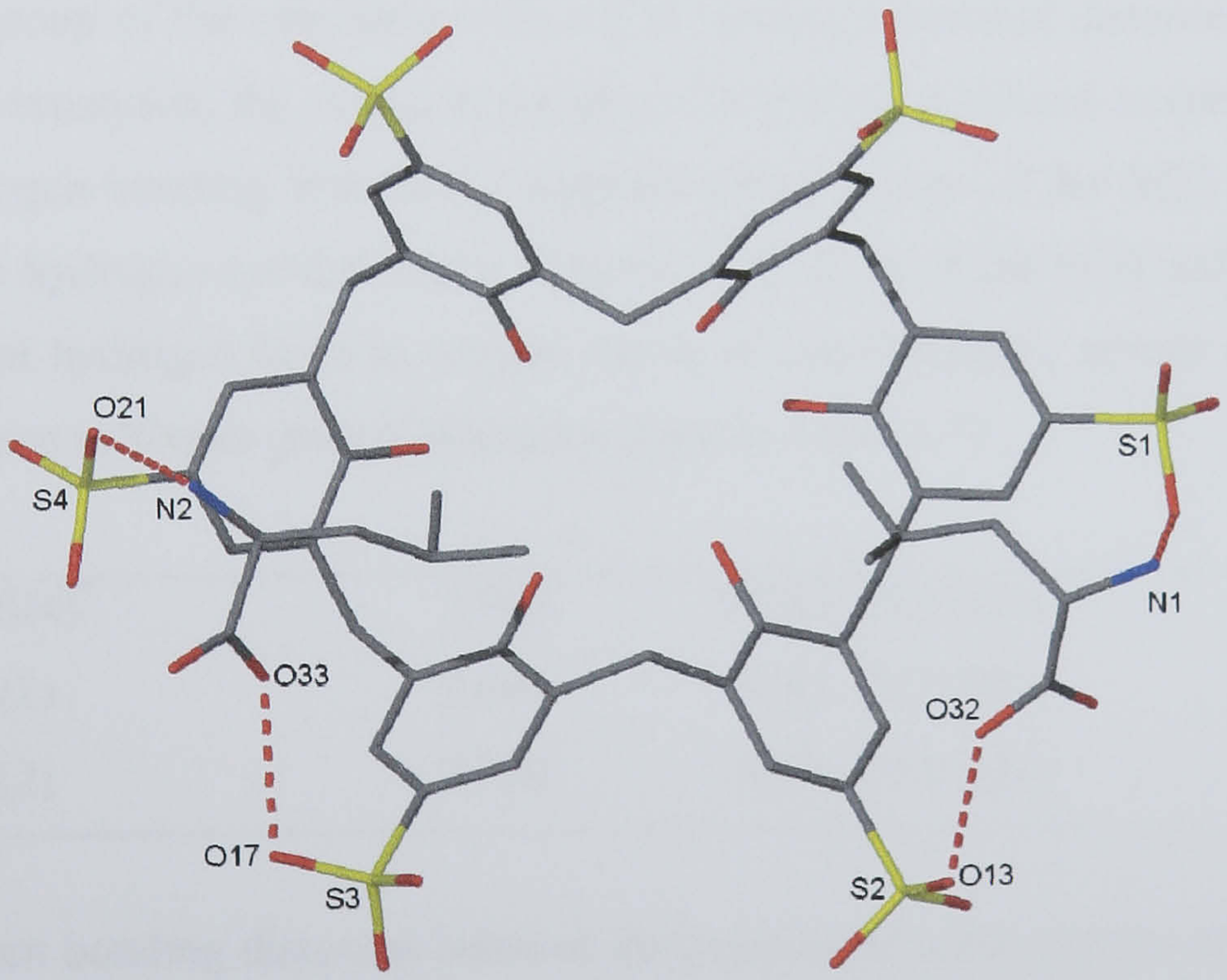

Figure 7.20 The hydrogen bonding found between the hydrophilic groups of the cavity bound L-leucine molecules and sulfonate groups of the *p*-sulfonatocalix[6]arene in the crystal structure of complex **7.4** (disordered sulfonate groups idealised for clarity). Selected atoms have been labelled.

There is one other CO···OS interaction between the O(38) atom of the N(4) $_{L}$-leucine molecule to a symmetry equivalent O(15) atom of a calixarene S(3) sulfonate group (COH···OS distance of 2.654 Å). The inability to locate of all the hydrogen atoms on carboxylic acid groups is likely attributable to the poor diffraction of the single crystals and that the structure is so large. Despite the fact that the data was collected at a low temperature (100(2) K) and on a stronger X-ray source (rotating anode at an output of 4.2 kW), disorder was still prevalent within the structure. The relatively poor diffraction also resulted in some ambiguity in some C-O bond lengths for the discrimination between the carbonyl and alcoholic oxygen atoms. Given this, no definite hydrogen bonding regimes incorporating all the amino acid molecules can be determined in the extended structure. A possible solution to the poor diffraction of the crystals and the problem of disorder would be a very low temperature synchotron data collection.

Although the assignment of the alcoholic and carbonyl oxygen atoms is problematic, several other interesting structural features based on hydrogen bonding between the $_{L}$-leucine protonated amine (NH_3^+) and calixarene sulfonate groups are evident. Complexes **7.1** and **7.2** showed *p*-sulfonatocalix[6]arene to assemble into bi-layer type chains when in the 'double cone' conformation. This feature is prevalent in complex **7.4** and the calixarenes pack through two crystallographically unique interactions; one π-stacking interaction with an aromatic centroid···centroid distance of 3.754 Å; one CH···π interaction between a methylene hydrogen atom and an aromatic group of the calixarene with a CH···aromatic centroid distance of 2.566 Å. Upon further symmetry expansion, the chains in complex **7.4** pack in a layered manner and are 'stitched together' by hydrogen bonding from the protonated amino groups of the N(3) and N(4) $_{L}$-leucine molecules to form hydrogen-bonded sheets (Figure 7.21). Each of the N(3) and N(4) NH_3^+ groups in this arrangement hydrogen bond to oxygen atoms of one symmetry unique and two symmetry equivalent calixarene sulfonate groups (distances listed in Table 7.7).

N(3)···O(21)S(4)†	2.989	N(4)···O(20)S(4)†	2.770
N(3)···O(4)S(1)	2.691	N(4)···O(11)S(2)	2.936
N(3)···O(9)S(2)	2.780	N(4)···O(28)S(6)	2.784

Table 7.7 Hydrogen bonding distances between the protonated amine groups of the N(3) and N(4) $_{L}$-leucine molecules and calixarene sulfonate groups in complex **7.4** (distances given in Å, † denotes a symmetry unique calixarene sulfonate group).

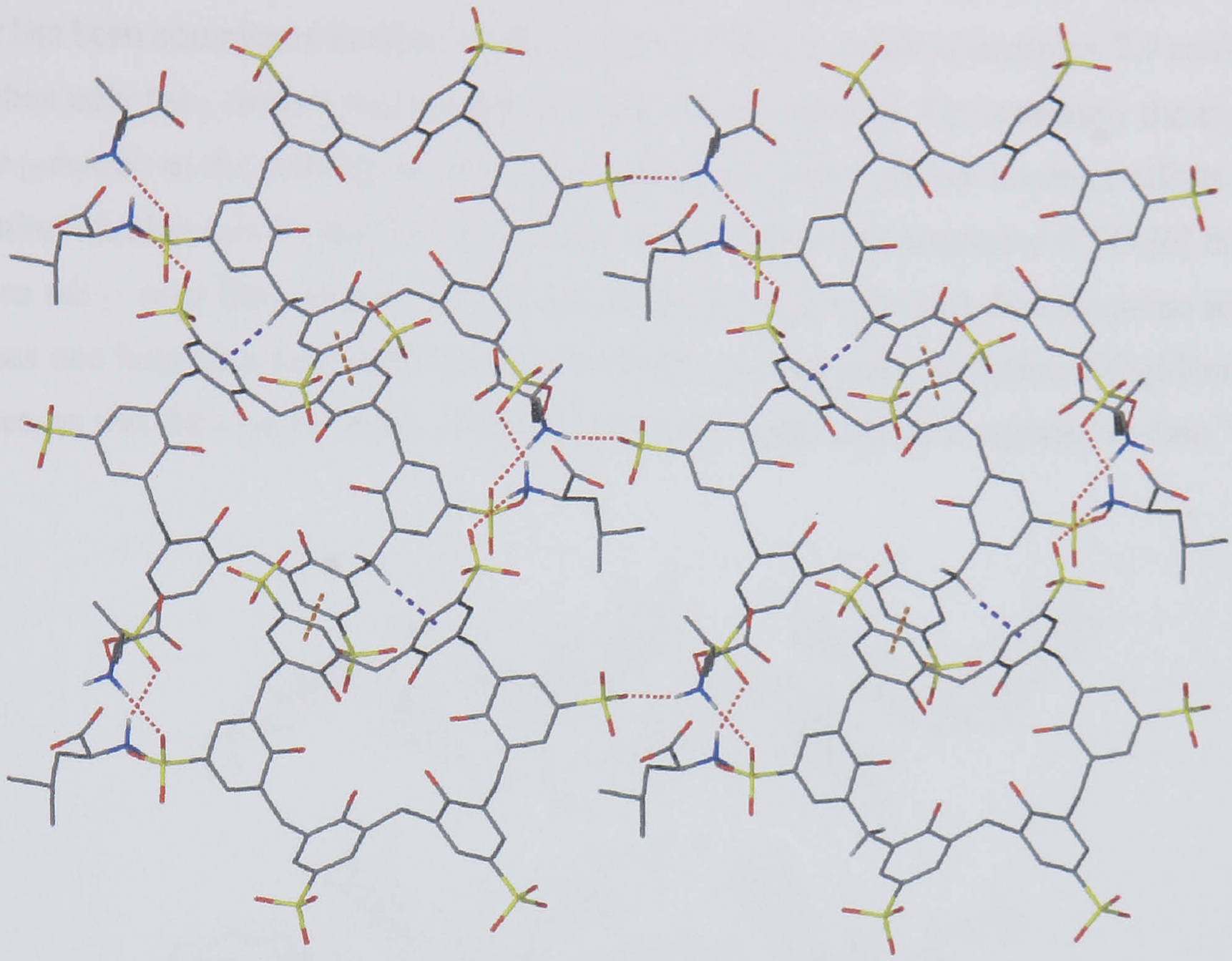

Figure 7.21 Partial packing diagram from the crystal structure of complex **7.4**. The *p*-sulfonatocalix[6]arene intra-chain π-stacking and CH···π interactions are shown as dashed orange and purple lines respectively. The NH_3^+/sulfonate hydrogen bonding 'stitches' formed between the N(3) or N(4) $_L$-leucine molecules and SO_3[6] chains are shown as dashed red lines (other $_L$-leucine molecules omitted and disordered calixarene sulfonate groups idealised for clarity).

In addition to the hydrogen bonding that links chains within sheets, there are numerous other hydrogen bonding contacts between $_L$-leucine protonated amine and carboxylic acid groups, waters of crystallisation and calixarene sulfonate groups. The extended structure reveals that some of the hydrophobic tails of the *exo* cavity $_L$-leucine molecules assemble proximate to one another in regions that are normally occupied by numerous water molecules or other hydrophilic functional groups that are present within *p*-sulfonatocalix[*n*]arene structures.

A notable feature of complex **7.4** is that SO_3[6] is able to selectively crystallise $_L$-leucine from a DL mixture of the amino acid (absolute structure parameter for complex **7.4** = 0.09(10)). As crystals of complex **7.4** grew, single crystals of a different morphology also grew and were structurally characterised to be $_L$-leucine hydrochloride. The formation of this compound is attributable to the presence of excess amino acid. A total of three data sets were collected for complex **7.4** and each found the $_L$-isomer to crystallise with SO_3[6] in the structural elucidation (all three data sets

collected on crystals from the racemic starting material). This does not determine whether or not the D-isomer has been complexed in other single crystals formed. Crystals of complex **7.4** could also be grown when only the L-isomer was employed in the reaction mixture. Unfortunately the experiment using the D-isomer as the starting material did not result in crystal growth however efforts continue to determine whether this is possible. Whilst that experiment would determine if SO_3[6] favourably complexes the L- over the D-isomer, it does not detract from the fact that the calixarene selectively crystallises one hand at a time rather than crystallising racemic pairs or sodium/SO_3[6]/amino acid complexes, as was the case for many of the SO_3[4] amino acid complexes reported to date.[59-62]

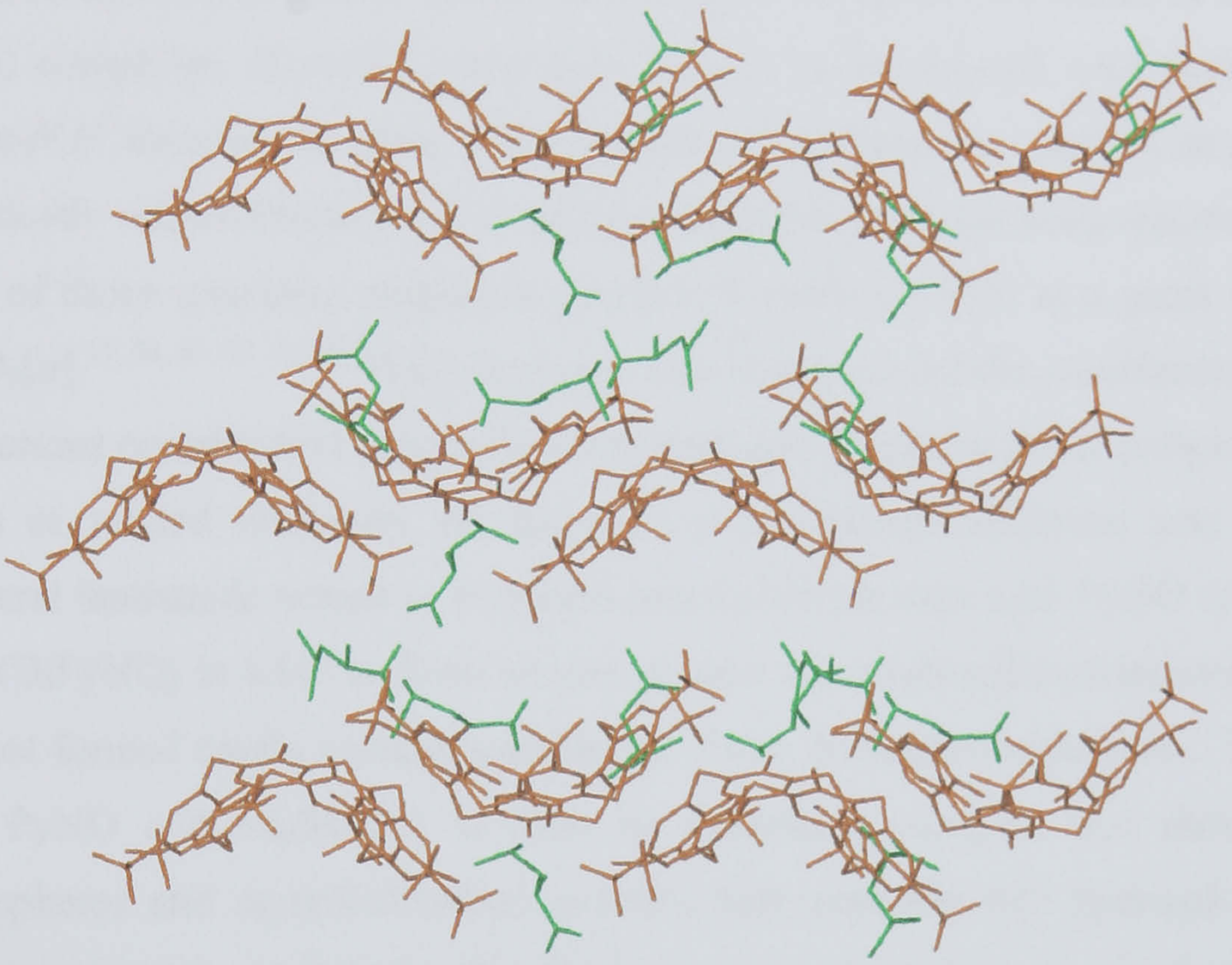

Figure 7.22 Partial packing diagram from the crystal structure of complex **7.4** showing the bi-layer type packing of *p*-sulfonatocalix[6]arene (orange, chains of which running across the page) and L-leucine molecules (green) that occupy the interstitial spaces within the lattice (cavity bound L-leucine molecules omitted and disordered calixarene sulfonate groups idealised for clarity).

7.2.2 Summary of solid state amino acid complexes of *p*-sulfonatocalix[6]arene.

Although solution studies by other research groups has shown complexation of amino acids by *p*-sulfonatocalix[6]arene, there have been no structurally reported examples of the phenomenon to date.[55, 56, 58] Of several amino acids selected, leucine was found to be the only one that formed single crystals with *p*-sulfonatocalix[6]arene at a pH <1. The structural solution showed the calixarene to adopt the 'double cone' conformation and to bear host to two L-leucine molecules in the pseudo-

calix[3]arene cavities. Complex **7.4** also showed that the calixarene complexes leucine selectively the L- and possibly D-form in different handed crystals. Although the number of structural examples of *p*-sulfonatocalix[6]arene adopting the 'double cone' conformation are limited (all in this chapter), they are all formed at a pH < 3. This pH range may help to maintain or stabilise the hydrogen bonding regime at the base of the calixarene and favour the 'double cone' conformation.

7.3 Metal/pyridine *N*-oxide (or 4,4'-dipyridine-*N,N'*-dioxide) complexes of *p*-sulfonatocalix[6]arene.

This section describes the formation and structural characterisation of a series of metal (lanthanide and transition) complexes of *p*-sulfonatocalix[6]arene that are formed with pyridine *N*-oxide or 4,4'-dipyridine-*N,N'*-dioxide. As described in the preceding chapters, a significant proportion of the crystallographically related literature of *p*-sulfonatocalix[*n*]arenes has been reported by Atwood *et al.* and many of those structures employed pyridine *N*-oxide (PyNO) as a guest molecule for the cavities of $SO_3[n]$.[17, 33, 35, 39, 41, 68] This chemistry was based around the *p*-sulfonatocalix[4,5]arenes and showed various coordination modes for lanthanide and transition metal complexes with PyNO. As analogous or related chemistry incorporating *p*-sulfonatocalix[6]arene was unexplored, we employed several lanthanide nitrate or transition metal chloride salts with PyNO or 4,4'-dipyridine-*N,N'*-dioxide (DiPyNO) in a bid to form interesting new supramolecular architectures with $SO_3[6]$. Four complexes formed single crystals suitable for X-ray diffraction techniques. Ytterbium nitrate reacted with PyNO and $Na_8SO_3[6]$ to form an interesting complex that shows varied metal coordination spheres and metal/calixarene moieties that assemble into hydrogen bonded sheets. When lanthanum nitrate is employed under identical conditions, only one unique metal coordination sphere is evident and the calixarene assembles in a new corrugated bi-layer motif. When nickel chloride is employed in excess, also under similar conditions, a bi-layer arrangement forms that shows free PyNO molecules to occupy 'partial cones' of $SO_3[6]$ whilst non-coordinating nickel hexa-aquo ions reside in the hydrophilic layers. Finally when PyNO is replaced by DiPyNO with europium nitrate and $Na_8SO_3[6]$, a bi-layer zig-zag coordination polymer forms that displays graphitic hydrogen bonded sheets in the extended structure.

7.3.1 Structure of the complex $[Yb(H_2O)_6$(pyridine *N*-oxide)(*p*-sulfonatocalix-[6]arene$)_{0.5}][Yb(H_2O)_5$(pyridine *N*-oxide$)_2$(*p*-sulfonatocalix[6]arene$)_{0.5}]\cdot 9H_2O\cdot$2pyridine *N*-oxide, 7.5.

Crystals of the complex $[Yb(H_2O)_6$(pyridine *N*-oxide)(*p*-sulfonatocalix-[6]arene$)_{0.5}][Yb(H_2O)_5$(pyridine *N*-oxide$)_2$(*p*-sulfonatocalix[6]arene$)_{0.5}]\cdot 9H_2O\cdot$2pyridine *N*-oxide,

7.5, grew upon standing over two days from an aqueous solution containing a 1:2.3:2 mixture of Na_8SO_3[6], pyridine *N*-oxide and ytterbium(III) nitrate pentahydrate (Equation 7.5). The complex was characterised by IR spectroscopy and single crystal X-ray crystallography. Complex 7.5 crystallises in a triclinic cell and the structural solution was performed in the space group $P\bar{1}$. Details of data collection and structure refinement are given in Table 7.17 of this chapter. A crystallographic information file containing all bond lengths and angles for complex 7.5 can be found in appendix 7.3.1 on the attached compact disc.

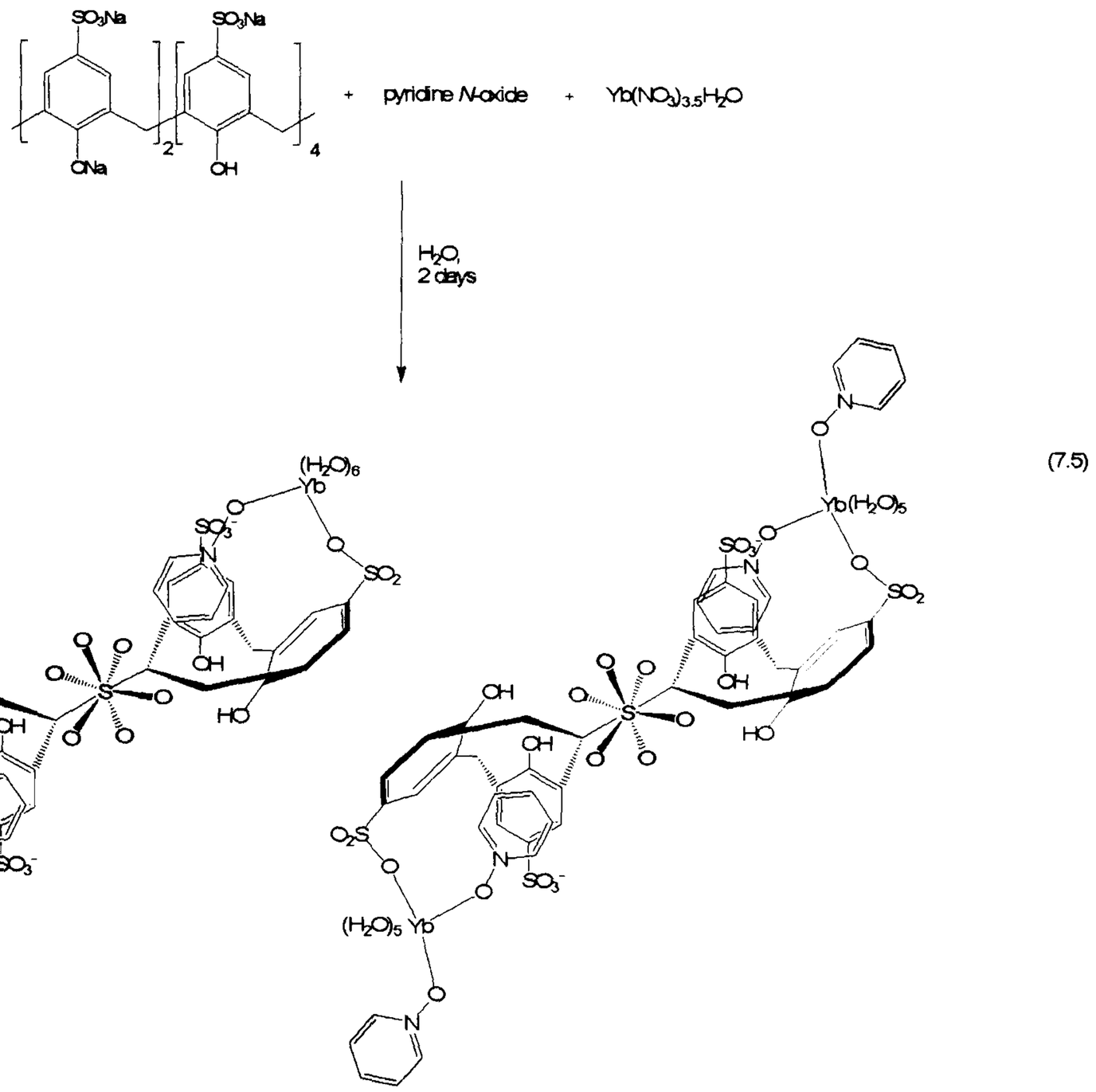

The asymmetric unit comprises primarily of two ytterbium/half SO_3[6] moieties. One ytterbium centre has five aquo ligands and two coordinated PyNO molecules. The other ytterbium centre has six aquo ligands and one coordinated PyNO molecule. In addition to this there are two free pyridine *N*-oxide molecules (one of which is disordered over two positions) and a total of nine solvent water molecules that are disordered over eleven positions (Figure 7.23). To aid discussion each ytterbium/half SO_3[6]/PyNO fragment shall be discussed separately as parts **A** and **B** (according to the labelling in Figure 7.23). Both of the calixarenes, when symmetry expanded are seen to adopt the up-down 'double partial cone' conformation. The two parts are linked (partly) through π-stacking and aromatic CH···π interactions between the coordinated and non-coordinating PyNO molecules and this shall be discussed further below.

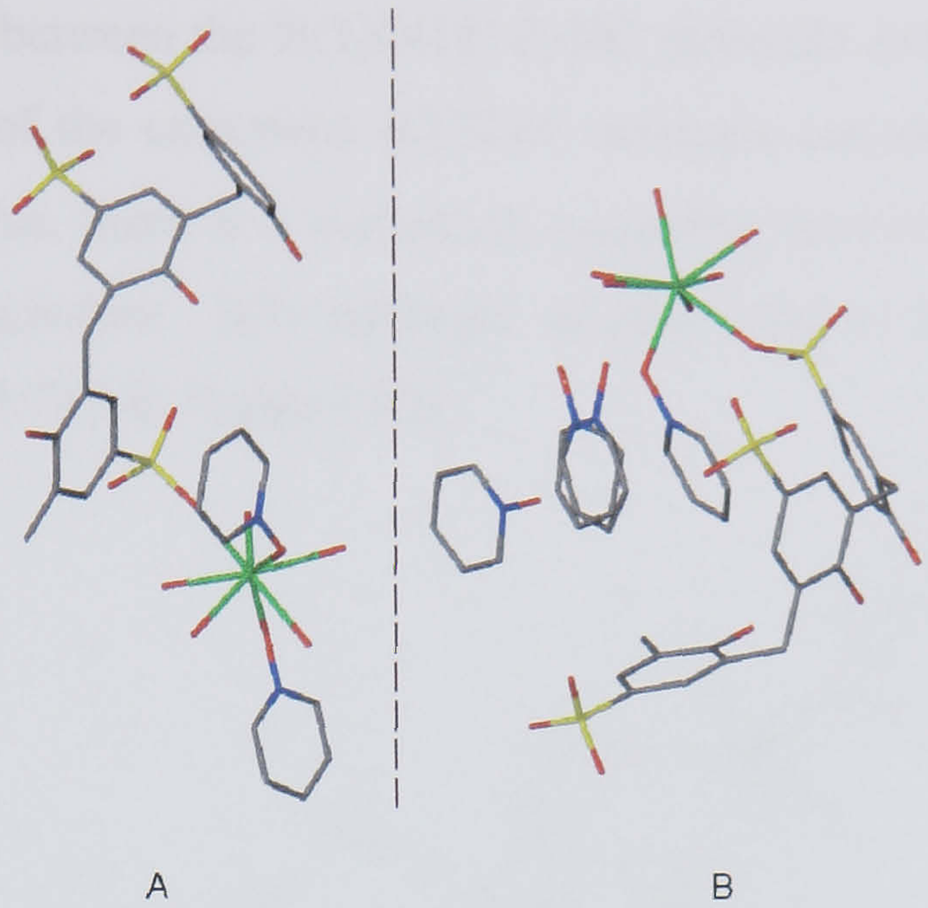

Figure 7.23 Stick representation of part of asymmetric unit from the crystal structure of complex **7.5**. The asymmetric unit diagram has been divided into two parts (**A** and **B**) to aid discussion.

The ytterbium metal centre of part **A** has five aquo ligands, two coordinated PyNO molecules and is of square anti-prismatic geometry (Figure 7.24). Bond lengths relating to the coordination sphere of Yb(2) are listed in Table 7.8. Both of the PyNO molecules are bound through the oxygen atoms of the polar *N*-oxide groups. The half SO_3[6] resides on a centre of inversion and symmetry expansion reveals the 'double partial cone' conformation. The N(1)O(18) PyNO molecule (and symmetry equivalent) is directed into the resultant partial cone whilst the N(2)O(19) PyNO molecule (and symmetry equivalent) is seen to point away from the asymmetric unit (Figure 7.25).

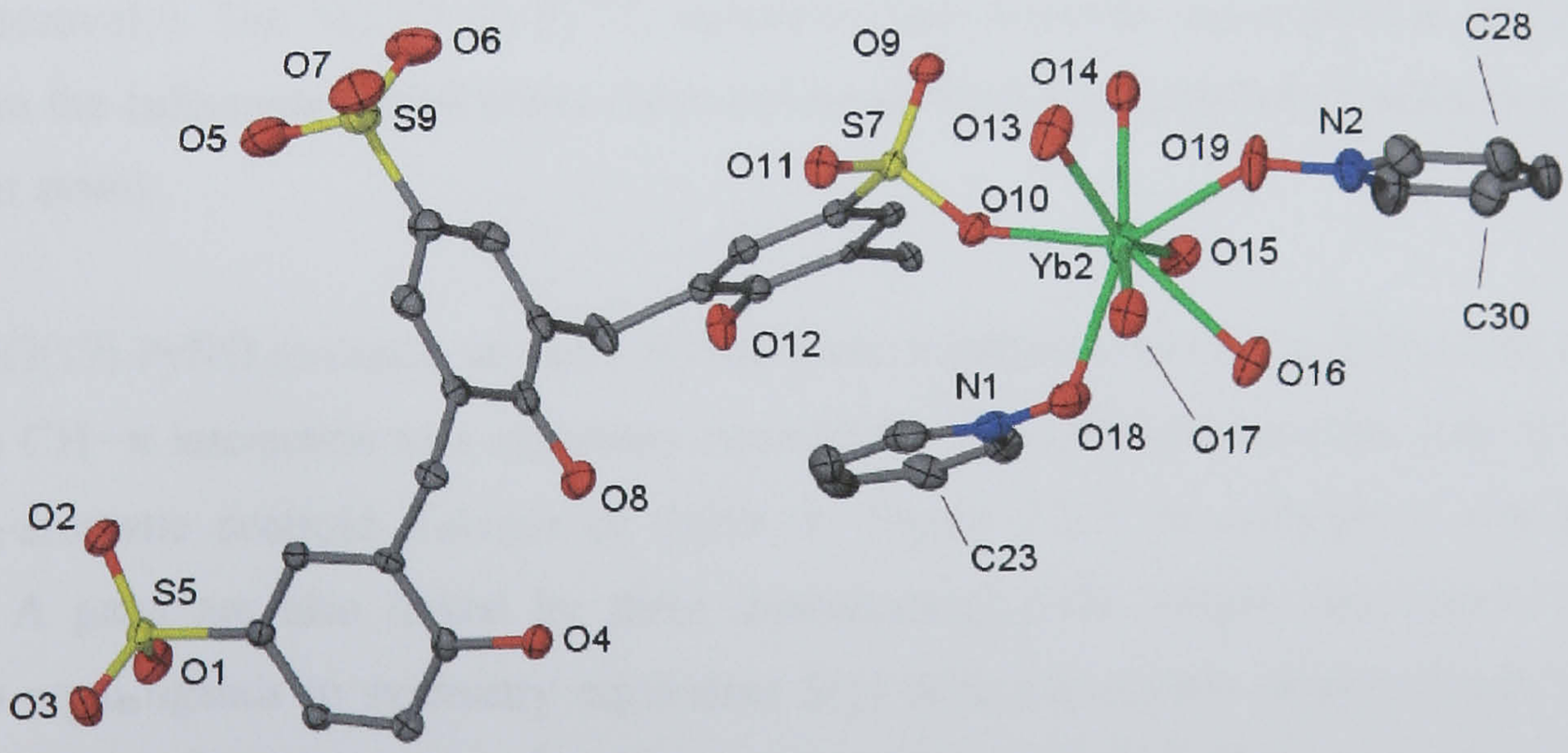

Figure 7.24 Part **A** of the asymmetric unit from the crystal structure of complex **7.5**, anisotropic displacement ellipsoids shown at the 50% probability level. Selected atoms have been labelled.

There is a ArH···π interaction between the N(1)O(18) PyNO molecule and a symmetry equivalent S(5) sulfonate aromatic ring of the calixarene (C(23)H···aromatic centroid distance of 2.742 Å, Figure 7.25). In addition to this, there is a π-stacking interaction between the N(1)O(18) PyNO molecule and a symmetry equivalent S(7) sulfonate aromatic ring of the calixarene (aromatic centroid···centroid distance of 3.748 Å, Figure 7.25).

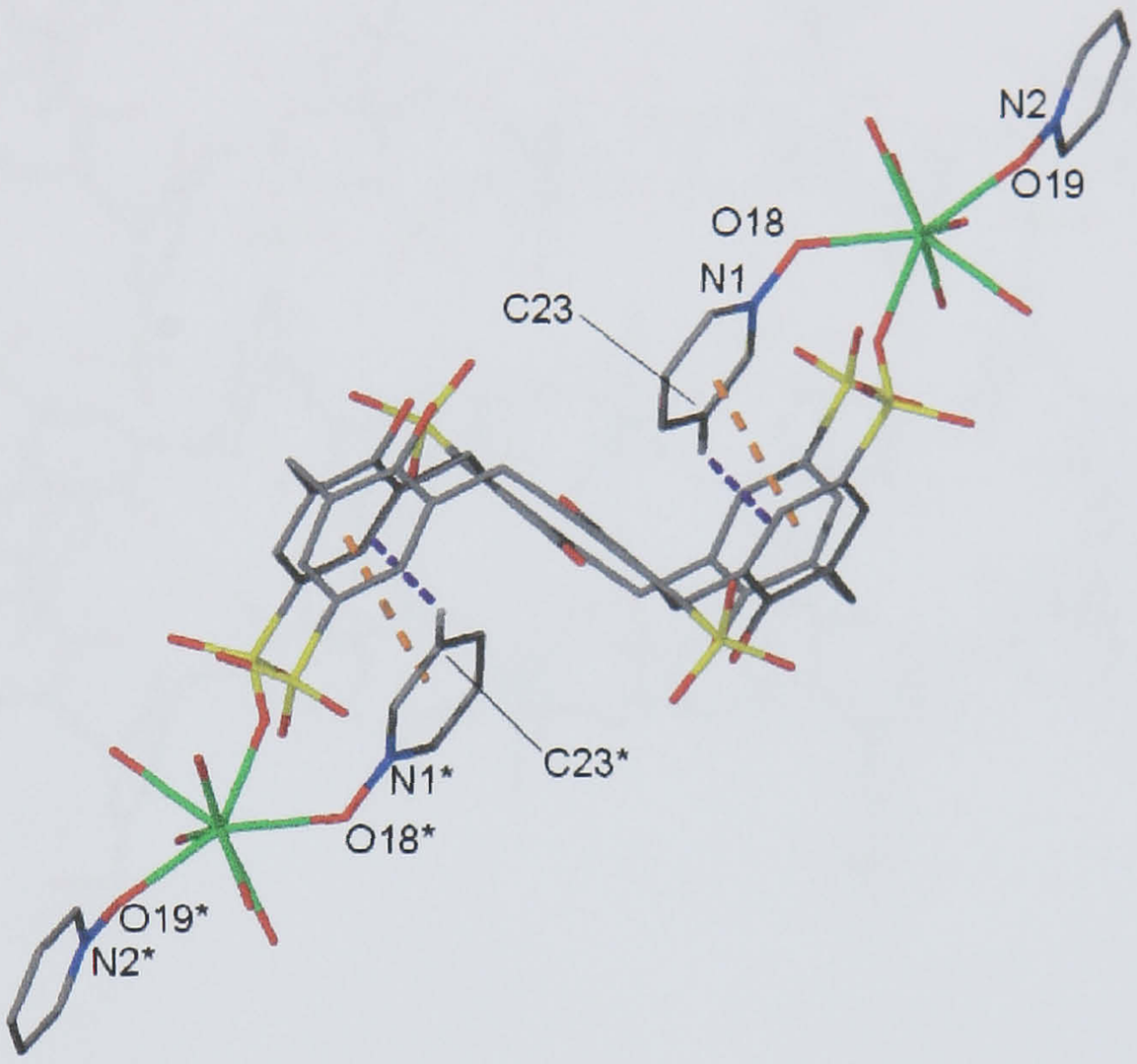

Figure 7.25 Symmetry expansion of part **A** from the crystal structure of complex **7.5**. The positioning of the N(1)O(18) PyNO molecule (and symmetry equivalent) and the CH···π and π-stacking interactions within the partial cone of the SO_3[6] are shown (dashed purple and orange lines respectively). The N(2)O(19) PyNO molecule (and symmetry equivalent) is shown to point away from the calixarene partial cones. Selected atoms have been labelled (* denotes a symmetry equivalent atom).

The N(2)O(19) PyNO molecule is partly directed into a partial cone of a neighbouring part **A** and there is a CH···π interaction to a symmetry equivalent S(9) sulfonate aromatic ring of an SO_3[6] (C(28)H···aromatic centroid distance of 2.659 Å, Figure 7.26). In addition to this interaction identical **A** parts are also linked by three crystallographically unique interactions from three ytterbium aquo ligands to symmetry equivalent S(5) sulfonate oxygen atoms (Figure 7.26). The Yb(2)O(15) aquo ligand hydrogen bonds to a symmetry equivalent O(1) atom with a YbO···OS distance of 2.792 Å. The Yb(2)O(16) aquo ligand hydrogen bonds to a symmetry equivalent O(1) atom (different to the one for the Yb(2)O(15) aquo ligand) with a YbO···OS distance of 2.707 Å. Finally, the Yb(2)O(17) aquo ligand hydrogen bonds to a symmetry equivalent O(2) atom with a YbO···OS distance of 2.829 Å.

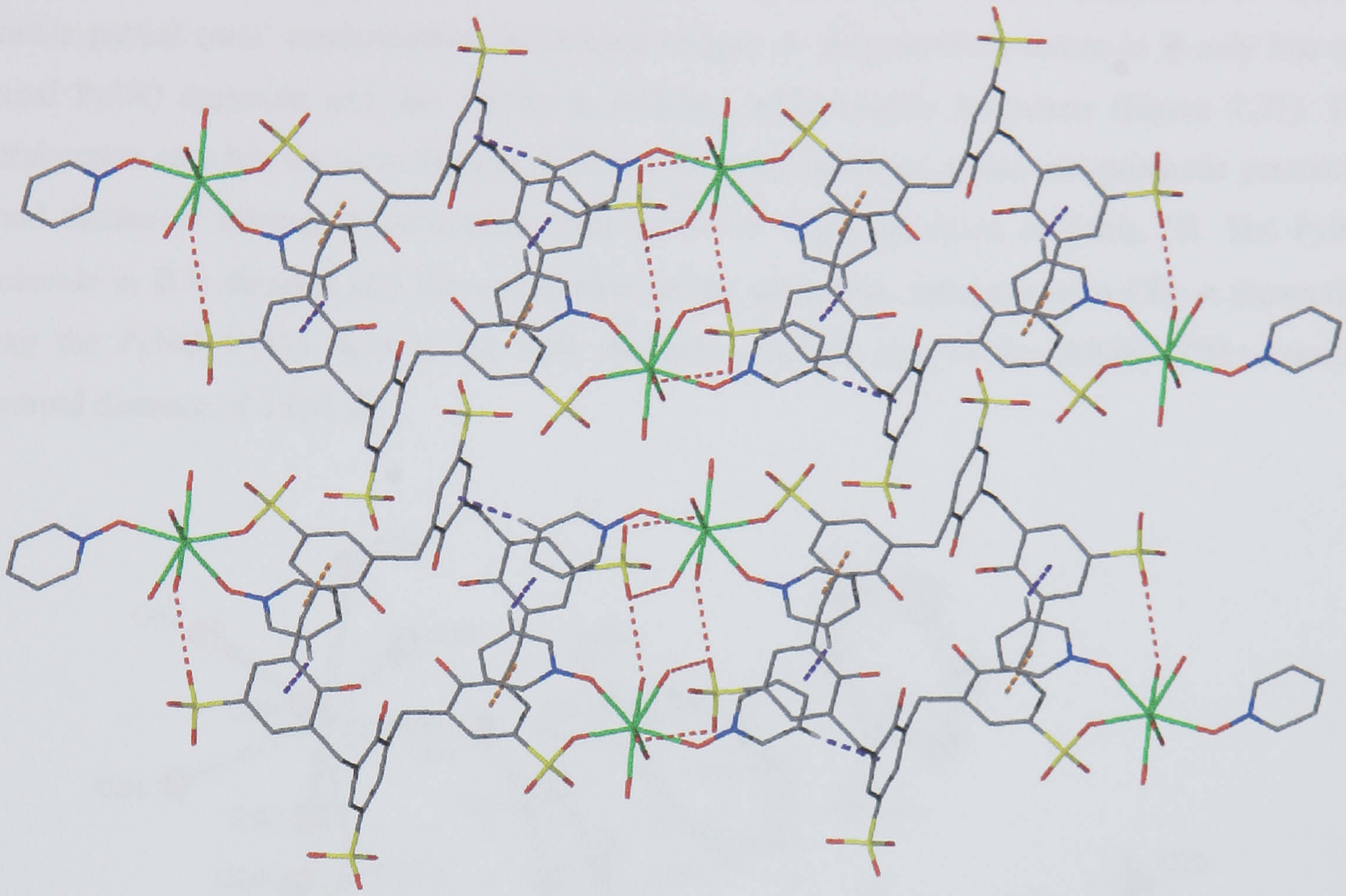

Figure 7.26 A hydrogen bonded sheet of part **A** from the crystal structure of complex **7.5**. The CH···π interactions between the N(2)O(19) PyNO molecules and the neighbouring host aromatic groups are shown (dashed purple line). The CH···π and π-stacking interactions for the N(1)O(18) PyNO molecule are also shown (as in Figure 7.25). The YbO···OS hydrogen bonds are shown as dashed red lines.

Yb(1)-O(28)	2.385(3)	Yb(1)-O(32)	2.279(4)
Yb(1)-O(33)	2.353(3)	Yb(1)-O(34)	2.335(4)
Yb(1)-O(35)	2.334(3)	Yb(1)-O(36)	2.402(3)
Yb(1)-O(37)	2.343(3)	Yb(1)-O(38)	2.260(4)
Yb(2)-O(10)	2.267(3)	Yb(2)-O(13)	2.349(4)
Yb(2)-O(14)	2.343(4)	Yb(2)-O(15)	2.359(4)
Yb(2)-O(16)	2.421(4)	Yb(2)-O(17)	2.354(4)
Yb(2)-O(18)	2.328(4)	Yb(2)-O(19)	2.259(4)

Table 7.8 Interatomic distances relating to the coordination sphere of the ytterbium metal centres in the crystal structure of complex **7.5** (distances given in Å with e.s.d. in parentheses).

The half SO_3[6] in part **B** also resides on a centre of inversion and symmetry expansion reveals the 'double partial cone' conformation. In contrast to part **A**, the ytterbium centre in **B** only has one bound PyNO molecule and this results in different self-assembly behaviour (Figure 7.27). The metal centre also has six aquo ligands, is octa-coordinate and is of square anti-prismatic geometry. Bond distances relating to the coordination sphere of Yb(1) are listed in Table 7.8. The PyNO molecule in **B** is directed into the partial cone of the calixarene and there is an CH···π interaction from the PyNO C(54) atom to the S(4) sulfonate aromatic ring of the SO_3[6] (CH···aromatic centroid distance of 3.091 Å).

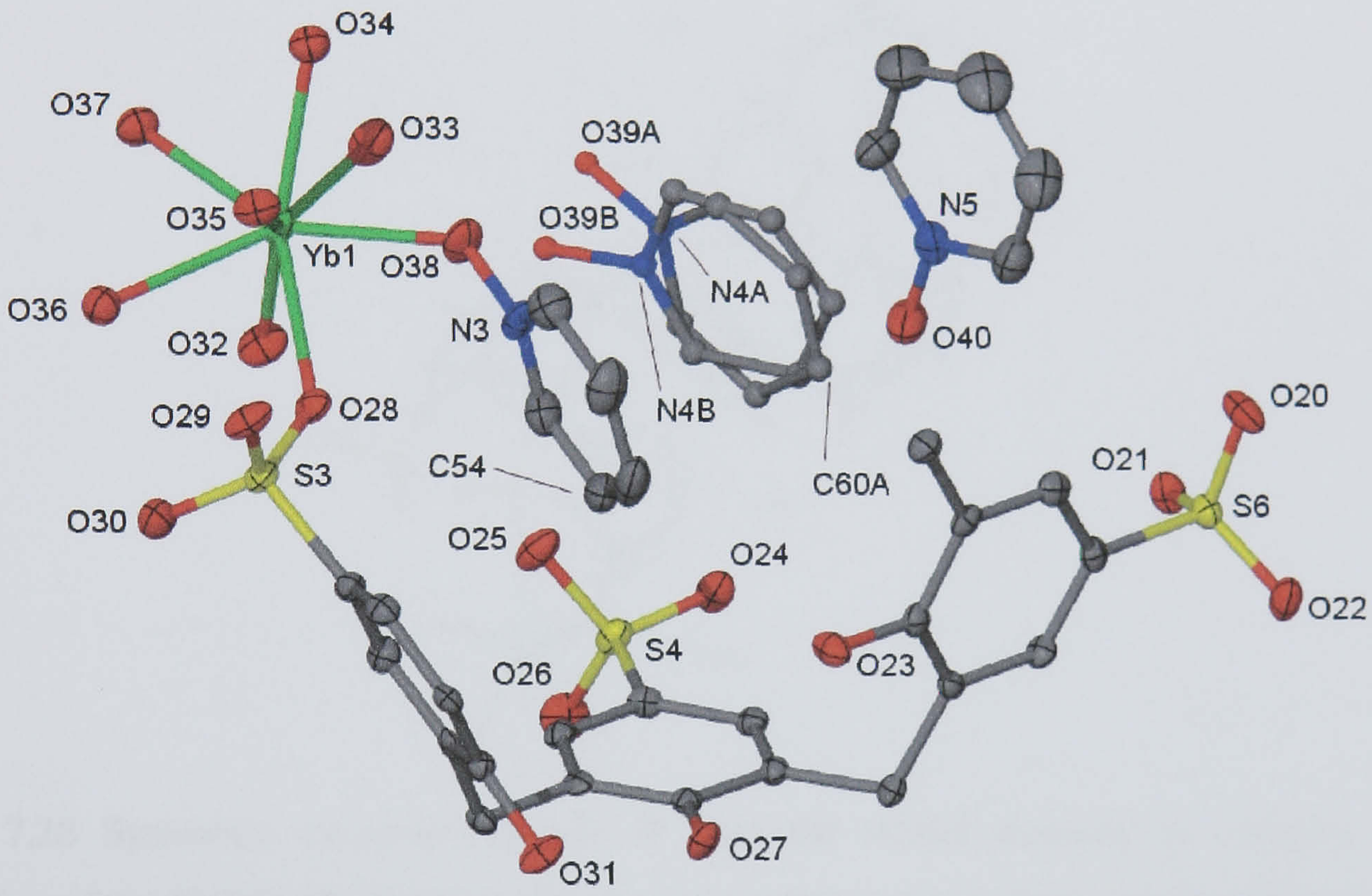

Figure 7.27 Part **B** of the asymmetric unit from the crystal structure of complex **7.5**, anisotropic displacement ellipsoids shown at the 50% probability level. The disordered pyridine *N*-oxide molecule is shown in ball and stick representation with a reduced atom radius for visual clarity. Selected atoms have been labelled.

The two remaining PyNO molecules (N(4A and B)O(39A and B) and N(5)O(40)) will be discussed in relation to the extended structure further below. As mentioned above, part **A** is seen to assemble into hydrogen bonded chains. The different number of coordinated PyNO molecules in **B** results in very different self-assembly behaviour, that being the formation of a hydrogen bonded sheet. Identical **B** parts within the sheet are partly linked by four crystallographically unique interactions from three ytterbium aquo ligands to symmetry equivalent sulfonate group oxygen atoms (Figure

7.29). The Yb(1)O(33) aquo ligand hydrogen bonds to a symmetry equivalent O(25) atom with a YbO···OS distance of 2.733 Å. The Yb(1)O(35) aquo ligand hydrogen bonds to a symmetry equivalent O(21) atom with a YbO···OS distance of 2.736 Å. The Yb(1)O(36) aquo ligand hydrogen bonds to a symmetry equivalent O(24) atom with a YbO···OS distance of 2.743 Å. Finally, the Yb(1)O(37) aquo ligand hydrogen bonds to a symmetry equivalent O(24) atom (different to the one for the Yb(1)O(36) aquo ligand) with a YbO···OS distance of 2.882 Å. Additional linking is in the form of one crystallographically unique hydrogen bond from a SO_3[6] 'base' hydroxyl group to a neighbouring calixarene sulfonate group (ArO(27)···O(22)S(6) distance of 2.783 Å).

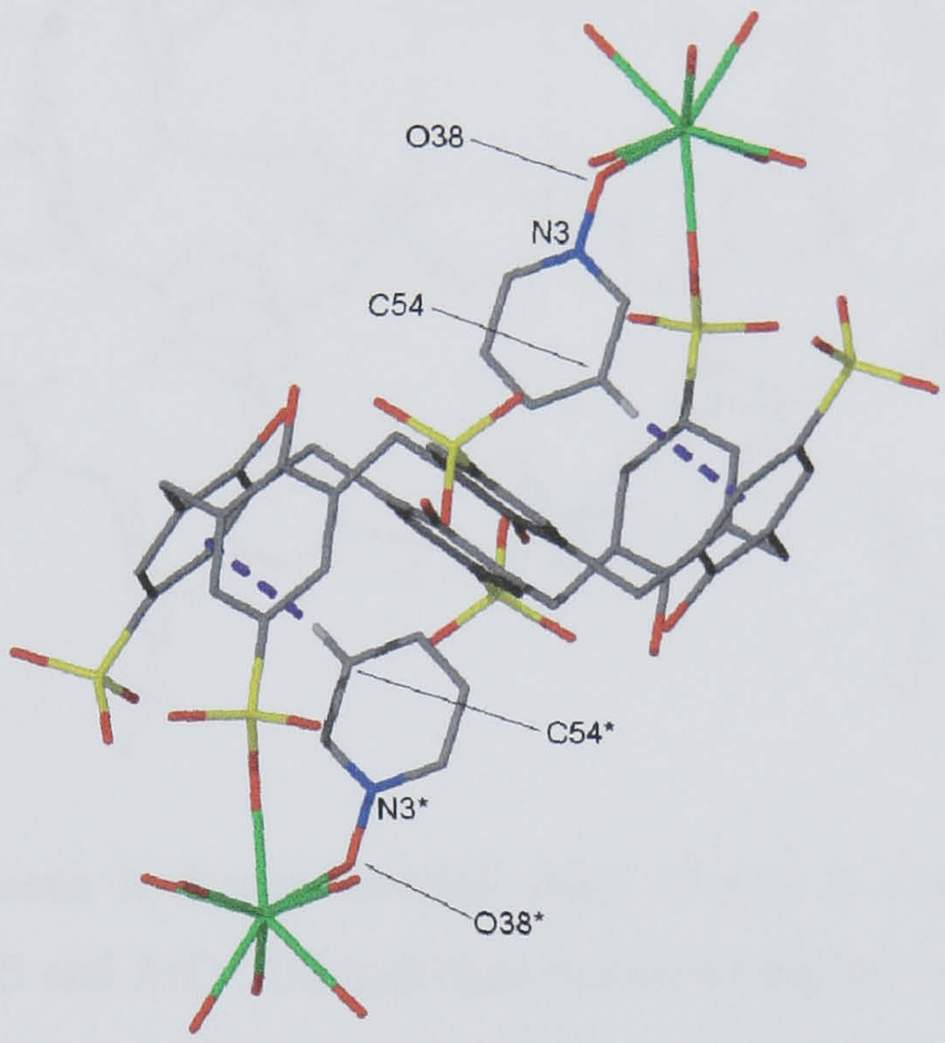

Figure 7.28 Symmetry expansion of part **B** from the crystal structure of complex **7.5**. The positioning of the N(3)O(38) PyNO molecule (and symmetry equivalent) and the CH···π interaction within the partial cone of the SO_3[6] are shown (dashed purple line, * denotes a symmetry equivalent atom, key operation for symmetry related atoms: 1-x, -y, -z).

When the extended structure is examine, the uni-composite sheets of **A** and **B** are linked by several π-stacking, hydrogen bonding and CH···π interactions. The non-coordinating PyNO molecules partake in a series of CH···π and π-stacking interactions with coordinated PyNO in **A** and **B** (Figure 7.29). There is on CH···π interaction between the PyNO that points away from the partial cone in A and the N(5)O(40) non-coordinating PyNO (PyH···aromatic centroid distance of 3.024 Å). The N(5)O(40) non-coordinating PyNO π-stacks with the disordered N(4)O(39) non-coordinating PyNO with an aromatic centroid···centroid distance of 3.661 Å. The link is completed by another π-stacking interaction between the non-coordinating N(4)O(39) and the coordinated with the N(3)O(38) PyNO with an aromatic centroid···centroid distance of 3.887 Å. The non-coordinating

PyNO molecules have several hydrogen bonding contacts with ytterbium aquo ligands of both A and B (YbO···OPy distances ranging from 2.637 – 2.933 Å).

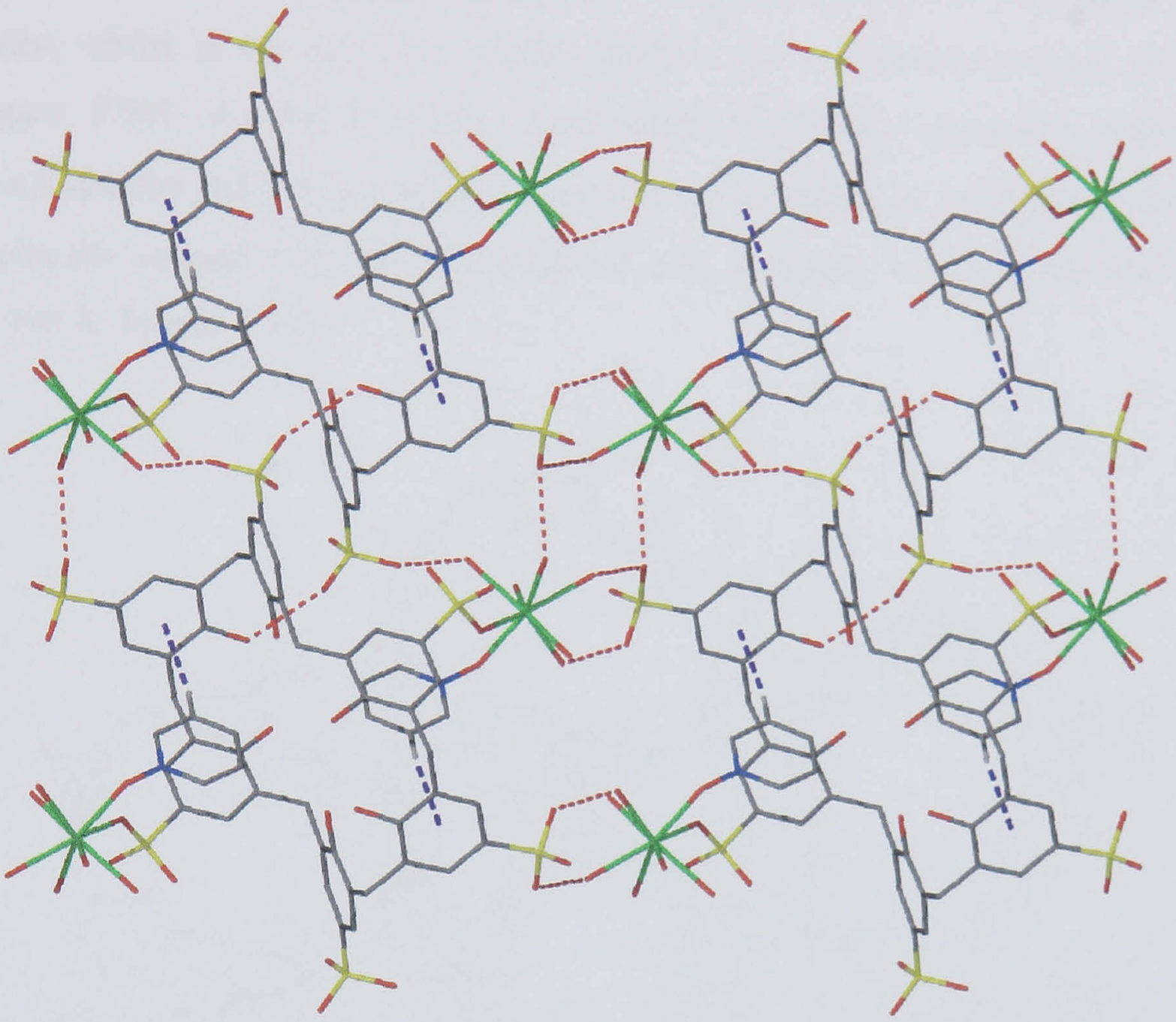

Figure 7.29 A uni-composite hydrogen bonded sheet of part B from the crystal structure of complex **7.5**. The YbO···OS and ArO···OS hydrogen bonds are shown as dashed red lines whilst the CH···π interactions are shown as dashed purple lines (as in Figure 7.28).

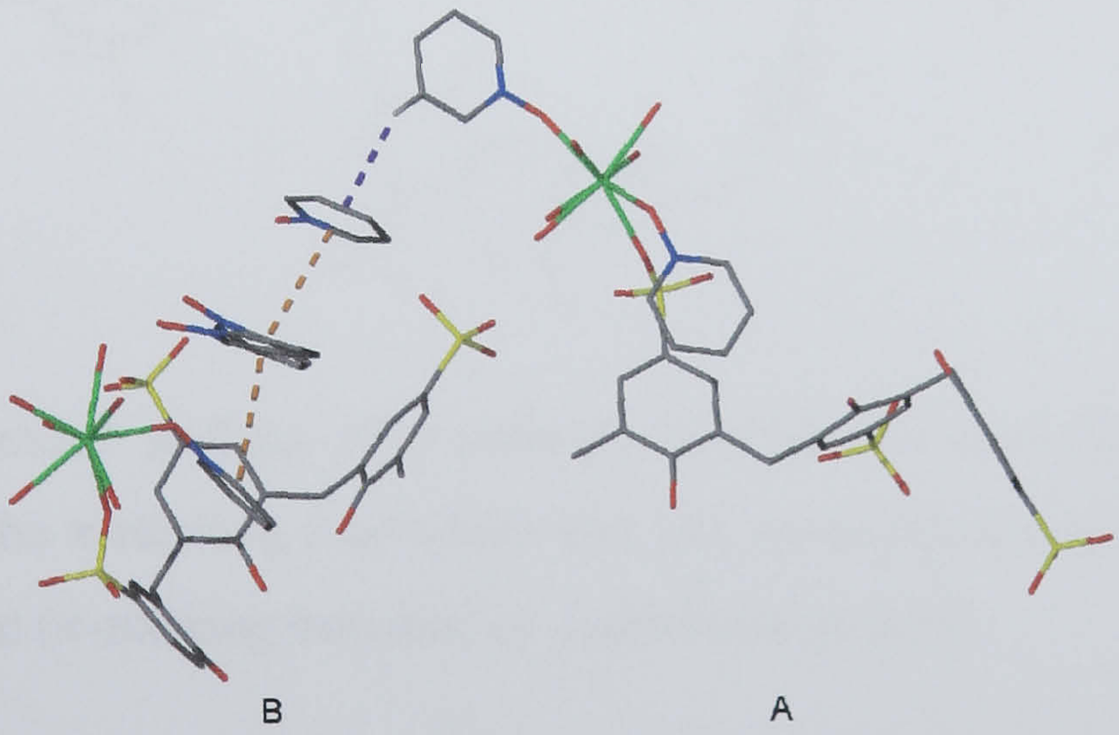

Figure 7.29 A link found between parts **A** and **B** from the crystal structure of complex **7.5**. The CH···π and π-stacking interactions are shown as dashed purple and orange lines respectively.

The extended structure displays a bi-layer motif that is similar to the one documented by Atwood *et al.* for the octa-sodium salt and sulfonic acid of SO_3[6].[69] Although reported, the bi-layer arrangement was not described in detail. In the octa-sodium salt, sulfonic acid and in complex **7.5**, the calixarenes, whilst in the up-down 'double partial cone' conformation pack in a hexagonal fashion (Figure 7.30). As for SO_3[4,5], *p*-sulfonatocalix[6]arene optimises hydrophobic and hydrophilic interactions and this is evident in complex **7.5** through four π-stacking interactions (two crystallographically unique π-stacking interactions with aromatic centroid···centroid distances of 3.947 and 3.990 Å, Figure 7.30).

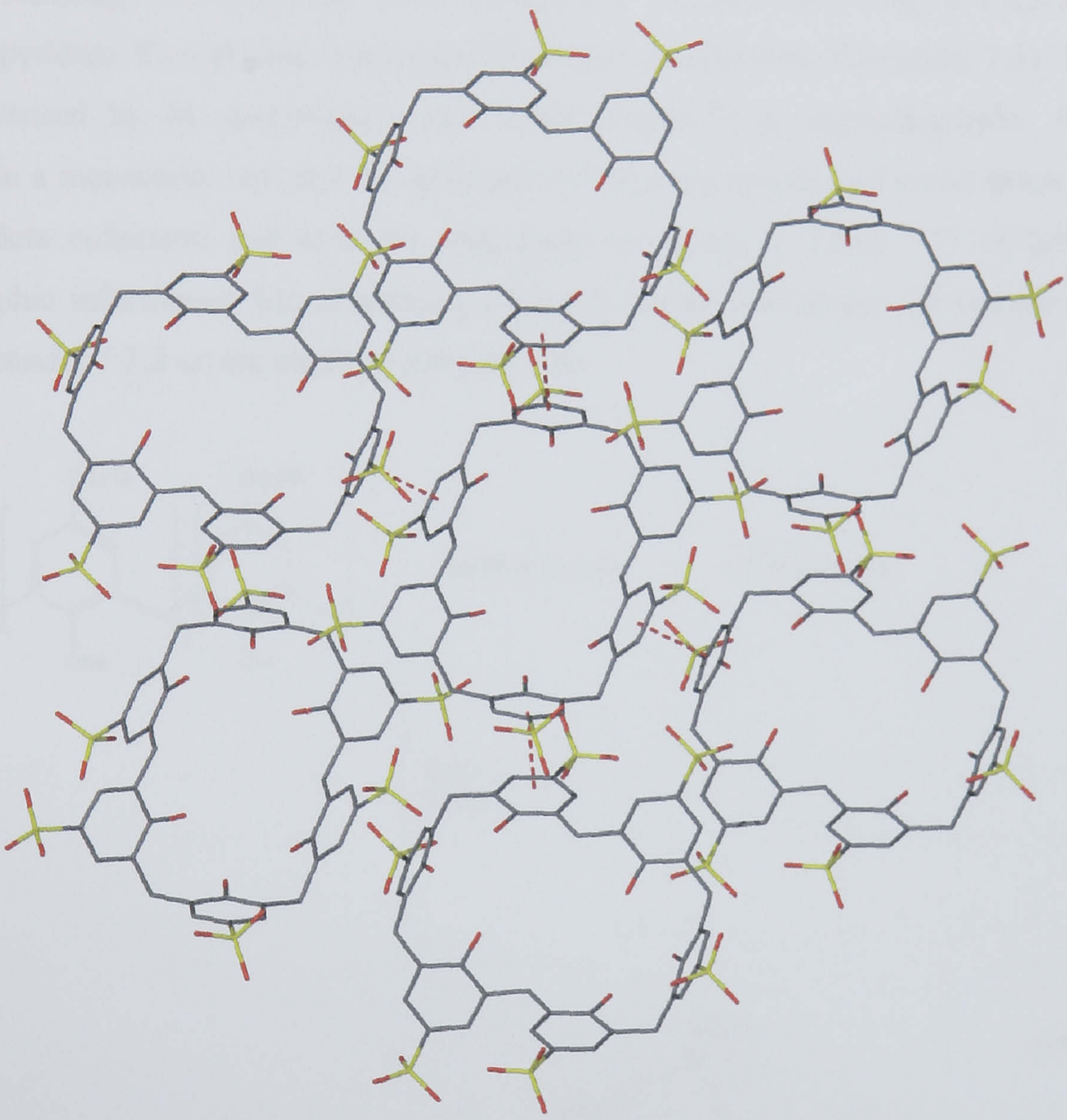

Figure 7.30 The extended packing of *p*-sulfonatocalix[6]arene from the crystal structure of complex **7.5** showing the π-stacking interactions that link uni-composite sheets of **A** and **B** within the bi-layer arrangement (π-stacking indicated by dashed orange lines).

In addition to all of the interactions described above, the numerous waters of crystallisation are in positions consistent with hydrogen bonding to ytterbium aquo ligands, PyNO molecules and *p*-sulfonatocalix[6]arene sulfonate groups. When ytterbium was replaced by lanthanum nitrate under identical molar ratios of reactants, a lanthanum/PyNO/SO_3[6] complex forms that shows only one

unique coordination sphere for the lanthanum metal centre but also shows the calixarenes to assemble in an unusual corrugated bi-layer arrangement that is very different to that shown for complex **7.5**.

7.3.2 Structure of the complex $[(La(H_2O)_7(\text{pyridine } N\text{-oxide}))_2(p\text{-sulfonatocalix-}[6]\text{arene})]\cdot 6H_2O$, 7.6.

Crystals of the complex $[(La(H_2O)_7(\text{pyridine } N\text{-oxide}))_2(p\text{-sulfonatocalix-}[6]\text{arene})]\cdot 6H_2O$, **7.6**, grew upon standing over two days from an aqueous solution containing a 1:2.3:2 mixture of $Na_8SO_3[6]$, pyridine *N*-oxide and lanthanum(III) nitrate hexahydrate (Equation 7.6). The complex was characterised by IR spectroscopy and single crystal X-ray crystallography. Complex **7.6** crystallises in a monoclinic cell and the structural solution was performed in the space group $P2_1/c$. Details of data collection and structure refinement are given in Table 7.17 of this chapter. A crystallographic information file containing all bond lengths and angles for complex **7.6** can be found in appendix 7.3.2 on the attached compact disc.

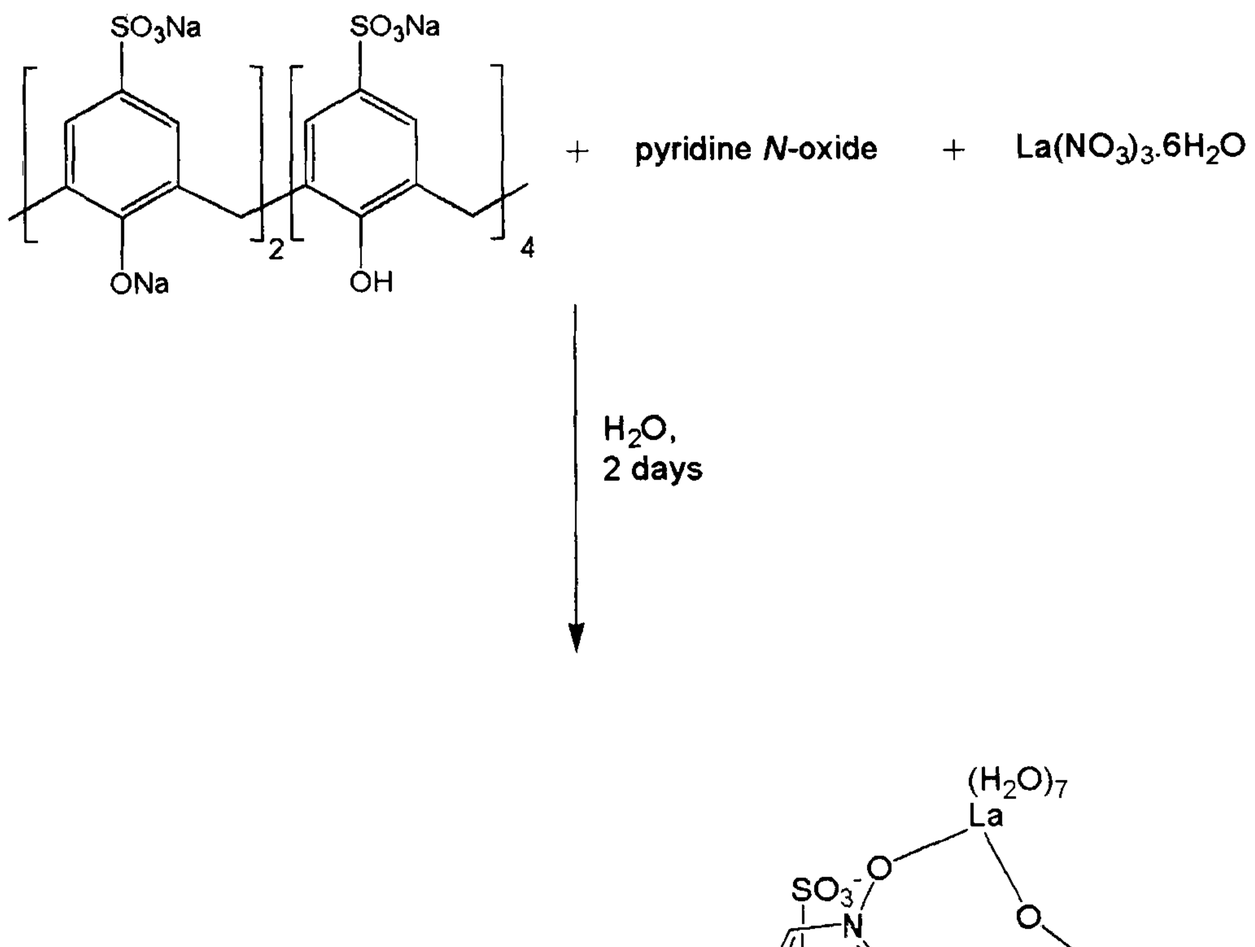

(7.6)

The asymmetric unit consists of one half of an SO_3[6] molecule and one sulfonate bound hepta-aqua lanthanum centre that also has a coordinated pyridine *N*-oxide molecule (Figure 7.31). In addition to this there are three waters of crystallisation all of which are at full occupancy. The lanthanum centre is nona-coordinate and has tri-capped trigonal prismatic geometry. The bond lengths relating to the coordination sphere of the lanthanum centre are listed in Table 7.9. The PyNO molecule that is coordinated to the lanthanum centre is directed into the 'partial cone' of the calixarene and there is a CH···π interaction from the C(22) atom to the S(1) sulfonate aromatic ring of the SO_3[6] (CH···aromatic centroid distance of 2.751 Å, Figure 7.32).

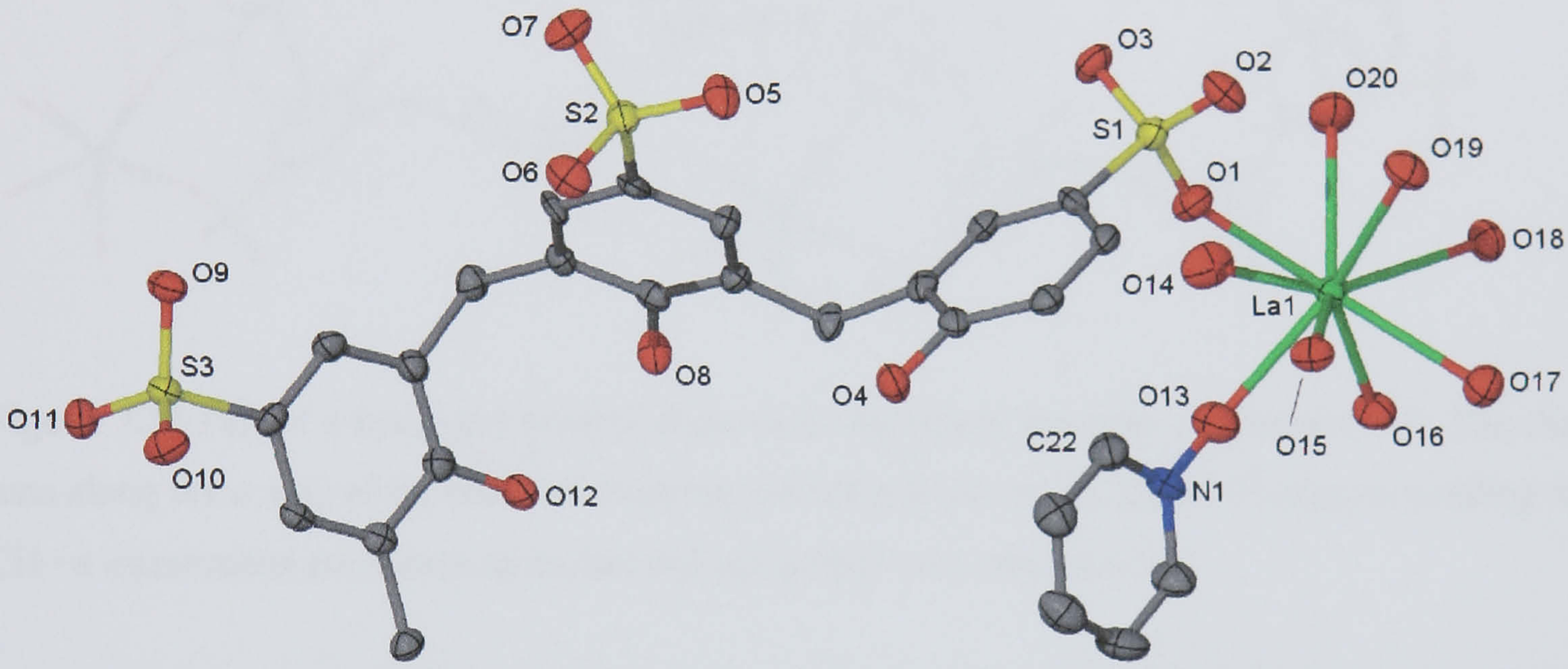

Figure 7.31 Part of the asymmetric unit from the crystal structure of complex **7.6**, anisotropic displacement ellipsoids shown at the 50% probability level. Selected atoms have been labelled.

La(1)-O(1)	2.486(5)	La(1)-O(13)	2.421(6)
La(1)-O(14)	2.630(6)	La(1)-O(15)	2.511(5)
La(1)-O(16)	2.585(5)	La(1)-O(17)	2.610(6)
La(1)-O(18)	2.571(5)	La(1)-O(19)	2.606(5)
La(1)-O(20)	2.656(6)		

Table 7.9 Interatomic distances relating to the coordination sphere of the ytterbium metal centres in the crystal structure of complex **7.6** (distances given in Å with e.s.d. in parentheses).

In order to better understand the extended structure, discrete hydrogen bonding regimes will be described separately. Upon symmetry expansion the asymmetric unit forms hydrogen bonded chains along the *a* axis of the unit cell (Figure 7.32). There are four crystallographically unique

hydrogen bonding contacts between lanthanum aquo ligands and symmetry equivalent calixarene sulfonate groups in the formation of the chains as shown in Figure 7.32 (LaO···OS distances listed in Table 7.10). Parallel chains are partially linked through two crystallographically unique inter-chain hydrogen bonds between lanthanum aquo ligands and symmetry equivalent calixarene sulfonate groups (LaO···OS distances listed in Table 7.10).

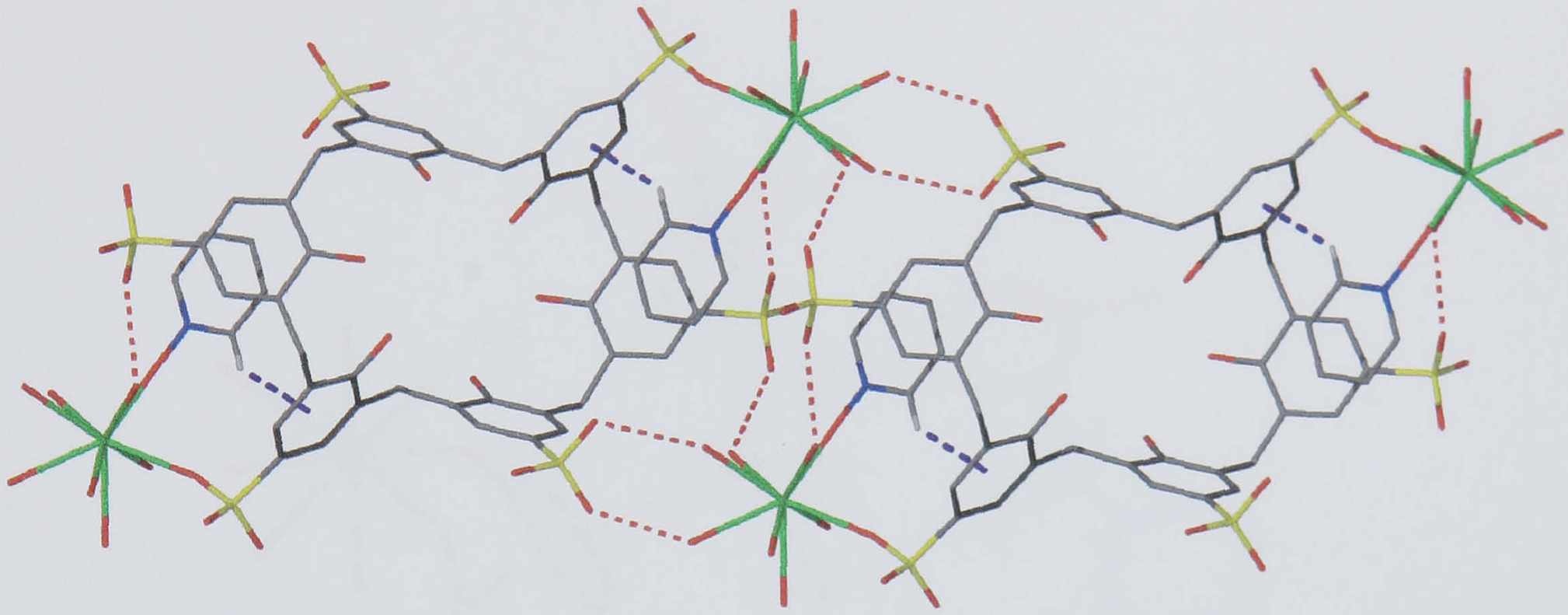

Figure 7.32 Part of a hydrogen bonded chain from the crystal structure of complex **7.6**. The chain runs along the *a* axis of the unit cell (running horizontally across the page). Hydrogen bonding and CH···π interactions are shown as dashed red and purple lines respectively.

INTRA-CHAIN		INTER-CHAIN	
La(1)-(O15)···O(10)-S(3)	2.669	La(1)-(O16)···O(11)-S(3)	2.756
La(1)-(O16)···O(9)-S(3)	2.851	La(1)-(O18)···O(9)-S(3)	2.682
La(1)-(O17)···O(6)-S(2)	2.915		
La(1)-(O17)···O(7)-S(2)	2.654		

Table 7.10 Crystallographically unique intra and inter-chain hydrogen bonding contacts between lanthanum aquo ligands and symmetry equivalent SO_3[6] sulfonate groups from the crystal structure of complex **7.6** (distances given in Å).

In addition to the LaO···OS hydrogen bonding described above, two of the waters of crystallisation also form hydrogen bonding motifs to form inter-chain connections (Figure 7.33). The water molecule O(23) is positioned so as to have four possible interactions with neighbouring atoms or asymmetric unit fragments. On of these is an OH···π interaction with the aromatic system of the lanthanum bound PyNO molecule (O···aromatic centroid distance of 3.399 Å). The water molecule hydrogen bonds to the O(3) atom of a symmetry equivalent S(1) sulfonate group with an O···OS

distance of 2.827 Å). There is a hydrogen bond from a symmetry equivalent O(14) lanthanum aquo ligand (LaO···O distance of 2.717 Å) and from the neighbouring O(22) water of crystallisation (O···O distance of 2.738 Å). The water molecule O(22) also hydrogen bonds to a symmetry equivalent O(2) atom of another symmetry equivalent S(1) sulfonate group with an O···OS distance of 2.998 Å).

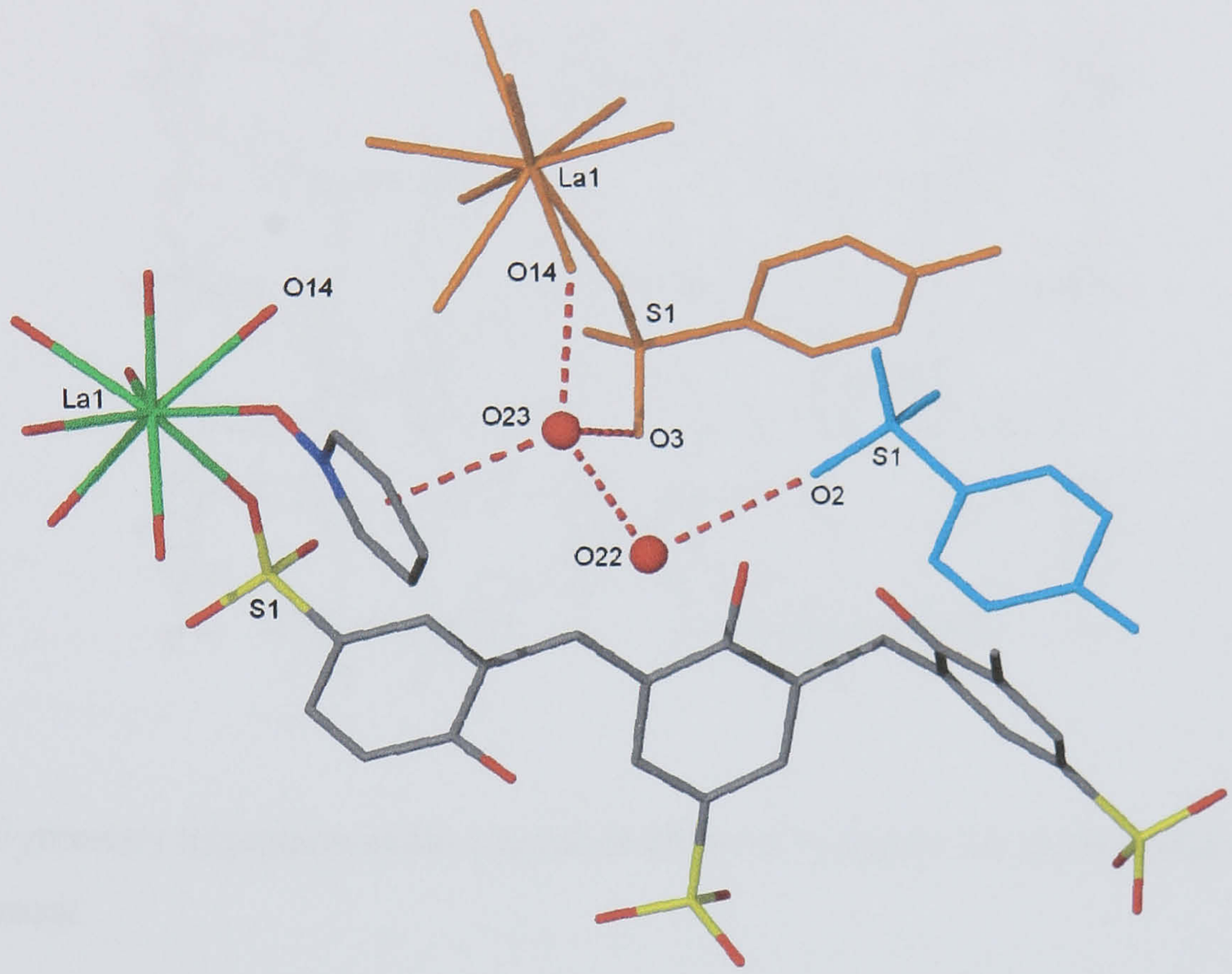

Figure 7.33 Hydrogen bonding interactions between two of the waters of crystallisation and neighbouring SO_3[6]/La/PyNO moieties from the crystal structure of complex **7.6**. The two partial asymmetric unit symmetry equivalent moieties are shown in blue and orange for clarity. Selected atoms have been labelled.

Within the extended structure the SO_3[6] molecules are seen to pack in a pseudo-hexagonal fashion similar to that shown in Figure 7.30 for complex **7.5**. In complex **7.6**, the calixarenes pack through only one crystallographically unique π-stacking interaction (compared with two in complex 7.5) with and aromatic centroid···centroid distance of 3.719 Å. The extended structure also shows the overall structure to adopt a new corrugated bi-layer arrangement that is markedly different to that found for SO_3[6] in complex **7.5** (indicated by the alternating positions of the lanthanum metal centres in Figure 7.34). When excess nickel(II) chloride is used in place of the lanthanide metal with PyNO and SO_3[6] present, a new complex forms that shows bi-layers of *p*-sulfonatocalix[6]arene (similar to those found in the octa-sodium salt) to host pyridine *N*-oxide

molecules that hydrogen bond to hexa-aqua nickel cations that reside in the hydrophilic layer of the extended structure.

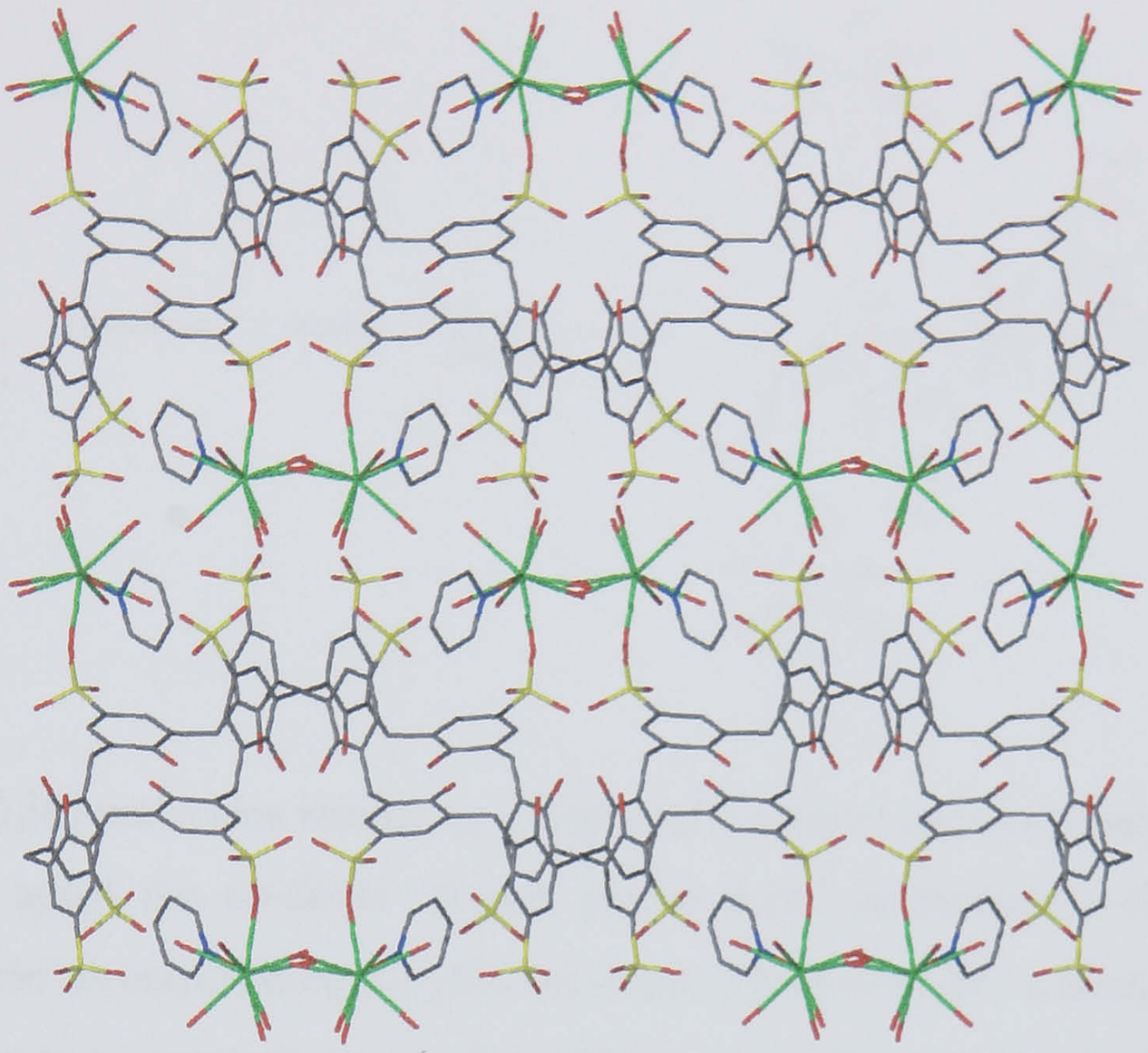

Figure 7.34 Symmetry expansion of the crystal structure of complex **7.6** showing the corrugated bi-layer arrangement.

7.3.3 Structure of the complex $[(Ni(H_2O)_6)_3][(\text{pyridine } N\text{-oxide})_2\subset(p\text{-sulfonatocalix-[6]arene})]\cdot 7H_2O$, 7.7.

Crystals of the complex $[(Ni(H_2O)_6)_3][(\text{pyridine } N\text{-oxide})_2\subset(p\text{-sulfonatocalix-[6]arene})]\cdot 7H_2O$, **7.7**, grew upon standing over several days from an aqueous solution containing a 1:2.3:5.2 mixture of Na_8SO_3[6], pyridine *N*-oxide and nickel(II) chloride hexahydrate (Equation 7.7). The complex was characterised by IR spectroscopy and single crystal X-ray crystallography. Complex **7.7** crystallises in a triclinic cell and the structural solution was performed in the space group $P\bar{1}$. Details of data collection and structure refinement are given in Table 7.18 of this chapter. A crystallographic information file containing all bond lengths and angles for complex **7.7** can be found in appendix 7.3.3 on the attached compact disc.

The asymmetric unit consists of two half SO_3[6] molecules, two non-coordinating pyridine *N*-oxide molecules and three hexa-aqua nickel cations (Figure 7.35). In addition to this there are seven waters of crystallisation all of which are at full occupancy. The three hexa-aqua nickel cations have

octahedral geometry and the bond lengths relating to the respective coordination spheres are listed in Table 7.11.

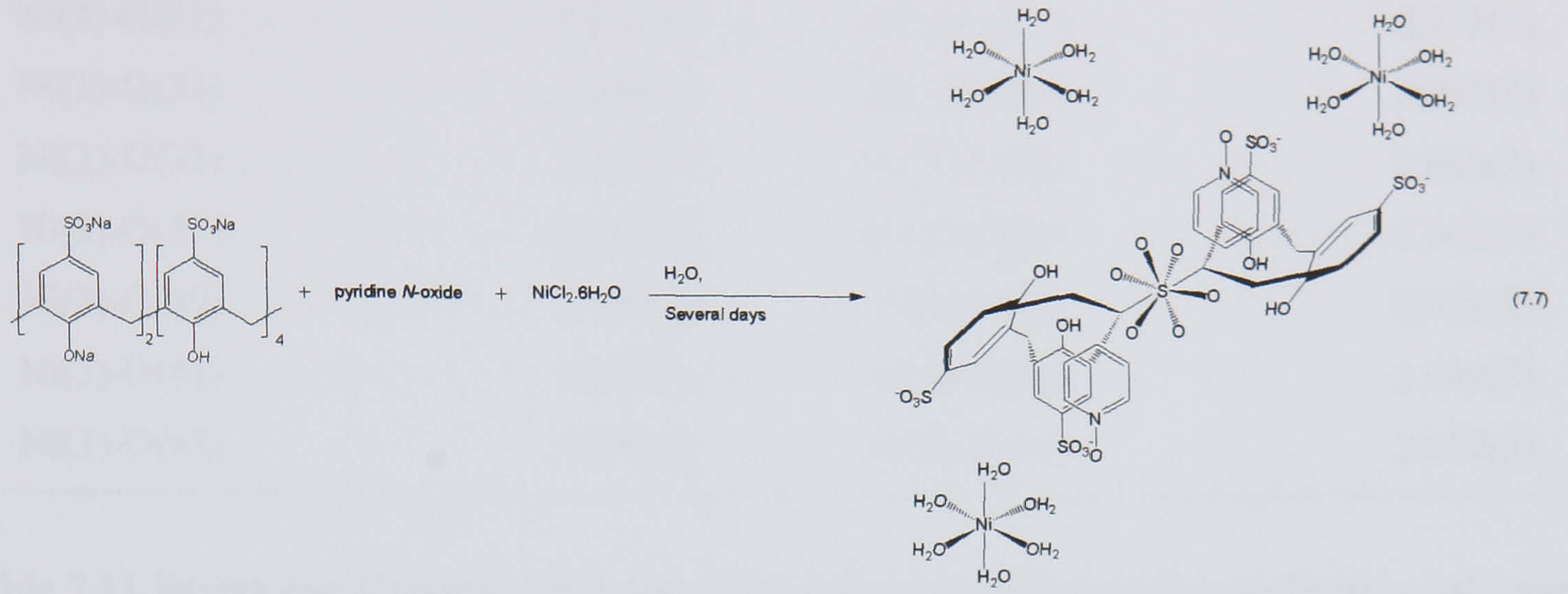

Each of the half SO_3[6] molecules resides on a centre of inversion and symmetry expansion reveals the calixarenes to adopt the up-down 'double partial cone' conformation (Figure 7.36). Each resultant 'partial cone' is occupied by a PyNO molecule. There is a CH···π interaction from each of the PyNO molecules to an aromatic group of an SO_3[6]. The CH···π interaction from the N(1)O(25) PyNO is from the C(44) atom to the S(6) sulfonate aromatic ring of the S(4) – S(6) half SO_3[6] molecule (CH···aromatic centroid distance of 2.724 Å). The CH···π interaction from the N(2)O(26) PyNO is from the C(51) atom to the S(2) sulfonate aromatic ring of the S(1) – S(3) half SO_3[6] molecule (CH···aromatic centroid distance of 2.839 Å).

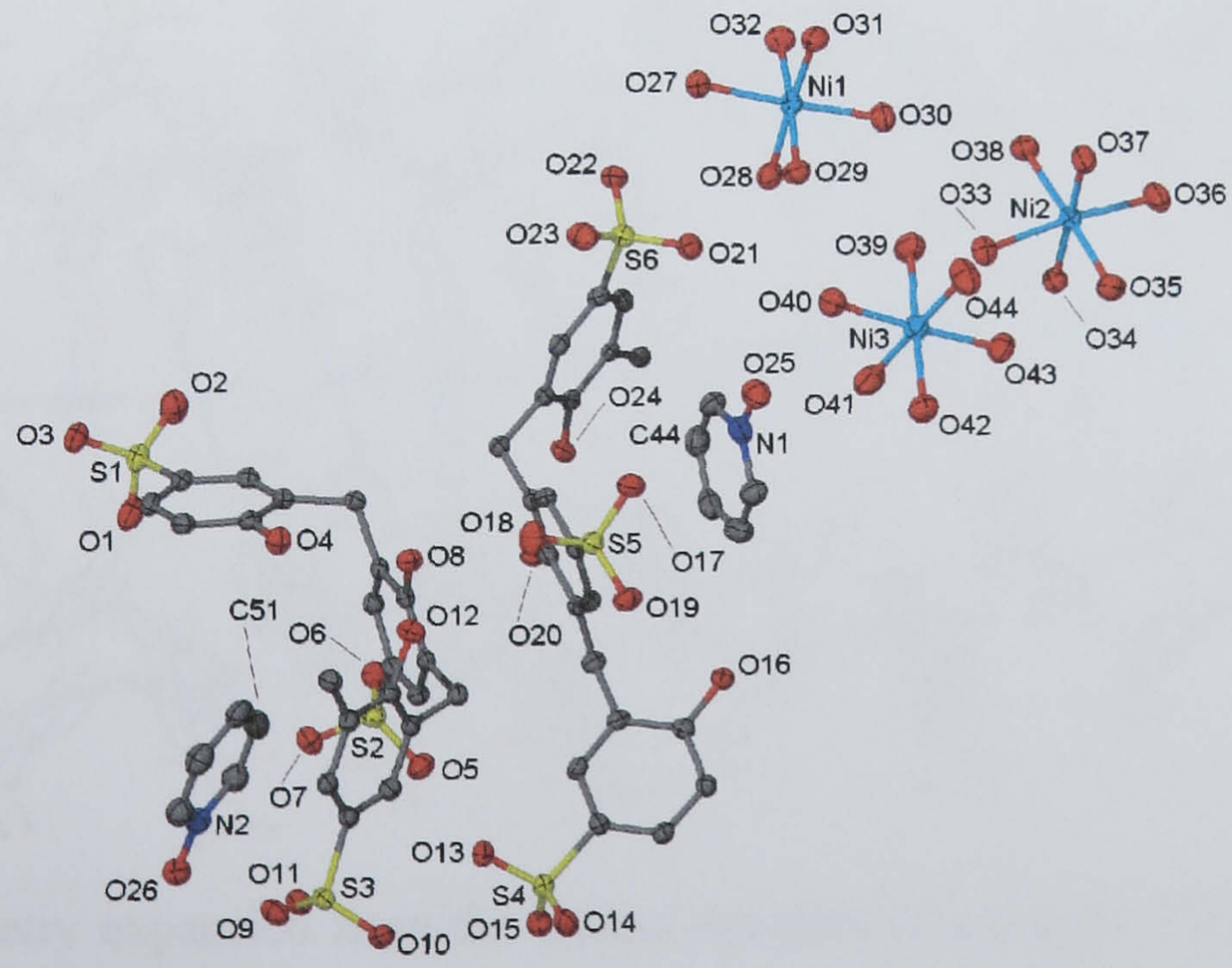

Figure 7.35 Part of the asymmetric unit from the crystal structure of complex **7.7**, anisotropic displacement ellipsoids shown at the 50% probability level. Selected atoms have been labelled.

Ni(1)-O(27)	2.062(3)	Ni(1)-O(28)	2.057(3)
Ni(1)-O(29)	2.073(3)	Ni(1)-O(30)	2.051(3)
Ni(1)-O(31)	2.027(3)	Ni(1)-O(32)	2.075(3)
Ni(2)-O(33)	2.108(3)	Ni(2)-O(34)	2.063(3)
Ni(2)-O(35)	2.035(3)	Ni(2)-O(36)	2.040(3)
Ni(2)-O(37)	2.067(3)	Ni(2)-O(38)	2.062(3)
Ni(3)-O(39)	2.083(3)	Ni(3)-O(40)	2.018(3)
Ni(3)-O(41)	2.027(3)	Ni(3)-O(42)	2.049(3)
Ni(3)-O(43)	2.040(3)	Ni(3)-O(44)	2.057(3)

Table 7.11 Interatomic distances relating to the coordination sphere of the ytterbium metal centres in the crystal structure of complex **7.7** (distances given in Å with e.s.d. in parentheses).

The extended structure shows the SO_3[6] molecules to pack to form a bi-layer arrangement similar to that found in both the octa-sodium salt and the sulfonic acid. This occurs through two crystallographically unique π-stacking interactions with aromatic centroid···centroid distances of 3.806 and 3.850 Å. Every partial cone in the extended structure is, as mentioned above occupied by a PyNO molecule and the polar *N*-oxide functionalities point into the hydrophilic layer generated by the sulfonate groups of the calixarenes (Figure 7.36).

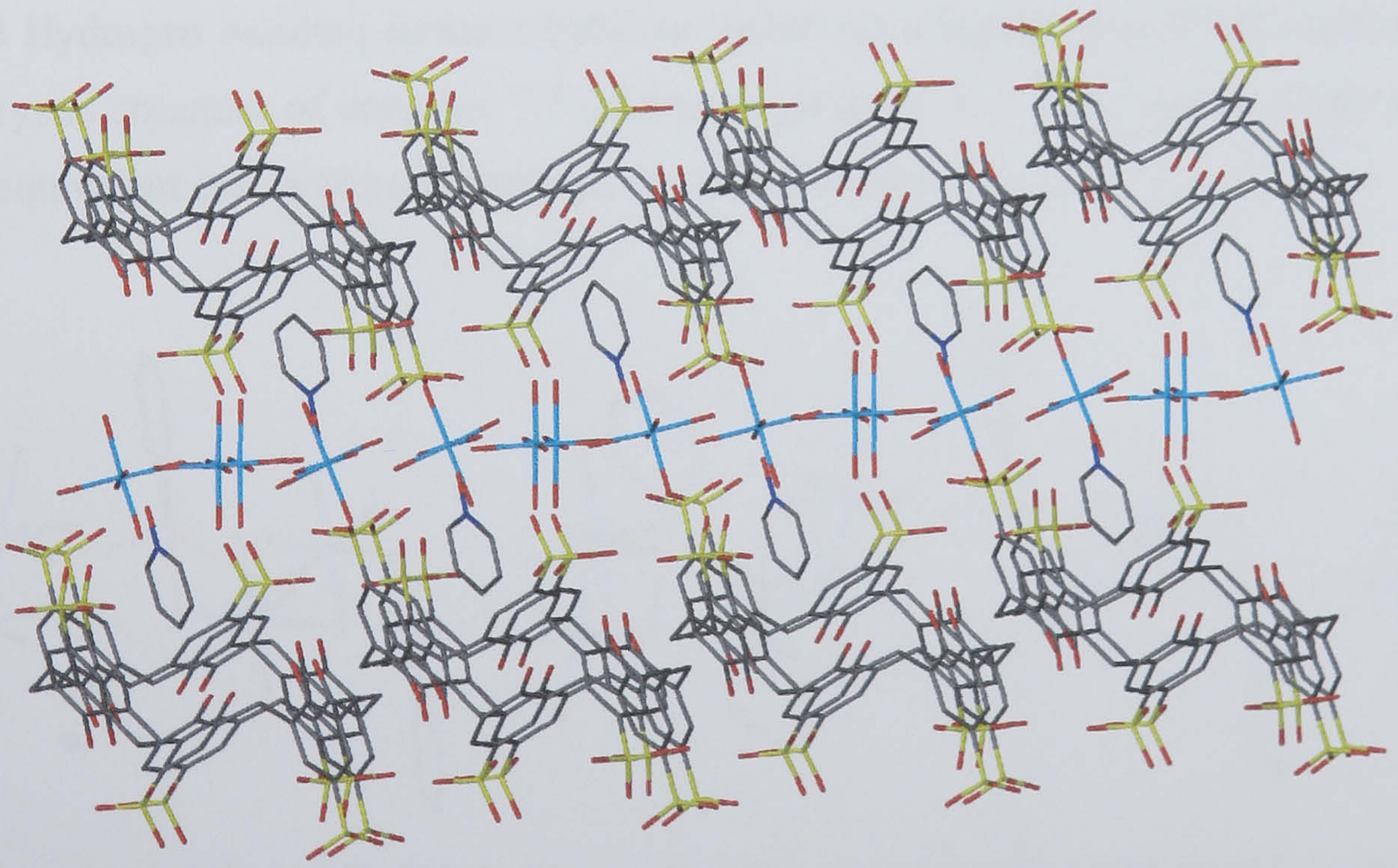

Figure 7.36 Symmetry expansion from the crystal structure of complex **7.7** showing the bi-layer arrangement and the positioning of the PyNO molecules and hexa-aqua nickel cations within the hydrophilic layer.

The hexe-aqua nickel(II) cations all reside in the hydrophilic layer of the extended structure and there are a total of twenty NiO···OS hydrogen bonds from nickel aquo ligands to oxygen atoms of calixarene sulfonate groups. The NiO···OS hydrogen bonding distances are listed in Table 7.12 and are all of a typical magnitude for such interactions.[152, 153] In addition to these interactions there are six hydrogen bonding contacts between nickel aquo ligands (from all three cations) and the oxygen atoms of the PyNO molecules within the hydrophilic layer (NiO···ON distances ranging from 2.664 – 3.031 Å, Figure 7.37). When the waters of crystallisation are accounted for, an extremely complicated hydrogen bonded regime is evident throughout the extended structure.

Ni(1)-(O27)···O(22)-S(6)	2.648	Ni(1)-(O28)···O(19)-S(5)*	2.723
Ni(1)-(O28)···O(15)-S(4)*	2.789	Ni(1)-(O29)···O(21)-S(6)	2.762
Ni(1)-(O29)···O(23)-S(6)*	2.715	Ni(1)-(O30)···O(1)-S(1)*	2.736
Ni(1)-(O31)···O(3)-S(1)*	2.709	Ni(1)-(O31)···O(17)-S(5)*	2.703
Ni(1)-(O32)···O(17)-S(5)*	2.814	Ni(2)-(O33)···O(5)-S(2)*	2.949
Ni(2)-(O33)···O(15)-S(4)*	2.728	Ni(2)-(O34)···O(13)-S(4)*	2.721
Ni(2)-(O34)···O(11)-S(3)*	2.734	Ni(2)-(O35)···O(7)-S(2)*	2.732
Ni(2)-(O35)···O(6)-S(2)†	2.793	Ni(2)-(O36)···O(11)-S(3)*	2.848
Ni(2)-(O37)···O(1)-S(1)*	2.686	Ni(2)-(O37)···O(9)-S(3)*	2.742
Ni(3)-(O40)···O(23)-S(6)*	2.889	Ni(3)-(O43)···O(5)-S(2)*	2.788

Table 7.12 Hydrogen bonding contacts between nickel aquo ligands and SO_3[6] sulfonate groups from the crystal structure of complex **7.7** (distances given in Å, * and † denote singly and doubly symmetry equivalent calixarene sulfonate groups respectively).

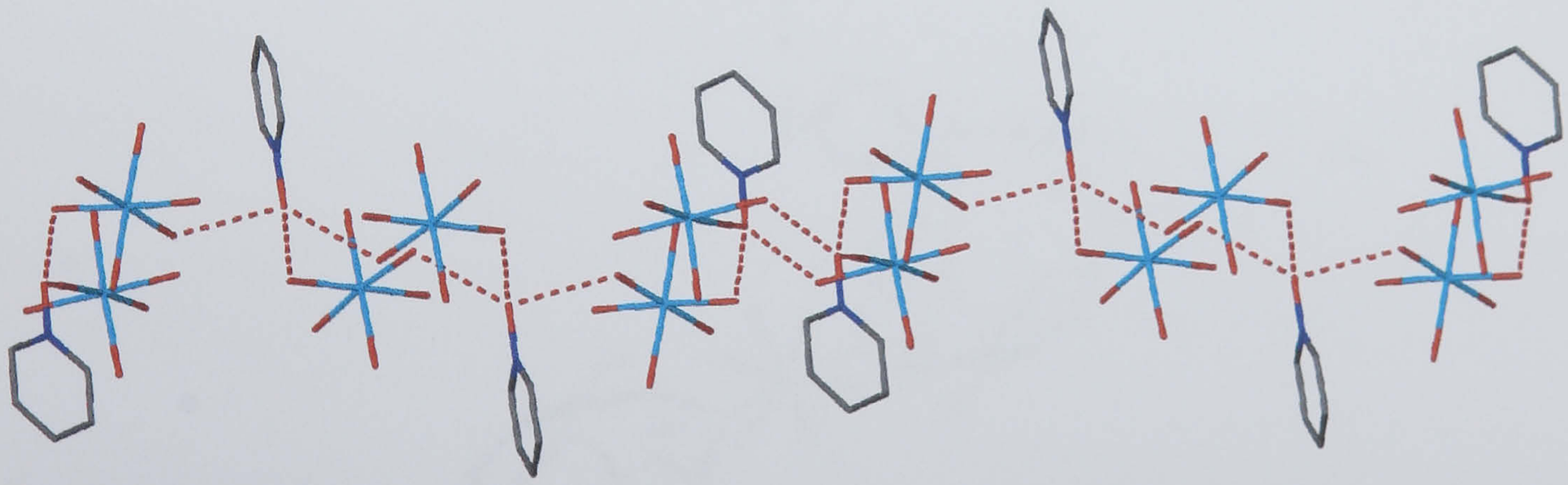

Figure 7.37 The nickel aquo/PyNO hydrogen bonding regime within a hydrophilic layer from the crystal structure of complex **7.7**.

Complexes **7.5** and **7.6** prove PyNO to be a good ligand for lanthanide metals in complex formation with *p*-sulfonatocalix[6]arene. Complex **7.7** shows that PyNO is a suitable guest for the partial cones of SO_3[6] in the absence of direct metal complexation in a transition metal complex. Given this, the larger related 4,4'-dipyridine-*N,N'*-dioxide (DiPyNO) was employed as a potential ligand for metal complexation with SO_3[6]. When europium(III) nitrate is reacted with DiPyNO an interesting coordination polymer forms that shows zig-zag chains of the complex to pack in a bi-layer fashion with concomitant formation of graphitic sheets of hydrogen bonds.

7.3.4 Structure of the coordination polymer $[(Eu(H_2O)_6)_2][$(4,4'-dipyridine-*N,N'*-dioxide)(*p*-sulfonatocalix[6]arene)$]\cdot 8H_2O$, 7.8.

Crystals of the complex $[(Eu(H_2O)_6)_2][$(4,4'-dipyridine-*N,N'*-dioxide)(*p*-sulfonatocalix[6]arene)$]\cdot 8H_2O$, **7.8**, grew upon standing over several days from an aqueous solution containing a 1:2.2:3 mixture of Na_8SO_3[6], 4,4'-dipyridine-*N,N'*-dioxide and europium(III) nitrate hydrate (Equation 7.8). The complex was characterised by IR spectroscopy, microanalysis and single crystal X-ray crystallography. Complex **7.8** crystallises in a monoclinic cell and the structural solution was performed in the space group $P2_1/c$. Details of data collection and structure refinement are given in Table 7.18 of this chapter. A crystallographic information file containing all bond lengths and angles for complex **7.8** can be found in appendix 7.3.4 on the attached compact disc.

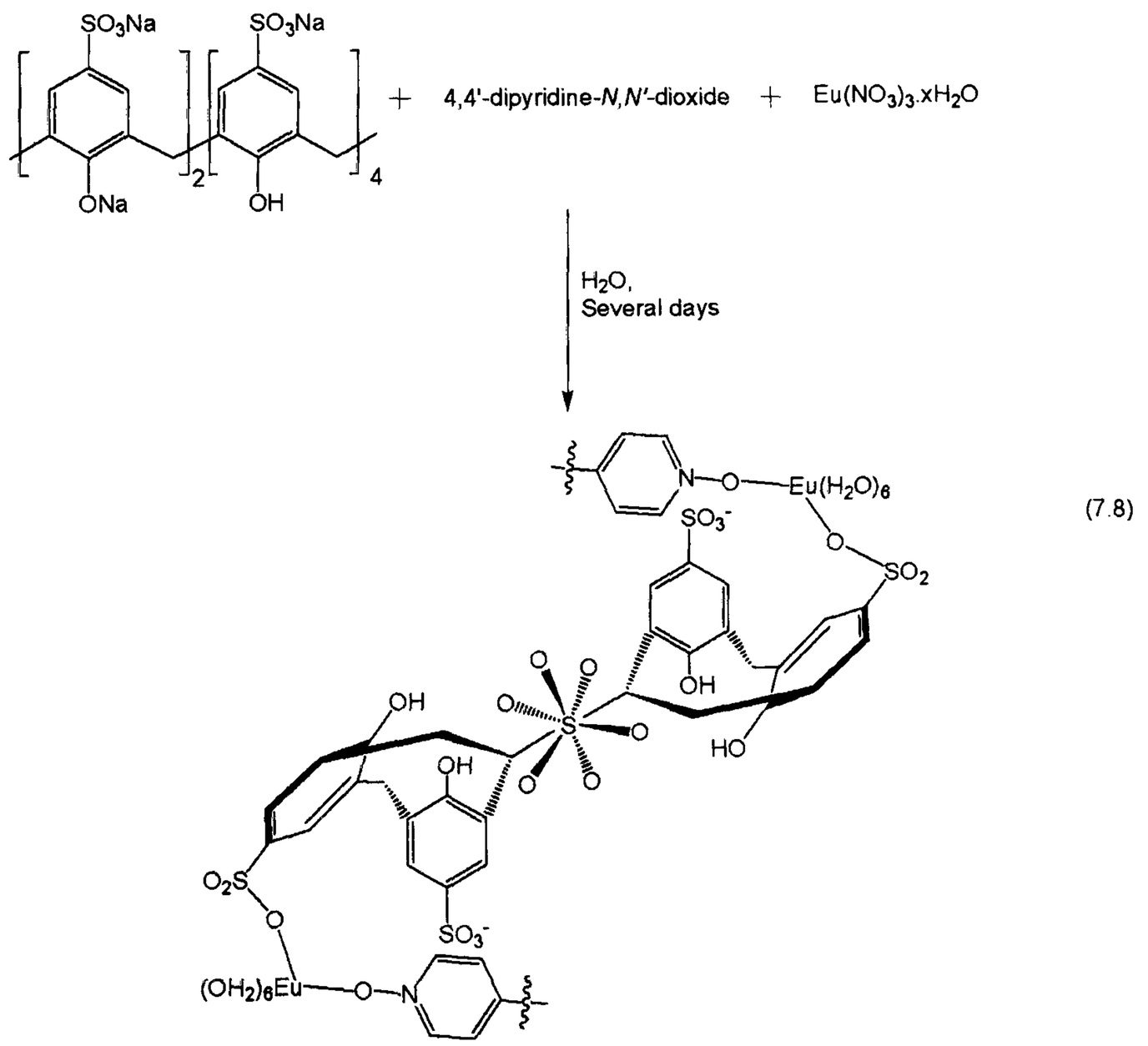

(7.8)

The asymmetric unit consists of one half SO_3[6] molecule, a hexa-aqua sulfonate bound europium centre and half of a DiPyNO molecule (Figure 7.38). In addition to this there are four full occupancy waters of crystallisation.

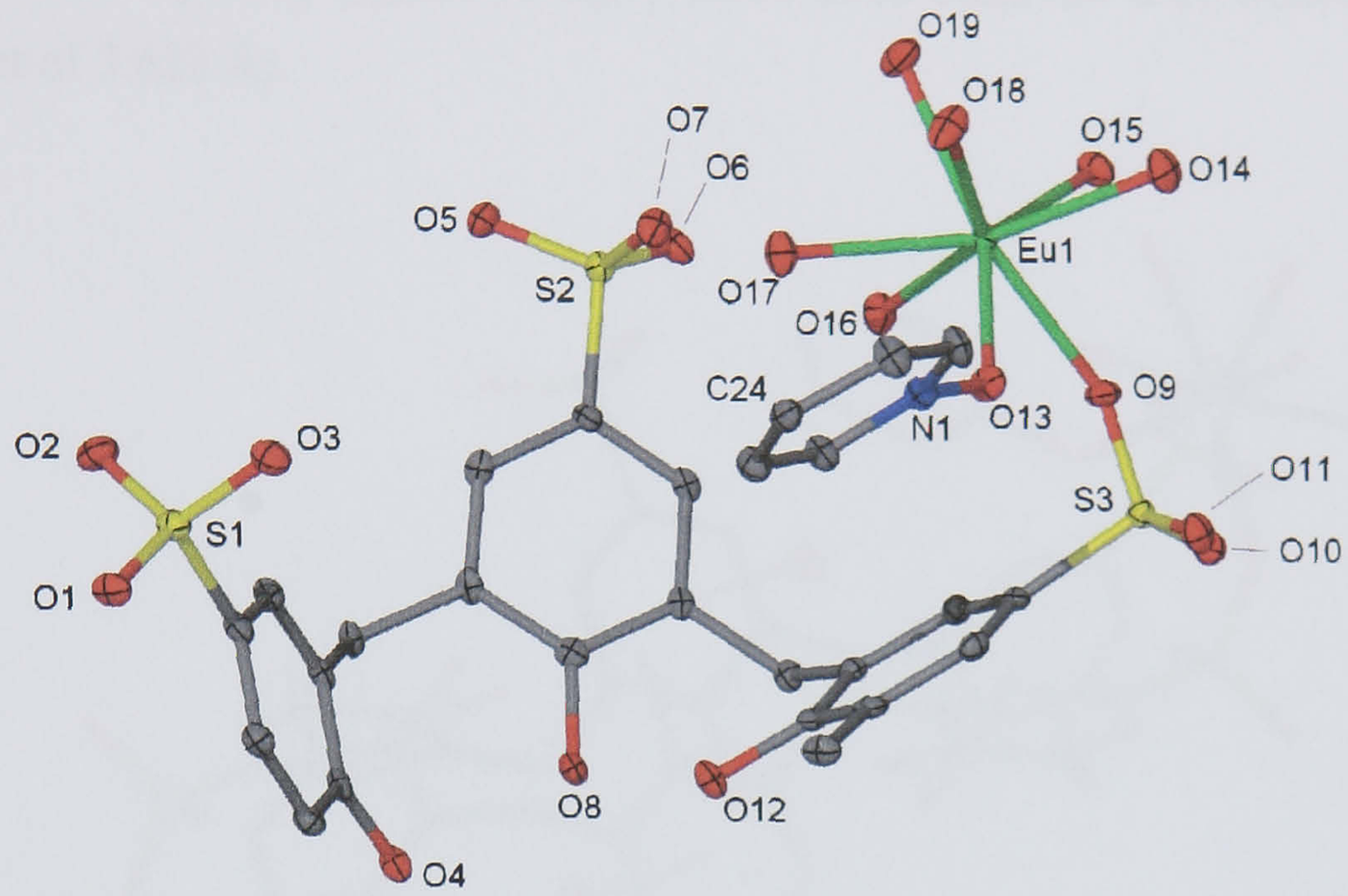

Figure 7.38 Part of the asymmetric unit from the crystal structure of complex **7.8**, anisotropic displacement ellipsoids shown at the 50% probability level. Selected atoms have been labelled.

The europium metal centre is bound to the O(9) atom of the S(3) calixarene sulfonate group, has six aquo ligands and has half of a bound DiPyNO molecule. The metal centre is eight-coordinate and is of square anti-prismatic geometry. Bond lengths relating to the europium coordination sphere are listed in Table 7.13.

Eu(1)-O(9)	2.397(2)	Eu(1)-O(13)	2.325(3)
Eu(1)-O(14)	2.384(3)	Eu(1)-O(15)	2.484(3)
Eu(1)-O(16)	2.386(3)	Eu(1)-O(17)	2.434(3)
Eu(1)-O(18)	2.449(3)	Eu(1)-O(19)	2.434(3)

Table 7.13 Interatomic distances relating to the coordination sphere of the europium metal centre in the crystal structure of complex **7.8** (distances given in Å with e.s.d. in parentheses).

Upon symmetry expansion of the asymmetric unit, several interesting structural features are evident. Firstly the calixarene is seen to adopt the up-down 'double partial cone' conformation and the half DiPyNO molecules point away from the partial cones of the calixarene. Within the extended calixarene moiety, the crystallographically unique cavity of the partial cone is occupied by

a water of crystallisation that is in a position consistent with OH···π hydrogen bonding interaction with one of the calixarene aromatic rings (Figure 7.39). Although the water molecule hydrogen atoms were not located in the Fourier difference map, the OH···aromatic centroid distance is consistent with those reported when a similar phenomenon observed with SO_3[4] (OH···aromatic centroid distance of 3.622 Å).

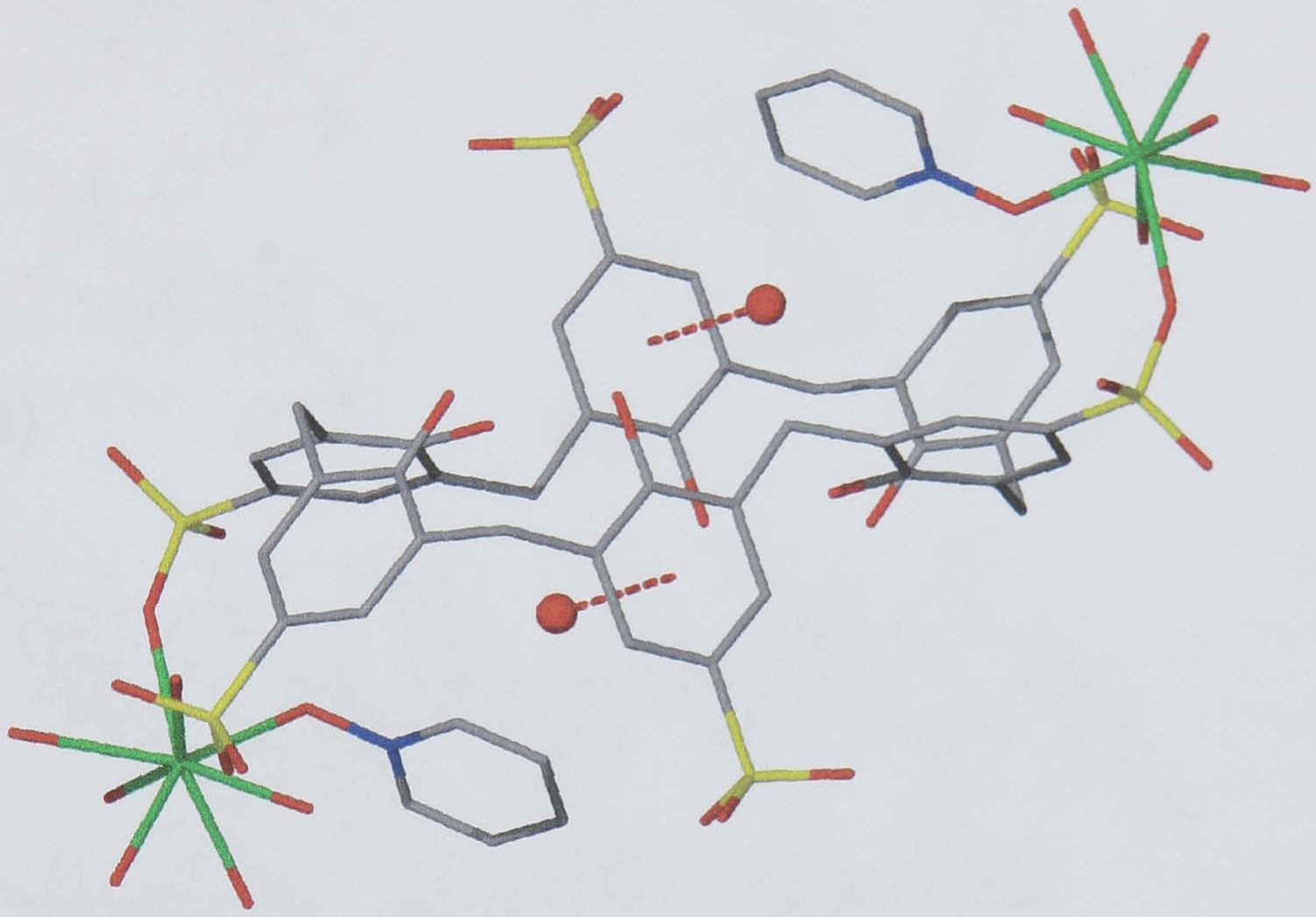

Figure 7.39 Part of the coordination polymer from the crystal structure of complex **7.8** showing the 'double partial cone' conformation of the SO_3[6] and the inclusion of the water molecules within the cavities (OH···π interaction shown as a dashed red line). All atoms except the cavity bound water molecules are shown in stick representation.

The units shown in Figure 7.39 are linked through the crystallographically unique half DiPyNO molecule and these units form a zig-zag chain in the extended structure (Figure 7.40). The calixarenes assemble in a bi-layer arrangement similar to that found in complex **7.5** through one crystallographically unique π-stacking interaction with an aromatic centroid···centroid distance of 3.719 Å (Figure 7.40c). The extended structure shows hydrogen bonding from europium aquo ligands to oxygen atoms of crystallographically unique and symmetry equivalent calixarene sulfonate groups. There are a total of eight EuO···OS hydrogen bonds from five metal aquo ligands to oxygen atoms of one crystallographically unique and three symmetry equivalent calixarene sulfonate groups (EuO···OS distances ranging from 2.679 to 2.943 Å). The result of the EuO···OS hydrogen bonding regime is that each europium centre 'sees' three neighbouring europium metal centres.

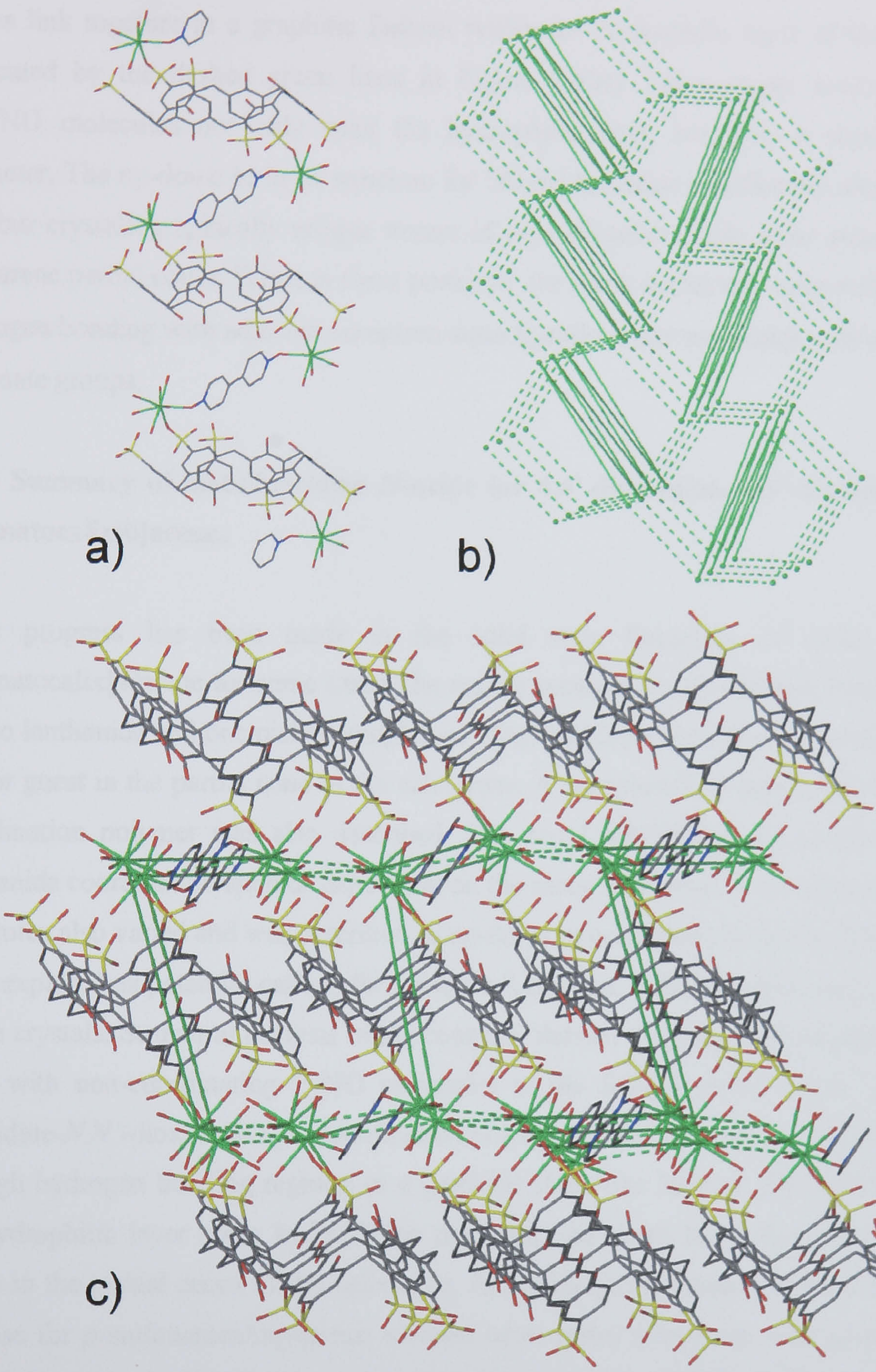

Figure 7.40 Symmetry expansion of part of the asymmetric unit from the crystal structure of complex **7.8**. a) The extended zig-zag coordination polymer shows the DiPyNO molecules to bridge the hydrophilic layer generated by the upper rim calixarene sulfonate groups. b) The coordination and hydrogen bonding network found in the topological diagram is shown (solid and dashed green lines respectively). c) The overall bi-layer arrangement shows the organisation of the coordination and hydrogen bonding network within the extended structure.

If each europium is thus treated as a three-connecting centre and connected as such, the zig-zag chains link together in a graphitic fashion within the hydrophilic layer of the extended structure (indicated by the dashed green lines in Figure 7.40c). Interestingly, complex **7.8** shows that DiPyNO molecules not only span the hydrophilic layer but give it significant hydrophobic character. The up-down bi-layer structure for SO_3[6] has been significantly altered and three out of the four crystallographically unique waters of crystallisation reside in or around the hydrophobic calixarene partial cones. When in these positions, the result is that the water molecules participate in hydrogen bonding with adjacent europium aquo ligands, water molecules, calixarene π-systems and sulfonate groups.

7.3.5 Summary of metal/pyridine *N*-oxide (or 4,4'-dipyridine-*N,N'*-dioxide) complexes of *p*-sulfonatocalix[6]arene.

Little progress has been made in the solid state formation of metal complexes of *p*-sulfonatocalix[4]arene for some time. The results presented in this section described the formation of two lanthanide and one nickel complex of SO_3[6] with pyridine *N*-oxide acting either as a ligand and or guest in the partial cone of the calixarene. A europium/4,4'-dipyridine-*N,N'*-dioxide/SO_3[6] coordination polymer was also described. The two Ln/PyNO/SO_3[6] complexes showed varied lanthanide coordination spheres depending on the metal employed. The calixarene packing in these structures also varied and was described as up-down or corrugated bi-layers. When transition metals were explored as potential cations for complex formation, nickel was the only metal found to form single crystals. Structural analysis of the complex showed the calixarene to pack in an up-down bi-layer with non-coordinating PyNO molecules in the SO_3[6] partial cones. The europium/4,4'-dipyridine-*N,N'*-dioxide/SO_3[6] coordination polymer formed as a zig-zag chain that self-assembled through hydrogen bonding regimes in a graphitic sheet-like fashion. The DiPyNO molecules give the hydrophilic layer some hydrophobic character, the result being that waters of crystallisation reside in the partial cones of the calixarene. In summary, the results reported in this section show promise for *p*-sulfonatocalix[6]arene to form other metal complexes with suitable ligands and or guests. Many such ligands/guests that have been used in similar studies with SO_3[4] could be employed in order to observe the difference in structural behaviour between the two calixarenes under similar chemical environments.

7.4 Alternative supramolecular structures incorporating *p*-sulfonatocalix[6]arene.

The sodium salts of the *p*-sulfonatocalix[4,5]arenes have been shown to form interesting complexes with various guest molecules in the absence of other metal cations.[40, 61, 62, 67] In addition to this, 3-

pyridine sulfonic acid ($PySO_3$) has been shown to form several interesting supramolecular architectures with various metal cations in the solid state.[137] As shown in Chapter 6, 3-pyridine sulfonic acid was investigated as a potential guest for the bowl shaped cavity of *p*-sulfonatocalix[5]arene. When sodium *p*-sulfonatocalix[5]arene is reacted with $PySO_3$, at a low pH (<1), a molecular capsule shrouding two $PySO_3$ molecules is formed. A similar experiment with octa-sodium *p*-sulfonatocalix[6]arene results in the formation of a coordination polymer that has near-linear poly-aquo sodium hexameric chains linking $PySO_3$ and SO_3[6] molecules. These chains assemble in a 'criss-cross' fashion in a very complicated hydrogen bonding network in the extended structure.

7.4.1 Synthesis of the coordination polymer [(3-pyridinium sulfonate)($Na_3(H_2O)_9$)(*p*-sulfonatocalix[6]arene)$_{0.5}$]·$1H_2O$, 7.9.

Crystals of the complex [(3-pyridinium sulfonate)($Na_3(H_2O)_9$)(*p*-sulfonatocalix[6]arene)$_{0.5}$]·$1H_2O$, **7.9**, grew upon slow evaporation of an acidic aqueous solution containing Na_8SO_3[6] and excess 3-pyridine sulfonic acid (Equation 7.9).

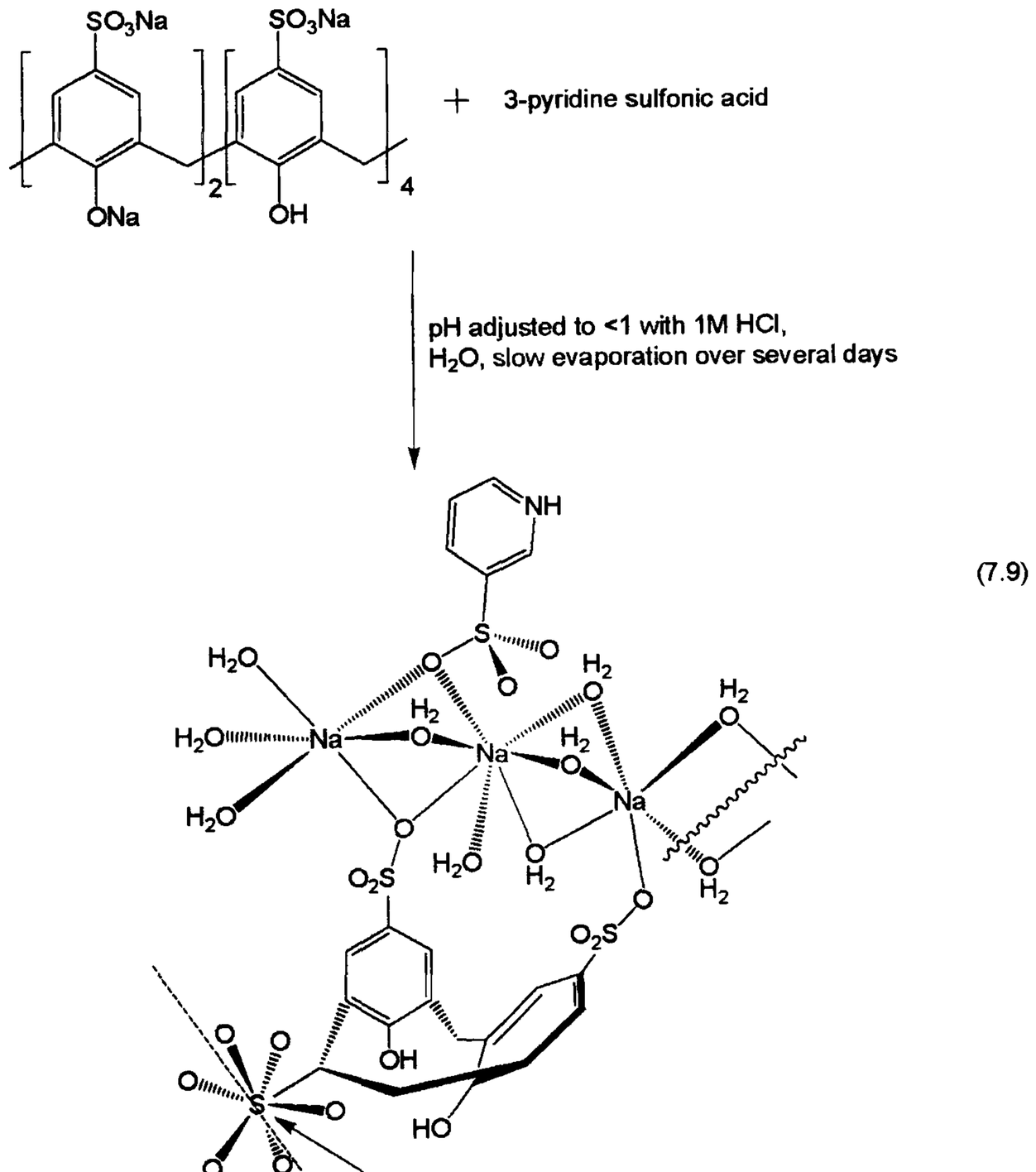

(7.9)

The complex was characterised by IR and NMR spectroscopy and single crystal X-ray crystallography. Complex **7.9** crystallises in a monoclinic cell and the structural solution was performed in the space group $P2_1/n$. Details of data collection and structure refinement are given in Table 7.19 of this chapter. A crystallographic information file containing all bond lengths and angles for complex **7.9** can be found in appendix 7.4.1 on the attached compact disc. The asymmetric unit consists of one half SO_3[6] molecule, three poly-aquo sodium centres and one pyridinium sulfonate molecule (protonated on the N(1) nitrogen atom) that is bound to two sodium centres through one sulfonate oxygen atom (Figure 7.41). In addition to this there is one full occupancy water molecule of crystallisation. Upon symmetry expansion, the crystallographically unique Na(1) and Na(3) are found to be hexa-coordinate and of octahedral geometry. The Na(2) sodium centre is found to be hepta-coordinate and has distorted capped trigonal prismatic geometry. Bond distances relating to the coordination spheres of the three crystallographically unique sodium centres are listed in Table 7.14. Symmetry expansion reveals the sodium centres to be arranged as near linear poly-aquo hexamers (Figure 7.42). Within the hexamer, Na(1) has five bridging aquo ligands whilst being tethered to the calixarene through the O(10) oxygen atom of the S(3) calixarene sulfonate group. The Na(2) is coordinated to the O(13) atom of the sulfonate group of the 3-pyridinium sulfonate molecule. In addition to this, Na(2) is also bound to a symmetry equivalent O(1) atom of an S(1) calixarene sulfonate group, has four bridging aquo ligands and one terminal aquo ligand (O(20), Figures 7.41 and 7.42). The third sodium centre, Na(3), is also coordinated to the O(13) atom of the sulfonate group of the 3-pyridinium sulfonate molecule (Figure 7.41). In addition, Na(3) is also bound to the same symmetry equivalent O(1) atom of an S(1) calixarene sulfonate group as Na(2), has one bridging aquo ligand and has three terminal ligands (O(22), O(23) and O(24), Figures 7.41 and 7.42).

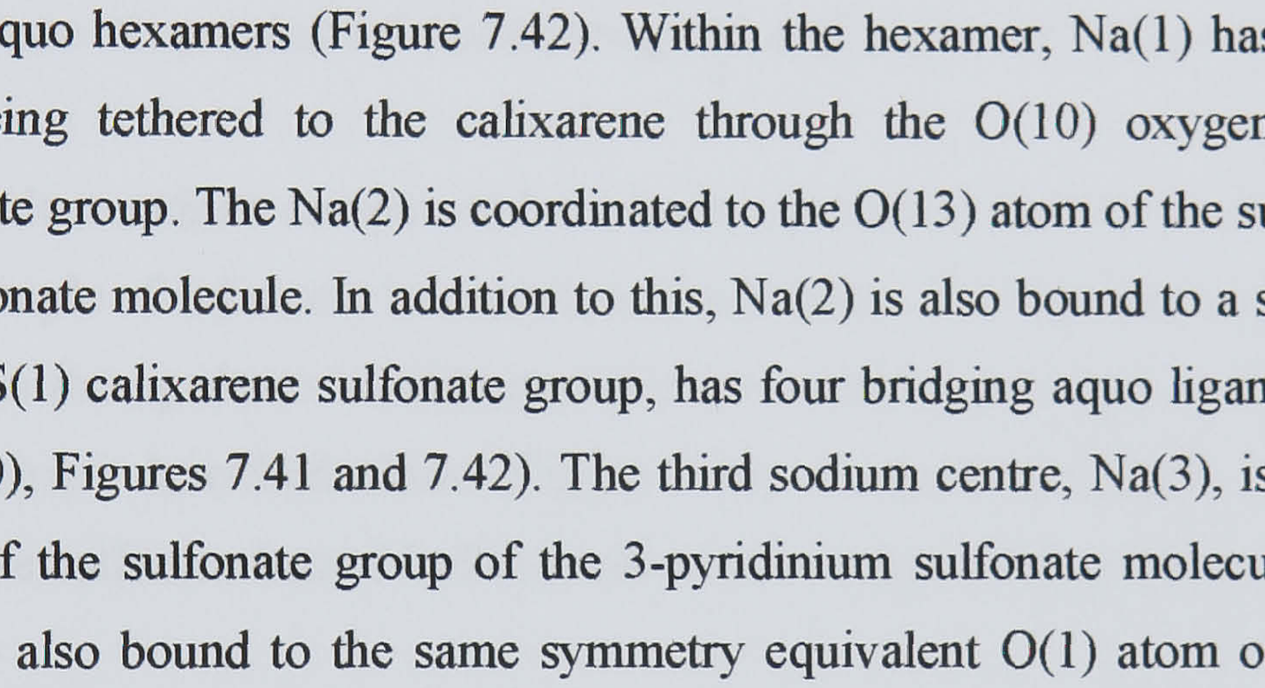

Figure 7.41 Part of the asymmetric unit from the crystal structure of complex **7.9**, anisotropic displacement ellipsoids shown at the 50% probability level. Selected atoms have been labelled.

Na(1)-O(10)	2.3661(18)	Na(1)-O(16)	2.388(2)
Na(1)-O(16)[(a)]	2.369(2)	Na(1)-O(17)	2.406(2)
Na(1)-O(18)	2.3699(19)	Na(1)-O(19)	2.412(2)
Na(2)-O(1)[(b)]	2.323(2)	Na(2)-O(13)	2.448(2)
Na(2)-O(17)	2.951(3)	Na(2)-O(18)	2.331(2)
Na(2)-O(19)	2.438(2)	Na(2)-O(20)	2.960(3)
Na(2)-O(21)	2.403(3)	Na(3)-O(1)[(b)]	2.6139(19)
Na(3)-O(13)	2.4494(19)	Na(3)-O(21)	2.379(2)
Na(3)-O(22)	2.351(2)	Na(3)-O(23)	2.425(2)
Na(3)-O(24)	2.4183(19)		

Table 7.14 Interatomic distances relating to the coordination sphere of the ytterbium metal centres in the crystal structure of complex **7.9** (distances given in Å with e.s.d. in parentheses).

numerous poly-nuclear sodium complexes have been reported to date but we believe that this is the first structural example of a discrete hexameric sodium chain.[139-143] Symmetry expansion reveals the calixarenes to be in the up-down 'double partial cone' conformation and to be linked by the poly-aquo sodium hexamers described above (Figure 7.42). These form infinite coordination polymer chains that have the sulfonate bound $PySO_3$ molecules arranged orthogonally to the direction of the chain.

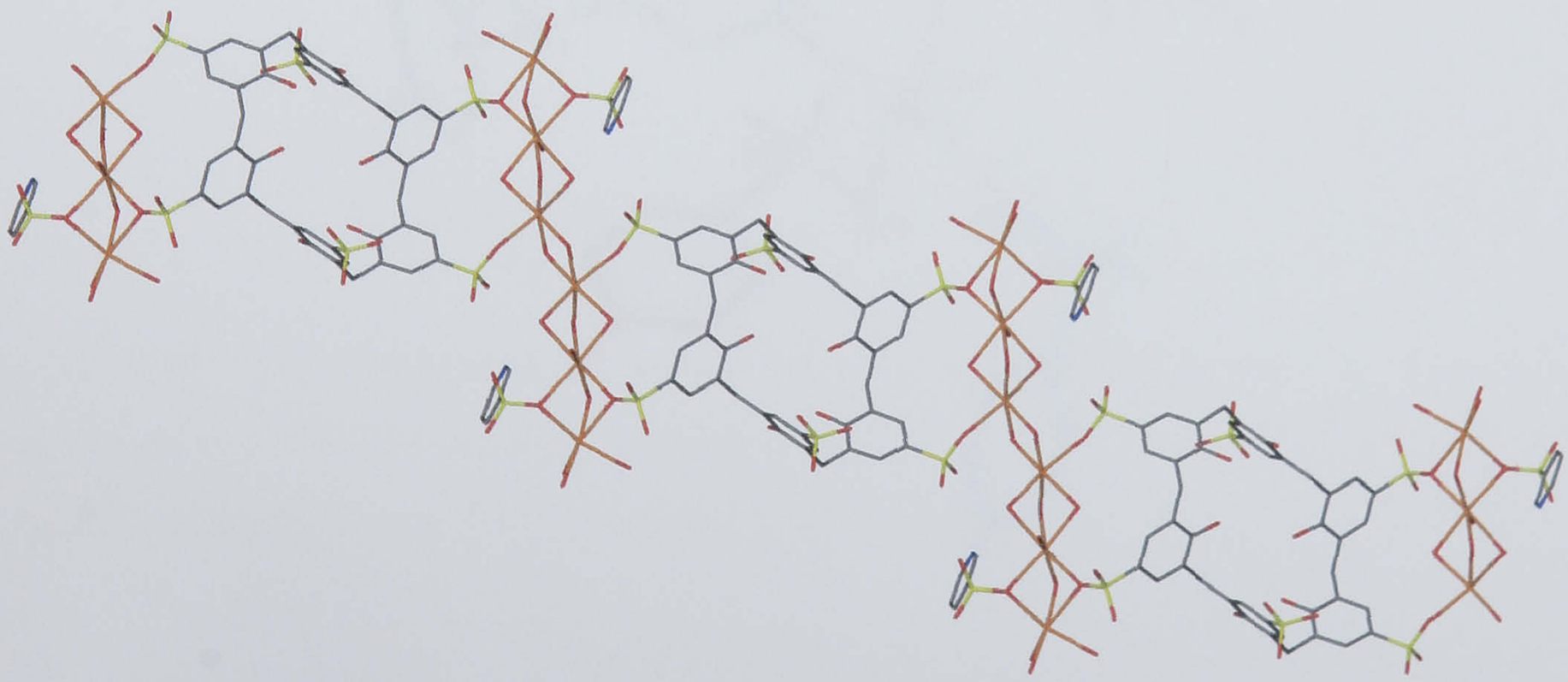

Figure 7.42 Part of a coordination polymer chain from the crystal structure of complex **7.9** showing the 'double partial cone' conformation of the SO_3[6] molecules, the poly-aquo sodium hexamers and the sodium/sulfonate coordination to the $PySO_3$ molecules.

The extended structure associated with these coordination polymer chains is complex and is best understood in parts. The quality of data collected for complex **7.9** was excellent and allowed the location and refinement of all hydrogen atoms of the metal aquo ligands and the water molecule of crystallisation (Figure 7.43). The hydrogen atom of the $PySO_3$ molecule was also located on the N(1) nitrogen atom and refined accordingly. This allows us to examine and further understand the exact hydrogen bonding and inter-chain interactions in the complex extended structure. There appear to be two significant points of inter-chain interaction. One of these is based around hydrogen bonding and CH···π interactions associated with the crystallographically unique water of crystallisation and $PySO_3$ (respectively) and neighbouring coordination polymer chains (Figure 7.43). The second of these is associated with neighbouring poly-aquo sodium hexamers and will be discussed further below (Figure 7.44). In the former of the two, one crystallographically unique chain is found to link through a series of intra and inter-chain interactions to three symmetry equivalent calixarenes of neighbouring chains. The intra-chain interactions consist of two hydrogen bonds. One is from the O(17) sodium aquo ligand to the O(25) water of crystallisation with an O···O distance of 2.868 Å (corresponding OH···O distance of 1.959 Å).

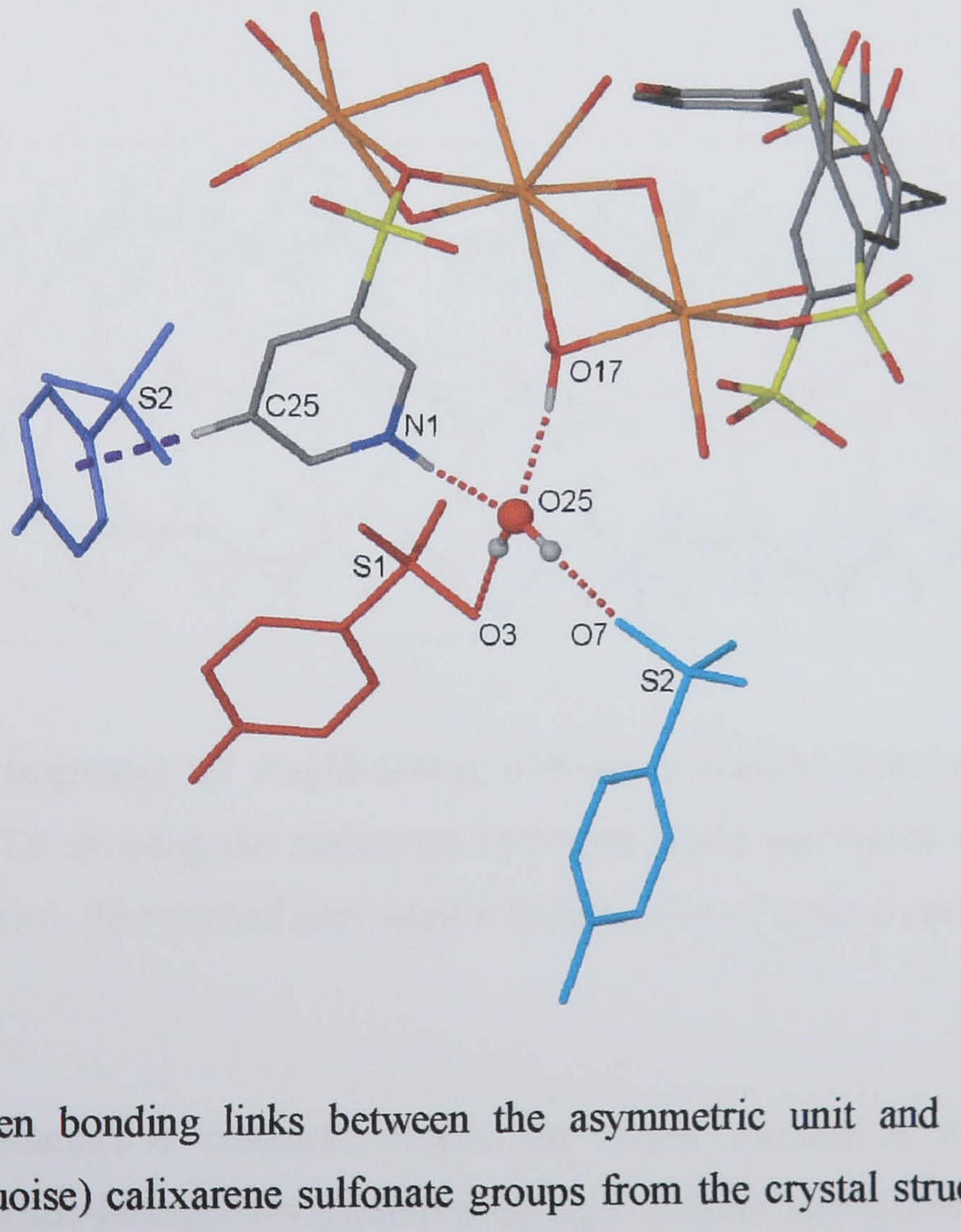

Figure 7.43 Hydrogen bonding links between the asymmetric unit and symmetry equivalent (purple, red and turquoise) calixarene sulfonate groups from the crystal structure of complex **7.9**. All atoms are in stick representation except for the O(25) water molecule that is in ball and stick representation.

The second hydrogen bond is from the protonated nitrogen atom of the $PySO_3$ molecule to O(25) with an N···O distance of 2.714 Å (corresponding NH···O distance of 1.776 Å). There are three inter-chain interactions and these are in the form of one CH···π and two OH···OS hydrogen bonds. The CH···π interaction is from the C(25) atom of the $PySO_3$ molecule to an aromatic ring of a section of a symmetry equivalent calixarene (S(2) calixarene fragment) with a CH···aromatic ring centroid distance of 2.450 Å (Figures 7.41 and 7.43). The O(25) water of crystallisation hydrogen bonds to the S(1) and S(2) sections of two symmetry equivalent calixarenes with O···OS distances of 2.877 and 2.696 Å (respective OH···OS distances of 1.968 and 1.790 Å).

The second point of inter-chain interaction is based solely around the poly-aquo sodium hexamers found in the extended structure (Figure 7.44). These are found to be arranged in a pseudo-hexagonally packed manner in a common plane (indicated by the different coloured hexamers and dashed grey line in Figure 7.44 respectively). There are a total of twenty, inter-hexamer OH···O and OH···OS hydrogen bonding interactions, five of which are crystallographically unique with O···O distances ranging from 2.767 to 3.116 Å (hydrogen bonds indicated by dashed red lines in Figure 7.44).

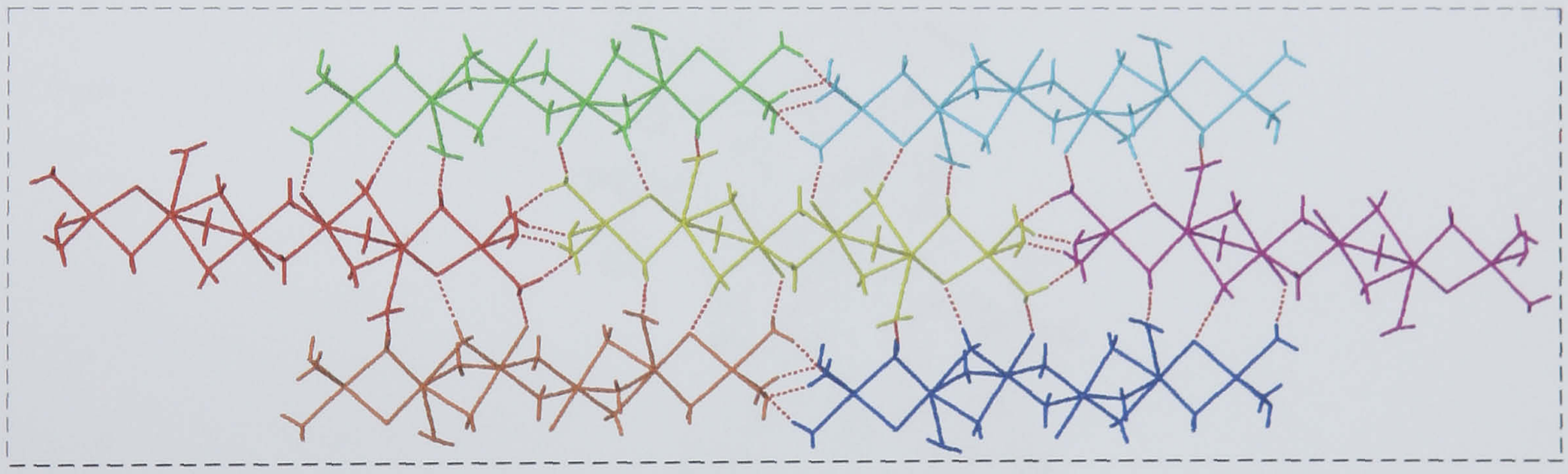

Figure 7.44 The arrangement of neighbouring poly-aquo sodium hexamers from the crystal structure of complex **7.9** showing the numerous hydrogen bonds associated with the sodium aquo ligands (dashed red lines). The dashed grey border is indicative of a plane and is for reference with Figure 7.45.

When the extended structure is examined further, the chains are seen to pack in a 'criss-cross' manner around the pseudo-hexagonally packed poly-aquo sodium arrangements that are shown in Figure 7.44 (indicated by the dashed grey lines in Figure 7.45). In one perspective, Figure 7.45b, the inter-chain hosting of $PySO_3$ molecules in cavities of calixarenes from adjacent dissimilar chains is

evident (indicated by the orange within green colour scheme in Figure 7.45 and vice versa). Although the extended structure is complex, the SO_3[6], in the up-down 'double partial cone' conformation retains the bi-layer arrangement and packs in a manner similar to the calixarene in complex **7.5**. This occurs through one crystallographically unique π-stacking interaction with an aromatic centroid···centroid distance of 3.665 Å.

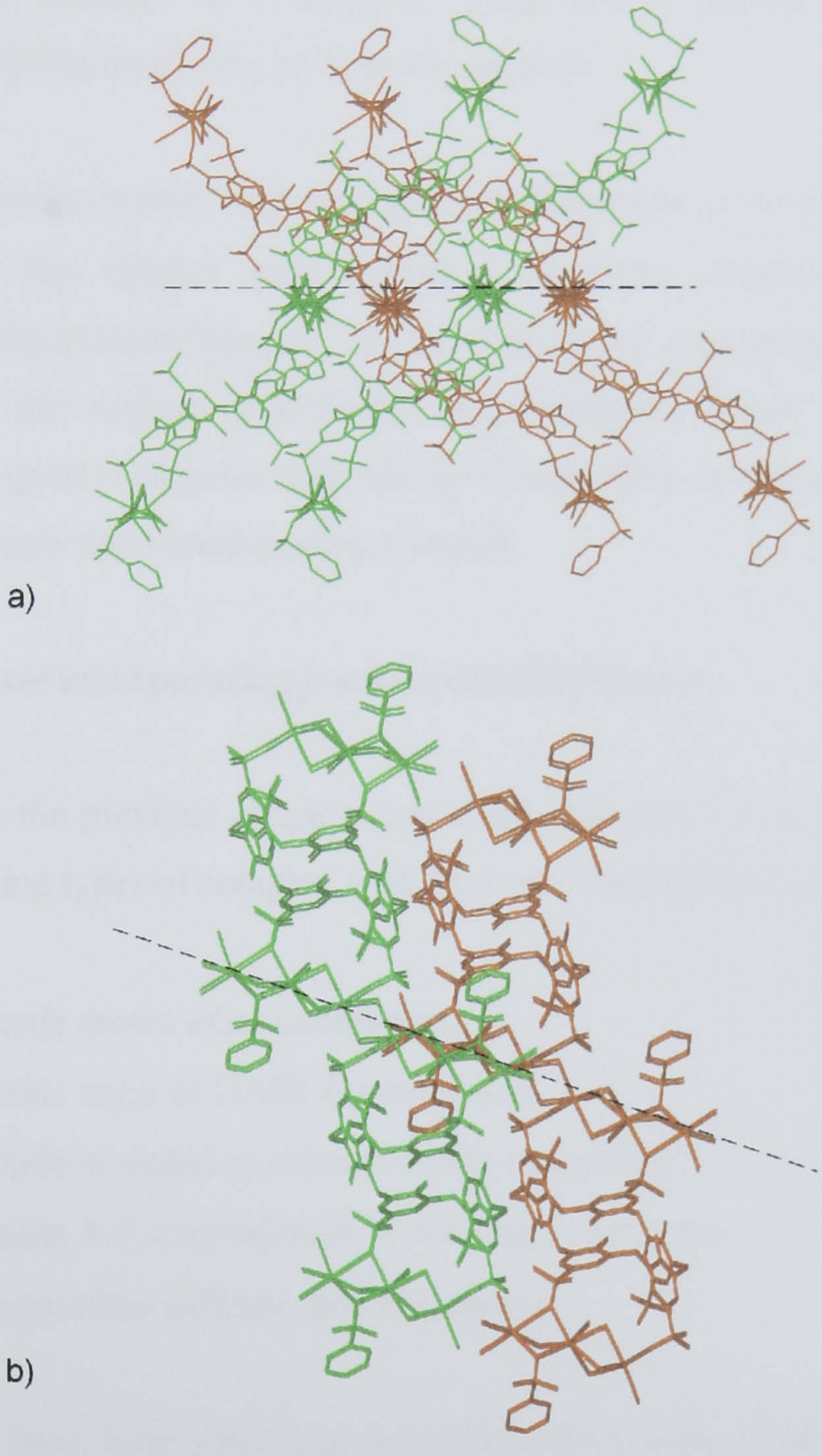

Figure 7.45 Two orientations of the packing of inter-digitated coordination polymer chains from the crystal structure of complex **7.9** (orange and green have been used to identify separate chains within the extended structure). The dashed line in both a) and b) represents the 'packing plane' of poly-aquo sodium hexamers as shown in Figure 7.44. a) The criss-cross arrangement of separate chains can be seen. b) The 'double partial cone' conformation of the SO_3[6] can be seen in addition to the 'orange within green' $PySO_3$:SO_3[6] hosting (and vice versa).

7.4.2 Summary of alternative supramolecular structures incorporating *p*-sulfonatocalix[6]arene.

The guest 3-pyridine sulfonic acid has been useful in forming supramolecular structures with the *p*-sulfonatocalix[5,6]arenes. This may be due to the fact that the molecule possesses some calixarene-like character with the presence of a sulfonate group that is capable of interacting with the calixarene in a hydrophilic/hydrophobic bi-layer successfully.

The presence of an aromatic system may also aid guest suitability as several of the supramolecular structures reported in this chapter have displayed numerous aromatic CH···π or π-stacking interactions with *p*-sulfonatocalix[6]arene. As the interesting supramolecular structures formed between $PySO_3$ and the sodium *p*-sulfonatocalix[5,6]arenes, future work could focus on incorporating different guest molecules with similar functionality in the cavities of the calixarenes with a view to forming new and varied structural motifs.

7.5 Solid state complexes incorporating *p*-sulfonatocalix[8]arene.

The work presented in the previous chapters combined with that shown above has described the formation of the following types of complex with the *p*-sulfonatocalix[4,5,6]arenes:

- Lanthanide crown ether complexes.
- Lanthanide crypt or DABCO complexes.
- Lanthanide or nickel pyridine *N*-oxide complexes.
- Lanthanide 4,4'-dipyridine-*N,N'*-dioxide complexes.
- Sodium pyridine sulfonic acid complexes.

Many guest molecules have been employed throughout the course of this work in a bid to form unusual and interesting new supramolecular architectures with the *p*-sulfonatocalix[4,5,6]arenes. Indeed many of these guests were also employed in analogous systems incorporating *p*-sulfonatocalix[8]arene but single crystals were not obtained. This particular host molecule has not been structurally characterised to date and often forms micro-crystalline material upon addition of a metal salt to a mixture containing SO_3[8] and a potential guest species. When DiPyNO was employed as a guest, addition of europium nitrate to the solution again resulted in the formation of a white needle-like precipitate but upon standing overnight, the precipitate re-dissolves with

concomitant growth of near cubic-shaped yellow single crystals. The crystals were weakly diffracting and required synchotron radiation to achieve a good quality of data. The resulting supramolecular structure was a very complex 3-D coordination polymer that incorporates SO_3[8] as a guest and linking unit. This is indeed the first structural authentication of the molecule to date and shows the host to adopt near meridional geometry in a 'pleated loop' conformation similar to that observed for *p-tert*-butylcalix[8]arene.[9]

7.5.1 Synthesis of the 3-Dcoordination polymer $\{[Eu(H_2O)_7]_{0.33}[Eu(H_2O)_4]_2[Eu(H_2O)_6]$(4,4'-dipyridine-*N,N'*-dioxide)$_{4.5}$(*p*-sulfonatocalix[8]arene-2H)$\}\cdot 1.5$(4,4'-dipyridine-*N,N'*-dioxide)$\cdot 8H_2O$, 7.10.

Crystals of the complex $\{[Eu(H_2O)_7]_{0.33}[Eu(H_2O)_4]_2[Eu(H_2O)_6]$(4,4'-dipyridine-*N,N'*-dioxide)$_{4.5}$(*p*-sulfonatocalix[8]arene-2H)$\}\cdot 1.5$(4,4'-dipyridine-*N,N'*-dioxide)$\cdot 8H_2O$, **7.10**, grew upon standing from an aqueous reaction mixture containing $Na_{10}SO_3$[8], DiPyNO and europium nitrate (Equation 7.10). The complex was characterised by IR spectroscopy and single crystal X-ray crystallography. Complex **7.10** crystallises in a triclinic cell and the structural solution was performed in the space group $P\bar{1}$. Details of data collection and structure refinement are given in Table 7.18 of this chapter. A crystallographic information file containing all bond lengths and angles for complex **7.10** can be found in appendix 7.5.1 on the attached compact disc.

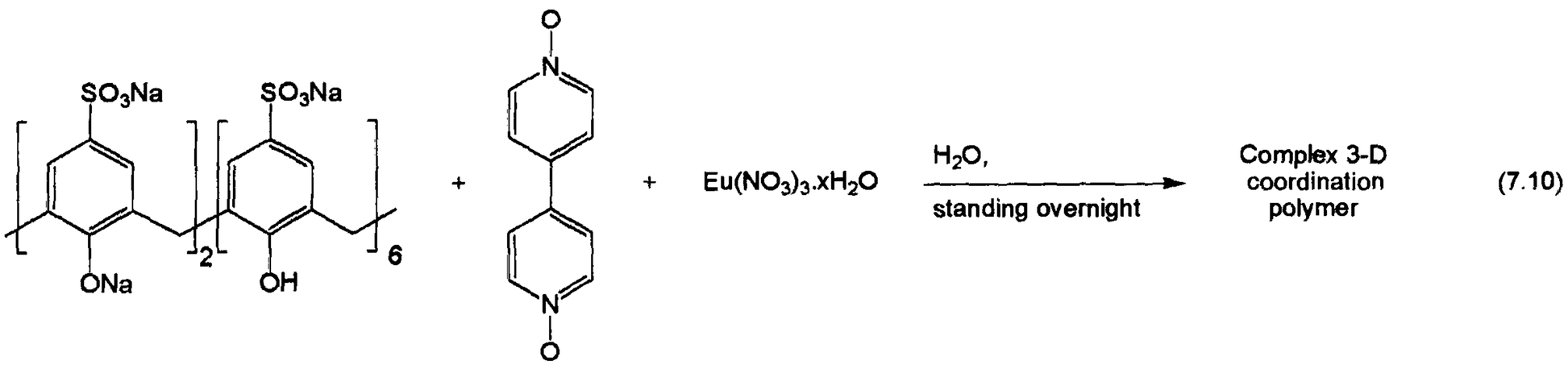

The asymmetric unit of complex 7.10 is large and comprises one deca-anionic *p*-sulfonato-calix[8]arene, a total of six DiPyNO molecules, three and a third poly-aquo europium centres and a total of eight water molecules of crystallisation that are disordered over twenty four positions. One DiPyNO molecule (at partial occupancy of 0.75), several europium aquo ligands and the oxygen atoms of two calixarene sulfonate groups were refined isotropically. Given that the asymmetric unit is complex, it will be described in parts before going on to describe the structural features of the extended 3-D coordination polymer (Figure 7.47).

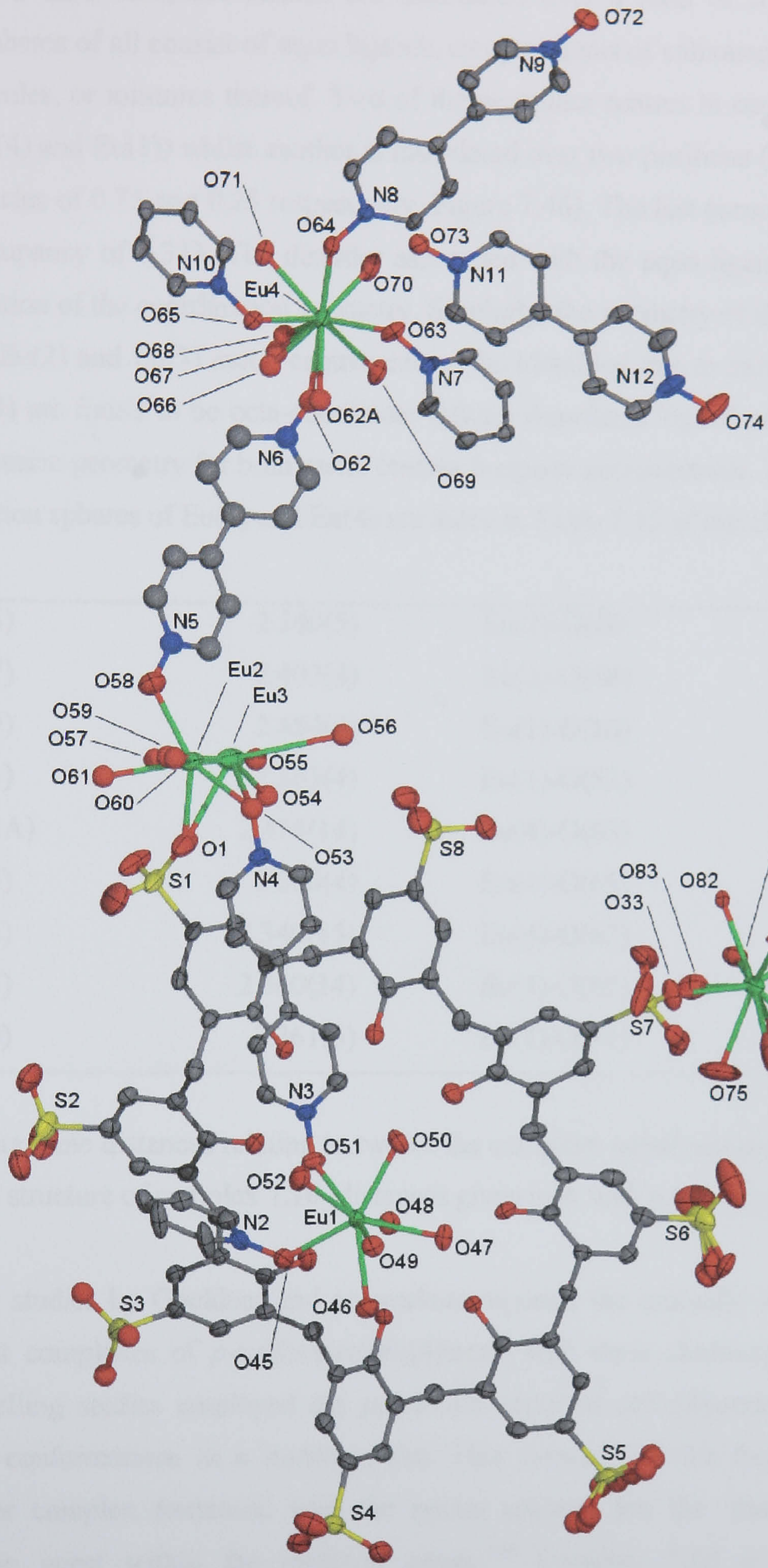

Figure 7.46 Part of the asymmetric unit from the crystal structure of complex **7.10**, anisotropic displacement ellipsoids shown at the 50% probability level. Selected atoms have been labelled. Isotropically refined atoms are shown in ball and stick representation.

The three and a third europium centres are disordered over a total of five positions and the coordination spheres of all consist of aquo ligands, oxygen atoms of calixarene sulfonate groups or DiPyNO molecules, or mixtures thereof. Two of the europium centres in complex **7.10** are at full occupancy (Eu(4) and Eu(1)) whilst another is disordered over two positions (Eu(2) and Eu(3) with partial occupancies of 0.75 and 0.25 respectively, Figure 7.46). The last europium centre (Eu(5)) is at a partial occupancy of 0.333. The disorder associated with the aquo ligands of Eu(5) does not allow identification of the coordination geometry. Similarly, the geometry of the entire coordination spheres of the Eu(2) and Eu(3) metal centres cannot be identified due to extensive disorder. Both Eu(1) and Eu(4) are found to be octa-coordinate (taking disordered ligand positions into account) and the coordination geometry for both metal centres is square anti-prismatic. Bond lengths relating to the coordination spheres of Eu(1) and Eu(4) are listed in Table 7.15 of this chapter.

Eu(1)-O(45)	2.340(5)	Eu(1)-O(46)	2.424(4)
Eu(1)-O(47)	2.402(4)	Eu(1)-O(48)	2.403(4)
Eu(1)-O(49)	2.454(4)	Eu(1)-O(50)	2.412(4)
Eu(1)-O(51)	2.361(4)	Eu(1)-O(52)	2.486(5)
Eu(4)-O(62A)	2.478(14)	Eu(4)-O(63)	2.374(4)
Eu(4)-O(64)	2.370(4)	Eu(4)-O(65)	2.366(4)
Eu(4)-O(66)	2.340(15)	Eu(4)-O(67)	2.407(12)
Eu(4)-O(68)	2.560(14)	Eu(4)-O(69)	2.471(4)
Eu(4)-O(70)	2.361(5)	Eu(4)-O(71)	2.493(5)

Table 7.15 Interatomic distances relating to two of the europium metal centre coordination spheres from the crystal structure of complex **7.10** (distances given in Å with e.s.d. in parentheses).

Recent solution studies by Goeldner and co-workers reported the mutually induced formation of some host-guest complexes of *p*-sulfonatocalix[8]arene with three cholinergic ligands.[154] Their molecular modelling studies employed the previously reported calix[8]arene 'pleated loop' and 'pinched cone' conformations as a starting point. This showed that the former of the two was unfavourable for complex formation with the guests selected but the 'pinched cone' allowed inclusion of the guest within the resultant cavity.[154] Complex **7.10** is the first structural authentication of *p*-sulfonatocalix[8]arene to date and shows the host to adopt a 'pleated loop' conformation similar to that of calix[8]arene as described above (indicated by two views in Figure 7.47).[9] When in this conformation, the host is of near meridional overall geometry and presents four 'grooves' on either side of the macrocycle that are generated by the kinking of the methylene bridging groups (Figure 7.47b).

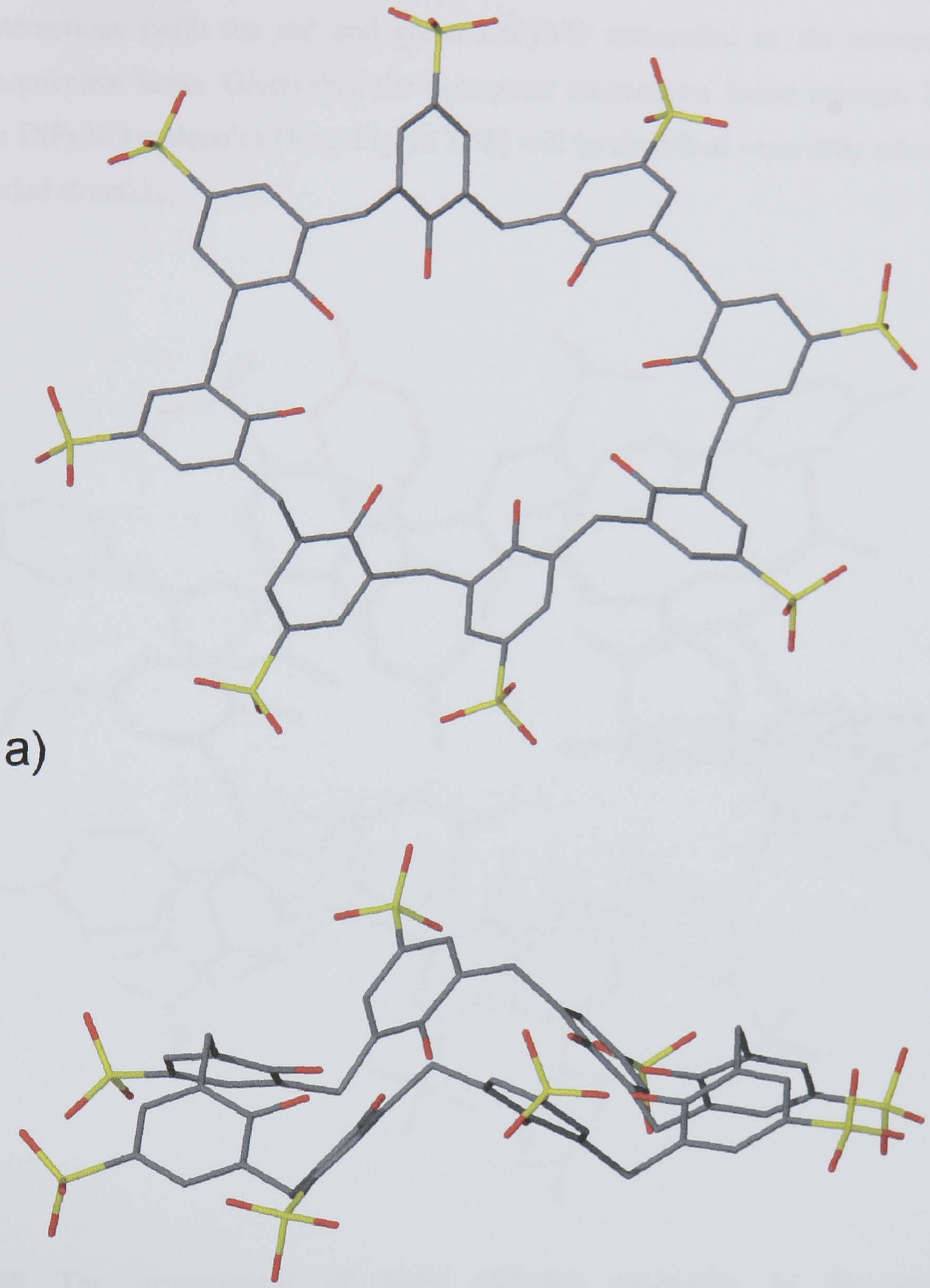

a)

b)

Figure 7.47 Top (a) and side (b) views of *p*-sulfonatocalix[8]arene from the crystal structure of complex **7.10** showing the 'pleated loop' conformation of the macrocycle (some disordered calixarene sulfonate oxygen atoms have been omitted for idealisation).

Examination of the 'grooves' formed by the 'pleated loop' conformation reveals each to be occupied by a DiPyNO molecule, four on either side of the host (as indicated by the red and green DiPyNO molecules in Figure 7.48). To aid clarity all the europium metal centres have been omitted from Figure 7.48 but will be included in latter discussion of the coordination polymer as a whole.

Upon symmetry expansion, each SO_3[8] is found to be linked through numerous CH···π and π-stacking interactions (with the red and green DiPyNO molecules) to six nearest neighbouring symmetry equivalent hosts. Given this, the host-guest interactions found between SO_3[8] and the red or green DiPyNO molecules (from Figure 7.48) will be described separately prior to description of the extended structure.

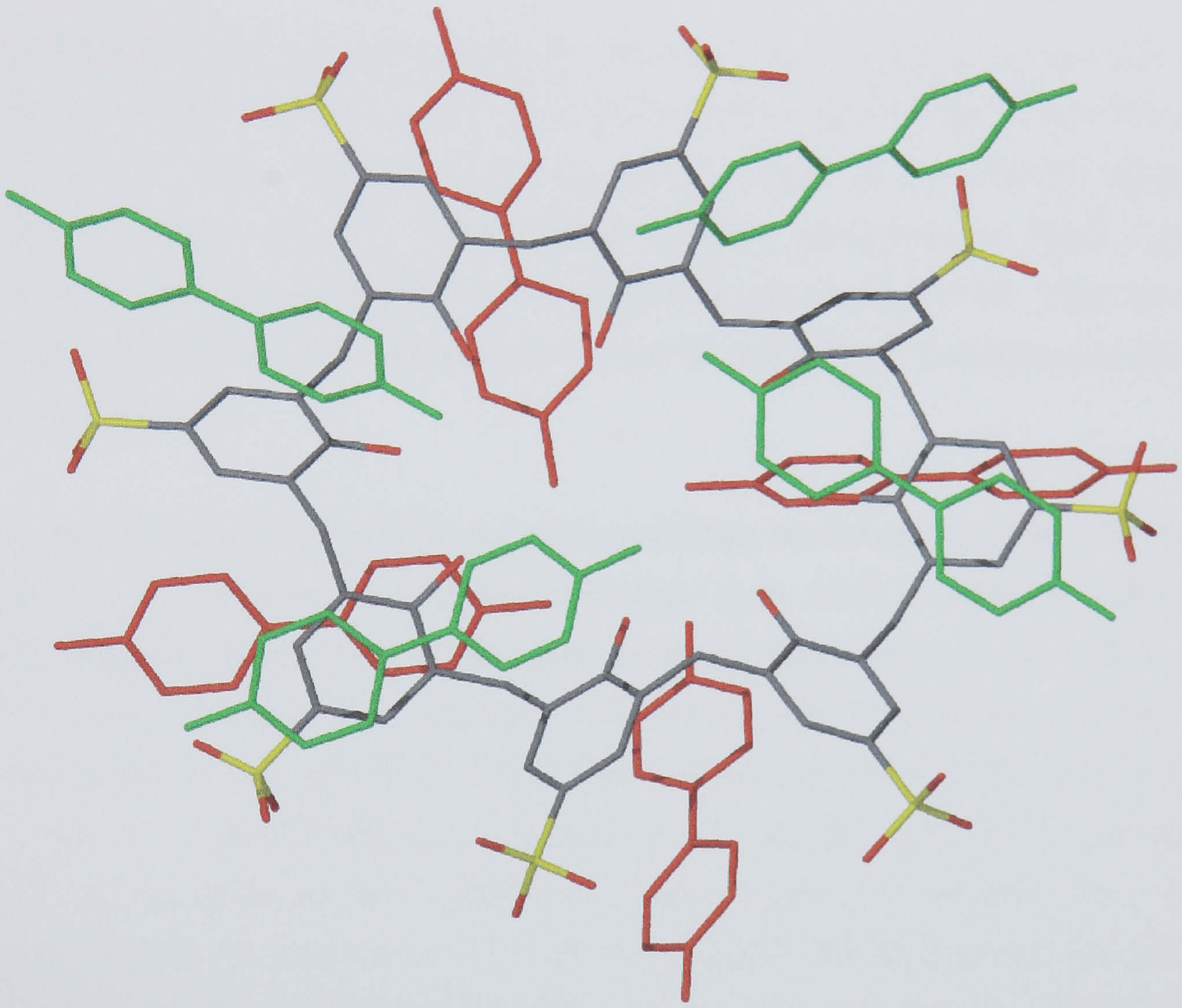

Figure 7.48 The arrangement of eight DiPyNO molecules in the grooves of *p*-sulfonatocalix[8]arene from the crystal structure of complex **7.10** (DiPyNO molecules shown completely in red or green). Four DiPyNO molecules reside on either side of the macrocycle as indicated by different guest colour. Some disordered calixarene sulfonate oxygen atoms have been omitted for idealisation and europium metal centres bound to DiPyNO molecules have also been omitted for clarity.

On one side of the host there are a total of four π-stacking and three CH···π interactions between the four green DiPyNO molecules and the aromatic rings of the SO_3[8] (Figure 7.49a, selected atoms labelled to aid relativity to the asymmetric unit in Figure 7.46). The aromatic centroid···centroid distances of the π-stacking interactions range from 3.762 to 3.925 Å whilst the CH···aromatic

centroid distances range from 2.745 to 3.045 Å. The green DiPyNO molecules are the host links to three symmetry equivalent SO_3[8] molecules through all four of the green DiPyNO guests (Figure 7.49). One SO_3[8]:SO_3[8] link forms through two of the four DiPyNO molecules (N(3)/N(4) and N(11)/N(12)) that are positioned around an inversion centre with one additional crystallographically unique DiPyNO/DiPyNO π-stacking interaction, aromatic centroid···centroid distance of 3.534 Å (Figure 7.49b).

The crystallographically unique host molecule (denoted by a # symbol in Figures 7.49 and 7.50) also links to two other SO_3[8] macrocycles *via* the N(1)/N(1)* and N(2)/N(2)* DiPyNO molecules but there are no other unique host-guest interactions. When the red DiPyNO molecules are examined in a similar fashion, a slightly different packing arrangement is found (Figure 7.50, selected atoms labelled to aid relativity to the asymmetric unit in Figure 7.46). There are a total of four π-stacking and four CH···π interactions between the red DiPyNO molecules and the aromatic rings of the calixarene.

The aromatic centroid···centroid distances of the π-stacking interactions range from 3.831 to 4.041 Å whilst the CH···aromatic centroid distances range from 2.716 to 2.864 Å. Although each crystallographically SO_3[8] links to three other symmetry equivalent hosts (as in the case of the green DiPyNO molecules), the calixarenes link through only three of the four red DiPyNO molecules (Figure 7.50). One SO_3[8]:SO_3[8] link is formed *via* the N(8)/N(9) DiPyNO molecule that π-stacks to a N(8)/N(9) symmetry equivalent with an aromatic centroid···centroid distance of 3.428 Å. The crystallographically unique SO_3[8] links to two other symmetry equivalent hosts through the N(7)/N(7)* and N(10)/N(10)* DiPyNO molecules but there are no other unique host-guest interactions. The N(5)/N(6) DiPyNO molecule plays no part in linking adjacent *p*-sulfonatocalix[8]arenes.

In order to fully understand the coordination polymer, only connecting europium centres and coordinated DiPyNO molecules will be considered initially. Of the five europium positions shown in Figure 7.46, Eu(1) – Eu(4) act as either two or three-connecting centres whilst Eu(5) is terminal and will be ignored at this point. When the above components are examined, symmetry expansion reveals a 2-D 'wavy brick wall' motif (Figure 7.51). Measurement between the three-connecting europium centres reveals each 'brick' to be ~ 5 x 2.5 nm in dimension (Figure 7.51b).

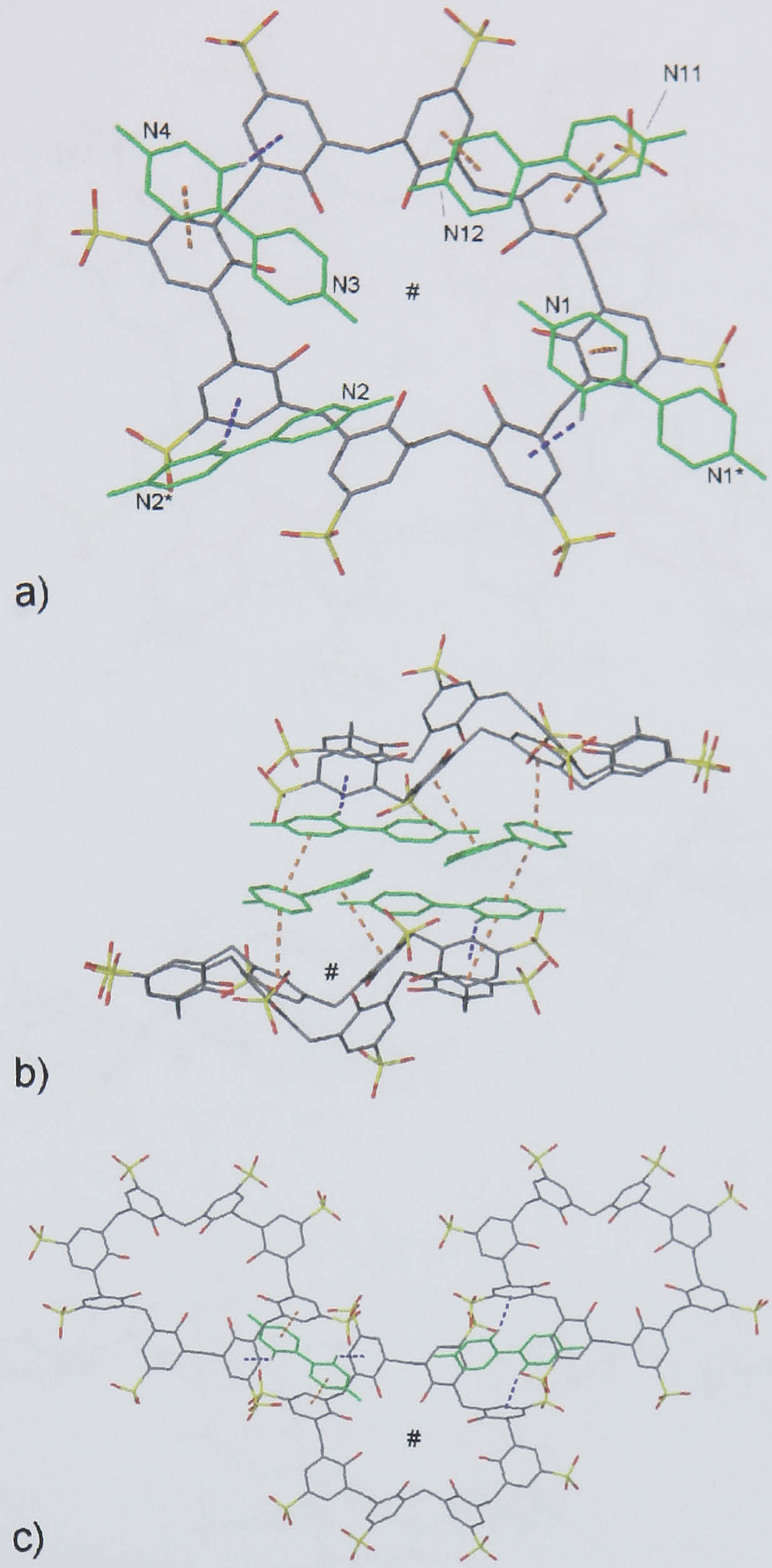

Figure 7.49 The intermolecular interactions and extended structure found between the green DiPyNO molecules (from Figure 7.48), the crystallographically unique, and neighbouring SO_3[8] from the crystal structure of complex **7.10** (CH···π and π-stacking interactions are shown as dashed purple and orange lines respectively throughout). a) The interactions found between the DiPyNO molecules occupying the grooves on one side of the SO_3[8] host (as in Figure 7.48). b) Two neighbouring SO_3[8] molecules are linked by four DiPyNO molecules through several intermolecular interactions. c) The crystallographically unique SO_3[8] links to two other symmetry equivalent macrocycles through other π-stacking and CH···π interactions. The crystallographically unique SO_3[8] is designated by a calixarene centralised # symbol in each diagram).

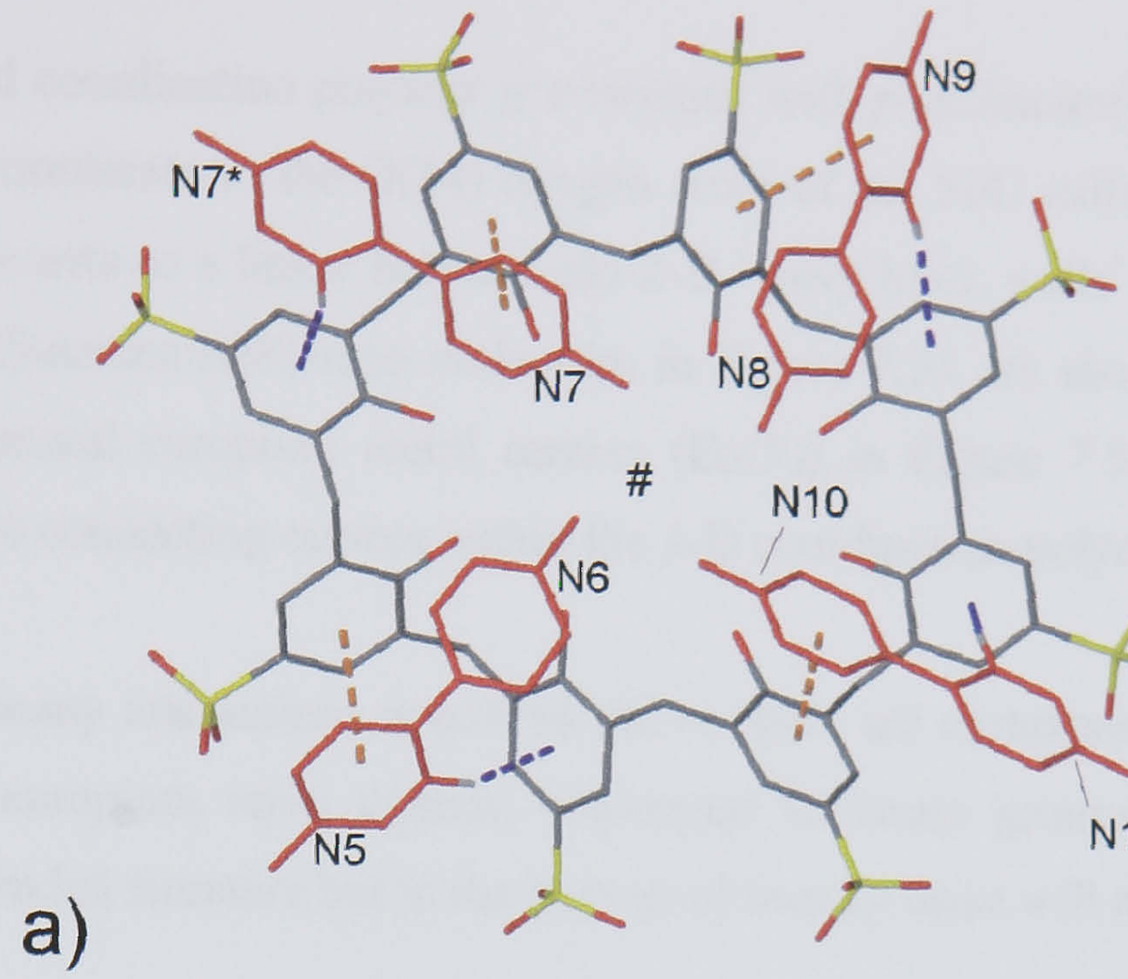

a)

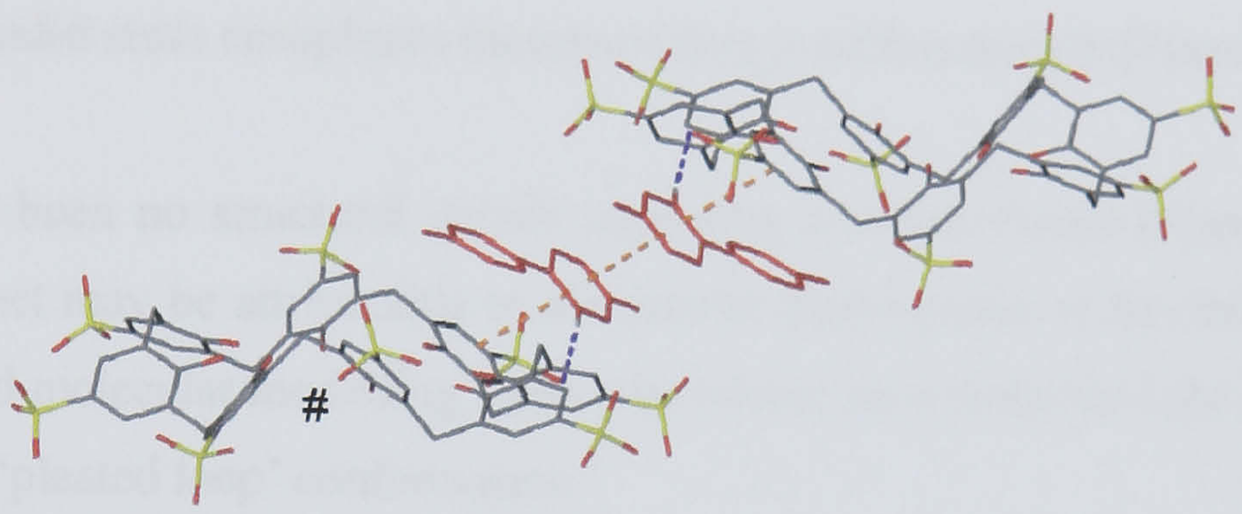

b)

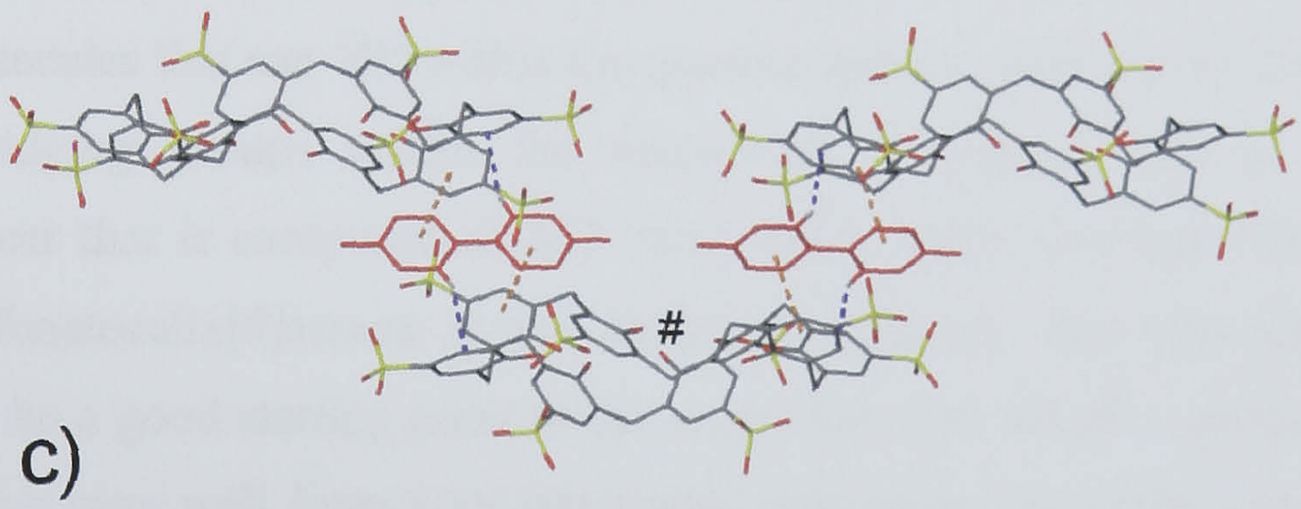

c)

Figure 7.50 The intermolecular interactions and extended structure found between the red DiPyNO molecules (from Figure 7.48), the crystallographically unique, and neighbouring SO_3[8] from the crystal structure of complex **7.10** (CH···π and π-stacking interactions are shown as dashed purple and orange lines respectively throughout). a) The interactions found between the DiPyNO molecules occupying the grooves on one side of the SO_3[8] host (as in Figure 7.48). b) Two neighbouring SO_3[8] molecules are linked by two DiPyNO molecules. c) The crystallographically unique SO_3[8] links to two other symmetry equivalent macrocycles through other π-stacking and CH···π interactions. The crystallographically unique SO_3[8] is designated by a calixarene centralised # symbol in each diagram).

When the extended coordination polymer is examined with *p*-sulfonatocalix[8]arenes incorporated, Eu(2) and Eu(3) coordinate to the O(14) oxygen atom of the S(4) sulfonate group. As this is the case, the calixarene acts as a linker between the 2-D 'wavy brick walls' (Figure 7.52). The carbon atoms of the *p*-sulfonatocalix[8]arene molecules in Figure 7.51 are shown in blue for clarity and emphasis. The terminal europium metal centres (Eu(5)) in Figure 7.52 are shown in purple to distinguish from the connecting centres within the 3-D coordination polymer.

In addition to the many interactions described above, there are numerous hydrogen bonds between water molecules, europium aquo ligands, calixarene sulfonate groups and DiPyNO molecules throughout the extended structure but in the interest of brevity these will not be described.

7.5.2 Summary of solid state complexes incorporating *p*-sulfonatocalix[8]arene.

To date there have been no structural details regarding *p*-sulfonatocalix[8]arene in the reported literature and this fact may be attributable to the greater conformational flexibility associated with SO_3[8]. Solution and molecular modelling studies by others have postulated the host to adopt either a 'pinched cone' or 'pleated loop' conformation.[9]

In complex **7.10**, SO_3[8] adopts a 'pleated loop' conformation and the calixarene is capable of bearing host to molecules that can 'fit' within the grooves that are generated by the kinking effect of the methylene bridging groups within the macrocycle. Complex **7.10** is an intricate 3-D coordination polymer that is composed of 2-D 'wavy brick walls' that both 'fit around' and link through the *p*-sulfonatocalix[8]arenes in the extended structure. The sterically suitable ligand DiPyNO may well be a good starting point in the search for other suitable guests that may interact with SO_3[8] and that may well form very interesting supramolecular architectures either as host-guest complexes, multi-guest molecular capsules, Ferris wheels, other coordination polymers or variations thereof. If it were possible to control the conformational flexibility of SO_3[8] so as to construct a multi-guest molecular capsule, the 'supermolecule' could be employed in the formation of larger nano-metre scale spheroidal arrays similar to those described in chapter five.

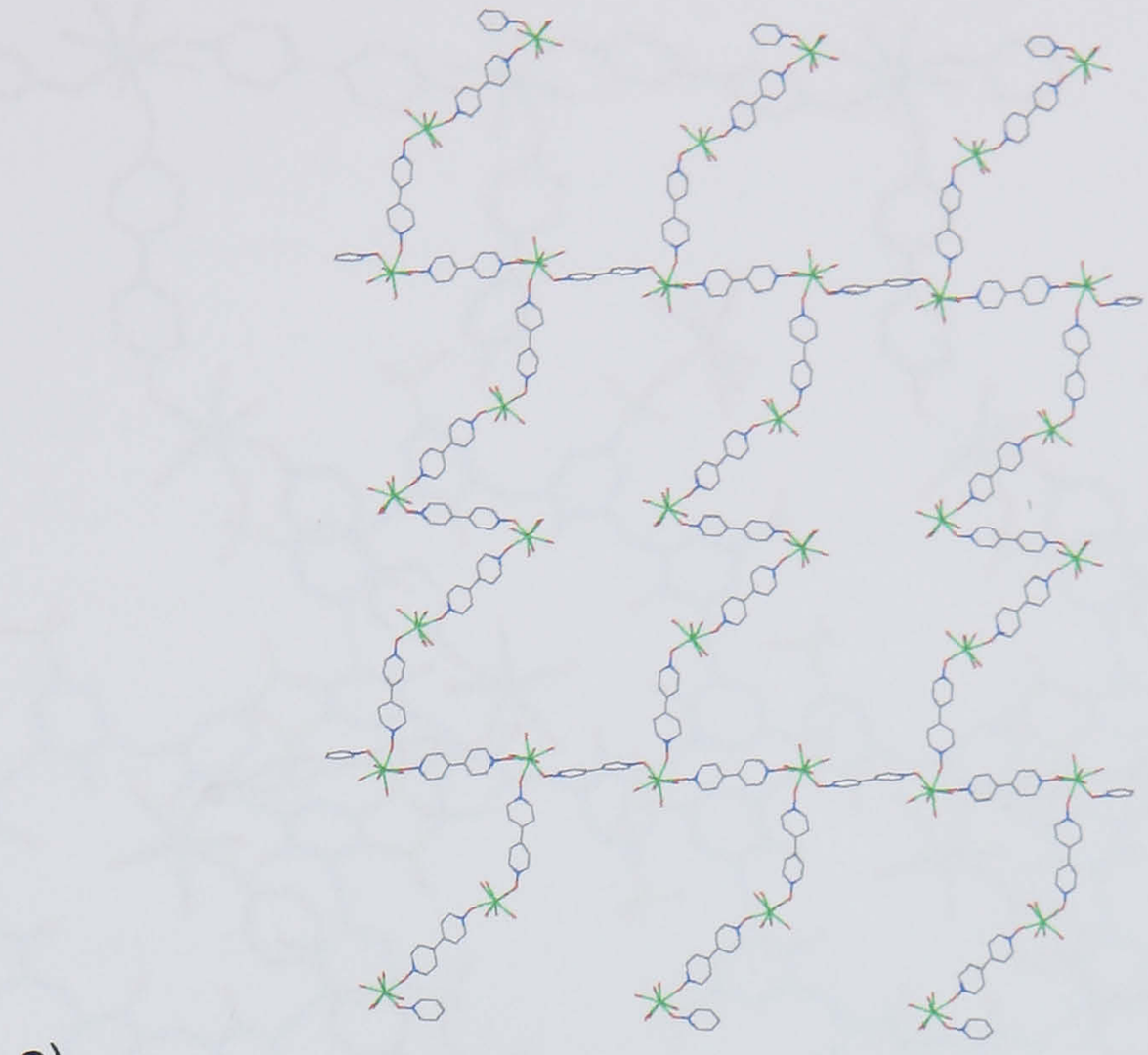

a)

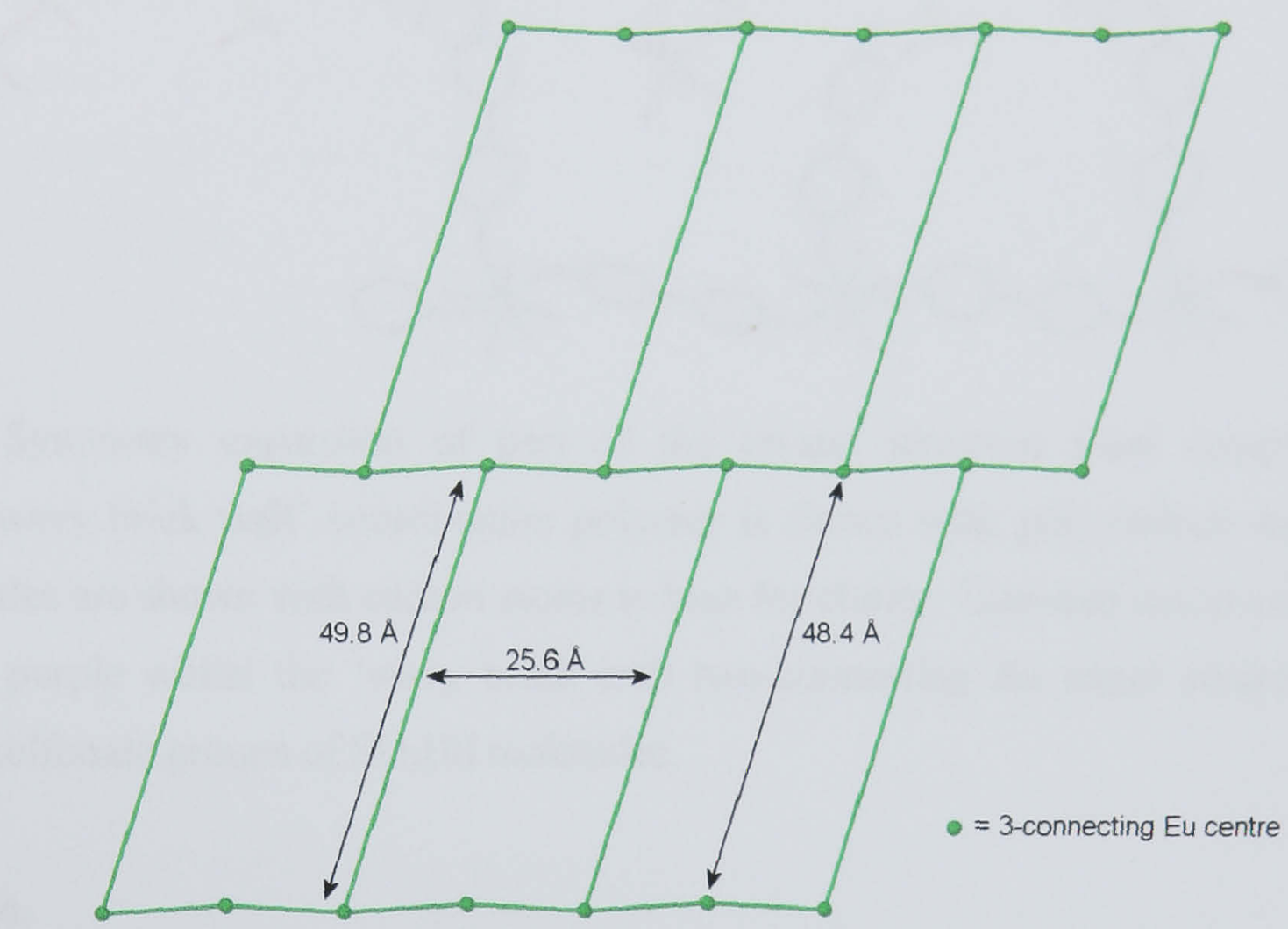

b)

Figure 7.51 The 'wavy brick wall' coordination polymer formed between europium metal centres and DiPyNO molecules from part of the crystal structure of complex **7.10** (terminal DiPyNO and other molecules omitted for clarity). a) The two and three connecting europium centres are seen to form the coordination polymer with DiPyNO. b) The 'wavy brick wall' topology of the extended coordination polymer is shown when three connecting europium centres are joined together (two connecting centres and DiPyNO molecules omitted for clarity). Approximate intra-brick wall dimensions are also shown.

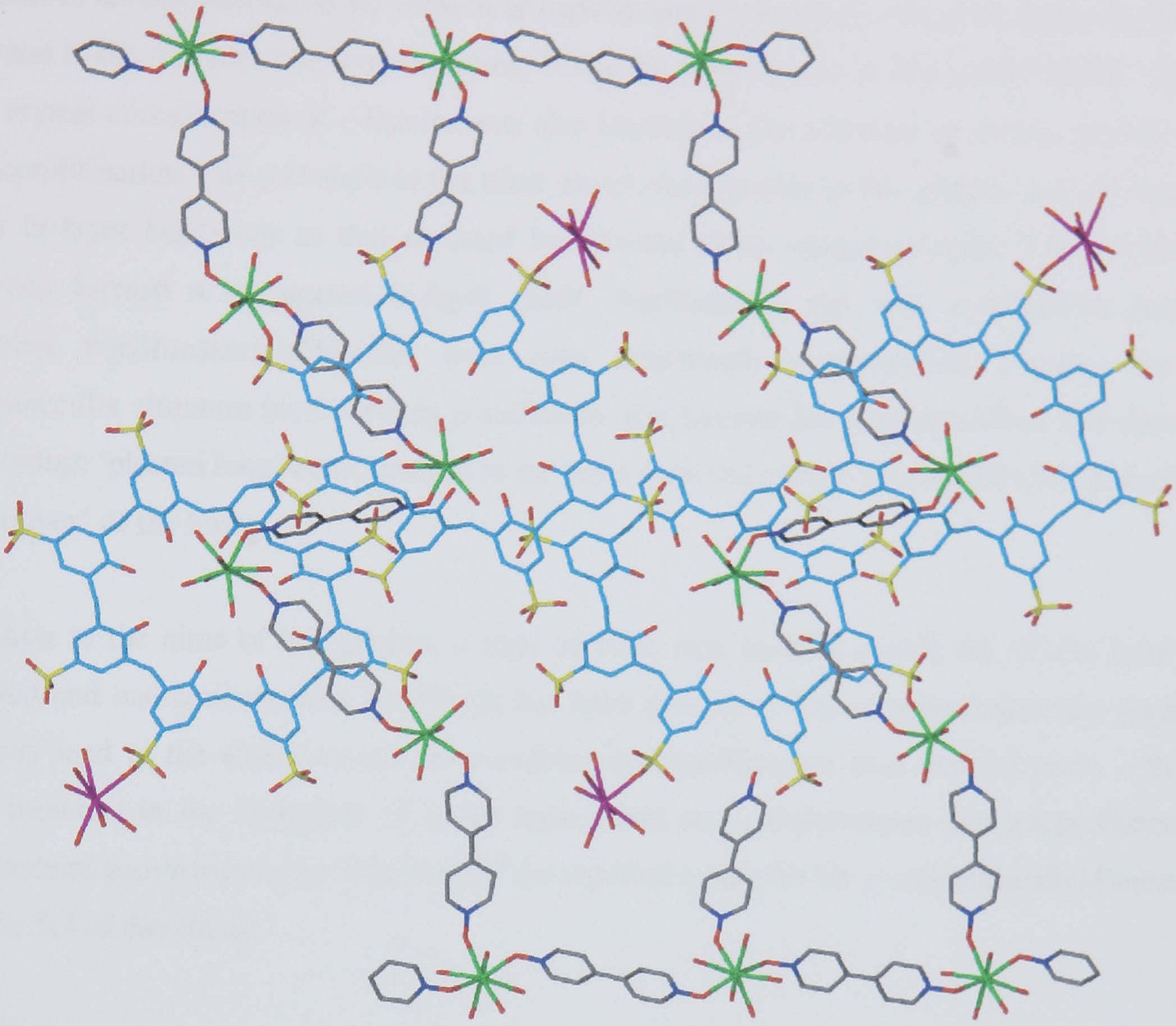

Figure 7.52 Symmetry expansion of part of the crystal structure from complex **7.10**. The Eu/DiPyNO 'wavy brick wall' coordination polymer is shown with grey carbon atoms whilst the SO_3[8] molecules are shown with carbon atoms in blue for clarity. Terminal europium metal centres are shown in purple whilst the 'wavy brick wall two-connecting Eu metal centres' are seen to coordinate to sulfonate groups of SO_3[8] molecules.

7.6 Conclusion.

For almost a decade the solid state supramolecular chemistry of *p*-sulfonatocalix[6]arene has remained in an embryonic state.[69] The analogous chemistry relating to *p*-sulfonatocalix[8]arene has been non-existent. The reason for this may possibly relate to the fact that much attention has been devoted to the tetrameric analogue that is particularly good at forming single crystalline material in bi-layer arrangements with a large number of guests and or metal cations.[25-27, 34, 35, 52, 59, 60, 110] Another reason may be the difficulty in controlling the conformational freedom of the larger hosts that may hinder the growth of single crystals suitable for X-ray diffraction studies. The results presented in this chapter have shown that the conformational freedom of *p*-sulfonatocalix[6]arene can be controlled through the formation of lanthanide crown ether complexes. This resulted in the

formation of an unprecedented *bis*-molecular capsule and a new Ferris wheel arrangement with the calixarene in the 'double cone' conformation. When the calixarene is in this conformation, selective single crystal complexation of L-leucine was also identified. The alternate up-down 'double partial cone' conformation was prevalent in the other structures reported in this chapter and all displayed similar bi-layer behaviour as that reported by Atwood et al. except complex **7.6** in which the calixarene formed a corrugated bi-layer motif. Additionally, the first coordination polymers containing *p*-sulfonatocalix[6]arene were also structurally characterised. Finally, the first supramolecular structure incorporating *p*-sulfonatocalix[8]arene has been described and shows the host to adopt 'pleated loop' conformation in the solid state and to bear host to DiPyNO molecules in the 'grooves' of the host.

In relation to the aims of this project, a total of three new packing motifs for SO_3[6] have been identified and one conformation for SO_3[8] has been described. The structural diversity present in both may lead to the ability to use the *p*-sulfonatocalix[6,8]arenes as a two (or more – SO_3[8]) vertex moieties in the formation of larger nano-metre scale architectures that adopt Platonic or Archimedean geometries as an extension to the reported examples for *p*-sulfonatocalix[4]arene and complex **5.2** of this thesis.

7.7 Experimental

The *p*-sulfonatocalix[6,8]arenes were synthesised by literature methods and purity was checked *via* ^{1}H NMR spectroscopy.[8] The pyridine *N*-oxide, 4,4'-dipyridine-*N,N'*-dioxide and 3-pyridine sulfonic acid, L-, D-, and DL-leucine were all purchased from Aldrich and used as supplied without further purification. X-ray data for complexes **7.1** – **7.3** and **7.6** – **7.9** were collected at 150(2) K on an Enraf-Nonius KappaCCD diffractometer with Mo-Kα radiation.

X-ray data for complex **7.4** was collected at 100(2) K on a Bruker-Nonius X8 diffractometer with Mo-Kα radiation. X-ray data for complex **7.5** was collected at 173(2) K on a Bruker Smart CCD diffractometer with Mo-Kα radiation. Finally the X-ray data for complex **7.10** was collected at 115(2) K on a Bruker Smart CCD diffractometer with synchotron radiation with a wavelength of 0.6903 Å. Data were corrected for Lorentz an polarisation effects and absorption corrections were applied using multi-scan techniques. The structures of complexes **7.1** – **7.9** were solved by direct methods using SHELXS-97 and refined with full-matrix least squares on F^2 using SHELXL-97. The structure of complex **7.10** was solved by direct methods using SHELXS-97 and refined with BLOC-matrix least squares on F^2 using SHELXL-97. Unless otherwise stated, hydrogen atoms

were placed at geometrically calculated positions in all complexes with the exception of aquo ligands and water molecules of crystallisation.

Complex number	**7.1**	**7.2**	**7.3**
Formula	$C_{54}H_{137}O_{71.50}S_6Tb_2$	$C_{54}H_{106}Eu_2O_{56}S_6$	$C_{66}H_{152}Eu_2O_{76}S_6$
*M*r	2440.84	2147.67	2658.16
Crystal system	Monoclinic	Orthorhombic	Triclinic
Space group	$P2_1/n$	$P2_12_12_1$	$P\bar{1}$
T/K	150(2)	150(2)	150(2)
a /Å	22.026(2)	17.1491(2)	14.6331(3)
b /Å	18.798(2)	17.9560(2)	21.2138(4)
c /Å	24.923(2)	26.9000(3)	21.5897(4)
α /°	90	90	110.254(1)
β /°	104.75(5)	90	103.205(1)
γ /°	90	90	105.409(1)
U Å^3	9979.02(16)	8283.30(16)	5668.40(19)
Z	4	4	2
F(000)	5036	4400	2756
ρ_{calc} /g cm^{-3}	1.625	1.722	1.557
μ /cm^{-1}	1.644	1.763	1.317
$\Theta_{min,\ max}$ /°	1.37, 26.0	1.64, 26.0	1.52, 25.0
Data collected	144919	58373	69386
Unique data	19568	16184	19411
R_{int}	0.1117	0.0691	0.1093
Obs data (I>2 $\sigma(I)$)	14892	13854	15493
Parameters	1303	1063	1322
Restraints	0	0	0
R_1 (observed data)	0.0942	0.0476	0.1505
ωR_2 (all data)	0.2181	0.1263	0.3639
S	1.255	1.039	1.123
Max/min residuals [eÅ^3]	1.619, -2.529	2.815, -1.142	4.695, -1.94

Table 7.16 Details of data collection and structure refinement for complexes **7.1** – **7.3**.

Infrared spectra were run either as a KBr disc or as a solid phase on a MIDAC FT-IR or Perkin-Elmer Spectrum One spectrometer respectively. In general, microanalyses were only performed on crystals of samples that did not show visual degradation upon removal from the mother liquor (complex **7.8**).

7.7.1 Synthesis of the *bis*-molecular capsule [{(H_2O⊂18-crown-6)·2H_2O}$_2$⊂[{($Tb(H_2O)_8$(*p*-sulfonatocalix[6]arene)}$_2$][$Tb(H_2O)_8$]$_2$]·23.5H_2O, 7.1.

Sulfonatocalix[6]arene (8 mg, 7 μmol), 18-crown-6 (8 mg, 30 μmol), and anhydrous terbium(III)chloride (10 mg, 38 μmol) were dissolved in distilled water (2 cm^3). Upon slow

evaporation over three days, small prismatic colourless crystals that were suitable for single crystal X-ray analysis formed. Yield 10 mg, 56 %. IR (solid phase, ν cm^{-1}): 3328s, 2890s, 1646m, 1471m, 1352m, 1248m, 1163m, 1103s, 1040s, 956s. The increase in the number of sulfonate group stretching frequencies suggests lanthanide/sulfonate coordination, as was found in the crystal structure solution. **X-ray crystallography**: The oxygen atoms of the S(6) calixarene sulfonate group were disordered and modelled over two positions with equal occupancies. The atoms of the S(2)/S(3) calixarene sulfonate group are disordered with partial occupancies of 0.7 and 0.3. Two of the Tb(1) aquo ligands are disordered over two positions with equal occupancies. The disordered oxygen of the S(2)/S(3) calixarene sulfonate group atoms and some disordered waters of crystallisation were refined isotropically. Residual electron density in complex **7.1** is located around 1 Å from the Tb(1) metal centre.

7.7.2 Synthesis of the Ferris wheel arrangement [(Eu(H$_2$O)$_2$⊂18-crown-6)∩(*p*-sulfonato-calix[6]arene)(Tb(H$_2$O)$_7$]·17H$_2$O, 7.2.

p-Sulfonatocalix[6]arene (10 mg, 8.9 μmol), 18-crown-6 (8 mg, 30 μmol), and anhydrous europium(III)chloride (10 mg, 39 μmol) were dissolved in distilled water (2 cm^3). Upon standing over three days, large purple/brown prismatic crystals that were suitable for single crystal X-ray analysis formed. Yield 15 mg, 77 %. IR (solid phase, ν cm^{-1}): 3368s, 2953m, 1637m, 1471w, 1155w, 1108m, 1071m, 1046s, 1039s, 962w. The increase in the number of sulfonate group stretching frequencies suggests lanthanide/sulfonate coordination, as was found in the crystal structure solution. **X-ray crystallography**: The largest residual electron density in complex **7.2** is associated with a possibly disordered aquo ligand of the Eu(2) metal centre. Other residual electron density is located around 1 Å from the Eu(1) metal centre.

7.7.3 Synthesis of the complex [Eu(H$_2$O)$_9$][{18-crown-6 ∩ (*p*-sulfonatocalix[6]-arene)$_{0.5}$}$_2$]·21.5H$_2$O, 7.3.

p-Sulfonatocalix[6]arene (10 mg, 8.9 μmol), 18-crown-6 (20 mg, 75 μmol), and anhydrous europium(III)chloride (8 mg, 31 μmol) were dissolved in distilled water (2 cm^3). Upon standing over three days, large colourless prismatic crystals that were suitable for single crystal X-ray analysis formed. Yield 17 mg, 73 %. IR (solid phase, ν cm^{-1}): 3370s, 2878s, 1647m, 1470m, 1451m, 1353m, 1250m, 1103s, 951m. The minor changes in sulfonate group stretching frequencies suggests that the calixarene is non-coordinating, as was found in the crystal structure solution. **X-ray crystallography**: The oxygen atoms of both the S(5) and S(6) calixarene sulfonate group were

disordered and modelled over two positions with equal occupancies. One Eu(2) aquo ligand is disordered over two positions with equal occupancies. The oxygen atoms of the S(3), S(5) and S(6) calixarene sulfonate groups, some disordered waters of crystallisation and one Eu(2) aquo ligand were refined isotropically. Residual electron density in complex **7.3** is located around 1Å from both europium metal centres.

7.7.4 Synthesis of the amino acid complex [($_L$-leucine + H^+)$_2$⊂*p*-sulfonatocalix[6]arene][$_L$-leucine + H^+)$_4$].3.25H_2O, 7.4.

1*M* hydrochloric acid was added to a solution containing octa-sodium *p*-sulfonatocalix[6]arene (15 mg, 11.5 μmol) and $_{DL}$-leucine (16 mg, 115 μmol) until the pH was adjusted to be < 1. Upon slow evaporation and consequent solution concentration, crystals of two morphologies that were suitable for X-ray diffraction studies formed. They were found to be complex **7.4** and $_L$-leucine hydrochloride. Given the formation of two crystal morphologies, NMR and IR spectroscopy could not be used to analyse the bulk sample.

Crystals of complex **7.4** were also grown from a solution containing *p*-sulfonatocalix[6]arene (15 mg, 11.5 μmol) and optically pure $_L$-leucine (16 mg, 115 μmol). Yield 10 mg, 45%. Both the unit cell and X-ray crystal structure of the crystals from the optically pure $_L$-leucine solution were very similar to that of complex **7.4**. Unfortunately the quality of precluded the acceptable location and resolution of all six L-leucine molecules within the lattice but the two crystal structures can be considered isostructural. NMR spectroscopy of the crystals obtained from the optically pure $_L$-leucine solution were analysed by both IR and NMR spectroscopy in order to verify the SO_3[6]:$_L$-leucine stoichiometry. IR (solid phase, ν cm^{-1}): 3398s, 2959s, 1581s, 1514s, 1405s, 1185s, 1168s, 1112s, 1048s. The minor changes in sulfonate group stretching frequencies suggests that the calixarene is non-coordinating, as was found in the crystal structure solution. NMR δ_H (250 MHz,, D2O): 7.54 (12H, s, ArH), 3.96, (12H, s, CH_2), 1.54 (18H, m, CH, CH_2), 0.65, (dd, CH_3). **X-ray crystallography (complex 7.4 {from the $_{DL}$-mixture})**: The oxygen atoms of the S(1) calixarene sulfonate group were disordered and modelled over two positions with partial occupancies of 0.8 and 0.2. In addition, the S(1) sulfonate oxygen atoms were refined with fixed thermal parameters. The oxygen atoms of the S(2) calixarene sulfonate group were disordered and modelled over two positions with partial occupancies of 0.9 and 0.1. In addition, the S(2) sulfonate oxygen atoms were refined with fixed thermal parameters. The N(4), N(5), N(6) and badly disordered N(7)/N(8) L-leucine molecules were refined isotropically. One methyl group of the N(5) $_L$-leucine molecule is disordered over two positions at partial occupancies of 0.6 and 0.4. Also, one of the methyl groups

of the N(4) L-leucine molecule is disordered over two positions with equal occupancies. All but two of the waters of crystallisation (both at a partial occupancy of 0.5) were refined isotropically. Some bond lengths between atoms of the L-leucine molecules were restrained to be chemically reasonable. Some bond lengths were restrained to be chemically meaningful.

Complex number	**7.4**	**7.5**	**7.6**
Formula	$C_{78}H_{120.50}N_6O_{39.25}S_6$	$C_{67}H_{95}N_5O_{49}S_6Yb_2$	$C_{26}H_{39}LaNO_{23}S_3$
Mr	1962.66	2292.92	968.67
Crystal system	Orthorhombic	Triclinic	Monoclinic
Space group	$P2_12_12_1$	$P\bar{1}$	$P2_1/c$
T/K	100(2)	173(2)	150(2)
a /Å	18.5302(8)	12.487(4)	17.2709(2)
b /Å	21.3013(8)	17.799(5)	18.4511(3)
c /Å	24.4166(11)	20.803(6)	11.9992(3)
α /°	90	113.601(4)	90
β /°	90	91.155(5)	108.716(1)
γ /°	90	91.297(5)	90
U Å^3	9637.7(7)	4234(2)	3621.55(12)
Z	4	2	4
F(000)	4162	2320	1964
ρ_{calc} /g cm^{-3}	1.353	1.799	1.777
μ /cm^{-1}	0.231	2.452	1.445
$\Theta_{min,\ max}$ /°	2.09, 25.18	1.63, 27.14	2.49, 26.0
Data collected	102169	37445	65215
Unique data	17229	18422	7107
R_{int}	0.1411	0.0434	0.1185
Obs data ($I>2\ \sigma(I)$)	8738	14123	6197
Parameters	1083	1197	482
Restraints	12	0	0
R_1 (observed data)	0.09	0.044	0.0646
ωR_2 (all data)	0.2378	0.1089	0.1618
S	1.216	1.028	1.14
Max/min residuals [eÅ^3]	0.695, -0.432	1.713, -1.466	3.132, -1.006

Table 7.17 Details of data collection and structure refinement for complexes **7.4 – 7.6**.

7.7.5 Synthesis of the complex [Yb(H$_2$O)$_6$(pyridine *N*-oxide)(*p*-sulfonatocalix-[6]arene)$_{0.5}$][Yb(H$_2$O)$_5$(pyridine *N*-oxide)$_2$(*p*-sulfonatocalix[6]arene)$_{0.5}$]·9H$_2$O·2pyridine *N*-oxide, 7.5.

Sodium *p*-sulfonatocalix[6]arene (30 mg, 23 μmol), pyridine *N*-oxide (5 mg, 53 μmol), and ytterbium(III) nitrate pentahydrate (21 mg , 46 μmol) were dissolved in distilled water (1.5 cm^3). Over three days, large colourless plates formed which were suitable for X-ray diffraction studies. Yield 19 mg, 37 %. IR (KBr disc, ν cm^{-1}): 3350s, 2943m, 2343m, 1647m, 1593m, 1473s, 1450m,

1219s, 1155s, 1111s, 1043s. The increase in the number of sulfonate group stretching frequencies suggests lanthanide/sulfonate coordination, as was found in the crystal structure solution. **X-ray crystallography**: One non-coordinating pyridine *N*-oxide molecule was disordered over two positions (at equal occupancies) and was refined isotropically. The hydrogen atoms of the calixarene base hydroxy groups were located in the difference map and refined accordingly.

Complex number	**7.7**	**7.8**
Formula	$C_{52}H_{90}N_2Ni_3O_{51}S_6$	$C_{26}H_{39}EuNO_{23}S_3$
*M*r	1927.75	981.72
Crystal system	Triclinic	Monoclinic
Space group	$P\bar{1}$	$P2_1/c$
T/K	150(2)	150(2)
a /Å	12.3959(3)	13.8169(2)
b /Å	17.6908(3)	12.2289(2)
c /Å	20.1012(4)	22.3563(4)
α /°	66.2390(1)	90
β /°	72.2680(1)	101.9011(3)
γ /°	71.2420(1)	90
U Å^3	3741.43(13)	3595.4(1)
Z	2	4
F(000)	2008	1988
ρ_{calc} /g cm^{-3}	1.711	1.814
μ /cm^{-1}	1.029	2.012
$\Theta_{min,\ max}$ /°	2.19, 27.47	2.54, 27.5
Data collected	65851	29098
Unique data	16881	8187
R_{int}	0.1087	0.0885
Obs data (I>2 $\sigma(I)$)	11980	6464
Parameters	1027	487
Restraints	0	0
R_1 (observed data)	0.0651	0.0362
ωR_2 (all data)	0.1956	0.0882
S	1.024	1.018
Max/min residuals [eÅ^3]	1.467, -1.364	0.805, -0.967

Table 7.18 Details of data collection and structure refinement for complexes **7.7** and **7.8**.

7.7.6 Synthesis of the complex [(La(H$_2$O)$_7$(pyridine *N*-oxide))$_2$(*p*-sulfonatocalix-[6]arene)]·6H$_2$O, 7.6.

Octa-sodium *p*-sulfonatocalix[6]arene hydrate (30 mg, 23 μmol), pyridine *N*-oxide (5 mg, 53 μmol), and lanthanum(III) nitrate hexa-hydrate (20 mg , 46 μmol) were dissolved in distilled water (1.5 cm^3). Over two days, colourless plates that were suitable for single crystal X-ray analysis formed. Yield 8 mg, 36 %. IR (KBr disc, ν cm^{-1}): 3250s, 2949m, 1642m, 1472s, 1448m, 1419w,

1364m, 1240s, 1149s, 1117s, 1103s, 1044s. The increase in the number of sulfonate group stretching frequencies suggests lanthanide/sulfonate coordination, as was found in the crystal structure solution. **X-ray crystallography**: Residual electron density in the crystal structure of complex **7.6** is located around 1 Å from a lanthanum metal centre.

Complex number	**7.9**	**7.10**
Formula	$C_{26}H_{50}NNa_3O_{25}S_4$	$C_{113.50}H_{134}Eu_{3.33}N_{11.50}O_{68.50}S_8$
Mr	973.88	3518.28
Crystal system	Monoclinic	Triclinic
Space group	$P2_1/n$	$P\bar{1}$
T/K	150(2)	123(2)
a /Å	17.854(4)	16.9935(8)
b /Å	12.266(3)	22.1127(11)
c /Å	18.081(4)	23.0089(11)
α /°	90	69.117(1)
β /°	106.53(3)	69.422(1)
γ /°	90	71.419(1)
U Å^3	3795.9(13)	7375.6(6)
Z	4	2
F(000)	2040	3563
ρ_{calc} /g cm^{-3}	1.704	1.584
μ /cm^{-1}	0.383	1.611
$\Theta_{min,\ max}$ /°	2.18, 27.49	1.79, 27.5
Data collected	68759	50036
Unique data	8691	35978
R_{int}	0.1137	0.0281
Obs data ($I>2\ \sigma(I)$)	6875	26702
Parameters	619	1946
Restraints	23	0
R_1 (observed data)	0.0413	0.0699
ωR_2 (all data)	0.1067	0.2151
S	1.042	1.026
Max/min residuals [eÅ^3]	0.653, -0.983	2.723, -3.113

Table 7.19 Details of data collection and structure refinement for complexes **7.9** and **7.10**.

7.7.7 Synthesis of the complex [(Ni(H$_2$O)$_6$)$_3$][(pyridine *N*-oxide)$_2$⊂(*p*-sulfonatocalix-[6]arene)]·7H$_2$O, 7.7.

Octa-sodium *p*-sulfonatocalix[6]arene hydrate (15 mg, 11.5 μmol), pyridine *N*-oxide (2.5 mg, 26.5 μmol), and nickel(II) chloride hexa-hydrate (14 mg , 60 μmol) were dissolved in distilled water (1.5 cm^3). Over several days, pale green plates that were suitable for single crystal X-ray analysis formed. Yield 10 mg, 45 %. IR (KBr disc, ν cm^{-1}): 3276s, 2965m, 1636m, 1473s, 1362m, 1211s, 1148s, 1045s. The minor changes in sulfonate group stretching frequencies suggests that the

calixarene is non-coordinating, as was found in the crystal structure solution. X-ray **crystallography**: Residual electron density in the crystal structure of complex **7.7** is located around 1 Å from a nickel metal centre.

7.7.8 Synthesis of the coordination polymer $[(Eu(H_2O)_6)_2][(4,4'\text{-dipyridine-}N,N'\text{-dioxide})(p\text{-sulfonatocalix[6]arene})]\cdot 8H_2O$, 7.8.

Octa-sodium *p*-sulfonatocalix[6]arene hydrate (15 mg, 11.5 μmol), 4,4'-dipyridine-*N,N'*-dioxide (5 mg, 25 μmol), and europium(III) nitrate hydrate (12 mg , 35 μmol) were dissolved in distilled water (2 cm^3). Over several days, small colourless plates that were suitable for single crystal X-ray analysis formed. Yield 5 mg, 44 %. IR (KBr disc, ν cm^{-1}): 3333s, 2941m, 1665s, 1478s, 1450m, 1431m, 1372m, 1215s, 1161s, 1116s, 1042s, 1039s. The increase in the number of sulfonate group stretching frequencies suggests lanthanide/sulfonate coordination, as was found in the crystal structure solution. Microanalysis calculated for $C_{26}H_{39}N_1O_{23}S_3Eu_1$: C, 31.81; H, 4.00; N, 1.43. Found: C, 31.35; H, 4.05; N, 1.55. **X-ray crystallography**: Hydrogen atoms were located on five of the europium aquo ligands and one water of crystallisation and refined accordingly.

7.7.9 Synthesis of the coordination polymer $[(3\text{-pyridinium sulfonate})(Na_3(H_2O)_9)(p\text{-sulfonatocalix[6]arene})_{0.5}]\cdot 1H_2O$, 7.9.

Octa-sodium *p*-sulfonatocalix[6]arene hydrate (15 mg, 11.5 μmol) and 3-pyridine sulfonic (, 11.5 μmol, XS) acid were dissolved in distilled water (1 cm^3). The pH of the solution was adjusted to be <1 *via* addition of 1M HCl. Upon slow evaporation over several days, large colourless crystals that were suitable for single crystal X-ray analysis formed. Yield 7 mg, 63 %.

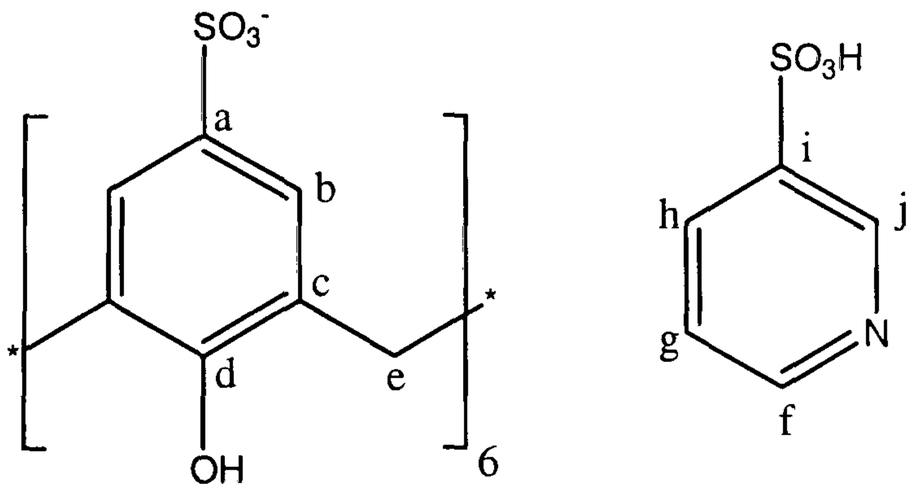

^1H NMR (250 MHz, D_2O) δ = 9.11 (s, 1H, C_jH), 8.83 (d, 1H, C_hH or C_fH), 8.80 (d, 1H, C_hH or C_fH), 8.05 (dd, 1H, C_gH), 7.50 (12H, C_bH), 3.93 (12H, C_eH). ^{13}C NMR (D_2O) δ = 153.4, 145.1,

144.6, 143.2, 170.2, 170.0, 136.2, 126.2, 126.0, 32.1 **X-ray crystallography**: Some OH (water of crystallisation and sodium aquo ligands) and the NH ($PySO_3$) bond lengths were restrained to be chemically reasonable.

7.7.10 Synthesis of the 3-Dcoordination polymer {$[Eu(H_2O)_7]_{0.33}[Eu(H_2O)_4]_2[Eu(H_2O)_6]$(4,4'-dipyridine-*N,N'*-dioxide)$_{4.5}$(*p*-sulfonatocalix[8]arene-2H)}·1.5(4,4'-dipyridine-*N,N'*-dioxide)·$8H_2O$, 7.10.

Sodium *p*-sulfonatocalix[8]arene (51 mg, 10 μmol) and 4,4'-dipyridine-*N,N'*-dioxide (45 mg, 0.24 mmol) were dissolved in distilled water (2 cm^3). Upon addition of europium(III) nitrate (50 mg , 0.15 mmol), a white precipitate formed which dissolved slowly overnight. Near cubic shaped yellow crystals suitable for X-ray diffraction studies grew from the resulting solution over a two day period. Yield 73 mg, 70%. IR (KBr disc, νcm^{-1}): 3408s, 2941m, 2361w, 1618m, 1591w, 1475s, 1429m, 1385w, 1223s, 1182s, 1160s, 1115s, 1043s. The increase in the number of sulfonate group stretching frequencies suggests lanthanide/sulfonate coordination, as was found in the crystal structure solution. **X-ray crystallography**: One europium centre is disordered over two positions (Eu(2) and Eu(3)) at partial occupancies of 0.75 and 0.25 respectively. The coordination sphere of Eu(3) is incomplete as it is believed that a DiPyNO molecule, that is at an occupancy of 0.75, occupies probable coordination points within the Eu(3) sphere. The oxygen atoms of both the S(5) and S(6) calixarene sulfonate groups were disordered and modelled over two positions with equal occupancies. The oxygen atoms of the S(7) calixarene sulfonate group were disordered and modelled over two positions with occupancies of 0.7 and 0.3. Several europium aquo ligands are disordered over two or three positions (all with equal occupancies). Some disordered waters of crystallisation, metal aquo ligands, one DiPyNO molecule (at a partial occupancy of 0.75), some europium aquo ligands and the oxygen atoms of two calixarene sulfonate groups (one of which is disordered) were all refined isotropically. The hydrogen atoms of the *p*-sulfonatocalix[8]arene base hydroxyl groups were calculated at positions suggested by residual electron density from the difference map. Residual electron density was located around 1 Å from the Eu(4) and Eu(5) metal centres. Additional residual electron density was located near a disordered aquo ligand of the Eu(3) metal centre and around 1 Å from the S(2) calixarene sulfur atom.

Concluding Remarks

The work presented in this thesis has shown that *p*-sulfonatocalix[4]arene is a highly versatile molecule that is capable of assembling into numerous interesting multi-faceted supramolecular architectures. The ability to control molecular capsule formation through the use of different pH regimes in the presence of lanthanide metals was demonstrated. Similarly, remarkable control can be achieved in the formation of nano-metre scale spheroids on the basis of the choice of guest molecule. A series of solution studies also showed SO_3[4]/crown ether complexation using Diffusion Ordered Spectroscopy.

Part of the work described above has furthered the supramolecular chemistry of *p*-sulfonatocalix[5]arene and characterised several new structural motifs for SO_3[5] in the presence of crown ethers or pyridine *N*-functionalised (or related) guest molecules and lanthanide metal cations.

The documented solid state supramolecular chemistry of *p*-sulfonatocalix[6]arene was scarce but work described here has explored this area and significantly increased the number of known structural motifs. At least four different solid state packing motifs have been identified and described for SO_3[6] and this was achieved through the use of several different guest molecules and or metal cations. Similarly, no solid state supramolecular chemistry has been documented for *p*-sulfonatocalix[8]arene and work described here has shown the first structural authentication of SO_3[8] to date as part of a complex coordination polymer.

Clearly the associated supramolecular chemistry of the *p*-sulfonatocalix[*n*]arenes is wide ranging with much still to be achieved. *p*-Sulfonatocalix[4]arene is the most widely studied of the class of molecules and it alone continues to provide continues to produce interesting results on a regular basis. The larger pentamer and hexamer were shown to assemble into *bis*-molecular capsule arrangements under particular conditions and these may prove useful in the isolation of other large nano-metre scale superstructures in the future.

References

1 J. M. Lehn, 'Supramolecular Chemistry: Concepts and Perspectives', VCH, 1995, Weinheim; and references therein.

2 A. M. Brouwer, C. Frochot, F. G. Gatti, D. A. Leigh, L. Mottier, F. Paolucci, S. Roffia, and G. W. H. Wurpel, *Science*, 2001, **291**, 2124

3 J. D. Badjic, V. Balzani, A. Credi, S. Silvi, and J. F. Stoddart, *Science*, 2004, **303**, 1845

4 K. S. Chichak, S. J. Cantrill, A. R. Pease, S.-H. Chiu, G. W. V. Cave, J. L. Atwood, and J. F. Stoddart, *Science*, 2004, **304**, 1308

5 J. V. Hernandez, E. R. Kay, and D. A. Leigh, *Science*, 2004, **306**.

6 T. LaBean, H. Yan, J. Kopatsch, F. Liu, E. Winfree, J. H. Reif, and N. C. Seeman, *J. Am. Chem. Soc.*, 2000, **122**, 1848

7 H. Yan, X. Zhang, S. Shen, and N. C. Seeman, *Nature*, 2002, **415**, 62

8 Z. Asfari, V. Böhmer, J. Harrowfield, and J. Vicens, 'Calixarenes 2001', Kluwer, 2001, Dordrecht; and references therein.

9 L. Mandolini and R. Ungaro, 'Calixarenes In Action', Imperial College Press, 2000, London; and references therein.

10 C. Janiak, *Dalton Trans.*, 2003, **14**, 2781

11 M. Eddaoudi, J. Kim, N. L. Rosi, D. T. Vodak, J. Wachter, M. O'Keeffe, and O. M. Yaghi, *Science*, 2002, **295**, 469.

12 N. L. Rosi, J. Eckert, M. Eddaoudi, D. T. Vodak, J. Kim, M. O'Keeffe, and O. M. Yaghi, *Science*, 2003, **300**, 1127.

13 L. Brammer, *Chem. Soc. Rev.*, 2004, **33**, 476.

14 J. W. Steed and J. L. Atwood, 'Supramolecular Chemistry', Wiley, 2000, Chichester; and references therein.

15 C. D. Gutsche, 'Calixarenes Revisited', The Royal Society of Chemistry, 1998, Cambridge; and references therein.

16 S. Shinkai, S. Mori, T. Tsubaki, T. Sone, and O. Manabe, *Tet. Lett.*, 1984, **25**, 5315.

17 G. W. Orr, L. J. Barbour, and J. L. Atwood, *Science*, 1999, **285**, 1049.

18 S. J. Harris, in 'Preparation of calixarene-based compounds having antibacterial, antifungal, anticancer, and anti-HIV activity', WO 9519974, 1995.

19 J. L. Atwood, R. J. Bridges, R. K. Juneja, and A. K. Singh, in 'Calixarene chloride-channel blockers', US. Ser. No. 748, 764, abandoned.

20 S. Shinkai, S. Mori, H. Koreishi, T. Tsubaki, and O. Manabe, *J. Am. Chem. Soc.*, 1986, **108**, 2409.

21 S. Shinkai, *Pure Appl. Chem.*, 1986, **58**, 1523.

22 S. Shinkai, K. Araki, H. Koreishi, T. Tsubaki, and O. Manabe, *Chem. Lett.*, 1986, 1351.

23 S. Shinkai, H. Koreishi, S. Mori, T. Sone, and O. Manabe, *Chem. Lett.*, 1985, 1033.

24 S. G. Bott, A. W. Coleman, and J. L. Atwood, *J. Am. Chem. Soc.*, 1988, **110**, 610.

25 A. W. Coleman, S. G. Bott, S. D. Morley, C. M. Means, K. D. Robinson, H. Zhang, and J. L. Atwood, *Angew. Chem. Int. Ed.*, 1988, **100**, 1412.

26 J. L. Atwood, A. W. Coleman, H. Zhang, and S. G. Bott, *J. Inclusion Phenom. Mol. Recognit. Chem.*, 1989, **7**, 203.

27 S. Shinkai, K. Araki, T. Matsuda, N. Nishiyama, H. Ikeda, I. Takasu, and M. Iwamoto, *J. Am. Chem. Soc.*, 1990, **112**, 9053.

28 J. L. Atwood, F. Hamada, K. D. Robinson, G. W. Orr, and R. L. Vincent, *Nature*, 1991, **349**, 683.

29 J. L. Atwood, G. W. Orr, F. Hamada, R. L. Vincent, S. G. Bott, and K. D. Robinson, *J. Am. Chem. Soc.*, 1991, **113**, 2760.

30 J. L. Atwood, G. W. Orr, F. Hamada, R. L. Vincent, S. G. Bott, and K. D. Robinson, *J. Inclusion Phenom. Mol. Recognit. Chem.*, 1992, **14**, 37.

31 J. L. Atwood, G. W. Orr, F. Hamada, S. G. Bott, and K. D. Robinson, *Supramol. Chem.*, 1992, **1**, 15.

32 J. L. Atwood, G. W. Orr, N. C. Means, F. Hamada, H. Zhang, S. G. Bott, and K. D. Robinson, *Inorg. Chem.*, 1992, **31**, 603.

33 J. L. Atwood, G. W. Orr, K. D. Robinson, and F. Hamada, *Supramol. Chem.*, 1992, **2**, 309.

34 M. J. Hardie and C. L. Raston, *Dalton Trans.*, 2000, 2483.

35 J. L. Atwood, L. J. Barbour, M. J. Hardie, and C. L. Raston, *Coord. Chem. Rev.* , 2001, **222**, 3.

36 J. L. Atwood, L. J. Barbour, P. C. Junk, and G. W. Orr, *Supramol. Chem.*, 1995, **5**, 105.

37 J. L. Atwood, L. J. Barbour, E. S. Dawson, P. C. Junk, and J. Kienzle, *Supramol. Chem.*, 1996, **7**, 271.

38 H. Iki, H. Tsuzuki, H. Kijima, I. Hamachi, and S. Shinkai, *Supramol. Chem.*, 1994, **4**, 223.

39 J. L. Atwood, G. W. Orr, R. K. Juneja, S. G. Bott, and F. Hamada, *Pure Appl. Chem.*, 1993, **65**, 1471.

40 L. J. Barbour, A. K. Damon, G. W. Orr, and J. L. Atwood, *Supramol. Chem.*, 1996, **7**, 209.

41 J. L. Atwood, G. W. Orr, and K. D. Robinson, *Supramol. Chem.*, 1994, **3**, 89.

42 K. M. Hwang, Y. M. Qi, and S. Y. Liu, in 'Method of treating viral infections with aryl macrocyclic compounds', Us, 1994.

43 K. M. Hwang, Y. M. Qi, S. Y. Liu, T. C. Lee, W. Choy, and J. Chen, in 'Antithrombotic treatment with calix(n)arene compounds', Wo, 1994.

44 A. Drljaca, M. J. Hardie, T. J. Ness, and C. L. Raston, *Eur. J. Inorg. Chem.* , 2000, 2221.

45 A. Drljaca, M. J. Hardie, C. L. Raston, and L. Spiccia, *Chem. Eur. J.*, 1999, **5**, 2295.

46 A. Drljaca, M. J. Hardie, and C. L. Raston, *J. Chem. Soc., Dalton Trans.*, 1999, 3639.

47 S. Airey, A. Drljaca, M. J. Hardie, and C. L. Raston, *Chem. Commun.*, 1999, 1137.

48 T. Ness, P. J. Nichols, and C. L. Raston, *Eur. J. Inorg. Chem.* , 2001, 1993.

49 M. J. Hardie, C. L. Raston, H. R. Webb, and J. A. Johnson, *Chem. Commun.*, 2000, 849.

50 A. Drljaca, M. J. Hardie, C. L. Raston, H. R. Webb, and J. A. Johnson, *Chem. Commun.*, 1999, 1135.

51 H. R. Webb, M. J. Hardie, and C. L. Raston, *Chem. Eur. J.*, 2001, **7**, 3616.

52 Y. Israeli, G. P. A. Yap, and C. Detellier, *Supramol. Chem.*, 2001, **12**, 457.

53 P. C. Leverd, P. Berthault, M. Lance, and M. Nierlich, *Eur. J. Org. Chem.* , 2000, 133.

54 E. Da Silva, F. Nouar, M. Nierlich, B. Rather, M. J. Zaworotko, C. Barbey, A. Navaza, and A. W. Coleman, *Cryst. Eng.*, 2003, **6**, 123.

55 N. Douteau-Guevel, A. W. Coleman, J.-P. Morel, and N. Morel-Desrosiers, *J. Phys. Org. Chem.* , 1998, **11**, 693.

56 N. Douteau-Guevel, A. W. Coleman, J.-P. Morel, and N. Morel-Desrosiers, *J. Chem. Soc., Perkin Trans. 2* 1999, 629.

57 O. I. Kalchenko, F. Perret, N. Morel-Desrosiers, and A. W. Coleman, *J. Chem. Soc., Perkin Trans. 2* 2001, 258.

58 E. Da Silva and A. W. Coleman, *Tetrahedron*, 2003, **59**, 7357.

59 M. Selkti, A. Tomas, A. W. Coleman, N. Douteau-Guevel, I. Nicolis, F. Villain, and C. de Rango, *Chem. Commun.*, 2000, 161.

60 A. Lazar, E. Da Silva, N. Alda, C. Barbey, and A. W. Coleman, *Chem. Commun.*, 2004, 2162.

61 J. L. Atwood, T. Ness, P. J. Nichols, and C. L. Raston, *Cryst. Growth Des.*, 2002, **2**, 171.

62 P. J. Nichols and C. L. Raston, *Dalton Trans.*, 2003, 2923.

63 M. Makha, C. L. Raston, A. N. Sobolev, and A. H. White, *Chem. Commun.*, 2004, 1066.

64 P. J. Nichols, C. L. Raston, and J. W. Steed, *Chem. Commun.*, 2001, 1062.

65 L. J. Barbour and J. L. Atwood, *Chem. Commun.*, 2001, 2020.

66 M. J. Hardie, M. Makha, and C. L. Raston, *Chem. Commun.*, 1999, 2409.

67 C. P. Johnson, J. L. Atwood, J. W. Steed, C. B. Bauer, and R. D. Rogers, *Inorg. Chem.*, 1996, **35**, 2602.

68 J. W. Steed, C. P. Johnson, C. L. Barnes, R. K. Juneja, J. L. Atwood, S. Reilly, R. L. Hollis, P. H. Smith, and D. L. Clark, *J. Am. Chem. Soc.*, 1995, **117**, 11426.

69 J. L. Atwood, D. L. Clark, R. K. Juneja, G. W. Orr, K. D. Robinson, and R. L. Vincent, *J. Am. Chem. Soc.*, 1992, **114**, 7558.

70 G. D. Andretti, F. Ugozzoli, A. Casnati, E. Ghidini, A. Pochini, and R. Ungaro, *Gazz. Chim. Ital.*, 1989, **119**, 47.

71 S. L. James, *Chem. Soc. Rev.*, 2003, **32**, 276.

72 P. J. Stang and B. Olenyuk, *Acc. Chem. Res.*, 1997, **30**, 502.

73 Y. K. Kryschenko, S. R. Seidel, D. C. Muddiman, A. I. Nepomuceno, and P. J. Stang, *J. Am. Chem. Soc.*, 2003, **125**, 9647.

74 Y. K. Kryschenko, S. R. Seidel, A. M. Arif, and P. J. Stang, *J. Am. Chem. Soc.*, 2003, **125**, 5193.

75 T. Yamaguchi, S. Tashiro, M. Tominaga, M. Kawano, T. Ozeki, and M. Fujita, *J. Am. Chem. Soc.*, 2004, **126**, 10818.

76 M. Tominaga, K. Suzuki, K. Masaki, T. Kusukawa, T. Ozeki, S. Sakamoto, Y. Kentaro, and M. Fujita, *Angew. Chem. Int. Ed.*, 2004, **43**, 2.

77 B. Moulton, J. Lu, A. Mondal, and M. J. Zaworotko, *Chem. Commun.*, 2001, 863.

78 H. Abourahma, A. W. Coleman, B. Moulton, B. Rather, P. Shahgaldian, and M. J. Zaworotko, *Chem. Commun.*, 2001, 2380.

79 G. J. McManus, Z. Wang, and M. J. Zaworotko, *Cryst. Growth Des.*, 2004, **4**, 11.

80 J. Lu, A. Mondal, B. Moulton, and M. J. Zaworotko, *Angew. Chem. Int. Ed.*, 2001, **40**, 2113.

81 A. Muller, *Science*, 2003, **300**, 749.

82 A. Muller, E. Beckmann, H. Bogge, M. Schmidtmann, and A. Dress, *Angew. Chem. Int. Ed.*, 2002, **41**, 1162.

83 A. Muller, E. Krickemeyer, S. K. Das, P. Kogerler, S. Sarkar, H. Bogge, M. Schmidtmann, and S. Sarkar, *Angew. Chem. Int. Ed.* , 2000, **39**, 1612.

84 A. Muller, S. Sarkar, S. Q. N. Shah, H. Bogge, M. Schmidtmann, S. Sarkar, P. Kogerler, B. Hauptfleisch, A. X. Trautwein, and V. Schunemann, *Angew. Chem. Int. Ed.*, 1999, **38**, 3238.

85 J. Kang and J. Rebek Jr., *Nature*, 1997, **385**, 50.

86 A. R. Far, A. Shivanyuk, and J. Rebek Jr., *J. Am. Chem. Soc.*, 2002, **124**, 2854.

87 A. Scarso, L. Trembleau, and J. Rebek Jr., *J. Am. Chem. Soc.*, 2004, **126**, 13512.

88 B. A. Roberts, G. W. V. Cave, Raston C. L., and J. L. Scott, *Green Chem.*, 2001, **3**, 280.

89 L. R. MacGillivray and J. L. Atwood, *Nature*, 1997, **389**, 469.

90 J. L. Atwood, L. J. Barbour, and A. Jerga, *Proc. Natl. Acad. Sci. U. S. A.*, 2002, **99**, 4837.

91 T. Gerkensmeier, W. Iwanek, C. Agena, R. Frohlich, S. Kotila, C. Nather, and J. Mattay, *Eur. J. Org. Chem.* , 1999, 2257.

92 G. W. V. Cave, Antesberger J., L. J. Barbour, R. M. McKinlay, and J. L. Atwood, *Angew. Chem. Int. Ed.*, 2004, **43**, 5263.

93 F. A. Cotton and G. Wilkinson, in 'Advanced Inorganic Chemistry 5th edn.' New York. 1988.

94 D.-L. Long, R. J. Hill, A. J. Blake, N. R. Champness, P. Hubbertsey, D. M. Proserpio, C. Wilson, and M. Schröder, *Angew. Chem. Int. Ed.*, 2004, **43**, 1851.

95 D.-L. Long, A. J. Blake, N. R. Champness, C. Wilson, and M. Schröder, *Angew. Chem. Int. Ed.*, 2001, **40**, 2444.

96 D.-L. Long, A. J. Blake, N. R. Champness, C. Wilson, and M. Schröder, *Chem. Eur. J.*, 2002, **8**, 2026.

97 L.-P. Zhang, M. Du, W.-J. Lu, and T. C. W. Mak, *Polyhedron*, 2004, **26**, 857.

98 L. Fielding, *Tetrahedron*, 2000, **56**, 6151.

99 J. Gómez-Lara, V. A. Basiuk, E. V. Basiuk, and S. Hernández-Ortega, *J. Chem. Cryst.*, 1999, **29**, 469.

100 H. R. Webb, 'Interaction of the rare earth ions with *p*-sulfonatocalix[4]arene and 18-crown-6', PhD Thesis, Monash University, Clayton, Australia, 2001.

101 K. R. Fewings and P. C. Junk, *Aust. J. Chem.*, 1999, **52**, 1109.

102 J. L. Atwood, L. J. Barbour, S. Dalgarno, C. L. Raston, and H. R. Webb, *J. Chem. Soc., Dalton Trans.*, 2002, 4351.

103 P. Thuéry and B. Masci, *Acta Cryst.*, 2002, **C58**, 556.

104 B. Masci, M. Nierlich, and P. Thuéry, *New J. Chem.*, 2002, **26**, 766.

105 G. B. Deacon, A. Gitlits, G. Zelensy, D. Stellfeldt, and G. Meyer, *Z. Anorg. Allg. Chem.*, 1999, **625**, 764.

106 H.-Y. Sun, Huang C.-H., G.-X. X.-S. Ma, and N.-C. Shi, *Polyhedron*, 1995, **14**, 947.

107 H. Maeda, S. Furuyoshi, Y. Nakatsuji, and M. Okahara, *Bull. Chem. Soc. Jpn.*, 1983, **56**, 212.

108 A. L. Spek, *Acta Cryst.*, 1990, **A46**, C34.

109 J. L. Atwood, L. J. Barbour, M. J. Hardie, C. L. Raston, M. N. Statton, and H. R. Webb, *CrystEngComm*, 2001, 1.

110 A. T. Yordanov, O. A. Gansow, M. W. Brechbiel, L. M. Rogers, and R. D. Rogers, *Polyhedron*, 1999, **18**, 1055.

111 S. Shinkai, *Tetrahedron*, 1993, **49**, 8933.

112 J.-M. Lehn, R. Meric, J.-P. Vigneron, M. Cesario, J. Guilhem, C. Pascard, Z. Asfari, and J. Vicens, *Supramol. Chem.*, 1995, **5**, 97.

113 D. Moras, K. W. Olsen, M. N. Sabesan, M. Buehner, G. C. Ford, and M. G. Rossmann, *J. Biol. Chem.*, 1975, **250**, 9137.

114 A. Gafni and Y. Cohen, *J. Org. Chem.* , 1997, **62**, 120.

115 L. Frish, F. Sansone, A. Casnati, R. Ungaro, and Y. Cohen, *J. Org. Chem.* , 2000, **65**, 5026.

116 L. Avram and Y. Cohen, *Org. Lett.* , 2003, **5**, 3329.

117 T. D. W. Claridge, 'High-Resolution NMR Techniques in Organic Chemistry'. ed. J. E. Baldwin, Williams, R. M., Pergamon, 1999, Oxford.

118 C. S. Johnson, *J. Magn. Reson. A*, 1993, **102**, 214.

119 K. S. Cameron and L. Fielding, *J. Org. Chem.* , 2001, **66**, 6891.

120 M. D. Pelta, H. Barjat, G. A. Morris, A. L. Davis, and S. J. Hammond, *Magn. Reson. Chem.*, 1998, **36**, 706.

121 K. S. Cameron and L. Fielding, *Magn. Reson. Chem.*, 2002, **40**, S106.

122 S. Shinkai, K. Araki, and O. Manabe, *J. Am. Chem. Soc.*, 1988, **110**, 7214.

123 S. Shinkai, K. Araki, T. Matsuda, and O. Manabe, *Bull. Chem. Soc. Jpn.* , 1989, **62**, 3856.

124 G. Arena, A. Contino, F. G. Gulino, A. Magri, F. Sansone, D. Sciotto, and R. Ungaro, *Tet. Lett.*, 1999, **40**, 1597.

125 G. Arena, A. Contino, F. G. Gulino, A. Magri, D. Sciotto, and R. Ungaro, *Tet. Lett.*, 2000, **41**, 9327.

126 N. Kon, N. Iki, and S. Miyano, *Organic & Biomolecular Chemistry*, 2003, **1**, 751.

127 G. Arena, A. Casnati, A. Contino, G. G. Lombardo, D. Sciotto, and R. Ungaro, *Chem. Eur. J.*, 1999, **5**, 738.

128 G. Arena, S. Gentile, F. G. Gulino, D. Sciotto, and C. Sgarlata, *Tetrahedron*, 2004, **45**, 7091.

129 C. Janiak, *J. Chem. Soc., Dalton Trans.*, 2000, **21**, 3885.

130 M. Nishio, *CrystEngComm*, 2004, **6**, 130.

131 L. J. Barbour, 'Cavity', Columbia, MO, 2001.

132 T. Douglas and M. Young, *Nature*, 1998, **393**, 152.

133 R. D. Rogers and A. N. Rollins, *J. Chem. Cryst.*, 1994, **24**, 321.

134 R. D. Rogers, A. N. Rollins, R. D. Etzenhouser, E. J. Voss, and C. B. Bauer, *Inorg. Chem.*, 1993, **32**.

135 R. B. King, *Inorg. Chim. Acta*, 1992, **198-200**, 841.

136 W. N. Lipscomb, *Science*, 1966, **153**, 373.

137 A. P. Côté and G. K. H. Shimizu, *Coord. Chem. Rev.* , 2003, **245**, 49.

138 M. G. Walawalkar, M. Ramaswamy, H. W. Roesky, I. Usón, and R. Kraetzner, *Inorg. Chem.*, 1998, **37**, 473.

139 H. Zhang, X. Wang, and B. K. Teo, *J. Am. Chem. Soc.*, 1996, **118**, 11813.

140 W. J. Dressick, C. George, S. L. Brandow, T. L. Schull, and D. A. Knight, *J. Org. Chem.*, 2000, **65**, 5059.

141 I. Abrahams, M. Lazell, M. Motavelli, S. A. A. Shah, and A. C. Sullivan, *J. Organomet. Chem.*, 1998, **553**, 23.

142 W. Klaui, A. Muller, W. Eberspach, R. Boese, and I. Goldberg, *J. Am. Chem. Soc.*, 1987, **109**, 164.

143 P. Sobota, M. Klimowicz, J. Utko, and L. B. Jerzykiewicz, *New J. Chem.*, 2000, **24**, 523.

144 Z. Asfari, J. Harrowfield, P. Thuery, and J. Vicens, *Supramol. Chem.*, 2003, **15**, 69.

145 R. Castro, L. A. Godinez, C. M. Crissm, S. G. Bott, and A. E. Kaifer, *Chem. Commun.*, 1997, 935.

146 E. Moret, F. Nicolo, D. Plancherel, P. Froidevaux, J.-C. G. Bunzli, and G. Chapuis, *Helv. Chim. Acta*, 1991, **74**, 65.

147 F. Nicolo, D. Plancherel, J.-C. G. Bunzli, and G. Chapuis, *Helv. Chim. Acta*, 1987, **70**, 1798.

148 H. Hassaballa, J. W. Steed, P. C. Junk, and M. R. J. Elsegood, *Inorg. Chem.*, 1998, **37**, 4666.

149 P. Starynowicz, *Polyhedron*, 2003, **22**, 337.

150 N. Douteau-Guevel, F. Perret, A. W. Coleman, J.-P. Morel, and N. Morel-Desrosiers, *J. Chem. Soc., Perkin Trans. 2* 2002, 524.

151 L. Memmi, A. Lazar, A. Brioude, V. Ball, and A. W. Coleman, *Chem. Commun.*, 2001, 2474.

152 E. J. Kosnic, E. L. McClymont, R. A. Hodder, and P. J. Squattrio, *Inorg. Chim. Acta*, 1992, **201**, 143.

153 A. J. Blake, M. T. Brett, N. R. Champness, A. N. Khlobystov, D.-L. Long, C. Wilson, and M. Schroder, *Chem. Commun.*, 2001, **21**, 2258.

154 A. Specht, P. Bernard, M. Goeldner, and L. Peng, *Angew. Chem. Int. Ed.* , 2002, **41**, 4706.